frontiers | Research Topics

Recent advances in the treatment of epilepsy

Edited by
Khojasteh Malekmohammad, Mahmoud Rafieian-Kopaei and Antonella Riva

Published in
Frontiers in Pharmacology
Frontiers in Neurology
Frontiers in Neuroscience

ISSN 1664-8714
ISBN 978-2-8325-5060-1
DOI 10.3389/978-2-8325-5060-1

About Frontiers

Frontiers is more than just an open access publisher of scholarly articles: it is a pioneering approach to the world of academia, radically improving the way scholarly research is managed. The grand vision of Frontiers is a world where all people have an equal opportunity to seek, share and generate knowledge. Frontiers provides immediate and permanent online open access to all its publications, but this alone is not enough to realize our grand goals.

Frontiers journal series

The Frontiers journal series is a multi-tier and interdisciplinary set of open-access, online journals, promising a paradigm shift from the current review, selection and dissemination processes in academic publishing. All Frontiers journals are driven by researchers for researchers; therefore, they constitute a service to the scholarly community. At the same time, the *Frontiers journal series* operates on a revolutionary invention, the tiered publishing system, initially addressing specific communities of scholars, and gradually climbing up to broader public understanding, thus serving the interests of the lay society, too.

Dedication to quality

Each Frontiers article is a landmark of the highest quality, thanks to genuinely collaborative interactions between authors and review editors, who include some of the world's best academicians. Research must be certified by peers before entering a stream of knowledge that may eventually reach the public - and shape society; therefore, Frontiers only applies the most rigorous and unbiased reviews. Frontiers revolutionizes research publishing by freely delivering the most outstanding research, evaluated with no bias from both the academic and social point of view. By applying the most advanced information technologies, Frontiers is catapulting scholarly publishing into a new generation.

What are Frontiers Research Topics?

Frontiers Research Topics are very popular trademarks of the *Frontiers journals series*: they are collections of at least ten articles, all centered on a particular subject. With their unique mix of varied contributions from Original Research to Review Articles, Frontiers Research Topics unify the most influential researchers, the latest key findings and historical advances in a hot research area.

Find out more on how to host your own Frontiers Research Topic or contribute to one as an author by contacting the Frontiers editorial office: frontiersin.org/about/contact

Recent advances in the treatment of epilepsy

Topic editors

Khojasteh Malekmohammad — Shiraz University, Iran

Mahmoud Rafieian-Kopaei — Shahrekord University of Medical Sciences, Iran

Antonella Riva — University of Genoa, Italy

Citation

Malekmohammad, K., Rafieian-Kopaei, M., Riva, A., eds. (2024). *Recent advances in the treatment of epilepsy*. Lausanne: Frontiers Media SA.

doi: 10.3389/978-2-8325-5060-1

Table of contents

05 Editorial: Recent advances in the treatment of epilepsy
Khojasteh Malekmohammad, Antonella Riva and Mahmoud Rafieian-Kopaei

08 Effects of ketogenic diet on the classification and functional composition of intestinal flora in children with mitochondrial epilepsy
Jing Wang, Lljuan Huang, Hua Li, Guohong Chen, Liming Yang, Dong Wang, Hong Han, Guo Zheng, Xu Wang, Jianmin Liang, Weijie He, Fang Fang, Jianxiang Liao and Dan Sun

17 Activated protein C in epilepsy pathophysiology
Linda Ines Zoungrana, Steven Didik, Hao Wang, Lily Slotabec and Ji Li

28 Population pharmacokinetics of everolimus in patients with seizures associated with focal cortical dysplasia
Jinha Park, Se Hee Kim, Jongsung Hahn, Hoon-Chul Kang, Sang-Guk Lee, Heung Dong Kim and Min Jung Chang

37 Lippia origanoides essential oil possesses anticonvulsant effect in pentylenetetrazol-induced seizures in rats: a behavioral, electroencephalographic, and electromyographic study
Daniella Bastos de Araújo, Anthony Lucas Gurgel do Amaral, Suzane Maia da Fonseca, Keyla Rodrigues de Souza, Allane Patrícia Santos da Paz, Vanessa Jóia de Mello, Gabriela Brito Barbosa, Maria Klara Otake Hamoy and Moisés Hamoy

48 Cenobamate as add-on therapy for drug resistant epilepsies: effectiveness, drug to drug interactions and neuropsychological impact. What have we learned from real word evidence?
Nicola Pietrafusa, Giovanni Falcicchio, Emilio Russo, Simona Lattanzi, Bianca Goffredo, Raffaele Simeoli, Sara Cairoli, Tiziana Corsetti, Roberta Roberti, Marina De Tommaso, Federico Vigevano, Angela La Neve and Nicola Specchio

60 Anti-seizure effects of JNJ-54175446 in the intra-amygdala kainic acid model of drug-resistant temporal lobe epilepsy in mice
Omar Mamad, Mona Heiland, Andreas U. Lindner, Thomas D. M. Hill, Ronan M. Ronroy, Kilian Rentrup, Amaya Sanz-Rodriguez, Elena Langa, Janosch P. Heller, Oscar Moreno, Jordi Llop, Anindya Bhattacharya, James A. Palmer, Marc Ceusters, Tobias Engel and David C. Henshall

71 Psychedelics, epilepsy, and seizures: a review
Ninon Freidel, Liliane Kreuder, Brenden Samuel Rabinovitch, Frank Yizhao Chen, Ryan S. T. Huang and Evan Cole Lewis

80 The interplay between microbiota and brain-gut axis in epilepsy treatment
Hanxiao Zhu, Wei Wang and Yun Li

106 Early life phenobarbital exposure dysregulates the hippocampal transcriptome
Seán Quinlan, Tahiyana Khan, David McFall, Carolina Campos-Rodriguez and Patrick A. Forcelli

122 Benzyl isothiocyanate ameliorates cognitive function in mice of chronic temporal lobe epilepsy
Chang Xiaoyu, Zhou Hongzhen, Peng Nan, Gao Tengwei, Gong Yanan, Guo Yan, La Haiyan, Ma Li, Wu Haiya, Wen Yujun and Zhang Rui

135 ADCY3: the pivotal gene in classical ketogenic diet for the treatment of epilepsy
Mingxing Lin, Jiayin Gong, Luyan Wu, Xin Lin, Yuying Zhang, Wanhui Lin, Huapin Huang and Chaofeng Zhu

154 Reproductive and fetal toxicity studies of histamine H3 receptor antagonist DL76 used in mice to prevent maximal electroshock-induced seizure
Salim M. Bastaki, Yousef M. Abdulrazzaq, Marwan Abdelrahim Zidan, Mohamed Shafiullah, Saif Ghdayer Alaryani, Fatima Awad Alnuaimi, Ernest Adeghate, Sahar Mohsin, Amal Akour, Agata Siwek, Dorota Łażewska, Katarzyna Kieć-Kononowicz and Bassem Sadek

frontiers | Frontiers in Pharmacology

TYPE Editorial
PUBLISHED 02 July 2024
DOI 10.3389/fphar.2024.1444138

OPEN ACCESS

EDITED AND REVIEWED BY
Nicholas M. Barnes,
University of Birmingham, United Kingdom

*CORRESPONDENCE
Mahmoud Rafieian-Kopaei,
rafieian@yahoo.com

RECEIVED 05 June 2024
ACCEPTED 07 June 2024
PUBLISHED 02 July 2024

CITATION
Malekmohammad K, Riva A and Rafieian-Kopaei M (2024), Editorial: Recent advances in the treatment of epilepsy. *Front. Pharmacol.* 15:1444138. doi: 10.3389/fphar.2024.1444138

Editorial: Recent advances in the treatment of epilepsy

Khojasteh Malekmohammad[1], Antonella Riva[2,3] and Mahmoud Rafieian-Kopaei[4]*

[1]Department of Biology, College of Sciences, Shiraz University, Shiraz, Iran, [2]IRCCS Istituto Giannina Gaslini Institute, Genoa, Italy, [3]Department of Neurosciences Rehabilitation, Ophthalmology, Genetics, Maternal and Child Health (DiNOGMI), University of Genoa, Genoa, Italy, [4]Medical Plants Research Center, Basic Health Sciences Institute, Shahrekord University of Medical Sciences, Shahrekord, Iran

KEYWORDS

epilepsy, seizure, drug-resistance, anti-seizure medications, ketogenic diet, neuroprotection

Editorial on the Research Topic
Recent advances in the treatment of epilepsy

Epilepsy is one of the World's oldest recognized neurological disorders, while its intricate mechanisms of pathogenesis, development, and treatment remain a conundrum. This Research Topic aimed to delve into the recent advancements in the treatment of epilepsy. It compiles unique studies from original research to review articles, covering the pathophysiological mechanisms underlying epilepsy with a special focus on the novel pharmacological and non-pharmacological therapeutic approaches.

Anti-seizure medications (ASMs) are the preferred first line of treatment to reduce neuronal excitability and seizure frequency. Various drugs, including brivaracetam, cannabidiol, cenobamate (CNB), everolimus (EVE), and fenfluramine have been employed in patients with epilepsy (Schmidt and Schachter, 2014; Perucca, 2021). Despite the wide usage of ASMs, about 30% of patients with epilepsy are refractory to treatment. Drug-Resistant Epilepsy (DRE) is a condition with long-term negative outcomes due to the unsatisfactory control over seizures (Gonzalez-Giraldo and Sullivan, 2020; Löscher et al., 2020).

Pietrafusa et al. reported that CNB, a drug acting both as a positive $GABA_A$ allosteric modulator and as an inhibitor of persistent sodium currents, could reduce the frequency of seizures in patients with drug-resistant focal-onset epilepsy. In their work the Authors provided pharmacokinetic evidence of drug-drug interactions and assessed CNB tolerability and efficacy. In line with these findings, Park et al. found that EVE, an inhibitor of the mammalian target of rapamycin complex 1 (mTORC1), could be a valuable adjunctive treatment for patients with seizures associated with focal cortical dysplasia.

Phenobarbital (PB) and levetiracetam (LEV) are generally the first choice for treating neonatal onset seizures. According to the intriguing research work of Quinlan et al. PB can cause long-term/adverse effects on the developing brain based on the transcriptomic analysis. Impaired synaptic development, behavioral and cognitive changes, and acute neurotoxicity are the most common manifestations of PB. LEV is safer than PB; it can prevent these changes in the brain. Mamad et al. research highlighted the anti-seizure effects of P2X7 receptor antagonist JNJ-47965567 in the treatment of drug-resistant Temporal Lobe Epilepsy (TLE). The JNJ-47965567 mechanisms of action in reducing spontaneous recurrent seizures can be based on decreasing astrogliosis, therefore reducing

neuroinflammation and changing the morphology of microglia processes in the CA3 region of the hippocampus. Research by Bastaki et al. revealed the anticonvulsant effect of histamine H3 receptor antagonist DL76 against maximal electroshock (MES)-induced seizure. Also, DL76, used at high doses, did not show urogenital and skeletal abnormalities and caudal malformation.

In line with the use of natural compound-based treatments, *Lippa origanoides* essential oil (LOEO) demonstrated to control seizures induced by pentylenetetrazol in rats. Also, *L. origanoides* essential oil had a synergistic anticonvulsant effect if associated to diazepam. A combination of LOEO with diazepam may be considered in the future as a neuroprotective therapeutic option for the treatment of epilepsy (Bastos de Araújo et al.).

Benzyl isothiocyanate (BITC), a natural component of cruciferous vegetables, exhibited its neuroprotective properties by improving the cognitive function, learning and memory abilities, and spatial cognition in the lithium-pilocarpine-induced chronic temporal lobe epileptic mice. BITC treatment increased the antioxidant capacity of the hippocampal tissue through activating of nuclear factor E2-related factor2/heme oxygenase 1 (Nrf2/HO-1) signaling pathway, along with increased glutathione peroxidase (GSH-Px) activity and decreased malondialdehyde (MDA) content (Xiaoyu et al.).

Zoungrana et al. reviewed the mechanisms involved in the induction, development, and pathogenesis of epilepsy. Also, they highlighted the Activated Protein C (APC) neuroprotective effects and the possible connection between APC and epileptic seizures. APC, as an anticoagulant protein, can reduce epilepsy pathogenesis by preventing blood-brain barrier dysfunction, decreasing neuroinflammation and apoptosis, and eventually increasing neurogenesis.

Freidel et al. shed light on the effects of different psychedelics, especially classical psychedelics, on non-epilepsy chronic seizure disorders. In their review paper, they provided a complete background about Psychedelic-assisted therapy (PAT) in the context of epilepsy and seizures. Usage of psychedelics such as Ketamine, lysergic acid diethylamide (LSD), 3,4 methylenedioxymethamphetamine (MDMA), and psilocybin "magic mushrooms" may be safe in patients with epilepsy under clinical supervision.

Drug resistance is a main challenge in the treatment of epilepsy. It is often related to uncontrolled tonic-colonic seizures that can result in sudden unexpected death (SUDEP). Neurostimulation techniques have gained more attention as novel non-pharmacological treatments for DRE patients. Particularly, Vagal Nerve Stimulation (VNS), Deep Brain Stimulation (DBS), and Responsive NeuroStimulation (RNS) are invasive techniques to modulate neuronal activity (Davis and Gaitanis, 2020; Riva et al., 2021). Also, there are 4 types of non-invasive neuromodulation for the treatment of epilepsy: transcutaneous vagus nerve stimulation (tVNS), trigeminal nerve stimulation (TNS), repetitive transcranial magnetic stimulation (rTMS), and Focused ultrasound method (Riva et al., 2021; Lescrauwaet et al., 2022).

The Ketogenic Diet (KD), a dietary approach with low-carbohydrate and high-fat content, has a pivotal role in the treatment of DRE along with surgery, ASMs, and neuromodulatory techniques. The KD and its variants, including the Classic Ketogenic Diet (KD), Medium-Chain Triglyceride Diet (MCTD), Modified Atkins Diet (MAD), and Low-Glycemic Index Treatment (LGIT) have already proven effective in seizure reduction through different anti-seizure mechanisms, such as elevating inhibitory neurotransmitters and reducing neuronal excitability, increasing brain energy production, and reducing production of proinflammatory and pro-apoptotic factors (Verrotti et al., 2020; Haridas and Kossoff, 2022).

The gut microbiota is also related to epilepsy through the gut-brain axis. Genetic factors, age, region, and diet are various factors that can affect the gut microbiota composition. The KD has been widely used in the treatment of refractory epilepsy. The antiepileptic effects of the KD on the gut microbiota have been studied through 16S rRNA sequencing in patients with mitochondrial epilepsy (Wang et al.).

Furthermore, the review by Zhu et al. marked a close relationship between the microbiota and the gut-brain by elucidating how the rebuilding of gut microbiota by KD, probiotics, and fecal microbiota transplantation could improve drug-resistant epilepsy. Indeed, the mechanisms through which the gut microbiota can be modulated for the treatment of epilepsy have been described.

Building upon the understanding of the molecular mechanisms of the KD in the treatment of epilepsy, in their study, Lin et al. investigated the mechanistic role of KD in treating epilepsy by assessing the Adenylate Cyclase 3 (ADCY3)-initiated cAMP signaling pathway. It was revealed that KD could improve epileptic seizures by regulating fatty acid metabolism, activating ADCY3-initiated cAMP signaling pathway, and enhancing neuronal inhibition. Also, Meta-analysis and animal experiments proved that KD was superior to other diets (i.e., routine diet) in contrast in treating epilepsy.

Therefore, the study of mechanisms underlying epilepsy and its novel treatments has become an intriguing scientific field. We hope that this special edition will present new insights into the current knowledge about ASMs and non-pharmacological therapeutic options involved in the treatment of epilepsy. We anticipate that the articles published on this Research Topic would be useful for clinicians and researchers in the field of neuroscience.

Author contributions

KM: Writing–original draft, Conceptualization. AR: Writing–review and editing. MR-K: Writing–review and editing, Conceptualization.

Funding

The author(s) declare that no financial support was received for the research, authorship, and/or publication of this article.

Conflict of interest

The authors declare that the research was conducted in the absence of any commercial or financial relationships that could be construed as a potential conflict of interest.

Publisher's note

References

Davis, P., and Gaitanis, J. (2020). Neuromodulation for the treatment of epilepsy: a review of current approaches and future directions. *Clin. Ther.* 42 (7), 1140–1154. doi:10.1016/j.clinthera.2020.05.017

Gonzalez-Giraldo, E., and Sullivan, J. E. (2020). Advances in the treatment of drug-resistant pediatric epilepsy. *Seminars neurology* 40 (2), 257–262. doi:10.1055/s-0040-1702941

Haridas, B., and Kossoff, E. H. (2022). Dietary treatments for epilepsy. *Neurol. Clin.* 40 (4), 785–797. doi:10.1016/j.ncl.2022.03.009

Lescrauwaet, E., Vonck, K., Sprengers, M., Raedt, R., Klooster, D., Carrette, E., et al. (2022). Recent advances in the use of focused ultrasound as a treatment for epilepsy. *Front. Neurosci.* 16, 886584. doi:10.3389/fnins.2022.886584

Löscher, W., Potschka, H., Sisodiya, S. M., and Vezzani, A. (2020). Drug resistance in epilepsy: clinical impact, potential mechanisms, and new innovative treatment options. *Pharmacol. Rev.* 72 (3), 606–638. doi:10.1124/pr.120.019539

Perucca, E. (2021). The pharmacological treatment of epilepsy: recent advances and future perspectives. *Acta Epileptol.* 3 (1), 22. doi:10.1186/s42494-021-00055-z

Riva, A., Golda, A., Balagura, G., Amadori, E., Vari, M. S., Piccolo, G., et al. (2021). New trends and most promising therapeutic strategies for epilepsy treatment. *Front. neurology* 12, 753753. doi:10.3389/fneur.2021.753753

Schmidt, D., and Schachter, S. C. (2014). Drug treatment of epilepsy in adults. *Bmj* 348, 2544–g318. doi:10.1136/bmj.g254

Verrotti, A., Iapadre, G., Di Francesco, L., Zagaroli, L., and Farello, G. (2020). Diet in the treatment of epilepsy: what we know so far. *Nutrients* 12 (9), 2645. doi:10.3390/nu12092645

frontiers | Frontiers in Neurology

TYPE Original Research
PUBLISHED 31 July 2023
DOI 10.3389/fneur.2023.1237255

OPEN ACCESS

EDITED BY
Khojasteh Malekmohammad,
Shiraz University, Iran

REVIEWED BY
Valentina Biagioli,
Giannina Gaslini Institute (IRCCS), Italy
Simone Perottoni,
Polytechnic University of Milan, Italy

*CORRESPONDENCE
Dan Sun
✉ Sundan@zgwhfe.com
Fang Fang
✉ 13910150389@163.com
Jianxiang Liao
✉ liaojianxiang@vip.sina.com

†These authors have contributed equally to this work

RECEIVED 09 June 2023
ACCEPTED 14 July 2023
PUBLISHED 31 July 2023

CITATION
Wang J, Huang L, Li H, Chen G, Yang L, Wang D, Han H, Zheng G, Wang X, Liang J, He W, Fang F, Liao J and Sun D (2023) Effects of ketogenic diet on the classification and functional composition of intestinal flora in children with mitochondrial epilepsy. *Front. Neurol.* 14:1237255. doi: 10.3389/fneur.2023.1237255

Effects of ketogenic diet on the classification and functional composition of intestinal flora in children with mitochondrial epilepsy

Jing Wang[1†], LIjuan Huang[1†], Hua Li[2], Guohong Chen[3], Liming Yang[4], Dong Wang[5], Hong Han[6], Guo Zheng[7], Xu Wang[8], Jianmin Liang[9], Weijie He[10], Fang Fang[11*], Jianxiang Liao[12*] and Dan Sun[1*]

[1]Department of Pediatric Neurology, Wuhan Children's Hospital, Tongji Medical College, Huazhong University of Science and Technology, Wuhan, Hubei, China, [2]Department of Epilepsy Center, Guangdong 999 Brain Hospital, Guangzhou, China, [3]Department of Neurology, Henan Provincial Children's Hospital, Zhengzhou, China, [4]Department of Neurology, Hunan Provincial Children's Hospital, Changsha, China, [5]Department of Neurology, Xi'an Children's Hospital, Xi'an, China, [6]Department of Neurology, Children's Hospital of Shanxi, Taiyuan, China, [7]Department of Neurology, Nanjing Children's Hospital, Nanjing, China, [8]Department of Neurology, Changchun Children's Hospital, Changchun, China, [9]Department of Neurology, The First Bethune Hospital of Jilin University, Changchun, China, [10]Aegicare (Shenzhen) Technology Co., Ltd., Shenzhen, China, [11]Department of Neurology, Beijing Children's Hospital, Capital Medical University, Beijing, China, [12]Department of Neurology, Shenzhen Children's Hospital, Shenzhen, China

The ketogenic diet (KD) has shown excellent performance in the treatment of refractory epilepsy, but how it works is not yet fully understood. Gut microbiota is associated with various neurological disorders through the brain-gut axis. Different dietary patterns have different effects on the composition and function of gut microbiota. Here, by analyzing fecal samples from some patients with mitochondrial epilepsy before and after KD treatment through 16SrRNA sequencing, we found that KD intervention reduced the abundance of *Firmicutes* in the patient's gut, while the abundance of *Bacteroidota* increased in the KD group. LefSe analysis showed that *Actinobacteriota*, *Phascolarctobacterium* had significant advantages in the control group, while Bacteroides increased significantly after KD intervention, especially *Bacteroides fragilis*. Functional analysis showed that there were significant differences in 12 pathways in level 3. These changes suggest that KD can change the composition and diversity of the gut microbiota in patients and affect their function. Changes in specific bacterial groups in the gut may serve as biomarkers for the therapeutic effects of KD on epilepsy.

KEYWORDS

mitochondrial epilepsy, ketogenic diet, gut microbiota, microbiota-gut-brain axis, *Bacteroides fragilis*

Introduction

The ketogenic diet is a low-carbohydrate, high-fat diet that induces the use of ketone bodies as the primary energy substrate by modulating intermediary metabolism. Developed in the 1920s (1), it has been widely used in the treatment of intractable epilepsy and has been shown to be safe and effective in this context (2–4). It is commonly believed that the KD plays an important role in mitochondrial biogenesis and function improvement (5), our previous studies have demonstrated that KD plays a significant role in the treatment of mitochondrial epilepsy (6) as well as in reducing oxidative stress (7–9). Increasing evidence suggests that the KD may also be involved in regulating brain excitability and epilepsy through pathways such as interrupting glutamate synaptic transmission (10), reducing glycolysis, and activating ATP-sensitive potassium channels (11). It is worth mentioning that due to its role in neuronal metabolism regulation, the KD has also been widely used in other neurological disorders such as Alzheimer's disease and autism spectrum disorders (12). However, it is still unclear how KD exactly exerts beneficial effects on brain activity and behavior. The classical KD relies on nearly complete elimination of dietary carbohydrates to induce ketosis, allowing long-chain fatty acids (LCFAs) in the liver to produce ketone bodies. Currently, alternative ketogenic supplements, such as medium-chain triglycerides (MCTs), can rapidly induce ketone production, leading to extensive neuroprotective effects (13).

As an intermediary between diet and host, the composition and abundance of gut microbiota are regulated by various factors, such as internal factors like genetics and age, and external factors like region and diet (14). We know that the composition of gut microbiota can change rapidly and persistently with dietary changes (15, 16). In recent years, more and more researchers have paid attention to the changes in gut microbiota in normal and diseased populations, and studies have shown that they play a regulatory role in the progression of various diseases in the human body. For example, in obese populations, there are significant changes in the phyla Bacteroidetes and Firmicutes (17, 18); in non-alcoholic fatty liver disease and type 2 diabetes, the gut microbiota also plays an important mediating role (19). The changes in gut microbiota induced by KD may affect metabolic and neural pathways related to epilepsy (16), and there is also evidence that the use of antibiotics increases the risk of epileptic seizures (20). This suggests that gut microbiota may play a key role in alleviating symptoms of epilepsy in ways that we are not yet clear about. Xie et al. (21) found significant differences in the gut microbiota composition between 14 epileptic children and 30 healthy individuals, and observed a decrease in the abundance of dominant pathogens (such as *Escherichia coli*, *Salmonella*, and *Vibrio*) and a significant increase in beneficial bacteria (such as *Bacteroides*) in the gut of epileptic children after KD treatment. Zhang et al. (22) analyzed the gut microbiota composition of 20 refractory epilepsy patients before and after KD treatment, and found that the α-diversity of gut microbiota was lower after KD treatment, with a significant decrease in the abundance of *Firmicutes* and an increase in the abundance of *Bacteroidetes*. Lindefeldt et al. (23) studied the gut microbiota of 12 drug-resistant epilepsy children and found that after 3 months of KD treatment, there was no significant change in the α-diversity of the gut microbiota, but the abundance of *Bifidobacterium* was significantly reduced, and the abundance of *Escherichia coli* increased. Based on these studies, although KD treatment was administered to all epilepsy patients, there were differences in the source of dietary fat and the timing of intervention, as well as differences in patient age, race, and epilepsy etiology, which led to variations in gut microbiota composition before and after KD treatment. Therefore, it is difficult to compare the results and establish a consensus based on these studies.

Here, we aimed to explore the relationship and potential altered pathways between ketosis, gut microbiota, and mitochondrial epilepsy. We performed 16S rRNA sequencing on samples obtained after following a KD, analyzed changes in microbial abundance and diversity in various populations, and conducted enrichment analysis of the potential functional pathways they may be involved in to reveal their relationship with the alleviation of epilepsy symptoms.

Materials and methods

Study cohort

Between January 2019 and December 2020, a total of 15 patients with mitochondrial diseases accompanied by epilepsy, ranging from newborns to 16 years old (Supplementary Table 1). Mitochondrial diseases were confirmed through genetic diagnosis (identifying pathogenic gene mutations in mtDNA or nDNA) and abnormal biomarkers (lactate and ketone bodies). The epilepsy condition was assessed using the International League Against Epilepsy (ILAE) classification system (24). Patients meeting the following criteria were excluded: those who had previously received KD treatment, other genetic metabolic disorders, immunodeficiency, severe gastrointestinal, cardiovascular, respiratory, hepatic, or urogenital diseases.

Experimental design

All eligible participants were randomly assigned to two groups (control group: regular diet + AED, study group: KD + AED) for treatment. During the enrollment period for starting KD, fecal samples were collected from the control group patients. Subsequently, KD was initiated at a 2:1 ratio of fat to non-fat components, with no fluid restriction and no fasting. The nutritionist calculated the daily energy requirements for each participant based on their age, height, and weight. Blood ketones and glucose levels were monitored every 6 h for the first 4 days. All side effects such as high ketone levels and low blood sugar were taken seriously and promptly addressed. Starting from the fifth day, energy intake was adjusted to meet daily requirements. During the baseline period, the nutritionist recorded the participants' conditions using an observation chart. The first month of KD, known as the efficacy observation period or titration period, was a critical time for adjustments. The doctor or nutritionist made adjustments to the KD ratio, daily energy intake, meal times, meal frequency, and calorie intake based on the patient's condition. At the end of the 12th week, the second fecal sample was collected. The

control group followed a regular diet plus standard AED for the first 4 weeks. Afterward, they underwent 12 weeks of KD treatment alongside the study group. Parents could decide to withdraw from the study at any time due to poor efficacy, poor tolerance, or other reasons. The doctor also had the authority to terminate KD if the participant experienced side effects or disease exacerbation.

To compare the gut microbiota composition between the KD group and the control group, 16S rRNA analysis was conducted. Further research was carried out using methods such as diversity analysis, differential analysis, and functional prediction to explore the differences in gut microbiota composition and functional pathways between the two groups.

Sample collection and storage

Fecal samples were obtained by parents using sterile cotton swabs and collection boxes. The first sample was collected before the initiation of KD. After 3 months of KD, a second sample was taken, which was then stored in a refrigerator for several hours until it was transported at low temperatures to the hospital. All samples were stored at −80°C.

Sample processing and sequencing

After sample collection, according to the instructions of the E.Z.N.A.® soil DNA kit (Omega Bio-tek, Norcross, GA, United States), microbial community total DNA extraction was performed. The 16S rRNA gene V3-V4 variable region was amplified by PCR using the primers 338F (5′-ACTCCTACGGGAGGCAGCAG-3′) and 806R (5′-GGACTACHVGGGTWTCTAAT-3′). After mixing the PCR products, the mixture was purified using a 2% agarose gel and the AxyPrep DNA Gel Extraction Kit (Axygen Biosciences, Union City, CA, United States). Library construction was performed using the NEXTFLEX Rapid DNA-Seq Kit, and sequencing was carried out using the Illumina NovaSeq PE250 platform.

Bioinformatics analysis

First, the software Trimmomatic v0.33 was used to filter the raw reads obtained from sequencing. Then, the software cutadapt 1.9.1 was used to identify and remove primer sequences, resulting in clean reads without primer sequences. The dada2 (25) method from QIIME2 2020.6 (26) was used for denoising, paired-end sequence merging, and removal of chimeric sequences, obtaining the final set of valid data (non-chimeric reads).

QIIME was also used for calculating the diversity of 16S rRNA gene sequencing analysis. Diversity indices (such as Shannon and Chao1) were used to evaluate the α-diversity of the samples. β-diversity was calculated based on the weighted Bray-Curtis distance matrix and visualized in principal coordinate analysis (PCoA). Linear discriminant analysis (LDA) effect size (LEfSe) was used to identify statistically significant differences in the relative abundance of taxa. Only LDA values >3 were considered significantly enriched. Functional prediction was performed using Tax4Fun, analyzing the composition and differences of metabolic pathways based on the KEGG database.

Statistical analysis

Data analysis was performed using SPSS statistical software (SPSS, Chicago, IL, United States). Student's *t*-test was used for comparing means between two groups, and the chi-square test was used for analyzing categorical variables. Measurement data are presented as mean ± standard deviation. Spearman correlation analysis was used to evaluate the relationship between gut microbiota and epilepsy ($p < 0.05$ considered significant).

Results

The demographic and clinical characteristics

Fifteen patients with mitochondrial epilepsy from 11 clinical centers participated in this study. They were randomly divided into two groups: eight in the KD group and seven in the control group. There were no significant differences in gender, age, duration of illness, medication, and number of seizures between the two groups ($p > 0.05$). We collected fecal samples from the patients at two time points: before starting KD and 3 months after starting KD. We obtained seven control group samples and eight KD group samples in total (Table 1).

Gut microbiota diversity

To investigate the effect of ketogenic intervention on gut microbiota in patients, alpha diversity and beta diversity were used to reflect the diversity of the microbial community within samples and the differences between samples, respectively. We observed that Shannon diversity was slightly higher in the control group than in the ketogenic intervention group, but this difference was not significant ($p > 0.05$), while Chao1 diversity showed that microbial diversity was significantly higher in the control group than in the KD group ($p < 0.05$; Figures 1A,B). Beta diversity PCoA analysis based on weighted Bray-Curtis distance showed differences in microbial composition between the KD group and the control group (Figure 1C). The cluster heatmap also showed clear distinctions between the two groups of samples (Figure 1D). At the phylum level, *Firmicutes* was the largest phylum in both the KD group and the control group, but its abundance was relatively lower in the KD group (42.76% in the KD group vs. 48.13% in the control group). The second-largest phylum, *Bacteroidota*, showed a significant increase in abundance in the KD group (36.93% in the KD group vs. 25.41% in the control group). Some low-abundance microbes showed an increasing trend in the control group, including *Actinobacteriota* (1.66% in the KD group vs. 7.64% in the control group), *Fusobacteriota* (0.68% in the KD group vs. 1.65% in the control group), and *Desulfobacterota* (0.15% in the KD group vs. 0.50% in the control group; Figure 2A). At the genus level, compared to the control group, *Bacteroides* showed a significant

TABLE 1 Demographic characteristics of the study population between the KD and control groups.

	KD group ($n = 8$)	Control group ($n = 7$)	p value
Age (year)	8.4 ± 4.8	4.7 ± 4.5	0.174
Sex			
Male	7 (87.5%)	6 (85.7%)	0.919
Female	1 (12.5%)	1 (14.3%)	
Age of onset (year)	6.9 ± 4.3	3.3 ± 3.8	0.135
Course of disease (year)	1.5 ± 1.0	1.3 ± 1.0	0.797
Seizure type			
Focal onset	4 (50.0%)	5 (71.4%)	0.398
Generalized onset	4 (50.0%)	2 (28.6%)	
Frequency (seizures per month)			
0–4	5 (62.5%)	2 (28.6%)	0.189
5–12	3 (37.5%)	5 (71.4%)	
Number of AEDs used (at the time of enrollment)			
0	3 (37.5%)	3 (42.8%)	0.966
1	1 (12.5%)	1 (14.3%)	
2	2 (25.0%)	2 (28.6%)	
4	2 (25.0%)	1 (14.3%)	

increase in the KD group (28.78% in the KD group vs. 9.51% in the control group; Figure 2B).

We used the Linear Discriminant Analysis (LDA) Effect Size (LEfSe) method proposed by Segata et al. (27) to confirm the differences between the KD group and the control group. In the control group, the abundance of *Actinobacteriota* increased significantly at the phylum level, while the abundance of *Firmicutes* and *Bacteroidota* changed without significant differences ($p > 0.05$). The abundance of *Phascolarctobacterium*, *Subdoligranulum*, *Agathobacter*, and *Erysipelotrichaceae_UCG_003* was relatively high at the genus level. In the KD group, the abundance of *Bacteroides* increased significantly at the genus level, mainly due to the significant increase of *Bacteroides fragilis* at the species level. We also observed an increase in *Blautia.s__Blautia_sp__N6H1_15* at the genus level and *Anaerotignum_lactatifermentans* at the species level in the KD group (Figures 3A,B).

Changes in gut microbiota function

Tax4Fun was used for functional prediction. In the comparison between the KD group and the control group, we found some obvious differences in three levels of KEGG pathways. Specifically, at each level, we found that some metabolic pathways, such as Environmental Information Processing and Cellular Processes, were slightly downregulated in the KD group, but not significantly. However, in level 2, some pathways showed significant differences between the two groups, with Infectious diseases: Bacterial and Signal transduction significantly elevated in the KD group. Particularly in level 3, a total of 320 pathways showed differences, mainly enriched in metabolic pathways such as Biosynthesis of secondary metabolites, Biosynthesis of antibiotics, Microbial metabolism in diverse environments, Two-component system, ABC transporters, Biosynthesis of amino acids, Carbon metabolism, Quorum sensing, Amino sugar and nucleotide sugar metabolism, and Purine metabolism. There are 12 pathways with significant differences in the group. The KD group shows an increased enrichment in pathways such as Citrate cycle (TCA cycle), Pertussis, Phosphatidylinositol signaling system, Biofilm formation—*Escherichia coli*, Penicillin and cephalosporin biosynthesis, Lysosome, and Glycosphingolipid biosynthesis—lacto and neolacto series. On the other hand, a decreasing trend is observed in pathways such as Quorum sensing, Bacterial secretion system, Nicotinate and nicotinamide metabolism, Legionellosis, and Arginine biosynthesis. Meanwhile, differences between the two groups are also observed in some other highly enriched pathways, such as Phenylalanine metabolism and Phenylalanine, tyrosine, and tryptophan biosynthesis, in which the former shows a decrease and the latter shows an increase after KD (Supplementary Table 2).

Discussion

Mitochondrial epilepsy is difficult to control with a single antiepileptic drug due to its diverse forms and types of seizures. Usually, a combination of drugs is used, but in this case, the mitochondrial toxicity of the drugs should be taken into consideration, and drugs that interfere with the respiratory chain should be used with caution (28). Therefore, the introduction of a KD to alleviate the symptoms of epilepsy is an effective solution. Since the classic KD was adopted in 1920, variants such as the Atkins diet (MAD) and the medium-chain triglyceride diet (MCT) have been developed based on palatability and compliance (29). Although researchers have been exploring the

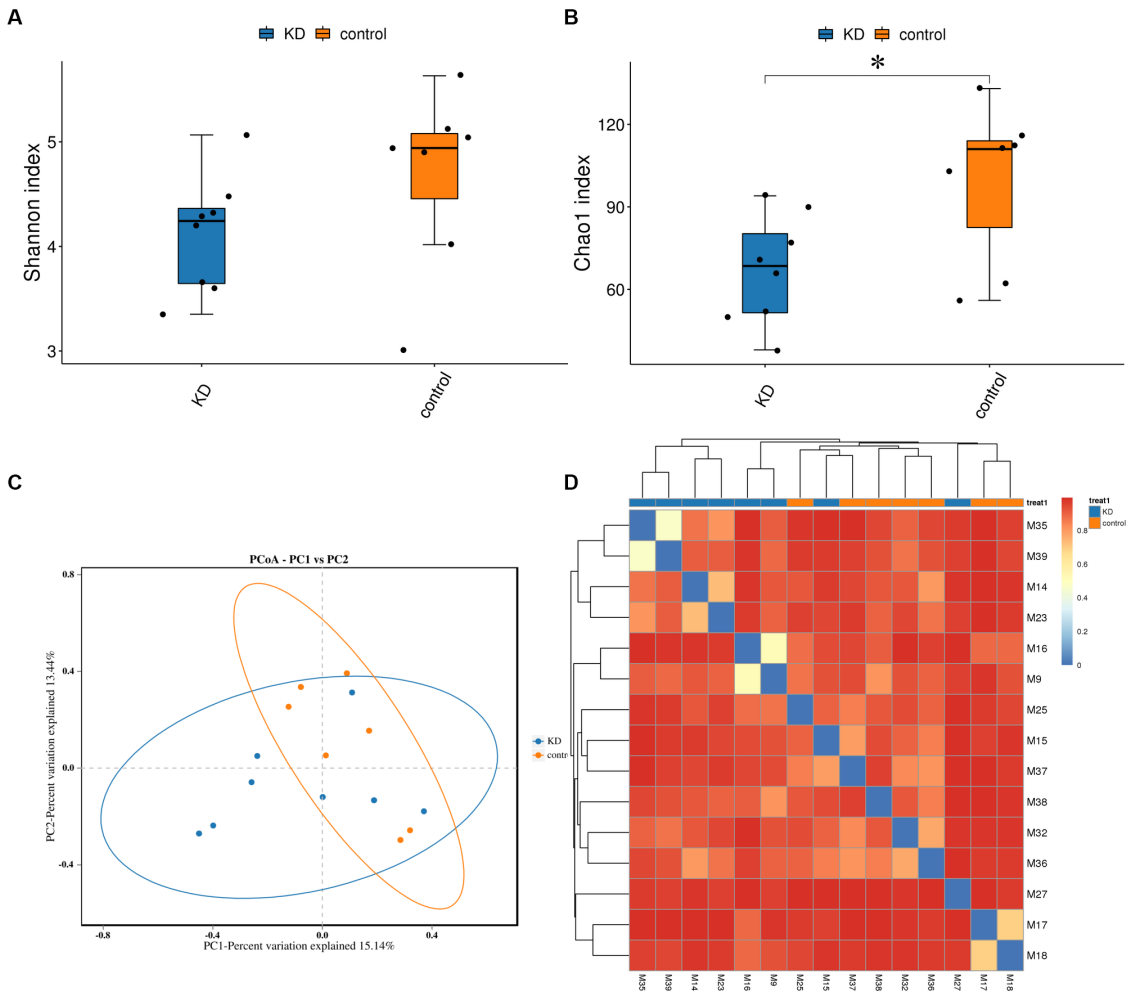

FIGURE 1
Diversity analysis of gut microbiota and microbial abundance in the KD group and the control group. **(A,B)** Alpha diversity (Shannon index) indicates no significant difference in gut microbiota diversity between the KD group and the control group ($p > 0.05$, calculated using Wilcoxon rank-sum test). Alpha diversity (Chao1 index) indicates significant difference in gut microbiota diversity between the KD group and the control group ($p < 0.05$). **(C)** Beta diversity PCoA analysis based on weighted Bray-Curtis distance indicates differences in gut microbiota composition between the KD group and the control group (blue dots represent the KD group, orange dots represent the control group). **(D)** Sample clustering heatmap based on weighted Bray-Curtis distance shows significant differences between the KD group and the control group. *$p < 0.05$.

molecular mechanisms of KD's effects, there is still no clear conclusion. In recent years, many researchers have attempted to study the anti-epileptic effects of KD in animal models. KD changed the gut microbiota of epileptic mice, and this change was necessary for the mice to cope with seizures (30). This was confirmed in a patient with Crohn's disease who was cured of epilepsy through fecal microbiota transplantation (FMT) and did not experience a recurrence of epilepsy in subsequent follow-ups (31). Meanwhile, in our previous research, 40.9% of participants achieved 50% seizure reduction after 3 month of diet intervention. The KD also showed high efficacy in participants with mitochondrial encephalopathy, lactic acidosis, and stroke-like episodes (MELAS) or pathogenic variants in mitochondrial DNA (mtDNA) (6).

We investigated the effects of a KD on the composition and abundance of gut microbiota in patients with mitochondrial epilepsy. All patients in the KD group underwent a 3-month intervention using a 2:1 KD. By analyzing the 16S rRNA sequencing of fecal samples, we found a significant increase in *Bacteroides* and its subspecies *Bacteroides fragilis* after the KD intervention, while *Firmicutes* showed a certain degree of decrease, which is consistent with the results of Alina Arulsamy et al. (32) (Figures 2A,B). Although there was no significant difference in alpha diversity between the two groups, the beta diversity and clustering heatmap indicated some differences between the two groups (Figures 1C,D). In the LEfSe results, we found a significant enrichment of *Bacteroides fragilis* in the KD group, which directly led to the increase in *Bacteroides* abundance (Figure 3A). Previous mouse experiments have shown that oral treatment with human commensal *Bacteroides fragilis* can correct intestinal permeability, change microbiota composition, and improve defects in ASD-related communication, stereotypy, anxiety-like, and sensorimotor behaviors in MIA offspring (33). The induced changes in the symbiotic microbiota and

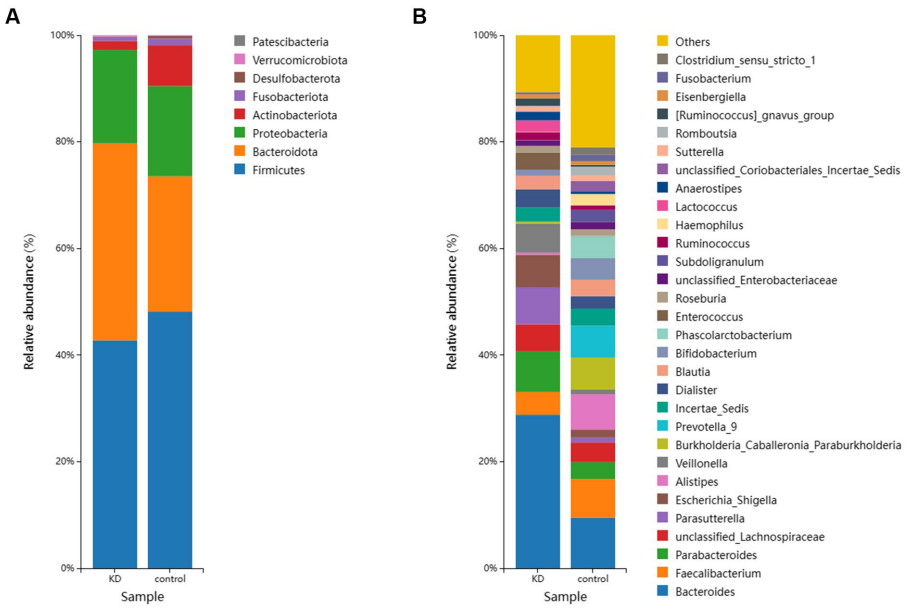

FIGURE 2
(A) The relative abundance of the top 10 microorganisms at the Phylum level in the KD group and the control group. **(B)** The relative abundance of the top 30 microorganisms at the genus level in the KD group and the control group.

serum metabolites may be the reason for this result. *Bacteroides fragilis* has been shown to play a significant role in other neurological diseases, and its bacterial capsule polysaccharide Ag can prevent autoimmune encephalitis (34). A previous study showed that compared to healthy individuals, the abundance of *Bacteroides fragilis* was lower in the gut of drug-resistant epilepsy patients (35). Similarly, this result was observed in a prospective study, in which *Bacteroides fragilis* played a significant role in the adjuvant treatment of drug-resistant epilepsy, with a reduction in seizure frequency of more than 53% in about 61% of patients (36). This suggests that *Bacteroides fragilis* may have a potential protective effect on seizures and may play a role as a key bacterium in the KD's efficacy in epilepsy treatment. In addition, *Actinobacteriota* was significantly enriched in the control group, and Kihyun Lee identified it as a biomarker for epilepsy patients at the phylum level (37). This result has also been confirmed in many other studies (38, 39).

In terms of functional enrichment in the microbiome, level 1 did not show significant differences, and only two pathways, Infectious diseases: Bacterial and Signal transduction, showed differential enrichment in level 2. In level 3, a total of 320 metabolic pathways showed varying degrees of changes, with 12 showing significant differences, some of which were significantly decreased in enrichment after KD. Of particular interest is the Purine metabolism pathway, which was severely affected—almost all enzymes showed varying degrees of changes (Supplementary Figure 1). In previous studies, purines have been found to play important roles not only as a crucial component of cellular metabolism, but also in signal transduction. Susan A. Masino's research has shown that the energy metabolism changes induced by the KD increase levels of ATP and adenosine, both of which may be the main mediators of the neuroprotective effects of the KD (40). Adenosine has been reported to be a powerful molecule for reducing seizures and providing neuroprotection (41). Our study only indirectly shows this possible effect, and more evidence is needed to prove changes in key substances or receptors. In Susan A. Masino's recent study, KD was found to reduce seizures in mice by increasing the activation of adenosine A1 receptors (A1Rs) (42). Several pathways, including Arginine biosynthesis, Cysteine and methionine metabolism, and Valine, leucine and isoleucine biosynthesis, were also affected to varying degrees in our KD-treated group, and it is not yet clear whether this is related to the amino acid metabolic disorders associated with epilepsy (43). As a pathway with a relatively high level of enrichment, ABC transporters were higher in the control group than in the KD group, but not significantly. In previous studies, drug-resistant epilepsy patients showed a significant increase in the abundance of ABC transporter proteins, which is consistent with our results (35).

In general, our study reveals the impact of the KD on the gut microbiota in mitochondrial epilepsy patients. These findings suggest its potential role in epilepsy relief. However, for this study, we collected a limited number of cases, and accumulating cases proved to be a challenging process. The limitation in sample size restricts the conclusions drawn from our research. One contributing factor is the difficulty in implementing the KD in clinical settings, considering patient compliance and adverse effects. It is necessary for us to further investigate the specific effects of microbiota changes at the metabolite level, as this could provide a more direct explanation for the interaction between the gut microbiota and the nervous system. Similarly, we are curious whether extending the duration of KD would have a more pronounced impact on the gut microbiota, but these results require further research and observation. We hope that subsequent studies can uncover the relationship between the gut microbiota and the nervous system, providing a theoretical basis for the treatment of mitochondrial epilepsy.

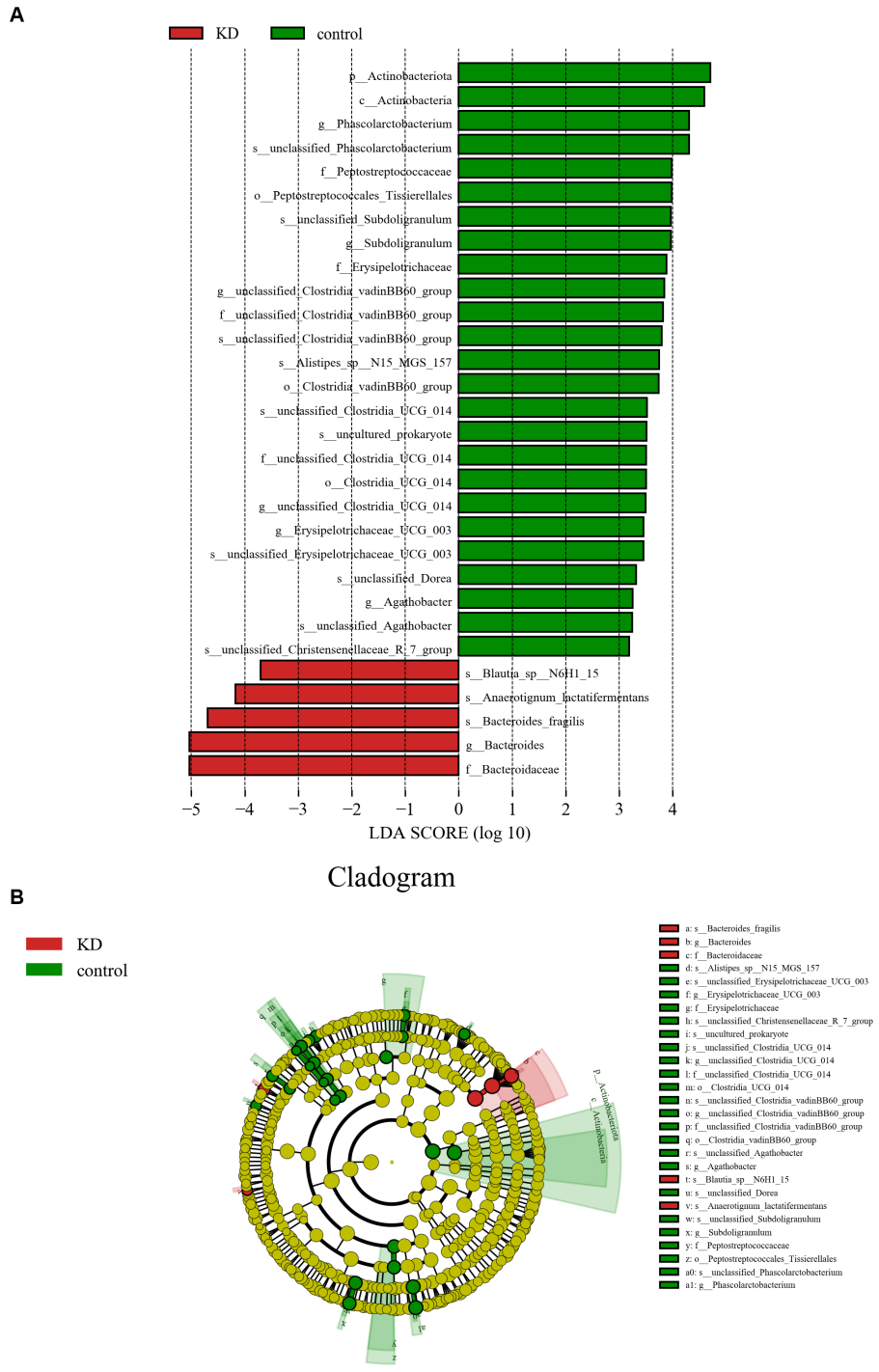

FIGURE 3
Analysis of differences in gut microbiota between KD group and control group. **(A)** LEfSe analysis: the length of the bars represents the logarithm of linear discriminant analysis (LDA). Green bars represent enriched microbiota in the control group; red bars represent enriched microbiota in the KD group (only species with LDA ≥ 3.0 are shown). **(B)** Cladogram of the phylogenetic distribution of microbes, microbes with an LDA value ≥3.0 in KD and control groups are marked with red and green.

Data availability statement

The original contributions presented in the study are included in the article/Supplementary material, further inquiries can be directed to the corresponding authors.

Ethics statement

The studies involving human participants were reviewed and approved by the Ethics Review Committee of Wuhan Children's Hospital and the ethics review number is 2021R048-F01. Written

informed consent to participate in this study was provided by the participants' legal guardian/next of kin.

Author contributions

DS, FF, JLiao, and LH designed the study and revised the manuscript accordingly. JW, HL, GC, LY, DW, HH, GZ, XW, JLiang, and WH participated in the study and provided case information. JW, LH, and DS drafted the manuscript. All authors contributed to the article and approved the submitted version.

Funding

This study was supported by the Fund of Futang Research Center of Pediatric Development (No. FTCSF-2018-05), the Fund of Shenzhen Zeneca Biotechnology Co., Ltd. (No. 20181208), China Association Against Epilepsy (CAAE) Research Fund Qitong Fund (No. CJ-B-2021-20) and the Foundation under the designation CJ-B-2021-20.

Acknowledgments

The authors appreciate and thank the parents and children who consented to KD therapy. The authors would like to thank the Futang Research Center of Pediatric Development and CAAE and thank Shenzhen Zeneca Biotechnology Co., Ltd. for technical support.

Conflict of interest

WH was employed by Aegicare (Shenzhen) Technology Co., Ltd.

The remaining authors declare that the research was conducted in the absence of any commercial or financial relationships that could be construed as a potential conflict of interest.

Publisher's note

Supplementary material

The Supplementary material for this article can be found online at: https://www.frontiersin.org/articles/10.3389/fneur.2023.1237255/full#supplementary-material

References

1. Freeman JM, Kossoff EH, Hartman AL. The ketogenic diet: one decade later. *Pediatrics*. (2007) 119:535–43. doi: 10.1542/peds.2006-2447

2. Martin-McGill KJ, Bresnahan R, Levy RG, Cooper PN. Ketogenic diets for drug-resistant epilepsy. *Cochrane Database Syst Rev*. (2020) 2020:CD001903. doi: 10.1002/14651858.CD001903.pub5

3. Kossoff EH, Zupec-Kania BA, Auvin S, Ballaban-Gil KR, Christina Bergqvist AG, Blackford R, et al. Optimal clinical management of children receiving dietary therapies for epilepsy: updated recommendations of the international ketogenic diet study group. *Epilepsia Open*. (2018) 3:175–92. doi: 10.1002/epi4.12225

4. Kang HC, Lee YM, Kim HD, Lee JS, Slama A. Safe and effective use of the ketogenic diet in children with epilepsy and mitochondrial respiratory chain complex defects. *Epilepsia*. (2007) 48:82–8. doi: 10.1111/j.1528-1167.2006.00906.x

5. Bough KJ, Wetherington J, Hassel B, Pare JF, Gawryluk JW, Greene JG, et al. Mitochondrial biogenesis in the anticonvulsant mechanism of the ketogenic diet. *Ann Neurol*. (2006) 60:223–35. doi: 10.1002/ana.20899

6. Huang L, Li H, Zhong J, Yang L, Chen G, Wang D, et al. Efficacy and safety of the ketogenic diet for mitochondrial disease with epilepsy: a prospective, open-labeled, controlled study. *Front Neurol*. (2022) 13:880944. doi: 10.3389/fneur.2022.880944

7. Stafford P, Abdelwahab MG, Kim DY, Preul MC, Rho JM, Scheck AC. The ketogenic diet reverses gene expression patterns and reduces reactive oxygen species levels when used as an adjuvant therapy for glioma. *Nutr Metab (Lond)*. (2010) 7:74. doi: 10.1186/1743-7075-7-74

8. Kim DY, Davis LM, Sullivan PG, Maalouf M, Simeone TA, van Brederode J, et al. Ketone bodies are protective against oxidative stress in neocortical neurons. *J Neurochem*. (2007) 101:1316–26. doi: 10.1111/j.1471-4159.2007.04483.x

9. Kim DY, Vallejo J, Rho JM. Ketones prevent synaptic dysfunction induced by mitochondrial respiratory complex inhibitors. *J Neurochem*. (2010) 114:130–41. doi: 10.1111/j.1471-4159.2010.06728.x

10. Yudkoff M, Daikhin Y, Melo TM, Nissim I, Sonnewald U, Nissim I. The ketogenic diet and brain metabolism of amino acids: relationship to the anticonvulsant effect. *Annu Rev Nutr*. (2007) 27:415–30. doi: 10.1146/annurev.nutr.27.061406.093722

11. Kim DY, Rho JM. The ketogenic diet and epilepsy. *Curr Opin Clin Nutr Metab Care*. (2008) 11:113–20. doi: 10.1097/MCO.0b013e3282f44c06

12. Stafstrom CE, Rho JM. The ketogenic diet as a treatment paradigm for diverse neurological disorders. *Front Pharmacol*. (2012) 3:59. doi: 10.3389/fphar.2012.00059

13. Bach AC, Babayan VK. Medium-chain triglycerides: an update. *Am J Clin Nutr*. (1982) 36:950–62. doi: 10.1093/ajcn/36.5.950

14. He Z, Shao T, Li H, Xie Z, Wen C. Alterations of the gut microbiome in Chinese patients with systemic lupus erythematosus. *Gut Pathog*. (2016) 8:64. doi: 10.1186/s13099-016-0146-9

15. David LA, Maurice CF, Carmody RN, Gootenberg DB, Button JE, Wolfe BE, et al. Diet rapidly and reproducibly alters the human gut microbiome. *Nature*. (2014) 505:559–63. doi: 10.1038/nature12820

16. Newell C, Bomhof MR, Reimer RA, Hittel DS, Rho JM, Shearer J. Ketogenic diet modifies the gut microbiota in a murine model of autism spectrum disorder. *Mol Autism*. (2016) 7:37. doi: 10.1186/s13229-016-0099-3

17. Ley RE, Turnbaugh PJ, Klein S, Gordon JI. Microbial ecology: human gut microbes associated with obesity. *Nature*. (2006) 444:1022–3. doi: 10.1038/4441022a

18. Turnbaugh PJ, Ley RE, Mahowald MA, Magrini V, Mardis ER, Gordon JI. An obesity-associated gut microbiome with increased capacity for energy harvest. *Nature*. (2006) 444:1027–31. doi: 10.1038/nature05414

19. Canfora EE, Meex RCR, Venema K, Blaak EE. Gut microbial metabolites in obesity, NAFLD and T2DM. *Nat Rev Endocrinol*. (2019) 15:261–73. doi: 10.1038/s41574-019-0156-z

20. Sutter R, Ruegg S, Tschudin-Sutter S. Seizures as adverse events of antibiotic drugs: a systematic review. *Neurology*. (2015) 85:1332–41. doi: 10.1212/WNL.0000000000002023

21. Xie G, Zhou Q, Qiu CZ, Dai WK, Wang HP, Li YH, et al. Ketogenic diet poses a significant effect on imbalanced gut microbiota in infants with refractory epilepsy. *World J Gastroenterol*. (2017) 23:6164–71. doi: 10.3748/wjg.v23.i33.6164

22. Zhang Y, Zhou S, Zhou Y, Yu L, Zhang L, Wang Y. Altered gut microbiome composition in children with refractory epilepsy after ketogenic diet. *Epilepsy Res*. (2018) 145:163–8. doi: 10.1016/j.eplepsyres.2018.06.015

23. Lindefeldt M, Eng A, Darban H, Bjerkner A, Zetterstrom CK, Allander T, et al. The ketogenic diet influences taxonomic and functional composition of the gut microbiota in children with severe epilepsy. *NPJ Biofilms Microbiomes*. (2019) 5:5. doi: 10.1038/s41522-018-0073-2

24. Fisher RS, Cross JH, French JA, Higurashi N, Hirsch E, Jansen FE, et al. Operational classification of seizure types by the international league against epilepsy: position paper of the ILAE Commission for Classification and Terminology. *Epilepsia*. (2017) 58:522–30. doi: 10.1111/epi.13670

25. Callahan BJ, McMurdie PJ, Rosen MJ, Han AW, Johnson AJ, Holmes SP. DADA2: high-resolution sample inference from Illumina amplicon data. *Nat Methods*. (2016) 13:581–3. doi: 10.1038/nmeth.3869

26. Bolyen E, Rideout JR, Dillon MR, Bokulich NA, Abnet CC, Al-Ghalith GA, et al. Reproducible, interactive, scalable and extensible microbiome data science using QIIME 2. *Nat Biotechnol*. (2019) 37:852–7. doi: 10.1038/s41587-019-0209-9

27. Segata N, Izard J, Waldron L, Gevers D, Miropolsky L, Garrett WS, et al. Metagenomic biomarker discovery and explanation. *Genome Biol*. (2011) 12:R60. doi: 10.1186/gb-2011-12-6-r60

28. Finsterer J, Zarrouk MS. Mitochondrial toxicity of antiepileptic drugs and their tolerability in mitochondrial disorders. *Expert Opin Drug Metab Toxicol*. (2012) 8:71–9. doi: 10.1517/17425255.2012.644535

29. Ye F, Li XJ, Jiang WL, Sun HB, Liu J. Efficacy of and patient compliance with a ketogenic diet in adults with intractable epilepsy: a meta-analysis. *J Clin Neurol*. (2015) 11:26–31. doi: 10.3988/jcn.2015.11.1.26

30. Olson CA, Vuong HE, Yano JM, Liang QY, Nusbaum DJ, Hsiao EY. The gut microbiota mediates the anti-seizure effects of the ketogenic diet. *Cells*. (2018) 173:1728–1741.e13. doi: 10.1016/j.cell.2018.04.027

31. He Z, Cui BT, Zhang T, Li P, Long CY, Ji GZ, et al. Fecal microbiota transplantation cured epilepsy in a case with Crohn's disease: the first report. *World J Gastroenterol*. (2017) 23:3565–8. doi: 10.3748/wjg.v23.i19.3565

32. Arulsamy A, Tan QY, Balasubramaniam V, O'Brien TJ, Shaikh MF. Gut microbiota and epilepsy: a systematic review on their relationship and possible therapeutics. *ACS Chem Neurosci*. (2020) 11:3488–98. doi: 10.1021/acschemneuro.0c00431

33. Hsiao EY, McBride SW, Hsien S, Sharon G, Hyde ER, McCue T, et al. Microbiota modulate behavioral and physiological abnormalities associated with neurodevelopmental disorders. *Cells*. (2013) 155:1451–63. doi: 10.1016/j.cell.2013.11.024

34. Ochoa-Reparaz J, Mielcarz DW, Ditrio LE, Burroughs AR, Begum-Haque S, Dasgupta S, et al. Central nervous system demyelinating disease protection by the human commensal *Bacteroides fragilis* depends on polysaccharide a expression. *J Immunol*. (2010) 185:4101–8. doi: 10.4049/jimmunol.1001443

35. Peng A, Qiu X, Lai W, Li W, Zhang L, Zhu X, et al. Altered composition of the gut microbiome in patients with drug-resistant epilepsy. *Epilepsy Res*. (2018) 147:102–7. doi: 10.1016/j.eplepsyres.2018.09.013

36. Yuhong D, Chuhui L., Dezhi CAO. The beneficial effect of Bacteroides Fragilis(BF839)as a supplementary treatment in drug-resistant epilepsy:a pilot study. *Journal of Epilepsy* (2021) 7:288–295. doi: 10.7507/2096-0247.20210046

37. Lee K, Kim N, Shim JO, Kim GH. Gut bacterial Dysbiosis in children with intractable epilepsy. *J Clin Med*. (2020) 10:5. doi: 10.3390/jcm10010005

38. Gong SZ, Qiu J, Wu LW, Tan LH. Change in intestinal flora after treatment in children with focal epilepsy. *Zhongguo Dang Dai Er Ke Za Zhi*. (2022) 24:290–6. doi: 10.7499/j.issn.1008-8830.2109134

39. Gong X, Liu X, Chen C, Lin J, Li A, Guo K, et al. Alteration of gut microbiota in patients with epilepsy and the potential index as a biomarker. *Front Microbiol*. (2020) 11:517797. doi: 10.3389/fmicb.2020.517797

40. Masino SA, Geiger JD. Are purines mediators of the anticonvulsant/neuroprotective effects of ketogenic diets? *Trends Neurosci*. (2008) 31:273–8. doi: 10.1016/j.tins.2008.02.009

41. Paleologou E, Ismayilova N, Kinali M. Use of the ketogenic diet to treat intractable epilepsy in mitochondrial disorders. *J Clin Med*. (2017) 6:56. doi: 10.3390/jcm6060056

42. Masino SA, Li T, Theofilas P, Sandau US, Ruskin DN, Fredholm BB, et al. A ketogenic diet suppresses seizures in mice through adenosine a (1) receptors. *J Clin Invest*. (2011) 121:2679–83. doi: 10.1172/JCI57813

43. Lee WT. Disorders of amino acid metabolism associated with epilepsy. *Brain Dev*. (2011) 33:745–52. doi: 10.1016/j.braindev.2011.06.014

frontiers | Frontiers in Neuroscience

TYPE Review
PUBLISHED 13 October 2023
DOI 10.3389/fnins.2023.1251017

OPEN ACCESS

EDITED BY
Antonella Riva,
University of Genoa, Italy

REVIEWED BY
Lu Cai,
University of Louisville, United States
Taixing Cui,
University of Missouri, United States

*CORRESPONDENCE
Ji Li
jli3@umc.edu

RECEIVED 30 June 2023
ACCEPTED 29 September 2023
PUBLISHED 13 October 2023

CITATION
Zoungrana LI, Didik S, Wang H, Slotabec L and Li J (2023) Activated protein C in epilepsy pathophysiology.
Front. Neurosci. 17:1251017.
doi: 10.3389/fnins.2023.1251017

Activated protein C in epilepsy pathophysiology

Linda Ines Zoungrana[1], Steven Didik[1], Hao Wang[2], Lily Slotabec[2] and Ji Li[2]*

[1]Department of Surgery, Morsani College of Medicine, University of South Florida, Tampa, FL, United States, [2]Department of Physiology and Biophysics, University of Mississippi Medical Center, Jackson, MS, United States

Epilepsy is one of the most common neurologic disorders that is characterized by recurrent seizures, and depending on the type of seizure, it could lead to a severe outcome. Epilepsy's mechanism of development is not fully understood yet, but some of the common features of the disease are blood-brain barrier disruption, microglia activation, and neuroinflammation. Those are also targets of activated protein C (APC). In fact, by downregulating thrombin, known as a pro-inflammatory, APC acts as an anti-inflammatory. APC is also an anti-apoptotic protein, instance by blocking p53-mediated apoptosis. APC's neuroprotective effect could prevent blood-brain barrier dysfunction by acting on endothelial cells. Furthermore, through the downregulation of proapoptotic, and proinflammatory genes, APC's neuroprotection could reduce the effect or prevent epilepsy pathogenesis. APC's activity acts on blood-brain barrier disruption, inflammation, and apoptosis and causes neurogenesis, all hallmarks that could potentially treat or prevent epilepsy. Here we review both Activated Protein C and epilepsy mechanism, function, and the possible association between them.

KEYWORDS

epilepsy, activated protein C, seizure, neuroprotection, neurologic disorders

Introduction

Epilepsy is one of the world's oldest recognized neurological disorders and the 4th most common neurologic disorder after migraine, cerebrovascular disease (stroke), and Alzheimer's disease (Johns Hopkins Medicine, 2020). Epilepsy, characterized by recurrent seizures, affects around 50 million people worldwide (Centers for Disease Control and Prevention, 2023). These seizures usually lead to the involuntary movement of part of

Abbreviations: APC, activated protein C; PC, protein C; SE, status epileptogenesis; TLE, temporal lobe epilepsy; BBB, blood-brain barrier; γ-GTP, γ-glutamyl transpeptidase; VEGFR1, vascular endothelial growth factor receptor 1; IgG, immunoglobulin G; TGF-βRs, transforming growth factor beta receptors; IL-1β, interleukin-1 beta; TLR, toll-like receptors; SMAD2/3, mothers against decapentaplegic Homolog 2/3; MMPs, matrix metalloproteases; NG2-glia, neuron-glia antigen 2-expressing glial cells; mTOR, mammalian target of rapamycin; TSC1, tuberous sclerosis complex 1; CX3CL1, chemokine (C-X3-C motif) ligand 1; GABA, gamma amino butyric acid; FOXP3, forkhead transcription factor 3; NMDA, *N*-methyl-D-aspartic acid; HMGB1, high mobility group box 1; RAGE, receptor for advanced glycation endproducts; MAPK, mitogen-activated protein kinase; BDNF, brain-derived neurotrophic factor; IkBα, inhibitor kappa B alpha; PTEN, phosphatase and tensin homolog; PGE2, prostaglandin E2; PAF, platelet-activating factor; GLA, γ-carboxyglutamic acid-rich; TF, tissue factor; TM, thrombomodulin; EPCR, endothelial protein C receptor; PAR1, protease-activated receptor 1; p-NF-kβ, phosphorylated nuclear FACTOR kappa B; NF-kβ, nuclear factor kappa B; TNF-α, tumor necrosis factor *alpha*; p75NTR, p75 neurotrophin receptor; GAL-1, galectin-1 (Gal-1).

the body or the entire body and could eventually lead to losing consciousness, temporary confusion, a staring spell, stiff muscles, uncontrollable jerking movements of the arms and legs, and abnormal movements (Sander, 2014; Centers for Disease Control and Prevention, 2023). There are two main types of epileptic seizures: generalized seizures, which affect the whole brain, and focal, or partial seizures, which affect just one part of the brain; temporal lobe seizures, or focal seizures, are the most common type of epilepsy (Centers for Disease Control and Prevention, 2020). The worst form of epilepsy is status epileptogenesis (SE), which is characterized by a seizure that is longer than 5 min or multiple seizures within a short period (Smith et al., 2018). This form of epilepsy required immediate attention as it could be life-threatening. Activated protein C (APC) is a natural anticoagulant protein that plays an important role in regulating blood clotting (Hayashi and Suzuki, 2015). It serves as a potent anticoagulant in the blood, mainly by inactivating coagulation factors Va and VIIIa (Alberelli and De Candia, 2014). This mechanism helps maintain blood fluidity and prevent excess production of blood clots (Alberelli and De Candia, 2014). In addition to its anticoagulant properties, APC also regulates the coagulation cascade, which ensures clot formation only when necessary (Shahzad et al., 2019). One of APC's biological functions is its fibrinolytic properties (Reda et al., 2019). Indeed, by acting on plasminogen activator inhibitor-1 (PAI-1), APC promotes the breakdown of existing blood clot formation, therefore preventing clot propagation (Reda et al., 2019). Furthermore, APC can modulate the immune response by reducing leukocyte adhesion to endothelial cells, suppressing the production involved in inflammation, and inhibiting the release of pro-inflammatory cytokines (Kant et al., 2020). APC also helps maintain the integrity of endothelial cells lining the blood vessels, as those cells regulate vascular tone, blood flow, and prevent clot formation (Ren et al., 2022). Lastly, APC preserves the integrity of various barriers in the body, including the blood-brain barrier, has cytoprotective properties, and activates several cell signaling pathways, including the activation of the protein C receptor (PAR-1) (Griffin et al., 2015). APC has been the focus of a few studies in which its cardioprotective, anti-inflammatory, and anti-apoptosis properties have been proven (Legrand and Tolwani, 2021). However, recently, APC's neuroprotective effects have been of research interest. Although epilepsy is one of the oldest neurological disorders, its mechanism of development is not fully understood. This review paper aims to highlight a few mechanisms involved in the induction and perpetuation of epileptic seizures. Furthermore, we will examine the role and mechanism of activated protein C. Additionally, we will explore the association between activated protein C and epileptic seizures.

Blood-brain barrier dysfunction

Brain function and neuronal environment are maintained within a specific homeostatic range, which is regulated by the blood-brain barrier (BBB) (Swissa et al., 2019). BBB is an element of the neurovascular unit composed of neurons, microglia, astrocytes, pericytes, and cerebral vessels in addition to BBB, and deregulation of these microunits is present in neurodegenerative diseases such as Alzheimer's disease or inflammatory-related diseases such as stroke or epilepsy (Rhea and Banks, 2019; Swissa et al., 2019). The BBB is composed of brain microvascular endothelial cells, the first interface between the blood and the brain (Persidsky et al., 2006). Those endothelial cells within the vessel function as osmoregulation, leukocyte trafficking, transport of nutrients, and a barrier, and to properly accomplish those functions, they have unique properties that include adherens junctions, tight junctions, and junctional adhesion molecules (Persidsky et al., 2006). The presence of adherens and tight junctions, or junctional adhesion molecules, composes the brain microvascular endothelial cells (Persidsky et al., 2006). Those elements have an increased number of mitochondria, which are essential for the transport of nutrients to the brain (Oldendorf et al., 1977; Persidsky et al., 2006). Enzymes such as aromatic acid decarboxylase, γ-glutamyl transpeptidase (γ-GTP), or alkaline phosphatase are present in high concentrations in the cerebral microvessels and metabolize bloodborne solutes, nutrients, and drugs, providing an enzymatic barrier (Abbott, 2005; Löscher and Potschka, 2005; Persidsky et al., 2006). These enzymes, as well as the polarity present between the abluminal and luminal surfaces of the brain microvasculature, provide a highly tightly regulated barrier (Persidsky et al., 2006). The extracellular matrix on which the endothelium cell lies also makes up the BBB structure. It provides anchors to the brain microvascular endothelial cells via collagen type IV, laminin, integrin, and other matrix proteins (Persidsky et al., 2006; Kadry et al., 2020). Disruption of the BBB extracellular matrix is associated with disordered development (Persidsky et al., 2006; Kangwantas et al., 2016). Next to the blood endothelial cell, there are the astrocytes that envelope the BBB endothelium, creating a tight interaction between them that influences their structure (Persidsky et al., 2006). Astrocytes represent the most abundant cell of the central nervous system (CNS), and whenever endothelial cells and astrocytes interact, the endothelial cell tight junctions are amplified, decreasing the gap in the area and increasing the number of astrocytic cells as well (Persidsky et al., 2006; Kadry et al., 2020). Astrocytes help maintain BBB function and tightness. In addition to astrocytes, pericytes are also part of the neurovascular unit, which plays an important role in BBB microvasculature stability, angiogenesis, and integrity (Peppiatt et al., 2006; Hall et al., 2014; Kadry et al., 2020). Due to their similar contractual ability to smooth muscle cells, pericytes can also control blood flow by regulating the capillary diameter (Sagare et al., 2013). Pericytes are closely connected to the endothelial cell and tight junction, which is unable to send cellular projection and react in the case of brain trauma or hypoxia (Dore-Duffy et al., 2000; Gonul et al., 2002; Persidsky et al., 2006). Pericytes regulate a few aspects of the neurovasculature (Heymans et al., 2020). For instance, Eilken et al. (2017) showed that the expression of vascular endothelial growth factor receptor 1 (VEGFR1) by pericytes could affect VEGF signaling, and depletion of pericyte activity could lead to an angiogenic defect, limited endothelial sprouting, and the enlargement of vessels (Persidsky et al., 2006). In summary, each of the components of the BBB plays an important role in the physiological aspect and function of the brain. Disruption of one of the components of the BBB could lead to neuroinflammation, neurological disorders, and neuronal hyperexcitability, including epilepsy. In fact, BBB association with epilepsy is not a new phenomenon, and decades of research have shown that BBB leakage can cause epilepsy and lead to status epilepticus.

BBB dysfunction in seizure

Years of research on BBB dysfunction have been reported in humans after brain injury, status epilepticus, as well as in temporal lobe epilepsy (TLE) animal models, induced by pilocarpine, kainic acid, or the electrical stimulation-induced seizure model (van Vliet et al., 2007; Wang et al., 2012; Yan et al., 2018; Mendes et al., 2019). This means that BBB dysfunction can occur because of epileptic seizures. In the animal model study, BBB leakages were observed in various regions of the brain, including the cortex, hippocampus, thalamus and amygdala. An intense seizure could lead to a change in the brain's electrical potential or reduce its electrical signaling (Dreier, 2011; van Vliet et al., 2015). These changes lead to a tone alteration of the blood vessel, which can lead to hypoperfusion or hyperperfusion and cause tissue damage (Winkler et al., 2012; van Vliet et al., 2015). Furthermore, this will lead to cellular damage and a decrease in blood pressure and pH, causing hypoxia and further enhancing BBB dysfunction (Stanimirovic and Friedman, 2012; van Vliet et al., 2015). SE has a high mortality rate, with survivors often experiencing complications that include epilepsy (Swissa et al., 2019). SE animal research has reported excitotoxicity, neuronal dysfunction, cell loss, and the development of epilepsy (Swissa et al., 2019). During the SE *in vivo* experimental model, a rapid increase in BBB permeability has been observed within the first 30 min in animals (Shrot et al., 2014; Swissa et al., 2019). In those research models, at 48 h, a quantifiable BBB leakage revealed that localized BBB dysfunction is highly sensitive to developing epilepsy on average 4 weeks later (Bar-Klein et al., 2017; Swissa et al., 2019). Whenever epilepsy was established, the histological analysis confirmed it with the presence of albumin, serum proteins, and IgG, as well as reactive microglia and astrocytes, neuroinflammation, and cellular damage (Swissa et al., 2019). These indicated SE animal models show BBB dysfunction and robust inflammatory response drugs that induce SE like, pilocarpine (Fujikawa, 1996; Tang et al., 2011; Swissa et al., 2019). The mechanism that underlies BBB dysfunction is not yet fully understood; however, there seems to be a close association between neuronal hyperactivity and BBB dysfunction (Milikovsky et al., 2017; Swissa et al., 2019). The extracellular level of glutamate is associated with SE, and glutamate, by binding with the brain endothelial cell, can alter tight junctions or reduce transcellular trafficking (Krizbai et al., 1998; Sharp et al., 2003; András et al., 2007; Swissa et al., 2019). The release and activation of glutamate also induce oxidative stress and increase intracellular calcium, which has been associated with increased BBB permeability (Brown and Davis, 2002; De Bock et al., 2013). Pericytes that have been found to secrete pro-inflammatory cytokines and actively participate in neuroinflammatory responses seem to be associated with BBB dysfunction during SE (Fabry et al., 1993; Armulik et al., 2010). Rearrangement and proliferation of pericytes were observed during epileptogenesis, and SE providing evidence of the association of pericytes with epilepsy (Klement et al., 2018; Swissa et al., 2019). After brain injury, BBB dysfunction is usually characterized by the extravasation of albumin circulating in the vessel (Swissa et al., 2019). Once in the extracellular space, albumin binds to the astrocytes through transforming growth factor beta receptors (TGF-βRs), causing Smad2/3 phosphorylation (Cacheaux et al., 2009). This phosphorylation leads to a transcriptional modification that results: (1) in a downregulation of the inward-rectifying potassium channel, which is responsible for maintaining the membrane resting potential and regulating the electrical excitation of neurons cells; (2) also a strong neuroinflammatory response with IL-1β, IL-6, and other pro-inflammatory cytokines being upregulated; (3) rearrangement and rewiring of the neuronal network, as well as synapse plasticity; (4) changes in the perineuronal microenvironment and upregulation of matrix metalloproteases (MMPs); and (5) excitatory synaptogenesis (Frigerio et al., 2012; Baronas and Kurata, 2014; Levy et al., 2015; Weissberg et al., 2015; Salar et al., 2016; Kim et al., 2017). These events are probably what enhance the seizure mechanism.

Microglia and glia activation in seizure

Neuroglia, or glia cells, are the majority composed of astrocytes, oligodendrocyte lineage cells, microglia, as well as progenitors NG2-glia (Jäkel and Dimou, 2017). Over the years, researchers have presented and shown the importance of glia cells in the nervous system; however, there is still much to know. Astrocytes have multiple functions, but as previously mentioned, they play a role in BBB integrity (Persidsky et al., 2006). Oligodendrocyte lineage cells have multiple functions and help in the formation of myelin sheaths found on nerve axons, as well as supporting axons' metabolic activity and neuroplasticity (Zhou et al., 2021). Progenitors NG2-glia are found in the white and gray matter of developing as well as the mature central nervous system. Little is known about their function, but they also have the ability to generate myelinating and non-myelinating cells, just like oligodendrocytes (Nishiyama et al., 2014). Microglia, the focus of this review, is known to be the immune cell of the CNS, capable of creating an inflammatory response; they play an important role in phagocytosis of debris and apoptotic cells; they provide neuronal support during development; they assist in synaptic organization; as well as neuronal excitability (Bachiller et al., 2018). Even though we have a lot of knowledge about microglial function under physiological conditions, little is known about the microglia's structure and function under SE conditions. Pioneers in the field have found an association between microglia and SE through their activation in regions of the brain affected by SE induced by drugs such as kainic acid or pilocarpine (Vezzani et al., 2015; Hiragi et al., 2018). Once activated, microglial cells release proinflammatory cytokines, creating an upregulation of glutamate, hyperexcitability, and the neurodegenerative hallmarks of epilepsy (Hiragi et al., 2018; Zhao H. et al., 2018; Andoh et al., 2020). Microglia most likely contribute to epileptogenesis and progress to Campbell et al. (1993) and Probert et al. (1997) were among the first to associate brain inflammation with epileptogenesis from their studies on transgenic mice, which showed overexpression of the cytokines IL-6 and TNF-α (Campbell et al., 1993; Probert et al., 1997). Since researchers have focused on proinflammatory cytokines and provided a timeline for their release. For instance, De Simoni et al. (2000) published in early 2000 that cytokines such as TNF-α, IL-1β, and IL-6 expression were elevated in the hippocampus on the first day of electric stimulation SE induction in rat models (Hiragi et al., 2018). On the other hand, TNF-α, IL-1β, and IL-6 expression increased 3 days after pilocarpine-induced SE (Benson et al., 2015;

Hiragi et al., 2018). It is important to mention that anti-inflammatory cytokines such as IL-10 and IL-4 were also increased in microglia in an epileptic brain (Hiragi et al., 2018). Toll-like receptors (TLR) also play a role in an epileptic brain; in fact, *in vitro* studies reported that microglia responded to TLR3, and TLR4 agonists lead to the production of cytokines (Olson and Miller, 2004; Hiragi et al., 2018). Gross et al. (2017) showed that a deficit in TLR3 reduces recurring seizures in pilocarpine-induced SE, and earlier, Maroso et al. (2010) recorded a reduction of acute seizures in KA-induced SE by blocking TLR4 activity (Maroso et al., 2010; Gross et al., 2017; Hiragi et al., 2018). Furthermore, the activation of TLR9 by microglia in the hippocampus can attenuate convulsive seizures, and a deficit in TLR9 aggravates seizure severity and leads to cognitive decline (Matsuda et al., 2015). Although a large majority of researchers agreed that microglial activation contributes to epileptogenesis through proinflammatory releases, other research showed microglia association with epileptogenesis without a proinflammatory signal. Zhao X. et al. (2018) by studying *Tsc1*Cx3cr1CKO mice, have shown microglia association with epileptogenesis without a proinflammatory signal (Hiragi et al., 2018; Kinoshita and Koyama, 2021). Elevated Mammalian target of rapamycin (mTOR) signaling has been observed in epileptogenic human and animal models, and tuberous sclerosis complex 1 (TSC1) is known to be a negative regulator of the mTOR pathway, so Zhao X. et al. (2018) used that to investigate the mTOR association with microglia and epilepsy (Chu-Shore et al., 2010; Franz and Capal, 2017). In their study, *Tsc1*Cx3cr1CKO mice had elevated mTOR signaling only in microglia cells, which exhibited an unusual increase in the activity of those cells, such as phagocytic activity. However, even though the expression of proinflammatory cytokines was elevated in the hippocampus of those mice, their microglia had a decreased expression of proinflammatory cytokines (Hiragi et al., 2018; Zhao X. et al., 2018). Interestingly, at 5 weeks, *Tsc1*Cx3cr1CKO mice develop spontaneous seizures, suggesting the upregulation of mTOR in microglia could induce a seizure and eventually lead to SE (Hiragi et al., 2018; Zhao X. et al., 2018). Some could argue that other glial cells could have played a role, like astrocytes. For instance, Bianco et al. (2005) showed that an increased ATP release observed during seizures from astrocytes induced IL-1β release from N9 microglial cells derived from mice's brains (Bianco et al., 2005; Stansley et al., 2012; Hiragi et al., 2018). Fractalkine chemokines like CX3CL1 also play a role in the epileptic brain. Primarily expressed by neurons, it binds to a CX3CR1 receptor present on the surface of microglia, and in epileptic patients, its protein levels are increased (Hiragi et al., 2018; Wyatt-Johnson and Brewster, 2020). In the pilocarpine-induced SE rats' model, CX3CL1 immunoreactivity increased within the first 3 h in the hippocampus region and decreases 3 days later, while CX3CR1 remained after the 3 days (Yeo et al., 2011; Hiragi et al., 2018). Although neuronal damage was reported 3 days after SE rescue, it was possible to give antibodies against CX3CL1 or CX3CR1 (Yeo et al., 2011; Hiragi et al., 2018). However, other studies suggested that CX3CL1 could decrease gamma-aminobutyric acid (GABA)-evoked currents in excitatory neurons, regulating the excitatory/inhibitory (E/I) balance of neural circuits in seizures (Xu et al., 2012; Roseti et al., 2013). However, no studies have reported a link during SE, and a lot remains to be studied. CXCR4 and CXCL12 seem to induce the microglial release of TNF-α as well as the astrocytic release of glutamate, leading to neuronal hyperexcitability, suggesting their possible contributions to epilepsy (Devinsky et al., 2013; Hiragi et al., 2018).

Pro-inflammatory gene activation in seizure

In addition to microglia activation, other inflammatory molecules have been associated with SE. VEGF, as previously mentioned, plays an important role in angiogenesis and BBB permeability, but an elevated level of VEGF protein and VEGFR expression has been observed in an epileptic seizure (Mukhtar, 2020). Nicoletti et al. (2008) found that after SE stimulation, VEGF might have a neuroprotective effect against SE. VEGFR was found to be stimulated on neuronal cells and upregulation of VEGF was observed on glial cells a day after pilocarpine-induced SE, preventing neuronal cell death (Rigau et al., 2007). The molecular mechanism of VEGF neuroprotection during SE is not fully understood; however, researchers suggest that the induction of the intracellular phosphatidylinositol 3-kinase/Akt pathway might block caspase-3 function, preventing apoptosis and increasing cell viability (Sun and Guo, 2005). Thus, depletion of VEGF during SE might enhance neuronal deterioration. We previously mentioned that TLR4 activity plays an important role in SE. Some studies suggest that forkhead transcription factor 3 (Foxp3) attenuates TLR4 signaling and inflammation, which then inactivates NR2B-containing *N*-methyl-D-aspartic acid (NMDA) receptors (Wang et al., 2017). This suggests that Foxp3 plays an important role in epileptogenesis (Wang et al., 2017; Mukhtar, 2020). Plus, the hyperacetylated form of high mobility group box 1 (HMGB1) regulates pro-inflammatory cytokines like IL-Iβ, and like Foxp3, it interacts with TLRs, TLR2, and TLR4 with receptors for advanced glycation endproducts (RAGE), its role in SE is still not fully understood (Mukhtar, 2020). Balosso et al. (2014) suggest HMGB1 augmented NMDA activity enhances excitotoxicity and aggravates Kainic acid seizure induced through activation of TLR4 in neurons located in the hippocampus (Mukhtar, 2020). When discussing neuroinflammation and seizures, NF-κB signaling pathway is one of the most important players. In fact, by interacting with other molecules such as COX-2, mTOR, and mitogen-activated protein kinase (MAPK), it can interact with other molecules such as HMGB1, TNF-α, and IL-1 and activate TLR-4, TNF receptor (TNFR), and IL-1R which are major players in the neuroinflammation process, but how is it associated with SE (Wang and Chen, 2018)? Lubin et al. (2007) have reported that the inhibition of the NF-κB signaling pathway significantly decreased brain-derived neurotrophic factor (bdnf) protein expression and inhibitor kappa B alpha (IκBα), in which an increase level is observed during seizure activity, suggesting NF-κB pathway involvement in the upregulation of these transcripts during SE. With its direct or indirect interaction with other molecules NF-κB plays an important role in neuroinflammation as well as being associated with SE.

Mammalian target of rapamycin plays an important role in cellular mechanism, and as we also mentioned earlier, it is no surprise that its activity could be associated with SE. Genetic deficits of cellular elements in the mTOR pathway, like TSC, phosphatase,

and tensin homolog (PTEN), are related to the development of epilepsy (Manning et al., 2002; Meikle et al., 2008; Zhou et al., 2009). It would explain that abnormal mTOR could result in SE. Previous studies have also reported that inhibition of the mTOR pathway could reduce seizures in SE and even restore BBB dysfunction, making it a potential treatment target for SE (van Vliet et al., 2016; Wang and Chen, 2018). Moreover, seizures could potentially activate NF-κB and other inflammatory molecules that could lead to SE (Wang and Chen, 2018; Mukhtar, 2020). MAPKs are composed of enzymes that play critical roles in the cellular response to various external stimuli and could be associated with SE (Wang and Chen, 2018). For instance, Yang et al. (2018) suggested that inhibition of p38 MAPK, a member of the MAPK family, could reduce the time to the first epileptic seizure and attenuate its severity in the pilocarpine-induced rat model of epilepsy. COX-2 and Prostaglandin E2 (PGE2) could lead to an increase in Ca^{2+}, causing neuronal damage, a neurologic deficit, and hyperexcitability, possibly associating COX-2 and PGE2 with SE further studies are required (Wang and Chen, 2018; Mukhtar, 2020). Matrix metalloproteinase-9 (MMP-9) is a protease released by microglia in the hippocampus, cerebellum, and cortex part of the brain, it releases accelerated cell loss through disruption of matrix-cell, excitotoxicity, apoptosis, and BBB dysfunction, and its upregulation could lead to epileptogenesis (Acar et al., 2015; Bronisz and Kurkowska-Jastrzębska, 2016; Mukhtar, 2020). Furthermore, platelet-activating factor (PAF), CD44, and NADPH oxidases (NOXs) expression are increased during SE induction, affecting neuronal plasticity, hippocampal synaptic reorganization, or microglial activations, all of which enhance SE (Meikle et al., 2008; Zhou et al., 2009; Mukhtar, 2020).

Protein C activation mechanism

Protein C (PC), a vitamin K-dependent serine protease zymogen, is a single-chain protein composed of a prepropeptide and a signal peptide and has its gene expression located on chromosome 2 (Plutzky et al., 1986; Brown et al., 2013). Synthesized in the male reproductive tract but mainly in the liver, it is a Ca^{2+}-binding zymogen with its three domains: an N-terminal epidermal growth factor (EGF)-like domain, a γ-Carboxyglutamic acid-rich (GLA) domain, and a catalytic domain (Brown et al., 2013). PC circulates as a single-chain zymogen in plasma with a concentration of 4 μg/mL and is then activated by the thrombin-thrombomodulin complex (Griffin et al., 1982; Brown et al., 2013; Ren et al., 2019). In the form of PC, it does not have any physiological function; in order to function, PC needs to be converted to activated protein C (APC) (Brown et al., 2013). Thrombin is the physiological enzyme that converts PC in its zymogen form to APC in its activated form (Brown et al., 2013). When thrombin is bound to thrombomodulin (TM), it is more effective in activating PC to APC, but the complex thrombin-thrombomodulin is not the only one responsible for PC activation (Brown et al., 2013). Indeed, PC needs to bind to endothelial protein C receptor (EPCR) through its Gla-domain binds in order to be converted to APC; in fact, PC is activated by the proteolysis at Arg169 in endothelial protein C receptor (EPCR)-bound protein C by thrombomodulin-bound thrombin (**Figure 1**; Esmon, 1993; Fukudome and Esmon, 1994; Stearns-Kurosawa et al., 1996; Brown et al., 2013; Ren et al., 2019). In the form of APC, this protein has cytoprotective effect, anticoagulant, anti-inflammatory, and neuroprotective effect, making it a possible target for epilepsy treatment.

Anticoagulant mechanism of APC

The most important defense mechanisms against bleeding include blood coagulation and platelet-dependent hemostasis (Dahlbäck and Villoutreix, 2005). The formation of platelets creates a plug that blocks the vascular lesion. At the same time, platelets are formed, and the coagulation mechanism is activated by tissue factor (TF) (Dahlbäck and Villoutreix, 2005). Once coagulation factor VIIa (FVIIa) binds to TF, it creates an FVIIa–TF complex that converts factor X (FX) and factor IX (FIX) to their active forms FIXa and Fxa (Schenone et al., 2004; Dahlbäck and Villoutreix, 2005). During the coagulation process, a very large amount of thrombin is generated as complex (FXa–FVa) converts prothrombin to thrombin, and thrombin can activate platelets, FVIII, FV, and convert fibrinogen to a fibrin clot, making thrombin an important procoagulant protein (Di Cera, 2003; Mann et al., 2003; Dahlbäck and Villoutreix, 2005). Blood coagulation is tightly controlled by anticoagulation proteins, and APC is one of them. One of APC's targets in the regulation of the coagulation pathway is the inhibition of thrombin production through the inactivation of procoagulant cofactors FVa and FVIIIa (**Figure 1**; Dahlbäck and Villoutreix, 2005; Brown et al., 2013). With protein S and intact factor V, APC can regulate coagulation pathways. To inactivate cofactors FVa, APC cleaves the peptide bonds; Arg306-Asn307, Arg506-Gly507 and Arg679-Lys680 and to inactivate FVIIIa, APC cleaves Arg336-Met337, Arg562-Gly563, and Arg740–Ser741 (Dahlbäck and Villoutreix, 2005; Brown et al., 2013). Through these cleavages, APC switches factors FVa and FVIIIa from procoagulant to anticoagulant roles.

Anti-inflammatory and cytoprotective effect

In addition to its anticoagulant and profibrinolytic functions, APC also has cytoprotective and anti- inflammatory properties. To activate APC's protective activity, APC requires the Gla domain-dependent interaction with EPCR. This interaction gives APC the possibility to cleave the exodomain of protease-activated receptor 1 (PAR-1) leading to the activation of anti-inflammatory and cytoprotective signaling in vascular endothelial cells. PAR1, with the other members PAR2, PAR3, and PAR4 are G protein-coupled receptors (GPCR) from the large Rhodopsin family (Joyce et al., 2001; Pompili et al., 2021). To be activated, PAR1's N-terminus, which contains a hirudin-like domain with a high-affinity binding site for thrombin, need to be cleaved (Vu et al., 1991; Pompili et al., 2021). In addition to thrombin, several proteases can cleave and activate PAR1, including APC, FXa, FVIIa, MMP2, MMP3, MMP8, MMP9, plasmin, trypsin, cathepsin-G, granzyme-A and B (Pompili et al., 2021). Thrombin cleaves PAR1's N-terminus at Arg 41 leading to a conformational change of PAR1 and causing its coupling with multiple Gα proteins such as Gαi, Gαq, and Gα12/13 (Pompili et al., 2021). After being activated, PAR1 can

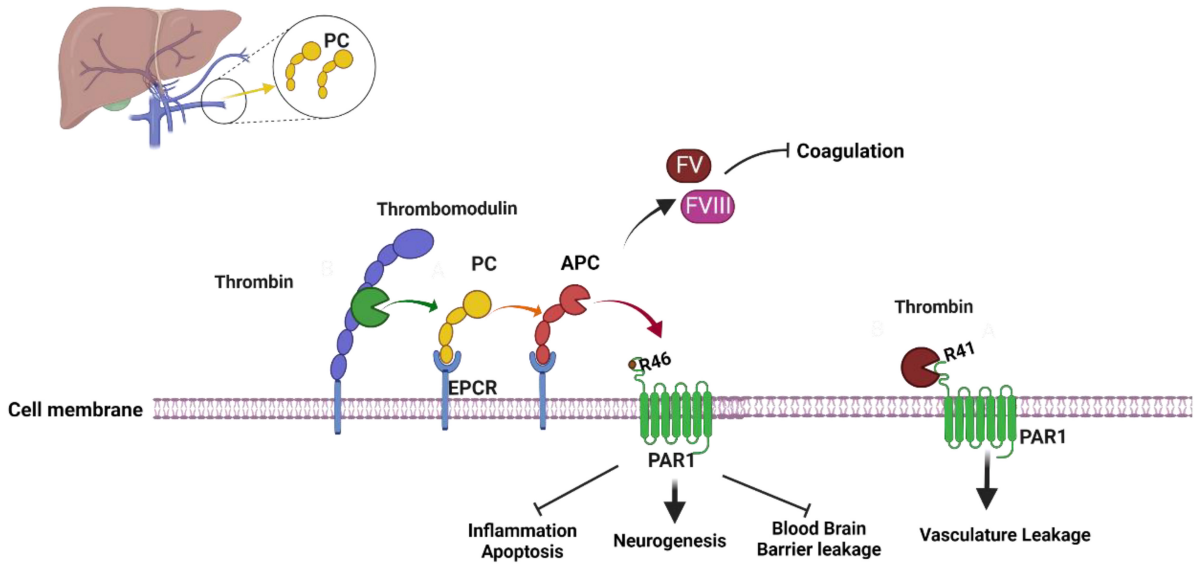

FIGURE 1
Activated protein C mechanism of activation and function. Thrombin-Thrombomodulin complex and endothelial protein C receptor (EPCR) are required to activate protein C to activated protein C which act as an anticoagulant. When activated protein C bind to protease activated receptor 1 (PAR1) it activated it neuroprotective mechanism. Thrombin interaction with PAR1 lead to vasculature leakage (see text for more information). The figure was prepared by software provided by Biorender.com (accessed 3 May, 2023).

recruit β-arrestin and activate Akt and Rac1 (Adams et al., 2011; Pompili et al., 2021). PAR1-Thrombin interaction initiated a pro-inflammatory mechanism that activated RhoA signaling pathway and phosphorylation of ERK1/2 (Mosnier et al., 2007, 2012; Ren et al., 2019). APC can also activate PAR1 by cleaving its N-terminus at Arg46 (**Figure 1**; Pompili et al., 2021). PAR1-APC interaction led to anti-inflammatory and cytoprotective mechanism activation. In fact, this activation leads to the downregulation of proapoptotic, and proinflammatory proteins such as NFκB or p53 and Bax, as well as the upregulation of antiapoptotic protein like Bcl-2 and anti-inflammatory proteins (Mosnier et al., 2007). The anti-inflammatory effect of APC involves its effect on leukocytes by limiting leukocyte adhesion and infiltration of tissues, maintaining vasculature integration, and inhibiting the release of pro-inflammatory cytokines and chemokines by leukocytes (Mosnier et al., 2007). Although APC activity is well known, its anti-inflammatory and cytoprotective mechanisms are not fully understood, creating limitations in the field.

Neuroprotective effect of APC

Our group, Ren et al. (2022) and other researchers established the APC cardioprotective effect and showed APC can prevent cardiac damage during I/R-induced stress, but recently the neuroprotective effect of APC has been a focus in the research field. In addition to its anticoagulant and cardioprotective effects, APC has a neuroprotective effect against neuropathology such as multiple sclerosis, ischemic stroke, and traumatic brain injury and the activation of the neuroprotective mechanism involves APC-PAR1 as well as PAR3 interaction (Griffin et al., 2018). Indeed, just like APC can induce a non-canonical activation of PAR1 by cleavage at Arg46 (**Figure 1**), APC can induce a non-canonical activation of PAR3 by cleavage at Arg41. Through their activation, they lead to signaling activation that would lead to stabilization of the BBB, up-regulation of neuronal antiapoptotic and anti-inflammatory proteins, as well as neurogenesis (Griffin et al., 2018). However, the detailed mechanism of the APC neuroprotective effect remains unclear, requiring more studies. Although APC's primary use has been to treat sepsis, its potential beneficial effects in the context of stroke, have been the focus of some research. Indeed, APC anti-inflammatory properties could be beneficial in reducing inflammation that occurs after stroke (Huuskonen et al., 2022). In fact, inflammation exacerbates brain injury after a stroke, and APC can help mitigate it (Lazic et al., 2019; Huuskonen et al., 2022). As mentioned above, APC has anticoagulation properties, and in an ischemic stroke caused by a blood clot, APC helps prevent it and improve blood flow in the affected area (Hall et al., 2014; Griffin et al., 2015; Huuskonen et al., 2022). APC antiapoptotic properties could limit cell death in stroke affected areas, regulate apoptosis, and inhibit cell death processes (Huuskonen et al., 2022). BBB is also one of the APC targets. In fact, APC helps maintain the integrity of the BBB, which could help reduce secondary damage following a stroke (Majid et al., 2020; Huuskonen et al., 2022; Wang et al., 2022). Lastly, APC can improve cerebral perfusion, and its neuroprotective effect can help reduce secondary damage following a stroke and reduce brain damage (Huuskonen et al., 2022; Wang et al., 2022). Despite those potential benefits, more research is needed to fully understand the effect of APC on stroke and to determine if it could be an effective treatment. As of right now, stroke treatment focuses on established therapies like thrombolytic drugs [like tissue plasminogen activator (tPA)], and due to its properties, it is understandable why APC could be a potential treatment target (Dong et al., 2019; Lazic et al., 2019).

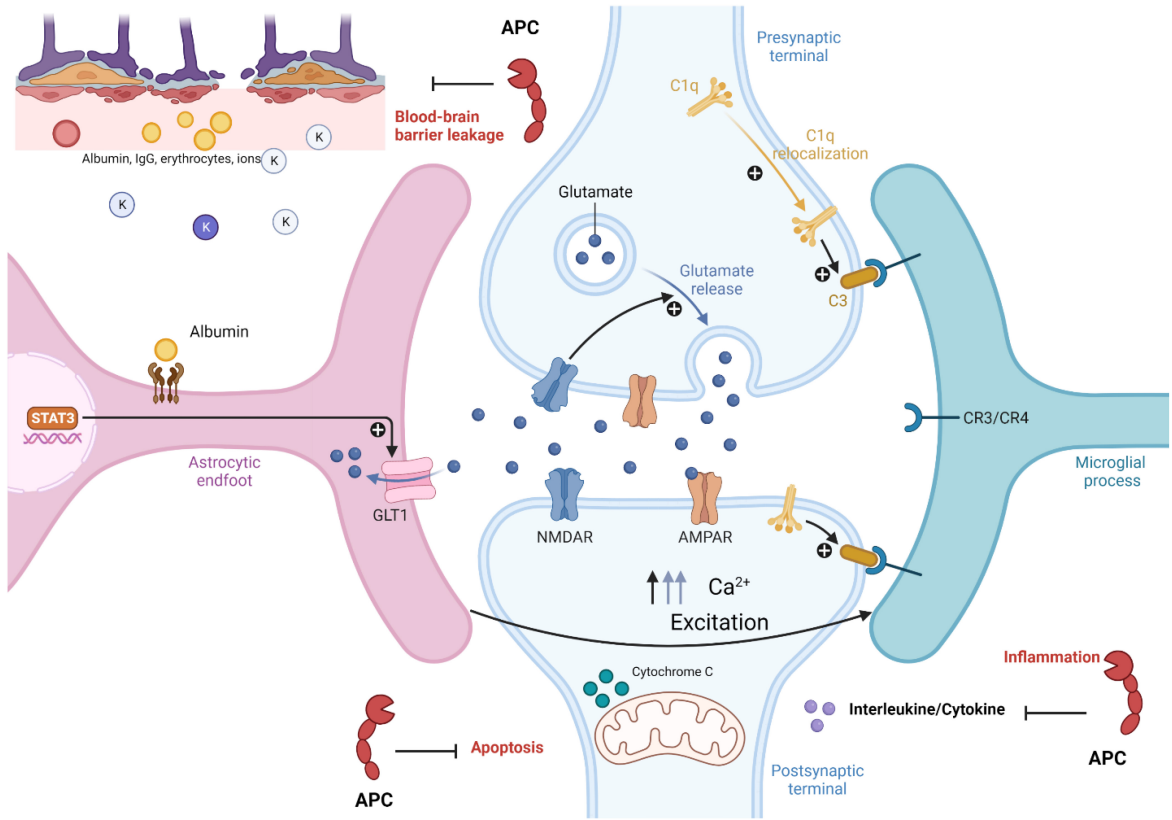

FIGURE 2
Role of activated protein C in epilepsy pathophysiology. Activated protein C neuroprotection in epilepsy pathophysiology inhibited blood brain barrier leakage, apoptosis, and inflammatory mechanism in disease development (see text for more information). The figure was prepared by software provided by Biorender.com (accessed 3 May, 2023).

Epilepsy and APC

Currently, in the field, there is still a lot to uncover regarding APC neuroprotective effects and the mechanism of epilepsy development; however, with the current knowledge, it is possible to make a connection between APC neuroprotective effects and epilepsy development. As mentioned earlier in this review, one of the hallmarks of epilepsy is BBB dysfunction, leading to reactive microglia and astrocytes, neuroinflammation, and cellular damage (Swissa et al., 2019). It is possible that the APC neuroprotective effect could prevent or treat epilepsy by initiating signaling effects on cells that could stabilize endothelial barrier functions like BBB, so in the presence of APC (**Figure 2**), BBB integrity remains intact (Griffin et al., 2018). As mentioned, inflammatory mediators could increase neuronal excitability and stimulate astrocytes and microglia activation during epilepsy, and since APC limited the release of pro-inflammatory cytokines and chemokines (**Figure 2**) by leukocytes in the vasculature, it could have an effect on microglia activation, limiting neuroinflammation during seizures (Mosnier et al., 2007; Kant et al., 2020; Mukhtar, 2020). In humans, neuronal cell death is one of the hallmarks of temporal lobe epilepsy. For instance, Bischoff et al. (2012) reported the death of interneurons in the pilocarpine seizure-inducing model and how Galectin-1 (Gal-1), a downstream effector of p75NTR, which triggers the disintegration of axons and cell death, plays a role in this mechanism (Bischoff et al., 2012). APC neurogenesis ability could reduce the effect of neuronal cell death through the replacement or creation of new neurons, particularly in the hippocampal region (Griffin et al., 2015, 2018). APC is not the only key element in its neuroprotective effect; PAR1 also plays an important role in this mechanism. PAR1 is in different regions of the brain, so its interaction with APC and other proteases could both be beneficial to the development of epilepsy or prevent it (Griffin et al., 2015, 2018; Heuberger and Schuepbach, 2019). For instance, Junge et al. (2003) reported in experimental brain ischemia that PAR1 activation by thrombin potentiates NMDA receptor responses and causes apoptosis in neurons, contributing to the pathological process (Junge et al., 2003). As outlined above, NMDA activity enhances excitotoxicity in epilepsy (Wang et al., 2017; Mukhtar, 2020). This suggests that increased interaction between PAR1 and thrombin might enhance seizure; however, APC-PAR1 might activate the neuroprotective mechanism (Griffin et al., 2018). There is still a lot to uncover about APC and the epilepsy association, even though APC has been proven to be an effective treatment target. In fact, in clinical studies, Wt-APC and 3K3A-APC have been given as treatments for ischemic stroke, sepsis, acute lung injury, diabetic ulcer wound healing, and more, and maybe with more research and a better understanding of their function, they could be used as a treatments or preventive methods for epilepsy.

Summary

Epilepsy is one of the world's oldest recognized neurological disorders and is characterized by recurrent seizures. A few of the mechanisms of development involved BBB disruption, neuroinflammation, and microglia activation. APC, well known for its anticoagulant properties, also has neuroprotective effects that could protect the BBB, activate anti-inflammatory and anti-apoptosis mechanisms, and lead to neurogenesis, all of which could help prevent or protect against epilepsy. In this review, we provided an overview of the possible association between APC and epilepsy, and a better understanding of both mechanisms is necessary to develop future therapies for current neurodevelopmental disorders.

Author contributions

LZ and JL conceptualized and wrote the review and carried out literature analysis. HW, SD, and LS reviewed and edited the article. JL acquired funding. All authors contributed to the article and approved the submitted version.

Funding

This work was supported by the Department of Veterans Affairs Merit Award I01BX005625 and I01CX002406 and the National Institute of Health grants P20GM1043577, P30GM149404, and R01HL158515.

Conflict of interest

The authors declare that the research was conducted in the absence of any commercial or financial relationships that could be construed as a potential conflict of interest.

Publisher's note

All claims expressed in this article are solely those of the authors and do not necessarily represent those of their affiliated organizations, or those of the publisher, the editors and the reviewers. Any product that may be evaluated in this article, or claim that may be made by its manufacturer, is not guaranteed or endorsed by the publisher.

Author disclaimer

The content is solely the responsibility of the authors and does not necessarily represent the official views of the National Institutes of Health, VA, or United States Government.

References

Abbott, N. J. (2005). Dynamics of CNS barriers: Evolution, differentiation, and modulation. *Cell. Mo. Neurobiol.* 25, 5–23. doi: 10.1007/s10571-004-1374-y

Acar, G., Tanriover, G., Acar, F., and Demir, R. (2015). Increased expression of matrix metalloproteinase-9 in patients with temporal lobe epilepsy. *Turkish Neuros.* 25, 749–756. doi: 10.5137/1019-5149.JTN.10738-14.0

Adams, M. N., Ramachandran, R., Yau, M. K., Suen, J. Y., Fairlie, D. P., Hollenberg, M. D., et al. (2011). Structure, function and pathophysiology of protease activated receptors. *Pharmacol. Ther.* 130, 248–282. doi: 10.1016/j.pharmthera.2011.01.003

Alberelli, M. A., and De Candia, E. (2014). Functional role of protease activated receptors in vascular biology. *Vascul. Pharmacol.* 62, 72–81. doi: 10.1016/j.vph.2014.06.001

Andoh, M., Ikegaya, Y., and Koyama, R. (2020). Microglia modulate the structure and function of the hippocampus after early-life seizures. *J. Pharmacol. Sci.* 144, 212–217. doi: 10.1016/j.jphs.2020.09.003

András, I. E., Deli, M. A., Veszelka, S., Hayashi, K., Hennig, B., and Toborek, M. (2007). The NMDA and AMPA/KA receptors are involved in glutamate-induced alterations of occludin expression and phosphorylation in brain endothelial cells. *J. Cereb. Blood Flow Metab.* 27, 1431–1443. doi: 10.1038/sj.jcbfm.9600445

Armulik, A., Genové, G., Mäe, M., Nisancioglu, M. H., Wallgard, E., Niaudet, C., et al. (2010). Pericytes regulate the blood–brain barrier. *Nature* 468, 557–561. doi: 10.1038/nature09522

Bachiller, S., Jiménez-Ferrer, I., Paulus, A., Yang, Y., Swanberg, M., Deierborg, T., et al. (2018). Microglia in neurological diseases: A road map to brain-disease dependent-inflammatory response. *Front. Cell. Neurosci.* 12:488. doi: 10.3389/fncel.2018.00488

Balosso, S., Liu, J., Bianchi, M. E., and Vezzani, A. (2014). Disulfide-containing high mobility group box-1 promotes N-methyl-D-aspartate receptor function and excitotoxicity by activating toll-like receptor 4-dependent signaling in hippocampal neurons. *Antioxidants Redox Signal.* 21, 1726–1740. doi: 10.1089/ars.2013.5349

Bar-Klein, G., Lublinsky, S., Kamintsky, L., Noyman, I., Veksler, R., Dalipaj, H., et al. (2017). Imaging blood–brain barrier dysfunction as a biomarker for epileptogenesis. *Brain* 140, 1692–1705. doi: 10.1093/brain/awx073

Baronas, V. A., and Kurata, H. T. (2014). Inward rectifiers and their regulation by endogenous polyamines. *Front. Physiol.* 5:325. doi: 10.3389/fphys.2014.00325

Benson, M. J., Manzanero, S., and Borges, K. (2015). Complex alterations in microglial M1/M2 markers during the development of epilepsy in two mouse models. *Epilepsia* 56, 895–905. doi: 10.1111/epi.12960

Bianco, F., Pravettoni, E., Colombo, A., Schenk, U., Möller, T., Matteoli, M., et al. (2005). Astrocyte-derived ATP induces vesicle shedding and IL-1β release from Microglia1. *J. Immunol.* 174, 7268–7277. doi: 10.4049/jimmunol.174.11.7268

Bischoff, V., Deogracias, R., Poirier, F., and Barde, Y. A. (2012). Seizure-induced neuronal death is suppressed in the absence of the endogenous lectin galectin-1. *J. Neurosci.* 32, 15590–15600. doi: 10.1523/JNEUROSCI.4983-11.2012

Bronisz, E., and Kurkowska-Jastrzębska, I. (2016). Matrix metalloproteinase 9 in epilepsy: The role of neuroinflammation in seizure development. *Mediat. Inflammat.* 2016:7369020. doi: 10.1155/2016/7369020

Brown, M. A., Stenberg, L. M., and Stenflo, J. (2013). Coagulation factor Xa. *Handb. Proteolytic Enzymes* 2013, 2908–2915.

Brown, R. C., and Davis, T. P. (2002). Calcium modulation of adherens and tight junction function: A potential mechanism for blood-brain barrier disruption after stroke. *Stroke* 33, 1706–1711. doi: 10.1161/01.str.0000016405.06729.83

Cacheaux, L. P., Ivens, S., David, Y., Lakhter, A. J., Bar-Klein, G., Shapira, M., et al. (2009). Transcriptome profiling reveals TGF-β signaling involvement in epileptogenesis. *J. Neurosci.* 29, 8927–8935. doi: 10.1523/JNEUROSCI.0430-09.2009

Campbell, I. L., Abraham, C. R., Masliah, E., Kemper, P., Inglis, J. D., Oldstone, M. B., et al. (1993). Neurologic disease induced in transgenic mice by cerebral overexpression of interleukin 6. *Proc. Natl. Acad. Sci. U.S.A.* 90, 10061–10065. doi: 10.1073/pnas.90.21.10061

Centers for Disease Control and Prevention (2020). *Types of seizures*. Atlanta, GA: Centers for Disease Control and Prevention.

Centers for Disease Control and Prevention (2023). *Epilepsy*. Atlanta, GA: Centers for Disease Control and Prevention.

Chu-Shore, C. J., Major, P., Camposano, S., Muzykewicz, D., and Thiele, E. A. (2010). The natural history of epilepsy in tuberous sclerosis complex. *Epilepsia* 51, 1236–1241. doi: 10.1111/j.1528-1167.2009.02474.x

Dahlbäck, B., and Villoutreix, B. O. (2005). The anticoagulant protein C pathway. *FEBS Lett* 579, 3310–3316. doi: 10.1016/j.febslet.2005.03.001

De Bock, M., Wang, N., Decrock, E., Bol, M., Gadicherla, A. K., Culot, M., et al. (2013). Endothelial calcium dynamics, connexin channels and blood–brain barrier function. *Prog. Neurobiol.* 108, 1–20. doi: 10.1016/j.pneurobio.2013.06.001

De Simoni, M. G., Perego, C., Ravizza, T., Moneta, D., Conti, M., Marchesi, F., et al. (2000). Inflammatory cytokines and related genes are induced in the rat hippocampus by limbic status epilepticus. *Eur. J. Neurosci.* 12, 2623–2633. doi: 10.1046/j.1460-9568.2000.00140.x

Devinsky, O., Vezzani, A., Najjar, S., De Lanerolle, N. C., and Rogawski, M. A. (2013). Glia and epilepsy: Excitability and inflammation. *Trends Neurosci.* 36, 174–184. doi: 10.1016/j.tins.2012.11.008

Di Cera, E. (2003). Thrombin interactions. *Chest* 124, 11S–17S. doi: 10.1378/chest.124.3_suppl.11s

Dong, X., Gao, J., Zhang, C. Y., Hayworth, C., Frank, M., and Wang, Z. (2019). Neutrophil membrane-derived nanovesicles alleviate inflammation to protect mouse brain injury from ischemic stroke. *ACS Nano* 13, 1272–1283. doi: 10.1021/acsnano.8b06572

Dore-Duffy, P., Owen, C., Balabanov, R., Murphy, S., Beaumont, T., and Rafols, J. A. (2000). Pericyte migration from the vascular wall in response to traumatic brain injury. *Microvasc. Res.* 60, 55–69. doi: 10.1006/mvre.2000.2244

Dreier, J. P. (2011). The role of spreading depression, spreading depolarization and spreading ischemia in neurological disease. *Nat. Med.* 17, 439–447. doi: 10.1038/nm.2333

Eilken, H. M., Diéguez-Hurtado, R., Schmidt, I., Nakayama, M., Jeong, H. W., Arf, H., et al. (2017). Pericytes regulate VEGF-induced endothelial sprouting through VEGFR1. *Nat. Commun.* 8, 1574. doi: 10.1038/s41467-017-01738-3

Esmon, C. T. (1993). Molecular events that control the protein C anticoagulant pathway. *Thromb. Haemost.* 70, 29–35. doi: 10.1055/s-0038-1646155

Fabry, Z., Fitzsimmons, K. M., Herlein, J. A., Moninger, T. O., Dobbs, M. B., and Hart, M. N. (1993). Production of the cytokines interleukin 1 and 6 by murine brain microvessel endothelium and smooth muscle pericytes. *J. Neuroimmunol.* 47, 23–34. doi: 10.1016/0165-5728(93)90281-3

Franz, D. N., and Capal, J. K. (2017). mTOR inhibitors in the pharmacologic management of tuberous sclerosis complex and their potential role in other rare neurodevelopmental disorders. *Orphanet J. Rare Dis.* 12:51. doi: 10.1186/s13023-017-0596-2

Frigerio, F., Frasca, A., Weissberg, I., Parrella, S., Friedman, A., Vezzani, A., et al. (2012). Long-lasting pro-ictogenic effects induced in vivo by rat brain exposure to serum albumin in the absence of concomitant pathology. *Epilepsia* 53, 1887–1897. doi: 10.1111/j.1528-1167.2012.03666.x

Fujikawa, D. G. (1996). The temporal evolution of neuronal damage from pilocarpine-induced status epilepticus. *Brain Res.* 725, 11–22. doi: 10.1016/0006-8993(96)00203-x

Fukudome, K., and Esmon, C. T. (1994). Identification, cloning, and regulation of a novel endothelial cell protein C/activated protein C receptor. *J. Biol. Chem.* 269, 26486–26491. doi: 10.1016/S0021-9258(18)47220-1

Gonul, E., Duz, B., Kahraman, S., Kayali, H., Kubar, A., and Timurkaynak, E. (2002). Early pericyte response to brain hypoxia in cats: An ultrastructural study. *Microvasc. Res.* 64, 116–119. doi: 10.1006/mvre.2002.2413

Griffin, J. H., Mosher, D. F., Zimmerman, T. S., and Kleiss, A. J. (1982). Protein C, an antithrombotic protein, is reduced in hospitalized patients with intravascular coagulation. *Blood* 60, 261–264.

Griffin, J. H., Zlokovic, B. V., and Mosnier, L. O. (2015). Activated protein C: Biased for translation. *Blood* 125, 2898–2907. doi: 10.1182/blood-2015-02-355974

Griffin, J. H., Zlokovic, B. V., and Mosnier, L. O. (2018). Activated protein C, protease activated receptor 1, and neuroprotection. *Blood* 132, 159–169. doi: 10.1182/blood-2018-02-769026

Gross, A., Benninger, F., Madar, R., Illouz, T., Griffioen, K., Steiner, I., et al. (2017). Toll-like receptor 3 deficiency decreases epileptogenesis in a pilocarpine model of SE-induced epilepsy in mice. *Epilepsia* 58, 586–596. doi: 10.1111/epi.13688

Hall, C. N., Reynell, C., Gesslein, B., Hamilton, N. B., Mishra, A., Sutherland, B. A., et al. (2014). Capillary pericytes regulate cerebral blood flow in health and disease. *Nature* 508, 55–60. doi: 10.1038/nature13165

Hayashi, T., and Suzuki, K. (2015). Changes of expression of the protein C pathway components in LPS-induced endotoxemia—Implication for sepsis. *Cardiovasc. Hematolo. Disord. Drug Targets* 15, 2–9. doi: 10.2174/1871529x15666150108110821

Heuberger, D. M., and Schuepbach, R. A. (2019). Protease-activated receptors (PARs): Mechanisms of action and potential therapeutic modulators in PAR-driven inflammatory diseases. *Thromb. J.* 17:4. doi: 10.1186/s12959-019-0194-8

Heymans, M., Figueiredo, R., Dehouck, L., Francisco, D., Sano, Y., Shimizu, F., et al. (2020). Contribution of brain pericytes in blood–brain barrier formation and maintenance: A transcriptomic study of cocultured human endothelial cells derived from hematopoietic stem cells. *Fluids Barriers CNS* 17:48. doi: 10.1186/s12987-020-00208-1

Hiragi, T., Ikegaya, Y., and Koyama, R. (2018). Microglia after seizures and in epilepsy. *Cells* 7:26. doi: 10.3390/cells7040026

Huuskonen, M. T., Wang, Y., Nikolakopoulou, A. M., Montagne, A., Dai, Z., Lazic, D., et al. (2022). Protection of ischemic white matter and oligodendrocytes in mice by 3K3A-activated protein C. *J. Exp. Med.* 219:e20211372. doi: 10.1084/jem.20211372

Jäkel, S., and Dimou, L. (2017). Glial cells and their function in the adult brain: A journey through the history of their ablation. *Front. Cell. Neurosci.* 11:24. doi: 10.3389/fncel.2017.00024

Johns Hopkins Medicine (2020). *Neurological disorders*. Baltimore, MA: Johns Hopkins Press Medicine.

Joyce, D. E., Gelbert, L., Ciaccia, A., DeHoff, B., and Grinnell, B. W. (2001). Gene expression profile of antithrombotic protein C defines new mechanisms modulating inflammation and apoptosis. *J. Biol. Chem.* 276, 11199–11203. doi: 10.1074/jbc.C100017200

Junge, C. E., Sugawara, T., Mannaioni, G., Alagarsamy, S., Conn, P. J., Brat, D. J., et al. (2003). The contribution of protease-activated receptor 1 to neuronal damage caused by transient focal cerebral ischemia. *Proc. Natl. Acad. Sci. U.S.A.* 100, 13019–13024. doi: 10.1073/pnas.2235594100

Kadry, H., Noorani, B., and Cucullo, L. (2020). A blood–brain barrier overview on structure, function, impairment, and biomarkers of integrity. *Fluids Barriers CNS* 17:69. doi: 10.1186/s12987-020-00230-3

Kangwantas, K., Pinteaux, E., and Penny, J. (2016). The extracellular matrix protein laminin-10 promotes blood–brain barrier repair after hypoxia and inflammation in vitro. *J. Neuroinflammat.* 13:25. doi: 10.1186/s12974-016-0495-9

Kant, R., Halder, S. K., Fernández, J. A., Griffin, J. H., and Milner, R. (2020). Activated protein C attenuates experimental autoimmune encephalomyelitis progression by enhancing vascular integrity and suppressing microglial activation. *Front. Neurosci.* 14:333. doi: 10.3389/fnins.2020.00333

Kim, S. Y., Senatorov, V. V., Morrissey, C. S., Lippmann, K., Vazquez, O., Milikovsky, D. Z., et al. (2017). TGFβ signaling is associated with changes in inflammatory gene expression and perineuronal net degradation around inhibitory neurons following various neurological insults. *Sci. Rep.* 7:7711. doi: 10.1038/s41598-017-07394-3

Kinoshita, S., and Koyama, R. (2021). Pro- and anti-epileptic roles of microglia. *Neural Regen. Res.* 16, 1369–1371. doi: 10.4103/1673-5374.300976

Klement, W., Garbelli, R., Zub, E., Rossini, L., Tassi, L., Girard, B., et al. (2018). Seizure progression and inflammatory mediators promote pericytosis and pericyte-microglia clustering at the cerebrovasculature. *Neurobiol. Dis.* 113, 70–81. doi: 10.1016/j.nbd.2018.02.002

Krizbai, I. A., Deli, M. A., Pestenácz, A., Siklós, L., Szabó, C. A., András, I., et al. (1998). Expression of glutamate receptors on cultured cerebral endothelial cells. *J. Neurosci. Res.* 54, 814–819. doi: 10.1002/(SICI)1097-4547(19981215)54:6<814::AID-JNR9<3.0.CO;2-3

Lazic, D., Sagare, A. P., Nikolakopoulou, A. M., Griffin, J. H., Vassar, R., and Zlokovic, B. V. (2019). 3K3A-activated protein C blocks amyloidogenic BACE1 pathway and improves functional outcome in mice. *J. Exp. Med.* 216, 279–293. doi: 10.1084/jem.20181035

Legrand, M., and Tolwani, A. (2021). Anticoagulation strategies in continuous renal replacement therapy. *Semin. Dial.* 34, 416–422. doi: 10.1111/sdi.12959

Levy, N., Milikovsky, D. Z., Baranauskas, G., Vinogradov, E., David, Y., Ketzef, M., et al. (2015). Differential TGF-β signaling in glial subsets underlies IL-6–mediated epileptogenesis in mice. *J. Immunol.* 195, 1713–1722. doi: 10.4049/jimmunol.1401446

Löscher, W., and Potschka, H. (2005). Role of drug efflux transporters in the brain for drug disposition and treatment of brain diseases. *Prog. Neurobiol.* 76, 22–76. doi: 10.1016/j.pneurobio.2005.04.006

Lubin, F. D., Ren, Y., Xu, X., and Anderson, A. E. (2007). Nuclear factor-κB regulates seizure threshold and gene transcription following convulsant stimulation. *J. Neuroch.* 103, 1381–1395. doi: 10.1111/j.1471-4159.2007.04863.x

Majid, Z., Tahir, F., Ahmed, J., Bin Arif, T. B., and Haq, A. (2020). Protein C deficiency as a risk factor for stroke in young adults: A review. *Cureus* 12:e7472. doi: 10.7759/cureus.7472

Mann, K. G., Brummel, K., and Butenas, S. (2003). What is all that thrombin for? *J. Thromb. Haemost.* 1, 1504–1514. doi: 10.1046/j.1538-7836.2003.00298.x

Manning, B. D., Tee, A. R., Logsdon, M. N., Blenis, J., and Cantley, L. C. (2002). Identification of the tuberous sclerosis complex-2 tumor suppressor gene product tuberin as a target of the phosphoinositide 3-kinase/akt pathway. *Mol. Cell* 10, 151–162. doi: 10.1016/s1097-2765(02)00568-3

Maroso, M., Balosso, S., Ravizza, T., Liu, J., Aronica, E., Iyer, A. M., et al. (2010). Toll-like receptor 4 and high-mobility group box-1 are involved in ictogenesis and can be targeted to reduce seizures. *Nat. Med.* 16, 413–419. doi: 10.1038/nm.2127

Matsuda, T., Murao, N., Katano, Y., Juliandi, B., Kohyama, J., Akira, S., et al. (2015). TLR9 signalling in microglia attenuates seizure-induced aberrant neurogenesis in the adult hippocampus. *Nat. Commun.* 6:6514. doi: 10.1038/ncomms7514

Meikle, L., Pollizzi, K., Egnor, A., Kramvis, I., Lane, H., Sahin, M., et al. (2008). Response of a neuronal model of tuberous sclerosis to mammalian target of rapamycin (mTOR) inhibitors: Effects on mTORC1 and Akt signaling lead to improved survival and function. *J. Neurosci.* 28, 5422–5432. doi: 10.1523/JNEUROSCI.0955-08.2008

Mendes, N. F., Pansani, A. P., Carmanhães, E. R. F., Tange, P., Meireles, J. V., Ochikubo, M., et al. (2019). The blood–brain barrier breakdown during acute phase of the pilocarpine model of epilepsy is dynamic and time-dependent. *Front. Neurol.* 10:382. doi: 10.3389/fneur.2019.00382

Milikovsky, D. Z., Kaufer, D., and Friedman, A. (2017). "Chapter 64. Blood–brain barrier disruption," in *Models of seizures and epilepsy*, 2nd Edn, eds A. Pitkänen, P. S. Buckmaster, A. S. Galanopoulou, and S. L. Moshé (Cambridge, MA: Academic Press), 951–959.

Mosnier, L. O., Sinha, R. K., Burnier, L., Bouwens, E. A., and Griffin, J. H. (2012). Biased agonism of protease-activated receptor 1 by activated protein C caused by noncanonical cleavage at Arg46. *Blood* 120, 5237–5246. doi: 10.1182/blood-2012-08-452169

Mosnier, L. O., Zlokovic, B. V., and Griffin, J. H. (2007). The cytoprotective protein C pathway. *Blood* 109, 3161–3172. doi: 10.1182/blood-2006-09-003004

Mukhtar, I. (2020). Inflammatory and immune mechanisms underlying epileptogenesis and epilepsy: From pathogenesis to treatment target. *Seizure* 82, 65–79. doi: 10.1016/j.seizure.2020.09.015

Nicoletti, J. N., Shah, S. K., McCloskey, D. P., Goodman, J. H., Elkady, A., Atassi, H., et al. (2008). Vascular endothelial growth factor is up-regulated after status epilepticus and protects against seizure-induced neuronal loss in hippocampus. *Neuroscience* 151, 232–241. doi: 10.1016/j.neuroscience.2007.09.083

Nishiyama, A., Suzuki, R., and Zhu, X. (2014). NG2 cells (polydendrocytes) in brain physiology and repair. *Front. Neurosci.* 8:133. doi: 10.3389/fnins.2014.00133

Oldendorf, W. H., Cornford, M. E., and Brown, W. J. (1977). The large apparent work capability of the blood–brain barrier: A study of the mitochondrial content of capillary endothelial cells in brain and other tissues of the rat. *Ann. Neurol.* 1, 409–417. doi: 10.1002/ana.410010502

Olson, J. K., and Miller, S. D. (2004). Microglia initiate central nervous system innate and adaptive immune responses through multiple TLRs1. *J. Immunol.* 173, 3916–3924. doi: 10.4049/jimmunol.173.6.3916

Peppiatt, C. M., Howarth, C., Mobbs, P., and Attwell, D. (2006). Bidirectional control of CNS capillary diameter by pericytes. *Nature* 443, 700–704. doi: 10.1038/nature05193

Persidsky, Y., Ramirez, S. H., Haorah, J., and Kanmogne, G. D. (2006). Blood–brain barrier: Structural components and function under physiologic and pathologic conditions. *J. Neuroimm. Pharmacol.* 1, 223–236. doi: 10.1007/s11481-006-9025-3

Plutzky, J., Hoskins, J. A., Long, G. L., and Crabtree, G. R. (1986). Evolution and organization of the human protein C gene. *Proc. Natl Acad. Sci. U.S.A.* 83, 546–550. doi: 10.1073/pnas.83.3.546

Pompili, E., De Franchis, V., Giampietri, C., Leone, S., De Santis, E., Fornai, F., et al. (2021). Protease activated receptor 1 and its ligands as main regulators of the regeneration of peripheral nerves. *Biomolecules* 11:1668. doi: 10.3390/biom1111668

Probert, L., Akassoglou, K., Kassiotis, G., Pasparakis, M., Alexopoulou, L., and Kollias, G. (1997). TNF-α transgenic and knockout models of CNS inflammation and degeneration. *J. Neuroimmunol.* 72, 137–141. doi: 10.1016/s0165-5728(96)00184-1

Reda, S., Winterhagen, F. I., Berens, C., Müller, J., Oldenburg, J., Pötzsch, B., et al. (2019). Circulating plasminogen activator inhibitor-1 (PAI-1) is reduced by in vivo thrombin generation and subsequent formation of activated protein C (APC). *Blood* 134(Suppl. 1), 2389–2389. doi: 10.1182/blood-2019-124731

Ren, D., Fedorova, J., Davitt, K., Van Le, T. N. V., Griffin, J. H., Liaw, P. C., et al. (2022). Activated protein C strengthens cardiac tolerance to ischemic insults in aging. *Circ. Res.* 130, 252–272. doi: 10.1161/CIRCRESAHA.121.319044

Ren, D., Giri, H., Li, J., and Rezaie, A. R. (2019). The cardioprotective signaling activity of activated protein C in heart failure and ischemic heart diseases. *Int. J. Mol. Sci.* 20:1762. doi: 10.3390/ijms20071762

Rhea, E. M., and Banks, W. A. (2019). Role of the blood–brain barrier in central nervous system insulin resistance. *Front. Neurosci.* 13:521. doi: 10.3389/fnins.2019.00521

Rigau, V., Morin, M., Rousset, M. C., de Bock, F., Lebrun, A., Coubes, P., et al. (2007). Angiogenesis is associated with blood–brain barrier permeability in temporal lobe epilepsy. *Brain* 130, 1942–1956. doi: 10.1093/brain/awm118

Roseti, C., Fucile, S., Lauro, C., Martinello, K., Bertollini, C., Esposito, V., et al. (2013). Fractalkine/CX3CL1 modulates GABAA currents in human temporal lobe epilepsy. *Epilepsia* 54, 1834–1844. doi: 10.1111/epi.12354

Sagare, A. P., Bell, R. D., Zhao, Z., Ma, Q., Winkler, E. A., Ramanathan, A., et al. (2013). Pericyte loss influences Alzheimer-like neurodegeneration in mice. *Nat. Commun.* 4:932. doi: 10.1038/ncomms3932

Salar, S., Lapilover, E., Müller, J., Hollnagel, J. O., Lippmann, K., Friedman, A., et al. (2016). Synaptic plasticity in area CA1 of rat hippocampal slices following intraventricular application of albumin. *Neurobiol. Dis.* 91, 155–165. doi: 10.1016/j.nbd.2016.03.008

Sander, J. W. (2014). "Epileptic seizures," in *Encyclopedia of the neurological sciences*, 2nd Edn, eds M. J. Aminoff and R. B. Daroff (Oxford: Academic Press), 175–177.

Schenone, M., Furie, B. C., and Furie, B. (2004). The blood coagulation cascade. *Curr. Opin. Hematol.* 11, 272–277. doi: 10.1097/01.moh.0000130308.37353.d4

Shahzad, K., Kohli, S., Al-Dabet, M. M., and Isermann, B. (2019). Cell biology of activated protein C. *Curr. Opin. Hematol.* 26, 41–50. doi: 10.1097/MOH.0000000000000473

Sharp, C. D., Hines, I., Houghton, J., Warren, A., Jackson, T. H., Jawahar, A., et al. (2003). Glutamate causes a loss in human cerebral endothelial barrier integrity through activation of NMDA receptor. *Am. J. Physio. Heart Circ. Physiol.* 285, H2592–H2598. doi: 10.1152/ajpheart.00520.2003

Shrot, S., Ramaty, E., Biala, Y., Bar-Klein, G., Daninos, M., Kamintsky, L., et al. (2014). Prevention of organophosphate-induced chronic epilepsy by early benzodiazepine treatment. *Toxicology* 323, 19–25. doi: 10.1016/j.tox.2014.05.010

Smith, Z. Z., Benison, A. M., Bercum, F. M., Dudek, F. E., and Barth, D. S. (2018). Progression of convulsive and nonconvulsive seizures during epileptogenesis after pilocarpine-induced status epilepticus. *J. Neurophysiol.* 119, 1818–1835. doi: 10.1152/jn.00721.2017

Stanimirovic, D. B., and Friedman, A. (2012). Pathophysiology of the neurovascular unit: Disease cause or consequence? *J. Cereb. Blood Flow Metab.* 32, 1207–1221. doi: 10.1038/jcbfm.2012.25

Stansley, B., Post, J., and Hensley, K. (2012). A comparative review of cell culture systems for the study of microglial biology in Alzheimer's disease. *J. Neuroinflamm.* 9:115. doi: 10.1186/1742-2094-9-115

Stearns-Kurosawa, D. J., Kurosawa, S., Mollica, J. S., Ferrell, G. L., and Esmon, C. T. (1996). The endothelial cell protein C receptor augments protein C activation by the thrombin-thrombomodulin complex. *Proc. Natl Acad. Sci. U.S.A.* 93, 10212–10216. doi: 10.1073/pnas.93.19.10212

Sun, F. Y., and Guo, X. (2005). Molecular and cellular mechanisms of neuroprotection by vascular endothelial growth factor. *J. Neurosci. Res.* 79, 180–184. doi: 10.1002/jnr.20321

Swissa, E., Serlin, Y., Vazana, U., Prager, O., and Friedman, A. (2019). Blood–brain barrier dysfunction in status epileptics: Mechanisms and role in epileptogenesis. *Epilepsy Behav.* 101:106285. doi: 10.1016/j.yebeh.2019.04.038

Tang, F. R., Loke, W. K., and Ling, E. A. (2011). Comparison of status epilepticus models induced by pilocarpine and nerve agents – A systematic review of the underlying aetiology and adopted therapeutic approaches. *Curr. Med. Chem.* 18, 886–899. doi: 10.2174/092986711794927720

van Vliet, E. A., Aronica, E., and Gorter, J. A. (2015). Blood–brain barrier dysfunction, seizures and epilepsy. *Semin. Cell Dev. Biol.* 38, 26–34. doi: 10.1016/j.semcdb.2014.10.003

van Vliet, E. A., da Costa Araújo, S., Redeker, S., van Schaik, R., Aronica, E., and Gorter, J. A. (2007). Blood–brain barrier leakage may lead to progression of temporal lobe epilepsy. *Brain* 130, 521–534. doi: 10.1093/brain/awl318

van Vliet, E. A., Otte, W. M., Wadman, W. J., Aronica, E., Kooij, G., de Vries, H. E., et al. (2016). Blood–brain barrier leakage after status epilepticus in rapamycin-treated rats II: Potential mechanisms. *Epilepsia* 57, 70–78. doi: 10.1111/epi.13245

Vezzani, A., Lang, B., and Aronica, E. (2015). Immunity and inflammation in epilepsy. *Cold Spring Harbor Perspect. Med.* 6, a022699. doi: 10.1101/cshperspect.a022699

Vu, T. K., Hung, D. T., Wheaton, V. I., and Coughlin, S. R. (1991). Molecular cloning of a functional thrombin receptor reveals a novel proteolytic mechanism of receptor activation. *Cell* 64, 1057–1068. doi: 10.1016/0092-8674(91)90261-v

Wang, F. X., Xiong, X. Y., Zhong, Q., Meng, Z. Y., Yang, H., and Yang, Q. W. (2017). Foxp3 exhibits antiepileptic effects in ictogenesis involved in TLR4 signaling. *FASEB J.* 31, 2948–2962. doi: 10.1096/fj.201600989R

Wang, L., Guo, H., Yu, X., Wang, S., Xu, C., Fu, F., et al. (2012). Responsive electrical stimulation suppresses epileptic seizures in rats. *PLoS One* 7:e38141. doi: 10.1371/journal.pone.0038141

Wang, M., and Chen, Y. (2018). Inflammation: A network in the pathogenesis of status epilepticus. *Front. Mol. Neurosci.* 11:341. doi: 10.3389/fnmol.2018.00341

Wang, Y., Kisler, K., Nikolakopoulou, A. M., Fernandez, J. A., Griffin, J. H., and Zlokovic, B. V. (2022). 3K3A-activated protein C protects the blood–brain barrier and neurons from accelerated ischemic injury caused by pericyte deficiency in mice. *Front. Neurosci.* 16:841916. doi: 10.3389/fnins.2022.841916

Weissberg, I., Wood, L., Kamintsky, L., Vazquez, O., Milikovsky, D. Z., Alexander, A., et al. (2015). Albumin induces excitatory synaptogenesis through astrocytic TGF-β/ALK5 signaling in a model of acquired epilepsy following blood–brain barrier dysfunction. *Neurobiol. Dis.* 78, 115–125. doi: 10.1016/j.nbd.2015.02.029

Winkler, M. K. L., Chassidim, Y., Lublinsky, S., Revankar, G. S., Major, S., Kang, E. J., et al. (2012). Impaired neurovascular coupling to ictal epileptic activity and

spreading depolarization in a patient with subarachnoid hemorrhage: Possible link to blood–brain barrier dysfunction. *Epilepsia* 53, 22–30. doi: 10.1111/j.1528-1167.2012.03699.x

Wyatt-Johnson, S. K., and Brewster, A. L. (2020). Emerging roles for microglial phagocytic signaling in epilepsy. *Epilepsy Curr.* 20, 33–38. doi: 10.1177/1535759719890336

Xu, Y., Zeng, K., Han, Y., Wang, L., Chen, D., Xi, Z., et al. (2012). Altered expression of CX3CL1 in patients with epilepsy and in a rat model. *Am. J. Pathol.* 180, 1950–1962. doi: 10.1016/j.ajpath.2012.01.024

Yan, B. C., Xu, P., Gao, M., Wang, J., Jiang, D., Zhu, X., et al. (2018). Changes in the blood–brain barrier function are associated with hippocampal neuron death in a kainic acid mouse model of epilepsy. *Front. Neurol.* 9:775. doi: 10.3389/fneur.2018.00775

Yang, Z., Wang, J., Yu, C., Xu, P., Zhang, J., Peng, Y., et al. (2018). Inhibition of p38 MAPK signaling regulates the expression of EAAT2 in the brains of epileptic rats. *Front. Neurol.* 9:925. doi: 10.3389/fneur.2018.00925

Yeo, S. I., Kim, J. E., Ryu, H. J., Seo, C. H., Lee, B. C., Choi, I. G., et al. (2011). The roles of fractalkine/CX3CR1 system in neuronal death following pilocarpine-induced status epilepticus. *J. Neuroimmunol.* 234, 93–102. doi: 10.1016/j.jneuroim.2011.03.005

Zhao, H., Zhu, C., and Huang, D. (2018). Microglial activation: An important process in the onset of epilepsy. *Am. J. Trans. Res.* 10, 2877–2889.

Zhao, X., Liao, Y., Morgan, S., Mathur, R., Feustel, P., Mazurkiewicz, J., et al. (2018). Noninflammatory changes of microglia are sufficient to cause epilepsy. *Cell Rep.* 22, 2080–2093. doi: 10.1016/j.celrep.2018.02.004

Zhou, B., Zhu, Z., Ransom, B. R., and Tong, X. (2021). Oligodendrocyte lineage cells and depression. *Mol. Psychiatry* 26, 103–117. doi: 10.1038/s41380-020-00930-0

Zhou, J., Blundell, J., Ogawa, S., Kwon, C. H., Zhang, W., Sinton, C., et al. (2009). Pharmacological inhibition of mTORC1 suppresses anatomical, cellular, and behavioral abnormalities in neural-specific Pten knockout mice. *J. Neurosci.* 29, 1773–1783. doi: 10.1523/JNEUROSCI.5685-08.2009

frontiers | Frontiers in Pharmacology

TYPE Original Research
PUBLISHED 24 November 2023
DOI 10.3389/fphar.2023.1197549

OPEN ACCESS

EDITED BY
Mahmoud Rafieian-Kopaei,
Shahrekord University of Medical Sciences, Iran

REVIEWED BY
Zhong Guoping,
Sun Yat-sen University, China
Ashwin Karanam,
Pfizer, United States

*CORRESPONDENCE
Heung Dong Kim,
hdkimmd@yuhs.ac
Min Jung Chang,
mjchang@yonsei.ac.kr

†These authors have contributed equally to this work and share first authorship

‡These authors have contributed equally to this work

RECEIVED 12 April 2023
ACCEPTED 01 November 2023
PUBLISHED 24 November 2023

CITATION
Park J, Kim SH, Hahn J, Kang H-C, Lee S-G, Kim HD and Chang MJ (2023), Population pharmacokinetics of everolimus in patients with seizures associated with focal cortical dysplasia. *Front. Pharmacol.* 14:1197549. doi: 10.3389/fphar.2023.1197549

Population pharmacokinetics of everolimus in patients with seizures associated with focal cortical dysplasia

Jinha Park[1,2†], Se Hee Kim[3†], Jongsung Hahn[4], Hoon-Chul Kang[3], Sang-Guk Lee[5], Heung Dong Kim[3,6*‡] and Min Jung Chang[1,2,7*‡]

[1]Department of Pharmaceutical Medicine and Regulatory Science, Colleges of Medicine and Pharmacy, Yonsei University, Seoul, Republic of Korea, [2]Department of Pharmacy, College of Pharmacy, Yonsei Institute of Pharmaceutical Sciences, Yonsei University, Seoul, Republic of Korea, [3]Pediatric Neurology, Department of Pediatrics, Yonsei University College of Medicine, Severance Children's Hospital, Epilepsy Research Institute, Seoul, Republic of Korea, [4]Department of Pharmacy, Jeonbuk National University, Jeonju, Republic of Korea, [5]Department of Laboratory Medicine, Severance Hospital, Yonsei University College of Medicine, Seoul, Republic of Korea, [6]Department of Pediatrics, Kangbuk Samsung Hospital, Sungkyunkwan University, Seoul, Republic of Korea, [7]Graduate Program of Industrial Pharmaceutical Science, Yonsei University, Incheon, Republic of Korea

Background: Everolimus is an inhibitor of mammalian target of rapamycin complex 1. As mutations in *TSC1* and *TSC2*, which cause partial-onset seizures associated with TSC, were found in focal cortical dysplasia type II (FCD II) patients, a clinical trial has been performed to explore the efficacy and safety of everolimus in FCD patients. However, no dosage regimen was determined to treat FCD II. To recommend an optimal dose regimen for FCD patients, a population pharmacokinetic model of everolimus in FCD patients was developed.

Methods: The data of everolimus were collected from September 2017 to May 2020 in a tertiary-level hospital in Korea. The model was developed using NONMEM® software version 7.4.1 (Icon Development Solutions, Ellicott City, MD, United States).

Results: The population pharmacokinetics of everolimus was described as the one-compartment model with first-order absorption, with the effect of BSA on clearance. The final model was built as follows: TVCL = 12.5 + 9.71 × (BSA/1.5), TVV = 293, and TVKA = 0.585. As a result of simulation, a dose higher than 7 mg/m^2 is needed in patients with BSA 0.5 m^2, and a dose higher than 6 mg/m^2 is needed in patients with BSA 0.7 m^2. A dose of 4.5 mg/m^2 is enough in the population with BSA higher than 1.5 m^2 to meet the target trough range of 5–15 ng/mL.

Conclusion: Based on the developed pharmacokinetics model, the optimal dose of everolimus in practice was recommended by considering the available strengths of Afinitor disperz®, 2 mg, 3 mg, and 5 mg.

KEYWORDS

everolimus, focal cortical dysplasia, epilepsy, population pharmacokinetics, non-linear mixed-effect modeling

1 Introduction

Everolimus is an inhibitor of mammalian target of rapamycin complex 1 (mTORC1), which play a role as an immunosuppressive and antineoplastic drug indicated for various organ transplantations and tumors. It inhibits the interaction between mTORC1 and FK506-binding protein-12 (FKBP-12) by binding to FKBP-12 with high affinity (Gabriele et al., 2004; Sánchez-Fructuoso, 2008). The downstream signaling related to cell cycle and glycolysis is altered, and the growth of tumor is inhibited consequently.

Based on the etiology of the tuberous sclerosis complex (TSC), which is related to mutations in oncogene suppressor *TSC1* and *TSC2* genes causing overactivation of mTOR, a randomized clinical trial examining Everolimus in a Study of Tuberous Sclerosis Complex (EXIST-3) was performed to evaluate the efficacy and safety of everolimus as an adjuvant treatment for seizures in TSC patients (French et al., 2016). As a result, in 2018, Afinitor disperz® (Novartis Pharmaceuticals Corporation) was approved for adjunctive treatment of adults and pediatrics older than 2 years with partial-onset seizure associated with TSC. The initial dose regimen was decided by age and the presence of the concomitant CYP3A4/P-glycoprotein inducer, which ranged from 3 mg/m^2 to 6 mg/m^2 once daily. The efficacy of reducing the frequency of seizures was shown in both low and high target trough concentration ranges, 3–7 ng/mL and 9–15 ng/mL, respectively.

Focal cortical dysplasia (FCD), which is characterized by abnormal development of the cerebral cortex, is one of the most important causes of refractory epilepsy which does not respond to conventional antiepileptic drugs in pediatrics (Sanjay et al., 2009). FCD is classified into three types by neuropathological features: FCD I presenting radial- and/or tangential-shaped dyslamination of the cortex, FCD II presenting cortical dyslamination and dysmorphic neurons, and FCD III related to other brain lesions (Blümcke et al., 2011).

There are many studies showing that FCD II is related to the hyperactivation of the mTOR pathway (Baybis et al., 2004; Miyata et al., 2004; Ljungberg et al., 2006). Furthermore, in 2017, mutations in *TSC1* and *TSC2* that cause partial-onset seizures associated with TSC were found in FCD II patients (Lim et al., 2015; Lim et al., 2017). Recently, a pilot study to determine the safety and mechanism of the action of everolimus in patients with TSC and FCD was reported (Fouladi et al., 2007; Dirk Jan et al., 2012; de Wit et al., 2016; Leitner et al., 2022). This allows us to hypothesize that everolimus, an mTOR inhibitor, can be used as a treatment of refractory seizures associated with FCD. The pharmacokinetics (PK) of everolimus was reported using both one- and two-compartment models (Atsuko Tanaka et al., 2016; Combes et al., 2018; Dirk Jan et al., 2012)). A population PK study based on EXIST-1, -2, and -3 reported that a two-compartment model with first-order absorption and body surface area showed that CYP3A or P-gp inducers increased the clearance of everolimus (Combes et al., 2018). However, no PK was reported in patients with FCD II, and no dosage regimen has been determined yet.

The purpose of this study is to develop a population pharmacokinetic model of everolimus in patients with seizures associated with focal cortical dysplasia (FCD) type II, analyzing clinical covariates to suggest an optimal dose regimen for this population.

2 Materials and methods

2.1 Study design and population

This analysis was performed with data available from a double-blinded crossover randomized clinical trial conducted at Severance Hospital in Seoul, Republic of Korea, from 2017 to 2020. The study protocol was approved by the Institutional Review Board (IRB NO. 4-2017-0299) of Severance Hospital. To obtain everolimus concentrations drawn at the time after dose from January 2020 to May 2020, an additional study protocol was approved by the Institutional Review Board (IRB NO. 4-2019-1232) of Severance Hospital. All participants and the legal surrogates provided written informed consent which explained the purpose and details of the study.

The inclusion and exclusion criteria for participants are described in the Supplementary Material. The clinical trial consists of the following four phases: baseline for 4 weeks, core I for 12 weeks, core II for 12 weeks, and extension phase for 29 weeks. After screening in the baseline phase for 4 weeks, patients were assigned randomly to one of two groups: everolimus (Afinitor disperz®, tablet for oral suspension) or placebo. After being administered with everolimus or placebo for core phase I, patients received the other treatment, by crossover, for core phase II. Only patients who agreed to participate in the extension phase were administered with everolimus until the completion of the trial.

2.2 Drug dosage and data collection

The initial dose of everolimus was 4.5 mg/m^2/day, which was used as an effective and safe dose in the EXIST-1 study (Franz et al., 2013). The target range of trough concentration was 5–15 ng/mL, and dose adjustment was performed through TDM for patients with a trough concentration lower or higher than the target range. The increase or decrease in the adjusted dose was 2 mg. Patients were administered with everolimus (Afinitor disperz®, tablet for oral suspension) once daily at the set time. Patients were also administered with more than one antiepileptic drug concomitantly. The specific products and doses of the concomitant antiepileptic drugs were not changed during the baseline and core phases.

The following data were collected from September 2017 to May 2020: the amount of everolimus administered, the actual time of administration, the actual time of sampling, the concentrations of everolimus, age, sex, weight (kg), body surface area (BSA, m^2), serum creatinine (mg/dL), ALT (IU/L), AST (IU/L), hemoglobin (g/dL), hematocrit (%), RBC (10^6/μL), albumin (g/dL), and the presence of concomitant CYP3A4 inducer and inhibitor (strong, moderate, and weak) (Supplementary Table S1).

2.3 Sampling strategy and bioanalysis

Blood samples for therapeutic drug monitoring were collected before administration and at weeks 2, 3, 4, and 8 in core phase I, at weeks 14, 15, 16, and 20 in core phase II, and at weeks 25, 28, and 40 in the extension phase. Additional blood samples were collected

at any time from 1 to 4 h after dose at weeks 24, 28, or 40 in the extension phase. Each drawn sample was 1 mL or 2 mL in volume for patients under or over the age of 6 years, respectively. Immediately after collection, the samples were placed in EDTA tubes.

The concentrations of everolimus were measured by validated high-performance liquid chromatography/tandem mass spectrometry (HPLC/MS/MS) using an Agilent 1260 (Agilent Technologies, CA, United States) coupled with an API 4000 (Sciex, Concord, Ontario, Canada). Then, 50 μL of deionized water and 50 μL of 0.1 M $ZnSO_4$ were added to 50 μL of sample, and the mixture was vortexed for 15 s. 5 μL each of ascomycin, sirolimus-d3, cyclosporin D, and everolimus-d4 as an internal standard and 130 μL of methanol were added to the mixture. After vortexing for 60 s, the mixture was centrifuged at 14,000 rpm for 10 min. Chromatographic separation was performed on a Guard column and a C_8 column (4 × 2.0 mm and 10 × 2.0 mm, respectively, Phenomenex, Torrance, CA, United States) with solvent A (deionized water with 2 mM ammonium acetate and 0.1% formic acid) and solvent B (100% methanol with 2 mM ammonium acetate and 0.1% formic acid) as the mobile phase. The gradient was as follows: 50:50 v/v for the first 0.1 min; 100% B for the next 1.1 min; and 50:50 v/v for the last 1.8 min. The flow rate was 650 μL/min for 3 min. The lower limit of quantification for everolimus was 1.1 ng/mL. The assay was validated within the range 1.1–41.6 ng/mL. The inter- and intra-assay coefficients of variation were below 7.3%.

2.4 Population pharmacokinetic analysis

Population pharmacokinetic modeling was conducted using the first-order conditional estimation method with the eta–epsilon interaction (FOCE + I) algorithm in NONMEM® software version 7.4.1 (Icon Development Solutions, Ellicott City, MD, United States) assisted by Perl-speaks-NONMEM (PsN, version 4.7.0), Pirana (version 2.9.7, Certara, NJ, United States), and Xpose4 (version 4.6.1) embedded in R (version 3.5.1; http://www.r-project.org/).

One- and two-compartmental PK models with first-order absorption were evaluated for a potential structural model using subroutines ADVAN2 TRANS2 and ADVAN4 TRANS4 in the NONMEM library, respectively. Inter-individual variability (η) was estimated with an exponential error model as follows:

$$\theta_i = \theta_{POP} \times \exp(\eta_i),$$

where θ_i is the individual PK parameter for the i^{th} individual, θ_{POP} is the population PK parameter, and η_i is a random variable of PK parameter which is assumed to follow a log-normal distribution with a mean of zero and a variance of ω^2.

Intra-individual variability (ε) was estimated with an additive, proportional, and a combined model as follows:

$$C_{ij} = C_{predij} + \varepsilon_{ij,additive},$$

$$C_{ij} = C_{predij} \times \left(1 + \varepsilon_{ij,proportional}\right),$$

$$C_{ij} = C_{predij} \times \left(1 + \varepsilon_{ij,proportional}\right) + \varepsilon_{ij,additive},$$

where C_{ij} is the j^{th} observed concentration for the i^{th} individual, C_{predij} is the corresponding predicted concentration, and $\varepsilon_{ij,additive}$ and $\varepsilon_{ij,proportional}$ are random variables which are assumed to follow a normal distribution with a mean of zero and a variance of σ^2. The best fitted base model was selected based on the minimum of the objective function value (OFV), which is statistically equivalent to the −2log likelihood, visual inspection on the basic goodness of fit plots, and the plausibility of relative standard errors. The criterion of a statistically significant decrease in OFV was 3.84 (χ^2 distribution, degrees of freedom = 1, p-value<0.05). The basic goodness-of-fit plots comprised four types of plots: observed concentration *versus* individual predicted concentration, observed concentration *versus* population predicted concentration, conditional weighted residuals (CWRES) *versus* population predicted concentration, and conditional weighted residuals (CWRES) *versus* time. Individual concentration–time plots and the eigenvalue of the models were also explored.

To explain the inter-individual variability of PK parameters, the following 14 potential covariates were evaluated: age (years), sex (0 for male; 1 for female), weight (kg), BSA (m^2), serum creatinine (mg/dL), ALT (IU/L), AST (IU/L), hemoglobin (g/dL), hematocrit (%), RBC (10^6/μL), albumin (g/dL), and the presence of at least one concomitant CYP3A4 strong inducer, weak inducer, and weak inhibitor (0 for absence; 1 for presence).

Continuous covariates (age, weight, BSA, serum creatinine, ALT, AST, hemoglobin, hematocrit, RBC, and albumin) centered on their median values were tested using linear, exponential, power, and proportional models. Moreover, for categorical covariates (sex and the presence of at least one concomitant CYP3A4 inducer or inhibitor), linear, exponential, power, and proportional models were used.

Covariates were analyzed using a stepwise method which consists of a forward selection step and a backward elimination step. In the forward selection step, a covariate was selected if the OFV of the model with added covariate decreased under 3.84 (χ^2-test, p-value<0.05) compared to the prior model. The procedure was performed until no more covariate reduced the OFV of the model significantly, and the full model was constructed with all influential covariates. In the backward elimination step, the covariate was retained in the final model if the OFV increased over 6.63 (χ^2-test, p-value<0.01) when each of the included covariates was deleted one by one. A decision on covariate selection was made at each step based on biological and clinical plausibility.

2.5 Final model validation

Validation of the final model was performed to evaluate its accuracy and robustness through bootstrap, goodness-of-fit plot, and prediction-corrected visual predictive check (pc-VPC). For bootstrap, 5,000 sets of data were resampled to validate the final model internally by comparing to estimates from the final model. Median values of estimates were calculated, and 95% confidence intervals were constructed by 2.5th and 97.5th percentiles from bootstrap results. Goodness-of-fit plots were examined to evaluate the fitting of predictions to observations. PC-VPC was performed with 1,000 simulations to diagnose the predictive performance of the final model graphically. Median, 2.5th, and 97.5th percentiles were visually assessed with 95% confidence interval.

TABLE 1 Baseline characteristics of study patients (n = 22).

Continuous variable	Median	IQR	Min., max.
Age (years)	13.5	12–17.75	4, 32
Body weight (kg)	50	35.5–60	13, 86
Body surface area (m^2)	1.5	1.23–1.7	0.6, 2
Serum creatinine (mg/dL)	0.67	0.48–0.76	0.33, 0.92
ALT (IU/L)	11	9–13	5, 67
AST (IU/L)	16	14–18	10, 44
Hemoglobin (g/dL)	13.15	12.7–14.3	10.3, 16.5
Hematocrit (%)	38.95	37.8–41.9	35, 47.8
RBC (10^6/mcL)	4.48	4.25–4.76	3.89, 5.19
Albumin (g/dL)	4.6	4.3–5	4.1, 5.2
Categorical variables	Number	Portion (%)	
Male	9	40.9	
CYP 3A4 inducer[a]			
Strong	1	4.5	
Moderate	0	0	
Weak	14	63.6	
CYP 3A4 inhibitor[a]			
Strong	2	9	
Moderate	1	4.5	
Weak	14	63.6	

ALT, alanine transaminase; AST, aspartate aminotransferase; CYP, cytochrome P450 enzyme; IQR, inter quantile range; min., minimum; max., maximum; RBC, red blood cell.
[a]The number of patients taking at least one CYP3A4 inducer/inhibitor with everolimus concomitantly.

2.6 Simulation

To predict the concentrations of everolimus at steady state using influential covariates, Monte Carlo simulation was performed based on the constructed final model. Dosages of 3 mg/m^2, 4.5 mg/m^2, 5 mg/m^2, 6 mg/m^2, 7 mg/m^2, and 9 mg/m^2 once daily were simulated for each BSA of 0.5 m^2, 1 m^2, 1.5 m^2, 1.7 m^2, and 2 m^2, which were the extracted values from the baseline range of patients in this study. Additionally, 3 mg/m^2, 4.5 mg/m^2, 5 mg/m^2, 6 mg/m^2, and 7 mg/m^2 were simulated for the groups with BSA 0.7 m^2 to explore the optimized dose regimen for FCD patients. A total of 35 scenarios are shown in Supplementary Table S2. Concentrations were generated for 1,000 subjects in each scenario assuming that concentrations of everolimus reach a steady state after 14 days.

3 Results

3.1 Patient characteristics

The demographics of the 22 total patients are described in Table 1. Continuous variables are shown in median with ranges as minimum, interquantile, and maximum. Categorical variables are shown in the numbers of patients, with portions in percentage. The median age was 13.5 years (range 4–32 years), and nine male patients (40.9%) were included. The median BSA was 1.5 m^2 (range 0.6–2 m^2), and the median albumin was 4.6 g/dL (range 4.1–5.2 g/dL). Only one patient was administered with CYP3A4 strong inducers concomitantly during this study, and another patient who was administered with a CYP3A4 moderate inducer concomitantly dropped out without valid everolimus concentrations.

3.2 Population pharmacokinetic model

A total of 152 observed everolimus concentrations of time after dose from 22 patients were included in the population PK modeling. The observed everolimus data were best described by the one-compartment model with the first-order absorption model. The clearance, volume of distribution, and absorption rate of the population were estimated as 21.9 L/h, 302 L, and 0.573 h^{-1}, respectively. The inter-individual variability of clearance (ω_{CL}^2) and volume of distribution (ω_V^2) were estimated as 0.0409 and 0.0602, which are correlated to 20.2% and 24.5% of the coefficient of variation, respectively. The inter-individual variability of the absorption rate (ω_{KA}^2) was fixed as zero. The residual variability (σ^2) was best explained by the proportional error model. The objective function value of the base model was 397.372.

TABLE 2 Parameter estimates and bootstrap confidence interval.

	Structural model (RSE%[b]) [shrinkage%]	Final model		
		TVCL = CL+ $\theta_{BSA\ on\ CL}$ × (BSA/1.5) TVV = VTVKA = KA		
		Final model (RSE%[a]) [shrinkage%]	Bootstrap (5,000 replicates)	
			Median	95% CI[b] (2.5%–97.5%)
Fixed effects				
CL (L/h)	21.9 (16)	12.5 (26)	12.04	5.46, 23.38
V (L)	302 (34)	293 (30)	287.7	72.0, 1454
KA (/h)	0.573 (34)	0.585 (30)	0.594	0.083, 1.195
$\theta_{BSA\ on\ CL}$	-	9.71 (33)	10.14	2.29, 26.54
Random effects				
Inter-individual variability (ω)				
ω_{CL}	0.2022 (51) [13]	0.1652 (47) [15]	0.1565	0.0728, 0.4535
ω_{V}	0.2454 (72) [38]	0.2083 (63) [39]	0.1977	0.0539, 1.2360
Residual variability (σ)				
$\sigma_{proportional}$	0.2922 (15) [7]	0.2943 (14) [6]	0.2888	0.2249, 0.3303
OFV				
$OFV_{Base\ model}$		$OFV_{Final\ model}$		Reduction of OFV
397.372		391.016		6.356

BSA, body surface area; CI, confidence interval; CL, clearance; KA, absorption rate; RSE, relative standard error; V, volume of distribution.
[a]RSE% = (standard error/parameter estimate) × 100.
[b]95% CI estimated from 5,000 resampled datasets by using the final population pharmacokinetic model.

All collected covariates were tested in a stepwise manner. For the first forward selection step, the linear model of BSA on clearance was selected, with the largest reduction of OFV (ΔOFV = −6.356). According to the clinical pharmacology review of the FDA (CDER, 2009), the clearance of everolimus increased linearly with BSA, which aligns well with this study. In the second step, the proportional model of albumin on clearance was selected, with a reduction of OFV (ΔOFV = −4.941). This can be explained by the protein-binding portion (75%) of everolimus. The proportional model of RBC on clearance and the power model of RBC on volume of distribution also reduced the OFV (ΔOFV = −5.6 and −4.095, respectively); however, RBC was excluded as a covariate because the bioassay of everolimus was performed with whole blood, meaning that RBC does not influence everolimus concentrations in this study. As a result, the full model had BSA and albumin on clearance.

When BSA was eliminated from the full model, OFV increased significantly (ΔOFV = 6.92), while the removal of albumin from the full model increased OFV to 4.941. The final PK model was constructed with BSA on clearance.

The estimated values of the parameters from the final population PK model are summarized in Table 2 with the medians derived from 5,000 bootstrapped samples in 95% confidence intervals. The estimated values were similar to the median values from the bootstrap result, within 95% confidence interval. The relative standard errors (RSEs) of the random effects were acceptable. All eta shrinkage values were under 40, except IIV of the absorption rate, which was fixed at zero.

Goodness-of-fit plots for the final PK model are shown in Figure 1. Individual predicted concentration (IPRED, (a)) and population predicted concentration (PRED, (b)) were uniformly distributed near the line, showing that observations equal predictions. Conditional weighted residuals (CWRES) by PRED (c) and time (d) were randomly distributed around zero, without specific trends.

The pc-VPC plot for the final PK model, which describes the 2.5th, median and 97.5th observed concentrations by lines, and each corresponding 95% confidence interval for the predicted estimates as given by the shaded areas are shown in Figure 2. Each line is well included in the shaded area, which was constructed from 1,000 simulated datasets from the final population PK model.

3.3 Simulations

Monte Carlo simulation based on the final PK model was performed to explore the optimal dose regimen in the population of FCD patients according to BSA, which influences everolimus concentration. Dosages were simulated based on BSA as follows: 3 mg/m^2, 4.5 mg/m^2, 5 mg/m^2, 6 mg/m^2, 7 mg/m^2, and 9 mg/m^2. The simulated concentration–time courses at steady state when BSA is 0.5 m^2, 0.7 m^2, 1 m^2, 1.5 m^2, 1.7 m^2, and 2 m^2 are presented in Supplementary Figures S1–S4. The target range of everolimus trough concentration in FCD was assumed to be from 5 to 15 ng/

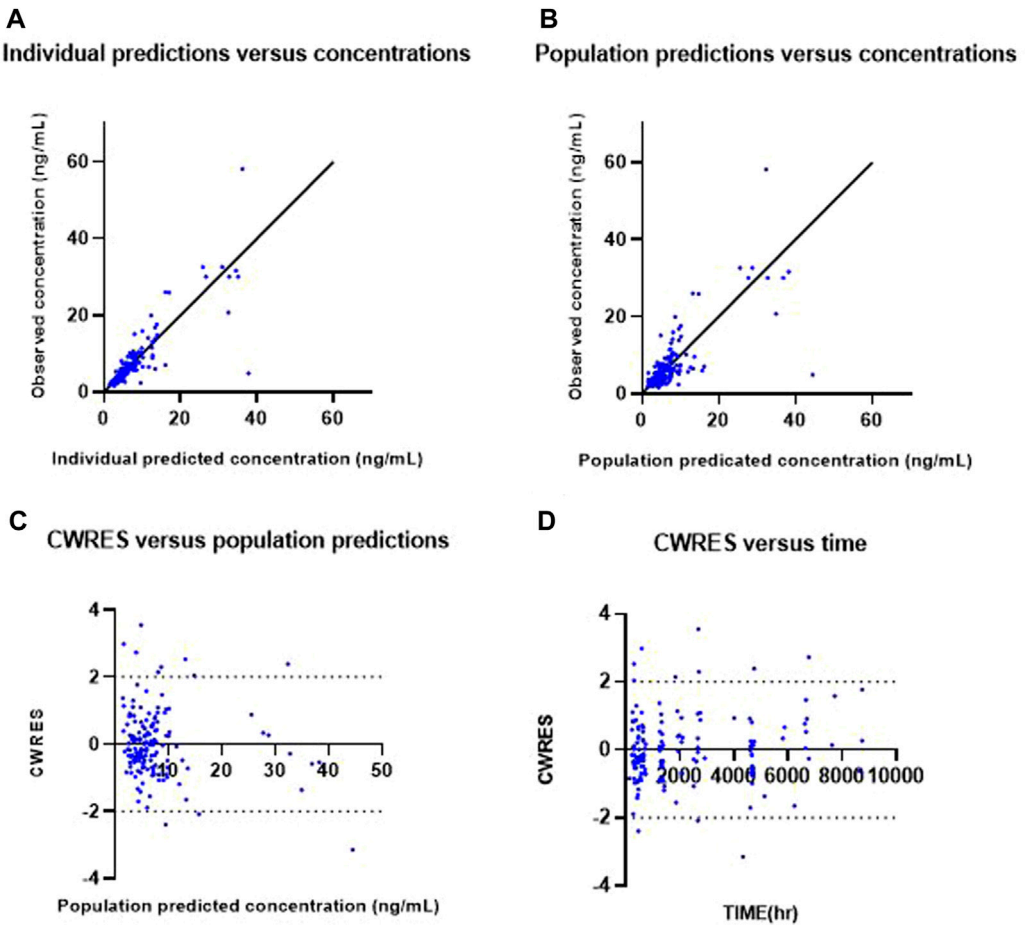

FIGURE 1
Goodness-of-fit plots of the final model. Observed everolimus concentration *versus* individual predicted (IPRED) concentration **(A)** and *versus* population predicted concentration (PRED) **(B)**. Conditional weighted residuals (CWRES) *versus* population predicted concentration **(C)** and *versus* time **(D)**.

mL, according to a previous clinical trial on TSC (Franz et al., 2013). Figure 3 describes the simulated trough concentrations based on the BSA level and various BSA-based dosage regimens after administering everolimus once a day for 2 weeks, which is enough time to reach the steady state. The target range 5–15 ng/mL is presented as a red dashed line, and the efficacious dose regimens that allow the trough concentrations to achieve the target range were explored according to each baseline of BSA. Furthermore, we decided the optimal initial doses by both mean trough concentrations and % of target concentrations as 60%. Based on the simulation results, Table 3 suggests an optimal initial dose of everolimus by the BSA range, and this can guide the efficacious dose for FCD individual patients according to their BSA value.

4 Discussion

The dosing regimen of everolimus and the target range of trough concentrations for treating seizures associated with FCD have not been decided yet, and a population pharmacokinetic model of everolimus in FCD patients was explored to optimize the dosage regimen. As a result, the model was described as a one-compartmental model with first-order absorption, and the final model revealed that the clearance of everolimus increased linearly as BSA increased. Target concentrations and clinical endpoints of everolimus in FCD were not determined, and we used those of TSC. This is the first study to develop a population pharmacokinetic model and suggest the optimal dosage of everolimus in patients with FCD.

The population pharmacokinetic model of everolimus for FCD patients is developed as a one-compartment model, different from other population PK models of everolimus, which are two-compartment models (Fouladi et al., 2007; Dirk Jan et al., 2012; Atsuko Tanaka et al., 2016; de Wit et al., 2016; Combes et al., 2018; Ter Heine et al., 2018). Only one study reported PK in FCD patients, reporting a two-compartment model with a similar CL (20.0 L/h) and a larger Vd (V2 219 L and V3 335.7 L) (Combes et al., 2018), where the CL was similar to that in our study, and the Vd was larger than that in our study. The difference in Vd may be due to differences in the study population, with the age of the subjects in Combes et al.'s study ranging from 19 to 74 years. Some studies reported on cancer and transplant patients. One study conducted on liver transplant patients reported that everolimus follows a one-compartment model, with a smaller CL and a similar Vd to this study, with covariates of body weight, total daily dose, fluconazole concomitant administration,

10.3389/fphar.2023.1197549

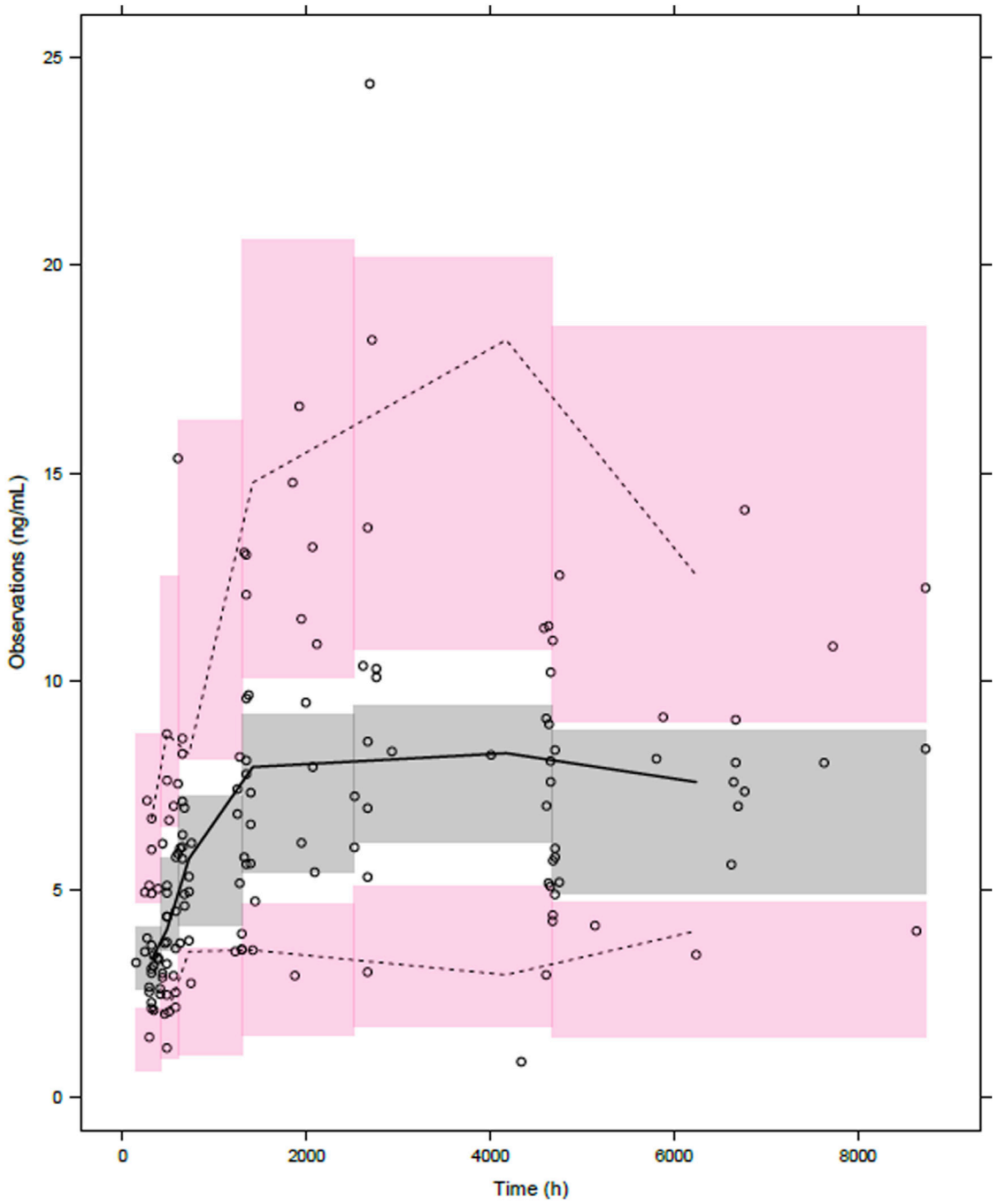

FIGURE 2
Prediction-corrected visual predictive check of the final model. Open circles, observed everolimus concentrations; solid line, median; lower and upper dashed lines, the 2.5th and 97.5th percentiles of the simulated data, respectively; and shaded areas, 95% confidence intervals for simulated predicted median, 2.5th percentile, and 97.5th percentile constructed from 1,000 simulated datasets of individuals from the original dataset.

eGFR, and sex (Itohara et al., 2022). Heine et al. developed a mechanistic two-compartment model for both transplant and cancer patients. As a result, a much higher CL (364 L/h) and a larger Vc (176 L) and Vp (577 L) were reported, and the dosage regimen was recommended according to the therapeutic ranges of each disease (Ter Heine et al., 2018). As described previously, different studies have shown different PK results, and more studies are needed to confirm trends, especially in patients with FCD.

Because the time points of sampling were sparse in this study, many assumptions regarding parameters were required to fit the data to the two-compartmental model. Therefore, a one-compartmental model was preferred for simplicity. The inter-individual variability of the rate constant of absorption (ka) was fixed at zero because there was not much information about the absorption phase from our data. The estimate of ka in this population was 0.585 h^{-1} in the final model, with the assumption that absorption

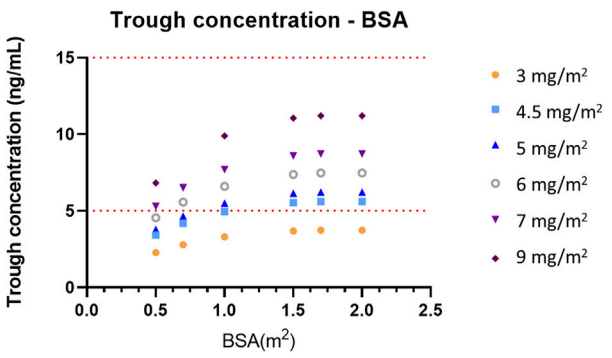

FIGURE 3
Simulated trough concentrations—BSA profiles according to the BSA-based dose regimen. The target range of trough concentrations, 5–15 ng/mL, is presented as a red dashed line.

TABLE 3 Optimal initial dose of everolimus by the BSA range.

BSA (m^2)	Initial dose regimen
0.5≤BSA< 1	7–9 mg/m^2 for the initial dose
1.5 ≤BSA	6–7 mg/m^2 for the initial dose

rates are the same among the patients. This estimate is lower than that of other populations, which ranged from 0.647 h^{-1} to 11.087 h^{-1}. Combes et al. reported the rate constant of absorption as 10.8 h^{-1} from the population pharmacokinetic model of everolimus in patients with seizures associated with TSC (Combes et al., 2018). The difference of rate constants between this study and the study of Combes might have resulted from differences in the range of age and the control of food effect (Kovarik et al., 2002).

From the simulation in this study, the initial dose of everolimus for FCD patients with refractory seizures was suggested by individual BSA. The optimal doses were found from the result of simulations by the BSA of 0.5 m^2, 0.7 m^2, 1 m^2, 1.5 m^2, 1.7 m^2, and 2 m^2. For FCD patients whose BSAs are less than 1 m^2, 7–9 mg/m^2 of everolimus is recommended. For patients with BSA between 1 and 2 m^2, 6–7 mg/m^2 of everolimus is recommended. The initial recommended doses are higher than those of our study, and this means that different dosage regimens should be considered in FCD patients. To suggest a practical dose regimen for FCD patients by BSA, the available strengths of everolimus should be considered; therefore, the actual dose which is obtained by the multiplication of BSA should be rounded to be useful in practice.

The recommended dosing regimens for FCD patients are similar to those for TSC patients, considering the correlation between age and BSA (Andre et al., 2016). The effect of concomitant use of CYP3A4/P-gp inducers was not analyzed in this study because of insufficient numbers of patients who have been administered strong CYP3A4/P-gp inducers. However, BSA is expected to enable more precise dosing for individuals such as obese children when compared to an only age-based dosing regimen.

There are some limitations in this study. First, it was not possible to estimate the inter-individual variability of the absorption rate and the effect of concomitant use of CYP3A4/P-gp inducers/inhibitors on the pharmacokinetics of everolimus because the number of samples was not enough. To suggest a more optimal dose regimen of everolimus for FCD patients, the reference range of target therapeutic concentration needs to be set first. The assumption that the therapeutic range of everolimus in FCD patients is similar to that of TSC patients was required to recommend the optimal dose in this study. Moreover, it is expected that the limit of maximum concentrations should be decided, and more precise dose regimens can be suggested for the FCD patient population using safety information from clinical studies.

5 Conclusion

The population pharmacokinetic model of everolimus for patients with refractory seizures associated with FCD was built as a one compartment model with first-order absorption and elimination. The linear effect of BSA on clearance was included in the final model. Based on the developed population pharmacokinetic model, the optimal dose regimen of everolimus for individuals with FCD was recommended by considering the BSA and strength of formulations in practice.

Data availability statement

Raw data with personal information removed can be provided upon request.

Ethics statement

The studies involving humans were approved by the Institutional Review Board (IRB NO. 4-2017-0299) of Severance Hospital. The studies were conducted in accordance with the local legislation and institutional requirements. Written informed consent for participation in this study was provided by the participants' legal guardians/next of kin.

Author contributions

Conception of the study: SK, H-CK, HK, and MC. Acquisition, analysis, and interpretation of data: JP, SK, JH, S-GL, and MC. Drafting the work: JP and SK. Revising the work: HK and MC. Providing approval for publication of the content: H-CK and HK. All authors contributed to the article and approved the submitted version.

Funding

This study analyzed data that were obtained during "A Study Investigating the Anti-epileptic Efficacy of Afinitor (Everolimus) in Patients with Refractory Seizures Who Have Focal Cortical Dysplasia Type II (FCD II) (NCT03198949)" funded by Novartis. This work was supported by a grant (No. 2023R1A2C1004568) from the National Research Foundation (NRF) of Korea, funded by the Korean government (Ministry of Science, ICT & Future Planning).

Conflict of interest

The authors declare that the research was conducted in the absence of any commercial or financial relationships that could be construed as a potential conflict of interest.

Publisher's note

All claims expressed in this article are solely those of the authors and do not necessarily represent those of their affiliated organizations, or those of the publisher, the editors, and the reviewers. Any product that may be evaluated in this article, or claim that may be made by its manufacturer, is not guaranteed or endorsed by the publisher.

Supplementary material

The Supplementary Material for this article can be found online at: https://www.frontiersin.org/articles/10.3389/fphar.2023.1197549/full#supplementary-material

References

Andre, F., Robbers-Visser, D., Helling-Bakki, A., Foll, A., Voss, A., Katus, H. A., et al. (2016). Quantification of myocardial deformation in children by cardiovascular magnetic resonance feature tracking: determination of reference values for left ventricular strain and strain rate. *J. Cardiovasc Magn. Reson* 19, 8. doi:10.1186/s12968-016-0310-x

Atsuko Tanaka, I. Y., Shinsako, K., Sato, E., Fukudo, M., Fukudo, M., Masuda, S., et al. (2016). Population pharmacokinetics of everolimus in relation to clinical outcomes in patients with advanced renal cell carcinoma. *Ther. Drug Monit.* 38, 663–669. doi:10.1097/FTD.0000000000000344

Baybis, M., Yu, J., Lee, A., Golden, J. A., Weiner, H., McKhann, G., 2nd, et al. (2004). mTOR cascade activation distinguishes tubers from focal cortical dysplasia. *Ann. neurology* 56, 478–487. doi:10.1002/ana.20211

Blümcke, I., Thom, M., Aronica, E., Armstrong, D. D., Vinters, H. V., Palmini, A., et al. (2011). The clinicopathologic spectrum of focal cortical dysplasias: a consensus classification proposed by an *ad hoc* Task Force of the ILAE Diagnostic Methods Commission. *Epilepsia* 52, 158–174. doi:10.1111/j.1528-1167.2010.02777.x

CDER (2009). *Clinical pharmacology and biopharmaceutics review*.

Combes, F. P., Baneyx, G., Coello, N., Zhu, P., Sallas, W., Yin, H., et al. (2018). Population pharmacokinetics-pharmacodynamics of oral everolimus in patients with seizures associated with tuberous sclerosis complex. *J. Pharmacokinet. Pharmacodyn.* 45, 707–719. doi:10.1007/s10928-018-9600-2

de Wit, D., Schneider, T. C., Moes, D. J., Roozen, C. F., den Hartigh, J., Gelderblom, H., et al. (2016). Everolimus pharmacokinetics and its exposure-toxicity relationship in patients with thyroid cancer. *Cancer Chemother. Pharmacol.* 78, 63–71. doi:10.1007/s00280-016-3050-6

Dirk Jan, A. R., Moes, R. R. P., Hartigh, J. den, de Fijter, J. W., de Fijter, J. W., and Guchelaar, H. J. (2012). Population pharmacokinetics and pharmacogenetics of everolimus in renal transplant patients. *Clin. Pharmacokinet.* 51, 467–480. doi:10.2165/11599710-000000000-00000

Fouladi, M., Laningham, F., Wu, J., O'Shaughnessy, M. A., Molina, K., Broniscer, A., et al. (2007). Phase I study of everolimus in pediatric patients with refractory solid tumors. *J. Clin. Oncol.* 25, 4806–4812. doi:10.1200/JCO.2007.11.4017

Franz, D. N., Belousova, E., Sparagana, S., Bebin, E. M., Frost, M., Kuperman, R., et al. (2013). Efficacy and safety of everolimus for subependymal giant cell astrocytomas associated with tuberous sclerosis complex (EXIST-1): a multicentre, randomised, placebo-controlled phase 3 trial. *Lancet* 381, 125–132. doi:10.1016/s0140-6736(12)61134-9

French, J. A., Lawson, J. A., Yapici, Z., Ikeda, H., Polster, T., Nabbout, R., et al. (2016). Adjunctive everolimus therapy for treatment-resistant focal-onset seizures associated with tuberous sclerosis (EXIST-3): a phase 3, randomised, double-blind, placebo-controlled study. *Lancet* 388, 2153–2163. doi:10.1016/s0140-6736(16)31419-2

GabrieleKirchner, I. I. M.-W., Manns, M. P., and Manns, M. P. (2004). Clinical pharmacokinetics of everolimus. *Clin. Pharmacokinet.* 43, 83–95. doi:10.2165/00003088-200443020-00002

Itohara, K., Yano, I., Nakagawa, S., Sugimoto, M., Hirai, M., Yonezawa, A., et al. (2022). Population pharmacokinetics of everolimus in adult liver transplant patients: comparison to tacrolimus disposition and extrapolation to pediatrics. *Clin. Transl. Sci.* 15, 2652–2662. doi:10.1111/cts.13389

Kovarik, J. M., Hartmann, S., Figueiredo, J., Rordorf, C., Golor, G., Lison, A., et al. (2002). Effect of food on everolimus absorption: quantification in healthy subjects and a confirmatory screening in patients with renal transplants. *Pharmacotherapy* 22, 154–159. doi:10.1592/phco.22.3.154.33542

Leitner, D. F., Kanshin, E., Askenazi, M., Siu, Y., Friedman, D., Devore, S., et al. (2022). Pilot study evaluating everolimus molecular mechanisms in tuberous sclerosis complex and focal cortical dysplasia. *PLoS One* 17, e0268597. doi:10.1371/journal.pone.0268597

Lim, J. S., Gopalappa, R., Kim, S. H., Ramakrishna, S., Lee, M., Kim, W. I., et al. (2017). Somatic mutations in TSC1 and TSC2 cause focal cortical dysplasia. *Am. J. Hum. Genet.* 100, 454–472. doi:10.1016/j.ajhg.2017.01.030

Lim, J. S., Kim, W. I., Kang, H. C., Kim, S. H., Park, A. H., Park, E. K., et al. (2015). Brain somatic mutations in MTOR cause focal cortical dysplasia type II leading to intractable epilepsy. *Nat. Med.* 21, 395–400. doi:10.1038/nm.3824

Ljungberg, M. C., Bhattacharjee, M. B., Lu, Y., Armstrong, D. L., Yoshor, D., Swann, J. W., et al. (2006). Activation of mammalian target of rapamycin in cytomegalic neurons of human cortical dysplasia. *Ann. neurology* 60, 420–429. doi:10.1002/ana.20949

Miyata, H., Chiang, A. C., and Vinters, H. V. (2004). Insulin signaling pathways in cortical dysplasia and TSC-tubers: tissue microarray analysis. *Ann. neurology* 56, 510–519. doi:10.1002/ana.20234

Sánchez-Fructuoso, A. I. (2008). Everolimus: an update on the mechanism of action, pharmacokinetics and recent clinical trials. *Expert Opin. drug metabolism Toxicol.* 4, 807–819. doi:10.1517/17425255.4.6.807

Sanjay, M., Sisodiya, S. F., Cross, J. H., and Thom, M. (2009). Focal cortical dysplasia type II: biological features and clinical perspectives. *Lancet Neurol.* 8, 830–843. doi:10.1016/S1474-4422(09)70201-7

Ter Heine, R., van Erp, N. P., Guchelaar, H. J., de Fijter, J. W., Reinders, M. E. J., van Herpen, C. M., et al. (2018). A pharmacological rationale for improved everolimus dosing in oncology and transplant patients. *Br. J. Clin. Pharmacol.* 84, 1575–1586. doi:10.1111/bcp.13591

frontiers | Frontiers in Pharmacology

TYPE Original Research
PUBLISHED 28 November 2023
DOI 10.3389/fphar.2023.1289336

OPEN ACCESS

EDITED BY
Mahmoud Rafieian-Kopaei,
Shahrekord University of Medical Sciences, Iran

REVIEWED BY
Hossein Amini-khoei,
Shahrekord University of Medical Sciences, Iran
Fatemeh Hoseinpour,
Razi University, Iran

*CORRESPONDENCE
Daniella Bastos de Araújo,
danivivaf@gmail.com
Moisés Hamoy,
hamoyufpa@gmail.com

RECEIVED 05 September 2023
ACCEPTED 30 October 2023
PUBLISHED 28 November 2023

CITATION
Bastos de Araújo D, Gurgel do Amaral AL, Maia da Fonseca S, Rodrigues de Souza K, Santos da Paz AP, Jóia de Mello V, Barbosa GB, Otake Hamoy MK and Hamoy M (2023), Lippia origanoides essential oil possesses anticonvulsant effect in pentylenetetrazol-induced seizures in rats: a behavioral, electroencephalographic, and electromyographic study. *Front. Pharmacol.* 14:1289336. doi: 10.3389/fphar.2023.1289336

Lippia origanoides essential oil possesses anticonvulsant effect in pentylenetetrazol-induced seizures in rats: a behavioral, electroencephalographic, and electromyographic study

Daniella Bastos de Araújo*, Anthony Lucas Gurgel do Amaral, Suzane Maia da Fonseca, Keyla Rodrigues de Souza, Allane Patrícia Santos da Paz, Vanessa Jóia de Mello, Gabriela Brito Barbosa, Maria Klara Otake Hamoy and Moisés Hamoy*

Laboratory of Pharmacology and Toxicology of Natural Products, Institute of Biological Science, Federal University of Pará, Belém, Brazil

Epilepsy is a neuronal disorder characterized by abnormal excitability of the brain, leading to seizures. Only around 66% of the epileptic patients respond adequately to treatment with existing conventional anticonvulsants, making it necessary to investigate new antiepileptic drugs. The growing research into natural products and their pharmacological properties has become increasingly promising, particularly in the study of essential oils, which are already widely used in popular culture for treating various diseases. The present study evaluated the anticonvulsant effects of Lippia origanoides essential oil (LOEO) (100 mg/kg i. p.) compared to diazepam (DZP) (5 mg/kg i. p.), and the combined administration of these two substances to control convulsions induced by pentylenetetrazol (PTZ) (60 mg/kg i. p.). This evaluation was carried out using 108 male Wistar rats, which were divided into two experiments. Experiment 1–Behavioral assessment: The animals were divided into 4 groups (n = 9): (I) saline solution + PTZ, (II) DZP + PTZ, (III) LOEO + PTZ, (IV) LOEO + DZP + PTZ. The convulsive behavior was induced 30 min after the administration of the tested anticonvulsant drugs, and the observation period lasted 30 min. Experiment 2- Electrocorticographic evaluation: The animals were divided into 8 groups (n = 9): (I) saline solution; (II) LOEO; (III) DZP; (IV) LOEO + DZP; (V) saline + PTZ, (VI) DZP + PTZ (VII) LOEO + PTZ, (VIII) LOEO + DZP + PTZ. PTZ was administered 30 min after LOEO and DZP treatments and electrocorticographic activity was assessed for 15 min. For the control groups, electromyographic recordings were performed in the 10th intercostal space to assess respiratory rate. The results demonstrated that Lippia origanoides essential oil increased the latency time for the appearance of isolated clonic seizures without loss of the postural reflex. The animals had a more intense decrease in respiratory rate when combined with LOEO + DZP. EEG recordings showed a reduction in firing amplitude in the LOEO-treated groups. The combining treatment with diazepam resulted in increased anticonvulsant

effects. Therefore, treatment with Lippia origanoides essential oil was effective in controlling seizures, and its combination with diazepam may represent a future option for the treatment of difficult-to-control seizures.

KEYWORDS

seizures, pentylenetetrazol, electrocorticographic recordings, essential oil, Lippia origanoides

1 Introduction

Epilepsy is a neurological disorder that affects around 45.9 million people globally and is characterized by a predisposition to suffer spontaneous seizures (Fisher et al., 2014). Its pathophysiology consists of the appearance of abnormal foci of cerebral electrical activity caused by the imbalance between excitatory and inhibitory neurotransmitters in the central nervous system, in such a way as to make it prone to functioning in an excessive oscillatory pattern. Conventional antiepileptic drugs act through these two pathways, either by enhancing inhibitory neurotransmitters or reducing excitatory signaling (Fisher et al., 2005; Sultana et al., 2021).

Currently available drug therapies are effective in only 66% of cases in developed countries (Duncan et al., 2006; Brodie et al., 2012) and are associated with various side effects (Perucca and Gilliam, 2012), highlighting the need for research to identify alternative treatments that target seizure mechanisms and have minimal side effects (Sultana et al., 2021).

One promising option is the use of essential oils (EOs) in the treatment of epilepsy. Essential oils are volatile substances extracted from plant parts, made up of a mixture of various components with therapeutic properties, widely used in popular culture to treat various ailments (de Almeida et al., 2011; Dobetsberger and Buchbauer, 2011). Recent studies have shown that several essential oils from aromatic plants have potential neuroprotective effects in age-related neurodegenerative diseases such as Alzheimer's and dementia and other neurological diseases such as anxiety, depression, epilepsy and seizures (Ayaz et al., 2017; Rashed et al., 2021; Sattayakhom et al., 2023).

Behavioral assessment and electrocorticography are of paramount importance in evaluating and comparing the changes caused by neuronal discharge that trigger seizures and epilepsy. In recent studies using natural products with potential anticonvulsant activities, data have shown that in the behavioral assessment, there were increases in seizure latencies and in the seizure threshold, confirmed by electrocorticographic records, along with a decrease in the peak and energy of the waves (Souza-Monteiro et al., 2015; Hamoy et al., 2018; Nascimento et al., 2022; Muto et al., 2022).

Lippia origanoides is a shrub with a strong aroma found mainly in the Amazon territory (Pascual et al., 2001; Oliveira et al., 2014) with medicinal properties well-known in popular culture (Siqueira-Lima et al., 2019). In Central America and Colombia, it is used to treat respiratory diseases, gastrointestinal discomfort such as gastralgia, nausea and antiseptic. In the countryside of Pará, in Brazil, Lippia origanoides, known as "salva-do-marajó," is commonly administered to combat intestinal colic, indigestion, diarrhea, burns, vaginal discharge, menstrual cramps, and fever (Oliveira et al., 2014). It is also notable for its use in food preparation, and in Venezuela, it is employed as an appetite stimulant (Morton, 1981).

Regarding the anticonvulsant properties of LOEO (Lippia origanoides essential oil), no studies have been found directly linking this plant to such effects. However, there are articles that suggest anticonvulsant effects of Lippia alba due to the high presence of flavonoids in its composition (Zétola et al., 2002; Neto et al., 2009; Siqueira-Lima et al., 2019), as well as L. Citriodora (Rashidian et al., 2016).

In this context, the objective of the present work was to evaluate the treatment with essential oil of *L. origanoides* in the control of seizures triggered by pentylenetetrazol and compare its effects with those of diazepam, through behavioral analysis, electrocorticography and assessment of respiratory movements (electromyogram).

2 Materials and methods

2.1 Animals

For the execution of this research, 108 adult Wistar rats were obtained from the Central Bioterium of the Federal University of Pará. All animals were housed under controlled conditions, with a temperature of approximately 23°C–25°C and a light-dark cycle of 12/12 h, receiving filtered water and rat food on free demand. The work was performed at the Laboratory of Pharmacology and Toxicology of Natural Products (Laboratório de Farmacologia e Toxicologia de Produtos Naturais)—ICB—UFPA. The project was approved by the Animal Ethics Committee (CEUA—UFPA) number 1395260821.

2.2 Drugs used

Lippia origanoides essential oil (LOEO) was purchased from Olinda pharmaceutical company (essential oils) and administered intraperitoneally at a dose of 100 mg/kg, while Diazepam (DZP) 10 mg/2 mL (União Química, Embu-Guaçu, SP, Brazil), was administered at a dose of 5 mg/kg intraperitoneally (i.p). Ketamine hydrochloride (50 mg/kg i. p.) was purchased from Köing Laboratory (Santana de Parnaíba, SP, Brazil), xylazine hydrochloride (5 mg/kg i. p) was purchased from Vallée Laboratory (Montes Claros, MG, Brazil), while the local anesthetic lidocaine was obtained from Hipolabor Laboratory (Sabará, MG, Brazil). Pentylenetetrazol (PTZ) was obtained from Sigma Chemical Co. (St. Louis, MO, United States) and administered intraperitoneally at a dose of 60 mg/kg (Santos et al., 2021; Muto et al., 2022).

2.3 Test to obtain the dose of LOEO used

To obtain the dose used of Lipia Origanoides extract (LOEO), a fixed time of 30 min was considered to achieve muscle relaxation

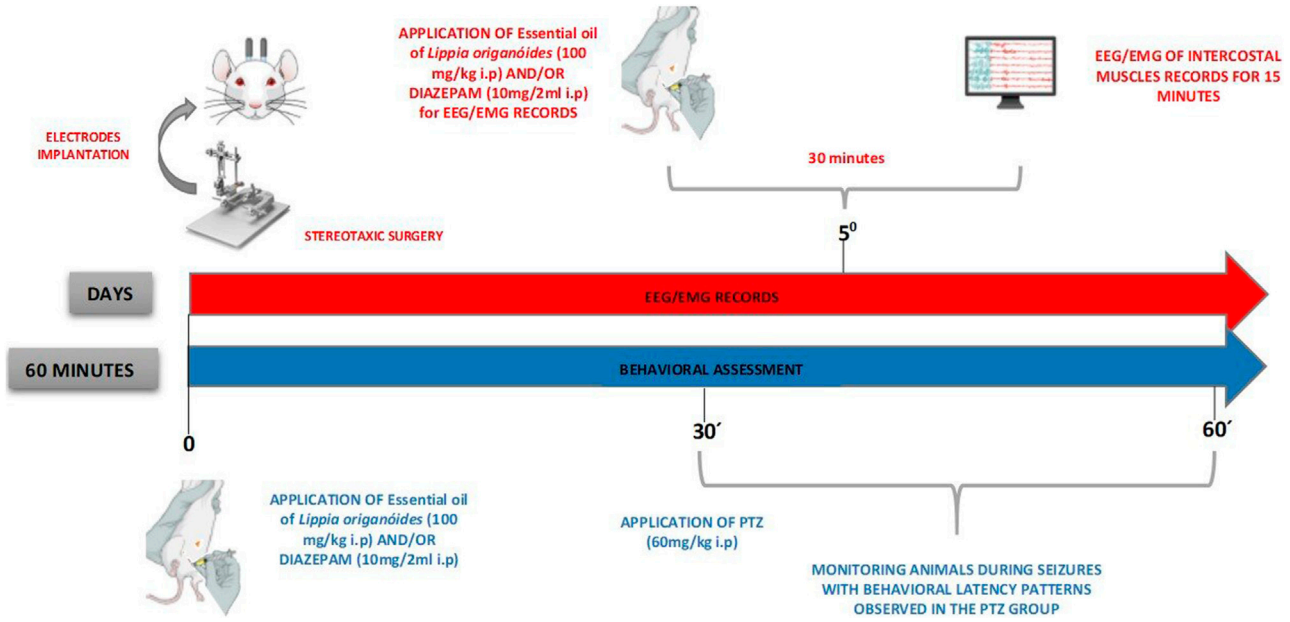

FIGURE 1
Experimental design. PTZ, pentylenetetrazol; EEG, electroencephalograph; EMG, electromyogram.

and animal sedation behavior at tested doses of 50 mg/kg, 100 mg/kg, 150 mg/kg, and 200 mg/kg i. p. the best response obtained was 100 mg/kg i. p. as higher doses caused myorelaxation with manifestation of respiratory depression. Therefore, a dose of 100 mg/kg i. p. was used 30 min before the onset of the seizure using PTZ (60 mg/kg).

2.4 Experimental design

The animals were kept at the research center for at least 7 days before the experiment for adaptation and acclimatization. The electrodes were implanted in the cortex 5 days before the application of the treatments. For the behavioral assessment the animals were divided into 4 groups (n = 9): (I) saline + PTZ, (II) DZP + PTZ, (III) LOEO + PTZ, (IV) LOEO + DZP + PTZ. The convulsant drug PTZ was administered 30 min after administration of the drugs tested as anticonvulsants and the observation time for behavior analysis was 30 min (Figure 1).

For electrocorticographic evaluation, animals were divided into 8 groups (n = 9): (I) saline; (II) LOEO; (III) DZP; (IV) LOEO + DZP; (V) saline + PTZ, (VI) DZP + PTZ (VII) LOEO + PTZ, (VIII) LOEO + DZP + PTZ. PTZ was administered 30 min after treatments and electrocorticographic activity was assessed for 15 min (Figure 1).

2.5 Evaluation of respiratory activity during sedation

For the analysis of respiratory frequency and muscle contraction power (Santos et al., 2021), electrodes were conjugated 2 mm apart and were prepared with a length of 2 mm and a diameter of 0.2 mm. These electrodes were inserted into the 10th intercostal space to record muscle activity. The recordings were conducted for a duration of 5 min for the Control, LOEO, DZP, and LOEO/DZP groups.

2.6 Description of seizure related behavior

The animals' behavior was monitored during the seizures and compared with latency patterns of behaviors observed in the PTZ-induced group (de Almeida. et al., 2020). Latency was measured concerning the initiation of the following behaviors: (I) whisker piloerection, (II) orofacial movements, (III) generalized tremor, (IV) anterior limb spasms, (V) isolated clonic seizures without loss of postural reflex, (VI) generalized clonic seizures with transient loss of postural reflex, and (VII) tonic-clonic seizures with complete loss of postural reflex.

2.7 Electrocorticographic recordings and data analysis

The animals were anesthetized and placed in a stereotaxic apparatus for the implantation of electrodes (with an exposed tip diameter of 1.0 mm) onto the dura mater above the prefrontal cortex at the coordinates of bregma–0.96 mm and ±1.0 mm lateral. The electrodes were secured using dental acrylic cement. Data were recorded using the electrodes with the assistance of a digital data acquisition system composed of a high-impedance amplifier (Grass Technologies, P511, United States), set with a filtering range of 0.3 Hz to 0.3 KHz. The data were monitored using an oscilloscope (Protek, Model 6510) and continuously digitized at a rate of 1 KHz by a computer equipped with a data acquisition board (National Instruments, Austin, TX).

During the recording sessions, the animals were confined within acrylic boxes (20 cm × 45 cm × 15 cm), and ECoG activity was recorded for 15 min immediately after the application of PTZ or physiological solution. The data collected through the digital data acquisition system were analyzed offline. The analyses were performed in frequencies up to 40 Hz and then divided into five bands: delta (1–4 Hz), theta (4–8 Hz), alpha (8–12 Hz), beta (12 Hz–28 Hz), and gamma (28 Hz–40 Hz) [30].

The characterization of the aspects of neuronal hyperexcitability in seizures caused by PTZ, as well as the reversal of the condition by the control drugs, were performed using the Signal ® 3.0 and Pyton 5.0 programs, which allowed the analysis of the frequency domain of brain waves, in addition to the visual inspection of wave patterns.

2.8 Chromatographic analysis of Lippia origanoides essential oil

Gas Chromatography-Mass Spectrometry (GC-MS) analysis, with Agilent Model MSD 5977B apparatus, was carried out by the company Olinda (essential oils) to certify the chromatographic analysis of *Lippia origanoides*. The analysis was performed on a batch with manufacturing date of February 2022, labeled as lot: 180002.

Organoleptic Properties: The essential oil appeared as a liquid with a golden-yellow color, free of impurities. It exhibited a pungent, fresh, and herbal scent, and had a density of 0.935 at 20°C. It originated from Brazil and was obtained through steam distillation.

The components were identified based on the Chemical Abstracts Service (CAS) registry number, which assigns a unique number to each chemical compound described in literature. The major components identified were Thymol (57.46%) and Carvacrol (1.42%).

2.9 Statistical analysis

The results were subjected to descriptive statistics, including mean and standard deviation. One-way Analysis of Variance (ANOVA) was employed, followed by Tukey's *post hoc* test. A significance level of $^{*}p < 0.05$, $^{**}p < 0.001$, and $^{***}p < 0.0001$ was adopted. The analyses were performed using GraphPad Prism, version 9 (GraphPad Software Inc., San Diego, CA, United States).

3 Results

3.1 Respiratory evaluation after administration of isolated and associated drugs

There was a reduction in respiratory rate when compared to the control group (60.22 ± 2.906/minute), LOEO group (52.44 ± 2.78/minute), DZP group (52.89 ± 3.480/minute) and LOEO/DZP group (45.33 ± 3.162/minute). The LOEO and DZP groups did not show a significant difference ($p = 0.990$), however, there was a decrease in respiratory frequency for the LOEO/DZP combination (Figures 2A–E).

To evaluate the muscle contraction power of the 10th intercostal muscle during treatment, it was observed that the control group had a mean power (3.215 ± 0.196 $mV^2/Hz \times 10–1$) and presented greater power compared to the other groups: LOEO group (2.254 ± 0.3382 $mV^2/Hz \times 10–1$), DZP group (2.523 ± 0.2479 $mV^2/Hz \times 10–1$) and LOEO/DZP group (1.976 ± 0.1767 $mV^2/Hz \times 10–1$). The LOEO and DZP groups did not show a significant difference ($p = 0.1181$). The LOEO and LOEO/DZP groups were also similar ($p = 0.1023$). The muscle contraction power of the DZP group was greater than that of the LOEO/DZP group (Figure 2F).

3.2 Behavioral assessment

The behavioral assessment of the animals was conducted to determine the progression of seizures (Table 1). Animals treated with PTZ rapidly progressed to tonic-clonic seizures with loss of postural reflex.

The group treated with DZP + PTZ exhibited the longest latency to the onset of convulsive seizures compared to the LOEO + PTZ group. However, when compared to the LOEO/DZP + PTZ combination, it showed significantly shorter latency. In the LOEO + PTZ group, animals did not progress to generalized clonic seizures. In the LOEO/DZP + PTZ group, animals only displayed whisker piloerection and generalized tremor, indicating greater stabilization of convulsive symptoms compared to DZP + PTZ. These results suggest that LOEO, when combined with DZP, can provide effective control of convulsive seizures by potentiating its effects.

3.3 Electrocorticographic evaluation

The animals in group I (physiological saline) exhibited amplitudes below 0.1 mV in the trace, and it can be observed in the corresponding spectrogram that the highest energy concentrations are below 10 Hz (Figure 3A). Group II (LOEO) showed little variation compared to the control group, although the spectrogram displayed greater intensity in oscillations up to 40 Hz (Figure 3B). Group III (DZP) displayed oscillations with amplitudes below 0.5 mV in the trace, with energy concentration below 10 Hz (Figure 3C). These groups did not maintain statistical differences and showed trace characteristics similar to the control group. In contrast, group IV (LOEO/DZP) (Figure 3D) displayed oscillations with amplitudes below 0.5 mV in the trace, and energy concentration below 15 Hz. On the other hand, group V (PTZ) exhibited significant alterations in the EEG trace, with peak amplitudes exceeding 0.5 mV, and activities characterized by constant levels of high-frequency and high-amplitude wave peaks (Figure 3E).

For group VI (LOEO + PTZ), the electrocorticographic trace did not show variations above 0.5 mV in amplitude, indicating seizure control. The spectrogram demonstrated an increase in power below 20 Hz (Figure 3F). For group VII (DZP + PTZ), the electrocorticographic trace did not show variations above 0.1 mV

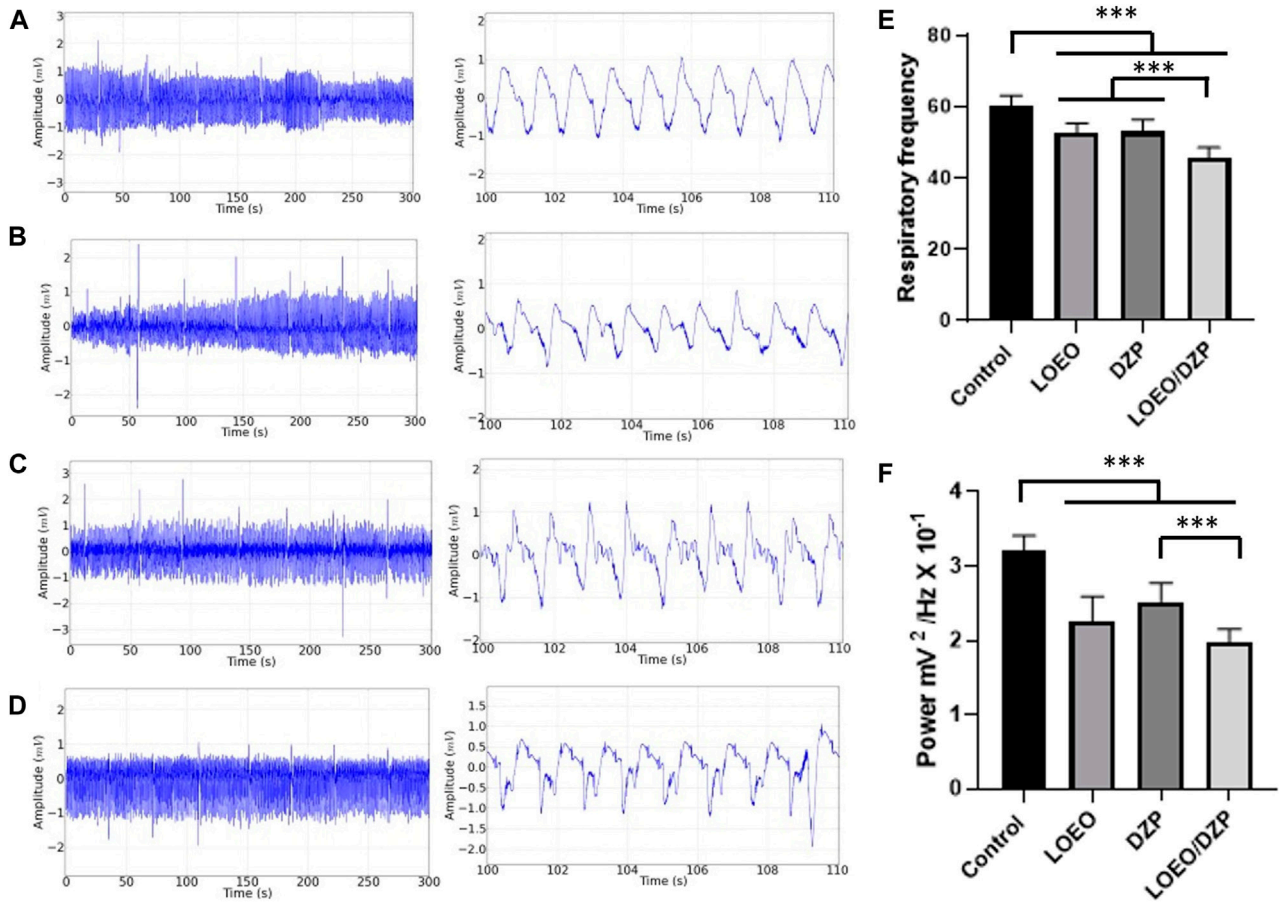

FIGURE 2
Demonstrations of electromyographic recordings performed in the 10th intercostal muscle of the rat. Control group **(A)**; Lippia origanoide group (LOEO) **(B)**; Diazepam group (DZP) **(C)**; LOEO/DZP group **(D)**; Graph showing the mean respiratory frequency for the groups during treatment **(E)**; Graph depicting the mean power of intercostal muscle contractions in animals subjected to treatment **(F)**. Recordings had a duration of 5 min. After ANOVA and Tukey's test, (***) $p < 0.0001$.

TABLE 1 Behavioral Characterization for Latencies of Excitability Behaviors Induced by PTZ (control group), Diazepam followed by PTZ application, and LOEO followed by PTZ application. (*) indicates statistical difference for the PTZ group, (#) represents statistical difference for the DZP + PTZ group, and (+) represents statistical difference for the LOEO group. After ANOVA followed by Tukey's test, a significance level of *$p < 0.05$, **$p < 0.001$, and ***$p < 0.0001$ was adopted.

Comportamento/ Latência (S)	Whisker piloerection	Orofaciais movements	Generalized tremor	Anterior limb espasms	Isolated clonic seizure without loss of postural reflex	Generalizes clonic seizure with transiente loss of postural reflex	Tonic-clonic seizure with loss of postural reflex
PTZ	59.0 ± 5.809	74.11 ± 8.738	84.67 ± 6.164	96.33 ± 4.637	113.1 ± 8.860	161.1 ± 22.74	207.43 ± 16.32
DZP + PTZ	131.6 ± 19.17***	180.9 ± 10.88***	242.6 ± 25.49***	304.2 ± 40.17***	—	—	—
LOEO + PTZ	117.7 ± 7.14***	153.0 ± 12.96***/###	193.4 ± 12.07***/###	280.3 ± 10.65***	338.7 ± 34.7***	—	—
LOEO/DZP + PTZ	172.0 ± 16.47***/ ###/+++	—	296.3 ± 21.17***/###/+++	—	—	—	—
F-value and *p*-value	F (3,34) = 108.9 $p < 0.0001$	F (2,24) = 228.3 $p < 0.0001$	F (2,24) = 228.2 $p < 0.0001$	F (2,24) = 199.8 $p < 0.0001$	—	—	—

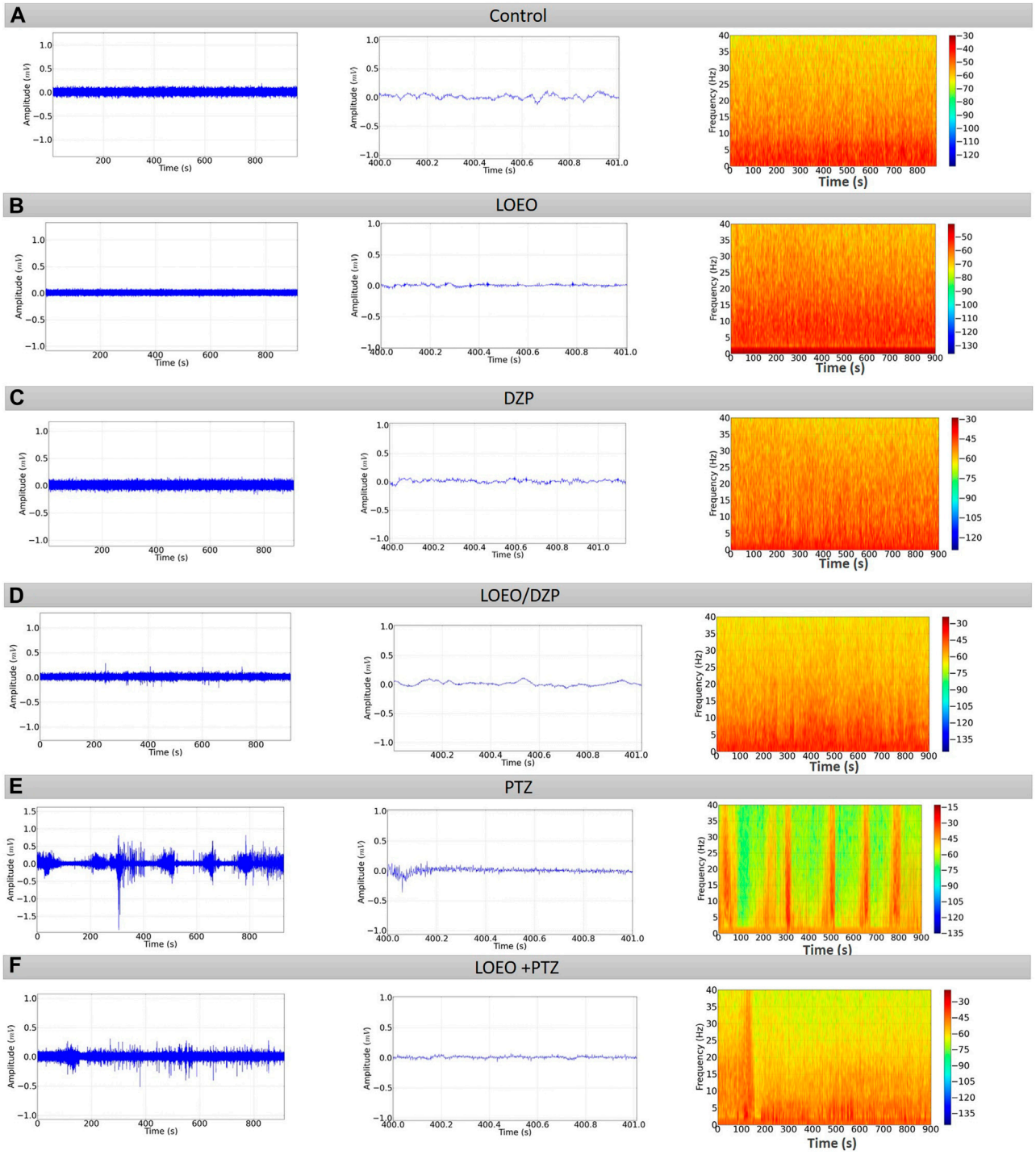

FIGURE 3
(Continued)

in amplitude, indicating seizure control. However, the spectrogram displayed an increase in power below 20 Hz (Figure 3G).

In group VIII, (LOEO/DZP + PTZ), the electrocorticographic trace did not show variations above 0.1 mV in amplitude, possibly indicating potentiation of the effect of DZP when combined with LOEO. The spectrogram displayed an increase in power below 15 Hz (Figure 3H).

Total power varied significantly between groups: group I 0.6268 ± 0.1064 $mV^2/Hz \times 10^{-3}$ and group II 0.1946 ± 0.06929 $mV^2/Hz \times 10^{-3}$ ($p = 0.0012$), group VI 0.9680 ± 0.1696 $mV^2/Hz \times 10^{-3}$ ($p = 0.0211$). However, groups III 0.5868 ± 0.06176 $mV^2/Hz \times 10^{-3}$ ($p > 0.9999$), group IV 0.6718 ± 0.1204 $mV^2/Hz \times 10^{-3}$ ($p = 0.9998$), group VII 0.7690 ± 0.1624 $mV^2/$

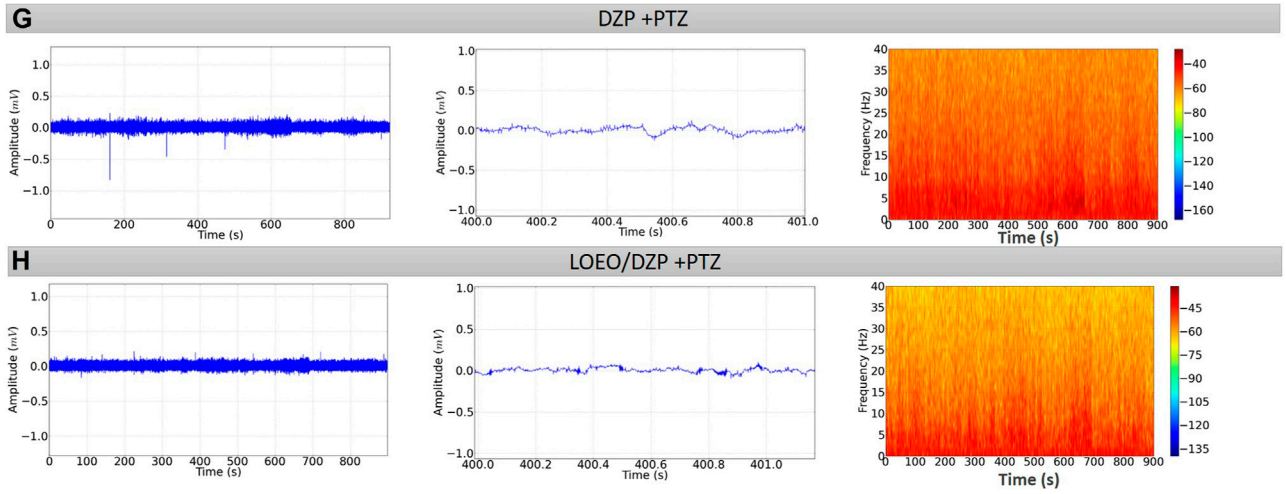

FIGURE 3
(Continued). Electrocorticography (ECoG) recording, representative 1s fragment (400–401 s) of the ECoG recording (center) and frequency spectrogram (right). Control group **(A)**; Lippia origanoides group (LOEO) **(B)**; Diazepam (DZP) **(C)**; LOEO + DZP group (LOEO + DZP) **(D)**; Pentylenetetrazol (PTZ) **(E)**, LOEO + PTZ **(F)**; DZP + PTZ **(G)** and LOEO/DZP + PTZ **(H)**.

Hz × 10^{-3} (p = 0.8363), and group VIII 0.4031 ± 0.09328 $mV^2/Hz \times 10^{-3}$ (p = 0.3313) no showed a difference to the saline control group. The administration of PTZ 2.215 ± 0.5042 $mV^2/Hz \times 10^{-3}$ (group V) resulted in a significant increase in power and presented a statistical difference in relation to all groups [F (7,64) = 77.25; p < 0.001] (Figure 4A).

Significant variation was found between groups II and VI (LOEO and LOEO + PTZ), groups II and VII (LOEO/DZP + PTZ), and between group VI and VIII (LOEO + PTZ and LOEO/DZP + PTZ).

For delta oscillations, the control group presented an average power of 0.1609 ± 0.02492 $mV^2/Hz \times 10^{-3}$, showing significant variation between the following groups: group II with 0.02884 ± 0.004213 $mV^2/Hz \times 10^{-3}$ (p = 0.0276) and group VII with 0.2948 ± 0.03959 $mV^2/Hz \times 10^{-3}$ (p = 0.0241). However, it was similar to groups III with 0.1624 ± 0.01824 $mV^2/Hz \times 10^{-3}$ (p > 0.9999), group IV with 0.1487 ± 0.03489 $mV^2/Hz \times 10^{-3}$ (p > 0.999) and group VIII with 0.1313 ± 0.03135 $mV^2/Hz \times 10^{-3}$ (p = 0.9949). However, significant differences were observed between groups V with 0.7095 ± 0.2105 $mV^2/Hz \times 10^{-3}$ and VI with 0.4827 ± 0.08197 $mV^2/Hz \times 10^{-3}$, for the other groups (Figure 4B).

For theta oscillations, group I presented an average power of 0.1626 ± 0.01493 $mV^2/Hz \times 10^{-3}$ and showed no statistical difference with group III 0.1272 ± 0.01868 $mV^2/Hz \times 10^{-3}$ (p = 0.3057), group IV 0.1275 ± 0.02840 $mV^2/Hz \times 10^{-3}$ (p = 0.3139) and group VI 0.2043 ± 0.03789 $mV^2/Hz \times 10^{-3}$ (p = 0,1322). Significant statistical differences were observed between groups II 0.1626 ± 0.01493 $mV^2/Hz \times 10^{-3}$, V 0.5975 ± 0.06429 $mV^2/Hz \times 10^{-3}$ and VII 0.2595 ± 0.03483 $mV^2/Hz \times 10^{-3}$ and group VIII 0.1142 ± 0.01620 $mV^2/Hz \times 10^{-3}$ (p = 0.0470) (Figure 4C).

For alpha oscillations, group I presented an average linear power of 0.07834 ± 0.01241 $mV^2/Hz \times 10^{-3}$ and showed no statistical difference with group III (0.06866 ± 0.01372 $mV^2/Hz \times 10^{-3}$, p = 0.9226), group VI (0.05895 ± 0.008050 $mV^2/Hz \times 10^{-3}$, p = 0.2384) and group VII (0.08349 ± 0.01473 $mV^2/Hz \times 10^{-3}$, p = 0.9980). Significant statistical differences were observed between groups II (0.02046 ± 0.002646 $mV^2/Hz \times 10^{-3}$), group IV (0.03024 ± 0.008092 $mV^2/Hz \times 10^{-3}$) and group V (0.3096 ± 0.03782 $mV^2/Hz \times 10^{-3}$) and group VIII (0.05244 ± 0.003926 $mV^2/Hz \times 10^{-3}$). The PTZ group had a higher mean linear power in alpha oscillations (Figure 4D).

For beta oscillations, the control group exhibited an average linear power of 0.08061 ± 0.01036 $mV^2/Hz \times 10^{-3}$, with no statistical difference observed in comparison to group III (0.08187 ± 0.01351 $mV^2/Hz \times 10^{-3}$, p > 0.9999), group IV (0.02291 ± 0.007150 $mV^2/Hz \times 10^{-3}$, p = 0.6753), group VI (0.08120 ± 0.01311 $mV^2/Hz \times 10^{-3}$, p > 0.9999), group VII (0.1060 ± 0.01166 $mV^2/Hz \times 10^{-3}$, p = 0.9948), and group VIII (0.06128 ± 0.01399 $mV^2/Hz \times 10^{-3}$, p = 0.9991). Significant statistical difference was observed only in group V (0.5655 ± 0.1993 $mV^2/Hz \times 10^{-3}$) (Figure 4E).

For gamma oscillations, the control group exhibited an average linear power of 0.02402 ± 0.004807 $mV^2/Hz \times 10^{-3}$, with no statistical difference observed for group II (0.007608 ± 0.003549 $mV^2/Hz \times 10^{-3}$, p = 0.9667), group III (0.03010 ± 0.004594 $mV^2/Hz \times 10^{-3}$, p > 0.9999), group IV (0.009768 ± 0.002647 $mV^2/Hz \times 10^{-3}$, p = 0.9849), group VI (0.01174 ± 0.001755 $mV^2/Hz \times 10^{-3}$, p = 0.9938), group VII (0.01953 ± 0.003204 $mV^2/Hz \times 10^{-3}$, p > 0.9999), and group VIII (0.01391 ± 0.002762 $mV^2/Hz \times 10^{-3}$, p = 0.9982). Significant statistical difference was observed only in group V (0.2121 ± 0.09447 $mV^2/Hz \times 10^{-3}$) (Figure 4F).

4 Discussion

In this study, we have demonstrated, for the first time, that the essential oil of Lippia origanoides was able to increase the convulsive threshold induced by PTZ in rats. This was achieved through the analysis of behavior, electroencephalographic (EEG) and electromyographic patterns after the administration of LOEO alone, as well as the evaluation of the LOEO/DZP combination and its response compared to diazepam.

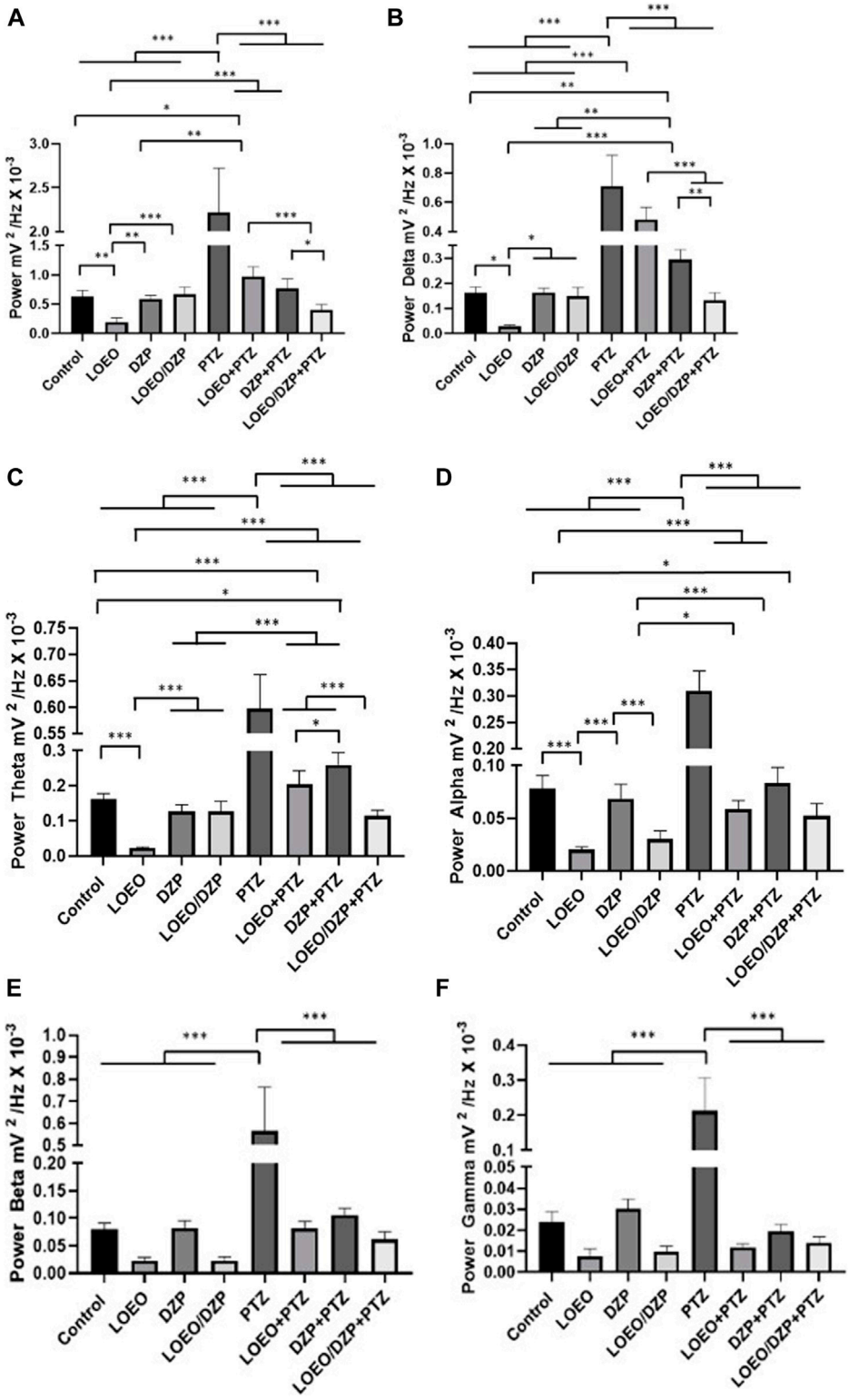

FIGURE 4
Total linear power analysis of brain waves up to 40 Hz **(A)** and quantitative linear frequency distribution of brain waves: **(B)** delta waves; **(C)** theta waves; **(D)** alpha waves; **(E)** beta waves and **(F)** gamma waves, recorded by electrocorticography. Data show drugs associated and not associated with pentylenetetrazole (*$p < 0.05$, **$p < 0.001$ and ***$p < 0.0001$).

The present study demonstrated significant differences in the respiratory frequency depression of the group treated with LOEO in combination with DZP compared to the other groups in relation to respiratory behavior patterns, as assessed through electromyography of the 10th intercostal muscle.

These respiratory depressant effects caused by the LOEO/DZP combination suggest various therapeutic targets. Some anesthetic medications are known respiratory depressants, such as propofol, sevoflurane, and midazolam, acting as GABA receptor agonists and NMDA receptor antagonists (Pattinson, 2008).

The depressant respiratory response shown in our results by the LOEO/DZP combination suggests the need for further investigations to elucidate the underlying mechanisms triggering the decrease in respiratory frequency after its combined administration.

In recent a study (Hamoy et al., 2018), behavioral and electrocorticographic assessments were extremely useful to evaluate and compare the changes arising from disordered neuronal excitability that generate seizures and consequent epileptic conditions. In this research, the electrocorticogram of rat cortex was examined and it was demonstrated that the administration of PTZ in rats presented continuous discharges and high amplitude waves, being this effect reversed by conventional anticonvulsants (phenobarbital, phenytoin and diazepam). Our results corroborate with the whole protocol of this study, using diazepam as conventional antiepileptic.

Thymol (2-isopropyl-5-methylphenol), the most abundant constituent (57.46%) in LOEO and several other essential oils, is an isomer of carvacrol (2-methyl-5-1 methylethylphenol), a monoterpene also present in LOEO (1.42%). Thymol can manifest as a white crystalline powder or colorless crystals and are constituents of the essential oils of several plants (Nunes et al., 2005; Guillen et al., 2007).

The effects of thymol that have been studied and described in the literature include its antimicrobial and antiseptic actions (Matos et al., 2000; Kachur and Suntres, 2020). Both carvacrol and thymol exhibit high antioxidant activity, serving as natural food preservatives that inhibit peroxidation of phospholipid liposomes and demonstrating antifungal activities (Milos et al., 2000; Teissedre and Waterhouse, 2000; Mastelic et al., 2008). Other natural monoterpenoids have a wide range of pharmacological properties, such as local anesthetic, anticancer, antihistaminic, anti-inflammatory, antiviral, and neuroprotective activities (Volcho et al., 2018).

In previous studies on the central action of carvacrol, its effects on experimental models of anxiety and depression in mice were demonstrated, suggesting involvement of the GABAergic system through the GABA-A receptor, similarly to benzodiazepines that have high affinity for these receptors. In evaluating the antidepressant effects of carvacrol, the mechanism of action was shown to be associated with the dopaminergic system, possibly through stimulation of D1 and D2 receptors (Melo et al., 2010; Melo et al., 2011). Other studies have also shown central nervous system actions of monoterpenes, exhibiting anxiolytic and antidepressant effects (Umezu and Morita, 2003; Silva et al., 2007).

In a study the authors suggested that the mechanism of action of the isomers carvacrol and thymol is related to the modulation of GABAergic ionotropic receptors with Cl^- channels, as the monoterpenes bound to GABA receptors increased the uptake of $^{36}Cl^-$ (Tong and Coats, 2010).

Analogues of carvone, such as carvacrol, were able to inhibit neuronal excitability in the sciatic nerve of rats, probably by blocking voltage-dependent sodium channels. The authors also observed that the structure of the compounds interfered with their ability to block channels. This capability of these compounds to alter their chemical structures can be effective in delivering drugs that act directly on their targets, without affecting other organisms (Gonçalves et al., 2010).

To evaluate the mechanisms by which carvacrol promoted the inhibition of neuronal excitability, the authors demonstrated through several tests that carvacrol is able to block neuronal excitability in a reversible and concentration-dependent manner through direct inhibition of voltage-dependent sodium channels, which suggests its effect as a local anesthetic (Joca et al., 2012).

Studies using oils and plant extracts have demonstrated the potentiation of GABAergic pathways in the control of convulsive crises triggered by pentylenetetrazole (de Oliveira et al., 2022; Muto et al., 2022; Nascimento et al., 2022). This effect is allosterically potentiated by benzodiazepines such as Diazepam, which favors the hyperpolarization of the neuronal membrane (Aburawi et al., 2021). LOEO demonstrated the ability to mitigate the intensity of PTZ-induced seizures, increasing the latency for the onset of behavior, as evidenced by ECoG. It was observed that the anticonvulsant activity of LOEO increased seizure control when associated with Diazepam, which demonstrated a potentiating effect on seizure control.

In summary, the outcomes of this study underscore the potential utility of LOEO in managing convulsive seizures, while its synergistic combination with DZP opens a promising pathway for the development of new agents targeting refractory epilepsy. Moreover, these findings contribute significantly to the deeper comprehension of the mechanisms underlying epilepsy.

5 Conclusion

The current study revealed that treatment with LOEO led to distinct alterations in electrocorticographic tracings, showcasing attributes of a potent anticonvulsant agent. Moreover, the combination of LOEO with diazepam yielded a more favorable response compared to any individual drug administration, resulting in increased convulsive threshold and respiratory depression. This finding holds significant implications, as the synergistic effect of Lippia origanoides essential oil with diazepam may represent a valuable therapeutic approach for the treatment of epilepsy, enhancing therapeutic efficacy while minimizing adverse effects.

Data availability statement

The original contributions presented in the study are included in the article/supplementary material, further inquiries can be directed to the corresponding authors.

Ethics statement

The animal study was approved by the Animal Ethics Committee (CEUA—UFPA) number 1395260821. The study was

conducted in accordance with the local legislation and institutional requirements.

Author contributions

Conceived and designed the experiments: D.B.d.A., M.H. Performed the experiments: D.B.d.A., A.L.G.d.A., G.B.B., M.K.O.H and M.H. Wrote the paper: all authors. Financial support and administrative support: M.H and V.J.d.M. All authors have read and agreed to the published version of the manuscript.

Funding

The author(s) declare financial support was received for the research, authorship, and/or publication of this article. This research was funded by Fundação Amazônia de Amparo a Estudos e Pesquisas do Estado do Pará (FAPESPA) and The APC was funded by Pró-Reitoria de Pesquisa e Pós-Graduação—PROPESP/UFPA.

Acknowledgments

The authors would like to acknowledge Fundação Amazônia de Amparo a Estudos e Pesquisas do Estado do Pará (FAPESPA) for their financial support provided of this research and Programa de Pós graduação em Farmacologia e Bioquímica (FARMABIO).

Conflict of interest

The authors declare that the research was conducted in the absence of any commercial or financial relationships that could be construed as a potential conflict of interest.

Publisher's note

References

Aburawi, S., Shushni, M., and Alkateb, M. (2021). Effect of Moringa Oleifera extract on the behavior of male albino rats. *AlQalam J. Med. Appl. Sci.* 4 (2), 1–12. doi:10.5281/zenodo.4667396

Ayaz, M., Sadiq, A., Junaid, M., Ullah, F., Subhan, F., and Ahmed, J. (2017). Neuroprotective and anti-aging potentials of essential oils from aromatic and medicinal plants. *Front. Aging Neurosci.* 9, 168. doi:10.3389/fnagi.2017.00168

Brodie, M. J., Barry, S. J., Bamagous, G. A., Norrie, J. D., and Kwan, P. (2012). Patterns of treatment response in newly diagnosed epilepsy. *Neurology* 78, 1548–1554. doi:10.1212/WNL.0b013e3182563b19

de Almeida, L. C. N., de Andrade Marques, B., Silva, R. L., Hamoy, A. O., de Mello, V. J., Borges, R. D. S., et al. (2020). New nanocarried phenobarbital formulation: maintains better control of pentylenetetrazole-Induced seizures. *Biotechnol. Rep. (Amst)* 9, e00539, e00539. doi:10.1016/j.btre.2020.e00539

de Almeida, R. N., Agra Mde, F., Maior, F. N., and de Sousa, D. P. (2011). Essential oils and their constituents: anticonvulsant activity. *Molecules* 16, 2726–2742. doi:10.3390/molecules16032726

de Oliveira, F. R., da Silva, N. M., Hamoy, M., Crespo-López, M. E., Ferreira, I. M., da Silva, E. O., et al. (2022). The GABAergic system and endocannabinoids in epilepsy and seizures: what can we expect from plant oils? *Molecules* 27 (11), 3595. doi:10.3390/molecules27113595

Dobetsberger, C., and Buchbauer, G. (2011). Actions of essential oils on the central nervous system: an updated review. *Flavour Fragr. J.* 26, 300–316. doi:10.1002/ffj.2045

Duncan, J. S., Sander, J. W., Sisodiya, S. M., and Walker, M. C. (2006). Adult epilepsy. *Lancet* 367, 1087–1100. doi:10.1016/S0140-6736(06)68477-8

Fisher, R. S., Acevedo, C., Arzimanoglou, A., Bogacz, A., Cross, J. H., Elger, C. E., et al. (2014). ILAE official report: a practical clinical definition of epilepsy. *Epilepsia* 55, 475–482. doi:10.1111/epi.12550

Fisher, R. S., Boas, W. V. E., Blume, W., Elger, C., Genton, P., Lee, P., et al. (2005). Epileptic seizures and epilepsy: definitions proposed by the international league against epilepsy (ILAE) and the international bureau for epilepsy (IBE). *Epilepsia* 46, 470–472. doi:10.1111/j.0013-9580.2005.66104.x

Gonçalves, J. C. R., Alves, A. M. H., Araújo, A. E. V., Cruz, J. S., and Araújo, D. A. M. (2010). Distinct effects of carvone analogues on the isolated nerve of rats. *Eur. J. Pharmacol.* 645, 108–112. doi:10.1016/j.ejphar.2010.07.027

Guillen, F. P. J., Zapata, D., Martinez-Romero, S., Castillo, M. S., and Valero, D. (2007). Improvement of the overall quality of table grapes stored under modified atmosphere packaging in combination with natural antimicrobial compounds. *J. Food Sci.* 72, 185–190. doi:10.1111/j.1750-3841.2007.00305.x

Hamoy, M., Batista, L. S., de Mello, V. J., Gomes-Leal, W., Farias, R. A. F., Batista, P. S., et al. (2018). Cunaniol-elicited seizures: behavior characterization and electroencephalographic analyses. *Toxicol. Appl. Pharmacol.* 360, 193–200. doi:10.1016/j.taap.2018.10.008

Joca, H. C., Cruz-Mendes, Y., Oliveira-Abreu, K., Maia-Joca, R. P. M., Barbosa, R., Lemos, T. L., et al. (2012). Carvacrol decreases neuronal excitability by inhibition of voltage-gated sodium channels. *J. Nat. Prod.* 75, 1511–1517. doi:10.1021/np300050g

Kachur, K., and Suntres, Z. (2020). The antibacterial properties of phenolic isomers, carvacrol and thymol. *Crit. Rev. Food Sci. Nutr.* 60, 3042–3053. doi:10.1080/10408398.2019.1675585

Mastelic, J., Jerković, I., Blazević, I., Poljak-Blazi, M., Borović, S., Ivancić-Baće, I., et al. (2008). Comparative study on the antioxidant and biological activities of carvacrol, thymol, and eugenol derivatives. *J. Agric. Food Chem.* 6, 3989–3996. doi:10.1021/jf073272v

Matos, F. J. A., Machado, M. I. L., Craveiro, A. A., Alencar, J. W., and Silva, M. G. V. (2000). Medicinal plants of Northeast Brazil containing thymol and carvacrol-*Lippia sidoides* Cham.and *L.gracilis* H.B.K (Verbenaceae). *J. Essent. Oil Res.* 11, 666–668. doi:10.1080/10412905.1999.9711990

Melo, F. H. C., Moura, B. A., Sousa, P. D., Vasconcelos, S. M. M., Macedo, D. S., Fonteles, M. M. F., et al. (2011). Antidepressant-like effect of Carvacrol (5-isopropyl-2-methylphenol) in mice: involvement of dopaminergic system. *Fundam. Clin. Pharmacol.* 25, 362–367. doi:10.1111/j.1472-8206.2010.00850.x

Melo, F. H. C., Venâncio, E. T., Sousa, D. P., Fonteles, M. M. F., Vasconcelos, S. M. M., Viana, G. S. B., et al. (2010). Anxiolytic-like effect of Carvacrol (5-isopropyl-2 methylphenol) in mice: involvement with GABAergic transmission. *Fundam. Clin. Pharmacol.* 24, 437–443. doi:10.1111/j.1472-8206.2009.00788.x

Milos, M., Mastelic, J., and Jerkovic, I. (2000). Chemical composition and antioxidante effect of glycosidically bound volatile compouds from orégano (*Origanum vulgare L. ssp hirtum*). *Food Chem.* 71, 79–83. doi:10.1016/S0308-8146(00)00144-8

Morton, J. F. (1981). *Atlas of medicinal plants of Middle America, Bahamas to yucatan*. Springfield (IL): C. Thomas.

Muto, N. A., Hamoy, M., da Silva Ferreira, C. B., Hamoy, A. O., Lucas, D. C. R., de Mello, V. J., et al. (2022). Extract of *Euterpe oleracea* martius stone presents anticonvulsive activity *via* the GABAA receptor. *Front. Cell Neurosci.* 11 (16), 872743. doi:10.3389/fncel.2022.872743

Nascimento, C. P., Ferreira, L. O., Silva, A. L. M., Silva, A. B. N., Rodrigues, J. C. M., Teixeira, L. L., et al. (2022). Combination of *curcuma longa* and diazepam attenuates seizures and subsequent hippocampal neurodegenaration. *Front. Cell. Neurosci.* 16, 884813. doi:10.3389/fncel.2022.884813

Neto, A. C., Netto, J. C., Pereira, P. S., Pereira, A. M. S., Taleb-Contini, S. H., França, S. C., et al. (2009). The role of polar phytocomplexes on anticonvulsant effects of leaf extracts of *Lippia alba* (Mill.) N.E. Brown chemotypes. *J. Pharm. Pharmacol.* 61, 933–939. doi:10.1211/jpp/61.07.0013

Nunes, R. S., Lira, A. M., Ximenes, E., Silva, J. A., and Santana, D. P. (2005). Characterization of the *Lippia sidoides* in vegetable raw material for pharmaceutical products. *Scentia Plena* 1, 182–184.

Oliveira, D. R., Leitão, G. G., Fernandes, P. D., and Leitão, S. G. (2014). Ethnopharmacological studies of Lippia origanoides. *Braz. J. Pharmacogn.* 24, 206–214. doi:10.1016/j.bjp.2014.03.001

Pascual, M. E., Slowing, K., Carretero, E., Sánchez Mata, D., and Villar, A. (2001). Lippia: traditional uses, chemistry and pharmacology: a review. *J. Ethnopharmacol.* 76, 201–214. doi:10.1016/s0378-8741(01)00234-3

Pattinson, K. T. S. (2008). Opioids and the control of respiration. *Br. J. Anaesth.* 100, 747–758. doi:10.1093/bja/aen094

Perucca, P., and Gilliam, F. G. (2012). Adverse effects of antiepileptic drugs. *Lancet Neurol.* 11, 792–802. doi:10.1016/S1474-4422(12)70153-9

Rashed, A. A., Rahman, A. Z. A., and Rathi, D. N. G. (2021). Essential oils as a potential neuroprotective remedy for age-related neurodegenerative diseases: a review. *Molecules* 19 (4), 1107. doi:10.3390/molecules26041107

Rashidian, A., Farhang, F., Vahedi, H., Dehpour, A. R., Mehr, S. E., Mehrzadi, S., et al. (2016). Anticonvulsant effects of *Lippia citriodora* (Verbenaceae) leaves ethanolic extract in mice: role of gabaergic system. *Int. J. Prev. Med.* 7, 97. doi:10.4103/2008-7802.187251

Santos, G. F. S., Ferreira, L. O., Gerrits Mattos, B., Fidelis, E. J., de Souza, A. S., Batista, P. S., et al. (2021). Electrocorticographic description of the effects of anticonvulsant drugs used to treat lidocaine-induced seizures. *Brain Behav.* 11 (2), e01940. doi:10.1002/brb3.1940

Sattayakhom, A., Wichit, S., and Koomhim, P. (2023). The effects of essential oils on the nervous system: a scoping review. *Molecules* 28 (9), 3771. doi:10.3390/molecules28093771

Silva, M. I. G., Neto, M. R. A., Neto, P. F. T., Moura, B. A., Amaral, J. F., Sousa, D. P., et al. (2007). Central nervous system activity of acute administration of isopulegol in mice. *Pharmacol. Biochem. Behav.* 88, 141–147. doi:10.1016/j.pbb.2007.07.015

Siqueira-Lima, P. S., Passos, F. R. S., Lucchese, A. M., Menezes, I. R. A., Coutinho, H. D. M., Lima, A. A. N., et al. (2019). Central nervous system and analgesic profiles of Lippia genus. *Braz. J. Pharmacogn.* 29, 125–135. doi:10.1016/j.bjp.2018.11.006

Souza-Monteiro, J. R., Hamoy, M., Santana-Coelho, D., Arrifano, G., Paraense, R. S. O., Costa-Malaquias, A., et al. (2015). Anticonvulsant properties of Euterpe oleracea in mice. *Neurochem. Int.* 90, 20–27. doi:10.1016/j.neuint.2015.06.014

Sultana, B., Panzini, M.-A., Veilleux Carpentier, A., Comtois, J., Rioux, B., Gore, G., et al. (2021). Incidence and prevalence of drug-resistant epilepsy: a systematic review and meta-analysis. *Neurology* 96, 805–817. doi:10.1212/WNL.0000000000011839

Teissedre, P. L., and Waterhouse, A. L. (2000). Inhibition of oxidation of human low-density lipoproteins by phenolic substances in different essential oils varieties. *J. Agric. Food Chem.* 48, 3801–3805. doi:10.1021/jf990921x

Tong, F., and Coats, J. R. (2010). Effects of monoterpenoid insecticides on [3H]-TBOB binding in house fly GABA receptor and 36Cl– uptake in American cockroach ventral nerve cord. *Biochem. Physiol.* 98, 317–324. doi:10.1016/j.pestbp.2010.07.003

Umezu, T., and Morita, M. (2003). Evidence for the involvement of dopamine in ambulation promoted by menthol in mice. *J. Pharmacol. Sci.* 91, 125–135. doi:10.1254/jphs.91.125

Volcho, K. P., Laev, S. S., Ashraf, G. M., Aliev, G., and Salakhutdinov, N. F. (2018). Application of monoterpenoids and their derivatives for treatment of neurodegenerative disorders. *Curr. Med. Chem.* 25, 5327–5346. doi:10.2174/0929867324666170112101837

Zétola, M., de Lima, T. C. M., Sonaglio, D., González-Ortega, D., Limberger, R. P., Petrovick, P. R., et al. (2002). CNS activities of liquid and spray-dried extracts from *Lippia alba* – verbenaceae (Brazilian false melissa). *J. Ethnopharmacol.* 82, 207–215. doi:10.1016/s0378-8741(02)00187-3

frontiers | Frontiers in Pharmacology

TYPE Original Research
PUBLISHED 21 December 2023
DOI 10.3389/fphar.2023.1239152

OPEN ACCESS

EDITED BY
Antonella Riva,
University of Genoa, Italy

REVIEWED BY
Dana Ekstein,
Hadassah Medical Center, Israel
Jagarlapudi M. Murthy,
Care Hospitals, India

*CORRESPONDENCE
Nicola Specchio,
nicola.specchio@opbg.net

RECEIVED 12 June 2023
ACCEPTED 06 December 2023
PUBLISHED 21 December 2023

CITATION
Pietrafusa N, Falcicchio G, Russo E, Lattanzi S, Goffredo B, Simeoli R, Cairoli S, Corsetti T, Roberti R, De Tommaso M, Vigevano F, La Neve A and Specchio N (2023), Cenobamate as add-on therapy for drug resistant epilepsies: effectiveness, drug to drug interactions and neuropsychological impact. What have we learned from real word evidence?
Front. Pharmacol. 14:1239152.
doi: 10.3389/fphar.2023.1239152

Cenobamate as add-on therapy for drug resistant epilepsies: effectiveness, drug to drug interactions and neuropsychological impact. What have we learned from real word evidence?

Nicola Pietrafusa [1], Giovanni Falcicchio [2], Emilio Russo [3], Simona Lattanzi [4], Bianca Goffredo [5], Raffaele Simeoli [5], Sara Cairoli[5], Tiziana Corsetti[6], Roberta Roberti [3], Marina De Tommaso [2], Federico Vigevano [7], Angela La Neve [2] and Nicola Specchio [1]*

[1]Clinical and Experimental Neurology, Full Member of European Reference Network EpiCARE, Bambino Gesù Children's Hospital, IRCCS, Rome, Italy, [2]Department of Translational Biomedicine and Neurosciences, University of Bari 'Aldo Moro', Bari, Italy, [3]Science of Health Department, University Magna Grecia of Catanzaro, Catanzaro, Italy, [4]Neurological Clinic, Department of Experimental and Clinical Medicine, Marche Polytechnic University, Ancona, Italy, [5]Division of Metabolic Diseases and Drug Biology, Bambino Gesù Children's Hospital, IRCCS, Rome, Italy, [6]Hospital Pharmacy Unit, Bambino Gesù Children's Hospital, IRCCS, Rome, Italy, [7]Head of Neurological Sciences and Rehabilitation Medicine Scientific Area, Bambino Gesù Children's Hospital, IRCCS, Rome, Italy

Background: Cenobamate (CNB) is an anti-seizure medication (ASM) approved in 2021 in Europe for adjunctive treatment of focal-onset seizures in adults who were not adequately controlled with at least two previous ASMs.

Methods: seizure outcome, treatment-emergent adverse events, neuropsychological profile, and blood levels of CNB and concomitant ASM were analyzed in a real world setting in two different Italian epilepsy centers in the context of CNB early access program. All patients performed a general cognitive evaluation, while 32 patients underwent the administration of a battery of neuropsychological tests at baseline and 6 months after CNB treatment. We performed CNB quantification in plasma in 31 patients at different doses in the range of 100–400 mg/day (65 measures).

Results: we enrolled 54 patients with a median age of 27.9 years. The mean follow-up was 10.7 months. Most (91%) completed the efficacy analysis. At last follow-up visit, a 69.5% median seizure reduction was registered. Thirty-two patients (59.2%) had a ≥50% reduction of seizures that was ≥75% in 20 (42.0%) cases, whilst 10 (20.2%) patients were seizure-free. The most common adverse events were somnolence (53.1%), dizziness (28.1%) and diplopia (12.5%). The correlation between CNB dose and plasma concentration, revealed a significant linear correlation (r = 0.86, p < 0.0001), and there was a significant difference in mean plasma concentration/dose administered ratio (C/D ratio) between patients taking or not at least one inducer (0.10 ± 0.04 [(μg/mL)/(mg/

day)]; n = 47 vs. 0.13 ± 0.05 [(μg/mL)/(mg/day)]; n = 18, p = 0.04). CNB dose was inversely correlated (r = −0.31, p = 0.02) to the C/D ratio of Carbamazepine blood levels. and positively correlated (r = 0.74, p < 0.0001) with an increased plasma concentration of the active Clobazam metabolite N-desmethylclobazam. General Anxiety Disorder-7 showed a significant improvement of score from baseline evaluation of 6.82 to follow-up 6 months evaluation of 4.53 (p = 0.03).

Conclusion: In this real-world study, we registered a clinically meaningful reduction in seizure frequency after CNB administration in most patients along with a good tolerability profile. CNB treatment is correlate to a reduction in symptom severity of anxiety score. Plasma levels measurements confirm that CNB acts both as "victim" and as "perpetrator" of drug-drug interactions.

KEYWORDS

cenobamate, epilepsy, focal-onset seizures, drug-resistance, blood levels, neuropsychology

Introduction

In the last decades, numerous anti-seizure medications (ASMs) with different mechanisms of action have been marketed representing new therapeutic alternatives for clinicians and for patients with epilepsy (Perucca et al., 2020). Despite the early use of new ASMs, up to 30% of patients will have inadequate seizure control (Kwan and Sander, 2004; Mohanraj and Brodie, 2005) with the chances to reach seizure freedom being lower with each treatment failed (Chen et al., 2018). The severity of epilepsy results in an urgent need for developing new and more effective pharmacologic treatments (Perucca et al., 2020). Cenobamate (CNB) is the latest ASM approved as adjunctive treatment for focal-onset seizures (FOS) in adult patients who have not been adequately controlled despite a history of treatment with at least two ASMs (Roberti et al., 2021). CNB has multiple mechanisms of action: it mainly inhibits the persistent component of the sodium current trough the inactivation of the neuronal voltage-gated sodium channels (Nakamura et al., 2019), and acts as a positive allosteric modulator of the γ-aminobutyric acid ($GABA_A$) ion channel binding at a non-benzodiazepine site (Sharma et al., 2020). Adjunctive CNB in adult patients with uncontrolled FOS has been associated with a greater reduction in seizure frequency than placebo in two pivotal multicenter, randomized, double-blind, placebo-controlled trials enrolling 659 patients (Lattanzi et al., 2020; Specchio et al., 2021). Interestingly, CNB treatment has been associated with seizure freedom rates which are considerably higher than those reported for other ASMs (Villani et al., 2022). A phase III, open-label, safety study (Sperling et al., 2021) further documented the safety of CNB when the drug is started at a lower dose (12.5 mg/day) and up-titrated bi-weekly. To date, only few real-world studies evaluated the efficacy and safety of CNB. Recently published series provided evidence about the efficacy and safety of CNB in both pediatric and adult patients, including patients with developmental and epileptic encephalopathies (DEEs) (Elliott et al., 2022; Makridis et al., 2022; Varughese et al., 2022; Beltrán-Corbellini et al., 2023; Friedo et al., 2023; Peña-Ceballos et al., 2023; Villanueva et al., 2023).

While data of safety and effectiveness are available, data on effects of CNB on neuropsychological functions are still lacking, moreover drug to drug interactions and blood levels of CNB are also missing. In the present study, we report the effectiveness, tolerability, neuropsychological outcomes, and occurrence of drug-drug interactions through the analysis of the CNB blood levels in a cohort of drug-resistant adult patients treated with CNB as adjunctive treatment.

Methods

Study design and population

We performed a retrospective study of consecutive patients treated with CNB attending two epilepsy centers, i.e., Rare and Complex epilepsy Unit of Bambino Gesù Children Hospital (Rome, Italy) and the Epilepsy Center of Bari University Hospital (Policlinico of Bari, Italy). All patients received CNB through Angelini Pharma's Early Access Program (EAP) between 2020 and 2022. We included all patients treated with add-on CNB for, aged ≥18 years and diagnosed with drug-resistant focal epilepsy. Patients with severe hepatic impairment or end-stage renal disease (including patients on hemodialysis), history of suicidal attempt, drug abuse or alcoholism, psychogenic or non-epileptic seizures and women with known (or planned) pregnancy were excluded. Written informed consent was obtained from patients or their legal representatives.

Patients underwent clinical evaluation every 3 months according to routine clinical practice or whenever clinically indicated (i.e., occurrence of adverse events [AEs] or need of therapeutic adjustments). Demographic, seizure- and treatment-related data were obtained from medical records and seizure diaries. CNB was started at the dose of 12.5 mg/day and up-titrated according to prescribing information until 200 mg/day. The maximum allowed daily dose was 400 mg/day. Duration of the titration period and CNB maximum achievable dose were at the epileptologists' discretion. Changes in the titration schedule of CNB and in the doses of concomitant ASMs were allowed if AEs occurred.

Assessment of efficacy

The 4 weeks before starting CNB were identified as the baseline period. Efficacy outcomes were evaluated at 3, 6, 9 and 12 months after the introduction of CNB. The primary efficacy endpoint was the percentage change in monthly baseline seizure frequency at the

last follow-up visit (LFV). The seizure frequency up to the LFV was calculated as the number of seizures recorded during the treatment with CNB (including both the titration and maintenance phase), divided by the number of days from the initiation of CNB to the LFV; the result was multiplied by 28 to obtain a monthly frequency. Both median and mean percentage change in monthly baseline seizure frequency at the LFV were calculated using the following formula: (seizure frequency through LFV − seizure frequency during baseline) × 100/seizure frequency during baseline.

Secondary efficacy endpoints were the percentages of patients who had ≥25%, ≥50%, ≥75%, or 100% reduction in baseline monthly seizure frequency at the LFV and over 3-month intervals (0–3; 3–6; 6–9; and 9–12 months). Seizure freedom was defined as no seizures since the prior visit. Patients with ≥50% reduction in baseline seizure frequency were defined as responders. Reduction in monthly seizure frequency <25% or any increase in baseline seizure frequency were also reported. The proportions of patients who were seizure-free at LFV or had no more than one seizure for six consecutive months were also considered.

Assessment of tolerability

Tolerability was summarized every 3 months. The number and percentage of individuals reporting AEs were recorded, considering the supposed causal relationship with the study drug. AEs were classified as mild (not interfering with normal everyday activities), moderate (interfering with normal everyday activities), or severe (preventing normal everyday activities). Serious AEs (SAEs) were summarized separately.

Considering the predicted higher incidence of AEs in patients tacking sodium channel blockers (SCBs) or clobazam, data was also analyzed comparing such subgroups (Table 5).

Neuropsychological evaluation

Neurocognitive outcomes were assessed at baseline and every 6 months through self- or parental-administered instruments: Progressive Matrices 38 IQ, the Trail Making Test (TMT), the Adaptive Behavior Assessment System, 2nd edition (ABAS-II), PHQ-9 (Patient Health Questionnaire), GAD-7 (Generalized Anxiety Disorder), Pediatric Quality of Life Inventory (PEDsQL) and QOLIE-31 (Quality of life in epilepsy-31 inventory).

Measurement of cenobamate plasma concentration by LC-MS/MS and other ASMs

Plasma concentrations of CNB and concomitant ASMs were performed every 3 months. Plasma laboratory analysis has all been performed in Rome (Bambino Gesù Children Hospital). Cenobamate plasma concentration was measured using an ultra-performance liquid chromatography (UPLC) 1,290 Infinity II system (Agilent Technologies) coupled to a 6,470 Mass Spectrometry system (Agilent Technologies) equipped with an ESI-JET-STREAM source operating in the positive ion (ESI+) mode. CNB powder was of analytical grade and was purchased from Spectra 2000 Srl (Rome, Italy). Detailed information on CNB methods for plasma concentration measurements is available as Supplementary Data.

Statistical analysis

Continuous data were summarized using descriptive statistics including means, standard deviations, medians, lower and upper quartiles, and ranges. Categorical variables were summarized with frequencies and percentages. Univariate comparisons were made by the chi-square test or the Fisher exact test for categorical variables and the Student's t test or Mann-Whitney U for continuous variables as appropriate; the analysis of variance was used to compare means across multiple groups.

A stepwise binomial logistic regression analysis was used to assess independent associations: in the final model, age at epilepsy onset, disease duration, numbers of previous ASMs, numbers of current ASMs, baseline seizure frequency and presence of focal to bilateral tonic-clonic seizures were the dependent variables and CNB response (≥50% seizure frequency reduction at LFV) was the independent variable. The model was validated by the Hosmer-Lemeshow test, and the stepwise entry method was used. We limited the number of independent variables to a minimum of 10:1 event per independent variable. Statistical significance was set at $p < 0.05$. Statistical analysis was performed using R version 3.2.3 (R Foundation for Statistical Computing, https://www.r-project.org/).

For measurement of plasma concentration of CNB by LC-MS/MS and other ASMs, all statistical analyses and graphs were performed using Graph-Pad Prism 9.0 (Graph-Pad software Inc., San Diego, CA). Cenobamate plasma concentrations were reported as median with range whereas ASMs plasma levels were expressed as median with interquartile range (IQR). D'Agostino & Pearson test was used to check data distribution normality.

Results

Fifty-four patients (31 F) with a median age of 27.9 years (IQR = 21.7-33.4) were enrolled. The mean follow-up duration was 10.7 months [range ±standard deviation (SD) 6.0-15.0 ± 2.1]. All patients presented FOS, 18 (33.3%) of them suffering from focal to bilateral tonic-clonic seizures. Patients were previously treated with a median of 9 ASMs (IQR = 7–9). When CNB was started, patients were taking a median of three ASMs (IQR = 1–4). The most common concomitant ASMs at the enrollment were carbamazepine (n = 24, 44.4%), clobazam (n = 22, 40.7%), and lacosamide (n = 17, 31.5%). Sixteen patients (29.6%) had vagal nerve stimulation therapy and 19 out of 54 patients (35.2%) had failed epilepsy surgery. Details of demographic and clinical characteristics of the study cohort are shown in Table 1.

Titration period up to 100 mg/day lasted for a mean period of 58.4 (range ±SD 30-151 ± 18.9) days; 107.7 (70-278 ± 40.3) days was the mean time to reach 200 mg/day and 167.9 (14-434 ± 109.7) days were needed to achieve the maximum dose of CNB (204 mg, 50-400 ± 90). At LFV, the mean dose of CNB was 201.8 mg/day (25-400 ± 96.9). In 9 patients (16.7%) CNB was withdrawn due to AEs

TABLE 1 Baseline demographics, clinical features (*N* = 54) and Efficacy data (*N* = 49).

	N (%) or Mean (ranges ±SD) or Median (Q1, Q3)
Patients	54
Sex	
Male	23 (42.6)
Female	31 (57.4)
Age at epilepsy onset (years)	5.8 (2.7, 8.9)
Age at enrolment (years)	27.9 (21.7, 33.4)
Disease duration (years)	22.5 (16.1, 28.4)
Etiology	
Unknown	17 (31.5)
Genetic	5 (9.2)
Genetic/Structural (TSC)	3 (5.5)
Structural	26 (48.1)
Infective	2 (3.7)
Autoimmune	1 (1.8)
Previous SE	7 (12.9)
Follow-up (months)	10.7 (6.0-15.0 ± 2.1)
Dose of CNB at last follow-up (mg/day)	201.8 (25-400 ± 96.9)
Weight (kg)	66.6 (30-121 ± 15.7)
Previous idiosyncratic reactions	5 (9.2)
Previous ASMs	9 (7, 12)
Concomitant ASMs (number)	3 (1, 4)
Other treatments	
VNS	16 (29.6)
Neurosurgery	19 (35.2)
KD	0 (0)
CNB dose (mg/day) mean	201.8 (25-400 ± 96.9)
CNB dose (mg/day) median	200 (100, 300)
Seizure type (n, %)	
Focal	54 (100)
Focal to bilateral	18 (33.3)
Other types of seizures	
Tonic	5 (9.2)
Atonic	3 (5.5)
Atypical absences	2 (3.7)
Spasms	2 (3.7)
Baseline seizure frequency	
Mean	23.5 (5-100 ± 25.7)
Median	11.7 (5.5, 31.9)
Titration period (days) at 100 mg/day	58.4 (30-151 ± 18.9)
Titration period (days) at 200 mg/day	107.7 (70-278 ± 40.3)
Titration period (days) at CNB maximum dose	167.9 (14-434 ± 109.7)
CNB withdraws (n, %)	9 (16.7)
Adverse events	5 (9.2)
Inefficacy	2 (3.7)
Increased seizure frequency	2 (3.7)

(Continued on following page)

TABLE 1 (*Continued*) Baseline demographics, clinical features (*N* = 54) and Efficacy data (*N* = 49).

	N (%) or Mean (ranges ±SD) or Median (Q1, Q3)
Last follow-up seizure frequency Mean Median	 10 (0-64 ± 15.5) 3.5 (0, 9.7)
Median duration of maintenance dose (months)	4.0 (2.3, 7.0)
Median percentage reduction in baseline seizure frequency at LFV	69.5 (20.8, 98.2)
≥50% reduction in seizure frequency at LFV	29 (59.2)
100% reduction in seizure frequency at LFV	10 (20.4)
N. of pts seizure-free for 6 consecutive months	
Baseline seizure frequency Mean Median	6 (13.3) 23.5 (5-100 ± 25.7) 11.7 (5.5, 31.9)
N. of pts nearly seizure freedom (one seizure in 6 consecutive months)	4 (8.9)

N, number; SD, standard deviation; Q1, first quartile; Q3, third quartile; TSC, tuberous sclerosis complex; SE, status epilepticus; CNB, cenobamate; VNS, vagal nerve stimulation; KD, ketogenic diet; LFV, last follow-up visit.

(*n* = 5; 9.2%), inefficacy (*n* = 2; 3.7%) or seizure worsening (*n* = 2; 3.7%).

Effectiveness

Data on seizure frequency were available for 49 patients (90.7%). The remaining patients (*n* = 5) dropped-out before 3 months of follow-up and they did not reach the 200 mg dose due to drug withdrawal (2 for seizure worsening and 3 for AEs) and were excluded from the efficacy analysis. The median monthly seizure frequency was 10.0 (IQR = 5.5–30.6) at baseline and 3.5 (IQR = 0–9.7) at LFV, with a corresponding median percentage reduction in baseline seizure frequency of 69.5% [IQR = 69.5 (20.8–98.2)]. At LFV, 29 out of 49 patients (59.2%) reported a ≥50% reduction in baseline seizure frequency with a mean CNB dose of 201.8 mg/day (25–400 ± 96.9), 42% of patients (n = 20) achieved ≥75% reduction, and 10 patients (20.2%) achieved seizure-freedom (Figure 1A). Six (13.3%) patients remained seizure-free and 4 (8.9%) experienced no more than one single seizure during at least 6 months. Responder rates over the 0–3 months, 3–6 months, 6–9 months, and 9–12 months intervals were 53.1%, 61.2%, 67.3%, and 65.3% respectively (Figure 1B). A low-CNB dosage (<200 mg per day) was used 17/49 patients (34.7%). The proportion of patients who experienced a 100%, ≥75%, or ≥50% reduction in seizure frequency at the last visit was not statistically significantly different in those receiving low-dose CNB (19.4%, 41.7%, and 58.3%, respectively) vs. those receiving high-dose CNB (20.3%, 45.5%, and 62.3%, respectively).

At 6 months, treatment retention for CNB was 100.0% (49/49), at 9 months, 81.6% (40/49, 6 patients with insufficient follow-up, 2 patients for lack of efficacy, 1 patient for AEs), and at 12 months, 95.2% (20/21 patients, 19 pts with insufficient follow-up, 1 patient for AEs). Binomial logistic regression failed to reveal any association among the efficacy outcome (seizure responder) and other parameters. Demographic and clinical characteristics were analyzed in responders and non-responders. We did not find significant differences in these two groups (see Supplementary Table).

Concomitant ASMs and pharmacokinetics evaluations and drug-drug interactions during cenobamate use in clinical practice

We analyzed the potential effect of concomitant ASMs on the efficacy outcomes. The coadministration of sodium-channel blockers (SCBs) resulted in higher percentage of responders (64.1%) if compared with patients not taking SCBs (40.0%) (p = 0.003). Considering clobazam (CLB), responders were 66.7% among patients taking CLB compared with 55.9% among patients not taking CLB as concomitant medication (p = 0.05) (Figure 1C). In thirty-two (59.2%) cases out of 54 patients we were able to reduce or withdraw one or more concomitant ASMs (Table 2; Supplementary Figure S1).

Regarding CNB quantification in plasma, 65 measures were performed in 31 patients at different doses in the range of 100–400 mg/day (details are reported in Table 3). In this group of patients, we analysed the correlation (Pearson test) between CNB dose and plasma concentration (Figure 2A), and we found a significant linear correlation (r = 0.86, p < 0.0001). We further analysed the effect of concomitant administration of inducer ASMs on CNB plasma concentration. We found a significant difference in mean plasma concentration/dose administered ratio (C/D ratio) of CNB between patients assuming at least one inducer and patients without an inducer as concomitant medication (0.10 ± 0.04 [(μg/mL)/(mg/day)]; n = 47 vs. 0.13 ± 0.05 [(μg/mL)/(mg/day)]; n = 18, p = 0.04) (Figure 2B). As concerns the impact of CNB on the plasma concentrations of other ASMs, we have analysed CBZ plasma levels over time. Specifically, in 19 patients, a significant (dose-dependent) effect of CNB has been observed. Increasing doses of CNB were inversely correlated (r = -0.31, p = 0.02) to the C/D ratio of CBZ (Figure 2C). Similarly, CNB dose was positively correlated (r = 0.74, p < 0.0001) with an increased plasma concentration of the active

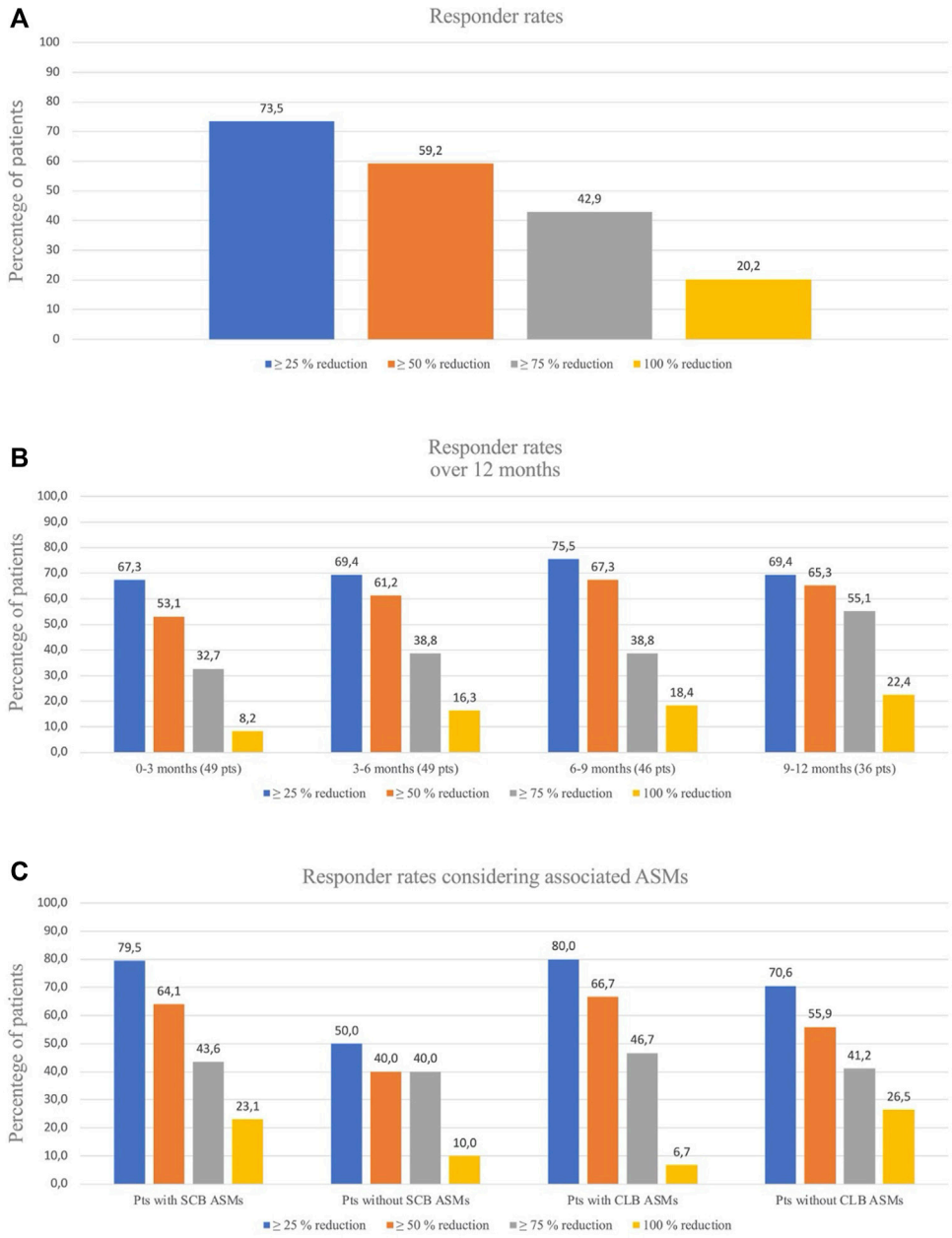

FIGURE 1
(A). Responder rates for seizures reduction al last follow-up visit. **(B)**. Responder rates over time for seizures frequency. At 0–3 months and 3–6 months, data were missing for 0 patients; at 6–9 months there were missing for 3 patients and at 9–12 months there were missing for 13 patients. **(C)**. Responder rates considering associated ASMs: patients with/without Sodium Channel Blockers (SCB) associated ASMs and patients with/without Clobazam (CLB) associated ASMs.

CLB metabolite N-desmethylclobazam (N-CLB) (Figure 2D). CNB dose of 200 mg/day resulted in a 2-fold increase of N-CLB plasma levels (Supplementary Figure S2), notably, the increase in N-CLB should be further explored since our data suggest a potential non-linear correlation at increasing doses. Correlations among CNB dose and plasma concentrations of other concomitant ASMs were not significant. Notably, C/D ratios of levetiracetam (2 patients), valproate (6 patients) and zonisamide (4 patients) were partially reduced with CNB increasing doses. Among other ASMs, drug level of lacosamide (10 patients), phenobarbital (6 patients), lamotrigine (7 patients), and perampanel (6 patients) did not change.

Neuropsychological evaluation

All patients had a general cognitive evaluation while 32 patients underwent the administration of a battery of neuropsychological tests at baseline and after 6 months since the start of treatment with CNB (Table 4). Administration of Raven's Progressive Matrices

TABLE 2 Concomitant ASMs modifications (*N* = 38).

Concomitant ASMs modifications	N (%)
Concomitant ASMs (type), n. of patients (%)	
CBZ	24 (44.4)
CLB	22 (40.7)
LCS	17 (31.5)
VPA	12 (22.2)
LTG	11 (20.3)
PB	11 (20.3)
PER	11 (20.3)
ZNS	6 (11.1)
BRV	6 (11.1)
LEV	5 (9.2)
OXC	4 (7.4)
RUF	3 (5.5)
TPM	3 (5.5)
GVG	3 (5.5)
CBD	3 (5.5)
PHT	1 (1.8)
ESL	1 (1.8)
CZP	1 (1.8)
NTZ	1 (1.8)
Patients who modified other ASMs with AEs	32/54 (59.2)
Patients who reduced 1 ASM	18/54 (33.3)
Patients who stopped 1 ASM	13/54 (24.0)
Patients who reduced/stopped 2 ASMs	1/54 (1.8)
Patients who reduced/stopped 3 ASMs	8/54 (14.8)
Patients who modified ASMs without AEs	7/54 (12.9)
Most frequent modified ASMs	
CBZ	7/54 (12.9)
LCS	5/54 (9.2)
CLB	8/54 (14.8)
LTG	3/54 (5.5)

N, number; ASMs, antiseizure medications; CNB, cenobamate; AEs, adverse events; CBZ, carbamazepine; CLB, clobazam; LCS, lacosamide; VPA, valproic acid; LTG, lamotrigine; PB, phenobarbital; PER, perampanel; ZNS, zonisamide; BRV, brivaracetam; LEV, levetiracetam; OXC, oxcarbazepine; RUF, rufinamide; TPM, topiramate; GVG, vigabatrin; CBD, cannabidiol; PHT, phenytoin; ESL, eslicarbazepine; CZP, clonazepam; NTZ, nitrazepam.

TABLE 3 Cenobamate plasma concentration across different doses and single dose group concentration/dose (C/D) ratio.

Dose (mg)	Number of Measures	Plasma concentration μg/mL (median; range)	C/D [(μg/mL)/mg/day)] (median; range)
100	10	8.28 (2.55–21.56)	0.08 (0.03–0.22)
150	13	21.38 (8.49–41.78)	0.14 (0.06–0.28)
200	28	18.61 (5.96–38.49)	0.09 (0.03–0.19)
250	3	24.38 (19.18–27.87)	0.10 (0.08–0.11)
300	6	27.78 (24.45–63.21)	0.095(0.08–0.21)
350	3	37.61 (36.33–57.21)	0.11 (0.10–0.16)
400	2	29.09 (24.64-33-54)	0.07 (0.06–0.08)

38 IQ showed a statistically significant improvement in total score (30.6 at baseline versus 41.56 at six-month evaluation, p = .05). General Anxiety Disorder-7 test shows a significant statistically improvement of final score (6.82 at baseline versus 4.53 at six-month evaluation, p = .03). A significant statistically improvement was observed also in TMT-A (68.31 at baseline versus 41.65 at six-month evaluation, p = .01) and ABAS II-DAP (91.59 at baseline versus 103.31 at six-month evaluation, p = .04). We did not find difference in mean GAD-7 final score responders versus non-responders (p = .08), moreover CNB dose and plasma levels did

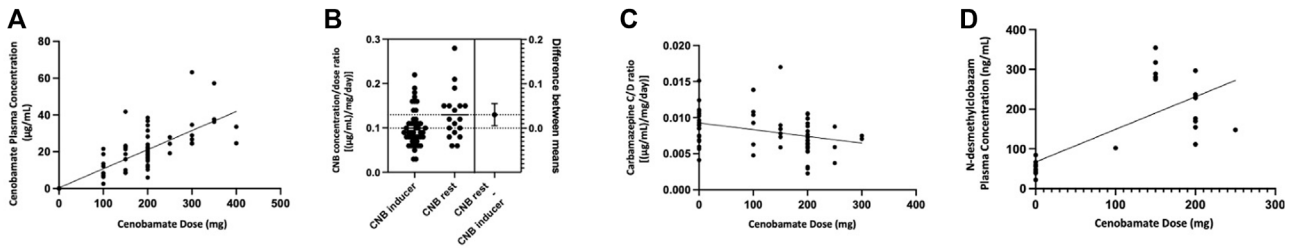

FIGURE 2
(A). Significant ($p < 0.0001$) linear correlation (Pearson test) between the daily dose and the plasma concentration of Cenobamate in the dose range 100–400 mg. **(B)**. Difference in mean concentration/dose ratio of Cenobamate with and without concomitant use of at least one inducer antiseizure medication. **(C)**. Correlation between Cenobamate dose and carbamazepine concentration/dose ratio. **(D)**. Correlation between Cenobamate dose and N-desmethylclobazam plasma concentration.

not correlate with GAD-7 final score ($r = 0.41$, $p = 0.07$ and $r = 0.47$, $p = 0.09$, respectively).

Safety

Data on safety were available for all patients (see Table 5). The most common AEs were somnolence ($n = 17$, 53.1%), dizziness ($n = 9$, 28.1%) and diplopia ($n = 4$, 12.5%). Dizziness and diplopia were more frequent in patients taking SCBs (36% and 16% versus 0% and 0% in patients without SCBs), while somnolence was more frequently reported by patients taking CLB (72.7%) compared with patients without CLB (42.8%) (Table 5). Somnolence was a temporary AE that most frequently resolved spontaneously, while the dose adjustment of concomitant ASMs or CNB was required in the other cases. The mean dose of CNB at the time of the occurrence of the AEs was 118.9 mg/day (12.5-250 ± 60.4). No patients presented SAEs or required hospitalization. AEs were observed in 63% of patients treated with low-dose CNB; 6.8% of patients discontinued treatment due to AEs.

Considering electrocardiogram monitoring, none of the patients experienced significant alterations of the QTc interval (ANOVA, $p = .47$). No significant blood tests alterations were registered.

Discussion

In this retrospective, real-world study of CNB treatment in patients with drug resistant focal epilepsies, add-on CNB provided a clinically significant reduction in seizure frequency in most of the patients. The results we found in the current study are consistent with those observed in previously published randomized controlled trials (RCTs) (Chung et al., 2020; Krauss et al., 2020) and real-life experiences (Elliott et al., 2022; Makridis et al., 2022; Varughese et al., 2022; Beltrán-Corbellini et al., 2023; Friedo et al., 2023; Peña-Ceballos et al., 2023; Villanueva et al., 2023).

Of note, this study allowed to obtain more information about the use of CNB in the context of the real-world practice, adopting a more flexible drug dosing regimen and providing data over a longer follow-up period if compared to earlier RCTs.

The median percentage reduction of seizure frequency of 69.5% and the responder rate of 59.2% were slightly higher compared to those reported in both pivotal studies: in C013 and in C017 trials, the reductions in median seizure frequency were 55.6% and 56% and the responder rates were 50.4% and 56% at CNB dose of 200 mg/day, respectively (Chung et al., 2020; Krauss et al., 2020; Lattanzi et al., 2020). The proportion of seizure-free patients in the present study was 20.4% at a mean CNB dose of 200 mg/day. This figure is lower if compared with the rate found in the C013 study (28% at maintenance dose of CNB 200 mg/day) (Chung et al., 2020), and higher than the rate reported in the C017 study (11% at maintenance dose of CNB 200 mg/day) (Krauss et al., 2020). Considering the different study designs, results in our cohort of patients seem to be slightly better if compared with the previous RCTs. This can be explained by the possibility of adjusting and personalizing the dose of CNB and concomitant ASMs, which may have given higher responder rates.

The results of this study were similar to results from other real-world studies of CNB, which also included patients with highly refractory epilepsy.

In a recent large series of patients with highly drug-resistant epilepsy, including 170 patients, the rate of seizure freedom was 13.3%; ≥90%, ≥75%, and ≥50% responder rates were 27.9%, 45.5%, and 63%, respectively. There was a significant reduction in the number of seizures per month (mean: 44.6%; median: 66.7%) between baseline and the last visit ($p < 0.001$) (Villanueva et al., 2023). Compared with this study (Villanueva et al., 2023), we observed a higher percentage of seizure-free patients (13.3% vs. 20.4%). This could be due to differences in the cohort composition, since our patients were slightly younger, and a lower number of previous treatments, suggesting that CNB could be associated with a better response when used earlier. Of note, we also found that 8.9% of patients were nearly to seizure freedom (patients with no more than one seizure during six consecutive months of the study period).

From a series of 45 adolescent and adult patients who had received a mean of 12 prior ASMs, Elliot et al. reported seizure freedom in 16% of patients and a ≥50% response in 60% (Elliot et al., 2022). A pediatric real-world study found a seizure freedom rate of 31% and a >50% response rate of 37.5% (Makridis et al., 2022). In another pediatric real-world study, 19% of patients achieved seizure freedom, 52% had a ≥75% response rate, and 63% had a ≥50% response rate (Varughese et al., 2022). Additionally, our results were in line with previous findings from an EAP in Ireland, which 57 patients with ultraresistant epilepsy and showed seizure

TABLE 4 Cognitive condition and neuropsychological evaluation.

	N (%)		
Cognitive condition (*N* = 54)			
No cognitive impairment	24 (44.4)		
Cognitive impairment	30 (55.5)		
Mild	11/30 (36.6)		
Moderate	12/30 (40.0)		
Severe	7/30 (12.9)		
Education (N = 54)			
No education	7 (27.8)		
Elementary school			
Middle school	3 (5.5)		
High school	26 (48.1)		
Graduation	10 (18.5)		
Neuropsychological tests (*N*= 32)	Baseline evaluation	Six months evaluation	*p*-value
Raven's Progressive Matrices 38 IQ	30.57	41.56	**0.05**
Trail-making test A	68.31 s	41.65 s	**0.01**
Trail-making test B	142.67 s	146.94 s	0.90
Patient Health Questionnaire-9	6.27	7.53	0.37
General Anxiety Disorder-7	6.82	4.53	**0.03**
ABAS II—GAC	92.63	99.5	0.36
ABAS II—DAC	93.19	89.38	0.45
ABAS II—DAS	90.68	96.88	0.42
ABAS II—DAP	91.59	103.31	**0.04**
PedsQL Total	74.27	71.35	0.51
Health	79.33	76.94	0.6
Emotion	69.11	66.76	0.71
Socialization	76.61	75.59	0.89
School	67.78	64.41	0.56
Qolie 31 Total	49.88	49.88	0.99
Seizure Worry	49.04	46.35	0.36
Quality of life	48.42	51.29	0.34
Wellbeing	50.92	50.35	0.80
Energy	53.15	50.24	0.34
Cognition	51.35	51.06	0.92
Medical effects	51.58	49.71	0.50
Social functions	47.04	45.12	0.44

ABAS II, Adaptive Behavior Assessment System—Second Edition; GAC, general adaptive composite; DAC, conceptual skills domain; DAS, social skills domain; DAP, practical skills domain; PedsQL, pediatric quality of life inventory; Qolie 31, Quality of Life Inventory in Epilepsy. Bold values denote statistical significance at the $p < 0.05$ level.

reduction in 75%–99% of the cohort in 42.1% of patients (Peña-Ceballos et al., 2022).

More recently, in the Beltran-Corbellini et al. study, in 51 patients with highly refractory focal epilepsy, retention rate at the last follow-up was 80.4% and the 50% responder rate in focal seizures was 56.5% and in focal to bilateral tonic-clonic seizures was 63.6% (Beltran-Corbellini et al., 2023).

Finally, a drug load reduction was possible in 12 patients with developmental and epileptic encephalopathies, thanks to CNB effectiveness, maintaining seizures reduction (Friedo et al., 2023).

Considering the responder rates, we found some differences in patients with and without concomitant SCBs: the concomitant use of SCBs increased the percentage of seizure free patients from 10% to 23% and the percentage of responders from 40% to 64%. Concomitant use of SCBs and CNB, should be carefully evaluated for tolerability issues. Although a similar increase of responders was seen in patients with and without concomitant CLB (67% versus 56%), the seizure freedom rate was higher among patients not taking concomitant CLB (26.5% versus 6.7%); we do not have a clear-cut explanation for this latter finding, which should be further investigated in future studies.

The longitudinal evaluation of efficacy revealed an increase in the responder rates from the first to the third trimester, going from 53% to 67.3% (≥50% responders) and from 8.2% to 18.4% (seizure

TABLE 5 Adverse events reported (*N* = 54).

	N (%) Total*	Pts with SCB (44/54) N (%)	Pts without SCB (10/54) N (%)	Pts with CLB (22/54) N (%)	Pts without CLB (32/54) N (%)
Patients with AEs	32 (100)	25 (100)	7 (100)	11 (100)	21 (100)
Somnolence	17/32 (53.1)	12/25 (48)	5/7 (71.4)	8/11 (72.7)	9/21 (42.8)
Dizziness	9/32 (28.1)	9/25 (36)	0/7 (0)	4/11 (36.4)	5/21 (23.8)
Diplopia	4/32 (12.5)	4/25 (16)	0/7 (0)	1/11 (9.1)	3/21 (14.3)
Ataxia	3/32 (9.4)	2/25 (8)	1/7 (14.3)	0/11 (0)	3/21 (14.3)
Headache	2/32 (6.5)	1/25 (4)	1/7 (14.3)	1/11 (9.1)	1/21 (4.8)
Vomiting	1/32 (3.1)	1/25 (4)	0/7 (0)	0/11 (0)	1/21 (4.8)
Urticaria	1/32 (3.1)	1/25 (4)	0/7 (0)	0/11 (0)	1/21 (4.8)
Diarrhea	1/32 (3.1)	0/25 (0)	1/7 (14.3)	0/11 (0)	1/21 (4.8)
Outcome					
Resolved	21/32 (65.6)	10/25 (40)	3/7 (42.8)	4/11 (36.4)	11/21 (52.4)
Not resolved/ongoing	8/32 (25)	5/25 (20)	3/7 (42.8)	3/11 (27.3)	5/21 (23.8)
Resolved with ASMs modification	3/32 (9.4)	10/25 (40)	1/7 (14.3)	4/11 (36.4)	5/21 (23.8)
Severity					
Mild	16/32 (50)	14/25 (56)	2/7 (28.6)	4/11 (36.4)	12/21 (57.1)
Moderate	9/32 (28.1)	5/25 (20)	4/7 (57.1)	4/11 (36.4)	5/21 (23.8)
Severe	7/32 (21.9)	6/25 (24)	1/7 (14.3)	3/11 (27.3)	4/21 (19.0)
SAEs	0 (0)	0 (0)	0 (0)	0 (0)	0 (0)
Hospitalization	0 (0)	0 (0)	0 (0)	0 (0)	0 (0)
CNB dose at time AEs (mg/kg/day)	118.9 (12.5-250 ± 60.4)	120.5 (12.5-250 ± 64.7)	100.0 (50-150 ± 40.8)	131.8 (50-200 ± 51.3)	107.7 (12.5-250 ± 65.1)
EKG				ANOVA $p = 0.47$	
QTc baseline (mean, msec)		408.3			
QTc at 3 months (mean, msec)		401.4			
QTc at 6 months (mean, msec)		409.5			
QTC at 9 months (mean, msec)		405.5			

N, number; Pts, patients; SCB, sodium channel blockers; CLB, clobazam; AEs, adverse events; ASMs, antiseizure medications; SAEs, serious adverse events; CNB, cenobamate; EKG, electrocardiogram; QTc, Corrected QT, Interval (QTc) with Fridericia correction formula.
*Patients can have more AE.

freedom). An improvement of the drug efficacy is seen over time, possibly related also to the increase in drug dosage, and clinicians should wait before considering CNB withdraw if the tolerability is kept, even if we have to acknowledge that—as it always happens in long term observation—the overall number of patients during time decrease making the results more attractive.

Reducing the load of concomitant ASMs is highly warranted in patients with drug resistant epilepsy: in the study cohort, most patients were taking a median of 3 ASMs and still experiencing a median of 11.7 seizures per month. In this regard, the 60% of the participants were able to reduce or withdraw one or more concomitant ASMs during the follow-up.

The incidence of AEs was higher if compared with literature data, even though a clear association with a specific CNB dose was not identified. Most AEs occurred at a relatively low dose of CNB (100 mg/day) and without the dose-related association registered in previous clinical trials (Chung et al., 2020; Krauss et al., 2020). A possible explanation of the poorer tolerability may be the use of multiple concomitant ASMs in our cohort of patients. Central nervous system-related side effects were the most reported as already found with the use of other currently available ASMs (Zaccara et al., 2013). Ataxia and diplopia were more frequent when a concomitant SCB was taken, likely as the result of the pharmacodynamic interaction that may occur among agents acting as SCBs.

In many cases, a reduction in the number and/or dose of concomitant ASMs was required to resolve AEs. SCBs and CLB were the most frequently modified concomitant drug regimens. A proactive lowering of ASMs with known pharmacodynamic (carbamazepine and lacosamide) and pharmacokinetic interactions (phenobarbital, phenytoin, CLB) with CNB may be indicated to prevent AEs and allow an optimal CNB dosing (Smith et al., 2022).

A linear correlation was shown between the daily dose and the plasma concentration of CNB in the dose range 100–400 mg/day. Dose-proportional increases in both maximum concentration and plasma exposure are confirmed by single and multiple ascending dose studies (Vernillet et al., 2020), but non-linear pharmacokinetics is expected at higher doses (more than 300 mg). In our cohort, the number of patients

treated with more than 300 mg of CNB was too small to assess any disproportionality in dose responses.

Plasma levels measurements confirm that CNB acts both as "victim" and as "perpetrator" of drug-drug interactions. Indeed, in patients treated with at least one inducer, the mean C/D ratio of CNB was significantly lower if compared with patients not taking an inducer. On the other hand, the reduction of CBZ plasma concentrations induced by CNB concomitant administration (Roberti et al., 2021) has been confirmed in our cohort. Also, the pharmacokinetic interactions involving CLB, and its metabolite have been confirmed, considering that we observed a 2-fold increase in N-CLB levels at CNB 200 mg/day. Such increase of N-CLB was associated with somnolence in our patients. Notably, a variable (between 145% and 1852%) increase in N-CLB serum concentration has been reported in a recent study (Elakkary et al., 2023). The authors suggest a potential role of the pharmacogenetics of the hepatic enzyme CYP2C19 to explain this high rate of variability and report fatigue as a direct consequence of N-CLB increase (Elakkary et al., 2023). In the same study, a synergistic interaction between CLB and CNB has been hypothesized, because both ASMs potentiate GABA transmission acting at different sites of the $GABA_A$ receptor (Elakkary et al., 2023).

Most notably, there was a certain degree of variability within the same dose among patients, therefore, TDM is likely recommended to better adjust therapy. This is also in agreement with our observation of the reduction of CNB concentration when inducer ASMs are concomitantly used, and the bidirectional influence observed.

The lack of a significant correlation among CNB doses and plasma concentrations of other concomitant ASMs may be due to the overall limited number of observations.

General Anxiety Disorder-7 test showed a significant improvement in symptom severity of anxiety score in our cohort. This result could be related to the reduction of seizures burden or to the CNB pharmacodynamic mechanism as positive allosteric modulator of the $GABA_A$ ion channel (Löscher et al., 2021). We failed to find any correlations between reduction of anxiety, the status of responder, and CNB blood concentrations. More studies should be performed to document and confirm if the reduction of anxiety is related to seizure's reduction or to the $GABA_A$ modulation. We observed an improvement in Raven's Progressive Matrices 38 IQ, TMT-A and ABAS-II probably due to the reduction of the concomitant drug load.

Study limitations

The limitations of this study are: the small sample size which does not allow internal statistical comparison; a potential selection bias considering the nature of patients selection, although, being an EAP, the selected patients represent a subgroup of patients with a high number of previous ASMs failures; the relatively short follow-up which does not allow the evaluation of long-term efficacy above all considering seizure freedom; the open-label design, the retrospective nature, and the lack of a control group.

Conclusion

If confirmed by future studies, the efficacy shown by CNB in reducing seizures in patients with FOS may support the indication to use CNB sooner in the treatment algorithm of focal epilepsy. We reported that lower doses of CNB may be as effective as those used in previous RCTs. Moreover, the use of add-on CNB allowed to reduce the overall load of concomitant ASMs.

Therapeutic drug monitoring could be a useful tool to improve CNB dosing and prevent possible AEs. CNB appears to reduce symptom severity of anxiety.

CNB was safe and provided sustained, clinically meaningful seizure reduction in this real-world study. More studies may better establish the long-term safety and efficacy of CNB and identify possible predictors of seizure control.

Data availability statement

The raw data supporting the conclusion of this article will be made available by the authors, without undue reservation.

Ethics statement

The studies involving humans were approved by the Bambino Gesù Children Hospital EC. The studies were conducted in accordance with the local legislation and institutional requirements. Written informed consent for participation in this study was provided by the participants' legal guardians/next of kin. Written informed consent was obtained from the individual(s) for the publication of any potentially identifiable images or data included in this article.

Author contributions

NP, NS, and AL conceived and designed the study, prepared the study protocol, and is responsible for study management and supervision. NP provided methodological and statistical knowledge. NP, GF, RS, RR, and SC are responsible for study conduction and monitoring. SL, ER, MG, TC, and RR contribute to the interpretation of results. NP, GF, and RS prepared the manuscript. SL, ER, MD, FV, and NS made the final review of the manuscript. All authors contributed to the article and approved the submitted version.

Funding

This work was supported also by the Italian Ministry of Health with Current Research funds.

Acknowledgments

We thank the patients and their families for participation in this study. This study was done also through a collaboration of Italian EpiCARE centers.

Conflict of interest

The authors declare that the research was conducted in the absence of any commercial or financial relationships that could be construed as a potential conflict of interest.

Publisher's note

All claims expressed in this article are solely those of the authors and do not necessarily represent those of their affiliated organizations, or those of the publisher, the editors and the reviewers. Any product that may be evaluated in this article, or claim that may be made by its manufacturer, is not guaranteed or endorsed by the publisher.

Supplementary material

The Supplementary Material for this article can be found online at: https://www.frontiersin.org/articles/10.3389/fphar.2023.1239152/full#supplementary-material

References

Beltrán-Corbellini, Á., Romeral-Jiménez, M., Mayo, P., Sánchez-Miranda Román, I., Iruzubieta, P., Chico-García, J. L., et al. (2023). Cenobamate in patients with highly refractory focal epilepsy: a retrospective real-world study. *Seizure* 111, 71–77. doi:10.1016/j.seizure.2023.07.026

Chen, Z., Brodie, M. J., Liew, D., and Kwan, P. (2018). Treatment outcomes in patients with newly diagnosed epilepsy treated with established and new antiepileptic drugs a 30-year longitudinal cohort study. *JAMA Neurol.* 75 (3), 279–286. doi:10.1001/jamaneurol.2017.3949

Chung, S. S., French, J. A., Kowalski, J., Krauss, G. L., Lee, S. K., Maciejowski, M., et al. (2020). Randomized phase 2 study of adjunctive cenobamate in patients with uncontrolled focal seizures. *Neurology* 94 (22), e2311–e2322. doi:10.1212/WNL.0000000000009530

Elakkary, S., Hagemann, A., Klimpel, D., Bien, C. G., and Brandt, C. (2023). A retrospective non-interventional study evaluating the pharmacokinetic interactions between cenobamate and clobazam. *Epilepsia* 64 (4), e36–e42. doi:10.1111/epi.17515

Elliott, T., Ridley-Pryor, T., Gienapp, A. J., and Wheless, J. W. (2022). Initial real-world experience with cenobamate in adolescents and adults: a single center experience. *Pediatr. Neurol.* 129, 19–23. doi:10.1016/j.pediatrneurol.2022.01.001

Friedo, A. L., Greshake, B., Makridis, K. L., and Straub, H. B. (2023). Cenobamate significantly improves seizure control in intellectually disabled patients with drug-resistant epilepsy and allows drug load reduction. *Front. Neurol.* 14, 1209487. doi:10.3389/fneur.2023.1209487

Krauss, G. L., Klein, P., Brandt, C., Lee, S. K., Milanov, I., Milovanovic, M., et al. (2020). Safety and efficacy of adjunctive cenobamate (YKP3089) in patients with uncontrolled focal seizures: a multicentre, double-blind, randomised, placebo-controlled, dose-response trial. *Lancet Neurol.* 19 (1), 38–48. doi:10.1016/S1474-4422(19)30399-0

Kwan, P., and Sander, J. W. (2004). The natural history of epilepsy: an epidemiological view. *J. Neurol. Neurosurg. Psychiatry* 75 (10), 1376–1381. doi:10.1136/jnnp.2004.045690

Lattanzi, S., Trinka, E., Zaccara, G., Striano, P., Del Giovane, C., Silvestrini, M., et al. (2020). Adjunctive cenobamate for focal-onset seizures in adults: a systematic review and meta-analysis. *CNS Drugs* 34 (11), 1105–1120. doi:10.1007/s40263-020-00759-9

Löscher, W., Sills, G. J., and White, H. S. (2021). The ups and downs of alkyl-carbamates in epilepsy therapy: how does cenobamate differ. *Epilepsia* 62 (3), 596–614. doi:10.1111/epi.16832

Makridis, K. L., Bast, T., Prager, C., Kovacevic-Preradovic, T., Bittigau, P., Mayer, T., et al. (2022). Real-world experience treating pediatric epilepsy patients with cenobamate. *Front. Neurol.* 13, 950171. doi:10.3389/fneur.2022.950171

Mohanraj, R., and Brodie, M. J. (2005). Pharmacological outcomes in newly diagnosed epilepsy. *Epilepsy Behav.* 6 (3), 382–387. doi:10.1016/j.yebeh.2005.01.008

Nakamura, M., Cho, J. H., Shin, H., and Jang, I. S. (2019). Effects of cenobamate (YKP3089), a newly developed anti-epileptic drug, on voltage-gated sodium channels in rat hippocampal CA3 neurons. *Eur. J. Pharmacol.* 855, 175–182. doi:10.1016/j.ejphar.2019.05.007

Peña-Ceballos, J., Moloney, P. B., Munteanu, T., Doyle, M., Colleran, N., Liggan, B., et al. (2023). Adjunctive cenobamate in highly active and ultra-refractory focal epilepsy: a "real-world" retrospective study. *Epilepsia*. 64(5):1225–1235. doi:10.1111/epi.17549

Perucca, E., Brodie, M. J., Kwan, P., and Tomson, T. (2020). 30 years of second-generation antiseizure medications: impact and future perspectives. *Lancet Neurol.* 19 (6), 544–556. doi:10.1016/S1474-4422(20)30035-1

Roberti, R., De Caro, C., Iannone, L. F., Zaccara, G., Lattanzi, S., and Russo, E. (2021). Pharmacology of cenobamate: mechanism of action, pharmacokinetics, drug-drug interactions and tolerability. *CNS Drugs* 35 (6), 609–618. doi:10.1007/s40263-021-00819-8

Sharma, R., Nakamura, M., Neupane, C., Jeon, B. H., Shin, H., Melnick, S. M., et al. (2020). Positive allosteric modulation of GABAA receptors by a novel antiepileptic drug cenobamate. *Eur. J. Pharmacol.* 879, 173117. doi:10.1016/j.ejphar.2020.173117

Smith, M. C., Klein, P., Krauss, G. L., Rashid, S., Seiden, L. G., Stern, J. M., et al. (2022). Dose adjustment of concomitant antiseizure medications during cenobamate treatment: expert opinion consensus recommendations. *Neurol. Ther.* 11 (4), 1705–1720. doi:10.1007/s40120-022-00400-5

Specchio, N., Pietrafusa, N., and Vigevano, F. (2021). Is cenobamate the breakthrough we have been wishing for. *Int. J. Mol. Sci.* 22 (17), 9339. doi:10.3390/ijms22179339

Sperling, M. R., Abou-Khalil, B., Aboumatar, S., Bhatia, P., Biton, V., Klein, P., et al. (2021). Efficacy of cenobamate for uncontrolled focal seizures: *post hoc* analysis of a Phase 3, multicenter, open-label study. *Epilepsia* 62 (12), 3005–3015. doi:10.1111/epi.17091

Varughese, R. T., Shah, Y. D., Karkare, S., and Kothare, S. V. (2022). Adjunctive use of cenobamate for pediatric refractory focal-onset epilepsy: a single-center retrospective study. *Epilepsy Behav.* 130, 108679. doi:10.1016/j.yebeh.2022.108679

Vernillet, L., Greene, S. A., and Kamin, M. (2020). Pharmacokinetics of cenobamate: results from single and multiple oral ascending-dose studies in healthy subjects. *Clin. Pharmacol. Drug Dev.* 9 (4), 428–443. doi:10.1002/cpdd.769

Villani, F., Cianci, V., Di Bonaventura, C., Di Gennaro, G., Galimberti, C. A., Guerrini, R., et al. (2022). Use of cenobamate for the treatment of focal epilepsy: an Italian expert opinion paper. *Expert Rev. Neurother.* 22 (11-12), 935–940. doi:10.1080/14737175.2023.2171291

Villanueva, V., Santos-Carrasco, D., Cabezudo-García, P., Gómez-Ibáñez, A., Garcés, M., Serrano-Castro, P., et al. (2023). Real-world safety and effectiveness of cenobamate in patients with focal onset seizures: outcomes from an Expanded Access Program. *Epilepsia Open* 8, 918–929. doi:10.1002/epi4.12757

Zaccara, G., Sisodiya, S. M., Giovannelli, F., Walker, M. C., Heaney, D. C., Angus-Leppan, H., et al. (2013). Network meta-analysis and the comparison of efficacy and tolerability of anti-epileptic drugs for treatment of refractory focal epilepsy. *Br. J. Clin. Pharmacol.* 76 (5), 827–828. doi:10.1111/bcp.12175

frontiers | Frontiers in Pharmacology

TYPE Original Research
PUBLISHED 08 January 2024
DOI 10.3389/fphar.2023.1308478

OPEN ACCESS

EDITED BY
Mahmoud Rafieian-Kopaei,
Shahrekord University of Medical Sciences, Iran

REVIEWED BY
Pablo Bascuñana,
San Carlos University Clinical Hospital, Spain
Wladyslaw—Lason,
Polish Academy of Sciences, Poland

*CORRESPONDENCE
David C. Henshall,
dhenshall@rcsi.ie

RECEIVED 06 October 2023
ACCEPTED 18 December 2023
PUBLISHED 08 January 2024

CITATION
Mamad O, Heiland M, Lindner AU, Hill TDM, Ronroy RM, Rentrup K, Sanz-Rodriguez A, Langa E, Heller JP, Moreno O, Llop J, Bhattacharya A, Palmer JA, Ceusters M, Engel T and Henshall DC (2024), Anti-seizure effects of JNJ-54175446 in the intra-amygdala kainic acid model of drug-resistant temporal lobe epilepsy in mice. *Front. Pharmacol.* 14:1308478. doi: 10.3389/fphar.2023.1308478

Anti-seizure effects of JNJ-54175446 in the intra-amygdala kainic acid model of drug-resistant temporal lobe epilepsy in mice

Omar Mamad[1,2], Mona Heiland[1,2], Andreas U. Lindner[1], Thomas D. M. Hill[1,2], Ronan M. Ronroy[3], Kilian Rentrup[2], Amaya Sanz-Rodriguez[1,2], Elena Langa[1,2], Janosch P. Heller[1,2,4], Oscar Moreno[5], Jordi Llop[5], Anindya Bhattacharya[6], James A. Palmer[6], Marc Ceusters[7], Tobias Engel[1,2] and David C. Henshall[1,2]*

[1]Department of Physiology and Medical Physics, RCSI University of Medicine and Health Sciences, Dublin, Ireland, [2]FutureNeuro SFI Research Centre, RCSI University of Medicine and Health Sciences, Dublin, Ireland, [3]Division of Population Health Sciences, RCSI University of Medicine and Health Sciences, Dublin, Ireland, [4]School of Biotechnology, Dublin City University, Dublin, Ireland, [5]CIC biomaGUNE, Basque Research and Technology Alliance (BRTA), San Sebastián, Spain, [6]Neuroscience, Janssen Pharmaceutical Research and Development, LLC, San Diego, CA, United States, [7]Neuroscience, Janssen Pharmaceutical Research and Development, Janssen Pharmaceutica NV, Beerse, Belgium

There remains a need for new drug targets for treatment-resistant temporal lobe epilepsy. The ATP-gated P2X7 receptor coordinates neuroinflammatory responses to tissue injury. Previous studies in mice reported that the P2X7 receptor antagonist JNJ-47965567 suppressed spontaneous seizures in the intraamygdala kainic acid model of epilepsy and reduced attendant gliosis in the hippocampus. The drug-resistance profile of this model is not fully characterised, however, and newer P2X7 receptor antagonists with superior pharmacokinetic profiles have recently entered clinical trials. Using telemetry-based continuous EEG recordings in mice, we demonstrate that spontaneous recurrent seizures in the intraamygdala kainic acid model are refractory to the common anti-seizure medicine levetiracetam. In contrast, once-daily dosing of JNJ-54175446 (30 mg/kg, intraperitoneal) resulted in a significant reduction in spontaneous recurrent seizures which lasted several days after the end of drug administration. Using a combination of immunohistochemistry and *ex vivo* radiotracer assay, we find that JNJ-54175446-treated mice at the end of recordings display a reduction in astrogliosis and altered microglia process morphology within the ipsilateral CA3 subfield of the hippocampus, but no difference in P2X7 receptor surface expression. The present study extends the characterisation of the drug-resistance profile of the intraamygdala kainic acid model in mice and provides further evidence that targeting the P2X7 receptor may have therapeutic applications in the treatment of temporal lobe epilepsy.

KEYWORDS

anti-seizure medicines, inflammation, interleukin 1β, drug-resistant epilepsy, hippocampal sclerosis

Introduction

Epilepsy is characterised by recurring spontaneous seizures and is among the most common and disabling brain diseases (Devinsky et al., 2018). Frontline treatment for epilepsy is based on small molecule drugs that target ion channels and neurotransmitter systems, including levetiracetam and other synaptic vesicle glycoprotein 2A (SV2A)-modulating compounds (Kwan et al., 2011; Loscher et al., 2016). Unfortunately, about one-third of patients fail to achieve seizure control and current anti-seizure medicines do not modify the underlying pathophysiology (Simonato et al., 2012; Loscher et al., 2020). Accordingly, new treatments are urgently required for treatment-resistant epilepsy, including patients with temporal lobe epilepsy (TLE) (Loscher et al., 2013).

Molecular and cellular analyses of resected brain tissue from patients, as well as from experimental models, has identified elevated inflammatory signalling in TLE (Vezzani et al., 2011; Aronica et al., 2017; Vezzani et al., 2019). This includes raised levels of cytokines and activation of capase-1, which catalyses maturation of interleukin 1β (IL-1β), a potent neuromodulator and activator of gliosis (Allan et al., 2005). The caspase-1/IL-1β system lies downstream of the surface expressed ATP-gated P2X7 receptor (Beamer et al., 2017; Dutta et al., 2022). In the brain, the P2X7 receptor is expressed by resident and activated microglia and has been reported to be present on other cell types, particular after injury (Sim et al., 2004; Anderson and Nedergaard, 2006; Kaczmarek-Hajek et al., 2018). Activation of the receptor coordinates neuroinflammatory responses that initially resolve tissue injury (Roth et al., 2014; Di Nunzio et al., 2021), but prolonged or excessive activation may contribute to pathological states of hyper-excitability (Aronica et al., 2017; Vezzani et al., 2019). Over-expression of the P2X7 receptor is found within the seizure focus in experimental and human epilepsy (Rappold et al., 2006; Jimenez-Pacheco et al., 2016; Wei et al., 2016), an observation recently extended by the use of P2X7 receptor radiotracers (Mikkelsen et al., 2023; Morgan et al., 2023). Antagonism or genetic disruption of the P2X7 receptor has been reported to reduce evoked seizures in rodents (Beamer et al., 2017). Recently, treatment of mice with the P2X7 receptor antagonist JNJ-47965567 was found to reduce the frequency of spontaneous seizures in a mouse TLE model (Jimenez-Pacheco et al., 2016). Notably, seizure suppression continued beyond the period of active dosing and was associated with reduced gliosis in the hippocampus (Jimenez-Pacheco et al., 2016), suggesting a potential disease-modifying effect.

The intraamygdala kainic acid (IAKA) model in mice has become increasingly adopted for studies on TLE (Henshall, 2017; Rusina et al., 2021; West et al., 2022). The status epilepticus triggered by IAKA causes damage to the ipsilateral hippocampus and within a few days the emergence of recurrent spontaneous seizures (Mouri et al., 2008). The model reflects aspects of the neuropathology and gene expression landscape of human TLE (Conte et al., 2020), has been adapted to various background strains and used to demonstrate effects of multiple genes, including the P2X7 receptor (Engel et al., 2012; Beamer et al., 2022). Recent studies show the epileptic seizures in the IAKA model are refractory to various conventional anti-seizure medicines (Welzel et al., 2020; West et al., 2022). The profile of levetiracetam in the model is unknown.

JNJ-54175446 is a recently discovered potent, selective and brain-penetrant P2X7 receptor antagonist which has entered clinical trials for other CNS disorders (Letavic et al., 2017; Recourt et al., 2020; Recourt et al., 2023). Here, we extend the characterization of the drug-resistance profile of the IAKA model by testing the effects of levetiracetam. We then assessed the effects of JNJ-54175446 on spontaneous seizures and analyzed gliosis in the brains of mice previously treated with JNJ-54175446. We report that the model is refractory to levetiracetam. In contrast, JNJ-54175446 resulted in a modest reduction in spontaneous seizures which was most apparent following the period of active dosing.

Materials and methods

Animals

All experimental procedures involving animals were carried out in accordance with the European Communities Council Directive (2010/63/EU). Procedures using adult male C57BL/6JOlaHsd mice (25–30 g, Harlan) were approved by the Research Ethics Committee (REC 1587) of the RCSI University of Medicine and Health Sciences, under license from the Ireland Health Products Regulatory Authority (AE19127/P057). Animals were housed on a 12 h light-dark cycle under controlled conditions (temperature: 20°C–25°C; humidity: 40%–60%). Food and water were available *ad libitum*.

Intraamygdala kainic acid (IAKA) model

Epilepsy was induced using the IAKA model technique (Jimenez-Pacheco et al., 2016). Briefly, male C57BL/6JOlaHsd mice (weight: 28–30 g; age 10 weeks) were anaesthetised with isoflurane (5% induction, 2% maintenance) and placed in a mouse-adapted stereotaxic frame. An EEG transmitter unit (model HDX-02; Data Systems International (DSI), MN, United States of America) was implanted under the skin in a subcutaneous pocket along the dorsal flank of the mouse. The EEG signal was recorded from skull-fixed screws over the dorsal hippocampi. A guide cannula was placed above the right basolateral amygdala (coordinates from adjusted Bregma: anterior-posterior (A/P) = −0.95 mm; lateral (L) = −2.85 mm). After 48 h recovery, all animals received an intraamygdala microinjection of KA (0.3 μg in 0.2 μL volume). Status epilepticus developed and was recorded using the surface EEG. After 40 min, all mice received an intraperitoneal (IP) injection of lorazepam (8 mg/kg; Pfizer) in order to reduce morbidity and mortality. Mice were returned to their home cages and stayed under climate-controlled conditions and video monitoring combined with telemetry. EEG was recorded from individually-housed, freely-moving mice for 24 h/day up to 5 weeks after KA injection. After the recording period, animals were transcardially perfused with phosphate-buffered saline (PBS) and whole brains were collected and directly flash-frozen.

EEG and seizure analysis

The number and duration of spontaneous seizures were determined by individually reviewing EEG records, as described

previously using LabChart 8 Reader (AD Instruments, Oxford, UK) (Jimenez-Pacheco et al., 2016). Spontaneous seizures were defined as high-frequency (>5 Hz), high-amplitude (more than two times baseline) polyspike discharges of ≥10 s duration that were present on both EEG channels. Seizure termination was defined as a return of EEG amplitude and frequency to baseline values with or without postictal amplitude suppression.

Drug administration

Due to solubility and oral bioavailability, delivery of levetiracetam to mice was achieved by dissolving in drinking water, guided by previous studies (Klitgaard et al., 1998; Russo et al., 2010). The ED_{50} (i.e., the dose protecting 50% of the animals) for levetiracetam in the pentylenetetrazol kindling test in mice is 36 mg/kg intraperitoneal (IP) and is 7 mg/kg (IP) in the corneal electroshock kindling the ED_{50} in mice. In rats, levetiracetam reduces pilocarpine-induced seizures at an ED_{50} of 17 mg/kg (IP) and protects against kainic acid seizures at an ED_{50} of 54 mg/kg (IP) (Klitgaard et al., 1998). Based on this, we aimed to reach dosing of ~80 mg/kg per day, by dissolving 200 mg of levetiracetam in 300 mL of drinking water. Drinking water bottles were covered to exclude light and prepared freshly twice a week. We confirmed this achieved suitable dosing by comparing plasma and brain levels of levetiracetam in mice after consuming the drinking water to the levels achieved following an acute IP injection. Blood samples for plasma analysis of levetiracetam were obtained via submandibular blood draws, as previously described (Brennan et al., 2020). The concentration of levetiracetam in samples was determined by LC-MS/MS.

JNJ-54175446 was dissolved in DMSO (10%) and PEG400 (90%). During the original characterization of JNJ-54175446, the EC_{50} for P2X7 receptor occupancy was a plasma concentration of 105 ng/mL (Letavic et al., 2017). Above 80% receptor occupancy occurs above 1000 ng/mL. An oral administration of 10 mg/kg JNJ-54175446 resulted in >80% receptor occupancy lasting 24 h (Letavic et al., 2017). To determine plasma and brain levels, a set of control and IAKA mice (2 week time-point) received a once daily IP injection of JNJ-54175446. The concentration of JNJ-54175446 was determined by LC-MS/MS. For dosing during epilepsy studies, mice were injected IP at a dose of 30 mg/kg once per day (Letavic et al., 2017) for five consecutive days (n = 8/group). To improve handling and reduce stress and potential displacement of EEG electrodes/telemetry, vehicle and JNJ-54175446-treated mice were briefly and lightly anaesthetised during each IP injection with isoflurane.

Histology

Whole brains were sectioned (12 μm coronal) on a cryostat (CM 1900, Leica), and mounted on glass slides. Slide-mounted sections were fixed using 4% paraformaldehyde (PFA), then permeabilized and blocked in bovine serum albumin followed by incubation with antibodies against glial fibrillary acidic protein (GFAP) (1:400; Sigma), and ionized calcium binding adaptor molecule 1 (IBA1) (1:400; GeneTex) overnight at 4°C. Sections were washed and then incubated with rabbit polyclonal secondary antibodies coupled to AlexaFluor 488 or AlexaFluor 568 (Invitrogen). To confirm specificity, additional sections were incubated without the primary antibody. Nuclei were labelled by staining with DAPI (4′,6′-diamidino-2-phenylindole dihydrochloride; Vector Laboratories), and sections were examined using a Leica DM4000 epifluorescence microscope. Counts of GFAP+ and IBA1+ cells were performed blind to treatment. One dorsal (−2.8 AP) and one ventral (−2.2 AP) representative region within each hippocampal subfield was selected, and cells were counted under ×20 lens magnification. Representative images of the GFAP/IBA1 staining were taken using the same exposure time without knowledge of the treatment group. We performed an additional analysis of the microglia in the CA3 subfield, by assessing the number and length of processes, as described (Young and Morrison, 2018).

Radiochemistry and *in vitro* autoradiography

Visualisation of P2X7 receptor binding in the brain was performed by autoradiography. ^{18}F-JNJ-64413739 synthesis was performed using a TRACERlab FX_{FN} synthesis module (GE Healthcare) following a previously described method with minor modifications (Morgan et al., 2023). In brief, $[^{18}F]F^-$ was generated in a Cyclone 18/9 cyclotron (IBA) by proton irradiation of ^{18}O-enriched water via the $^{18}O(p,n)^{18}F$ nuclear reaction, and trapped on a preconditioned Sep-Pak Accell Plus QMA Light cartridge (Waters). The trapped $[^{18}F]F^-$ was eluted with a solution of Kryptofix $K_{2.2.2}/K_2CO_3$ in a mixture of acetonitrile/water (2:1, 1.5 mL). After complete elimination of the solvent by azeotropic evaporation, a solution containing the precursor (JNJ-64410047, 4 mg) in DMSO (0.7 mL) was added, and the mixture was heated at 120°C for 15 min. After cooling to room temperature, the mixture was purified by high-performance liquid chromatography (HPLC) using a Phenomenex Luna C18 (250 mm) column as the stationary phase and water (0.1% trifluoroacetic acid [TFA])/acetonitrile (65/35, vol/vol) as the mobile phase (flow rate = 4 mL/min). The desired fraction (retention time = 18.0 min) was collected, diluted with a sodium ascorbate solution, and reformulated using a C-18 light cartridge (Sep-Pak Plus, Waters). The resulting ethanol solution (1 mL) was directly used for the *in vitro* studies. Chemical and radiochemical purity were determined by radio-HPLC, and identity of the desired tracer was confirmed by co-elution with reference standard. An Agilent Eclipse XBD-C18 (4.6 × 150 mm, 5 μm) was used as the stationary phase and water (0.1% TFA)/acetonitrile (70/30, vol/vol) as the mobile phase at a flow rate of 1 mL/min (retention time = 12.5 min). Decay-corrected radiochemical yield was 6.9% ± 0.5% (total synthesis time: 90 min). Radiochemical purity was >99% and a molar activity of 47.3 GBq/μmol was obtained at the end of the synthesis.

Coronal brain slices (12 μm) were thawed and pre-incubated for 15 min with Tris-HCl buffer (50 mM, pH 7.4, supplemented with 1 mM $MgCl_2$, 1 mM $CaCl_2$, 2 mM KCl and 1% of bovine serum albumin) at room temperature. Subsequently, the slices (four to six slices per animal, 5 animals per group) were incubated with 1.4 nM of ^{18}F-JNJ-64413739 in buffer solution during 30 min at room temperature. For the determination of non-specific binding,

successive slices were incubated with the same radioligand solution containing 10 μM of non-labelled JNJ-64413739 (homologous blocking). After incubation, the slices were removed from the baths, washed twice in ice-cold buffer (50 mM Tris-HCl, pH 7.4, 4°C) and dipped once in ice-cold ultra-pure water. After drying over a heating plate (40°C), the slices were exposed to a phosphor sensitive plate for 5 min and the plate was scanned in a phosphor imager (Amersham Typhoon 5, GE, United States of America) at the highest resolution (10 μm). For image quantification, a region of interest was defined in the whole coronal brain slice with a specific software (ImageQuantTL, GE, United States of America) and a mean pixel intensity value was obtained for each slice. For each pair of slices, the percentage of blocking (specific binding) was calculated as [(No block- Block)/No block)] x 100. Statistical analysis (Nested *t*-test) was performed using Graphpad Prism (version 9).

Statistics

The effects of JNJ-54175446 on spontaneous seizures were analysed with Stata Release 16.1. Ordinal logistic regression was used to test for the effect of treatment on seizure count within each of the three trial periods. Regression models included a term for day of trial and used robust variance estimation to account for clustering of observations within animals. Data was also separately graphed for data visualisation purposes. For other data, statistical analyses were performed using GraphPad Prism (version 9). Data were tested for normal distribution using D'Agostino and Pearson omnibus normality test or Shapiro-Wilk test for small n numbers. Parametric statistics used an unpaired two-tailed Student's t-test (with Welch correction when assuming non-equal standard error of mean (SEM)) and data are presented as mean ± SEM. Non-parametric analyses used Mann-Whitney U test and data are presented as median ± interquartile range. For comparison of data with multiple parameters, a two-way repeated measures ANOVA was used. The individual tests used for each comparison are specified in the text. Data was considered significant at p-value ≤0.05.

Results

Spontaneous seizures in the IAKA model are refractory to levetiracetam

The pharmacological profile of the IAKA model has recently been explored and includes resistance to phenytoin and carbamazepine, and partial responses to phenobarbital, valproate and diazepam (West et al., 2022). Prior to testing JNJ-54175446, we sought to extend this characterisation by testing the response to levetiracetam, a common first-line drug to treat TLE (Kwan et al., 2011). Injection of 40 and 60 mg/kg levetiracetam (IP) resulted in plasma levels of 4000–5000 ng/mL at 4 h which declined to ~1000 ng/mL by 8 h (Figure 1A). Next, mice were given levetiracetam dissolved in the drinking water and after 10 or 20 days, brain and plasma levels were determined. Dissolving 200 mg levetiracetam per 300 mL resulted in plasma and brain levels in mice similar to those achieved following IP dosing which are known to suppress seizures in various animal models (Figures 1B,C).

We next subjected a group of mice to IAKA. All mice developed status epilepticus and, within a few days, began displaying spontaneous seizures, consistent with the known profile in the model (Jimenez-Pacheco et al., 2016). Two weeks after IAKA when chronic epilepsy is established, the drinking water was switched to contain levetiracetam and rates of spontaneous seizures were followed for another week. Spontaneous seizures continued in mice after being switched to levetiracetam (Figure 1D). Rates were not statistically different when comparing 2 days before treatment to 2 days after (Figures 1D,E). These findings demonstrate that the spontaneous seizures in the IAKA model of TLE are largely refractory to levetiracetam.

Plasma and brain levels of JNJ-54175446 after IP dosing

JNJ-54175446 was delivered via once-daily IP dosing at 30 mg/kg (Letavic et al., 2017). We first checked whether the presence of epilepsy would affect uptake in the brain, since the original pharmacokinetics studies were performed in healthy rodents (Letavic et al., 2017). Naïve mice and IAKA mice (2-week time-point) received a 30 mg/kg IP injection of JNJ-54175446. Brain and plasma samples were collected 3 hours after IP injection and processed for measurement of JNJ-54175446. Analysis revealed the IP injection of JNJ-54175446 (30 mg/kg) produced a high concentration of JNJ-54175446 in both the plasma and brain of control and epileptic mice, above what has been shown to produce 80% receptor occupancy level (Letavic et al., 2017). (Figures 2A,B). Thus, IP injection of JNJ-54175446 at 30 mg/kg to mice provides brain exposures that produce high levels of antagonism of the P2X7 receptor.

JNJ-54175446 reduces spontaneous seizures in the IAKA model

To investigate the effect of JNJ-54175446 in the model, spontaneous seizures were recorded until day 14 after status epilepticus. Then, mice began to receive once-daily IP injections of JNJ-54175446 (30 mg/kg) or vehicle for 5 days. Dosing was then terminated and spontaneous seizures recorded for a further 13 days to allow drug wash-out, with mice killed on day 14.

Spontaneous recurrent seizures emerged within a few days of status epilepticus, consistent with the normal course of epilepsy in the model, and there was a small increase in seizure frequency over time between the first and second week (Figure 2C; Supplementary Figure S1A). At baseline, there were no differences in spontaneous recurrent seizures between the mice in the vehicle group and the mice that would go on to receive JNJ-54175446 (Figures 2C,D; Supplementary Figures S1A, B). During active dosing with JNJ-54175446, there was a small but non-significant reduction in spontaneous seizure rates in mice (Figures 2C,D; Supplementary Figures S1A, B). After dosing with JNJ-54175446/vehicle finished, spontaneous seizures continued to be monitored. Seizures in vehicle-treated mice continued at an average of ~10 per day. In contrast, seizure rates in JNJ-54175446-treated mice remained low and there was a significant difference between JNJ-54175446-treated mice and vehicle-treated mice during the washout period

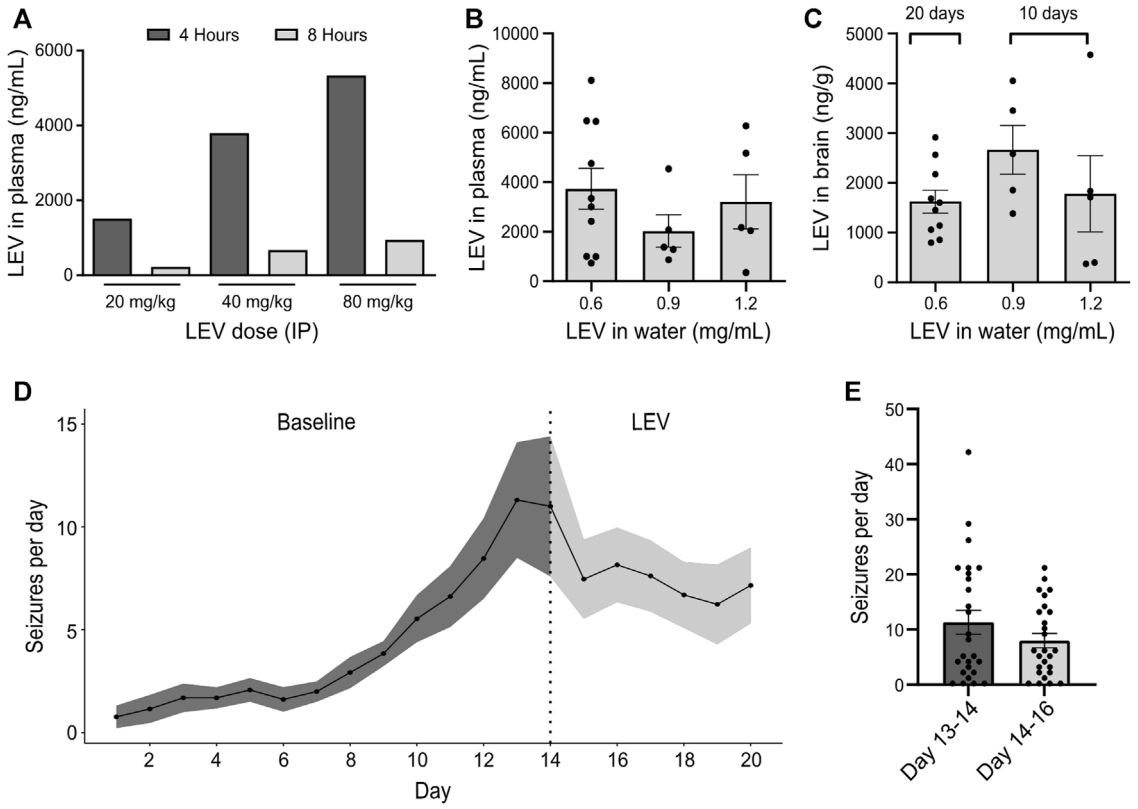

FIGURE 1
Effect of levetiracetam in the IAKA model of TLE **(A)** Dose range-finding pilot to gauge plasma levels of levetiracetam (LEV) 4 and 8 h following IP injection at various doses (n = 1/group). **(B)** Quantification of levetiracetam in plasma following 10 days of oral administration at different doses dissolved in water. Note that a dose of 0.6 mg/mL drinking water was sufficient to reach plasma levels comparable to those following an IP dose of 40 mg/kg (p = 0.437, one-way ANOVA, n = 5–10/group). **(C)** Summary of levetiracetam concentration in the brain following oral administration. Note that brain levels following a water concentration of 0.6 mg/mL was sufficient to reach brain levels of above 1000 ng/g, a concentration previously known to reduce seizure activity. **(D)** Spontaneous seizures following IAKA (n = 13). Note seizures continue after beginning levetiracetam treatment. **(E)** Graph comparing spontaneous seizure rates during the last 2 days of the baseline to the rates during the 2 days after treatment with levetiracetam. The change was not statistically significant (p = 0.191, unpaired t-test, seizure counts collected from n = 13 animals/day).

(Figures 2C,D; Supplementary Figures S1A, B). That is, there was no difference in the seizure rate during the baseline phase (p = 0·858). In the treatment phase, the JNJ-54175446 group had a marginally lower overall seizure rate but this was not statistically significant (p = 0·096). However, in the post-treatment phase, the JNJ-54175446 group had a significantly lower seizure rate (p = 0·022). There was no effect of JNJ-54175446 on seizure durations during the dosing period or after dosing (Supplementary Figure S2).

Effects of JNJ-54175446 on gliosis in the IAKA model

Previous studies showed a 5-day treatment with JNJ-47965567 attenuates astrogliosis and microgliosis in the IAKA model (Jimenez-Pacheco et al., 2016). Accordingly, we analysed hippocampal sections from the vehicle and JNJ-54175446-treated mice at the end of recordings. Semi-quantitative analysis of astrogliosis in the hippocampus of vehicle control mice using GFAP immunostaining identified strong staining, particularly around the CA3 subfield ipsilateral to the site of IAKA (Figures 3A–E). GFAP staining was similar in brains from JNJ-54175446-treated mice in the CA1 and dentate gyrus, but was significantly reduced in the CA3 subfield (Figures 3A–E). Microgliosis was assessed by staining for IBA1. Strong staining for IBA1 was detected in the CA3 subfield of mice in both groups, as well as staining in both the CA1 and dentate gyrus but there were no differences in cell counts between vehicle- and JNJ-54175446-treated mice (Figures 3F–J). Consequently, we performed a further analysis of the morphology of IBA1-positive microglia processes, which may reflect differences in activation state (Paolicelli et al., 2022), in the CA3 subfield. This revealed IBA1-positive microglia in JNJ-54175446-treated mice displayed higher numbers of endpoints and longer process lengths compared to vehicle-treated mice (Supplementary Figure S3).

Ex vivo autoradiography

Finally, to complement and extend the histologic findings, we sought to visualise P2X7 receptor levels in the brains of the mice. Here we employed an *ex vivo* radiotracer approach using ^{18}F-JNJ-64413739 that we recently used to demonstrate enhanced P2X7 receptor levels in brain sections from patients with TLE (Morgan et al., 2023). The radiotracer ^{18}F-JNJ-64413739 was applied to brain tissue sections from either vehicle or JNJ-

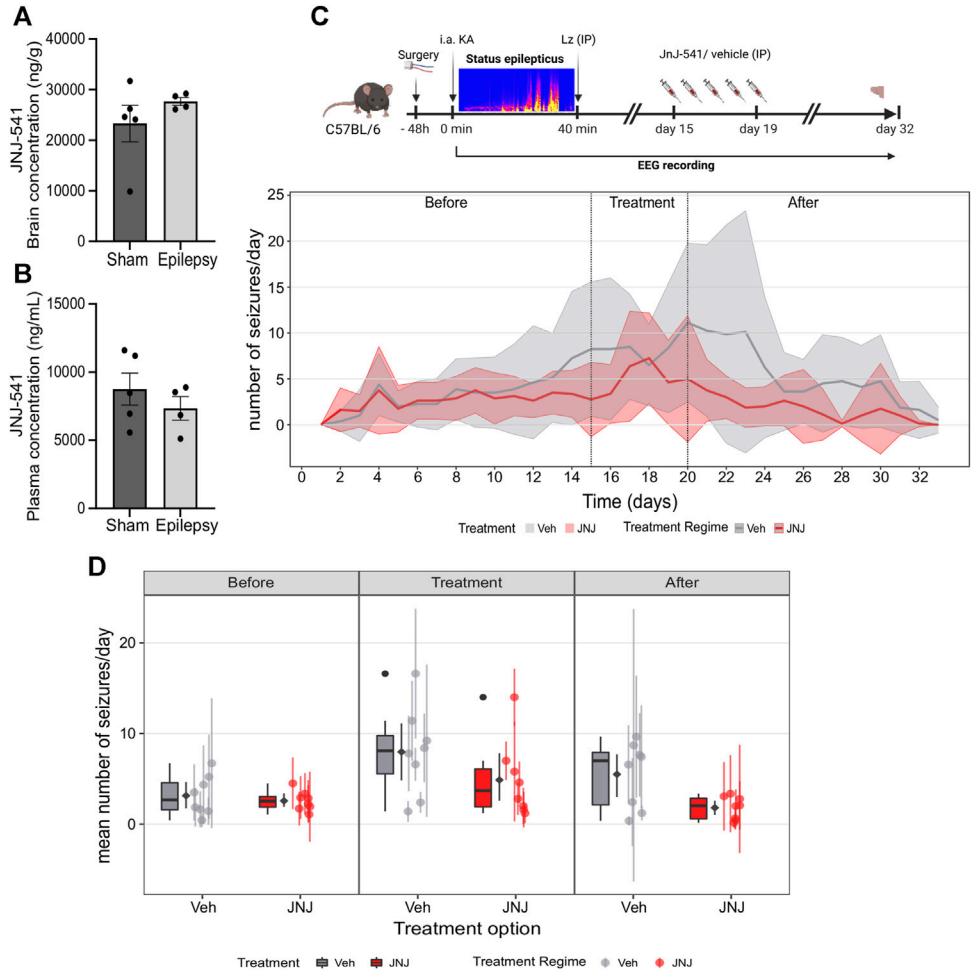

FIGURE 2
Effect of JNJ-54175446 on spontaneous seizures in the IAKA model. **(A)** Plasma levels of JNJ-54175446 (JNJ-541) measured 3 hours following a 30 mg/kg IP injection of the drug in naïve and IAKA animals (p = 0.387, unpaired t-test, n = 4–5/group). Levels exceed what has been shown to produce 80% receptor occupancy level. **(B)** Levels of JNJ-54175446 in the brain showed no difference (p = 0.299, unpaired t-test, n = 4–5/group) between naïve and IAKA animals following the same 30 mg/kg IP injection. **(C)** Schematic of experiment and (below) graph showing spontaneous seizures in the two groups. During JNJ-54175446 dosing there was a non-significant reduction in seizure frequency, but following drug washout, seizure frequency in JNJ-54175446-treated mice remained significantly lower than in vehicle-treated counterparts (n = 8/group). **(D)** Mean number of seizures for vehicle vs. JNJ-54175446-treated mice, showed a significantly lower seizure frequency in JNJ-54175446-treated mice following drug washout. Coloured scatters show animals median ± mad; diamond scatter indicates mean ± sd of mean values. Dark scatters show outliers excluded from mean, box and whiskers.

54175446 groups and specific binding was confirmed under homologous blocking conditions (Figure 4A, Supplementary Figures S4A, S5). This revealed variable staining intensity between individual mice and groups. Semi-quantification of the tracer levels in whole brain sections revealed no statistical difference between groups in specific ^{18}F-JNJ-64413739 labeling (Figures 4B,C). Similar results were obtained when the hippocampus and neocortex were separately analysed (Supplementary Figure S4B).

Discussion

Attenuating neuroinflammation is a promising strategy for treatment-resistant epilepsies. Here we show that JNJ-54175446, a potent and selective antagonist of the P2X7 receptor, has anti-seizure effects in the IAKA model of treatment-resistant TLE in mice. We also extend the characterisation of the pharmacoresistance profile of the model, reporting the spontaneous seizures in the model are largely refractory to levetiracetam. Together, these findings support further investigation into the use of P2X7 receptor antagonists for the treatment of drug-resistant TLE and perhaps other epilepsies associated with a neuroinflammatory component.

Ongoing studies support neuroinflammation as a pathomechanism in treatment-resistant epilepsy and thus a target to achieve disease-modifying effects which are currently not provided by frontline anti-seizure medicines (Aronica et al., 2017; Beamer et al., 2017; Vezzani et al., 2019; Vezzani et al., 2022). This has led to recent clinical studies targeting the caspase-1/IL-1β system for treatment-resistant seizures, particularly where an inflammatory component is known or suspected (Lai et al., 2020; Yamanaka et al., 2021). The optimal approach to safe and protective modulation of neuroinflammation in epilepsy remains uncertain. Here, we tested

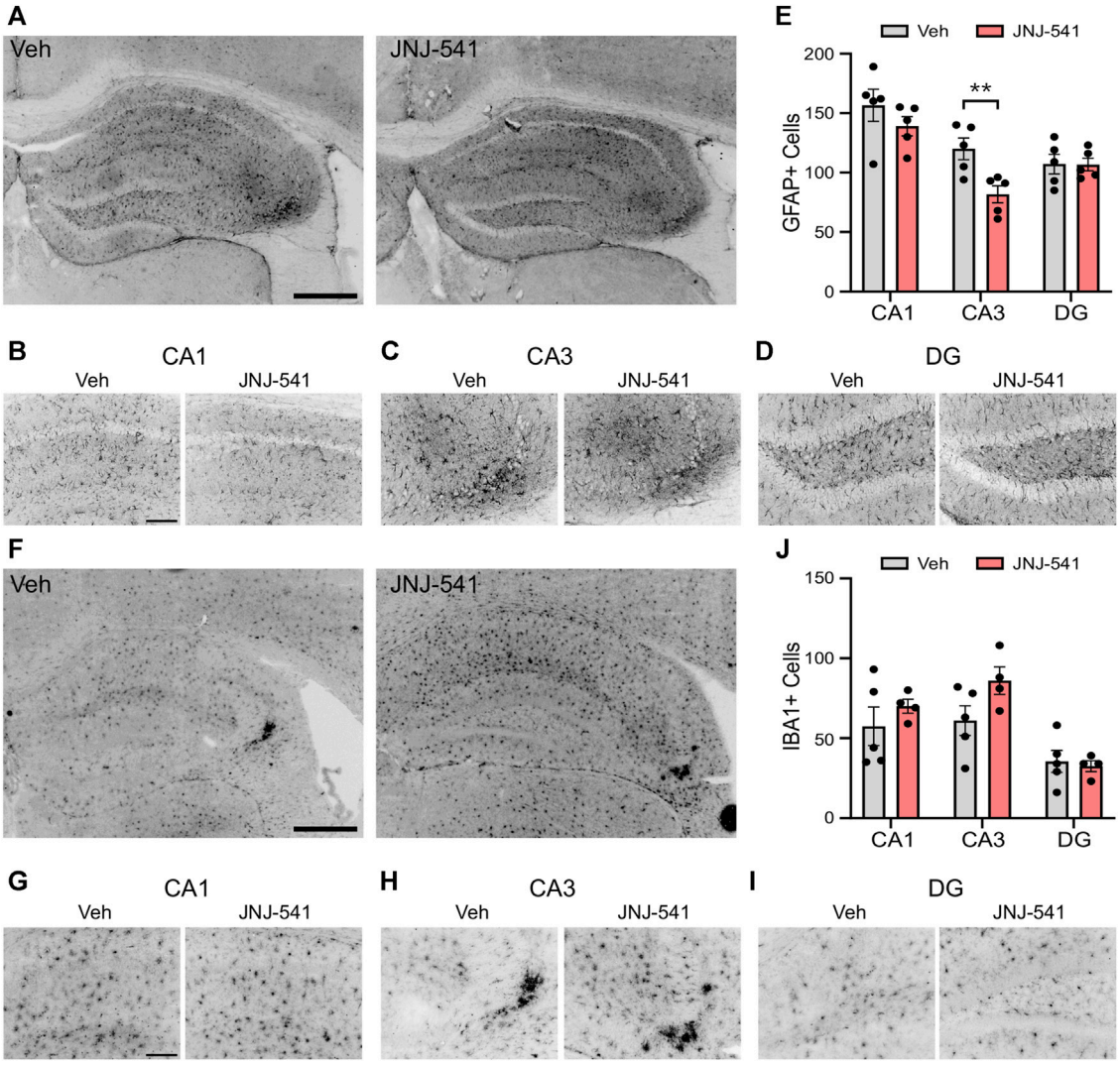

FIGURE 3
Gliosis in mice treated with JNJ-54175446 in the IAKA model. **(A–D)** Photomicrographs of representative GFAP staining in the hippocampus from vehicle and JNJ-54175446 (JNJ-541)-treated epileptic mice at the end of the experiment, showing ×5 field views (A) and ×20 lens magnifications **(B–D)** of individual subfields from the same animal. Note, lower numbers of GFAP + cells in the CA3 region of mice treated with JNJ-54175446 compared to mice treated with vehicle. Astrogliosis was similar in other subfields. **(E)** Quantification of GFAP + cells in each hippocampal subfield from vehicle and JNJ-54175446-treated mice, perfused 2 weeks after drug washout at the end of recordings (p = 0.034, two-way repeated measures ANOVA, n = 5/group). **(F–I)** Photomicrographs of representative IBA1 staining in the hippocampus from vehicle- and JNJ-54175446-treated epileptic mice, showing ×5 field views (F) and ×20 lens magnifications **(G–I)** of individual subfields from the same animal. Note similar staining between mice treated with vehicle as compared with JNJ-54175446. **(J)**, Quantification of IBA1+ cells found in each hippocampal subfield from vehicle- and JNJ-54175446-treated mice perfused 14 days after drug washout at the end of recordings (p = 0.219, mixed-effects analysis, n = 4–5/group). Scale bars: **(A,F)**, 500 µm; **(B–D)**, **(G–I)**, 100 µm.

an antagonist of the P2X7 receptor in a model of treatment-resistant TLE in mice. The P2X7 receptor represents a promising target since it lies upstream of the IL-1β pathway and is activated by high concentrations of extracellular ATP which likely occur mainly in the setting of tissue damage or excessive neuronal excitation (Beamer et al., 2017). This potentially avoids off-target effects of blocking the receptor outside the seizure focus or site of neuropathology (Beamer et al., 2017). The present study employed a potent, selective and brain-penetrant P2X7 receptor antagonist that has recently entered clinical trials (Letavic et al., 2017; Recourt et al., 2020; Recourt et al., 2023). The main finding here was that mice in the IAKA model treated with a short course of once-daily IP injections of JNJ-54175446 had fewer spontaneous seizures compared to vehicle-treated animals. This indicates that pharmacological blockade of the P2X7 receptor may be a suitable strategy for treatment-resistant epilepsy. If translated to a human trial setting, the observed three-fold lower seizure rates produced by JNJ-54175446 may represent a clinically-meaningful improvement in symptom control. Taking account of changes in the vehicle group, the main effect of JNJ-54175446 may have been to blunt the normal progression in seizure frequency in the model. Moreover, JNJ-54175446 was not superior to the previously tested P2X7 receptor antagonist JNJ-47965567 in the same (Jimenez-Pacheco et al., 2016). This raises the possibility that a ceiling has been reached with the amount of seizure suppression that can be achieved by targeting this

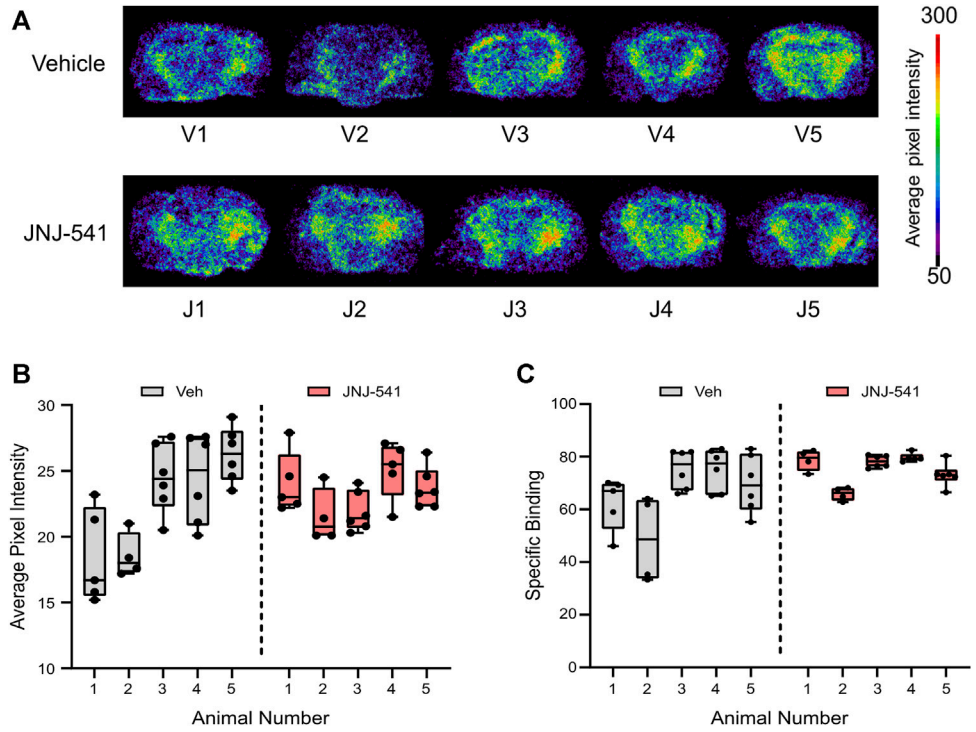

FIGURE 4
Ex vivo P2X7 receptor radiotracer binding after long-term recordings **(A)** Phosphor imaging of whole brain coronal slices showing localized average pixel intensity of bound P2X7 receptor radiotracer (n = 5/group). V1-V5 were treated with vehicle while J1-J5 were treated with the specific P2X7 receptor antagonist JNJ-54175446. **(B)** Average pixel intensity under non-blocking conditions of bound P2X7 receptor radiotracer on several whole brain slices of vehicle–and JNJ-54175446-treated epileptic mice. Nested *t*-test showed no statistically significant differences between groups. **(C)** Specific binding of P2X7 receptor radiotracer given as percentage of blocking ([(No block-block)/No block)] x 100).

receptor. Nevertheless, other properties including the requirement for less frequent dosing needed with JNJ-54175446 might influence decisions on selection for further development. A notable finding was that anti-seizure effects of JNJ-54175446 were most apparent at later time points, a delay also found in tests with JNJ-47965567 (Jimenez-Pacheco et al., 2016). As with the previous study (Jimenez-Pacheco et al., 2016), we did not observe an effect of P2X7 receptor inhibition on the duration of spontaneous seizures. Thus, antagonism of the P2X7 receptor appears to reduce the likelihood of a seizure occurring but does not influence the features of the event once a seizure is underway in this model. This contrasts with studies that found antagonism of the P2X7 receptor reduced the severity but not the frequency of spontaneous seizures in rats (Amhaoul et al., 2016). The explanation for the difference is unclear and may relate to the species, model, compound tested or dosing regimen. Regardless, the present study extends the evidence that targeting the P2X7 receptor can reduce seizures in experimental treatment-resistant TLE. Any preclinical development should take account of species-specific differences in the properties of rodent and human P2X7 receptors (Roger et al., 2010). In this regard, future studies could explore the present compound or subsequent iterations in other rodent or large animal models. For example, canines with naturally-occurring epilepsy would offer a potential translational model before moving to human studies (Loscher, 2022). Results with P2X7 receptor antagonists in other models (Fischer et al., 2016; Smith et al., 2023) suggest it may also be relevant to explore whether dosing with JNJ-54175466 immediately after status epilepticus has anti-epileptogenic effects in the model.

The mechanism of seizure suppression by JNJ-54175446 is unknown and was not explored presently. Since gliosis is an important driver of epileptogenesis and ictogenesis, the observed effects may derive from attenuation of gliosis. Indeed, both here and previously (Jimenez-Pacheco et al., 2016), we observed reductions in gliosis in mice after dosing with a P2X7 receptor antagonist. The model features select neuronal loss and gliosis, particularly within the ipsilateral CA3 subfield (Mouri et al., 2008; Jimenez-Pacheco et al., 2016), which is probably the site of ictogenesis (Li et al., 2008). Notably, this is the area where astrogliosis was reduced in the JNJ-54175446-treated mice. Moreover, the time-frame of the anti-seizure effects, emerging several days after dosing began, is slower than observed for conventional anti-seizure medicines in the model which have neuron-based mechanisms of action (West et al., 2022), and is more consistent with other cell type or higher-scale changes to network function. The reduction in astrogliosis may be secondary to reduced production of IL-1β, which is a potent trigger of astrogliosis (Allan et al., 2005; Vezzani et al., 2022). Here, JNJ-54175446 did not reduce microgliosis, as evidenced by microglia counts and indirectly via radiotracer studies for the P2X7 receptor. This was unexpected since microglia are the predominant cell type expressing the P2X7 receptor in mice (Kaczmarek-Hajek et al., 2018) and P2X7 receptor activation promotes microgliosis (Monif et al., 2009). We did, however, note a difference in the morphology of microglial

processes which may be relevant to their influence on pathophysiology (Paolicelli et al., 2022). The finding contrasts the reduced microgliosis observed after dosing with JNJ-47965567 (Jimenez-Pacheco et al., 2016), and may be accounted for by a later end-point in the present study and waning of the anti-seizure effect re-provoking microgliosis. Non-glial-based mechanisms are also possible for the effects of JNJ-54175446 in the present study. While the function of neuron-based P2X7 receptor activity is uncertain (Armstrong et al., 2002; Sperlagh et al., 2002; Papp et al., 2004), studies have reported that the P2X7 receptor is over-expressed in neurons within a seizure focus (Rappold et al., 2006; Jimenez-Pacheco et al., 2016; Wei et al., 2016; Mikkelsen et al., 2023; Morgan et al., 2023). The delayed and net outcome of P2X7 receptor antagonism may therefore be a combination of effects of blocking the receptor on different cell types and longer-term changes secondary to resolving gliosis. This could be teased apart in future studies, for example, by studying the development and progression of epilepsy in mice lacking *P2rx7* in different cell types.

The IAKA model of TLE in mice displays a drug-resistance profile suitable to identify novel anti-seizure and disease-modifying therapies (Welzel et al., 2020; West et al., 2022). Previously, high-dose levetiracetam was shown to reduce the number of spontaneous seizure-like events and block generalized convulsive seizures in the intrahippocampal kainate model in mice (Klein et al., 2015). Here, we found that the spontaneous seizures in the intraamygdala kainic acid model are largely resistant to levetiracetam, extending work which showed resistance to both phenytoin and carbamazepine and partial responses to diazepam, phenobarbital and valproate (West et al., 2022). The finding is important, therefore, since levetiracetam has a different mechanism of action to these, acting via modulation of SV2A and neurotransmitter release rather than ion channels and neurotransmitter receptors. Nevertheless, levetiracetam, as with the other compounds, has a neuro-centric mechanism of action. Since gliosis is a critical pro-epileptogenic stimuli (Ortinski et al., 2010; Robel et al., 2015), compounds which attenuate gliosis such as P2X7 receptor antagonists, are important additions to the drug armamentarium. Targeting the P2X7 receptor may have applications in other focal epilepsies. That is, non-TLE forms of treatment-resistant epilepsy also associated with gliosis and neuroinflammatory signaling (Wei et al., 2016; Iffland et al., 2017).

There are a number of limitations to consider in the present study. We did not perform combined video-EEG monitoring which could have provided information on whether the drug mitigates behavioral components of spontaneous seizures. We did not explore whether JNJ-54175446 affected levels of the P2X7 receptor at earlier time-points or prove the anti-seizure effects are specifically through targeting the P2X7 receptor, for example, via attenuation of IL-1β responses. We may not have achieved optimal dosing with JNJ-54175446. While the pharmacokinetics of JNJ-54175446 suggest that a once-daily IP injection of 30 mg/kg should achieve sufficient receptor occupancy in the brain, different routes, earlier introduction of the drug relative to the inciting status epilepticus, repeating administration or higher doses may have produced greater or more lasting suppression of seizures. Although we have asserted the model is refractory to levetiracetam, the drug appeared to blunt the rising number of spontaneous seizures. We expect to have achieved a sufficient brain level of levetiracetam in our studies but cannot exclude that higher doses or delivery via another route would have produced different results. Finally, it is unclear whether antagonism of the P2X7 receptor alone will be sufficient to achieve complete seizure suppression, even when dosing is fully optimized. It would be interesting, therefore, to explore whether a period of treatment with JNJ-54175446 or another P2X7 receptor antagonist would enhance the effects of a conventional anti-seizure medicine such as levetiracetam. Indeed, studies suggest that a combinatorial approach blocking P2X7 receptor activity may render mice more susceptible to the anti-convulsant effects of benzodiazepines in models of status epilepticus (Beamer et al., 2022). Such a combination would also hold translational value since any future clinical trial of a P2X7 receptor antagonist would no doubt require add-on dosing with an existing anti-seizure medicine (Simonato et al., 2012).

In summary, the present study supports the targeting of the P2X7 receptor for the treatment of drug-resistant TLE and extends the evidence for the pharmacoresistance profile of the IAKA model in mice. Future studies could explore optimal dosing, perhaps in combination with a conventional anti-seizure medicine, and explore the cell type-specific effects of antagonism of the receptor.

Data availability statement

The original contributions presented in the study are included in the article/Supplementary Material, further inquiries can be directed to the corresponding author.

Ethics statement

The animal study was approved by the Research Ethics Committee (REC 1587) of the RCSI University of Medicine and Health Sciences, under license from the Ireland Health Products Regulatory Authority (AE19127/P057). The study was conducted in accordance with the local legislation and institutional requirements.

Author contributions

OmM: Conceptualization, Writing–review and editing, Formal Analysis, Investigation, Methodology. MH: Formal Analysis, Writing–review and editing, Visualization. AL: Formal Analysis, Visualization, Writing–review and editing. TH: Formal Analysis, Visualization, Writing–review and editing, Conceptualization, Investigation, Methodology. RR: Formal Analysis, Methodology, Visualization, Writing–review and editing. KR: Formal Analysis, Methodology, Visualization, Writing–review and editing, Investigation. AS-R: Investigation, Methodology, Writing–review and editing, Data curation. EL: Data curation, Methodology, Writing–review and editing, Visualization. JH: Methodology, Visualization, Writing–review and editing. OsM: Methodology, Visualization, Writing–review and editing, Formal Analysis. JL: Formal Analysis, Methodology, Visualization, Writing–review and editing. AB: Methodology, Writing–review and editing, Conceptualization, Funding acquisition. JP: Funding acquisition, Writing–review and editing, Supervision. MC: Funding acquisition, Writing–review and editing, Conceptualization, Methodology. TE: Conceptualization, Writing–review and editing, Supervision. DH:

Conceptualization, Supervision, Writing–review and editing, Funding acquisition, Project administration, Writing–original draft.

Funding

The author(s) declare financial support was received for the research, authorship, and/or publication of this article. This publication has emanated from research supported in part by a research grant from Science Foundation Ireland (SFI) under Grant Number 16/RC/3948 and 21/RC/10294 and co-funded under the European Regional Development Fund, with co-funding from Janssen Pharmaceutical Research and Development. TE was supported by Science Foundation Ireland under Grant Number 17/CDA/4708 and from the European Union's Horizon 2020 research and innovation programme under the Marie Sklowdowska-Curie grant agreement (No. 766124). JH was supported by funding from the Irish Research Council (EpiGlymph) under grant IRCLA/2022/3828. JL was supported by Grant PID 2020-117656RB-I00 funded by the Ministerio de Ciencia e Innovación/Agencia Estatal de Investigación (MCIN/AEI) 10.13039/501100011033. OM was supported by Grant PRE 2019-089068 funded by MCIN/AEI.

Acknowledgments

The authors would like to thank staff in the biomedical research facilities at RCSI and the operations team at FutureNeuro. We also thank Jordan Higgins for support with data analysis.

Conflict of interest

Authors AB, JP and MC are/were employees by Neuroscience, Janssen Pharmaceutical Research and Development, LLC.

The remaining authors declare that the research was conducted in the absence of any commercial or financial relationships that could be construed as a potential conflict of interest.

The authors declare that this study received funding from Janssen Pharmaceutical Research & Development. The funder had the following involvement in the study: original conceptualization and experimental design, selection of methodology, provision of JNJ-54175446 and measurement of plasma and brain concentrations of JNJ-54175446 and levetiracetam, researcher supervision, reviewing and editing the manuscript, and acquisition of funding.

Publisher's note

Supplementary material

The Supplementary Material for this article can be found online at: https://www.frontiersin.org/articles/10.3389/fphar.2023.1308478/full#supplementary-material

References

Allan, S. M., Tyrrell, P. J., and Rothwell, N. J. (2005). Interleukin-1 and neuronal injury. *Nat. Rev. Immunol.* 5, 629–640. doi:10.1038/nri1664

Amhaoul, H., Ali, I., Mola, M., Van Eetveldt, A., Szewczyk, K., Missault, S., et al. (2016). P2X7 receptor antagonism reduces the severity of spontaneous seizures in a chronic model of temporal lobe epilepsy. *Neuropharmacology* 105, 175–185. doi:10.1016/j.neuropharm.2016.01.018

Anderson, C. M., and Nedergaard, M. (2006). Emerging challenges of assigning P2X7 receptor function and immunoreactivity in neurons. *Trends Neurosci.* 29, 257–262. doi:10.1016/j.tins.2006.03.003

Armstrong, J. N., Brust, T. B., Lewis, R. G., and Macvicar, B. A. (2002). Activation of presynaptic P2X7-like receptors depresses mossy fiber-CA3 synaptic transmission through p38 mitogen-activated protein kinase. *J. Neurosci.* 22, 5938–5945.

Aronica, E., Bauer, S., Bozzi, Y., Caleo, M., Dingledine, R., Gorter, J. A., et al. (2017). Neuroinflammatory targets and treatments for epilepsy validated in experimental models. *Epilepsia* 58 (3), 27–38. doi:10.1111/epi.13783

Beamer, E., Fischer, W., and Engel, T. (2017). The ATP-gated P2X7 receptor as a target for the treatment of drug-resistant epilepsy. *Front. Neurosci.* 11, 21. doi:10.3389/fnins.2017.00021

Beamer, E., Morgan, J., Alves, M., Menendez Mendez, A., Morris, G., Zimmer, B., et al. (2022). Increased expression of the ATP-gated P2X7 receptor reduces responsiveness to anti-convulsants during status epilepticus in mice. *Br. J. Pharmacol.* 179, 2986–3006. doi:10.1111/bph.15785

Brennan, G. P., Bauer, S., Engel, T., Jimenez-Mateos, E. M., Del Gallo, F., Hill, T. D. M., et al. (2020). Genome-wide microRNA profiling of plasma from three different animal models identifies biomarkers of temporal lobe epilepsy. *Neurobiol. Dis.* 144, 105048. doi:10.1016/j.nbd.2020.105048

Conte, G., Parras, A., Alves, M., Olla, I., De Diego-Garcia, L., Beamer, E., et al. (2020). High concordance between hippocampal transcriptome of the mouse intra-amygdala kainic acid model and human temporal lobe epilepsy. *Epilepsia* 61, 2795–2810. doi:10.1111/epi.16714

Devinsky, O., Vezzani, A., O'brien, T. J., Jette, N., Scheffer, I. E., De Curtis, M., et al. (2018). Epilepsy. *Nat. Rev. Dis. Prim.* 4, 18024. doi:10.1038/nrdp.2018.24

Di Nunzio, M., Di Sapia, R., Sorrentino, D., Kebede, V., Cerovic, M., Gullotta, G. S., et al. (2021). Microglia proliferation plays distinct roles in acquired epilepsy depending on disease stages. *Epilepsia* 62, 1931–1945. doi:10.1111/epi.16956

Dutta, S. S., Andonova, A. A., Woellert, T., Hewett, S. J., and Hewett, J. A. (2022). P2X7-dependent constitutive Interleukin-1β release from pyramidal neurons of the normal mouse hippocampus: evidence for a role in maintenance of the innate seizure threshold. *Neurobiol. Dis.* 168, 105689. doi:10.1016/j.nbd.2022.105689

Engel, T., Gomez-Villafuertes, R., Tanaka, K., Mesuret, G., Sanz-Rodriguez, A., Garcia-Huerta, P., et al. (2012). Seizure suppression and neuroprotection by targeting the purinergic P2X7 receptor during status epilepticus in mice. *FASEB J.* 26, 1616–1628. doi:10.1096/fj.11-196089

Fischer, W., Franke, H., Krügel, U., Müller, H., Dinkel, K., Lord, B., et al. (2016). Critical evaluation of P2X7 receptor antagonists in selected seizure models. *PloS One* 11, e0156468. doi:10.1371/journal.pone.0156468

Henshall, D. C. (2017). "Poststatus epilepticus models: focal kainic acid," in *Models of seizures and epilepsy*. Editors A. Pitkanen, A. S. Galanopoulou, and S. L. Moshe (Academic Press), 611–624.

Iffland, P. H., and Crino, P. B. (2017). Focal cortical dysplasia: gene mutations, cell signaling, and therapeutic implications. *Annu. Rev. Pathol.* 12, 547–571. doi:10.1146/annurev-pathol-052016-100138

Jimenez-Pacheco, A., Diaz Hernandez, M., Arribas-Blázquez, M., Sanz-Rodriguez, A., Olivos-Oré, L. A., Artalejo, A. R., et al. (2016). Transient P2X7 receptor antagonism produces lasting reductions in spontaneous seizures and gliosis in experimental temporal lobe epilepsy. *J. Neurosci.* 36, 5920–5932. doi:10.1523/JNEUROSCI.4009-15.2016

Kaczmarek-Hajek, K., Zhang, J., Kopp, R., Grosche, A., Rissiek, B., Saul, A., et al. (2018). Re-evaluation of neuronal P2X7 expression using novel mouse models and a P2X7-specific nanobody. *Elife* 7, e36217. doi:10.7554/eLife.36217

Klein, S., Bankstahl, M., and Loscher, W. (2015). Inter-individual variation in the effect of antiepileptic drugs in the intrahippocampal kainate model of mesial temporal lobe epilepsy in mice. *Neuropharmacology* 90, 53–62. doi:10.1016/j.neuropharm.2014.11.008

Klitgaard, H., Matagne, A., Gobert, J., and Wulfert, E. (1998). Evidence for a unique profile of levetiracetam in rodent models of seizures and epilepsy. *Eur. J. Pharmacol.* 353, 191–206. doi:10.1016/s0014-2999(98)00410-5

Kwan, P., Schachter, S. C., and Brodie, M. J. (2011). Drug-resistant epilepsy. *N. Engl. J. Med.* 365, 919–926. doi:10.1056/NEJMra1004418

Lai, Y. C., Muscal, E., Wells, E., Shukla, N., Eschbach, K., Hyeong Lee, K., et al. (2020). Anakinra usage in febrile infection related epilepsy syndrome: an international cohort. *Ann. Clin. Transl. Neurol.* 7, 2467–2474. doi:10.1002/acn3.51229

Letavic, M. A., Savall, B. M., Allison, B. D., Aluisio, L., Andres, J. I., De Angelis, M., et al. (2017). 4-Methyl-6,7-dihydro-4H-triazolo[4,5-c]pyridine-Based P2X7 receptor antagonists: optimization of pharmacokinetic properties leading to the identification of a clinical candidate. *J. Med. Chem.* 60, 4559–4572. doi:10.1021/acs.jmedchem.7b00408

Li, T., Ren, G., Lusardi, T., Wilz, A., Lan, J. Q., Iwasato, T., et al. (2008). Adenosine kinase is a target for the prediction and prevention of epileptogenesis in mice. *J. Clin. Invest.* 118, 571–582. doi:10.1172/JCI33737

Loscher, W. (2022). Dogs as a natural animal model of epilepsy. *Front. Vet. Sci.* 9, 928009. doi:10.3389/fvets.2022.928009

Loscher, W., Gillard, M., Sands, Z. A., Kaminski, R. M., and Klitgaard, H. (2016). Synaptic vesicle glycoprotein 2A ligands in the treatment of epilepsy and beyond. *CNS Drugs* 30, 1055–1077. doi:10.1007/s40263-016-0384-x

Loscher, W., Klitgaard, H., Twyman, R. E., and Schmidt, D. (2013). New avenues for anti-epileptic drug discovery and development. *Nat. Rev. Drug Discov.* 12, 757–776. doi:10.1038/nrd4126

Loscher, W., Potschka, H., Sisodiya, S. M., and Vezzani, A. (2020). Drug resistance in epilepsy: clinical impact, potential mechanisms, and new innovative treatment options. *Pharmacol. Rev.* 72, 606–638. doi:10.1124/pr.120.019539

Mikkelsen, J. D., Aripaka, S. S., Kaad, S., Pazarlar, B. A., Pinborg, L., Finsen, B., et al. (2023). Characterization of the novel P2X7 receptor radioligand [(3)H]JNJ-64413739 in human brain tissue. *ACS Chem. Neurosci.* 14, 111–118. doi:10.1021/acschemneuro.2c00561

Monif, M., Reid, C. A., Powell, K. L., Smart, M. L., and Williams, D. A. (2009). The P2X7 receptor drives microglial activation and proliferation: a trophic role for P2X7R pore. *J. Neurosci.* 29, 3781–3791. doi:10.1523/JNEUROSCI.5512-08.2009

Morgan, J., Moreno, O., Alves, M., Baz, Z., Menendez Mendez, A., Leister, H., et al. (2023). Increased uptake of the P2X7 receptor radiotracer (18) F-JNJ-64413739 in the brain and peripheral organs according to the severity of status epilepticus in male mice. *Epilepsia* 64, 511–523. doi:10.1111/epi.17484

Mouri, G., Jimenez-Mateos, E., Engel, T., Dunleavy, M., Hatazaki, S., Paucard, A., et al. (2008). Unilateral hippocampal CA3-predominant damage and short latency epileptogenesis after intra-amygdala microinjection of kainic acid in mice. *Brain Res.* 1213, 140–151. doi:10.1016/j.brainres.2008.03.061

Ortinski, P. I., Dong, J., Mungenast, A., Yue, C., Takano, H., Watson, D. J., et al. (2010). Selective induction of astrocytic gliosis generates deficits in neuronal inhibition. *Nat. Neurosci.* 13, 584–591. doi:10.1038/nn.2535

Paolicelli, R. C., Sierra, A., Stevens, B., Tremblay, M. E., Aguzzi, A., Ajami, B., et al. (2022). Microglia states and nomenclature: a field at its crossroads. *Neuron* 110, 3458–3483. doi:10.1016/j.neuron.2022.10.020

Papp, L., Vizi, E. S., and Sperlagh, B. (2004). Lack of ATP-evoked GABA and glutamate release in the hippocampus of P2X7 receptor-/- mice. *Neuroreport* 15, 2387–2391. doi:10.1097/00001756-200410250-00017

Rappold, P. M., Lynd-Balta, E., and Joseph, S. A. (2006). P2X7 receptor immunoreactive profile confined to resting and activated microglia in the epileptic brain. *Brain Res.* 1089, 171–178. doi:10.1016/j.brainres.2006.03.040

Recourt, K., De Boer, P., Van Der Ark, P., Benes, H., Van Gerven, J. M. A., Ceusters, M., et al. (2023). Characterization of the central nervous system penetrant and selective purine P2X7 receptor antagonist JNJ-54175446 in patients with major depressive disorder. *Transl. Psychiatry* 13, 266. doi:10.1038/s41398-023-02557-5

Recourt, K., Van Der Aart, J., Jacobs, G., De Kam, M., Drevets, W., Van Nueten, L., et al. (2020). Characterisation of the pharmacodynamic effects of the P2X7 receptor antagonist JNJ-54175446 using an oral dexamphetamine challenge model in healthy males in a randomised, double-blind, placebo-controlled, multiple ascending dose trial. *J. Psychopharmacol.* 34, 1030–1042. doi:10.1177/0269881120914206

Robel, S., Buckingham, S. C., Boni, J. L., Campbell, S. L., Danbolt, N. C., Riedemann, T., et al. (2015). Reactive astrogliosis causes the development of spontaneous seizures. *J. Neurosci.* 35, 3330–3345. doi:10.1523/JNEUROSCI.1574-14.2015

Roger, S., Gillet, L., Baroja-Mazo, A., Surprenant, A., and Pelegrin, P. (2010). C-terminal calmodulin-binding motif differentially controls human and rat P2X7 receptor current facilitation. *J. Biol. Chem.* 285, 17514–17524. doi:10.1074/jbc.M109.053082

Roth, T. L., Nayak, D., Atanasijevic, T., Koretsky, A. P., Latour, L. L., and Mcgavern, D. B. (2014). Transcranial amelioration of inflammation and cell death after brain injury. *Nature* 505, 223–228. doi:10.1038/nature12808

Rusina, E., Bernard, C., and Williamson, A. (2021). The kainic acid models of temporal lobe epilepsy. *eNeuro* 8. ENEURO.0337-20.2021. doi:10.1523/eneuro.0337-20.2021

Russo, E., Citraro, R., Scicchitano, F., De Fazio, S., Di Paola, E. D., Constanti, A., et al. (2010). Comparison of the antiepileptogenic effects of an early long-term treatment with ethosuximide or levetiracetam in a genetic animal model of absence epilepsy. *Epilepsia* 51, 1560–1569. doi:10.1111/j.1528-1167.2009.02400.x

Sim, J. A., Young, M. T., Sung, H. Y., North, R. A., and Surprenant, A. (2004). Reanalysis of P2X7 receptor expression in rodent brain. *J. Neurosci.* 24, 6307–6314. doi:10.1523/JNEUROSCI.1469-04.2004

Simonato, M., Loscher, W., Cole, A. J., Dudek, F. E., Engel, J., Jr., Kaminski, R. M., et al. (2012). Finding a better drug for epilepsy: preclinical screening strategies and experimental trial design. *Epilepsia* 53, 1860–1867. doi:10.1111/j.1528-1167.2012.03541.x

Smith, J., Menendez Mendez, A., Alves, M., Parras, A., Conte, G., Bhattacharya, A., et al. (2023). The P2X7 receptor contributes to seizures and inflammation-driven long-lasting brain hyperexcitability following hypoxia in neonatal mice. *Br. J. Pharmacol.* 180, 1710–1729. doi:10.1111/bph.16033

Sperlagh, B., Kofalvi, A., Deuchars, J., Atkinson, L., Milligan, C. J., Buckley, N. J., et al. (2002). Involvement of P2X7 receptors in the regulation of neurotransmitter release in the rat hippocampus. *J. Neurochem.* 81, 1196–1211. doi:10.1046/j.1471-4159.2002.00920.x

Vezzani, A., Balosso, S., and Ravizza, T. (2019). Neuroinflammatory pathways as treatment targets and biomarkers in epilepsy. *Nat. Rev. Neurol.* 15, 459–472. doi:10.1038/s41582-019-0217-x

Vezzani, A., French, J., Bartfai, T., and Baram, T. Z. (2011). The role of inflammation in epilepsy. *Nat. Rev. Neurol.* 7, 31–40. doi:10.1038/nrneurol.2010.178

Vezzani, A., Ravizza, T., Bedner, P., Aronica, E., Steinhauser, C., and Boison, D. (2022). Astrocytes in the initiation and progression of epilepsy. *Nat. Rev. Neurol.* 18, 707–722. doi:10.1038/s41582-022-00727-5

Wei, Y. J., Guo, W., Sun, F. J., Fu, W. L., Zheng, D. H., Chen, X., et al. (2016). Increased expression and cellular localization of P2X7R in cortical lesions of patients with focal cortical dysplasia. *J. Neuropathol. Exp. Neurol.* 75, 61–68. doi:10.1093/jnen/nlv003

Welzel, L., Schidlitzki, A., Twele, F., Anjum, M., and Loscher, W. (2020). A face-to-face comparison of the intra-amygdala and intrahippocampal kainate mouse models of mesial temporal lobe epilepsy and their utility for testing novel therapies. *Epilepsia* 61, 157–170. doi:10.1111/epi.16406

West, P. J., Thomson, K., Billingsley, P., Pruess, T., Rueda, C., Saunders, G. W., et al. (2022). Spontaneous recurrent seizures in an intra-amygdala kainate microinjection model of temporal lobe epilepsy are differentially sensitive to antiseizure drugs. *Exp. Neurol.* 349, 113954. doi:10.1016/j.expneurol.2021.113954

Yamanaka, G., Ishida, Y., Kanou, K., Suzuki, S., Watanabe, Y., Takamatsu, T., et al. (2021). Towards a treatment for neuroinflammation in epilepsy: interleukin-1 receptor antagonist, Anakinra, as a potential treatment in intractable epilepsy. *Int. J. Mol. Sci.* 22, 6282. doi:10.3390/ijms22126282

Young, K., and Morrison, H. (2018). Quantifying microglia morphology from photomicrographs of immunohistochemistry prepared tissue using ImageJ. *J. Vis. Exp.* 136, 57648. doi:10.3791/57648

frontiers | Frontiers in Pharmacology

TYPE Mini Review
PUBLISHED 12 January 2024
DOI 10.3389/fphar.2023.1326815

OPEN ACCESS

EDITED BY
Mahmoud Rafieian-Kopaei,
Shahrekord University of Medical Sciences, Iran

REVIEWED BY
Janosch P. Heller,
Dublin City University, Ireland

*CORRESPONDENCE
Brenden Samuel Rabinovitch,
brenden.rabinovitch@uhn.ca,
brenden.rabinovitch@mail.utoronto.ca

†These authors share first authorship

‡These authors share senior authorship

RECEIVED 24 October 2023
ACCEPTED 07 December 2023
PUBLISHED 12 January 2024

CITATION
Freidel N, Kreuder L, Rabinovitch BS, Chen FY, Huang RST and Lewis EC (2024), Psychedelics, epilepsy, and seizures: a review.
Front. Pharmacol. 14:1326815.
doi: 10.3389/fphar.2023.1326815

Psychedelics, epilepsy, and seizures: a review

Ninon Freidel[1,2†], Liliane Kreuder[1,3†], Brenden Samuel Rabinovitch[1,4,5*], Frank Yizhao Chen[1,6], Ryan S. T. Huang[1,7] and Evan Cole Lewis[1,8‡]

[1]Department of Clinical Research, Numinus Toronto, Toronto, ON, Canada, [2]Department of Neuroscience, University of British Columbia Djavad Mowafaghian Centre for Brain Health, Vancouver, BC, Canada, [3]Department of Medical Biophysics, University of Toronto Temerty Faculty of Medicine, Toronto, ON, Canada, [4]Krembil Research Institute, University Health Network, Toronto, ON, Canada, [5]Department of Physiology, University of Toronto Temerty Faculty of Medicine, Toronto, ON, Canada, [6]Department of Research, Jamaican Medical Cannabis Corporation, Toronto, ON, Canada, [7]Department of Medicine, University of Toronto Temerty Faculty of Medicine, Toronto, ON, Canada, [8]Department of Pediatrics, University of Toronto Temerty Faculty of Medicine, Toronto, ON, Canada

Psychedelic compounds have been utilized by humans for centuries for medicinal, religious, and tribal purposes. Clinical trial data starting from the early 2000s and continuing today indicates that psychedelics are a clinically efficacious treatment for a variety of neurological and psychiatric disorders. However, all clinical trials examining these substances have excluded any individual with a past or current history of seizures, leaving a large cohort of epilepsy and non-epilepsy chronic seizure disorder patients without anywhere to turn for psychedelic-assisted therapy. These exclusions were made despite any significant evidence that clinically supervised psychedelic use causes or exacerbates seizures in this population. To date, no clinical trial or preclinical seizure model has demonstrated that psychedelics induce seizures. This review highlights several cases of individuals experiencing seizures or seizure remission following psychedelic use, with the overall trend being that psychedelics are safe for use in a controlled, supervised clinical setting. We also suggest future research directions for this field.

KEYWORDS

psychedelics, seizures, epilepsy, LSD, psilocybin, magic mushrooms, MDMA, ketamine

1 Introduction

Psychedelic-assisted therapy (PAT) has emerged as a clinically efficacious treatment for an array of psychiatric disorders including treatment-resistant depression (TRD) (Carhart-Harris et al., 2016a; Stroud et al., 2018; Palhano-Fontes et al., 2019; Goodwin et al., 2022), major depressive disorder (MDD) (Davis et al., 2021; Sloshower et al., 2023), end-of-life psychiatric distress (Bossis et al., 2016; Agin-Liebes et al., 2020; Rosa et al., 2022), anxiety (Davis et al., 2019), post-traumatic stress disorder (PTSD) (Mithoefer et al., 2018; Mithoefer et al., 2019) and obsessive-compulsive disorder (OCD) (Rodriguez et al., 2013; Kelmendi et al., 2022). PAT has also effectively treated tobacco addiction and alcohol dependence (Krebs and Johansen, 2012; Bogenschutz et al., 2015; Johnson et al., 2017; Sessa et al., 2019). In these clinical trials, both classical psychedelics, such as psilocybin and lysergic acid diethylamide (LSD), and atypical psychedelics, such as ketamine and 3,4-methylenedioxymethamphetamine (MDMA) were integrated into therapy sessions. These forms of PAT are well-tolerated by patients in clinical settings. Recently, psychedelic treatment has been used to treat functional neurological disorder (FND), an umbrella of neurological symptoms including functional movement disorders

(FMDs), functional sensory disorders (FSDs), and functional seizures (Butler et al., 2020; Stewart et al., 2020; Argento et al., 2023).

Although psychedelics have shown strong efficacy in treating a diverse array of symptoms, one specific cohort of patients has been excluded from all PAT clinical trials: individuals with a past or current history of seizures.

Individuals with chronic seizure disorders, such as epilepsy and some mitochondrial encephalopathies, have a reduced quality of life and experience disproportionate rates of anxiety and depression compared to the general population (Carhart-Harris and Nutt, 2017; López-Giménez and González-Maeso, 2018). Additionally, ~10% of individuals with epilepsy experience functional seizures (also referred to as psychogenic, non-epileptic seizures [PNES]), which are not treatable with traditional anti-epileptic pharmacological therapies or surgical interventions due to their psychological underpinnings. These patients require novel, alternative therapies, with conjunctive psychological treatment, such as in PAT.

There is sparse and conflicting published data regarding the safety of psychedelics in the context of chronic and acute seizures. We will demonstrate that most reports are case studies of individuals taking psychedelics recreationally in unsupervised non-clinical settings. The few controlled studies support classical psychedelics as safe and tolerable under clinical supervision, even in patients with a history of epilepsy who currently experience spontaneous, recurrent seizures (SRS).

The safety profile of classical psychedelics in individuals with epilepsy must be characterized to determine if these compounds are safe for use to treat functional seizures and co-morbid neuropsychiatric conditions. Although this review will focus on epilepsy, the data we present is also relevant to individuals with non-epilepsy chronic seizure disorders, such as mitochondrial encephalopathies. This review aims to summarize the complex mosaic of psychedelics in the context of epilepsy and seizures.

2 Methods

2.1 Databases and search terms

All data were extracted from public databases including PubMed, Google Scholar, and ResearchGate. The following search terms were used in different combinations: epilepsy, psychedelics, psilocybin, magic mushrooms, mescaline, LSD, lysergide, lysergic acid diethylamide, MDMA, 3,4-methylenedioxymethamphetamine, methylenedioxymethamphetamine, molly, ecstasy, seizures, chronic seizures, acute seizures, serotonergic psychedelics, and hallucinogen.

2.2 Screening process

2.2.1 Results screening

Search results were screened by reviewing titles and abstracts. The full text of screened abstracts was reviewed to confirm inclusions.

2.2.2 Inclusion criteria

The inclusion criteria were: 1) any explicit mention of classical and/or atypical psychedelics in the context of acute and/or chronic seizures, and 2) case reports and/or clinical trials involving classical and/or atypical psychedelic use in any seizure disorder or in patients with acute seizures.

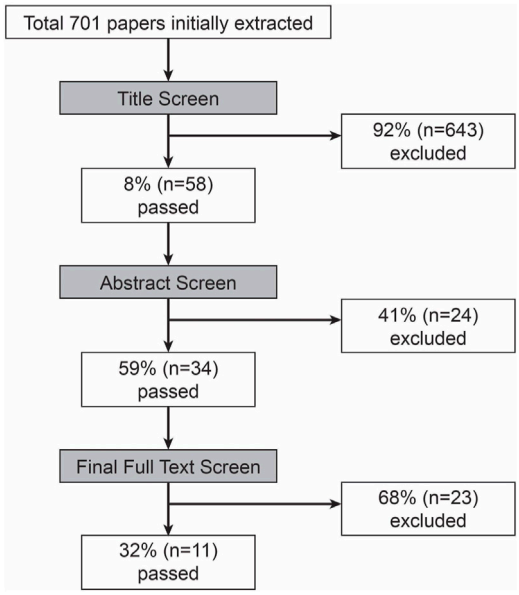

FIGURE 1
Process of screening papers with initial and final inclusions.

3 Results

3.1 Search results

A total of 701 papers were collected. 34 papers passed the title and abstract screens. From there, 11 papers passed the full text screen and were included in the analysis (Figure 1).

3.2 Overview of psychedelic actions and mechanisms

3.2.1 Classical psychedelics

The classical psychedelics psilocybin, LSD, and mescaline are agonists of the 5-hydroxytryptamine (5-HT) 2A and 2C receptors (López-Giménez and González-Maeso, 2018). The neural circuitry effects of LSD and psilocybin include changes in resting-state functional connectivity (RSFC) between and within distinct brain regions. Most notably, these compounds increase inter-network RSFC, between the default mode network (DMN), executive network (EN), and salience network (SN) structures, while decreasing intra-network RSFC within each set of structures (Carhart-Harris et al., 2014; Carhart-Harris and Nutt, 2017). The precise neurobiological underpinnings of these functional network changes are still not completely understood.

3.2.2 MDMA

MDMA is an atypical psychedelic, referred to as an empathogen and entactogen (National Academies of Sciences et al., 2022).

TABLE 1 KAT treatment regimen and timeline from Argento et al., (2023). Adapted from Argento et al., (2023) Figure 2.

Weeks	Sublingual dose	Intranasal dose	Treatment type	Therapy administered?
1	100 mg	30 mg	KAT session	Yes
2	-	-	Break	No
3	150 mg	45 mg	KAT session	Yes
4	200 mg	60 mg	KAT session	Yes
5	100 mg	30 mg	Ketamine maintenance session	Yes
6	100 mg	30 mg	Ketamine maintenance session	Yes
7	100 mg	30 mg	Ketamine maintenance session	Yes
8	150 mg	30 mg	Ketamine maintenance session	Yes
9	-	-	Break	No
10	150 mg	30 mg	Ketamine maintenance session	Yes
11	-	-	Break	Yes
12	150 mg	30 mg	Break	Yes
13	-	-	Interval update	No
14	-	-	Break	Yes
15	150 mg	30 mg	Ketamine maintenance session	Yes
16	150 mg	-	Ketamine maintenance session	Yes
17	-	-	Interval update	No
18	-	-	Break	No
19	150 mg	-	Ketamine maintenance session	Yes
20	-	-	Break	No
21	-	-	Break	No
22	-	-	Break	No
23	150 mg	-	Ketamine maintenance session	Yes

Although MDMA is serotonergic, it acts via a different mechanism from the classical psychedelics and also possesses some dopaminergic activity (Schenk and Highgate, 2021). MDMA has several mechanisms of action, including increasing presynaptic serotonin release to the synaptic cleft, inhibiting serotonin reuptake at the presynaptic terminal, and some monoamine oxidase inhibition (Kalant, 2001). The subjective effects of MDMA are reported as less hallucinogenic than the classical psychedelics, with increased feelings of empathy and lovingness both outwardly to others and inwardly to oneself (Dumont et al., 2009; Bedi et al., 2010).

3.2.3 Ketamine

Ketamine, an atypical psychedelic and dissociative anesthetic, is an N-methyl-D-aspartate (NMDA) receptor antagonist. The neurobiological mechanisms underlying ketamine's effects are still being investigated, as ketamine has several mechanisms of action. Ketamine preferentially binds to the NMDA receptors on GABAergic inhibitory interneurons (Gerhard et al., 2020). Ketamine also binds extra-synaptic NMDA receptors on glutamatergic excitatory neurons at lower subanaesthetic doses (Zorumski et al., 2016). At anaesthetic doses, ketamine binds to NMDA receptors on glutamatergic excitatory neurons, inducing overall reduced excitatory transmission, leading to loss of consciousness. Moreover, ketamine may also induce its rapid and persistent anti-depressive effects through its metabolism into hydroxynorketamine (HNK), which is an antagonist of the excitatory α-amino-3-hydroxy-5-methyl-4-isoxazolepropionic acid (AMPA) receptor (Zanos et al., 2016), which glutamate is an agonist of.

3.3 Psychedelic use and seizures

We identified 10 case reports from 1992 to 2023 in which patients experienced seizures after ingesting a classical or atypical psychedelic substance. Reports in each subsection are ordered by date (oldest to newest). One additional paper, which was not a case report (Serafetinides, 1965) is also described, though this paper is an open-label trial of LSD in individuals with epilepsy who undergo neurosurgery.

TABLE 2 Summary of all reports described in the results section. Abbreviations used in this table exclusively: years-old (yo); months-old (mo); generalized tonic-clonic seizure (GTC); not applicable (N/A).

Citation	Drug(s) used	Doses	Age (sex)	Clinical features	Final outcome
Hall et al. (1996)	MDMA	Unknown	26yo (male)	- GTC	Complete recovery
				- Hypotension	
				- Disseminated intravascular coagulation (DIC)	
				- Acute renal and hepatic failure	
				- Rhabdomyolysis	
				- Respiratory distress	
Cooper et al. (1997)	MDMA, amoxicillin	Unknown	2yo (female)	- Agitation	Complete recovery
				- High fever	
				- Rapid heart rate	
				- Dilated pupils	
Magee et al. (1998)	MDMA, alcohol	Unknown	17yo (female)	- GTC	Complete recovery
				- Drowsiness	
				- Incoherent speech	
				- Hypotension	
				- Reduced urine sodium levels (115 mmol/L)	
				- Severe dilutional hyponatremia leading to secondary seizure and stupor	
Huntjens et al., (2022)	MDMA	Unknown	14 months (male)	- GTC	Complete recovery
Pauwels et al. (2023)	MDMA	Unknown	19 months (male)	- Mowing arm gestures	Complete recovery
				- Staring	
				- Eye turning	
	MDMA	Unknown	20 months (female)	- Convulsions	Complete recovery
				- Hyperthermia	
				- Tachycardia	
				- Rigidity	
Picker et al. (1992)	LSD, fluoxetine	- Unknown (LSD); - 20 mg/day (Fluoxetine)	16yo (male)	- Initial focal seizure involving left arm and face that progressed to a GTC	Complete recovery
Legriel et al. (2008)	LSA	Unknown	39yo (male)	- GTC	Complete recovery
				- Dilated pupils	
				- Rapid heart rate	
				- Hypertension	
Aakeroy et al. (2021)	LSD, DMT, methamphetamine, amphetamine, MDMA	–300 µg (LSD); - unknown (DMT, methamphetamine, amphetamine, MDMA)	Late teens (male)	- GTC	Severe cerebral sequelae 1-year post incident
				- Vomiting	
				- Cyanosis	
				- Cardiorespiratory arrest	
Serafetinides (1965)	LSD	1 µg/kg (LSD)	20 patients (12 male, 8 female)	–17 patients had no change in post-operation epileptic activity	N/A

(Continued on following page)

TABLE 2 (*Continued*) Summary of all reports described in the results section. Abbreviations used in this table exclusively: years-old (yo); months-old (mo); generalized tonic-clonic seizure (GTC); not applicable (N/A).

Citation	Drug(s) used	Doses	Age (sex)	Clinical features	Final outcome
				–2 patients had decreased epileptic activity	
				–1 patient had increased	
Blond et al. (2023)	Psilocybin (magic mushrooms)	3.6 g (mushrooms)	31yo (male)	–32 long episodes of prolonged epileptiform activity recorded by implanted responsive neurostimulation system	N/A
Argento et al. (2023)	Ketamine	Variable (See Table 1)	51yo (female)	N/A	Remission of symptoms following treatment with ketamine (see subsection *3.3.4*)

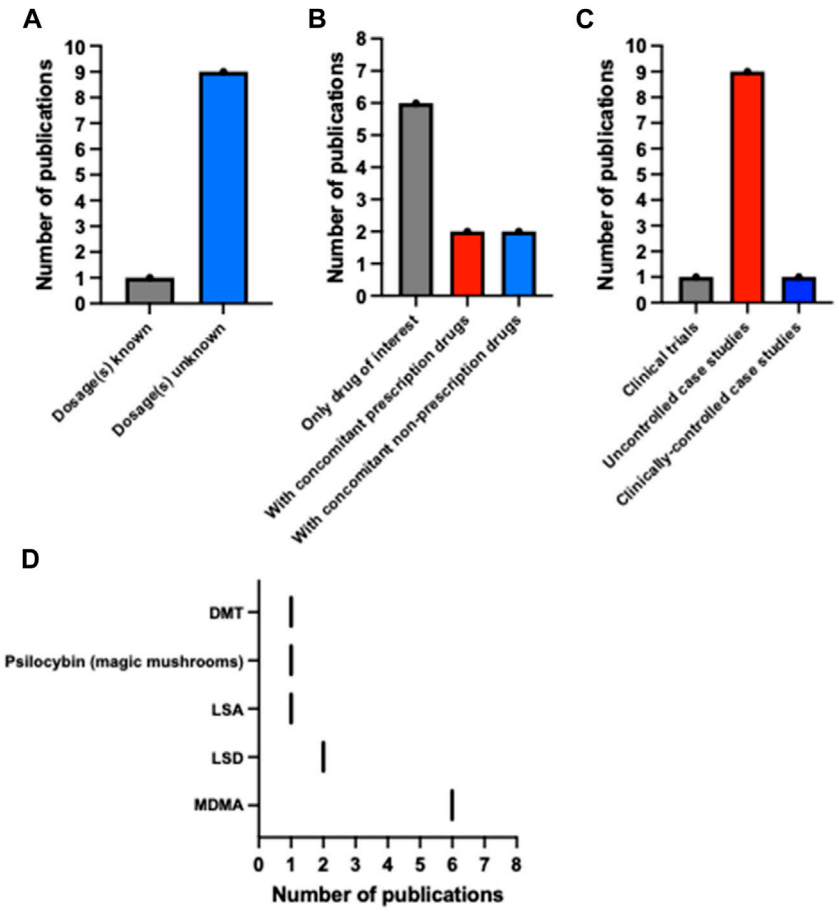

FIGURE 2
Descriptive statistics of the psychedelic and epilepsy literature. Bar plots of the number of publications describing reports where **(A)** drug dosages were known, **(B)** multiple drugs (prescription and non-prescription) were ingested, and **(C)** there was clinical supervision. **(D)** The number of publications based on the psychedelics ingested in each report. These data highlight variability and sparsity in the literature. Note: Pauwels et al. (2023) counted as n = 2 in this figure due to its reporting of two separate and unrelated cases. **(A,B)** Do not include Serafetinides (1965) due to this study being a clinical trial. This figure was made using GraphPad Prism 10.

3.3.1 Reports involving MDMA

Hall et al. (1996) reported a 26-year-old paraplegic male experiencing generalized seizures following the ingestion of an ecstasy (MDMA) tablet (of unknown dosage) alongside concurrent alcohol consumption (Hall et al., 1996). He was treated with 50 mg of intravenous diazepam, dantrolene and anaesthesia (thiopentone, alfentanil and suxamethonium), successfully halting the generalized tonic-clonic seizure. Subsequently, the patient developed hypotension,

disseminated intravascular coagulation (DIC), acute renal failure, gross rhabdomyolysis, adult respiratory distress syndrome and hepatic failure. Despite the severity of his condition, he was discharged 17 days later and achieved a complete recovery.

Cooper et al. (1997) reported an accidental ingestion of MDMA (of unknown dosage) resulting in febrile convulsion in a 2-year-old female with a history of speech delay (Cooper and Egleston, 1997). At the time, the patient was undergoing treatment with amoxicillin for an upper respiratory tract infection, but the duration of treatment was not specified. The patient displayed agitation, high fever, rapid heart rate and dilated pupils. She was treated with oxygen, rectal paracetamol, and intravenous diazepam resulting in a full recovery without complications. Initially, the mother did not indicate that the patient ingested any substance, until she was questioned about the patient's abnormal teeth grinding and oculogyric crisis. Following this, the patient's urine was analyzed, and the findings showed MDMA and MDA (the metabolite of MDMA) presence. The mother then admitted that the patient had accidently ingested MDMA, which delayed the delivery of treatment. The exact timecourse of the urine analysis and treatment was not described, but it was noted that the patient was admitted to the hospital and underwent the aforementioned treatments prior to the parent's admission (Cooper and Egleston, 1997).

Magee et al. (1998) reported the case of a 17-year-old female who exhibited generalized seizures 5 and 12 h following the ingestion of an ecstasy (MDMA) tablet (of unknown dosage) with concurrent alcohol consumption (Magee et al., 1998). The patient's symptoms included drowsiness, incoherent speech, hypotension, and reduced urine sodium levels (115 mmol/L). These symptoms indicated severe dilutional hyponatremia leading to secondary seizure and stupor. The significant salt and water loss resulting from vigorous dancing was effectively treated with intravenous isotonic saline, resulting in a complete recovery.

Huntjens et al. (2022) reported accidental MDMA intoxication in a 14-month-old male toddler with an unremarkable medical history (Huntjens et al., 2022). The patient presented to the emergency department with a generalized tonic-clonic seizure. 2.0 mg (0.2 mg/kg) of intraosseous midazolam was administered, but seizures persisted until the patient received 400 mg (42.5 mg/kg) of intravenous levetiracetam, which successfully terminated the status epilepticus. Blood serum analysis revealed an MDMA concentration of 0.48 mg/L[33].

Pauwels et al. (2023), reported two independent incidents where a young child accidently ingested ecstasy (MDMA) and subsequently began experiencing seizures (Pauwels et al., 2013). *Patient 1* was a 19-month-old male with an unremarkable medical history who was taken to the hospital due to mowing arm gestures, staring, and eye turning. Urine analysis showed 7.8 mg/L 3,4-methylenedioxyamphetamine (MDA) concentration and 183 mg/L MDMA concentration approximately 1–3 h after initial intoxication. The patient was eventually discharged from the hospital without complications.

Patient 2 was a 20-month-old female with a history of convulsions after a fall on the head. She was taken to the hospital presenting with hyperthermia, tachycardia, and rigidity. Urine analysis revealed a 6 mg/L MDA and 119 mg/L MDMA concentration, along with trace amounts of cocaine (Pauwels et al., 2013). It should be noted, however, that although this report explicitly described trace amounts of cocaine being present in the main text, the table displaying the toxicology results showed a negative result in the cocaine assay, without any urine concentration listed.

3.3.2 Reports involving LSD

Several case studies describe adults experiencing seizures following the recreational use of psychedelics without clinical supervision.

Picker et al. (1992) reported a potential interaction between LSD and fluoxetine, a selective serotonin reuptake inhibitor (SSRI) after a 16-year-old male undergoing 20 mg/day of fluoxetine treatment for approximately 1 year experienced a focal seizure that progressed to a generalized tonic-clonic seizure after ingesting two "blotters" containing LSD at an unknown dosage (Picker et al., 1992). Interestingly, this may have been a case of serotonin syndrome, which is an acute constellation of symptoms caused by excessive serotonin levels. Serotonin syndrome is often reported when different serotonergic drugs are taken concomitantly, such as an SSRI with a large dose of LSD (Boyer and Shannon, 2005; Foong et al., 2018; Francescangeli et al., 2019).

Legriel et al. (2008) reported the case of a 39-year-old male with a history of depression and chronic alcohol abuse (Legriel et al., 2008). The medication history included 75 mg/kg of clomipramine daily to control depression symptoms, which was discontinued after 6 months. The patient reported experiencing a generalized tonic-clonic seizure 3 years prior following ingestion of lysergic acid amine (LSA), which is structurally similar to LSD. The patient was taken to a hospital and experienced mental confusion and mydriasis. Vital signs included a 120 beats/min heart rate, and 185/130 mmHg blood pressure. At the hospital, the patient experienced another seizure that lasted over 10 min, which did cease following intravenous clonazepam administration. The patient was subsequently intubated and mechanically ventilated and was successfully extubated 3 days after admission. The dose of LSA taken was unknown, and the purity was not determined (Legriel et al., 2008).

Aakeroy et al. (2021), reported a male in his late teens with an unremarkable medical history who arrived at the hospital following ingestion of a "blotter" containing LSD and small amounts of N,N-dimethyl tryptamine (DMT), methamphetamine, amphetamine, and MDMA that resulted in the patient experiencing a tonic seizure and other adverse events including vomiting and cyanosis (Aakerøy et al., 2021). Emergency personnel arrived 25 min after the initial onset of symptoms and found the patient in cardiorespiratory arrest. The patient was intubated and received cardiopulmonary resuscitation (CPR) therapy. A comprehensive drug analysis was conducted on a blotter sample identical to the one the patient ingested, which revealed a dosage of 300 μg LSD. Serum and urine samples were collected 3 h after the initial onset of symptoms and LSD was found to have a serum concentration of 4 ng/mL (12.4 nmol/L) and 1.3 ng/mL (4.0 nmol/L) urine concentration (Aakerøy et al., 2021). For comparison, clinical trial LSD dosing is standardized at or around 75 μg, which induces significant mind-altering effects compared to placebo, with observable changes in functional brain activity, detected by functional magnetic resonance imaging (fMRI) (Carhart-Harris et al., 2016b).

3.3.2.1 Reports involving LSD in a clinically-controlled trial

Serafetinides (1965) examined the effect of LSD in 20 individuals with a temporal lobectomy to treat their epileptic seizures. 1 μg/kg LSD was given to patients (orally) 2–3 days before, and 1 month after their temporal lobectomy surgeries (Serafetinides, 1965). Scalp

electroencephalograph (EEG) recordings were taken during the LSD administration to determine changes in brain waves and epileptic activity. During the pre-operation recordings, 12 patients had no change in epileptic activity, while 5 had a decrease and 1 had increased epileptic EEG activity. During the post-operation recordings, 17 patients had no change in epileptic activity, while 2 had decreased and 1 had increased epileptic activity. Overall, this study indicates LSD may be safe for use in individuals with epilepsy (Serafetinides, 1965).

3.3.3 Reports involving psilocybin ("magic mushrooms")

Lastly, a case study by Blond et al. (2023), reported a significant exacerbation in epileptic seizures following the ingestion of a large dose (3.6 g) of psychedelic mushrooms in a 31-year-old male with a history of refractory frontal epilepsy (Blond and Schindler, 2023). In order to treat the unilateral right temporal epilepsy, the patient had been previously implanted with a responsive neurostimulation system (RNS) that improved morbidity although he continued to experience several focal seizures without awareness per week. According to his RNS data, ingestion of psilocybin at high doses (3.6 g) resulted in 32 long episodes (30 s of prolonged epileptiform activity) while ingestion at low doses (1.5 g) did not change baseline seizure frequency (Blond and Schindler, 2023).

3.3.4 Reports involving ketamine

Recently, Argento et al. (2023) reported the case of a 51-year-old female with refractory functional seizures with a daily frequency (Argento et al., 2023). The patient's medical history included MDD and PTSD. After years of failing behavioural and pharmacological therapies, she enrolled in a ketamine-assisted therapy program. The patient underwent 3 weeks of ketamine-assisted therapy followed by 20 weeks of intermittent therapy and ketamine sessions. During weeks 1, 3, and 4, the patient received 100, 150, and 200 mg of ketamine sublingually, respectively, with an additional 35, 45, and 60 mg intranasal dose, respectively. See Table 1 for the complete KAT treatment regimen. The type of therapy used was psychotherapy by a clinical psychologist specializing in trauma and somatization disorders. Following the treatment, the patient went into remission for the functional seizures, depressive symptoms, and functional movement symptoms (Argento et al., 2023).

4 Discussion

4.1 Conclusion

In conclusion, there is a deficit of published data on preclinical and clinical uses of psychedelics in the context of epilepsy and non-epilepsy seizure disorders. Most data are case reports of individuals taking unspecified amounts of untested psychedelic drugs in an uncontrolled recreational setting (see Figure 2). Although adverse events were reported, including convulsive seizures, it is unclear whether these events resulted from the psychedelic use, or whether other confounding factors played a role, such as simultaneous alcohol or other drug consumption and concomitant medication, all of which were reported in several cases (see Table 2). Several reports described both accidental and intentional ingestion of other substances, such as cocaine and non-MDMA amphetamines concomitantly with the psychedelic substance (Cooper and Egleston, 1997; Boyer and Shannon, 2005; Huntjens et al., 2022). Additionally, the case reports involving young children ingesting MDMA, though concerning, do not indicate that MDMA induces seizures in individuals with chronic seizure conditions when taken in a controlled clinical setting with appropriate dosing.

It should be noted, however, that in all reports of psychedelic use while under clinical supervision, such as Argento et al. (2023) and Serafetinides (1965), no significant serious adverse events were reported in the individuals who have epilepsy. Although further research is needed, the data we describe in this review indicate that psychedelics may be safe for use in the epilepsy population when taken under clinical supervision in a clinical setting, such as with psychedelic-assisted therapy.

4.2 Future research directions

Future research should focus on studying classical psychedelics in preclinical animal and human-derived organoid models of chronic and acute seizures. If it is established that classical psychedelics do not exacerbate seizures in animals, then randomized double-blind placebo-controlled trials should be completed to determine if there is any therapeutic benefit of psychedelics in patients with epilepsy or other chronic seizure disorders to treat their seizures, both epileptic and functional. The field of epilepsy and seizure research is ripe for new data testing classical psychedelic use in acute and chronic seizure disease models. More data is essential to inform clinicians of the potential adverse events or therapeutic benefits of these substances.

Author contributions

NF: Data curation, Writing–original draft, Writing–review and editing. LK: Data curation, Writing–original draft, Writing–review and editing. BR: Writing–review and editing, Conceptualization, Data curation, Formal Analysis, Methodology, Project administration, Supervision, Validation, Visualization, Writing–original draft. FC: Writing–review and editing. RH: Writing–review and editing, Visualization. ECL: Supervision, Writing–review and editing.

Funding

The author(s) declare that no financial support was received for the research, authorship, and/or publication of this article.

Acknowledgments

The authors thank Maria Paz De Barros Barrento Scavone for her contribution to this work. She assisted in collecting and sorting papers for review. We are grateful to JMCC for their continued support of NCT's research program.

Conflict of interest

Author FC was employed by Jamaican Medical Cannabis Corporation. Author ECL is employed by Numinus.

The remaining authors declare that the research was conducted in the absence of any commercial or financial relationships that could be construed as a potential conflict of interest.

Publisher's note

References

Aakerøy, R., Brede, G. I., Stolen, S. B., Krabseth, H. M., Michelsen, L. S., Andreassen, T. N., et al. (2021). Severe neurological sequelae after a recreational dose of LSD. *J. Anal. Toxicol.* 45, e1–e3. doi:10.1093/jat/bkaa145

Agin-Liebes, G. I., Malone, T., Yalch, M. M., Mennenga, S. E., Ponté, K. L., Guss, J., et al. (2020). Long-term follow-up of psilocybin-assisted psychotherapy for psychiatric and existential distress in patients with life-threatening cancer. *J. Psychopharmacol. (Oxf.)* 34, 155–166. doi:10.1177/0269881119897615

Argento, E., Omene, E., Jaeger, A. H., Kertes, A., Mitchell, K. A., Necyk, C., et al. (2023). Case report: improvement in refractory functional seizures, depression, and quality of life with ketamine-assisted therapy. *Front. Neurosci.* 17, 1197409. doi:10.3389/fnins.2023.1197409

Bedi, G., Hyman, D., and de Wit, H. (2010). Is ecstasy an 'empathogen'? Effects of ±3,4-methylenedioxymethamphetamine on prosocial feelings and identification of emotional states in others. *Biol. Psychiatry* 68, 1134–1140. doi:10.1016/j.biopsych.2010.08.003

Blond, B. N., and Schindler, E. A. D. (2023). Case report: psychedelic-induced seizures captured by intracranial electrocorticography. *Front. Neurol.* 14, 1214969. doi:10.3389/fneur.2023.1214969

Bogenschutz, M. P., Forcehimes, A. A., Pommy, J. A., Wilcox, C. E., Barbosa, P. C. R., and Strassman, R. J. (2015). Psilocybin-assisted treatment for alcohol dependence: a proof-of-concept study. *J. Psychopharmacol. (Oxf.)* 29, 289–299. doi:10.1177/0269881114565144

Bossis, A., Ross, S., Guss, J., Agin-Liebes, G., Malone, T., Cohen, B., et al. (2016). Rapid and sustained symptom reduction following psilocybin treatment for anxiety and depression in patients with life-threatening cancer: a randomized controlled trial. *J. Psychopharmacol. (Oxf.)* 30, 1165–1180. doi:10.1177/0269881116675512

Boyer, E. W., and Shannon, M. (2005). The serotonin syndrome. *N. Engl. J. Med.* 352, 1112–1120. doi:10.1056/NEJMra041867

Butler, M., Seynaeve, M., Nicholson, T. R., Pick, S., Kanaan, R. A., Lees, A., et al. (2020). Psychedelic treatment of functional neurological disorder: a systematic review. *Ther. Adv. Psychopharmacol.* 10, 2045125320912125. doi:10.1177/2045125320912125

Carhart-Harris, R., Leech, R., Hellyer, P. J., Shanahan, M., Feilding, A., Tagliazucchi, E., et al. (2014). The entropic brain: a theory of conscious states informed by neuroimaging research with psychedelic drugs. *Front. Hum. Neurosci.* 8, 20. doi:10.3389/fnhum.2014.00020

Carhart-Harris, R. L., Bolstridge, M., Rucker, J., Day, C. M. J., Erritzoe, D., Kaelen, M., et al. (2016a). Psilocybin with psychological support for treatment-resistant depression: an open-label feasibility study. *Lancet Psychiatry* 3, 619–627. doi:10.1016/S2215-0366(16)30065-7

Carhart-Harris, R. L., Kaelen, M., Bolstridge, M., Williams, T. M., Williams, L. T., Underwood, R., et al. (2016b). The paradoxical psychological effects of lysergic acid diethylamide (LSD). *Psychol. Med.* 46, 1379–1390. doi:10.1017/S0033291715002901

Carhart-Harris, R. L., and Nutt, D. J. (2017). Serotonin and brain function: a tale of two receptors. *J. Psychopharmacol. Oxf. Engl.* 31, 1091–1120. doi:10.1177/0269881117725915

Cooper, A. J., and Egleston, C. V. (1997). Accidental ingestion of Ecstasy by a toddler: unusual cause for convulsion in a febrile child. *J. Accid. Emerg. Med.* 14, 183–184. doi:10.1136/emj.14.3.183

Davis, A. K., Barrett, F. S., May, D. G., Cosimano, M. P., Sepeda, N. D., Johnson, M. W., et al. (2021). Effects of psilocybin-assisted therapy on major depressive disorder: a randomized clinical trial. *JAMA Psychiatry* 78, 481–489. doi:10.1001/jamapsychiatry.2020.3285

Davis, A. K., So, S., Lancelotta, R., Barsuglia, J. P., and Griffiths, R. R. (2019). 5-methoxy-N,N-dimethyltryptamine (5-MeO-DMT) used in a naturalistic group setting is associated with unintended improvements in depression and anxiety. *Am. J. Drug Alcohol Abuse* 45, 161–169. doi:10.1080/00952990.2018.1545024

Dumont, G. J. H., Sweep, F. C. G. J., van der Steen, R., Hermsen, R., Donders, A. R. T., Touw, D. J., et al. (2009). Increased oxytocin concentrations and prosocial feelings in humans after ecstasy (3,4-methylenedioxymethamphetamine) administration. *Soc. Neurosci.* 4, 359–366. doi:10.1080/17470910802649470

Foong, A.-L., Grindrod, K. A., Patel, T., and Kellar, J. (2018). Demystifying serotonin syndrome (or serotonin toxicity). *Can. Fam. Physician* 64, 720–727.

Francescangeli, J., Karamchandani, K., Powell, M., and Bonavia, A. (2019). The serotonin syndrome: from molecular mechanisms to clinical practice. *Int. J. Mol. Sci.* 20, 2288. doi:10.3390/ijms20092288

Gerhard, D. M., Pothula, S., Liu, R. J., Wu, M., Li, X. Y., Girgenti, M. J., et al. (2020). GABA interneurons are the cellular trigger for ketamine's rapid antidepressant actions. *J. Clin. Invest.* 130, 1336–1349. doi:10.1172/JCI130808

Goodwin, G. M., Aaronson, S. T., Alvarez, O., Arden, P. C., Baker, A., Bennett, J. C., et al. (2022). Single-dose psilocybin for a treatment-resistant episode of major depression. *N. Engl. J. Med.* 387, 1637–1648. doi:10.1056/NEJMoa2206443

Hall, A. P., Lyburn, I. D., Spears, F. D., and Riley, B. (1996). An unusual case of Ecstasy poisoning. *Intensive Care Med.* 22, 670–671. doi:10.1007/BF01709744

Huntjens, D. W., Weersink, E. P. S., Hilarius, D. L., Ran, N. C., and Franssen, E. J. F. (2022). Severe epileptic seizures after accidental MDMA exposure in a 14-month-old child. *Clin. Toxicol. Phila. Pa* 60, 657. doi:10.1080/15563650.2021.1999464

Johnson, M. W., Garcia-Romeu, A., and Griffiths, R. R. (2017). Long-term follow-up of psilocybin-facilitated smoking cessation. *Am. J. Drug Alcohol Abuse* 43, 55–60. doi:10.3109/00952990.2016.1170135

Kalant, H. (2001). The pharmacology and toxicology of "ecstasy" (MDMA) and related drugs. *CMAJ Can. Med. Assoc. J.* 165, 917–928.

Kelmendi, B., Kichuk, S. A., DePalmer, G., Maloney, G., Ching, T. H. W., Belser, A., et al. (2022). Single-dose psilocybin for treatment-resistant obsessive-compulsive disorder: a case report. *Heliyon* 8, e12135. doi:10.1016/j.heliyon.2022.e12135

Krebs, T. S., and Johansen, P.-Ø. (2012). Lysergic acid diethylamide (LSD) for alcoholism: meta-analysis of randomized controlled trials. *J. Psychopharmacol. (Oxf.)* 26, 994–1002. doi:10.1177/0269881112439253

Legriel, S., Bruneel, F., Spreux-Varoquaux, O., Birenbaum, A., Chadenat, M. L., Mignon, F., et al. (2008). Lysergic acid amide-induced posterior reversible encephalopathy syndrome with status epilepticus. *Neurocrit. Care* 9, 247–252. doi:10.1007/s12028-008-9096-5

López-Giménez, J. F., and González-Maeso, J. (2018). Hallucinogens and serotonin 5-ht2a receptor-mediated signaling pathways. *Curr. Top. Behav. Neurosci.* 36, 45–73. doi:10.1007/7854_2017_478

Magee, C., Staunton, H., Tormey, W., and Walshe, J. J. (1998). Hyponatraemia, seizures and stupor associated with ecstasy ingestion in a female. *Ir. Med. J.* 91, 178.

Mithoefer, M. C., Feduccia, A. A., Jerome, L., Mithoefer, A., Wagner, M., Walsh, Z., et al. (2019). MDMA-assisted psychotherapy for treatment of PTSD: study design and rationale for phase 3 trials based on pooled analysis of six phase 2 randomized controlled trials. *Psychopharmacol. (Berl.)* 236, 2735–2745. doi:10.1007/s00213-019-05249-5

Mithoefer, M. C., Mithoefer, A. T., Feduccia, A. A., Jerome, L., Wagner, M., Wymer, J., et al. (2018). 3,4-methylenedioxymethamphetamine (MDMA)-assisted psychotherapy for post-traumatic stress disorder in military veterans, firefighters, and police officers: a randomised, double-blind, dose-response, phase 2 clinical trial. *Lancet Psychiatry* 5, 486–497. doi:10.1016/S2215-0366(18)30135-4

National Academies of Sciences, et al. (2022). "History and current status of psychedelics and entactogens for the treatment of psychiatric disorders," in *Exploring psychedelics and entactogens as treatments for psychiatric disorders: proceedings of a workshop* (Washington, DC: National Academies Press US).

Palhano-Fontes, F., Barreto, D., Onias, H., Andrade, K. C., Novaes, M. M., Pessoa, J. A., et al. (2019). Rapid antidepressant effects of the psychedelic ayahuasca in treatment-resistant depression: a randomized placebo-controlled trial. *Psychol. Med.* 49, 655–663. doi:10.1017/S0033291718001356

Pauwels, S., Lemmens, F., Eerdekens, K., Penders, J., Poesen, K., Desmet, K., et al. (2013). Ecstasy intoxication as an unusual cause of epileptic seizures in young children. *Eur. J. Pediatr.* 172, 1547–1550. doi:10.1007/s00431-013-2080-x

Picker, W., Lerman, A., and Hajal, F. (1992). Potential interaction of LSD and fluoxetine. *Am. J. Psychiatry* 149, 843–844. doi:10.1176/ajp.149.6.843b

Rodriguez, C. I., Kegeles, L. S., Levinson, A., Feng, T., Marcus, S. M., Vermes, D., et al. (2013). Randomized controlled crossover trial of ketamine in obsessive-compulsive disorder: proof-of-concept. *Neuropsychopharmacol. Off. Publ. Am. Coll. Neuropsychopharmacol.* 38, 2475–2483. doi:10.1038/npp.2013.150

Rosa, W. E., Sager, Z., Miller, M., Bernstein, I., Doerner Rinaldi, A., Addicott, K., et al. (2022). Top ten tips palliative care clinicians should know about psychedelic-assisted therapy in the context of serious illness. *J. Palliat. Med.* 25, 1273–1281. doi:10.1089/jpm.2022.0036

Schenk, S., and Highgate, Q. (2021). Methylenedioxymethamphetamine (MDMA): serotonergic and dopaminergic mechanisms related to its use and misuse. *J. Neurochem.* 157, 1714–1724. doi:10.1111/jnc.15348

Serafetinides, E. A. (1965). The EEG effects of LSD-25 in epileptic patients before and after temporal lobectomy. *Psychopharmacologia* 7, 453–460. doi:10.1007/BF00402367

Sessa, B., Sakal, C., O'Brien, S., and Nutt, D. (2019). First study of safety and tolerability of 3,4-methylenedioxymethamphetamine (MDMA)-assisted psychotherapy in patients with alcohol use disorder: preliminary data on the first four participants. *BMJ Case Rep. CP* 12, e230109. doi:10.1136/bcr-2019-230109

Sloshower, J., Skosnik, P. D., Safi-Aghdam, H., Pathania, S., Syed, S., Pittman, B., et al. (2023). Psilocybin-assisted therapy for major depressive disorder: an exploratory placebo-controlled, fixed-order trial. *J. Psychopharmacol. (Oxf.)* 37, 698–706. doi:10.1177/02698811231154852

Stewart, B., Dean, J. G., Koek, A., Chua, J., Wabl, R., Martin, K., et al. (2020). Psychedelic-assisted therapy for functional neurological disorders: a theoretical framework and review of prior reports. *Pharmacol. Res. Perspect.* 8, e00688. doi:10.1002/prp2.688

Stroud, J. B., Freeman, T. P., Leech, R., Hindocha, C., Lawn, W., Nutt, D. J., et al. (2018). Psilocybin with psychological support improves emotional face recognition in treatment-resistant depression. *Psychopharmacol. (Berl.)* 235, 459–466. doi:10.1007/s00213-017-4754-y

Zanos, P., Moaddel, R., Morris, P. J., Georgiou, P., Fischell, J., Elmer, G. I., et al. (2016). NMDAR inhibition-independent antidepressant actions of ketamine metabolites. *Nature* 533, 481–486. doi:10.1038/nature17998

Zorumski, C. F., Izumi, Y., and Mennerick, S. (2016). Ketamine: NMDA receptors and beyond. *J. Neurosci.* 36, 11158–11164. doi:10.1523/JNEUROSCI.1547-16.2016

frontiers | Frontiers in Pharmacology

TYPE Review
PUBLISHED 26 January 2024
DOI 10.3389/fphar.2024.1276551

OPEN ACCESS

EDITED BY
Khojasteh Malekmohammad,
Shiraz University, Iran

REVIEWED BY
Alina Arulsamy,
Monash University, Malaysia
Satoshi Taksugi,
Meiji, Japan
Shahin Hakimian,
University of Washington, United States

*CORRESPONDENCE
Hanxiao Zhu,
zhu_hanxiao1109@163.com
Yun Li,
ly@dali.edu.cn

†These authors have contributed equally to this work

RECEIVED 12 August 2023
ACCEPTED 12 January 2024
PUBLISHED 26 January 2024

CITATION
Zhu H, Wang W and Li Y (2024), The interplay between microbiota and brain-gut axis in epilepsy treatment.
Front. Pharmacol. 15:1276551.
doi: 10.3389/fphar.2024.1276551

The interplay between microbiota and brain-gut axis in epilepsy treatment

Hanxiao Zhu[1,2*†], Wei Wang[3†] and Yun Li[1,2*]

[1]Department of Neurology, The First Affiliated Hospital of Dali University, Dali, China, [2]Clinical Medical School, Dali University, Dali, China, [3]Neurobiology Laboratory, China Agricultural University, Beijing, China

The brain-gut axis plays a vital role in connecting the cognitive and emotional centers of the brain with the intricate workings of the intestines. An imbalance in the microbiota-mediated brain-gut axis extends far beyond conditions like Irritable Bowel Syndrome (IBS) and obesity, playing a critical role in the development and progression of various neurological disorders, including epilepsy, depression, Alzheimer's disease (AD), and Parkinson's disease (PD). Epilepsy, a brain disorder characterized by unprovoked seizures, affects approximately 50 million people worldwide. Accumulating evidence suggests that rebuilding the gut microbiota through interventions such as fecal microbiota transplantation, probiotics, and ketogenic diets (KD) can benefit drug-resistant epilepsy. The disturbances in the gut microbiota could contribute to the toxic side effects of antiepileptic drugs and the development of drug resistance in epilepsy patients. These findings imply the potential impact of the gut microbiota on epilepsy and suggest that interventions targeting the microbiota, such as the KD, hold promise for managing and treating epilepsy. However, the full extent of the importance of microbiota in epilepsy treatment is not yet fully understood, and many aspects of this field remain unclear. Therefore, this article aims to provide an overview of the clinical and animal evidence supporting the regulatory role of gut microbiota in epilepsy, and of potential pathways within the brain-gut axis that may be influenced by the gut microbiota in epilepsy. Furthermore, we will discuss the recent advancements in epilepsy treatment, including the KD, fecal microbiota transplantation, and antiseizure drugs, all from the perspective of the gut microbiota.

KEYWORDS

epilepsy, brain-gut-microbiota axis, viscerosensory pathway, endocrine pathway, immune pathway

1 Introduction

Epilepsy is a neurological disease characterized by recurrent, unprovoked epileptic seizures, temporary neurological dysfunction, and a host of other adverse effects (Fisher et al., 2014; Thijs et al., 2019). Seizures are transient clinical manifestations arising from synchronized, high-frequency, or abnormal excessive neuronal activity in the central nervous system (CNS). They can stem from a diverse range of etiologies associated with congenital or acquired brain malformations, structural injuries or lesions, and other brain diseases or disorders (Fisher et al., 2017a; Balestrini et al., 2021; Zhu et al., 2023). Recent study has revealed that the prevalence of active epilepsy worldwide stands at 6.38 per 1,000 individuals, whereas the lifetime prevalence is estimated at 7.60 per

1,000 individuals (Fiest et al., 2017). The annual incidence rate of epilepsy is 6.144 per 10,000 people, with an alarming long-term recurrence rate of 83.6% within a decade (Beretta et al., 2017; Fiest et al., 2017; Zhu et al., 2022). Moreover, it has been found to be linked with patient stigmatization, concurrent neurological and psychiatric disorders, as well as exorbitant medical expenses, all of which significantly impair the patient's wellbeing and quality of life, especially in low-income nations.

The elaborate relationship between the brain and the gut is commonly referred to as the "brain-gut axis," serving as the central nexus that connects the cognitive and emotional centers in the brain to gut function. This connection begins during development and persists throughout a person's lifetime (Borre et al., 2014; Furness et al., 2014). Recent advancements in research have expanded our understanding of the brain-gut axis beyond its role in functional gastrointestinal disorders. Furthermore, these studies are dedicated to elucidating the impact of gut dysbiosis on the structure and function of this axis. The "brain-gut-microbiota axis" has been coined to describe this form of gut microbial involvement in brain-gut communication (Cryan and Dinan, 2012). Gut microbiota influence brain-gut interactions primarily through nerve, endocrine, immune and metabolic signaling mechanisms, spanning early life stages to neurodegenerative pathologies, and from the gut lumen to the CNS (Quigley, 2017).

Dysfunction within the brain-gut-microbiota axis may contribute to the pathogenesis and pathophysiology of gastrointestinal disorders such as IBS and obesity. Additionally, it also plays a role in the development of numerous neurological disorders, including epilepsy, depression, AD, autism spectrum disorder (ASD), Parkinson's disease, and more (Amaral et al., 2008; Mayer, 2011; Cryan and Dinan, 2012; Park et al., 2013; Sampson et al., 2016; Vuong and Hsiao, 2017; Ding et al., 2021). In recent years, numerous studies have provided evidence supporting a close connection between the gut and epilepsy, both in clinical observations and animal experiments (Peng et al., 2018; Zhang et al., 2018; Lindefeldt et al., 2019; Gong et al., 2020; Citraro et al., 2021; Ding et al., 2021; Eor et al., 2021; Lee et al., 2021). For instance, significant differences in fecal microbial composition have been observed between individuals with epilepsy and healthy subjects, as well as before and after KD treatment in epilepsy patients and in animal models of epilepsy (Lindefeldt et al., 2019; Gong et al., 2020; Eor et al., 2021; Lee et al., 2021).

Understanding the interactions between the brain and the gut in individuals with epilepsy holds immense significance in unraveling the mechanisms of communication between these vital centers of activity in the body and the underlying pathophysiology of epilepsy. This exploration not only has the potential to identify novel therapeutic targets for epilepsy treatment but also strives to develop tailored preventive strategies for this condition. Numerous previous reviews have delved into the connection between gut microbiota and epilepsy (De Caro et al., 2019a; Dahlin and Prast-Nielsen, 2019; Fan et al., 2019; Ułamek-Kozioł et al., 2019; Holmes et al., 2020; Amlerova et al., 2021; Chatzikonstantinou et al., 2021; Ding et al., 2021; Tang et al., 2021; Arulsamy and Shaikh, 2022; Fusco et al., 2022; Iannone et al., 2022; Russo, 2022; Yue et al., 2022; Özcan et al., 2022; Wang et al., 2023), but this paper stands out as the most comprehensive analysis to date. We have curated an extensive body of clinical and animal evidence that supports the involvement of the brain-gut-microbiota axis in epilepsy and drug-resistant epilepsy. Furthermore, we meticulously outline potential pathways through which gut flora mediate epilepsy pathology. Our primary focus is on elucidating the mechanisms by which gut microbiota can be harnessed for epilepsy therapy, thereby contributing to a more profound comprehension of this critical aspect of the condition.

2 The close relationship between the gut microbiota and epilepsy

Several population-based studies have revealed differences in gut microbiota between individuals with epilepsy and healthy controls, albeit in relatively limited sample sizes. In a bi-directional Mendelian randomization study, researchers explored the causal relationship and identified specific gut microbe taxa associated with epilepsy, using genome-wide association study (GWAS) data of epilepsy, gut microbiota, and gut microbiota-dependent metabolites such as trimethylamine N-oxide and its predecessors. Following multiple-testing correction, the study identified a suggestive association of host-genetic-driven increase in class Melainabacteria with a lower risk of generalized epilepsy with tonic-clonic seizures, class Betaproteobacteria and order Burkholderiales with a lower risk of juvenile myoclonic epilepsy, and family Veillonellaceae with a higher risk of childhood absence epilepsy (Ouyang et al., 2022).

In order to gain a better understanding of the changes in gut microbiota in children with focal epilepsy before and after drugs treatment, Zhou et al. conducted a study that involved dividing 10 children with newly diagnosed focal epilepsy into a pre-treatment subgroup and a post-treatment subgroup (treated with oral oxcarbazepine), and included 14 healthy children of the same age as controls. The study revealed significant differences in α diversity between the pre-treatment subgroup and the control group. The relative abundance of Actinobacteria phylum, and *Escherichia/Shigella*, *Collinsella*, *Streptococcus*, and *Megamonas* genus was notably higher in the pre-treatment subgroup, while *Faecalibacterium* and *Anaerostipes* were enriched in the control group. After 3 months of antiseizure treatment, no significant differences were found in α diversity between the post-treatment and pre-treatment subgroups. Additionally, the differences in bacterial composition between the post-treatment children and controls were not significant. However, the relative abundance of Actinobacteria phylum notably declined after treatment compared to the pre-treatment subgroup, and the proportion of certain genera, such as *Escherichia/Shigella*, *Collinsella*, *Streptococcus*, and *Megamonas*, also decreased significantly (Zhou et al., 2022). Similarly, Gong S.Z. et al. also found higher levels of Actinobacteria phylum and the genus *Escherichia/Shigella*, *Collinsella*, *Streptococcus*, and *Megamonas* in children with focal epilepsy. After treatment with Oxcarbazepine, patients exhibited lower levels of Actinobacteria phylum and the genus *Escherichia/Shigella*, *Collinsella*, *Streptococcus*, and *Megamonas* (Gong, et al., 2022). These findings were consistent with the results of the study by Zhou et al. (2022).

In a separate study examining the gut microbiota composition, 30 patients with idiopathic focal epilepsy and 10 healthy subjects

TABLE 1 Alterations in gut microbiota in patients with epilepsy.

Participants	Age (years)	Treatment	Alteration in gut microbiota	References
Children with refractory epilepsy	0.5–3.2	KD	Lower alpha diversity; increased levels of Bacteroidetes phylum and decreased abundance of Firmicutes phylum	Zhang et al. (2018)
Children with therapy-resistant epilepsy	2.8–15.3	KD	No changes in alpha diversity; decreased the genus Bifidobacterium (the species *Bifidobacterium longum* and *B. adolescentis*) as well as *Eubacterium rectale* and genus *Dialister*; increased abundance in *Escherichia coli*	Lindefeldt et al. (2019)
Childhood absence epilepsy	—	—	Host-genetic-driven increase in family Veillonellaceae with a higher risk of childhood absence epilepsy	Ouyang et al. (2022)
Generalized epilepsy with tonic-clonic seizures	—	—	Host-genetic-driven increase in class Melainabacteria with a lower risk of generalized epilepsy with tonic-clonic seizures	Ouyang et al. (2022)
Juvenile myoclonic epilepsy	—	—	Host-genetic-driven increase in class Betaproteobacteria and order Burkholderiales with a lower risk of juvenile myoclonic epilepsy	Ouyang et al. (2022)
Paediatric patients with cerebral palsy and epilepsy	70.43 ± 20.93 months	—	Higher microbial diversity; incaresed genera *Bifidobacterium*, *Streptococcus*, *Akkermansia*, *Enterococcus*, *Prevotella*, *Veillonella*, *Rothia*, and *Clostridium IV*; reduced genera *Bacteroides*, *Faecalibacterium*, *Blautia*, *Ruminococcus*, *Roseburia*, *Anaerostipes*, and *Parasutterella*	Huang et al. (2019)
Children with focal epilepsy	Mean age 6.35	Oral antiepileptics	Pre-reatment vs. Control: significant differences in alpha diversity; higer Actinobacteria phylum; increased genera *Escherichia/Shigella*, *Streptococcus*, *Collinsella*, and *Megamonas*; decaresed genera *Faecalibacterium* and *Anaerostipes*; Post-treatment vs. Pre-treatment: reduced Actinobacteria phylum and genera *Escherichia/Shigella*, *Streptococcus*, *Collinsella*, and *Megamonas*	Zhou et al. (2022)
Children with cerebral palsy and epilepsy	4–14	—	*Bifidobacterium*, *Bacteroidetes*, and *Prevotella* were the top three abundant genera	Huang et al. (2022)
Infants with epilepsy	0–2	—	Lower abundance of Proteobacteria phylum and higher abundance of *Bifidobacterium* genus	Liu et al. (2023)
Children with cerebral palsy and epilepsy	3–15	Fluid diet	Liquid diet vs. General diet: significant differences in Bacteroidetes and Actinobacteria phylum; increased genera *Bifidobacterium* and *Collinsella*; decreased genera *Prevotella*, *Roseburia*, *Lactobacillus*, and *Faecalibacterium*	Huang et al. (2021)
Childhood Epilepsy	2–11	—	Higer the genera *Flavobacterium*, *Holdemania*, and *Hyphomicrobium*; the genera *Megamonas* and *Coriobacterium* were observed only in the epilepsy	Türay et al. (2023)
Children with drug refractory epilepsy	26.33 ± 12.05	—	Increased richness and diversity, and Actinobacteria phylum and the genus *Enterococcus*, *Anaerostipes*, *Bifidobacterium*, *Bacteroides*, and *Blautia*	Gong et al. (2021)
Children with drug refractory epilepsy	26.33 ± 12.05	KD	Decreased the genus *Bifidobacterium*, *Akkermansia*, *Enterococcaceae* and *Actinomyces*, and increased the genus *Subdoligranulum*, *Dialister*, *Alloprevotella*	Gong et al. (2021)

(Continued on following page)

TABLE 1 (*Continued*) Alterations in gut microbiota in patients with epilepsy.

Participants	Age (years)	Treatment	Alteration in gut microbiota	References
An ASD patient with a history of generalized seizures	17-year-old	KD	A reduction in Firmicutes, Bacteroidetes, and Proteobacteria phylum;	Bertuccioli et al. (2022)
An ASD patient with a history of generalized seizures	17-year-old	Monosaccharides and polyols diet	Increased alpha biodiversity; Decreased Actinobacteria, Firmicutes, Lactobacilli, and Bifidobacteria, and the Firmicutes/Bacteroidetes ratio	Bertuccioli et al. (2022)
Children with epilepsy	3–16	—	Reduced trend of bacterial abundances and biodiversity; increased abundance in *Akkermansia* spp. and Proteobacteria and a decreased relative abundance in *Faecalibacterium* spp.	Ceccarani et al. (2021)
Participants with cryptogenic epilepsy	53 ± 6.72	VPA treatment	Increased the ratio of phylum Firmicutes/Bacteriodetes;	Gong et al. (2022a)
Temporal lobe epilepsy patients with anxiety disorders	31.3 ± 7.2	—	Higher abundances of Firmicutes (phylum), Proteobacteria (phylum), Lachnospirales (order), Enterobacterales (order), Lachnospiraceae (family), Enterobacteriaceae (family), Gammaproteobacteria (class), and lower abundances of Clostridia (class), *Escherichia-Shigella* (genus), and *Ruminococcus* (genus); more abundant in fungi: Saccharomycetales fam. incertae sedis (family), Saccharomycetales (order), Saccharomycetes (class), and Ascomycota (phylum)	Wei et al. (2023)
Patients with drug-resistant epilepsy	16–50	Ciprofloxacin	Increased Bacteroidetes/Firmicutes ratio	Cheraghmakani et al. (2021)
Children with cerebral palsy and epilepsy	8.8 (4.5–16.9)	—	Decreased abundances of *Bacteroides fragilis* and *Dialister invisus*; increased abundances of *Phascolarctobacterium faecium* and *Eubacterium limosum*	Peng et al. (2023)
Children with cerebral palsy and drug-resistant epilepsy	9.7 (4.5–15.4)	—	Higher abundances of *Veillonella parvula*	Peng et al. (2023)
Patients with epilepsy	31.6 ± 12.2	—	Increased the genus *Fusobacterium*, *Megasphaera*, *Alloprevotella*, and *Sutterella*	Dong et al. (2022)
Children with focal epilepsy	6 (5, 9)	—	Higher Actinobacteria phylum and the genus *Escherichia/Shigella*, *Collinsella*, *Streptococcus*, and *Megamonas*	Gong et al. (2022)
Children with focal epilepsy	6 (5, 9)	Oxcarbazepine	Lower Actinobacteria phylum Actinobacteria phylum and the genus *Escherichia/Shigella*, *Collinsella*, *Streptococcus*, and *Megamonas*	Gong et al. (2022)
Drug-resistant epilepsy patients	27.70 ± 13.32	—	Lower microbial diversity; higher the Phylum Firmicutes and the class Bacilli	Dai et al. (2022)
Rasmussen encephalitis with focal intractable seizures	18	Probiotic kefir supplementation	Increased *Lactobacillus* and *Bifidobacterium* species	Lemos et al. (2022)
Children with Intractable Epilepsy	1.16–6.92	—	Lower microbiota richness; higher abundance of Actinobacteria and lower abundance of Bacteroidetes	Lee et al. (2020)
Pediatric patients with refractory epilepsy	1.95 ± 3.10	—	Increased abundance of the Firmicutes and Proteobacteria phylum; decreased abundance of Bacteroidetes and Actinobacteria; elevated abundance of *Cronobacter*, and decreased the relative abundance of beneficial genera such as *Bacteroides*, *Prevotella*, and *Bifidobacterium*	Xie et al. (2017)

(Continued on following page)

TABLE 1 (*Continued*) Alterations in gut microbiota in patients with epilepsy.

Participants	Age (years)	Treatment	Alteration in gut microbiota	References
Pediatric patients with refractory epilepsy	1.95 ± 3.10	KD	Increased abundance of the *Bacteroides* and *Prevotella*; decreased abundance of the *Cronobacter*, *Erysipelatoclostridium*, *Streptococcus*, *Alistipes*, *Ruminiclostridium*, *Barnesiella* and *Enterococcus*	Xie et al. (2017)
Patients with idiopathic focal epilepsy	41.3 ± 12.2	—	Higher levels of the Proteobacteria phylum, which included genera such as *Campylobacter*, *Delftia*, *Lautropia*, *Haemophilus*, and *Neisseria*	Şafak et al. (2020)
Patients with drug- responsive epilepsy	44 ± 17.2	—	Increased relative abundance of *Bacteroides finegoldii* and *Ruminococcus_g2*	Lee et al. (2021)
Patients with drug-resistant epilepsy	41 ± 13.6	—	Increased relative abundance of *Negativicutes*	Lee et al. (2021)
Patients with drug-resistant epilepsy	28.4 ± 12.4	—	Greater microbial community richness and evenness; higher abundance of the Firmicutes phylum and relatively lower abundance of the Bacteroidetes phylum; elevated abundance of numerous rare bacteria, including *Clostridium XVIII*, *Fusobacterium*, *Methanobrevibacter*, *Atopobium*, *Holdemania*, *Delftia*, *Coprobacillus*, *Dorea*, *Saccharibacteria*, *Paraprevotella*, *Gemmiger*, *Akkermansia*, *Ruminococcus*, *Neisseria*, *Coprococcus*, *Phascolarctobacterium*, and *Roseburia*	Peng et al. (2018)
Patients diagnosed with epilepsy	26.33 ± 12.05	—	Increased levels of Actinobacteria and Verrucomicrobia phylum and decreased levels of Proteobacteria phylum; increased *Prevotella_9*, *Blautia*, *Bifidobacterium*, and others genus	Gong et al. (2020)
Patients with drug-resistant epilepsy	26.33 ± 12.05	—	Increased Actinobacteria, Verrucomicrobia, and Nitrospirae phylum and several genera including *Blautia*, *Subdoligranulum*, *Bifidobacterium*, *Dialister*, and *Anaerostipes*	Gong et al. (2020)

were analyzed (Şafak et al., 2020). Patients with epilepsy exhibited higher levels of the Proteobacteria phylum, which included genera such as *Campylobacter*, *Delftia*, *Lautropia*, *Haemophilus*, and *Neisseria*. Conversely, the healthy controls had lower abundance of this phylum. The *Clostridium* phylum, specifically *Leptotrichia* and *Fusobacterium*, were found in 10.6% of epileptic patients but were absent in the healthy controls. Moreover, the levels of the Firmicutes, Actinobacteria, and Bacteroidetes phylum were higher in the healthy control group compared to epileptic patients. At the genus level, *Blautia*, *Coprococcus*, *Faecalibacterium* and *Ruminococcus* genus of the Firmicutes phylum, *Bifidobacterium* and *Collinsellagenus* of the Actinobacteria phylum, *Bacteroides* and *Parabacteroides* genus of the Bacteroidetes phylum were significantly higher in the healthy volunteer group than in the epilepsy group (Şafak et al., 2020).

Furthermore, Huang et al. conducted a study to investigate the gut microbiota characteristics in 25 children with both cerebral palsy and epilepsy, comparing them with 21 healthy children. The results revealed that pediatric patients with cerebral palsy and epilepsy exhibited significantly higher microbial diversity and enrichment of *Bifidobacterium*, *Streptococcus*, *Akkermansia*, *Enterococcus*, *Prevotella*, *Veillonella*, *Rothia*, and *Clostridium IV* genera, while there was a noticeable reduction in *Bacteroides*, *Faecalibacterium*, *Blautia*, *Ruminococcus*, *Roseburia*, *Anaerostipes*, and *Parasutterella* genera (Huang et al., 2019). Moreover, a separate study by Liu et al. (2023) found that neonates aged 0–2 years with epilepsy showed a lower abundance of Proteobacteria phylum and a higher abundance of *Bifidobacterium* genus. These findings, in conjunction with the data presented in Tables 1, 2, suggest a potential association between epilepsy and alterations in gut microbiota. Notably, these studies have too few subjects and risk for over fitting if the data. It is crucial for future research to utilize larger and more diverse samples in order to ensure the generalizability of the findings. Additionally, researchers should employ appropriate statistical techniques to avoid overfitting and ensure the robustness of their results.

However, a significant portion of current research aimed at understanding the role of gut flora in epilepsy has primarily focused on patients with drug-resistant epilepsy, which refers to cases where seizures cannot be effectively controlled with antiseizure drugs. Drug-resistant epilepsy, where approximately 30%–40% of individuals with epilepsy are resistant to multiple anti-seizure drugs, presents a significant challenge in treatment (Tang et al., 2017). To investigate potential factors contributing to drug resistance, a study analyzed the gut microbiota of 42 patients with drug-resistant epilepsy, 49 with drug-sensitive epilepsy, and 65 healthy controls. The results revealed that patients with drug-

TABLE 2 Alterations in gut microbiota in animal models of epilepsy.

Animals	Age (years)	Treatment	Alteration in gut microbiota	References
Dogs with idiopathic epilepsy	1–11	—	No changes in α-diversity and *Lactobacillus* genus	Muñana et al. (2020)
Epileptic dogs	2–6	—	Reduced abundance of *Pseudomonadales*, *Pseudomonadaceae*, *Pseudomonas*, *Pseudomona_graminis*, *Peptococcaceae*, *Ruminococcaceae*, *Anaerotruncus* as well as *Prevotellaceae*	García-Belenguer et al. (2021)
Epileptic dogs	5.6 ± 1.9	—	Higher abundance of *Lactobacillus*	García-Belenguer et al. (2023)
Epileptic dogs	5.6 ± 1.9	Ketogenic medium chain triglycerides (MCT)- enriched diet	Higher abundance of *Negativicutes* and *Selenomonadales*	García-Belenguer et al. (2023)
Dogs with drug-refractory epilepsy	6.8 ± 1.8	MCT diet	Increased the abundance of Firmicutes; decreased the abundance of Bacteroidetes and Fusobacteria	García-Belenguer et al. (2023)
The PTZ-induced kindled rats	90 days	Prednisolone administration	Increased abundance of Verrucomicrobia, Actinobacteria, and *Saccharibacteria*	de Lima et al. (2022)
Chronic PTZ-kindled model rats	7–8 weeks	Anticonvulsant chemical Q808	Increased abundance of *Lactobacillus*, *Roseburia*, *Alloprevptella*, *Prevotellaceae_NK3B31_group*, *Prevotellaceae_UCG-001*, and *Prevotella_9*	Li et al. (2022)
Lithium chloride-pilocarpine-induced epilepsy rats	—	—	Reduced the genus *Helicobacter*, *Prevotellaceae_UCG-001*, and Ruminococcaceae_*UCG-005*	Gong et al. (2022b)
Rats with Lithium-Pilocarpine-Induced Temporal Lobe Epilepsy	60-day-old	—	Lower species richness; increased phylum Desulfobacterota and decreased Patescibacteria	Oliveira et al. (2022)
Neonatal rat model of infantile spasms syndrome (IS)	Four days after birth	Switching KD to a normal diet	lower abundance of the genus *Streptococcus*, *Staphylococcus* and higher *Rothia*; reduced *Streptococcus thermophilus* and *Streptococcus azizii* species; increased *Enterococcus faecium* species	Shearer et al. (2023)
Rat model of symptomatic IS	Four days after birth	KD and antibiotic administration	Increased abundance of *Streptococcus thermophilus* and *Lactococcus lactis*	Mu et al. (2022a)
WAG/Rij rats (a genetic animal model of absence epilepsy)	1, 4, and 8 months of age	—	lower Bacteroidetes/Firmicutes ratio	Citraro et al. (2021)
WAG/Rij rats (a genetic animal model of absence epilepsy)	6 months of age	FMT from Wistar non-epileptic donors	Increased *Coprococcus* (*C eutactus*) and *Phascolarctobacterium* (*P succinatutens*) genera, and decreased *Flexispira* genera	Citraro et al. (2021)
Wistar rats	6 months of age	FMT from WAG/Rij rats	Decreased the relative abundance of *C eutactus* and an increase of *Bacteroides* (*B dorei* and *B eggerthii*), *Parabacteroides* (*P distasonis*), and *Akkermansia* (*A muciniphila*)	Citraro et al. (2021)
Mouse model of refractory epilepsy	3–4 week old	KD	Decreased alpha-diversity; Increases *A. muciniphila* and *Parabacteroides*	Olson et al. (2018)
The *Kcna1*$^{-/-}$ mouse model for generalized tonic-clonic seizures	3–4 week old	KD	Increases *A. muciniphila* and *Parabacteroides*	Olson et al. (2018)
The DBA/1 mouse model of sudden unexpected death in epilepsy	—	High-tryptophan diet	Increased richness and diversity and Proteobacteria and Actinobacteria phylum	Yue et al. (2021)
Kainic acid (KA)-induced mouse model	—	Lipopolysaccharide (LPS) injections for 4 consecutive days	Increased the abundance of *Ruminococcus*	Ding et al. (2022)
Dravet mice	14–26 days after birth	—	Reduced species richness; increased ratio of Firmicutes and Bacteroidetes phylum;	Miljanovic and Potschka (2021)

(Continued on following page)

TABLE 2 (*Continued*) Alterations in gut microbiota in animal models of epilepsy.

Animals	Age (years)	Treatment	Alteration in gut microbiota	References
Dravet mice	P14–26 days after birth	KD	Increased the abundance of Firmicutes and decreased the abundance of Bacteroidetes phylum; elevated in *Clostridium*, Oscillospira, Acetatifactor, and Enterohabdus abundance	Miljanovic and Potschka (2021)
Mouse model of trimethyltin chloride-induced epilepsy-like seizure	—	Oral gavage of chlorogenic acid	Increased abundance of *Lactobacillus* genus	Xi et al. (2022)

resistant epilepsy showcased an altered gut microbiome composition, characterized by a pronounced increase in the abundance of various rare bacteria. In contrast, the gut microbiota of patients with drug-sensitive epilepsy closely resembled that of healthy controls (Peng et al., 2018). At a higher taxonomic level, patients with drug-resistant epilepsy exhibited greater microbial community richness and evenness. Specifically, they displayed relatively higher abundance of the Firmicutes phylum and relatively lower abundance of the Bacteroidetes phylum. Additionally, several rare phylum demonstrated an increasing trend in patients with drug-resistant epilepsy. For instance, the phylum Verrucomicrobia was also more abundant in drug-resistant epilepsy patients compared to both drug-sensitive epilepsy patients and healthy controls. Moreover, at the genus level, patients with drug-sensitive epilepsy showed significantly higher abundance of Bacteroidetes and two genera, *Bacteroides* and *Barnesiella*. In contrast, the microbial composition of drug-resistant epilepsy patients was characterized by an elevated abundance of numerous rare bacteria, including *Clostridium XVIII*, *Fusobacterium*, *Methanobrevibacter*, *Atopobium*, *Holdemania*, *Delftia*, *Coprobacillus*, *Dorea*, *Saccharibacteria*, *Paraprevotella*, *Gemmiger*, *Akkermansia*, *Ruminococcus*, *Neisseria*, *Coprococcus*, *Phascolarctobacterium*, and *Roseburia* (Peng et al., 2018). Gong et al. (2020) examined the fecal microbiota of 55 patients diagnosed with epilepsy and 46 healthy individuals to unravel the intricate interplay between gut microbiome and epilepsy. Differences were observed in the structure and composition of the fecal microbiota among patients with various clinical prognoses, as well as between patients and healthy controls. For instance, Verrucomicrobia, and Nitrospirae phylum and several genera including *Blautia*, *Subdoligranulum*, *Bifidobacterium*, *Dialister*, and *Anaerostipes* were enriched in patients with drug-resistant epilepsy. The alterations in the microbiome observed in patients with epilepsy included increased levels of Actinobacteria and Verrucomicrobia phylum, while the levels of Proteobacteria phylum were decreased. In addition, *Prevotella_9*, *Blautia*, *Bifidobacterium*, and other genera were found to be increased in epilepsy patients. Notably, the models constructed based on the gut microbiome were capable of distinguishing between drug-resistant and drug-sensitive epilepsy (Gong et al., 2020). Interestingly, an exploratory study found that patients with drug-resistant epilepsy and drug-sensitive epilepsy did not show significant differences in alpha and beta diversity analyses, but the composition of the gut microbiota did. In particular, the drug-sensitive group showed an increased relative abundance of *Bacteroides finegoldii* and *Ruminococcus_g2*, whereas the drug-resistant group showed an increased relative abundance of *Negativicutes*, a phylum belonging to the Firmicutes (Lee et al., 2021).

A comprehensive analysis of the fecal microbiota in pediatric patients with refractory epilepsy has unveiled significant differences in the diversity of their intestinal microbiota compared to age-matched healthy infants (Xie et al., 2017). For example, infants with refractory epilepsy exhibited a notable increase in the abundance of the Firmicutes and Proteobacteria phylum, while experiencing a decrease in the presence of Bacteroidetes and Actinobacteria in their fecal microbiota. Delving deeper into the microbial composition at the genus level, infants with epilepsy displayed a significant rise in the abundance of *Cronobacter*, a potential pathogenic bacterium, while concurrently experiencing a decrease in the relative abundance of beneficial genera such as *Bacteroides*, *Prevotella*, and *Bifidobacterium* (Xie et al., 2017). In addition, Lindefeldt et al. (2019) investigated the fecal microbiota of 12 children with therapy-resistant epilepsy and unraveled compelling alterations in the relative abundance of key phylum within the intestinal microbiota. The patients with epilepsy exhibited a significant decrease in the presence of the Bacteroidetes and Proteobacteria phylum. Inversely, there was a substantial increase in the relative abundance of the Actinobacteria and Firmicutes phylum. Consistently, Lee et al. conducted a study focusing on the gut microbiome of 8 children with intractable epilepsy and 32 age-matched healthy participants. The results also revealed lower microbiota richness in the epilepsy children compared to the healthy controls. The epilepsy group exhibited higher abundance of Actinobacteria and lower abundance of Bacteroidetes compared to the healthy controls. What is more, *Enterococcus faecium*, *Bifidobacterium longum*, and *Eggerthella lenta* emerged as strong potential biomarkers in the refractory epilepsy patients (Lee et al., 2020).

In addition to clinical studies, evidence from animal models of epilepsy supports the relationship between gut microbiota and the pathophysiology of epilepsy. Sprague-Dawley (SD) rats exposed to chronic restraint stress exhibited heightened vulnerability to seizures, as even a minimal amount of basolateral amygdala stimulation was sufficient to trigger complete and persistent seizures. Furthermore, when fecal contents from stressed donors were transplanted into the gastrointestinal tract of specific pathogen-free (SPF) rats, the recipients displayed an amplified susceptibility to seizure-inducing stimuli, along with prolonged seizure duration. SPF rats receiving fecal transplants from sham-stressed subjects exhibited increased seizure thresholds and shortened seizure duration. On the contrary, the implantation of intestinal microbiota from non-stressed rats into stressed animals

demonstrated a noteworthy reduction in the duration of epileptic seizures within the stressed group of rats (Medel-Matus et al., 2018). The induction of intestinal inflammation through the intracolonic administration of 2,4,6-trinitrobenzene sulfonic acid (TNBS) in adult male rats resulted in an augmented susceptibility to pentylenetetrazole (PTZ) seizures, which exhibited a strong correlation with the severity and progression of intestinal inflammation (Riazi et al., 2008). Central antagonism of TNF alpha using a monoclonal antibody successfully prevented the increase in seizure susceptibility. Analysis of the gut microbiota between WAG/Rij rats (a recognized genetic model of absence epilepsy) and non-epileptic Wistar rats revealed notable differences in beta diversity and specific phylotypes across all age groups, as well as significant variations in the Bacteroidetes/Firmicutes ratio (Citraro et al., 2021). Importantly, fecal microbiota transplantation (FMT) from both Wistar and ethosuximide-treated WAG/Rij donors to WAG/Rij rats resulted in a significant reduction in the frequency and duration of seizures. Further, histological findings further highlighted that WAG/Rij rats displayed intestinal villi disruption and inflammatory infiltrates as early as 1 month of age, prior to the onset of seizures. FMT partially restored intestinal morphology while also significantly modifying the gut microbiota, leading to a concurrent reduction in absence seizures (Citraro et al., 2021).

Similarly, the dextran sulfate sodium (DSS)-induced intestinal inflammation in mice led to an increased susceptibility to PTZ-induced seizures (De Caro et al., 2019b). Reducing intestinal inflammation through the administration of alpha-lactoalbumin (ALAC) and sodium butyrate (NaB) exhibited significant anti-seizure effects in mice, but failed to demonstrate efficacy as anti-seizure agents in control mice without colitis at the same doses. Notably, in DSS-treated mice, the anti-seizure efficacy of valproic acid (VPA) was compromised compared to its ability to prevent seizures in non-DSS-treated mice (De Caro et al., 2019b). Then again, mice receiving microbiota from epileptic animals exhibited a higher propensity to develop status epilepticus compared to recipients of "healthy" microbiota, particularly after receiving subclinical doses of pilocarpine. This indicates an increased susceptibility to seizures influenced by the microbiota (Mengoni et al., 2021).

In brief, a wealth of clinical and animal experimental evidence (along with Tables 1, 2) supports the hypothesis of a close relationship between gut microbiota and epilepsy.

3 The role of gut microbiota-mediated visceral sensory pathways in epilepsy

The Enteric nervous system (ENS) is a peripheral nervous system substructure that directly controls the gastrointestinal tract and plays a vital role in the reflex physiological control of the body (Costa et al., 2000). Comprising over 100 million interconnected neurons, the ENS is a highly complex microcircuit designed to function autonomously, independent of the CNS and spinal cord (Gershon, 2010).

While the ENS is capable of autonomous behavior, it maintains bidirectional communication with the CNS. This communication is usually through the sympathetic nervous system via afferent sensory pathways in the vagus nerve and efferent motor pathways in the prevertebral ganglion, respectively (Khlevner et al., 2018). The ENS innervates visceral smooth muscle and other organs involved in gastrointestinal secretory, sensory, motor, endocrine, and immune functions. It transmits sensory signals through the spinal cord and vagus nerve to the brainstem and sensorimotor brain circuits, with modulation from affective and cognitive networks (bottom-up pathways) (Craig, 2003). Additionally, the autonomic nervous system's sympathetic and parasympathetic efferent branches directly connect emotional arousal and autonomic brain circuits to the ENS (top-down pathway) (Mayer, 2011; Van Oudenhove et al., 2016). The brain and gastrointestinal tract have a complex bidirectional interaction to regulate normal digestive processes and integrate them with the organism's emotional and physiological states (Craig, 2002).

Interestingly, emerging evidence suggests that the gut microbiota plays a significant role in regulating the brain-gut axis. The microbiota has the ability to influence the CNS directly through the vagus nerve or indirectly by modulating the ENS (Bercik et al., 2011) (see Figure 1). On the side, an essential player in the communication between the brain and gut is 5-hydroxytryptamine (5-HT). It is present in both the ENS and CNS, acting as a crucial mediator in brain-gut communication. As a hormone throughout the loop, further highlighting its importance in this intricate system (Wikoff et al., 2009).

Remarkably, vagus nerve stimulation (VNS) has emerged as a widely utilized therapy for epilepsy since its initial discovery in 1988 (Attenello et al., 2015). The electrical stimulation of vagal afferent fibers has been found to have an effect on the brain's concentrations of various neurotransmitters, such as 5-hydroxytryptamine, gamma-aminobutyric acid (GABA), and glutamate. This alteration in neurotransmitter levels may provide an explanation for the effectiveness of vagus nerve stimulation in treating epilepsy (Ressler and Mayberg, 2007). Besides that, recent studies have shed light on the connection between gut stimulation and modulation of brain activity through the autonomic nervous system. In mice administered live *Campylobacter* jejuni, it was observed that the c-fos gene expression is upregulated in the vagus sensory ganglia and the nucleus of the solitary tract (nTS), which serves as the primary sensory relay nucleus for the vagus. This finding suggests that gut stimulation may have the ability to influence brain activity through the autonomic nervous system (Goehler et al., 2005). Specifically, the enteroendocrine cells (EECs) can detect signals released by gut microbiota through various receptors, and interact with neurotransmitters like GABA, glutamate, 5-hydroxytryptophan, and norepinephrine, which are released by gut microbiota. The signals from the EECs are then transmitted through vagal synapses to neurons, ultimately modulating the excitability of the CNS (Wang and Powley, 2007; Kaelberer et al., 2018; Gribble and Reimann, 2019; Kuwahara et al., 2020; Yu et al., 2020) (see Figure 1). For instance, Kaelberer et al. (2018) discovered the presence of intestinal endocrine cells, known as neuropod cells, that can synapse with vagal neurons and utilize glutamate as a neurotransmitter to rapidly transmit intestinal luminal signals on a millisecond scale. These neuroepithelial circuits establish a direct connection between the gut lumen and the brainstem, creating a physical conduit for the brain to perceive gut stimuli with remarkable temporal precision and topographical resolution.

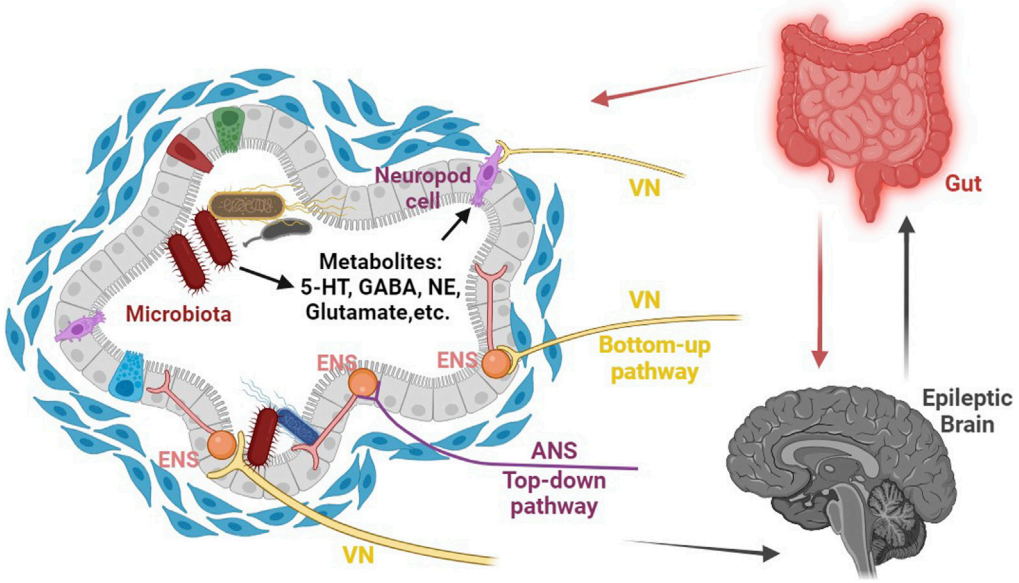

FIGURE 1
Schematic representation of the role of gut microbiota-mediated visceral sensory pathways in epilepsy. The gut microbiota possesses the remarkable capacity to directly affect the CNS through the vagus nerve, as well as indirectly by influencing the enteric nervous system (ENS) and generating essential metabolites (such as 5-HT, NE, glutamate, GABA, and more) that can traverse the blood-brain barrier, ultimately regulating epilepsy susceptibility by modulating the excitability of the CNS. Abbreviations: CNS, central nervous system; ENS, enteric nervous system; ANS, autonomic nervous system; VN, vagus nerve; NE, norepinephrine.

4 The role of gut microbiota-mediated endocrine pathways in epilepsy

4.1 Endocrine pathways in brain-gut signaling

The intricate mechanisms through which the brain and gut interact involve the release of endocrine mediators primarily derived from the hypothalamic-pituitary-adrenal (HPA) axis (Mayer et al., 2015). Part of the limbic system, the HPA axis is typically activated by stressors or systemic pro-inflammatory cytokines, and it primarily regulates emotional responses. Stress, in particular, induces emotional responses and stimulates hypothalamic activity. This stimulation triggers the secretion of corticotropin-releasing factor (CRF) (Stengel and Tache, 2010), which, in turn, stimulates the release of adrenocorticotropic hormone (ACTH) from the pituitary gland. ACTH then acts on the adrenal glands to promote the secretion of cortisol. Elevated levels of cortisol, a crucial stress hormone, interact with the gut to modulate various aspects of gastrointestinal function, visceral sensation, autonomic activity, and behavior (Ulrich-Lai and Herman, 2009).

At the intestinal level, these effector molecules exert effects on motility and secretion, intestinal permeability, local and systemic immune function and inflammation, as well as microbiota composition and function. For instance, increased intestinal permeability can disrupt the intestinal microbiota, resulting in elevated levels of pro-inflammatory cytokines (such as tumor necrosis factor α29) and the release of serotonin (5-HT) from enteroendocrine cells (Liebregts et al., 2007; Collins et al., 2012). These processes can enhance the sensitivity of visceral afferent nerves, amplifying stress-induced changes in motility, secretion, and permeability, which further heightens afferent signaling from the ENS (Keightley et al., 2015).

Both animal and human studies indicate that chronic or prolonged stress may lead to a sustained increase in the responsiveness of the brain's central stress loop, ultimately resulting in functional and affective disturbances. Moreover, chronic or prolonged stress has been associated with the onset and exacerbation of symptoms in IBS (Whitehead et al., 1992). Patients with IBS often exhibit stress-induced alterations in gastrointestinal motility, gut sensation, autonomic regulation, and the response of the HPA axis (Whitehead et al., 2002). Over time, disruptions in the HPA axis can result in dysregulation of stress responses, pain modulation, and various other brain circuits, creating a maladaptive and mutually reinforcing cycle of brain-gut interactions.

Additionally, a diverse array of peptide hormones secreted by intestinal endocrine cells play a key role in regulating brain-gut signaling (Steinert et al., 2017). These intestinal peptides not only regulate gastrointestinal motility and sensitivity but also homeostatic brain circuits in the brainstem and hypothalamus through vagal afferent-terminal receptors. By doing so, they regulate food intake and energy homeostasis based on the body's energy resources and nutritional needs. And then this regulatory neural network is involved in the motivational, emotional, and learning aspects of food reward (Alonso-Alonso et al., 2015). The combination of sensory signals from the gut, along with oral (taste) and extra-sensory inputs such as vision and odor, ultimately determines the rewarding value of food, thereby influencing appetite and feeding behavior (Weltens et al., 2014). Under normal circumstances, these gut peptides maintain a balance with the homeostatic network established by brain regions. However,

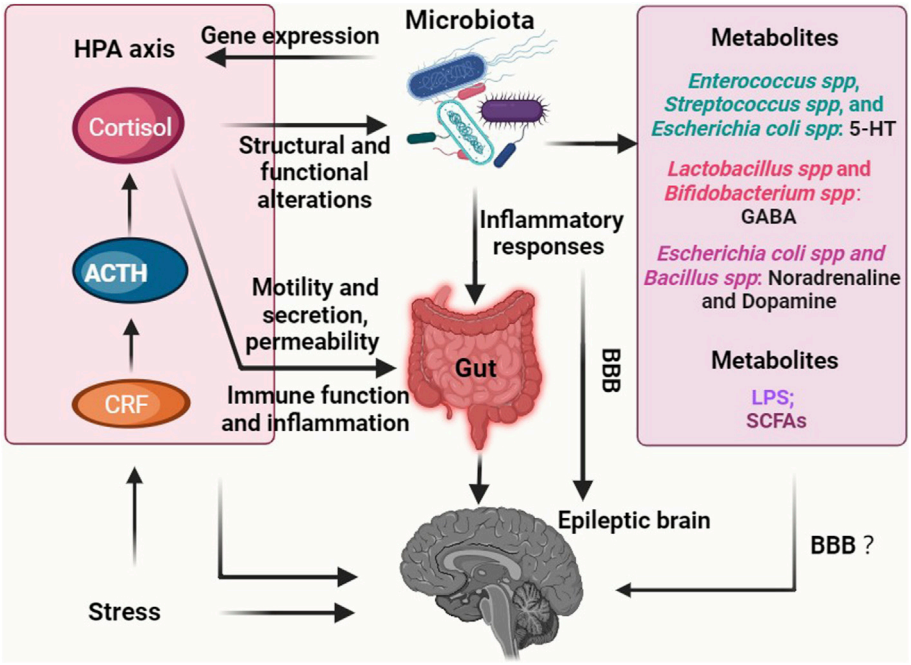

FIGURE 2
Overview of role of gut microbiota-mediated endocrine pathways in epilepsy. Chronic stress has emerged as a potential catalyst for disrupted gut microbiota, which, in turn, can upregulate the production of metabolites (such as LPS) that promote epilepsy. Additionally, these imbalances in the gut microbiota can trigger the secretion of inflammatory factors, further exacerbating the condition. Consequently, an abnormal GABA/glutamate ratio ensues, ultimately leading to the onset of epilepsy. Conversely, a healthy gut microbiota has the ability to generate beneficial metabolites like SCFAs and 5-HT, which play a crucial role in inhibiting the occurrence of epilepsy. Furthermore, the interaction between the microbiota-gut-brain axis and epilepsy involves the HPA axis, thereby highlighting its significance in this intricate relationship. Notably, the question of whether metabolites, including neurotransmitters, produced through the metabolism or regulation by the gut microbiota can permeate the BBB, and whether their effects on epilepsy are direct, indirect, or both, remains an unresolved inquiry. Abbreviations: HPA axis, hypothalamic-pituitary-adrenal axis; CRF, corticotropin-releasing factor; ACTH, adrenocorticotropic hormone; LPS, lipopolysaccharide; SCFAs, short-chain fatty acids; BBB, blood-brain barrier.

when dysfunction occurs at any level of the brain-gut axis, this balance can be disrupted, leading to abnormal processing of signals, both physiological and noxious. Prolonged enhancement of afferent visceral signals may even impact mood, fear, anxiety, and other emotional processes (Berthoud and Morrison, 2008; Mayer et al., 2015).

4.2 Endocrine signaling between the gut microbiota and the brain plays a vital role in epilepsy

Stress has the potential to trigger seizures, and the HPA axis is the primary regulatory system in the stress response (Cano-López and González-Bono, 2019). Different hormones have distinct effects on seizures: glucocorticoid levels are elevated in epilepsy patients, while deoxycorticosterone, an anticonvulsant drug, exhibits beneficial effects; Corticotropin-releasing hormone (CRH) and corticosterone promote the signaling of excitatory neurotransmitters like glutamate, which can induce seizures (Baram and Schultz, 1991; Reddy and Rogawski, 2002; Werner and Coveñas, 2017). Recent research has revealed a correlation between gut microbiota and the HPA axis. For instance, structural and functional changes in the gut microbiota due to stressful conditions regulate the expression of genes associated with the colonic CRH pathway (Vodička et al., 2018) (see Figure 2). Nevertheless, further investigation is required to understand the mechanism connecting gut microbiota, the HPA axis, and epilepsy.

Congruent lines of evidence have proposed that imbalances in neurotransmitters have been strongly linked to the development of epilepsy, with epileptic foci often exhibiting decreased levels of inhibitory neurotransmitters, such as GABA, and elevated levels of excitatory neurotransmitters like glutamate, dopamine, and norepinephrine (Singh and Goel, 2016). For instance, the disrupted balance of GABA and glutamate in brain tissue has been observed in patients with epilepsy (Fisher et al., 2017b). GABA is an inhibitory neurotransmitter widely distributed in the nervous system, and a decrease in GABA levels can lead to changes in neuronal cell permeability to synaptic interstitial chloride ions. This alteration can result in lower seizure thresholds and an increased susceptibility to epilepsy (Barrett et al., 2012; Peng et al., 2018). It has been found that various types of gut microbiome are capable of metabolizing and producing distinct neurotransmitters. For example, *Enterococcus* spp., *Streptococcus* spp., and *Escherichia coli* spp. can produce serotonin. *Lactobacillus* spp. and *Bifidobacterium* spp. are responsible for synthesizing GABA. *Escherichia coli* spp. and *Bacillus* spp., on the other hand, produce noradrenaline and dopamine (Tsavkelova et al., 2000; Özoğul, 2004; Shishov et al., 2009; Barrett et al., 2012; Özoğul

et al., 2012; Strandwitz, 2018) (see Figure 2). Recent studies have shown the relative abundance of intestinal *Ruminococcus* and *Coprococcus* was positively correlated with brain tissue glutamate and glutamine levels (Sun et al., 2016; Zhang et al., 2021; Binh Tran et al., 2023). The gut microbiota, specifically the presence of beneficial bacteria such as *A. mucinophilia* and *Parabacteroides*, may provide protective benefits against seizures by modulating brain neurotransmitter levels, including GABA and glutamate in the hippocampus. Bacterial dysbiosis may alter GABA levels, leading to an exacerbation of seizures (Galland, 2014; McDonald et al., 2018). In addition, Barrett et al. investigated that *Bifidobacterium* spp., an important probiotic in the gut, not only stimulates inflammatory responses and boosts the immune system's defenses against external pathogens but also secretes GABA that may traverse the blood-brain barrier (BBB) and enter the CNS. Notably, when mice were colonized with Ackermannia and Paramycetes in their gastrointestinal tracts, it led to reduced levels of excitatory amino acids (glutamate) in both the serum and intestines, along with increased expression of GABA in the hippocampus. This colonization exerted anti-seizure effects (Olson et al., 2018). However, current research has yet to confirm the direct entry of neurotransmitters produced by gut microbiota into the brain across the BBB and their role in shaping brain structure and function.

Previous studies have demonstrated that approximately 90% of 5-HT is produced and distributed in intestinal enterochromaffin cells (ECs), but the intestinal microbiota can play a role in its production and secretion process (Yano et al., 2015; Lu et al., 2021). The commensal microbiota has the ability to directly utilize luminal tryptophan to synthesize serotonin. Various bacteria including *Lactococcus*, *Lactobacillus*, *Streptococcus*, *Escherichia coli*, and *Klebsiella* have been found to produce serotonin by expressing tryptophan synthetase. Specifically, strains such as *Lactococcus lactis subsp. Cremoris (MG 1363)*, *Lactococcus lactis subsp. Lactis (IL 1403)*, *Lactobacillus plantarum (FI8595)*, *Streptococcus thermophilus (NCFB2392)*, *Eschericchia coli K-12*, *Morganella morganii (NCIMB, 10466)*, *Klebisella pneumoniae (NCIMB, 673)*, and *Hafnia alvei (NCIMB, 11999)* have been identified as capable of serotonin production. Furthermore, it has been observed that commensal bacteria, particularly spore-forming bacteria found in the mouse and human microbiota, can enhance serotonin biosynthesis in colonic ECs through a metabolite or cell component-dependent mechanism (Williams and Chryssanthopoulos, 1997; Sudo et al., 2004; O'Mahony et al., 2015; Yano et al., 2015; Clark and Mach, 2016; Eisenstein, 2016; Mandic et al., 2019). For instance, specific microbiota within the intestines of mice have been found to promote the production of 5-HT by regulating the rate-limiting enzyme responsible for its synthesis, tryptophan hydroxylase 1 (TPH1) (Yano et al., 2015). Depletion of 5-HT induced by reserpine reduces the threshold for seizures triggered by electrical stimulation in rats, thereby increasing their susceptibility to seizures (Wenger et al., 1973). Therefore, it is reasonable to hypothesize that the intestinal microbiota modulates the production and release of 5-HT from endocrine cells, subsequently affecting the electrical activity of the intestinal vagus nerve and the immune-inflammatory response. This modulation, in turn, leads to an increased susceptibility to epilepsy. Besides, studies have revealed a reduction in brain tissue N-acetylaspartate (NAA) levels in both epileptic patients and animal models of epilepsy (Ferrier et al., 2000; Gomes et al., 2007).

Specific intestinal microbiota, such as Firmicutes and Bacteroidetes, have the ability to ferment and break down insoluble dietary fiber, leading to the production of important metabolites known as short-chain fatty acids (SCFAs), including acetate, propionate, and butyrate (den Besten et al., 2013) (see Figure 2). These SCFAs play a significant role in promoting the maturation of microglia, and changes in microglial function and BBB permeability have been linked to seizure susceptibility (De Caro et al., 2019a). It is worth noting that in this context, patients with drug-resistant epilepsy exhibited significantly different levels of Firmicutes and Bacteroidetes phylum compared to those with drug-sensitive epilepsy and healthy controls, as demonstrated in studies by Xie et al. (2017), Peng et al. (2018), Lindefeldt et al. (2019), Lee et al. (2020), Şafak et al. (2020), and Lee et al. (2021). A rat model of post-traumatic epilepsy caused by lateral fluid percussion injury showed that the trauma itself did not result in significant alterations in the gut microbiota. However, the risk of developing post-traumatic seizure was strongly correlated with the disruption of gut microbiota and a decrease in intestinal SCFAs content prior to the traumatic event (Medel-Matus et al., 2022). In an absence seizure model using WAG/Rij rats, it was observed that brain tissue levels of SCFAs were significantly reduced, whereas the supplementation of butyrate effectively controlled their absence seizures. This can be attributed to the ability of butyrate to enhance mitochondrial function, protect brain tissue from oxidative stress, and prevent neuronal apoptosis, ultimately increasing the seizure threshold and reducing seizure intensity (Li et al., 2021a). As such, propionate supplementation has been shown to attenuate mitochondrial damage, hippocampal apoptosis, and neurological deficits, leading to a decrease in seizure intensity and an increase in seizure latency (Cheng et al., 2019). Furthermore, the KD has been utilized for nearly a century as a treatment for drug-resistant epilepsy in both children and adults (Xie et al., 2017; Olson et al., 2018; Zhang et al., 2018; Lindefeldt et al., 2019; Eor et al., 2021; Gong et al., 2021; Miljanovic and Potschka, 2021; Shearer et al., 2023). A high consumption of cruciferous and leafy vegetables, berries, and nuts on the KD has been linked to a positive impact on the profile of SCFAs produced by the gut microbiome (Gudan et al., 2022).

5 The role of gut microbiota-mediated immune pathways in epilepsy

5.1 Gut microbiota in the immune system

The gut microbiota plays a crucial role in maintaining the balance of the host immune system. Research conducted on mouse models of multiple sclerosis and stroke has highlighted the involvement of gut microbes in the regulation of autoimmunity, particularly impacting the development and function of CNS-resident immune cells, such as microglia M1 (Ochoa-Reparaz et al., 2010; Wang et al., 2014b; Benakis et al., 2016). For instance, when adult SPF mice were treated with antibiotics to remove bacteria, microglia reverted to an immature state. However, subsequent restoration to a normal state was

possible through allogeneic gut microbiota transplantation, demonstrating the intimate connection between gut microbial signaling and the maintenance of a mature microglial state (Erny et al., 2015). Plus, disruptions in T cell subset homeostasis, including Th1, Th2, Th17, and Treg, due to intestinal malnutrition, can contribute to the development of autoimmune and inflammatory disorders (Lee and Kim, 2017).

Th1 cells, which secrete pro-inflammatory cytokines like IL-2, IL-12, TNF-alpha, and IFN-γ, play a critical role in promoting cellular immune responses (Luckheeram et al., 2012). Recent research has shown that alterations in the gut microbiota composition leads to the accumulation of specific amino acids, such as phenylalanine and isoleucine, which in turn promote the differentiation and proliferation of Th1 cells. Consequently, Th1 immune cells infiltrate the brain and engage in local communication with M1 microglia, causing a shift towards a pro-inflammatory state. This cascade ultimately contributes to neuroinflammation and cognitive dysfunction associated with conditions like AD (Wang et al., 2019).

IL-17, which is produced by Th17 and γδT cells during acute infections, has been shown to contribute to the pro-inflammatory response. Interestingly, in stroke models, there is an enrichment of γδT cells in the gut, which are then transported to the delicate membranes of the brain. This suggests a potential link between gut inflammation and the onset of stroke (Weaver et al., 2007). On the other hand, Treg cells play a crucial role in maintaining immune homeostasis by secreting the anti-inflammatory cytokine IL-10, which helps to suppress excessive immune responses (Zhu et al., 2010). Animal models of stroke have demonstrated that the deletion of Treg cells leads to a significant increase in the activation of resident and infiltrating inflammatory cells, including microglia and T cells. This heightened activation consequently attenuates the post-ischemic inflammatory response (Liesz et al., 2009). Moreover, Treg cells have been found to inhibit the differentiation of Th17 cells and the proliferation of γδT cells in the gut, thereby contributing to the maintenance of an anti-inflammatory environment (Huber et al., 2011).

Fecal calprotectin, a protein involved in intestinal inflammation, has emerged as a potential regulator of the inflammatory response in neurodegenerative diseases like AD and PD. A study showed that fecal calprotectin levels were elevated in nearly 70% of AD patients, suggesting its role in promoting neuroinflammation (Leblhuber et al., 2015). Similarly, elevated levels of fecal calreticulin in PD patients led to changes in the integrity of the intestinal epithelial barrier and the immune system (Mulak et al., 2017). Calreticulin is a calcium-binding protein consisting of the S100A8 and S100A9 heterodimer, which make up a significant proportion of the soluble protein content of neutrophils. Both S100A8 and S100A9 are capable of producing amyloid proteins and can form associations with other amyloids like β-amyloid (Aβ) and alpha-synuclein (α-syn), as well as amyloid oligomers and protofibrils (Wang et al., 2014a; Walsham and Sherwood, 2016). Macrophages and microglia secrete S100A9 during amyloid plaque formation, leading to its expression in neuronal cells. These effector molecules interact with Toll-like Receptor 4 (TLR4) and Receptor for Advanced Glycation End Products (RAGE) pathways, further activating microglia. The increased levels of calreticulin in cerebrospinal fluid (CSF) and the brain of AD patients may facilitate its co-aggregation with Aβ and amyloid formation (Wang et al., 2014a).

Among the intestinal microbiota amyloids, the curli protein (curli) produced by *Escherichia coli* is currently the most extensively studied. It shares similarities in primary and tertiary structures with CNS amyloids and forms biofilms with bacterial cells, providing resistance against physical and immunological factors (Cherny et al., 2005; Zhao et al., 2015). Exposure to intestinal bacterial amyloid can activate the immune system, thereby enhancing the response to endogenous amyloid production in the brain (Friedland and Chapman, 2017). It has been demonstrated that exposure of rats to bacteria capable of producing frizzled protein leads to increased α-syn deposition in neurons, as well as higher numbers of microglia and astrocytes in both the gut and brain. This exposure also results in elevated expression of Toll-like Receptor 2 (TLR2), interleukin-6 (II-6), and tumor necrosis factor (TNF) in the brain (Chen et al., 2016).

5.2 Involvement of the gut microbiota-mediated immune response in epilepsy pathology

A cohort study conducted in northern Denmark, encompassing children born between 1998 and 2008, revealed a significant link between maternal infection during pregnancy and an increased risk of epilepsy in their offspring (Nørgaard et al., 2012). It is worth noting that this outcome is not specific to any particular pathogens or drugs but rather can be attributed to common processes associated with infections. Corroborating this finding, another cohort study examining Danish births from 1982 to 2012 reported a noteworthy 78% surge in the prevalence of epilepsy among children and young adults who had been hospitalized for an infection (Ahlers et al., 2019). The infants affected by *group B streptococcus* (GBS) infection, a leading cause of neonatal infections, faced a significantly elevated risk of developing epilepsy or other neurological disorders later in life (Yeo et al., 2019). The impact of infectious diseases on epilepsy is further amplified by epidemiological investigations from Norway, which demonstrated a significant rise in the incidence of infection-associated febrile seizures following the 2009 influenza A (H1N1) outbreak (Bakken et al., 2015). Furthermore, an association has been established between human herpesvirus type 6 (HHV-6) and medial temporal lobe sclerosis, a common cause of refractory epilepsy. For instance, infected individuals with medial temporal lobe sclerosis experience more frequent seizures and exhibit higher viral DNA loads indicative of HHV-6 involvement in the development of this condition through the induction of an aberrant immune-inflammatory response (Kawamura et al., 2015; Leibovitch and Jacobson, 2015). These findings collectively emphasize the critical role that infections (or immune-inflammatory response), both during pregnancy and throughout early life, play in shaping the risk and development of epilepsy.

Evidence from animal models further supports the notion that infections heighten the risk of developing epilepsy by engaging immunoinflammatory pathways, involving factors such as TNF-α, monocyte chemoattractant protein-1 (MCP-1), and others (Lv et al., 2014; Cusick et al., 2017; Patel et al., 2017; Sewal et al., 2017; Medel-

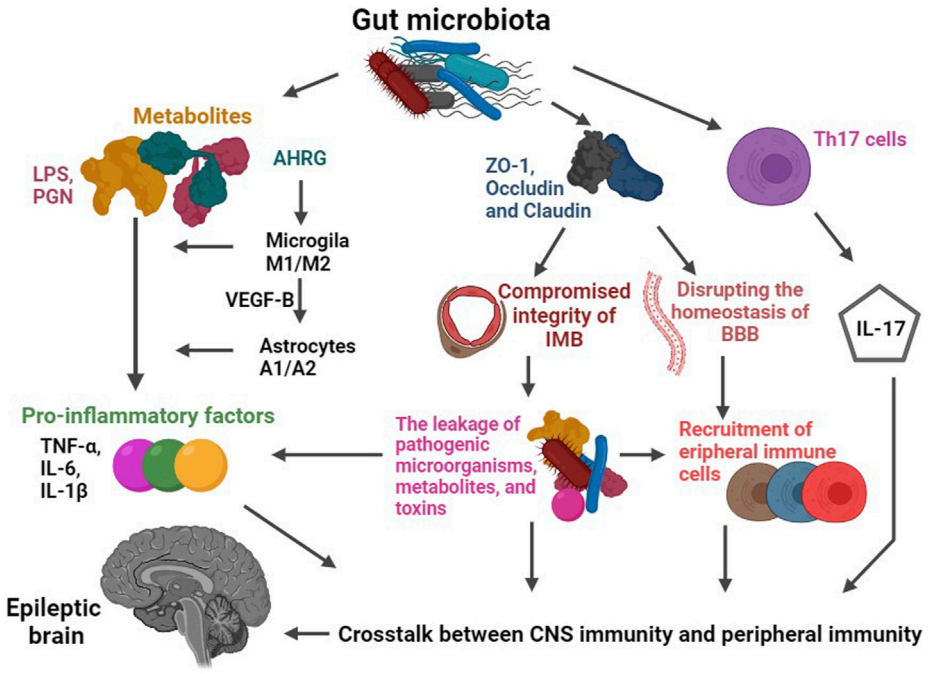

FIGURE 3
Schematic diagram of the role of gut microbiota-mediated immune pathways in epilepsy. The gut microbiota plays a crucial regulatory role in the expression of key proteins responsible for maintaining the integrity of the intestinal mucosal barrier (IMB) and blood-brain barrier (BBB), such as Occludin and Claudin. When the permeability of these barriers is increased, it paves the way for the escape of pathogenic microorganisms, metabolites (such as LPS and PGN), and toxins from the intestinal tract. Consequently, compromised barriers allow for a significant influx of immune cells (including peripheral monocytes or macrophages, T-cells) and inflammatory factors (such as TNF-A and IL-1b) to enter the CNS. These immune cells and inflammatory factors then interact with central immune components like microglia and astrocytes, ultimately triggering seizures. Furthermore, specific intestinal microbiota, such as those belonging to the Bacteroidetes phylum, can modulate the secretion of IL-17. These gut bacteria have the ability to influence the activation and differentiation of Th17 cells, leading to alterations in the secretion of IL-17. Abbreviations: LPS, lipopolysaccharide; PGN, peptidoglycan; AHRG, aryl hydrocarbon receptor agonist; VEGF-B, vascular endothelial growth factor-B; IMB, intestinal mucosal barrier; BBB, blood-brain barrier.

Matus et al., 2018). For instance, studies utilizing rodent models have demonstrated that the injection of lipopolysaccharide, a component found in bacterial cell walls, triggers an upsurge in pro-inflammatory factors like TNF-α, IL-6, and IL-1β within brain tissue. This inflammatory response consequently lowers the threshold for seizures induced by chemical (PTZ) and electrical stimulation (Kołosowska et al., 2014; Russo et al., 2014; Leo et al., 2020; Hu et al., 2022) (see Figure 3). Intracerebral infection of C57BL/6J mice with the Daniels (DA) strain of Theiler's murine encephalomyelitis virus (TMEV) leads to approximately 50% of the mice exhibiting acute behavioral seizures. The primary pathophysiological mechanism involves elevated levels of inflammatory factors in the hippocampus and limbic system, particularly IL-6 and TNF-α (Cusick et al., 2017). Remarkably, when IL-6 and TNF receptor 1 (TNFR1) and TNF receptor 2 (TNFR2) knockout mice were injected with TMEV, a significant reduction in seizures was observed, highlighting the key role of these inflammatory factors in the epileptic process (Cusick et al., 2017).

Th17 cells, identified as $CD4^+$ T cell subset, hold a pivotal role in orchestrating the adaptive immune response (Weaver et al., 2007; Chow and Mazmanian, 2009; Huber et al., 2011; Lee and Kim, 2017). Their production of IL-17 can be modulated by specific intestinal flora, such as those belonging to the Bacteroidetes phylum. These gut bacteria can influence the activation and differentiation of Th17 cells, consequently altering the secretion of IL-17 (Ivanov et al., 2008) (see Figure 3). Notably, patients suffering from epilepsy exhibit markedly elevated levels of IL-17 in both cerebrospinal fluid and peripheral blood. In line with this, alterations in the expression of IL-17 showcase a positive correlation with both seizure frequency and severity. This intriguing link suggests that the gut flora may influence epilepsy susceptibility by intricately mediating the IL-17 pathway (Mao et al., 2013).

The pathogenesis of epilepsy is intertwined with the inflammatory pathways that are regulated by the brain-gut-microbiota axis (Gong et al., 2022b; Ding et al., 2022; Gernone et al., 2022; Mu et al., 2022). For instance, the composition of the gut flora may influence the immune function and modulate the susceptibility of hosts to seizures (Wu et al., 2016; Li et al., 2021b) (see Figure 3). Specifically, gut microbiota metabolizes dietary tryptophan into an aryl hydrocarbon receptor agonist. This agonist, in turn, interacts with microglia receptors, promoting their migration, apoptosis, and phagocytosis, ultimately leading to increased release of inflammatory factors (Ochoa-Reparaz et al., 2010; Wang et al., 2014a; Benakis et al., 2016; Rothhammer et al., 2018). Additionally, the activation of microglia further upregulates the expression of transforming growth factor-alpha (TGF-α) and vascular endothelial growth factor-B (VEGF-B) in astrocytes. As a consequence, an

inflammatory response is triggered within astrocytes (Rothhammer et al., 2018). The crosstalk between astrocytes and microglia can potentiate an enhanced inflammatory response and disrupt the homeostasis of the BBB, facilitating the entry of peripheral blood immune cells and inflammatory factors into the CNS. This chronic inflammation, in turn, significantly elevates the risk of epilepsy (Rothhammer et al., 2018). Experimental evidence supports the role of gut flora in maintaining microglial immune function (Erny et al., 2015; Rothhammer et al., 2016). For instance, observations in mice reared in a sterile environment or treated with antibiotics to suppress gut flora reveal that microglia in these animals exhibit morphological, functional, differentiation, and activation defects, leading to innate immunodeficiencies against pathogens. Since there is no evidence to support that this pathological elimination of microbiomes does not affect the absorption of nutrients, exclusion of toxins, migration of cells, or other effects at a gut level, which could potentially have a multistep downstream effect on microglia. Therefore, it is reasonable to hypothesize that microglial changes are primarily an indirect result of changes in the microbiota. However, upon recolonization of the gastrointestinal tract, the immune function of these microglia is restored, underscoring the criticality of gut microbiota in regulating microglial function (Rothhammer et al., 2016). Moreover, abnormalities in the function of peripheral immune cells have been implicated in the development of epilepsy. T-lymphocytes and monocytes, upon migration to the CNS, can differentiate into macrophages and invade brain tissue, ultimately inducing seizures (Erny et al., 2015). Lin et al. (2021) demonstrated an increase in gut *Klebsiella pneumoniae* in patients with epilepsy. Subsequent animal studies have shed light on the impact of *Klebsiella pneumoniae* in the intestinal tract on seizure susceptibility and the activation of microglial cells to release inflammatory factors (Lin et al., 2021). This discovery highlights the intricate interplay between neuroinflammation and epilepsy pathogenesis. All told, the deep involvement of gut flora in both peripheral and neuroinflammation strongly suggests that gut flora-mediated neuroinflammation may play an important role in epileptogenesis that must not be overlooked (see Figure 3).

Intestinal microbiota exerts a regulatory role on the expression of key proteins involved in the integrity of the intestinal mucosal barrier, such as Occludin and Claudin. Animal studies have demonstrated a significant increase in BBB permeability in mice reared in a germ-free environment or treated with antibiotics to inhibit gut microbiota (Amasheh et al., 2011; Braniste et al., 2014). Dysbiosis of gut microbiota may downregulate the expression of Occludin and Claudin, leading to compromised integrity of the intestinal mucosal and BBB (see Figure 3). Consequently, this increased permeability facilitates the leakage of pathogenic microorganisms, metabolites, and toxins from the intestinal tract, and then the compromised barriers allow a large influx of immune cells and inflammatory factors to enter the CNS, ultimately triggering seizures (Rahman et al., 2018; Vezzani et al., 2019; Welcome, 2019). For instance, studies have found reduced expression levels of occludin and ZO-1, crucial components of the tight junctions in the BBB, in patients with drug-resistant temporal lobe epilepsy (Castañeda-Cabral et al., 2020). Besides that, the gut harbors a vast population of bacteria, many of which possess cell wall components, such as peptidoglycan (PGN) (Clarke et al., 2010). PGN and its fragments possess strong proinflammatory properties, signaling through Toll-like receptors (TLR), NOD-like receptors (NLR), and specialized PGN recognition proteins (such as PGLYRP1-4) (Laman et al., 2020). Alterations in the permeability of the intestinal mucosal barrier allow flora-associated metabolites, including PGN, to cross into the CNS. As a consequence, chronic inflammation is induced within the CNS, further contributing to the pathogenesis of epilepsy (Gales and Prayson, 2017). The collective findings from the aforementioned studies strongly implicate the involvement of intestinal flora in the regulation of epilepsy susceptibility through its influence on barrier permeability and immune-inflammatory responses. Although these studies provide valuable insights, it is important to note that only a limited number have investigated the intricate relationship between gut microbiota, immune-inflammatory responses, and epilepsy. Therefore, further well-designed studies are imperative to corroborate and expand upon these findings, in order to fully elucidate the role of the brain-gut-microbiota axis in the pathogenesis of epilepsy.

Significantly, epidemiological studies have established a clear association between inflammatory gastrointestinal diseases (GI) and the incidence of epilepsy. For instance, patients with epilepsy have been found to have up to eight times higher incidence of peptic ulcers compared to the general population (Keezer et al., 2016). Furthermore, a perforated peptic ulcer can trigger or complicate a generalized tonic-clonic seizure (Magon, 2010). Huang et al. (2010) demonstrated that even mild gastroenteritis could precede the development of benign infantile convulsions. Neurological complications are also observed in a considerable percentage of patients with inflammatory bowel disease (IBD), ranging from 0.25% to 47.50%. In severe cases of IBD, seizures of all types, including status epilepticus, can occur during the clinical course (Ferro and Oliveira Santos, 2021). Based on this evidence, it is plausible to hypothesize that some cases of epilepsy may be caused by autoimmune disorders that have manifestations in both the gut and the brain, with the direction of causality attributed to an extraneous factor (i.e., neither epilepsy nor the gut microbiome). Consider the example of Celiac disease, a well-documented systemic autoimmune condition characterized by gluten-triggered autoimmune intestinal villous atrophy, malabsorption, and a range of systemic and gastrointestinal symptoms. Approximately 10% of individuals with celiac disease experience neurological complications, including seizures. Conversely, about 0.78%–9.10% of epilepsy patients develop celiac disease (Djurić et al., 2012; Işıkay and Kocamaz, 2014). The precise mechanism behind these neurological manifestations remains poorly understood, likely linked to immune mechanisms. This hypothesis is supported by the presence of anti-Purkinje cells and anti-ganglioside antibodies in individuals with celiac disease who develop neurological symptoms (Pratesi et al., 2003). Moreover, drug-resistant epilepsy is more prevalent in children with celiac disease as a comorbidity. Remarkably, adherence to a gluten-free diet has led to the resolution of epilepsy in many celiac disease patients. Furthermore, maintaining a gluten-free diet alongside appropriate antiseizure medications has shown to reduce seizure frequency and severity in individuals with celiac disease and drug-resistant epilepsy (Swartwood et al., 2021). In these scenarios, it is plausible that a reduction in the inflammatory state, possibly through dietary

changes, may significantly impact both gut microbiota and the severity of epilepsy. Nevertheless, these hypotheses necessitate further research to validate their potential implications.

6 Gut microbiota in epilepsy treatment

6.1 The KD is a highly promising dietary intervention strategy with extraordinary potential for seizure control

Dr. Russell Wilder in the 1920s noted that seizures were halted during states of absolute fasting (Wheless, 2008; Winesett et al., 2015). With this observation, Dr. Wilder formulated a diet that emulated the effects of fasting by relying on a high-fat, moderate-protein, and low-carbohydrate composition. Specifically, the KD adheres to a calculated ratio of fat to the combined intake of proteins and carbohydrates, typically ranging between 2:1 and 4:1. To illustrate, a 4:1 ratio involves consuming four servings of fat for every one serving of proteins and carbohydrates. Therefore, 90% of the body's required calories are derived from fat, while adequate protein is included to prevent the utilization of lean body mass. By metabolizing fat into ketone bodies, the brain is provided with an alternative fuel source to glucose, which is typically utilized when carbohydrates are consumed in excess.

Over the years, the dietary regimen developed by Dr. Wilder remains the foundation of KD therapy used today. Simultaneously, less strict variations of the original diet have also been introduced, including the Modified Atkins diet (MAD) and low glycemic index treatment (LGIT) (Kossoff and Doward, 2008; Pfeifer et al., 2008). Further, extensive exploration into the potential applications of the KD has expanded its use beyond epilepsy to other neurological disorders such as Alzheimer's disease and Parkinson's disease, among others. In recent years, the diet has even been investigated as a potential therapeutic intervention for non-neurological diseases. However, its foremost role remains as an effective treatment for epilepsy (Winesett et al., 2015; Xie et al., 2017; Olson et al., 2018; Zhang et al., 2018; Lindefeldt et al., 2019; Li et al., 2021b; Eor et al., 2021; Gong et al., 2021; Miljanovic and Potschka, 2021; Gudan et al., 2022; Shearer et al., 2023). In the pediatric age group, the KD has demonstrated significant benefits. In one study, it resulted in a 50% reduction in seizure frequency for at least 56% of patients, a 90% reduction in seizures for 32% of patients, and complete cessation of seizures in 16% of patients (Lefevre and Aronson, 2000). In a 2008 clinical trial conducted in England, children were randomly assigned either to receive the KD after a 1-month delay (treatment arm) or to undergo a 4-month delay (control arm) with no changes to their anticonvulsant medications. Five out of 54 patients in the treatment arm experienced a remarkable 90% reduction in seizures, while none of the patients in the control arm achieved such a response at the 4-month mark. Moreover, a greater than 50% decrease in seizures was observed in 38% of the patients in the treatment arm, compared to only 6% in the control arm. It is important to note that these findings were particularly significant considering the patients in the study were classified as quite refractory, having previously failed multiple antiseizure drugs (Neal et al., 2008).

Another study by Guzel et al. examined the effects of a 1-year KD intervention on 389 patients with drug-resistant epilepsy. The results revealed a significant improvement in the anti-seizure effect of the KD, with sustained efficacy over time. At 1, 3, 6, and 12 months, 65.8%, 74.7%, 70.6%, and 83.1% of the patients, respectively, demonstrated a positive response to the treatment (Guzel et al., 2019). The broad efficacy of the KD in treating various seizure types and childhood epilepsy syndromes, including symptomatic generalized, partial, and genetic epilepsies, is worth noting (Hartman, 2008; Hara et al., 2018). In fact, certain subgroups of epilepsy syndromes exhibit a particularly favorable response to the KD compared to available pharmacological treatments. One such remarkable subgroup is patients with glucose transporter (Glut-1) deficiency syndrome, where the efficacy of the KD may exceed 80% (Hartman, 2008; Leen et al., 2010). Recent research has delved into the effectiveness of combining the MAD with standard drug therapy (SDT) in the treatment of drug-resistant epilepsy. The findings of the study revealed that the combination of MAD and SDT was superior to SDT alone in reducing seizure frequency and improving overall outcomes, at the 6-month mark in adolescents and adults with non-surgical drug-resistant epilepsy (Manral et al., 2023). Moreover, the KD has demonstrated benefits beyond seizure control. It has been found to have a positive impact on the cognitive, emotional, verbal, and intellectual development of children (Zhu et al., 2016). However, KD or dietary treatment for seizures has thus far only shown effectiveness in pediatric populations. There is currently a lack of concrete evidence to support its benefits or effectiveness in adult populations. As a result, all the KD-related patients we discuss below are from studies focused on pediatric epilepsy.

6.2 Anti-seizure effects of the KD mediated by the gut microbiota

A growing body of evidence suggests that the gut microbiota may play a significant role in the therapeutic effects of the KD for epilepsy (Olson et al., 2018; Spinelli and Blackford, 2018; Dahlin and Prast-Nielsen, 2019; Lindefeldt et al., 2019; Pittman, 2020; Ding et al., 2021; Yue et al., 2022; Özcan et al., 2022; García-Belenguer et al., 2023; Kundu et al., 2023; Shearer et al., 2023) (see Figure 4). A cross-sectional study conducted with 12 children suffering from drug-refractory epilepsy examined the impact of a 6-month KD treatment. The results were remarkable, with one patient experiencing complete cessation of seizures, three patients achieving a staggering 90%–99% reduction in seizure frequency, and five out of twelve children achieving a reduction of over 50% in seizure frequency. Cognitive and motor function improvements were observed in ten out of twelve children after 6 months on the KD. Importantly, a comparison of fecal samples taken before and after the 6-month KD intervention showcased that there was a notable decrease in the abundance of *Bifidobacterium*, *Akkermansia*, *Enterococcaceae*, and *Actinomyces*, along with a significant increase in the abundance of *Subdoligranulum*, *Dialister*, *Alloprevotella*, and *Bifidobacterium* (Gong et al., 2021). Another study conducted with 20 children suffering from refractory epilepsy who followed a KD for 6 months also yielded similar results. Two patients became completely seizure-free, three experienced a seizure reduction of

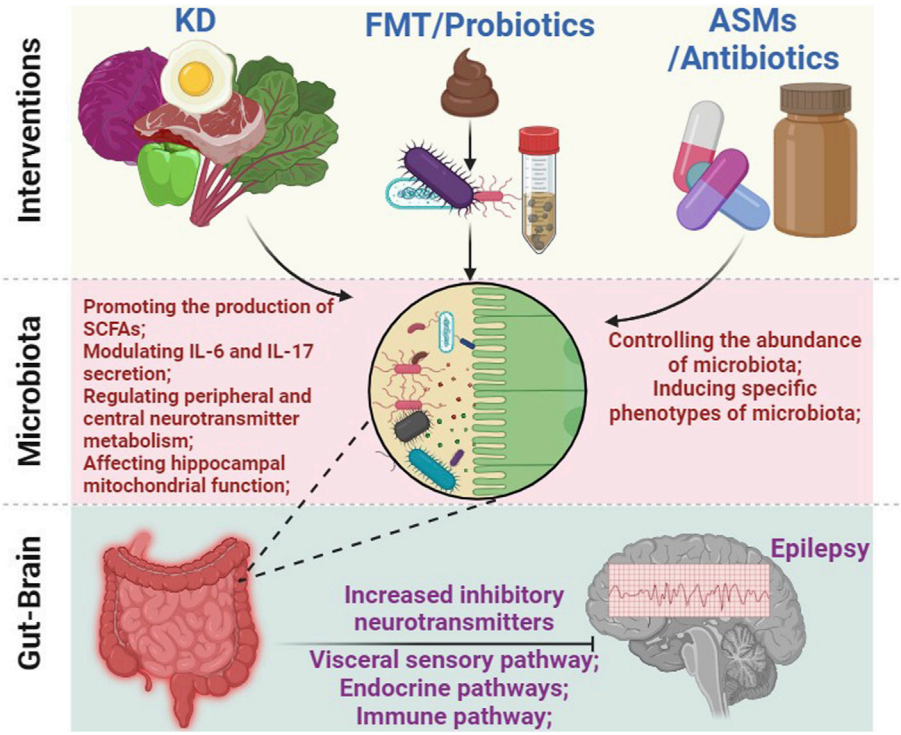

FIGURE 4
The intricate connection between gut microbiota and the treatment of epilepsy. Various approaches, including KD, FMT, probiotics, antibiotics, and ASMs, can affect the composition and function of gut microbiota. This, in turn, triggers a cascade of effects leading to alterations in inflammation response, peripheral and central metabolites (such as short-chain fatty acids, 5-HT, and GABA, among others), as well as the activity of the ENS, ultimately modulating brain function and effectively controlling seizures. Abbreviations: KD, ketogenic diet; FMT, fecal microbiota transplantation; ASMs, anti-seizure medications; ENS, enteric nervous system; SCFAs, short-chain fatty acids.

90% or more, five achieved a reduction between 50%–89%, and ten saw a reduction of less than 50%. Remarkably, all ten responders showed an improvement in their electroencephalogram (EEG) readings. In addition, analysis of fecal microbial profiles revealed a lower alpha diversity after KD therapy, along with significantly decreased abundance of Firmicutes and increased levels of Bacteroidetes (Zhang et al., 2018).

A significant increase in the abundance of the Bacteroidetes phylum within the intestinal flora was observed following KD treatment. This shift in microbial composition has been associated with the modulation of interleukin 6 and interleukin 17 secretion in dendritic cells, as well as promoting the production of SCFAs. These alterations play a key role in the reduction of seizure severity (Olson et al., 2018; Lindefeldt et al., 2019). Animal studies have also provided evidence supporting the efficacy of the KD in increasing seizure thresholds. In mice with a 6-Hz-induced refractory seizure model, the KD demonstrated the ability to raise seizure thresholds (Samala et al., 2008; Hartman et al., 2010; Olson et al., 2018). The KD also induced rapid and significant changes in the composition of the mouse gut microbiota. For instance, it led to an increase in the relative abundance of *Akkermansia muciniphila* and *Parabacteroides* (Samala et al., 2008; Hartman et al., 2010; Olson et al., 2018). To delve deeper into the relationship between the gut microbiota and the protective effects of the KD, Olson et al. conducted experiments involving germ-free feeding or antibiotic treatment (consisting of ampicillin, vancomycin, neomycin, and metronidazole) followed by 6 Hz electrical stimulation to induce epilepsy modeling. The results revealed that the protective effects of the KD were attenuated in germ-free fed and antibiotic-treated mice. However, when germ-free fed mice received the intestinal microbiota from normal mice, the seizure-protective efficacy was restored to that observed in normal mice receiving the KD. These findings strongly suggest that the presence of a healthy gut microbiota is necessary for the KD to exert its seizure-protective effects (Olson et al., 2018). Further investigations have indicated co-administration of *Akkermansia muciniphila* and *Parabacteroides* to the gastrointestinal tracts of germ-free or antibiotic-treated mice resulted in a notable increase in seizure thresholds upon 6 Hz electrical stimulation, supporting that the enriched intestinal flora associated with the KD possess anti-seizure properties (Frost et al., 2014; Vuong et al., 2017; Olson et al., 2018). Interestingly, colonization with only *Akkermansia muciniphila* or *Parabacteroides* alone did not restore the protective effect of the KD. This indicates that the presence of both bacteria is necessary for the anti-seizure effect of the KD (Olson et al., 2018). The metabolomic studies have suggested that administration of the KD resulted in decreased peripheral blood γ-D-glutamine levels, which was associated with an increase in the hippocampal GABA/glutamate ratio in mice, suggesting that the gut flora may modulate peripheral metabolites and central neurotransmitter metabolism, ultimately regulating seizure susceptibility (Frost et al., 2014; Vuong et al., 2017; Olson et al.,

2018). The transplantation of KD-associated intestinal flora (*Akkermansia muciniphila* and *Parabacteroides*) into the gut of *Kcna1*$^{-/-}$ sudden epileptic death model mice demonstrated elevated seizure thresholds, reduced seizure frequency, and shortened seizure duration. Instead, inhibition of both bacteria with antibiotics led to an increase in spontaneous tonic-clonic seizures in mice. These results highlight the broad applicability of the anti-seizure effects of the intestinal flora to various seizure types and model mice (Fenoglio-Simeone et al., 2009; Olson et al., 2018).

Remarkably, the manipulation of intestinal flora in models of IS using a KD and antibiotics has been shown to impact hippocampal mitochondrial function and subsequently alter epilepsy susceptibility. This observation suggests that targeting mitochondrial function-related flora could hold promise as a potential therapeutic strategy for epilepsy (Mu et al., 2022b). The major metabolite of ginsenosides Rb1, Rb2, and Rc in the intestinal microbiota, Ginsenoside compound K (GCK), has been found to have beneficial effects in a rat model of PTZ-induced epilepsy. GCK increases the levels of GABA, ultimately leading to a reduction in the intensity and prolongation of seizure latency (Zeng et al., 2018).

The disparities observed between animals in a germ-free environment and control animals are indeed fascinating (Fenoglio-Simeone et al., 2009; Frost et al., 2014; Vuong et al., 2017; Olson et al., 2018). However, it is crucial to approach the physiological effects of a germ-free environment with caution, as it represents an extreme condition that profoundly impacts the health and wellbeing of animals. Hence, it is imperative to build on these studies by conducting a thorough evaluation of the significance of the findings and delving deeper into the causation that precedes the observed factors.

6.3 FMT, probiotics and epilepsy treatment

FMT is an increasingly promising strategy for reconstructing the gut microbiota and has shown efficacy in various disease, such as epilepsy, *Clostridium difficile* infection, IBD, constipation, and other related disorders (Hartman et al., 2010; Borody and Khoruts, 2011; Surawicz et al., 2013; Reinisch, 2017; Olson et al., 2018). In a notable case study, a patient with both Crohn's disease and refractory epilepsy underwent fecal transplantation, resulting in remarkable improvements. Following three consecutive transplants, the Crohn's disease activity index (CDAI) significantly decreased from 361 to 131. Also, the patient's seizures were completely controlled without the need for anti-seizure drugs 20 months after the fecal transplantation (He et al., 2017). However, this case is unique because it potentially involves an autoimmune etiology of Crohn's disease as well as epilepsy. In another study, the administration of a probiotic mixture consisting of *Lactobacillus acidophilus DSM32241*, *Lactobacillus plantarum DSM32244*, *Lactobacillus casei DSM32243*, *Lactobacillus helveticus DSM32242*, *Lactobacillus brevis DSM11988*, *Bifidobacterium lactis DSM32246*, *B. lactis DSM32247*, and *Streptococcus salivarius* subsp. *thermophilus DSM32245* in patients with drug-resistant epilepsy for four consecutive months yielded promising outcomes. Notably, 28.9% of the patients experienced a significant reduction of more than 50% in the frequency of seizures (Gómez-Eguílaz et al., 2018). Furthermore, the administration of probiotics, specifically *Saccharomyces boulardii* or *Lactobacillus casei*, to neonates within 24 h of birth has displayed promising effects in reducing the risk of seizures. This effect was observed regardless of whether the infants were infected with rotavirus or not. Conversely, rotavirus-infected infants who did not receive probiotics exhibited an increased risk of seizures (Yeom et al., 2019). One potential mechanism underlying the anti-seizure effect of *Saccharomyces boulardii* in rotavirus-infected infants involves the inhibition of rotavirus non-structural protein 4 (NSP4). NSP4 has been implicated in increasing reactive oxygen species (ROS) production, white matter damage, and immune-inflammatory responses. By inhibiting NSP4, *Saccharomyces boulardii* may mitigate these detrimental effects, thereby reducing the frequency and severity of seizures in these infants (Buccigrossi et al., 2014; Yeom et al., 2019) (see Figure 4).

Animal models have also provided evidence for the anti-seizure effects of probiotics (see Figure 4). Studies involving rat and mouse brain tissues have shown that the application of *Lactobacillus rhamnosus* and/or *Bifidobacterium longum* leads to increased expression of GABA and its receptor GABAR, resulting in a reduction in seizures (Bravo et al., 2011; Liang et al., 2017). Furthermore, the administration of probiotic supplements containing *Lactobacillus rhamnosus*, *Lactobacillus reuteri*, and *Bifidobacterium infantis* to PTZ-induced epilepsy model rat for 3 weeks demonstrated favorable outcomes. The intervention resulted in a decrease in epileptic activity levels, a significant reduction in seizure severity, and a partial improvement in spatial learning and memory in the epileptic rats. Importantly, the probiotic treatment also led to decreased concentrations of pro-inflammatory cytokines IL-6 and TNF-α, reduced levels of nitric oxide (NO) and malondialdehyde (MDA), increased total antioxidant capacity (TAC), and elevated levels of GABA in the brain tissue (Bagheri et al., 2019; Aygun et al., 2022a; Aygun et al., 2022b). Additional research utilizing animal models of epilepsy has corroborated the anti-seizure effects of probiotics. For instance, the supplementation of probiotics and NS (N-stearoyl-L-tyrosine) reduced population spike-long-term potentiation (PS-LTP) in kindled rats, thereby improving seizure-induced cognitive impairment (Gong et al., 2020). Other animal models have also demonstrated the potential anti-seizure effects of probiotics (Tahmasebi et al., 2020; Eor et al., 2021; Kilinc et al., 2021; Sabouri et al., 2021; Mu et al., 2022b; Wang et al., 2022; Ciltas et al., 2023).

6.4 Gut microbiota and anti-seizure medications

Anti-seizure medications (ASMs) are typically the first line of treatment for controlling seizures in patients with epilepsy. However, a significant portion of these patients, estimated to be around 30%–40%, do not respond to at least two ASMs. Drug-resistant epilepsy patients also tend to exhibit dysregulation in their gastrointestinal ecological system, highlighting the potential involvement of the gut microbiota in epilepsy treatment (Peng et al., 2018). Drug-resistant patients have been found to possess higher alpha diversity, indicating a greater number of unique microbial types compared to drug-sensitive patients. Furthermore, specific microbiota has been associated with drug

response. For instance, drug-sensitive patients tend to have a greater relative abundance of *Bacteroides* and *Ruminococcus*, while members of the *Negativicute*s group are overrepresented in drug-resistant epilepsy patients (Peng et al., 2018; Lee et al., 2021). Further evidence supporting the role of the gut microbiota in drug-resistant epilepsy comes from both animal models and pediatric cohort studies. These studies have demonstrated that the microbiota-based modulation of the anticonvulsant properties of the KD has shown promise in improving seizure control in these patients (Olson et al., 2018; Lindefeldt et al., 2019) (see Figure 4).

Previous research has demonstrated that intestinal inflammation can reduce the effectiveness of VPA, while therapy with SCFAs can effectively reduce inflammation, thereby enhancing the efficacy of VPA treatment (De Caro et al., 2019b). In animal models of epilepsy, the administration of lithium, valproate, and aripiprazole has been found to significantly increase the richness and diversity of microbial species. At the phylum level, valproate treatment has been shown to induce an increase in Actinobacteria and Firmicutes, while simultaneously decreasing the abundance of Bacteroidetes. At the genus level, several species including *Clostridium*, *Peptoclostridium*, *Intestinibacter*, and *Christenellaceae* were found to be increased following treatment with lithium, valproate, and aripiprazole compared to the control rats (Cussotto et al., 2019). Additionally, valproate treatment in rat models has been shown to decrease the relative abundance of *S24-7 uncultbact* and increase the relative abundance of *Ruminococcaceae* uncultured. Interestingly, VPA was also found to decrease the levels of two important SCFAs, namely, propionate and butyrate, in the cecum, while increasing the levels of isovalerate (Cussotto et al., 2019). Notably, mice exposed to sodium valproate demonstrated an increased ratio of Bacteroidetes to Firmicutes when compared to control mice (Sgritta et al., 2019). In clinical studies, it has been observed that the ratio of the phylum Firmicutes to Bacteriodetes is significantly higher in patients with new-onset epilepsy after 3 months of VPA treatment (Gong et al., 2022a). These findings provide further support for the role of gut microbiota composition in epilepsy and suggest that alterations in microbial populations may be associated with the effects of VPA therapy.

The anti-seizure drug lamotrigine and its ammonium salt complexes exhibit strong antibacterial activity against Gram-positive bacteria such as *B. subtilis*, *S. aureus*, and *S. faecalis* (Qian et al., 2009). Clonazepam, another anti-seizure drug, is metabolized by intestinal flora, which can potentially increase the drug's toxic effects (Zimmermann et al., 2019). Then carbamazepine has been found to induce specific phenotypes in gut microbiota (Watkins et al., 2017; Gong et al., 2022; Ilhan et al., 2022). In a study involving epilepsy patients, after 3 months of carbamazepine treatment, the frequency of seizures was reduced by more than 50%. The abundance of Actinobacteria at the phylum level, which was initially higher in epileptic patients compared to healthy controls, decreased significantly after treatment. At the genus level, the abundances of bacteria such as *Escherichia/Shigella*, *Streptococcus*, *Collinsella*, and *Megamonas* were significantly higher in epilepsy patients before treatment but decreased significantly after treatment (Gong et al., 2022).

ASMs typically possess a narrow therapeutic window and are associated with numerous adverse effects, particularly impacting the gastrointestinal tract. Between 10% and 30% of epilepsy patients experienced intolerable side effects from these medications, leading them to discontinue treatment, particularly when undergoing polytherapy (Wiebe et al., 2008). Many ASMs have a direct impact on the enteric nervous system, influencing gut motility, which is evident in the gastrointestinal adverse effects of these medications (Jahromi et al., 2011; Minton et al., 2011; Al-Beltagi, 2021; Al-Beltagi and Saeed, 2022; Nevitt et al., 2022). For example, carbamazepine can lead to a range of gastrointestinal adverse effects, including dry mouth, mouth sores, glossitis, loss of appetite, dysphagia, nausea, vomiting, heartburn, gastritis, stomach/abdominal pain, constipation, and diarrhea (Anttila and Valtonen, 1992). Similarly, ethosuximide can induce anorexia, nausea, vomiting, gastric pain, diarrhea, and gastric and intestinal atony with decreased peristaltic activity (Kristev et al., 1994; Zagorchev et al., 1998). Phenobarbital can result in sore throat, diarrhea, swelling of the tongue/throat, nausea, vomiting, constipation, dysphagia, and heartburn (Jahromi et al., 2011; Al-Beltagi and Saeed, 2022). Phenytoin can cause changes in taste sensation, gingival overgrowth, sore throat, mouth ulcers, diarrhea, nausea, vomiting, constipation, dysphagia, heartburn, and reduced gastrointestinal absorption of calcium (Bell et al., 1979). Valproate also leads to gastrointestinal adverse effects, including diarrhea, nausea, vomiting, constipation, dysphagia, and gastritis with heartburn (Abdullah and Mousheer, 2020). This influence on the gut may significantly contribute to alterations in the gut microbiome. However, despite our comprehensive review of the existing research literature, we have found a lack of studies specifically examining the microbiota alterations induced by the gastrointestinal adverse effects of ASMs.

Carbamazepine, lamotrigine, and topiramate have been found to inhibit the growth of more than ten strains of bacteria when combined with the syrup excipient propyl-paraben. Ilhan et al. (2022) studied the effects of sweeteners and benzoates commonly found in ASM syrup. They found that the impact of these chemicals was concentration-dependent, with parabens and sweeteners showing increased toxicity or proliferation with higher concentrations. *Bifidobacterium species* were negatively affected by high concentrations of propyl-paraben, while methyl-paraben did not have the same effect. These results align with previous research by Crovetto et al., who reported a greater toxic effect of propyl- and butyl-parabens compared to methyl-paraben on *E. coli* and *Staphylococcus aureus* under aerobic conditions (Cussotto et al., 2019). Interestingly, the presence of various artificial sweeteners in ASMs formulations stimulated the growth of certain gut bacterial strains. The active ingredients that exhibited greater toxicity towards bacterial strains also displayed toxicity towards HT-29 cells (Watkins et al., 2017; Ilhan et al., 2022). Notably, previous studies have suggested that common food and drug additives, including artificial sweeteners, can alter the composition and function of the gut microbiota in batch-culture systems (Gerasimidis et al., 2020). Aspartame and benzoate have been shown to increase the relative abundance of *Bifidobacterium* in these mixed cultures, indicating a potential prebiotic effect (Gerasimidis et al., 2020). In addition, the supernatant of *Bifidobacterium longum* was found to reduce the cytotoxic effects of carbamazepine and lamotrigine. Similarly, the supernatants of *Akkermansia muciniphila* or mixed bacterial communities reduced the expression of drug resistance genes in HT-29 cell lines (Ilhan

et al., 2022). In conclusion, these findings reveal that medications targeted for humans may inadvertently affect the gut microbiome, potentially exerting anti-commensal effects. This highlights the complex relationship between human-targeted medications and the gut microbiome, emphasizing the importance of understanding and modulating the microbiome to optimize treatment outcomes.

In general, the gut microbiota appears to play a significant role in the functioning and development of fundamental physiological processes, and it may also have an impact on central neural processes through the microbiota-gut-brain (MGB) axis. Both preclinical and clinical studies suggest that the microbiome could potentially modulate seizures and contribute to the pathogenesis of epilepsy. Various interventions, such as changes in diet, supplementation, and medication, have the potential to directly and indirectly affect the MGB axis. Researching the effects of these interventions could lead to a better understanding of epilepsy, the identification of biomarkers, and the development of new therapeutic options. That's where our interest in the field lies. However, investigating the MGB axis and the role of gut supplementation in epilepsy is challenging due to the numerous potential pathways and variables involved. To date, only a few limited studies have been conducted, making it premature to draw conclusions. We also acknowledge that it is essential to conduct studies with the same rigor as pharmaceutical drug development trials, including taxa and metabolomic analyses using standard methodologies.

7 The association of gut microbiota with potential differences in behavioral characteristics of epileptic patients

Given the bidirectional relationship between the brain and the gut, it is important to note that neurological disorders may have a significant impact on the gastrointestinal tract. This impact can manifest in various ways, including the occurrence of sialorrhea, dysphagia, anorexia, gastroparesis, and motility disorders such as diarrhea, intestinal pseudo-obstruction, fecal incontinence, and constipation (Camilleri, 2021). Consequently, epilepsy can also affect the gastrointestinal tract in different forms, including abdominal aura, epilepsy with abdominal pain, and the adverse effects of medications on the gut and the gut microbiota.

An epigastric aura, also known as a visceral aura, is a somatosensory phenomenon often characterized by a growing sensation in the upper abdomen. This type of aura can manifest as visceral sensations, such as abdominal discomfort, visceromotor symptoms like vomiting, borborygmi, or tachycardia, as well as vegetative symptoms, including blushing or sweating. The occurrence of epigastric aura is linked to abnormal neuronal activation and discharges in the sensory cortex that represent the abdominal viscera (Schmitt and Ebner, 2000; Blom, 2010; Al-Beltagi and Saeed, 2022). Notably, this type of aura is frequently observed in epilepsy, with epigastric auras being the most common aura in medial temporal lobe epilepsy. Epilepsy with abdominal pain is a relatively rare condition characterized by recurrent paroxysms of abdominal and periumbilical pain, often accompanied by symptoms such as nausea and vomiting. This form of temporal lobe epilepsy typically presents with abdominal auras and can occur in both children and adults (Kshirsagar et al., 2012). Following these episodes, individuals may experience characteristic postictal manifestations, including lethargy, drowsiness, blindness, headache, paraesthesia, or even convulsions. For example, Remick et al. (1980) described three patients who experienced postictal hyperphagia. In some cases, postictal hyperphagia and compulsive water drinking have been reported, particularly in patients with secondary epilepsy due to temporal lobe lesions, showing a notable response to carbamazepine (Ott, 1991). Similar manifestations have also been observed in secondary epilepsy due to frontal lobe lesions (Mittal et al., 2001).

Epilepsy may have a significant impact on the microbiota, which may be due to various social, physical, and dietary differences between patients with epilepsy and normal controls. For example, patients with epilepsy may experience excessive sleepiness, have different dietary preferences due to comorbid autism, have mobility limitations, aspirate food more frequently, rely on mechanically soft diets, and consume more processed foods. Gastroesophageal reflux disease (GERD) is a common comorbidity in children with neurological problems like cerebral palsy and epilepsy. The presence of GERD in such patients can complicate their management and mimic refractory seizures, making it difficult to diagnose and treat the underlying condition (Bayram et al., 2016). Peptic ulcers are also more common in patients with epilepsy than in the general population, with some studies reporting up to eight times higher prevalence rates (Keezer et al., 2016). Similarly, the incidence of IBS is five times higher in patients with epilepsy than in controls (Camara-Lemarroy et al., 2016). Children with epilepsy also have a higher incidence of functional gastrointestinal disorders, including IBS, compared to their matched controls (Aydemir et al., 2020). Additionally, children with autism, who have a high rate of celiac disease and gut dysbiosis, are more likely to develop epilepsy. Abnormal EEG results are present in 60% of children with autism, compared to only 6%–7% of typically developed children, while epilepsy is present in 10%–30% of children with autism.

Furthermore, epilepsy may manifest with postictal states that exhibit gastrointestinal symptoms, including postictal hypersalivation, compulsive water drinking, and hyperphagia (Ott, 1991; Mittal et al., 2001; Al-Beltagi and Saeed, 2022). These postictal manifestations, particularly prevalent in patients with medication-refractory epilepsy and comorbid conditions such as cerebral palsy, have the potential to significantly impact the composition and functionality of the gut microbiota. Despite this, there remains a gap in understanding how the social, psychological, and dietary characteristics of individuals with epilepsy, either alone or in conjunction with other disorders, contribute to alterations in gut microbes. Closing this knowledge gap is crucial for developing a comprehensive understanding of the intricate interplay between epilepsy, comorbid conditions, and the gut microbiome.

8 Conclusion

The brain-gut-microbiota axis plays a critical role in maintaining a delicate balance between the brain and gut,

primarily through visceral sensory, endocrine, and immune pathways. It is intricately involved in the pathophysiological mechanisms of gastrointestinal and neurological disorders, with a particular focus on epilepsy. In recent years, a growing body of evidence from animal models and clinical studies has highlighted the significant role of gut microbiota in epilepsy. Not only does it contribute to the occurrence of seizures through various pathways, including visceral sensory, endocrine, and immune mechanisms, but it also influences the therapeutic effects of epilepsy drugs and KD. Disparities in fecal microbial composition have been observed in both epilepsy patients and animal models before and after treatment with a KD. This underscores the increasing number of studies that are investigating the gut microbiota as a crucial factor in epilepsy. However, the current research presents a complex and sometimes contradictory picture, with discrepancies observed in the gut microbiota composition across different epilepsy models, as well as variations in clinical evidence. Furthermore, there is a lack of comprehensive mechanistic studies that would definitively establish the important role of gut microbiota in epileptogenesis and disease progression. Nevertheless, this growing body of evidence also suggests that targeting the gut microbiota, along with dietary interventions, holds significant potential for the prevention, diagnosis, treatment, and prognosis of epilepsy.

Author contributions

HZ: Conceptualization, Funding acquisition, Writing–original draft, Methodology, Project administration, Resources, Software, Supervision, Writing–review and editing. WW: Methodology, Supervision, Writing–review and editing. YL: Conceptualization, Funding acquisition, Methodology, Resources, Supervision, Writing–review and editing, Project administration.

Funding

The authors declare financial support was received for the research, authorship, and/or publication of this article. This research was funded by a grant (2022J0703) from the Scientific Research Fund Project of Yunnan Provincial Department of Education, a grant from the Science and Technology Talent Project (Reserve talent) of the First Affiliated Hospital of Dali University, a grant from the Yunnan Basic Research Program Joint Special Project of Local Universities-Youth Project, and a grant (2021KBG047, 2022KBG035) from the Dali Science and Technology Bureau Project.

Conflict of interest

The authors declare that the research was conducted in the absence of any commercial or financial relationships that could be construed as a potential conflict of interest.

Publisher's note

References

Abdullah, A. T., and Mousheer, Z. T. (2020). Vitamin D status in epileptic children on valproic acid; a case-control study. *Arch. Acad. Emerg. Med.* 8, e13.

Ahlers, F. S., Benros, M. E., Dreier, J. W., and Christensen, J. (2019). Infections and risk of epilepsy in children and young adults:a nationwide study. *Epilepsia* 60, 275–283. doi:10.1111/epi.14626

Al-Beltagi, M. (2021). Autism medical comorbidities. *World J. Clin. Pediatr.* 10, 15–28. doi:10.5409/wjcp.v10.i3.15

Al-Beltagi, M., and Saeed, N. K. (2022). Epilepsy and the gut: perpetrator or victim? *World J. Gastrointest. Pathophysiol.* 13, 143–156. doi:10.4291/wjgp.v13.i5.143

Alonso-Alonso, M., Woods, S. C., Pelchat, M., Grigson, P. S., Stice, E., Farooqi, S., et al. (2015). Food reward system: current perspectives and future research needs. *Nutr. Rev.* 73, 296–307. doi:10.1093/nutrit/nuv002

Amaral, F. A., Sachs, D., Costa, V. V., Fagundes, C. T., Cisalpino, D., Cunha, T. M., et al. (2008). Commensal microbiota is fundamental for the development of inflammatory pain. *Proc. Natl. Acad. Sci. U. S. A.* 105, 2193–2197. doi:10.1073/pnas.0711891105

Amasheh, S., Fromm, M., and Günzel, D. (2011). Claudins of intestine and nephron:a correlation of molecular tight junction structure and barrier function. *Acta Physiol(Oxf)* 201, 133–140. doi:10.1111/j.1748-1716.2010.02148.x

Amlerova, J., Šroubek, J., Angelucci, F., and Hort, J. (2021). Evidences for a role of gut microbiota in pathogenesis and management of epilepsy. *Int. J. Mol. Sci.* 22, 5576. doi:10.3390/ijms22115576

Anttila, V. J., and Valtonen, M. (1992). Carbamazepine-induced eosinophilic colitis. *Epilepsia* 33, 119–121. doi:10.1111/j.1528-1157.1992.tb02293.x

Arulsamy, A., and Shaikh, M. F. (2022). Epilepsy-associated comorbidities among adults: a plausible therapeutic role of gut microbiota. *Neurobiol. Dis.* 165, 105648. doi:10.1016/j.nbd.2022.105648

Attenello, F., Amar, A. P., Liu, C., and Apuzzo, M. L. (2015). Theoretical basis of vagus nerve stimulation. *Prog. Neurol. Surg.* 29, 20–28. doi:10.1159/000434652

Aydemir, Y., Carman, K. B., and Yarar, C. (2020). Screening for functional gastrointestinal disorders in children with epilepsy. *Epilepsy Behav.* 111, 107267. doi:10.1016/j.yebeh.2020.107267

Aygun, H., Akin, A. T., Kızılaslan, N., Sumbul, O., and Karabulut, D. (2022a). Electrophysiological, histopathological, and biochemical evaluation of the protective effect of probiotic supplementation against pentylenetetrazole-induced seizures in rats. *Eur. J. Neurol.* 30, 3540–3550. doi:10.1111/ene.15359

Aygun, H., Akin, A. T., Kızılaslan, N., Sumbul, O., and Karabulut, D. (2022b). Probiotic supplementation alleviates absence seizures and anxiety- and depression-like behavior in WAG/Rij rat by increasing neurotrophic factors and decreasing proinflammatory cytokines. *Epilepsy Behav.* 128, 108588. doi:10.1016/j.yebeh.2022.108588

Bagheri, S., Heydari, A., Alinaghipour, A., and Salami, M. (2019). Effect of probiotic supplementation on seizure activity and cognitive performance in PTZ-induced chemical kindling. *Epilepsy Behav.* 95, 43–50. doi:10.1016/j.yebeh.2019.03.038

Bakken, I. J., Aaberg, K. M., Ghaderi, S., Gunnes, N., Trogstad, L., Magnus, P., et al. (2015). Febrile seizures after 2009 influenza A (H1N1) vaccination and infection:a nationwide registry-based study. *BMC Infect. Dis.* 15, 506. doi:10.1186/s12879-015-1263-7

Balestrini, S., Arzimanoglou, A., Blümcke, I., Scheffer, I. E., Wiebe, S., Zelano, J., et al. (2021). The aetiologies of epilepsy. *Epileptic Disord.* 23, 1–16. doi:10.1684/epd.2021.1255

Baram, T. Z., and Schultz, L. (1991). Corticotropin-releasing hormone is a rapid and potent convulsant in the infant rat. *Brain Res. Dev. Brain Res.* 61, 97–101. doi:10.1016/0165-3806(91)90118-3

Barrett, E., Ross, R. P., O'Toole, P. W., Fitzgerald, G. F., and Stanton, C. (2012). γ-Aminobutyric acid production by culturable bacteria from the human intestine. *J. Appl. Microbiol.* 113, 411–417. doi:10.1111/j.1365-2672.2012.05344.x

Bayram, A. K., Canpolat, M., Karacabey, N., Gumus, H., Kumandas, S., Doğanay, S., et al. (2016). Misdiagnosis of gastroesophageal reflux disease as epileptic seizures in children. *Brain Dev.* 38, 274–279. doi:10.1016/j.braindev.2015.09.009

Bell, R. D., Pak, C. Y., Zerwekh, J., Barilla, D. E., and Vasko, M. (1979). Effect of phenytoin on bone and vitamin D metabolism. *Ann. Neurol.* 5, 374–378. doi:10.1002/ana.410050411

Benakis, C., Brea, D., Caballero, S., Faraco, G., Moore, J., Murphy, M., et al. (2016). Commensal microbiota affects ischemic stroke outcome by regulating intestinal γδ T cells. *Nat. Med.* 22, 516–523. doi:10.1038/nm.4068

Bercik, P., Denou, E., Collins, J., Jackson, W., Lu, J., Jury, J., et al. (2011). The intestinal microbiota affect central levels of brain-derived neurotropic factor and behavior in mice. *Gastroenterology* 141, 599–609. doi:10.1053/j.gastro.2011.04.052

Beretta, S., Carone, D., Zanchi, C., Bianchi, E., Pirovano, M., Trentini, C., et al. (2017). Long-term applicability of the new ILAE definition of epilepsy. Results from the PRO-LONG study. *Epilepsia* 58, 1518–1523. doi:10.1111/epi.13854

Berthoud, H. R., and Morrison, C. (2008). The brain, appetite, and obesity. *Annu. Rev. Psychol.* 59, 55–92. doi:10.1146/annurev.psych.59.103006.093551

Bertuccioli, A., Cardinali, M., Di Pierro, F., Zonzini, G. B., and Matera, M. R. (2022). Ketogenic and low FODMAP diet in therapeutic management of a young autistic patient with epilepsy and dysmetabolism poorly responsive to therapies: clinical response and effects of intestinal microbiota. *Int. J. Mol. Sci.* 23, 8829. doi:10.3390/ijms23158829

Binh Tran, T. D., Nguyen, H., Sodergren, E., Addiction, CFSNO., Dickson, P. E., Wright, S. N., et al. (2023). Microbial glutamate metabolism predicts intravenous cocaine self-administration in diversity outbred mice. *Neuropharmacology* 226, 109409. doi:10.1016/j.neuropharm.2022.109409

Blom, J. D. (2010). *A dictionary of hallucinations*. New York, NY: Springer.

Borody, T. J., and Khoruts, A. (2011). Fecal microbiota transplantation and emerging applications. *Nat. Rev. Gastroenterol. Hepatol.* 9, 88–96. doi:10.1038/nrgastro.2011.244

Borre, Y. E., O'Keeffe, G. W., Clarke, G., Stanton, C., Dinan, T. G., and Cryan, J. F. (2014). Microbiota and neurodevelopmental windows: implications for brain disorders. *Trends Mol. Med.* 20, 509–518. doi:10.1016/j.molmed.2014.05.002

Braniste, V., Al-Asmakh, M., Kowal, C., Anuar, F., Abbaspour, A., Tóth, M., et al. (2014). The gut microbiota influences bloodbrain barrier permeability in mice. *Sci. Transl. Med.* 6, 263ra158. doi:10.1126/scitranslmed.3009759

Bravo, J. A., Forsythe, P., Chew, M. V., Escaravage, E., Savignac, H. M., Dinan, T. G., et al. (2011). Ingestion of Lactobacillus strain regulates emotional behavior and central GABA receptor expression in a mouse via the vagus nerve. *Proc. Natl. Acad. Sci. U. S. A.* 108, 16050–16055. doi:10.1073/pnas.1102999108

Buccigrossi, V., Laudiero, G., Russo, C., Miele, E., Sofia, M., Monini, M., et al. (2014). Chloride secretion induced by rotavirus is oxidative stress-dependent and inhibited by Saccharomyces boulardii in human enterocytes. *PLoS One* 9, e99830. doi:10.1371/journal.pone.0099830

Camara-Lemarroy, C. R., Escobedo-Zúñiga, N., Ortiz-Zacarias, D., Peña-Avendaño, J., Villarreal-Garza, E., and Díaz-Torres, M. A. (2016). Prevalence and impact of irritable bowel syndrome in people with epilepsy. *Epilepsy Behav.* 63, 29–33. doi:10.1016/j.yebeh.2016.05.041

Camilleri, M. (2021). Gastrointestinal motility disorders in neurologic disease. *J. Clin. Invest.* 131, e143771. doi:10.1172/JCI143771

Cano-López, I., and González-Bono, E. (2019). Cortisol levels and seizures in adults with epilepsy:a systematic review. *Neurosci. Biobehav Rev.* 103, 216–229. doi:10.1016/j.neubiorev.2019.05.023

Castañeda-Cabral, J. L., Colunga-Durán, A., Ureña-Guerrero, M. E., Beas-Zárate, C., Nuñez-Lumbreras, M. L. A., Orozco-Suárez, S., et al. (2020). Expression of VEGF- and tight junction-related proteins in the neocortical microvasculature of patients with drug-resistant temporal lobe epilepsy. *Microvasc. Res.* 132, 104059. doi:10.1016/j.mvr.2020.104059

Ceccarani, C., Viganò, I., Ottaviano, E., Redaelli, M. G., Severgnini, M., Vignoli, A., et al. (2021). Is gut microbiota a key player in epilepsy onset? A longitudinal study in drug-naive children. *Front. Cell Infect. Microbiol.* 11, 749509. doi:10.3389/fcimb.2021.749509

Chatzikonstantinou, S., Gioula, G., Kimiskidis, V. K., McKenna, J., Mavroudis, I., and Kazis, D. (2021). The gut microbiome in drug-resistant epilepsy. *Epilepsia Open* 6, 28–37. doi:10.1002/epi4.12461

Chen, S. G., Stribinskis, V., Rane, M. J., Demuth, D. R., Gozal, E., Roberts, A. M., et al. (2016). Exposure to the functional bacterial amyloid protein curli enhances alpha-synuclein aggregation in aged fischer 344 rats and *Caenorhabditis elegans*. *Sci. Rep.* 6, 34477. doi:10.1038/srep34477

Cheng, Y., Mai, Q., Zeng, X., Wang, H., Xiao, Y., Tang, L., et al. (2019). Propionate relieves pentylenetetrazol-induced seizures, consequent mitochondrial disruption, neuron necrosis and neurological deficits in mice. *Biochem. Pharmacol.* 169, 113607. doi:10.1016/j.bcp.2019.08.009

Cheraghmakani, H., Rezai, M. S., Valadan, R., Rahimzadeh, G., Moradi, M., Jahanfekr, V., et al. (2021). Ciprofloxacin for treatment of drug-resistant epilepsy. *Epilepsy Res.* 176, 106742. doi:10.1016/j.eplepsyres.2021.106742

Cherny, I., Rockah, L., Levy-Nissenbaum, O., Gophna, U., Ron, E. Z., and Gazit, E. (2005). The formation of *Escherichia coli* curli amyloid fibrils is mediated by prion-like peptide repeats. *J. Mol. Biol.* 352, 245–252. doi:10.1016/j.jmb.2005.07.028

Chow, J., and Mazmanian, S. K. (2009). Getting the bugs out of the immune system: do bacterial microbiota "fix" intestinal T cell responses? *Cell Host Microbe* 5, 8–12. doi:10.1016/j.chom.2008.12.006

Ciltas, A. C., Toy, C. E., Güneş, H., and Yaprak, M. (2023). Effects of probiotics on GABA/glutamate and oxidative stress in PTZ-induced acute seizure model in rats. *Epilepsy Res.* 195, 107190. doi:10.1016/j.eplepsyres.2023.107190

Citraro, R., Lembo, F., De Caro, C., Tallarico, M., Coretti, L., Iannone, L. F., et al. (2021). First evidence of altered microbiota and intestinal damage and their link to absence epilepsy in a genetic animal model, the WAG/rij rat. *Epilepsia* 62, 529–541. doi:10.1111/epi.16813

Clark, A., and Mach, N. (2016). Exercise-induced stress behavior, gut-microbiota-brain axis and diet: a systematic review for athletes. *J. Int. Soc. Sports Nutr.* 13, 43. doi:10.1186/s12970-016-0155-6

Clarke, T. B., Davis, K. M., Lysenko, E. S., Zhou, A. Y., Yu, Y., and Weiser, J. N. (2010). Recognition of peptidoglycan from the microbiota by Nod1 enhances systemic innate immunity. *Nat. Med.* 16, 228–231. doi:10.1038/nm.2087

Collins, S. M., Surette, M., and Bercik, P. (2012). The interplay between the intestinal microbiota and the brain. *Nat. Rev. Microbiol.* 10, 735–742. doi:10.1038/nrmicro2876

Costa, M., Brookes, S. J., and Hennig, G. W. (2000). Anatomy and physiology of the enteric nervous system. *Gut* 47, iv15–9. doi:10.1136/gut.47.suppl_4.iv15

Craig, A. D. (2002). How do you feel? Interoception: the sense of the physiological condition of the body. *Nat. Rev. Neurosci.* 3, 655–666. doi:10.1038/nrn894

Craig, A. D. (2003). Interoception: the sense of the physiological condition of the body. *Curr. Opin. Neurobiol.* 13, 500–505. doi:10.1016/s0959-4388(03)00090-4

Cryan, J. F., and Dinan, T. G. (2012). Mind-altering microorganisms: the impact of the gut microbiota on brain and behaviour. *Nat. Rev. Neurosci.* 13, 701–712. doi:10.1038/nrn3346

Cusick, M. F., Libbey, J. E., Doty, D. J., DePaula-Silva, A. B., and Fujinami, R. S. (2017). The role of peripheral interleukin-6 in the development of acute seizures following virus encephalitis. *J. Neurovirol* 23, 696–703. doi:10.1007/s13365-017-0554-8

Cussotto, S., Strain, C. R., Fouhy, F., Strain, R. G., Peterson, V. L., Clarke, G., et al. (2019). Differential effects of psychotropic drugs on microbiome composition and gastrointestinal function. *Psychopharmacology* 236, 1671–1685. doi:10.1007/s00213-018-5006-5

Dahlin, M., and Prast-Nielsen, S. (2019). The gut microbiome and epilepsy. *EBioMedicine* 44, 741–746. doi:10.1016/j.ebiom.2019.05.024

Dai, Y., Wang, M., Zhong, D., and Xu, X. (2022). Bacillus subtilis plays a role in the inhibition of transporter ABCB1 in Caco-2 cells. *Epilepsy Res.* 183, 106925. doi:10.1016/j.eplepsyres.2022.106925

De Caro, C., Iannone, L. F., Citraro, R., Striano, P., De Sarro, G., Constanti, A., et al. (2019a). Can we 'seize' the gut microbiota to treat epilepsy? *Neurosci. Biobehav Rev.* 107, 750–764. doi:10.1016/j.neubiorev.2019.10.002

De Caro, C., Leo, A., Nesci, V., Ghelardini, C., di Cesare Mannelli, L., Striano, P., et al. (2019b). Intestinal inflammation increases convulsant activity and reduces antiepileptic drug efficacy in a mouse model of epilepsy. *Sci. Rep.* 9, 13983. doi:10.1038/s41598-019-50542-0

de Lima, A. M. D. L., de Lima Rosa, G., Müller Guzzo, E. F., Padilha, R. B., Costa da Silva, R., Silveira, A. K., et al. (2022). Gut microbiota modulation by prednisolone in a rat kindling model of pentylenetetrazol (PTZ)-induced seizure. *Microb. Pathog.* 163, 105376. doi:10.1016/j.micpath.2021.105376

den Besten, G., van Eunen, K., Groen, A. K., Venema, K., Reijngoud, D. J., and Bakker, B. M. (2013). The role of short-chain fatty acids in the interplay between diet, gut microbiota, and host energy metabolism. *J. Lipid Res.* 54, 2325–2340. doi:10.1194/jlr.R036012

Ding, M., Lang, Y., Shu, H., Shao, J., and Cui, L. (2021). Microbiota-gut-brain Axis and epilepsy: a review on mechanisms and potential therapeutics. *Front. Immunol.* 12, 742449. doi:10.3389/fimmu.2021.742449

Ding, X., Zhou, J., Zhao, L., Chen, M., Wang, S., Zhang, M., et al. (2022). Intestinal flora composition determines microglia activation and improves epileptic episode progress. *Front. Cell Infect. Microbiol.* 12, 835217. doi:10.3389/fcimb.2022.835217

Djurić, Z., Nagorni, A., Jocić-Jakubi, B., Dimić, M., Novak, M., Milićević, R., et al. (2012). Celiac disease prevalence in epileptic children from Serbia. *Turk J. Pediatr.* 54, 247–250.

Dong, L., Zheng, Q., Cheng, Y., Zhou, M., Wang, M., Xu, J., et al. (2022). Gut microbial characteristics of adult patients with epilepsy. *Front. Neurosci.* 16, 803538. doi:10.3389/fnins.2022.803538

Eisenstein, M. (2016). Microbiome: bacterial broadband. *Nature* 533, 104–106. doi:10.1038/533S104a

Eor, J. Y., Son, Y. J., Kim, J. Y., Kang, H. C., Youn, S. E., Kim, J. H., et al. (2021). Neuroprotective effect of both synbiotics and ketogenic diet in a pentylenetetrazol-induced acute seizure murine model. *Epilepsy Res.* 174, 106668. doi:10.1016/j.eplepsyres.2021.106668

Erny, D., Hrabě de Angelis, A. L., Jaitin, D., Wieghofer, P., Staszewski, O., David, E., et al. (2015). Host microbiota constantly control maturation and function of microglia in the CNS. *Nat. Neurosci.* 18, 965–977. doi:10.1038/nn.4030

Fan, Y., Wang, H., Liu, X., Zhang, J., and Liu, G. (2019). Crosstalk between the ketogenic diet and epilepsy: from the perspective of gut microbiota. *Mediat. Inflamm.* 2019, 8373060. doi:10.1155/2019/8373060

Fenoglio-Simeone, K. A., Wilke, J. C., Milligan, H. L., Allen, C. N., Rho, J. M., and Maganti, R. K. (2009). Ketogenic diet treatment abolishes seizure periodicity and improves diurnal rhythmicity in epileptic Kcna1-null mice. *Epilepsia* 50, 2027–2034. doi:10.1111/j.1528-1167.2009.02163.x

Ferrier, C. H., Alarcón, G., Glover, A., Koutroumanidis, M., Morris, R. G., Simmons, A., et al. (2000). N-Acetylaspartate and creatine levels measured by (1)H MRS relate to recognition memory. *Neurology* 55, 1874–1883. doi:10.1212/wnl.55.12.1874

Ferro, J. M., and Oliveira Santos, M. (2021). Neurology of inflammatory bowel disease. *J. Neurol. Sci.* 424, 117426. doi:10.1016/j.jns.2021.117426

Fiest, K. M., Sauro, K. M., Wiebe, S., Patten, S. B., Kwon, C. S., Dykeman, J., et al. (2017). Prevalence and incidence of epilepsy: a systematic review and meta-analysis of international studies. *Neurology* 88, 296–303. doi:10.1212/WNL.0000000000003509

Fisher, R. S., Acevedo, C., Arzimanoglou, A., Bogacz, A., Cross, J. H., Elger, C. E., et al. (2014). ILAE official report: a practical clinical definition of epilepsy. *Epilepsia* 55, 475–482. doi:10.1111/epi.12550

Fisher, R. S., Cross, J. H., D'Souza, C., French, J. A., Haut, S. R., Higurashi, N., et al. (2017b). Instruction manual for the ILAE 2017 operational classification of seizure types. *Epilepsia* 58, 531–542. doi:10.1111/epi.13671

Fisher, R. S., Cross, J. H., French, J. A., Higurashi, N., Hirsch, E., Jansen, F. E., et al. (2017a). Operational classification of seizure types by the international league against epilepsy: position paper of the ILAE commission for classification and terminology. *Epilepsia* 58, 522–530. doi:10.1111/epi.13670

Friedland, R. P., and Chapman, M. R. (2017). The role of microbial amyloid in neurodegeneration. *PLoS Pathog.* 13, e1006654. doi:10.1371/journal.ppat.1006654

Frost, G., Sleeth, M. L., Sahuri-Arisoylu, M., Lizarbe, B., Cerdan, S., Brody, L., et al. (2014). The short-chain fatty acid acetate reduces appetite via a central homeostatic mechanism. *Nat. Commun.* 5, 3611. doi:10.1038/ncomms4611

Furness, J. B., Callaghan, B. P., Rivera, L. R., and Cho, H. J. (2014). The enteric nervous system and gastrointestinal innervation: integrated local and central control. *Adv. Exp. Med. Biol.* 817, 39–71. doi:10.1007/978-1-4939-0897-4_3

Fusco, F., Perottoni, S., Giordano, C., Riva, A., Iannone, L. F., De Caro, C., et al. (2022). The microbiota-gut-brain axis and epilepsy from a multidisciplinary perspective: clinical evidence and technological solutions for improvement of *in vitro* preclinical models. *Bioeng. Transl. Med.* 7, e10296. doi:10.1002/btm2.10296

Gales, J. M., and Prayson, R. A. (2017). Chronic inflammation in refractory hippocampal sclerosis-related temporal lobe epilepsy. *Ann. Diagn Pathol.* 30, 12–16. doi:10.1016/j.anndiagpath.2017.05.009

Galland, L. (2014). The gut microbiome and the brain. *J. Med. Food* 17, 1261–1272. doi:10.1089/jmf.2014.7000

García-Belenguer, S., Grasa, L., Palacio, J., Moral, J., and Rosado, B. (2023). Effect of a ketogenic medium chain triglyceride-enriched diet on the fecal microbiota in canine idiopathic epilepsy: a pilot study. *Vet. Sci.* 10, 245. doi:10.3390/vetsci10040245

García-Belenguer, S., Grasa, L., Valero, O., Palacio, J., Luño, I., and Rosado, B. (2021). Gut microbiota in canine idiopathic epilepsy: effects of disease and treatment. *Animals* 11, 3121. doi:10.3390/ani11113121

Gerasimidis, K., Bryden, K., Chen, X., Papachristou, E., Verney, A., Roig, M., et al. (2020). The impact of food additives, artificial sweeteners and domestic hygiene products on the human gut microbiome and its fibre fermentation capacity. *Eur. J. Nutr.* 59, 3213–3230. doi:10.1007/s00394-019-02161-8

Gernone, F., Uva, A., Silvestrino, M., Cavalera, M. A., and Zatelli, A. (2022). Role of gut microbiota through gut-brain axis in epileptogenesis:a systematic review of human and veterinary medicine. *Biology* 11, 1290. doi:10.3390/biology11091290

Gershon, M. D. (2010). Developmental determinants of the independence and complexity of the enteric nervous system. *Trends Neurosci.* 33, 446–456. doi:10.1016/j.tins.2010.06.002

Goehler, L. E., Gaykema, R. P., Opitz, N., Reddaway, R., Badr, N., and Lyte, M. (2005). Activation in vagal afferents and central autonomic pathways:early responses to intestinal infection with Campylobacter jejuni. *Brain Behav. Immun.* 19, 334–344. doi:10.1016/j.bbi.2004.09.002

Gomes, W. A., Lado, F. A., de Lanerolle, N. C., Takahashi, K., Pan, C., and Hetherington, H. P. (2007). Spectroscopic imaging of the pilocarpine model of human epilepsy suggests that early NAA reduction predicts epilepsy. *Magn. Reson Med.* 58, 230–235. doi:10.1002/mrm.21310

Gómez-Eguílaz, M., Ramón-Trapero, J. L., Pérez-Martínez, L., and Blanco, J. R. (2018). The beneficial effect of probiotics as a supplementary treatment in drug-resistant epilepsy: a pilot study. *Benef. Microbes* 9, 875–881. doi:10.3920/BM2018.0018

Gong, S. Z., Qiu, J., Wu, L. W., and Tan, L. H. (2022). Change in intestinal flora after treatment in children with focal epilepsy. *Zhongguo Dang Dai Er Ke Za Zhi* 24, 290–296. doi:10.7499/j.issn.1008-8830.2109134

Gong, X., Cai, Q., Liu, X., An, D., Zhou, D., Luo, R., et al. (2021). Gut flora and metabolism are altered in epilepsy and partially restored after ketogenic diets. *Microb. Pathog.* 155, 104899. doi:10.1016/j.micpath.2021.104899

Gong, X., Liu, L., Li, X., Xiong, J., Xu, J., Mao, D., et al. (2022b). Neuroprotection of cannabidiol in epileptic rats: gut microbiome and metabolome sequencing. *Front. Nutr.* 9, 1028459. doi:10.3389/fnut.2022.1028459

Gong, X., Liu, X., Chen, C., Lin, J., Li, A., Guo, K., et al. (2020). Alteration of gut microbiota in patients with epilepsy and the potential index as a biomarker. *Front. Microbiol.* 11, 517797. doi:10.3389/fmicb.2020.517797

Gong, X., Liu, Y., Liu, X., Li, A. Q., Guo, K. D., Zhou, D., et al. (2022a). Analysis of gut microbiota in patients with epilepsy treated with valproate: results from a three months observational prospective cohort study. *Microb. Pathog.* 162, 105340. doi:10.1016/j.micpath.2021.105340

Gribble, F. M., and Reimann, F. (2019). Function and mechanisms of enteroendocrine cells and gut hormones in metabolism. *Nat. Rev. Endocrinol.* 15, 226–237. doi:10.1038/s41574-019-0168-8

Gudan, A., Skonieczna-Żydecka, K., Palma, J., Drozd, A., and Stachowska, E. (2022). Effects of dietary components on intestinal short-chain fatty acids (SCFAs) synthesis in healthy adult persons following a ketogenic diet. *Rocz. Panstw Zakl. Hig.* 73, 51–69. doi:10.32394/rpzh.2022.0196

Guzel, O., Uysal, U., and Arslan, N. (2019). Efficacy and tolerability of olive oil-based ketogenic diet in children with drug-resistant epilepsy: a single center experience from Turkey. *Eur. J. Paediatr. Neurology* 23, 143–151. doi:10.1016/j.ejpn.2018.11.007

Hara, T., Mihara, T., Ishibashi, M., Kumagai, T., and Joh, T. (2018). Heat-killed Lactobacillus casei subsp. casei 327 promotes colonic serotonin synthesis in mice. *J. Funct. Foods* 47, 585–589. doi:10.1016/j.jff.2018.05.050

Hartman, A. L. (2008). Does the effectiveness of the ketogenic diet in different epilepsies yield insights into its mechanism? *Epilepsia* 49, 53–56. doi:10.1111/j.1528-1167.2008.01835.x

Hartman, A. L., Zheng, X., Bergbower, E., Kennedy, M., and Hardwick, J. M. (2010). Seizure tests distinguish intermittent fasting from the ketogenic diet. *Epilepsia* 51, 1395–1402. doi:10.1111/j.1528-1167.2010.02577.x

He, Z., Cui, B. T., Zhang, T., Li, P., Long, C. Y., Ji, G. Z., et al. (2017). Fecal microbiota transplantation cured epilepsy in a case with Crohn's disease: the first report. *World J. Gastroenterol.* 23, 3565–3568. doi:10.3748/wjg.v23.i19.3565

Holmes, M., Flaminio, Z., Vardhan, M., Xu, F., Li, X., Devinsky, O., et al. (2020). Cross talk between drug-resistant epilepsy and the gut microbiome. *Epilepsia* 61, 2619–2628. doi:10.1111/epi.16744

Hu, A., Yuan, H., Qin, Y., Zhu, Y., Zhang, L., Chen, Q., et al. (2022). Lipopolysaccharide (LPS) increases susceptibility to epilepsy via interleukin-1 type 1 receptor signaling. *Brain Res.* 1793, 148052. doi:10.1016/j.brainres.2022.148052

Huang, C., Chu, C., Peng, Y., Zhang, N., Yang, Z., You, J., et al. (2022). Correlations between gastrointestinal and oral microbiota in children with cerebral palsy and epilepsy. *Front. Pediatr.* 10, 988601. doi:10.3389/fped.2022.988601

Huang, C., Li, X., Wu, L., Wu, G., Wang, P., Peng, Y., et al. (2021). The effect of different dietary structure on gastrointestinal dysfunction in children with cerebral palsy and epilepsy based on gut microbiota. *Brain Dev.* 43, 192–199. doi:10.1016/j.braindev.2020.09.013

Huang, C., Li, Y., Feng, X., Li, D., Li, X., Ouyang, Q., et al. (2019). Distinct gut microbiota composition and functional category in children with cerebral palsy and epilepsy. *Front. Pediatr.* 7, 394. doi:10.3389/fped.2019.00394

Huang, T. S., Lu, X. G., Li, B., Chen, Y., Wen, J. L., Hu, Y., et al. (2010). Benign infantile convulsions with mild gastroenteritis: clinical analysis of 40 cases. *Zhongguo Dang Dai Er Ke Za Zhi* 12, 533–535.

Huber, S., Gagliani, N., Esplugues, E., O'Connor, W., Jr., Huber, F. J., Chaudhry, A., et al. (2011). Th17 cells express interleukin-10 receptor and are controlled by Foxp3^{-} and Foxp3+ regulatory CD4+ T cells in an interleukin-10-dependent manner. *Immunity* 34, 554–565. doi:10.1016/j.immuni.2011.01.020

Iannone, L. F., Gómez-Eguílaz, M., and De Caro, C. (2022). Gut microbiota manipulation as an epilepsy treatment. *Neurobiol. Dis.* 174, 105897. doi:10.1016/j.nbd.2022.105897

Ilhan, Z. E., Brochard, V., Lapaque, N., Auvin, S., and Lepage, P. (2022). Exposure to anti-seizure medications impact growth of gut bacterial species and subsequent host response. *Neurobiol. Dis.* 167, 105664. doi:10.1016/j.nbd.2022.105664

Işıkay, S., and Kocamaz, H. (2014). Prevalence of celiac disease in children with idiopathic epilepsy in southeast Turkey. *Pediatr. Neurol.* 50, 479–481. doi:10.1016/j.pediatrneurol.2014.01.021

Ivanov, I. I., Frutos Rde, L., Manel, N., Yoshinaga, K., Rifkin, D. B., Sartor, R. B., et al. (2008). Specific microbiota direct the differentiation of IL-17-producing T-helper cells

in the mucosa of the small intestine. *Cell Host Microbe* 4, 337–349. doi:10.1016/j.chom.2008.09.009

Jahromi, S. R., Togha, M., Fesharaki, S. H., Najafi, M., Moghadam, N. B., Kheradmand, J. A., et al. (2011). Gastrointestinal adverse effects of antiepileptic drugs in intractable epileptic patients. *Seizure* 20, 343–346. doi:10.1016/j.seizure.2010.12.011

Kaelberer, M. M., Buchanan, K. L., Klein, M. E., Barth, B. B., Montoya, M. M., Shen, X., et al. (2018). A gut-brain neural circuit for nutrient sensory transduction. *Science* 361, eaat5236. doi:10.1126/science.aat5236

Kawamura, Y., Nakayama, A., Kato, T., Miura, H., Ishihara, N., Ihira, M., et al. (2015). Pathogenic role of human herpesvirus 6B infection in mesial temporal lobe epilepsy. *J. Infect. Dis.* 212, 1014–1021. doi:10.1093/infdis/jiv160

Keezer, M. R., Sisodiya, S. M., and Sander, J. W. (2016). Comorbidities of epilepsy: current concepts and future perspectives. *Lancet Neurol.* 15, 106–115. doi:10.1016/S1474-4422(15)00225-2

Keightley, P. C., Koloski, N. A., and Talley, N. J. (2015). Pathways in gut–brain communication: evidence for distinct gut-to-brain and brain-to-gut syndromes. *Aust. N. Z. J. Psychiatry* 49, 207–214. doi:10.1177/0004867415569801

Khlevner, J., Park, Y., and Margolis, K. G. (2018). Brain-gut Axis: clinical implications. *Gastroenterol. Clin. North Am.* 47, 727–739. doi:10.1016/j.gtc.2018.07.002

Kilinc, E., Ankarali, S., Ayhan, D., Ankarali, H., Torun, I. E., and Cetinkaya, A. (2021). Protective effects of long-term probiotic mixture supplementation against pentylenetetrazole-induced seizures, inflammation and oxidative stress in rats. *J. Nutr. Biochem.* 98, 108830. doi:10.1016/j.jnutbio.2021.108830

Kołosowska, K., Maciejak, P., Szyndler, J., Turzyńska, D., Sobolewska, A., and Płaźnik, A. (2014). The role of interleukin-1β in the pentylenetetrazole-induced kindling of seizures, in the rat hippocampus. *Eur. J. Pharmacol.* 731, 31–37. doi:10.1016/j.ejphar.2014.03.008

Kossoff, E. H., and Doward, J. L. (2008). The modified atkins diet. *Epilepsia* 49, 37–41. doi:10.1111/j.1528-1167.2008.01831.x

Kristev, A., Sirakov, V., Kostadinova, I., and Lukanov, J. (1994). The ethosuximide-induced hyperpolarization of smooth muscle tissues--a cause of functional changes in the gastrointestinal tract of rats--is provoked by CA(2+)-dependent K(+)-efflux. *Folia Med. Plovdiv.* 36, 13–22.

Kshirsagar, V. Y., Nagarsenkar, S., Ahmed, M., Colaco, S., and Wingkar, K. C. (2012). Abdominal epilepsy in chronic recurrent abdominal pain. *J. Pediatr. Neurosci.* 7, 163–166. doi:10.4103/1817-1745.106468

Kundu, S., Nayak, S., Rakshit, D., Singh, T., Shukla, R., Khatri, D. K., et al. (2023). The microbiome-gut-brain axis in epilepsy: pharmacotherapeutic target from bench evidence for potential bedside applications. *Eur. J. Neurol.* 30, 3557–3567. doi:10.1111/ene.15767

Kuwahara, A., Matsuda, K., Kuwahara, Y., Asano, S., Inui, T., and Marunaka, Y. (2020). Microbiota-gut-brain axis: enteroendocrine cells and the enteric nervous system form an interface between the microbiota and the central nervous system. *Biomed. Res.* 41, 199–216. doi:10.2220/biomedres.41.199

Laman, J. D., 't Hart, B. A., Power, C., and Dziarski, R. (2020). Bacterial peptidoglycan as a driver of chronic brain inflammation. *Trends Mol. Med.* 26, 670–682. doi:10.1016/j.molmed.2019.11.006

Leblhuber, F., Geisler, S., Steiner, K., Fuchs, D., and Schütz, B. (2015). Elevated fecal calprotectin in patients with Alzheimer's dementia indicates leaky gut. *J. Neural Transm. (Vienna)* 122, 1319–1322. doi:10.1007/s00702-015-1381-9

Lee, H., Lee, S., Lee, D. H., and Kim, D. W. (2021). A comparison of the gut microbiota among adult patients with drug-responsive and drug-resistant epilepsy: an exploratory study. *Epilepsy Res.* 172, 106601. doi:10.1016/j.eplepsyres.2021.106601

Lee, K., Kim, N., Shim, J. O., and Kim, G. H. (2020). Gut bacterial dysbiosis in children with intractable epilepsy. *J. Clin. Med.* 10, 5. doi:10.3390/jcm10010005

Lee, N., and Kim, W. U. (2017). Microbiota in T-cell homeostasis and inflammatory diseases. *Exp. Mol. Med.* 49, e340. doi:10.1038/emm.2017.36

Leen, W. G., Klepper, J., Verbeek, M. M., Leferink, M., Hofste, T., van Engelen, B. G., et al. (2010). Glucose transporter-1 deficiency syndrome: the expanding clinical and genetic spectrum of a treatable disorder. *Brain* 133, 655–670. doi:10.1093/brain/awp336

Lefevre, F., and Aronson, N. (2000). Ketogenic diet for the treatment of refractory epilepsy in children: a systematic review of efficacy. *Pediatrics* 105, E46. doi:10.1542/peds.105.4.e46

Leibovitch, E. C., and Jacobson, S. (2015). Human herpesvirus 6 as a viral trigger in mesial temporal lobe epilepsy. *J. Infect. Dis.* 212, 1011–1013. doi:10.1093/infdis/jiv162

Lemos, V. R., Aires, R., Côco, L. Z., Domingues, R. B., Meyrelles, S. S., Vasquez, E. C., et al. (2022). Benefits of multi-day supplementation with probiotic kefir in Rasmussen encephalitis: the first case report. *Nutr. Neurosci.* 25, 2390–2397. doi:10.1080/1028415X.2021.1970299

Leo, A., Nesci, V., Tallarico, M., Amodio, N., Gallo Cantafio, E. M., De Sarro, G., et al. (2020). IL-6 receptor blockade by tocilizumab has anti-absence and anti-epileptogenic effects in the WAG/rij rat model of absence epilepsy. *Neurotherapeutics* 17, 2004–2014. doi:10.1007/s13311-020-00893-8

Li, D., Bai, X., Jiang, Y., and Cheng, Y. (2021a). Butyrate alleviates PTZ-induced mitochondrial dysfunction, oxidative stress and neuron apoptosis in mice via Keap1/Nrf2/HO-1 pathway. *Brain Res. Bull.* 168, 25–35. doi:10.1016/j.brainresbull.2020.12.009

Li, X., Wang, Q., Wu, D., Zhang, D. W., Li, S. C., Zhang, S. W., et al. (2022). The effect of a novel anticonvulsant chemical Q808 on gut microbiota and hippocampus neurotransmitters in pentylenetetrazole-induced seizures in rats. *BMC Neurosci.* 23, 7. doi:10.1186/s12868-022-00690-3

Li, Y., Yang, X., Zhang, J., Jiang, T., Zhang, Z., Wang, Z., et al. (2021b). Ketogenic diets induced glucose intolerance and lipid accumulation in mice with alterations in gut microbiota and metabolites. *mBio* 12, e03601–e03620. doi:10.1128/mBio.03601-20

Liang, L., Zhou, H., Zhang, S., Yuan, J., and Wu, H. (2017). Effects of gut microbiota disturbance induced in early life on the expression of extrasynaptic GABA-A receptor α5 and δ subunits in the hippocampus of adult rats. *Brain Res. Bull.* 135, 113–119. doi:10.1016/j.brainresbull.2017.09.014

Liebregts, T., Adam, B., Bredack, C., Röth, A., Heinzel, S., Lester, S., et al. (2007). Immune activation in patients with irritable bowel syndrome. *Gastroenterology* 132, 913–920. doi:10.1053/j.gastro.2007.01.046

Liesz, A., Suri-Payer, E., Veltkamp, C., Doerr, H., Sommer, C., Rivest, S., et al. (2009). Regulatory T cells are key cerebroprotective immunomodulators in acute experimental stroke. *Nat. Med.* 15, 192–199. doi:10.1038/nm.1927

Lin, P., Lin, A., Tao, K., Yang, M., Ye, Q., Chen, H., et al. (2021). Intestinal *Klebsiella pneumoniae* infection enhances susceptibility to epileptic seizure which can be reduced by microglia activation. *Cell Death Discov.* 7, 175. doi:10.1038/s41420-021-00559-0

Lindefeldt, M., Eng, A., Darban, H., Bjerkner, A., Zetterström, C. K., Allander, T., et al. (2019). The ketogenic diet influences taxonomic and functional composition of the gut microbiota in children with severe epilepsy. *NPJ Biofilms Microbiomes* 5, 5. doi:10.1038/s41522-018-0073-2

Liu, T., Jia, F., Guo, Y., Wang, Q., Zhang, X., Chang, F., et al. (2023). Altered intestinal microbiota composition with epilepsy and concomitant diarrhea and potential indicator biomarkers in infants. *Front. Microbiol.* 13, 1081591. doi:10.3389/fmicb.2022.1081591

Lu, Y., Zhang, Z., Tong, L., Zhou, X., Liang, X., Yi, H., et al. (2021). Mechanisms underlying the promotion of 5-hydroxytryptamine secretion in enterochromaffin cells of constipation mice by Bifidobacterium and Lactobacillus. *Neurogastroenterol. Motil.* 33, e14082. doi:10.1111/nmo.14082

Luckheeram, R. V., Zhou, R., Verma, A. D., and Xia, B. (2012). CD4⁺T cells: differentiation and functions. *Clin. Dev. Immunol.* 2012, 925135. doi:10.1155/2012/925135

Lv, R., Xu, X., Luo, Z., Shen, N., Wang, F., and Zhao, Y. (2014). Pyrrolidine dithiocarbamate (PDTC) inhibits the overexpression of MCP-1 and attenuates microglial activation in the hippocampus of a pilocarpine-induced status epilepticus rat model. *Exp. Ther. Med.* 7, 39–45. doi:10.3892/etm.2013.1397

Magon, P. (2010). Abdominal epilepsy misdiagnosed as peptic ulcer pain. *Indian J. Pediatr.* 77, 916. doi:10.1007/s12098-010-0141-y

Mandic, A. D., Woting, A., Jaenicke, T., Sander, A., Sabrowski, W., Rolle-Kampcyk, U., et al. (2019). Clostridium ramosum regulates enterochromaffin cell development and serotonin release. *Sci. Rep.* 9, 1177. doi:10.1038/s41598-018-38018-z

Manral, M., Dwivedi, R., Gulati, S., Kaur, K., Nehra, A., Pandey, R. M., et al. (2023). Safety, efficacy, and tolerability of modified atkins diet in persons with drug-resistant epilepsy: a randomized controlled trial. *Neurology* 100, e1376–e1385. doi:10.1212/WNL.0000000000206776

Mao, L. Y., Ding, J., Peng, W. F., Ma, Y., Zhang, Y. H., Fan, W., et al. (2013). Interictal interleukin-17A levels are elevated and correlate with seizure severity of epilepsy patients. *Epilepsia* 54, e142–e145. doi:10.1111/epi.12337

Mayer, E. A. (2011). Gut feelings: the emerging biology of gut-brain communication. *Nat. Rev. Neurosci.* 12, 453–466. doi:10.1038/nrn3071

Mayer, E. A., Labus, J. S., Tillisch, K., Cole, S. W., and Baldi, P. (2015). Towards a systems view of IBS. *Nat. Rev. Gastroenterol. Hepatol.* 12, 592–605. doi:10.1038/nrgastro.2015.121

McDonald, T. J. W., Henry-Barron, B. J., Felton, E. A., Gutierrez, E. G., Barnett, J., Fisher, R., et al. (2018). Improving compliance in adults with epilepsy on a modified Atkins diet: a randomized trial. *Seizure* 60, 132–138. doi:10.1016/j.seizure.2018.06.019

Medel-Matus, J. S., Lagishetty, V., Santana-Gomez, C., Shin, D., Mowrey, W., Staba, R. J., et al. (2022). Susceptibility to epilepsy after traumatic brain injury is associated with preexistent gut microbiome profile. *Epilepsia* 63, 1835–1848. doi:10.1111/epi.17248

Medel-Matus, J. S., Shin, D., Dorfman, E., Sankar, R., and Mazarati, A. (2018). Facilitation of kindling epileptogenesis by chronic stress may be mediated by intestinal microbiome. *Epilepsia Open* 3, 290–294. doi:10.1002/epi4.12114

Mengoni, F., Salari, V., Kosenkova, I., Tsenov, G., Donadelli, M., Malerba, G., et al. (2021). Gut microbiota modulates seizure susceptibility. *Epilepsia* 62, e153–e157. doi:10.1111/epi.17009

Miljanovic, N., and Potschka, H. (2021). The impact of Scn1a deficiency and ketogenic diet on the intestinal microbiome: a study in a genetic Dravet mouse model. *Epilepsy Res.* 178, 106826. doi:10.1016/j.eplepsyres.2021.106826

Minton, G. C., Miller, A. D., Bookstaver, P. B., and Love, B. L. (2011). Topiramate: safety and efficacy of its use in the prevention and treatment of migraine. *J. Cent. Nerv. Syst. Dis.* 3, 155–168. doi:10.4137/JCNSD.S4365

Mittal, S., Farmer, J. P., Rosenblatt, B., Andermann, F., Montes, J. L., and Villemure, J. G. (2001). Intractable epilepsy after a functional hemispherectomy: important lessons from an unusual case. Case report. *J. Neurosurg.* 94, 510–514. doi:10.3171/jns.2001.94.3.0510

Mu, C., Nikpoor, N., Tompkins, T. A., Choudhary, A., Wang, M., Marks, W. N., et al. (2022a). Targeted gut microbiota manipulation attenuates seizures in a model of infantile spasms syndrome. *JCI Insight* 7, e158521. doi:10.1172/jci.insight.158521

Mu, C., Tompkins, T. A., Rho, J. M., Scantlebury, M. H., and Shearer, J. (2022b). Gut based manipulations spur hippocampal mitochondrial bioenergetics in a model of pediatric epilepsy. *Biochim. Biophys. Acta Mol. Basis Dis.* 1868, 166446. doi:10.1016/j.bbadis.2022.166446

Mu, X., Zhang, X., Gao, H., Gao, L., Li, Q., and Zhao, C. (2022). Crosstalk between peripheral and the brain-resident immune components in epilepsy. *J. Integr. Neurosci.* 21, 9. doi:10.31083/j.jin2101009

Mulak, A., Budrewicz, S., Panek-Jeziorna, M., Koszewicz, M., Jasinska, M., Marczak-Karpina, B., et al. (2017). Fecal biomarkers of gut inflammation and intestinal barrier dysfunction in Parkinson's disease. *Gastroenterology* 152, S924. doi:10.1016/s0016-5085(17)33152-9

Muñana, K. R., Jacob, M. E., and Callahan, B. J. (2020). Evaluation of fecal Lactobacillus populations in dogs with idiopathic epilepsy: a pilot study. *Anim. Microbiome* 2, 19. doi:10.1186/s42523-020-00036-6

Neal, E. G., Chaffe, H., Schwartz, R. H., Lawson, M. S., Edwards, N., Fitzsimmons, G., et al. (2008). The ketogenic diet for the treatment of childhood epilepsy: a randomised controlled trial. *Lancet Neurol.* 7, 500–506. doi:10.1016/S1474-4422(08)70092-9

Nevitt, S. J., Sudell, M., Cividini, S., Marson, A. G., and Tudur Smith, C. (2022). Antiepileptic drug monotherapy for epilepsy: a network meta-analysis of individual participant data. *Cochrane Database Syst. Rev.* 4, CD011412. doi:10.1002/14651858.CD011412.pub4

Nørgaard, M., Ehrenstein, V., Nielsen, R. B., Bakketeig, L. S., and Sørensen, H. T. (2012). Maternal use of antibiotics, hospitalisation for infection during pregnancy, and risk of childhood epilepsy:a populationbased cohort study. *PLoS One* 7, e30850. doi:10.1371/journal.pone.0030850

Ochoa-Reparaz, J., Mielcarz, D. W., Ditrio, L. E., Burroughs, A. R., Begum-Haque, S., Dasgupta, S., et al. (2010). Central nervous system demyelinating disease protection by the human commensal Bacteroides fragilis depends on polysaccharide A expression. *J. Immunol.* 185, 4101–4108. doi:10.4049/jimmunol.1001443

Oliveira, M. E. T., Paulino, G. V. B., Dos Santos Júnior, E. D., da Silva Oliveira, F. A., Melo, V. M. M., Ursulino, J. S., et al. (2022). Multi-omic analysis of the gut microbiome in rats with lithium-pilocarpine-induced temporal lobe epilepsy. *Mol. Neurobiol.* 59, 6429–6446. doi:10.1007/s12035-022-02984-3

Olson, C. A., Vuong, H. E., Yano, J. M., Liang, Q. Y., Nusbaum, D. J., and Hsiao, E. Y. (2018). The gut microbiota mediates the anti-seizure effects of the ketogenic diet. *Cell* 173, 1728–1741. doi:10.1016/j.cell.2018.04.027

O'Mahony, S. M., Clarke, G., Borre, Y. E., Dinan, T. G., and Cryan, J. F. (2015). Serotonin, tryptophan metabolism and the brain-gut-microbiome axis. *Behav. Brain Res.* 277, 32–48. doi:10.1016/j.bbr.2014.07.027

Ott, B. R. (1991). Bulimia in a patient with temporal lobe epilepsy. *J. Neurol. Neurosurg. Psychiatry* 54, 1020–1021. doi:10.1136/jnnp.54.11.1020

Ouyang, Y., Chen, Y., Wang, G., Song, Y., Zhao, H., Xiao, B., et al. (2022). Genetically proxied gut microbiota, gut metabolites with risk of epilepsy and the subtypes: a bi-directional Mendelian randomization study. *Front. Mol. Neurosci.* 15, 994270. doi:10.3389/fnmol.2022.994270

Özcan, E., Lum, G. R., and Hsiao, E. Y. (2022). Interactions between the gut microbiome and ketogenic diet in refractory epilepsy. *Int. Rev. Neurobiol.* 167, 217–249. doi:10.1016/bs.irn.2022.06.002

Özoğul, F. (2004). Production of biogenic amines by *Morganella morganii*, *Klebsiella pneumoniae* and Hafnia alvei using a rapid HPLC method. *Eur. Food Res. Technol.* 219, 465–469. doi:10.1007/s00217-004-0988-0

Özoğul, F. K. E., Özoğul, Y., Özoğul, I., and Özoğul, İ. (2012). The function of lactic acid bacteria on biogenic amines production by food-borne pathogens in arginine decarboxylase broth. *Food Sci. Technol. Res.* 18, 795–804. doi:10.3136/fstr.18.795

Park, A. J., Collins, J., Blennerhassett, P. A., Ghia, J. E., Verdu, E. F., Bercik, P., et al. (2013). Altered colonic function and microbiota profile in a mouse model of chronic depression. *Neurogastroenterol. Motil.* 25, 733–e575. doi:10.1111/nmo.12153

Patel, D. C., Wallis, G., Dahle, E. J., McElroy, P. B., Thomson, K. E., Tesi, R. J., et al. (2017). Hippocampal TNFα signaling contributes to seizure generation in an infection-induced mouse model of limbic epilepsy. *eNeuro* 4, 0105–0117. doi:10.1523/ENEURO.0105-17.2017

Peng, A., Qiu, X., Lai, W., Li, W., Zhang, L., Zhu, X., et al. (2018). Altered composition of the gut microbiome in patients with drug-resistant epilepsy. *Epilepsy Re.* 147, 102–107. doi:10.1016/j.eplepsyres.2018.09.013

Peng, Y., Chiu, A. T. G., Li, V. W. Y., Zhang, X., Yeung, W. L., Chan, S. H. S., et al. (2023). The role of the gut-microbiome-brain axis in metabolic remodeling amongst children with cerebral palsy and epilepsy. *Front. Neurol.* 14, 1109469. doi:10.3389/fneur.2023.1109469

Pfeifer, H. H., Lyczkowski, D. A., and Thiele, E. A. (2008). Low glycemic index treatment: implementation and new insights into efficacy. *Epilepsia* 40, 33–36.

Pittman, Q. J. (2020). A gut feeling about the ketogenic diet in epilepsy. *Epilepsy Res.* 166, 106409. doi:10.1016/j.eplepsyres.2020.106409

Pratesi, R., Modelli, I. C., Martins, R. C., Almeida, P. L., and Gandolfi, L. (2003). Celiac disease and epilepsy: favorable outcome in a child with difficult to control seizures. *Acta Neurol. Scand.* 108, 290–293. doi:10.1034/j.1600-0404.2003.00082.x

Qian, Y., Lv, P. C., Shi, L., Fang, R. Q., Song, Z. C., and Zhu, H. L. (2009). Synthesis, antimicrobial activity of lamotrigine and its ammonium derivatives. *J. Chem. Sci.* 121, 463–470. doi:10.1007/s12039-009-0055-2

Quigley, E. M. M. (2017). Microbiota-brain-gut Axis and neurodegenerative diseases. *Curr. Neurol. Neurosci. Rep.* 17, 94. doi:10.1007/s11910-017-0802-6

Rahman, M. T., Ghosh, C., Hossain, M., Linfield, D., Rezaee, F., Janigro, D., et al. (2018). IFN-γ, IL-17A, or zonulin rapidly increase the permeability of the blood-brain and small intestinal epithelial barriers: relevance for neuro-inflammatory diseases. *Biochem. Biophys. Res. Commun.* 507, 274–279. doi:10.1016/j.bbrc.2018.11.021

Reddy, D. S., and Rogawski, M. A. (2002). Stress-induced deoxycorticosteronederived neurosteroids modulate GABA(A)receptor function and seizure susceptibility. *J. Neurosci.* 22, 3795–3805. doi:10.1523/JNEUROSCI.22-09-03795.2002

Reinisch, W. (2017). Fecal microbiota transplantation in inflammatory bowel disease. *Dig. Dis.* 35, 123–126. doi:10.1159/000449092

Remick, R. A., Jones, M. W., and Campos, P. E. (1980). Postictal bulimia. *J. Clin. Psychiatry* 41, 256.

Ressler, K. J., and Mayberg, H. S. (2007). Targeting abnormal neural circuits in mood and anxiety disorders: from the laboratory to the clinic. *Nat. Neurosci.* 10, 1116–1124. doi:10.1038/nn1944

Riazi, K., Galic, M. A., Kuzmiski, J. B., Ho, W., Sharkey, K. A., and Pittman, Q. J. (2008). Microglial activation and TNFalpha production mediate altered CNS excitability following peripheral inflammation. *Proc. Natl. Acad. Sci. U. S. A.* 105, 17151–17156. doi:10.1073/pnas.0806682105

Rothhammer, V., Borucki, D. M., Tjon, E. C., Takenaka, M. C., Chao, C. C., Ardura-Fabregat, A., et al. (2018). Microglial control of astrocytes in response to microbial metabolites. *Nature* 557, 724–728. doi:10.1038/s41586-018-0119-x

Rothhammer, V., Mascanfroni, I. D., Bunse, L., Takenaka, M. C., Kenison, J. E., Mayo, L., et al. (2016). Type I interferons and microbial metabolites of tryptophan modulate astrocyte activity and central nervous system inflammation via the aryl hydrocarbon receptor. *Nat. Med.* 22, 586–597. doi:10.1038/nm.4106

Russo, E. (2022). The gut microbiota as a biomarker in epilepsy. *Neurobiol. Dis.* 163, 105598. doi:10.1016/j.nbd.2021.105598

Russo, E., Andreozzi, F., Iuliano, R., Dattilo, V., Procopio, T., Fiume, G., et al. (2014). Early molecular and behavioral response to lipopolysaccharide in the WAG/Rij rat model of absence epilepsy and depressive-like behavior, involves interplay between AMPK, AKT/mTOR pathways and neuroinflammatory cytokine release. *Brain Behav. Immun.* 42, 157–168. doi:10.1016/j.bbi.2014.06.016

Sabouri, S., Kangi, S., Najimi, S., and Rahimi, H. R. (2021). Effects of probiotics on pentylenetetrazol-induced convulsions in mice. *Epilepsy Res.* 176, 106723. doi:10.1016/j.eplepsyres.2021.106723

Şafak, B., Altunan, B., Topçu, B., and Eren Topkaya, A. (2020). The gut microbiome in epilepsy. *Microb. Pathog.* 139, 103853. doi:10.1016/j.micpath.2019.103853

Samala, R., Willis, S., and Borges, K. (2008). Anticonvulsant profile of a balanced ketogenic diet in acute mouse seizure models. *Epilepsy Res.* 81, 119–127. doi:10.1016/j.eplepsyres.2008.05.001

Sampson, T. R., Debelius, J. W., Thron, T., Janssen, S., Shastri, G. G., Ilhan, Z. E., et al. (2016). Gut microbiota regulate motor deficits and neuroinflammation in a model of Parkinson's disease. *Cell* 167, 1469–1480. doi:10.1016/j.cell.2016.11.018

Schmitt, J. J., and Ebner, A. (2000). Anatomic substrate of epigastric aura: case report. *Nervenarzt* 71, 485–488. doi:10.1007/s001150050612

Sewal, R. K., Modi, M., Saikia, U. N., Chakrabarti, A., and Medhi, B. (2017). Increase in seizure susceptibility in sepsis like condition explained by spiking cytokines and altered adhesion molecules level with impaired blood brain barrier integrity in experimental model of rats treated with lipopolysaccharides. *Epilepsy Res.* 135, 176–186. doi:10.1016/j.eplepsyres.2017.05.012

Sgritta, M., Dooling, S. W., Buffington, S. A., Momin, E. N., Francis, M. B., Britton, R. A., et al. (2019). Mechanisms underlying microbialmediated changes in social behavior in mouse models of autism spectrum disorder. *Neuron* 101, 246–259. doi:10.1016/j.neuron.2018.11.018

Shearer, J., Scantlebury, M. H., Rho, J. M., Tompkins, T. A., and Mu, C. (2023). Intermittent vs continuous ketogenic diet: impact on seizures, gut microbiota, and mitochondrial metabolism. *Epilepsia* 64, e177–e183. doi:10.1111/epi.17688

Shishov, V. A., Kirovskaia, T. A., Kudrin, V. S., and Oleskin, A. V. (2009). Amine neuromediators, their precursors, and oxidation products in the culture of *Escherichia coli* K-12. *Prikl. Biokhim Mikrobiol.* 45, 550–554.

Singh, T., and Goel, R. K. (2016). Evidence in support of using a neurochemistry approach to identify therapy for both epilepsy and associated depression. *Epilepsy Behav.* 61, 248–257. doi:10.1016/j.yebeh.2016.05.005

Spinelli, E., and Blackford, R. (2018). Gut microbiota, the ketogenic diet and epilepsy. *Pediatr. Neurol. Briefs* 32, 10. doi:10.15844/pedneurbriefs-32-10

Steinert, R. E., Feinle-Bisset, C., Asarian, L., Horowitz, M., Beglinger, C., and Geary, N. (2017). Ghrelin, CCK, GLP-1, and PYY(3-36): secretory controls and physiological roles in eating and glycemia in health, obesity, and after RYGB. *Physiol. Rev.* 97, 411–463. doi:10.1152/physrev.00031.2014

Stengel, A., and Tache, Y. (2010). Corticotropin-releasing factor signaling and visceral response to stress. *Exp. Biol. Med.* 235, 1168–1178. doi:10.1258/ebm.2010.009347

Strandwitz, P. (2018). Neurotransmitter modulation by the gut microbiota. *Brain Res.* 1693, 128–133. doi:10.1016/j.brainres.2018.03.015

Sudo, N., Chida, Y., Aiba, Y., Sonoda, J., Oyama, N., Yu, X. N., et al. (2004). Postnatal microbial colonization programs the hypothalamic-pituitary-adrenal system for stress response in mice. *J. Physiol.* 558, 263–275. doi:10.1113/jphysiol.2004.063388

Sun, Y., Su, Y., and Zhu, W. (2016). Microbiome-metabolome responses in the cecum and colon of pig to a high resistant starch diet. *Front. Microbiol.* 7, 779. doi:10.3389/fmicb.2016.00779

Surawicz, C. M., Brandt, L. J., Binion, D. G., Ananthakrishnan, A. N., Curry, S. R., Gilligan, P. H., et al. (2013). Guidelines for diagnosis, treatment, and prevention of *Clostridium difficile* infections. *Am. J. Gastroenterol.* 108, 478–498. doi:10.1038/ajg.2013.4

Swartwood, S., Wilkes, J., Bonkowsky, J. L., and Trandafir, C. C. (2021). Celiac disease in children: an association with drug-resistant epilepsy. *Pediatr. Neurol.* 120, 12–17. doi:10.1016/j.pediatrneurol.2021.03.003

Tahmasebi, S., Oryan, S., Mohajerani, H. R., Akbari, N., and Palizvan, M. R. (2020). Probiotics and Nigella sativa extract supplementation improved behavioral and electrophysiological effects of PTZ-induced chemical kindling in rats. *Epilepsy Behav.* 104, 106897. doi:10.1016/j.yebeh.2019.106897

Tang, F., Hartz, A. M. S., and Bauer, B. (2017). Drug-resistant epilepsy: multiple hypotheses, few answers. *Front. Neurol.* 8, 301. doi:10.3389/fneur.2017.00301

Tang, Y., Wang, Q., and Liu, J. (2021). Microbiota-gut-brain axis: a novel potential target of ketogenic diet for epilepsy. *Curr. Opin. Pharmacol.* 61, 36–41. doi:10.1016/j.coph.2021.08.018

Thijs, R. D., Surges, R., O'Brien, T. J., and Sander, J. W. (2019). Epilepsy in adults. *Lancet* 393, 689–701. doi:10.1016/S0140-6736(18)32596-0

Tsavkelova, E. A., Botvinko, I. V., Kudrin, V. S., and Oleskin, A. V. (2000). Detection of neurotransmitter amines in microorganisms with the use of high-performance liquid chromatography. *Dokl. Biochem.* 372, 115–117.

Türay, S., Cangür, Ş., Kahraman, G., Kayabaşı, E., Çetiner, Ö. F., Aydın, B., et al. (2023). Can the gut microbiota serve as a guide to the diagnosis and treatment of childhood epilepsy? *Pediatr. Neurol.* 145, 11–21. doi:10.1016/j.pediatrneurol.2023.04.006

Ułamek-Kozioł, M., Czuczwar, S. J., Januszewski, S., and Pluta, R. (2019). Ketogenic diet and epilepsy. *Nutrients* 11, 2510. doi:10.3390/nu11102510

Ulrich-Lai, Y. M., and Herman, J. P. (2009). Neural regulation of endocrine and autonomic stress responses. *Nat. Rev. Neurosci.* 10, 397–409. doi:10.1038/nrn2647

Van Oudenhove, L., Levy, R. L., Crowell, M. D., Drossman, D. A., Halpert, A. D., Keefer, L., et al. (2016). Biopsychosocial aspects of functional gastrointestinal disorders: how central and environmental processes contribute to the development and expression of functional gastrointestinal disorders. *Gastroenterology* 150, 1355–1367.e2. doi:10.1053/j.gastro.2016.02.027

Vezzani, A., Balosso, S., and Ravizza, T. (2019). Neuroinflammatory pathways as treatment targets and biomarkers in epilepsy. *Nat. Rev. Neurol.* 15, 459–472. doi:10.1038/s41582-019-0217-x

Vodička, M., Ergang, P., Hrnčíř, T., Mikulecká, A., Kvapilová, P., Vagnerová, K., et al. (2018). Microbiota affects the expression of genes involved in HPA axis regulation and local metabolism of glucocorticoids in chronic psychosocial stress. *Brain Behav. Immun.* 73, 615–624. doi:10.1016/j.bbi.2018.07.007

Vuong, H. E., and Hsiao, E. Y. (2017). Emerging roles for the gut microbiome in autism spectrum disorder. *Biol. Psychiatry* 81, 411–423. doi:10.1016/j.biopsych.2016.08.024

Vuong, H. E., Yano, J. M., Fung, T. C., and Hsiao, E. Y. (2017). The microbiome and host behavior. *Annu. Rev. Neurosci.* 40, 21–49. doi:10.1146/annurev-neuro-072116-031347

Walsham, N. E., and Sherwood, R. A. (2016). Fecal calprotectin in inflammatory bowel disease. *Clin. Exp. Gastroenterol.* 9, 21–29. doi:10.2147/CEG.S51902

Wang, C., Klechikov, A. G., Gharibyan, A. L., Wärmländer, S. K., Jarvet, J., Zhao, L., et al. (2014a). The role of pro-inflammatory S100A9 in Alzheimer's disease amyloid-neuroinflammatory cascade. *Acta Neuropathol.* 127, 507–522. doi:10.1007/s00401-013-1208-4

Wang, F. B., and Powley, T. L. (2007). Vagal innervation of intestines:afferent pathways mapped with new *en bloc* horseradish peroxidase adaptation. *Cell Tissue Res.* 329, 221–230. doi:10.1007/s00441-007-0413-7

Wang, X., Sun, G., Feng, T., Zhang, J., Huang, X., Wang, T., et al. (2019). Sodium oligomannate therapeutically remodels gut microbiota and suppresses gut bacterial amino acids-shaped neuroinflammation to inhibit Alzheimer's disease progression. *Cell Res.* 29, 787–803. doi:10.1038/s41422-019-0216-x

Wang, X., Yang, C., Yang, L., and Zhang, Y. (2022). Modulating the gut microbiota ameliorates spontaneous seizures and cognitive deficits in rats with kainic acid-induced status epilepticus by inhibiting inflammation and oxidative stress. *Front. Nutr.* 9, 985841. doi:10.3389/fnut.2022.985841

Wang, Y., Telesford, K. M., Ochoa-Repáraz, J., Haque-Begum, S., Christy, M., Kasper, E. J., et al. (2014b). An intestinal commensal symbiosis factor controls neuroinflammation via TLR2-mediated CD39 signalling. *Nat. Commun.* 5, 4432. doi:10.1038/ncomms5432

Wang, Y., Zhuo, Z., and Wang, H. (2023). Epilepsy, gut microbiota, and circadian rhythm. *Front. Neurol.* 14, 1157358. doi:10.3389/fneur.2023.1157358

Watkins, C., Murphy, K., Yen, S., Carafa, I., Dempsey, E. M., O'Shea, C. A., et al. (2017). Effects of therapeutic hypothermia on the gut microbiota and metabolome of infants suffering hypoxic-ischemic encephalopathy at birth. *Int. J. Biochem. Cell Biol.* 93, 110–118. doi:10.1016/j.biocel.2017.08.017

Weaver, C. T., Hatton, R. D., Mangan, P. R., and Harrington, L. E. (2007). IL-17 family cytokines and the expanding diversity of effector T cell lineages. *Annu. Rev. Immunol.* 25, 821–852. doi:10.1146/annurev.immunol.25.022106.141557

Wei, S., Mai, Y., Hu, L., Zheng, R., Zheng, D., Chen, W., et al. (2023). Altered gut microbiota in temporal lobe epilepsy with anxiety disorders. *Front. Microbiol.* 14, 1165787. doi:10.3389/fmicb.2023.1165787

Welcome, M. O. (2019). Gut microbiota disorder, gut epithelial and bloodbrain barrier dysfunctions in etiopathogenesis of dementia:molecular mechanisms and signaling pathways. *Neuromolecular Med.* 21, 205–226. doi:10.1007/s12017-019-08547-5

Weltens, N., Zhao, D., and Van Oudenhove, L. (2014). Where is the comfort in comfort foods? Mechanisms linking fat signaling, reward, and emotion. *Neurogastroenterol. Motil.* 26, 303–315. doi:10.1111/nmo.12309

Wenger, G. R., Stitzel, R. E., and Craig, C. R. (1973). The role of biogenic amines in the reserpine-induced alteration of minimal electroshock seizure thresholds in the mouse. *Neuropharmacology* 12, 693–703. doi:10.1016/0028-3908(73)90122-6

Werner, F. M., and Coveñas, R. (2017). Classical neurotransmitters and neuropeptides involved in generalized epilepsy in a multineurotransmitter system: how to improve the antiepileptic effect? *Epilepsy Behav.* 71, 124–129. doi:10.1016/j.yebeh.2015.01.038

Wheless, J. (2008). History of the ketogenic diet. *Epilepsia* 49, 3–5. doi:10.1111/j.1528-1167.2008.01821.x

Whitehead, W. E., Crowell, M. D., Robinson, J. C., Heller, B. R., and Schuster, M. M. (1992). Effects of stressful life events on bowel symptoms: subjects with irritable bowel syndrome compared with subjects without bowel dysfunction. *Gut* 33, 825–830. doi:10.1136/gut.33.6.825

Whitehead, W. E., Palsson, O., and Jones, K. R. (2002). Systematic review of the comorbidity of irritable bowel syndrome with other disorders: what are the causes and implications? *Gastroenterology* 122, 1140–1156. doi:10.1053/gast.2002.32392

Wiebe, S., Téllez-Zenteno, J. F., and Shapiro, M. (2008). An evidence-based approach to the first seizure. *Epilepsia* 49, 50–57. doi:10.1111/j.1528-1167.2008.01451.x

Wikoff, W. R., Anfora, A. T., Liu, J., Schultz, P. G., Lesley, S. A., Peters, E. C., et al. (2009). Metabolomics analysis reveals large effects of gut microflora on mammalian blood metabolites. *Proc. Natl. Acad. Sci. U. S. A.* 106, 3698–3703. doi:10.1073/pnas.0812874106

Williams, C., and Chryssanthopoulos, C. (1997). Pre-exercise food intake and performance. *World Rev. Nutr. Diet.* 82, 33–45. doi:10.1159/000059648

Winesett, S., Bessone, S., and Kossoff, E. (2015). The ketogenic diet in pharmacoresistant childhood epilepsy. *Expert Rev. Neurother.* 15, 621–628. doi:10.1586/14737175.2015.1044982

Wu, J., Zhang, Y., Yang, H., Rao, Y., Miao, J., and Lu, X. (2016). Intestinal microbiota as an alternative therapeutic target for epilepsy. *Can. J. Infect. Dis. Med. Microbiol.* 2016, 9032809. doi:10.1155/2016/9032809

Xi, Y., Li, H., Yu, M., Li, X., Li, Y., Hui, B., et al. (2022). Protective effects of chlorogenic acid on trimethyltin chloride-induced neurobehavioral dysfunctions in mice relying on the gut microbiota. *Food Funct.* 13, 1535–1550. doi:10.1039/d1fo03334d

Xie, G., Zhou, Q., Qiu, C. Z., Dai, W. K., Wang, H. P., Li, Y. H., et al. (2017). Ketogenic diet poses a significant effect on imbalanced gut microbiota in infants with refractory epilepsy. *World J. Gastroenterol.* 23, 6164–6171. doi:10.3748/wjg.v23.i33.6164

Yano, J. M., Yu, K., Donaldson, G. P., Shastri, G. G., Ann, P., Ma, L., et al. (2015). Indigenous bacteria from the gut microbiota regulate host serotonin biosynthesis. *Cell* 161, 264–276. doi:10.1016/j.cell.2015.02.047

Yeo, K. T., Lahra, M., Bajuk, B., Hilder, L., Abdel-Latif, M. E., Wright, I. M., et al. (2019). Long-term outcomes after group B streptococcus infection:a cohort study. *Arch. Dis. Child.* 104, 172–178. doi:10.1136/archdischild-2017-314642

Yeom, J. S., Park, J. S., Kim, Y. S., Kim, R. B., Choi, D. S., Chung, J. Y., et al. (2019). Neonatal seizures and white matter injury: role of rotavirus infection and probiotics. *Brain Dev.* 41, 19–28. doi:10.1016/j.braindev.2018.07.001

Yu, Y., Yang, W., Li, Y., and Cong, Y. (2020). Enteroendocrine cells: sensing gut microbiota and regulating inflammatory bowel diseases. *Inflamm. Bowel Dis.* 26, 11–20. doi:10.1093/ibd/izz217

Yue, Q., Cai, M., Xiao, B., Zhan, Q., and Zeng, C. (2021). A high-tryptophan diet reduces seizure-induced respiratory arrest and alters the gut microbiota in DBA/1 mice. *Front. Neurol.* 12, 762323. doi:10.3389/fneur.2021.762323

Yue, Q., Cai, M., Xiao, B., Zhan, Q., and Zeng, C. (2022). The microbiota-gut-brain Axis and epilepsy. *Cell Mol. Neurobiol.* 42, 439–453. doi:10.1007/s10571-021-01130-2

Zagorchev, P., Sirakov, V., Uchikov, A., and Sirakov, N. (1998). Ethosuximide inducted changes in the gastrointestinal tract. *Folia Med. Plovdiv.* 40, 28–33.

Zeng, X., Hu, K., Chen, L., Zhou, L., Luo, W., Li, C., et al. (2018). The effects of ginsenoside compound K against epilepsy by enhancing the γ-aminobutyric acid signaling pathway. *Front. Pharmacol.* 9, 1020. doi:10.3389/fphar.2018.01020

Zhang, Y., Zhao, M., Jiang, X., Qiao, Q., Liu, T., Zhao, C., et al. (2021). Comprehensive analysis of fecal microbiome and metabolomics in hepatic fibrosis rats reveal hepatoprotective effects of yinchen wuling powder from the host-microbial metabolic Axis. *Front. Pharmacol.* 12, 713197. doi:10.3389/fphar.2021.713197

Zhang, Y., Zhou, S., Zhou, Y., Yu, L., Zhang, L., and Wang, Y. (2018). Altered gut microbiome composition in children with refractory epilepsy after ketogenic diet. *Epilepsy Res.* 145, 163–168. doi:10.1016/j.eplepsyres.2018.06.015

Zhao, Y., Dua, P., and Lukiw, W. J. (2015). Microbial sources of amyloid and relevance to amyloidogenesis and Alzheimer's disease (AD). *J. Alzheimers Dis. Park.* 5, 177. doi:10.4172/2161-0460.1000177

Zhou, C., Gong, S., Xiang, S., Liang, L., Hu, X., Huang, R., et al. (2022). Changes and significance of gut microbiota in children with focal epilepsy before and after treatment. *Front. Cell Infect. Microbiol.* 12, 965471. doi:10.3389/fcimb.2022.965471

Zhu, D., Wang, M., Wang, J., Yuan, J., Niu, G., Zhang, G., et al. (2016). Ketogenic diet effects on neurobehavioral development of children with intractable epilepsy: a prospective study. *Epilepsy Behav.* 55, 87–91. doi:10.1016/j.yebeh.2015.12.011

Zhu, H., Li, Y., Yang, X., Chu, Y., Guo, W., Chen, R., et al. (2023). Demographics and clinical characteristics of patients with neurocysticercosis: a retrospective study from Dali, China. *Saudi J. Med. Med. Sci.* 11, 283–291. doi:10.4103/sjmms.sjmms_298_23

Zhu, H., Wang, W., and Li, Y. (2022). Molecular mechanism and regulation of autophagy and its potential role in epilepsy. *Cells* 11, 2621. doi:10.3390/cells11172621

Zhu, J., Yamane, H., and Paul, W. E. (2010). Differentiation of effector CD4 T cell populations. *Annu. Rev. Immunol.* 28, 445–489. doi:10.1146/annurev-immunol-030409-101212

Zimmermann, M., Zimmermann-Kogadeeva, M., Wegmann, R., and Goodman, A. L. (2019). Separating host and microbiome contributions to drug pharmacokinetics and toxicity. *Science* 363, eaat9931. doi:10.1126/science.aat9931

frontiers | Frontiers in Pharmacology

TYPE Original Research
PUBLISHED 28 March 2024
DOI 10.3389/fphar.2024.1340691

OPEN ACCESS

EDITED BY
Mahmoud Rafieian-Kopaei,
Shahrekord University of Medical Sciences, Iran

REVIEWED BY
Amin Mottahedin,
University of Oxford, United Kingdom
Govindaiah Vinukonda,
New York Medical College, United States

*CORRESPONDENCE
Patrick A. Forcelli,
paf22@georgetown.edu

RECEIVED 05 December 2023
ACCEPTED 01 March 2024
PUBLISHED 28 March 2024

CITATION
Quinlan S, Khan T, McFall D, Campos-Rodriguez C and Forcelli PA (2024), Early life phenobarbital exposure dysregulates the hippocampal transcriptome.
Front. Pharmacol. 15:1340691.
doi: 10.3389/fphar.2024.1340691

Early life phenobarbital exposure dysregulates the hippocampal transcriptome

Seán Quinlan[1], Tahiyana Khan[1,2], David McFall[1,2], Carolina Campos-Rodriguez[1] and Patrick A. Forcelli[1,2,3]*

[1]Department of Physiology and Pharmacology, Georgetown University, Washington, DC, United States, [2]Interdisciplinary Program in Neuroscience, Georgetown University, Washington, DC, United States, [3]Department of Neuroscience, Georgetown University, Washington, DC, United States

Introduction: Phenobarbital (PB) and levetiracetam (LEV) are the first-line therapies for neonates with diagnosed seizures, however, a growing body of evidence shows that these drugs given during critical developmental windows trigger lasting molecular changes in the brain. While the targets and mechanism of action of these drugs are well understood-what is not known is how these drugs alter the transcriptomic landscape, and therefore molecular profile/gene expression during these critical windows of neurodevelopment. PB is associated with a range of neurotoxic effects in developing animals, from cell death to altered synaptic development to lasting behavioral impairment. LEV does not produce these effects.

Methods: Here we evaluated the effects of PB and Lev on the hippocampal transcriptome by RNA sequencing. Neonatal rat pups were given a single dose of PB, Lev or vehicle and sacrificed 72 h later-at time at which drug is expected to be cleared.

Results: We found PB induces broad changes in the transcriptomic profile (124 differentially expressed transcripts), as compared to relatively small changes in LEV-treated animals (15 transcripts). PB exposure decreased GABAergic and oligodendrocyte markers *pvalb* and *opalin*, and increased the marker of activated microglia, *cd68* and the astrocyte- associated gene *vegfa*. These data are consistent with the existing literature showing developmental neurotoxicity associated with PB, but not LEV.

Discussion: The widespread change in gene expression after PB, which affected transcripts reflective of multiple cell types, may provide a link between acute drug administration and lasting drug toxicity.

KEYWORDS

neonatal, seizure, phenobarbital, levetiracetam, toxicity

1 Introduction

A large and growing body of evidence suggests that exposure to anti-seizure medications (ASMs) during defined and vulnerable periods of brain development induces long-lasting alterations in brain structure and function (Farwell et al., 1990; Ikonomidou et al., 2007; Meador et al., 2009; Meador et al., 2012; Meador et al., 2013; Forcelli et al., 2012a; Forcelli et al., 2012b; Al-Muhtasib et al., 2018). This is of particular concern for the treatment of neonatal seizures, which are often aggressively treated with

AMSs. Phenobarbital (PB) and levetiracetam (LEV) are two of the most common therapies for neonatal seizures (Pressler et al., 2023). The most recent consensus guidance from the International League Against Epilepsy recommends PB as first line therapy, and LEV as a second-line therapy based on clinical evidence for efficacy. However, both clinical and preclinical evidence suggests that they have different safety profiles for the developing brain (Kim et al., 2007; Kaushal et al., 2016; Sharpe et al., 2020).

PB induces a profound increase in apoptosis in both developing grey and white matter when given to neonatal rats (Bittigau et al., 2002; Forcelli et al., 2011; Kaushal et al., 2016) or macaques (Ikonomidou et al., 2019; 2022). Levetericatam does not, even at doses several times those that are therapeutically relevant (Manthey et al., 2005; Kim et al., 2007). A single exposure to PB produces a disruption in synaptic development that far outlasts the period of drug exposure, reducing both excitatory and inhibitory synaptic connections in the striatum (Forcelli et al., 2012a), and hippocampus (Al-Muhtasib et al., 2018). Levetericatam does not. Both brief, and prolonged early postnatal exposure to PB produce robust and lasting deficits in learning and memory, sensorimotor gatings, and anxiety-like responses in rodents (Pick and Yanai, 1984; Pereira de Vasconcelos et al., 1990; Rogel-Fuchs et al., 1992; Frankel et al., 1995; Stefovska et al., 2008; Forcelli et al., 2012b; Bhardwaj et al., 2012; Gutherz et al., 2014). Phenobarbital also suppresses postnatal neurogenesis (Stefovska et al., 2008; Chen et al., 2009). LEV is less studied for behavioral teratogenesis, but existing evidence suggests that its profile is more benign (Manent et al., 2008; Ozyurek et al., 2010). Clinically, PB exposure in the early life period has been associated with reduced IQ (Farwell et al., 1990; Reinisch et al., 1995; Sulzbacher et al., 1999), and a metanalysis indicates better neurodevelopmental outcomes associated with LEV and compared to PB (Qiao et al., 2021).

How then, does acute drug exposure lead to long lasting changes in circuit function? One study has taken a proteomic approach and identified a set of changes in the cortical proteome immediately, 1 week, and 4 weeks following a single exposure to PB. Alterations in astrocyte markers, and synaptic proteins were observed, some lasting across time-points (Kaindl et al., 2008). A direct head-to-head comparison between a PB and LEV, has also yet to be performed. To address this gap, we turned to a transcriptomic approach. We compared the hippocampal transcriptome after a single exposure to PB, LEV, or vehicle in postnatal day (P)7 in rats. We found a robust and large set of differentially regulated genes in PB-exposed animals, and a smaller set of differentially regulated genes in LEV exposed rats 72 h after drug exposure. These data provide a link between acute drug effects, intermediate-term changes gene expression, and long term-changes in brain function.

2 Materials and methods

2.1 Drug treatments

Timed pregnant female Sprague Dawley (E15) rats were purchased from Envigo/Charles River, at postnatal day 7 (P7) male pups were weighed and randomly assigned to treatment group. Animals were purchased over two orders and one animal per litter was taken per treatment group, one for RNA sequencing and one for qPCR and immunofluorescent analysis. The P7 time point represents the period of peak vulnerability to drug-induced apoptosis (Bittigau et al., 2002) and roughly corresponds to the peak of the "brain growth spurt," which equates to the late third trimester through early infancy in humans (Dobbing and Sands, 1979).

Treatments were balanced within litter. Animals were housed in the Division of Comparative Medicine in a temperature-controlled room (21°C) on a standard 12:12 h light-dark cycle (Lights on 0700). Dams had *ad libitium* access to food (LabDiet #5001) and water. Pups were treated with an intraperitoneal injection of LEV (200 mg/kg; 20 mg/mL), PB (75 mg/kg, 7.5 mg/mL) or vehicle (saline), and then returned to dam. LEV was purchased from Sigma-Aldrich (Product # L8668), as was phenobarbital (Product #1636). Animals were numbered using a marker on the back and tail, which was refreshed daily as needed until euthanasia (or weaning, see below).

For experiments in adult animals that received neonatal drug treatment, animals were treated as above, weaned into same-sex cages on postnatal day 21, ear tagged, and maintained in housing rooms until euthanasia at postnatal day 90.

This study was conducted under a protocol approved by the Georgetown University Animal Care and Use Committee (2016-1306) and in accordance with the Guide for the Care and Use of Laboratory Animals (National Research Council, 2011).

The dose of PB (75 mg/kg) falls at the high end of the anticonvulsant dose range in neonatal rats, induces neuronal apoptosis in developing rats, impairs both hippocampal and striatal synaptic development, and is associated with lasting behavioral changes (Kubova and Mares, 1991; Bittigau et al., 2003; Forcelli et al., 2011). Clinically, reports have found PB to be effective on a range of doses from 15 to 80 mg/kg (Kubova and Mares, 1991; Velísek et al., 1992; Polásek et al., 1996; Johne et al., 2021). On the basis of body surface area scaling the dose we used (75 mg/kg) would fall within the human 20–25 mg/kg bolus dose range (Tien et al., 2015). This dose produces plasma levels that fall within the human target range over a period of 24 h (Sanchez Brualla et al., 2023). Importantly, changes in transcriptome outlast the duration of drug action in our present study as the half-life of PB is ~12 h.

The dose of LEV (200 mg/kg) was selected to fall at a supratherapeutic dose. This dose is expected to produce peak plasma levels in the range of 300 ug/mL, on the basis of studies in adult rats (Coles et al., 2023), which is well beyond peak levels typically observed in humans. However, LEV has a short half-life as compared to PB (e.g., ~3 vs. 12 h). Thus, a single dose was expected to produce anti-seizure relevant effects for at least 12 h (4 half-lives). Moreover, given that prior studies have demonstrated that even supratherapeutic doses of LEV do not induce cell death or disrupt synaptic development (Manthey et al., 2005; Kim et al., 2007; Kaushal et al., 2016), this dose level provided the most robust test for a safety signal.

2.2 mRNA sequencing

At P10 pups were euthanized with overdose of sodium pentobarbital (Euthasol), transcardially perfused with cold PBS and hippocampi were dissected and placed in Trizol. Tissue was

collected between 0900 and 1800, depending on the time of the initial treatment. Total RNA was extracted from the hippocampus using the Trizol method. RNA quantity was measured using a Nanodrop Spectrophotometer (Thermo Fisher Scientific, Waltham, MA, United States). Only samples with an absorbance ratio at 260/280 between 1.8 and 2.2 were considered acceptable. RNA degradation was assessed using bio-analyzer, all samples sent for sequencing had an RNA Integrity Number (RIN value) > 9.0.

Samples were sent to Novogene ltd. (Ca.) for sequencing. 1 mg of RNA per samples was used to generate libraries using NEBNext Ultra RNA Library Prep Kit for Illumina® (NEB, United States), the library preparations were sequenced on an Illumina platform (NovaSeq 6000) and 150 bp paired-end reads were generated for an average of 24.6 M reads per sample.

Bioinformatic analyses were performed by SQ and PAF using the PartekFlow bioinformatic platform (Chesterfield, MO). Raw reads were (fastq files) were processed for QA/QC assessment (removing adaptor sequences, poly-N reads and low-quality reads) and mapped to reference rat (*rattus norvegicus*, rn6) genome using the STAR (STAR 2.7.3a) method (Dobin et al., 2013). Aligned transcripts were quantified to the rn6 annotation model using the quantify to annotation model (Partek E/M) module in PartekFlow.

For cell-type specific gene lists, we drew GABA neuron genes from (Seol et al., 2023). We added Sst, which was included in their neuron list but not in the GABA neuron list, on the basis of its strong expression in a subpopulation of interneurons. The microglial and oligodendrocyte gene lists were drawn from the same source without alteration. We used a gene list encompassing the top 50% of genes identified as most selective for astrocytes from (McKenzie et al., 2018). The meta-analysis they performed for astrocyte gene lists was much more comprehensive. These lists were not used for quantitative analysis, but rather to highlight a subset of differentially expressed genes across common CNS cell types. The final transcript lists for each cell type are shown in Supplementary Table S1.

2.3 qPCR

For qPCR analyses, a separate cohort of animals were treated with ASMs at P7 and sacrificed at P10- as with RNA sequencing. Total RNA was extracted with Trizol as for RNA sequencing, and cDNA synthesized using SuperScriptIV (Invitrogen) and random hexamer primers as per the manufacturers protocol. PCR reactions were prepared in duplicate using a SensiFASTTM Probe No-ROX Kit mix (Bioline, Meridian BioScience, United States) and multiplexed analyses of multiple mRNA targets within the same reaction (i.e., *actb*, *gad1* and *pvalb*) with Fluorophore containing primers from Bio-Rad, in a Mic qPCR system (Bio Molecular Systems, Australia) (Supplementary Table S5). Cycle threshold (cT) was automatically determined and averaged across replicates by the cycler manager software (Bio Molecular Sciences). Fold changes were determined using the $2^{-\Delta\Delta CT}$ method, with expression of all transcripts normalized to *actb* levels in the control group.

2.4 Immunofluorescence

Animals were anesthetized with pentobarbital (>100 mg/kg) and transcardially perfused with cold PBS, followed by 4% paraformaldehyde (PFA, 18,505, Ted Pella Inc.). Brains were extracted and post-fixed in PFA overnight. Following post-fixation, brains were cryoprotected overnight in 15% sucrose, and then overnight 30% sucrose in PBS before flash-freezing on dry ice.

Brains were sectioned at 30 µm on a cryostat (CM 1850, Leica Biosystems) and immediately mounted on charged slides. Sections were permeabilized in PBS +0.5% TritonX100 and then blocked in a solution of PBS +2.5% normal goat serum. Sections were incubated in primary antibody overnight (Supplementary Table S6). Slices were washed and then incubated at room temperature for 1 h with secondary antibodies (Supplementary Table S6) and coverslipped with Fluoromount mounting medium containing DAPI.

Fluorescent photomicrographs were collected on a Zeiss AxioScope M2 Microscope with an Apotome optical sectioning device using Microlucida software. Images were taken at ×10 magnification (1.124 mm^2 region). For parvalbumin positive cell counting analyses, a ×10 image was taken of the hippocampus on 3–4 non-consecutive slices (90 µm apart) and counts within CA1, CA3, and dentate gyrus were averaged per individual brain. To provide a whole-hippocampus view for presentation purposes, hippocampal sections were also scanned using a Leica Mica workstation. For CD68 and Opalin fluorescent intensity analysis, 4–6 ×10 over-lapping images were taken of the corpus collosum from the CA1 to the CA3 regions on the hippocampus on 3–4 non-consecutive slices and results were averaged per individual sample. For GFAP fluorescent intensity analysis, one 10X image was taken on the apex of the CA1 and CA3 regions and one of the dentate gyrus/hilar regions of the hippocampus (representative images of the CA3 region only) and intensity was averaged over entire hippocampal region per brain slice, with 3–4 slices per sample. Histological analysis was performed while blind to treatment status of the animal.

2.5 Statistics

For RNA sequencing, one sample from the control condition was excluded due to its average coverage (58.34) being double the samples (25.82–28.68), with the genomic coverage (4.939) half that of the rest of the samples (9.02–10.932). This resulted in final sample sizes for the groups of: VEH = 13, PB = 14, LEV = 14. Data were batch-normalized using a linear model function in PartekFlow to remove both main effects of batch and batch-by-treatment interactions. Differential expression analysis on the normalized data was performed using DESeq2 package (Love et al., 2014) in PartekFlow (PB v VEH; LEV v VEH). *p*-values were adjusted with the Benjamini and Hochberg approach for controlling the False Discovery Rate (FDR). Transcripts found by DESeq2 with an adjusted *p*-value <0.05 and a fold change <1.25 were considered differentially expressed.

qPCR and immunofluorescence results were analyzed by one way analysis of variance with Holm-Sidak corrected post-tests in GraphPad Prism. *p*-values <0.05 were considered statistically significant.

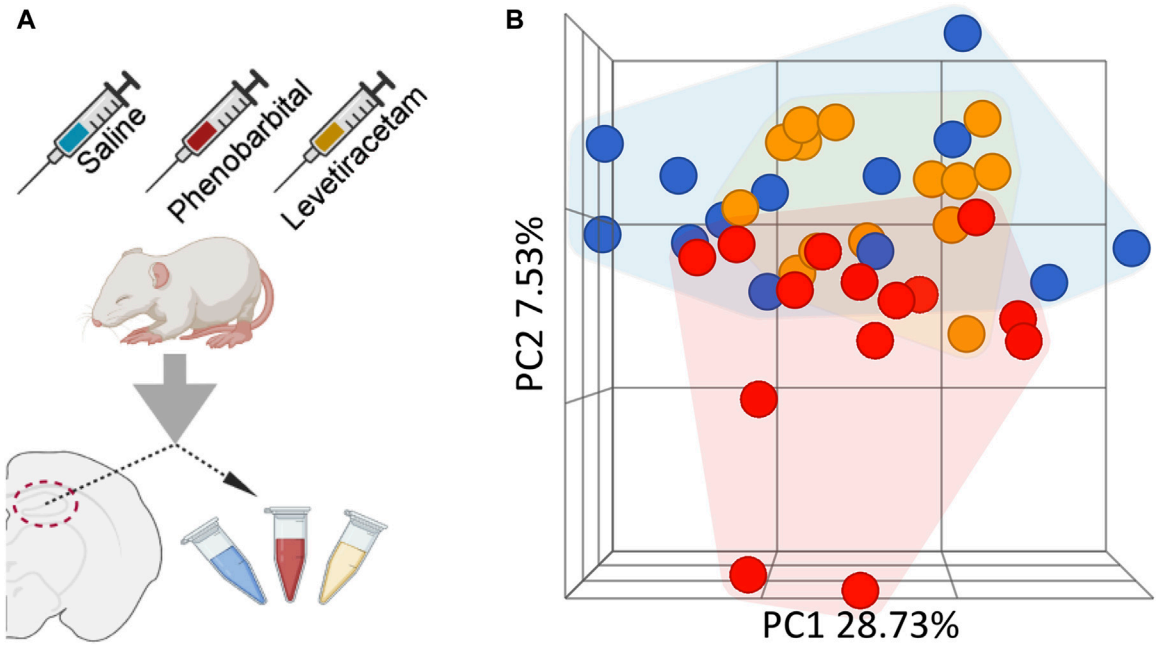

FIGURE 1
Overview of experimental design and processing. **(A)** Neonatal P7 Sprague Dawley pups treated with vehicle, PB or LEV. Schematic of P7 animals treated with drug and hippocampi harvested and RNA extracted and sequenced. **(B)** Principal component analysis of vehicle, PB and LEV treated animals.

3 Results

3.1 Quality control and clustering

To identify changes following anti-seizure drug administration (PB or LEV vs. vehicle control, VEH), RNA sequencing was performed on hippocampi 72 h after drug treatment (Figure 1A). Pre-alignment quality assessment and control showed a minimum of 20 million reads of 150 base pair read length transcripts per sample, with average read quality >35.0. Over 90% of aligned reads were uniquely paired. Principal component analysis (PCA) showed relatively clear clustering with the VEH and PB groups, however LEV group showed overlap with both PB and LEV groups (Figure 1B).

3.2 Differential gene expression following ASM exposure

To identify significantly differentially expressed genes (DEGs) regulated by ASM treatment, we performed differential expression analysis using the DESeq2 package. Genes with fold change ± 1.25 and an adjusted *p*-value of 0.05 were considered differentially expressed. In PB-treated animals, 124 transcripts were significantly altered as compared to controls (80 upregulated, 44 downregulated; Figure 2A). By contrast, in LEV-treated animals, we identified only 15 transcripts that were significantly altered (6 upregulated, 9 downregulated; Figure 2B). A heatmap showing the pattern of expression across groups is shown in Figure 2C. The top 10 up and downregulated genes for PB and LEV are shown in Table 1, 2. Full lists of transcripts are shown in Supplementary Table S2; differentially expressed transcripts following PB treatment are shown in Supplementary Table S3; differentially expressed transcripts following LEV treatment are shown in Supplementary Table S4.

3.3 Pathway analysis

We next entered the differentially expressed transcripts into a gene set enrichment analysis against the KEGG pathway database (Kanehisa and Goto, 2000; Kanehisa et al., 2023). After adjusting for multiple comparisons, the only pathway with significant enrichment was the neuroactive ligand-receptor interaction pathway (rno04080) with an enrichment score of 9.3 (*adj. p-value* = 0.03) for differentially expressed genes in the PB treated group (Figure 3). 3.6% (11 of 305) of genes in the set were differentially expressed following PB treatment.

3.4 GABAergic neuron associated transcripts are downregulated following PB treatment

We had previously reported altered GABAergic synaptic development in the hippocampus after exposure to PB (Al-Muhtasib et al., 2018). Given this prior finding, and the presence of GABA-neuron related genes in our KEGG analysis (above), we next sought to evaluate the impact of PB and LEV on GABAergic markers. Figure 4A shows a volcano plot with genes from a GABA neuron gene list for the PB condition (Supplementary Table S1). Four of 88 genes were downregulated in PB-exposed animals (Sst, Pvalb, Vip, Tac3). Calb2 fell just under the fold-change cutoff (1.24) for increased expression in PB-exposed animals. No transcripts were altered in the LEV-exposed condition.

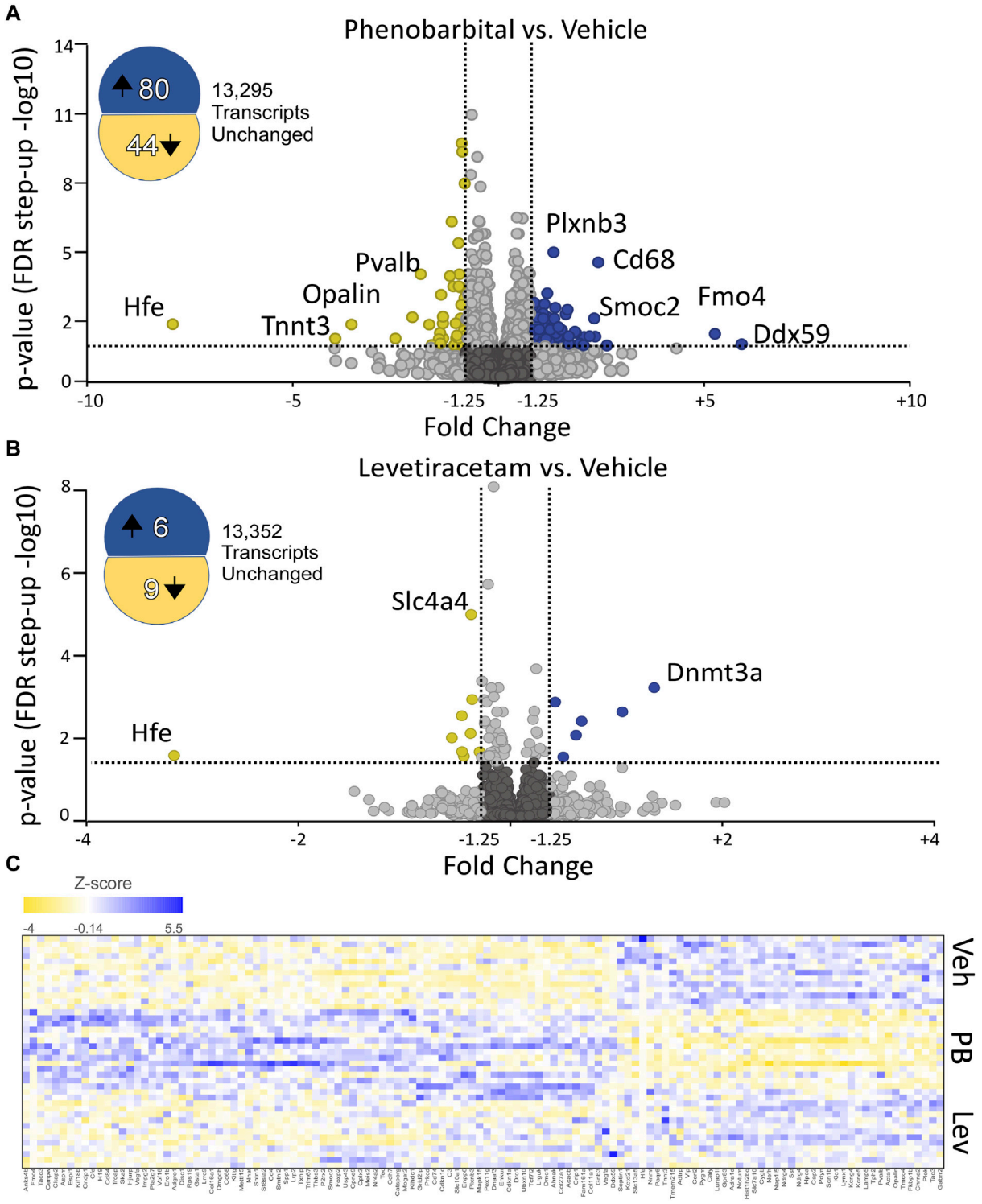

FIGURE 2
Phenobarbital robustly dysregulates the hippocampal transcriptome, while levetiracetam does not. **(A)** Volcano plot showing differential expression (PB vs. VEH). PB exposure resulted in 8- upregulated and 44 downregulated transcripts. FDR cutoff = 0.05, Fold change cutoff: -1.25 to 1.25. **(B)** Volcano plot showing differential expression (LEV vs. VEH). LEV exposure upregulated 6 transcripts and downregulated 9 transcripts. The top 10 up and downregulated genes for PHB and LEV are shown in Tables 1, 2. Full lists of transcripts are shown in Supplementary Table S2; differentially expressed transcripts following PB treatment are shown in Supplementary Table S3; differentially expressed transcripts following LEV treatment are shown in Supplementary Table S4. **(C)** Heatmap showing similar expression patterns between VEH and LEV, which differs from the pattern observed with PB.

TABLE 1 Top differentially expressed genes after PB exposure.

Top downregulated genes after PB exposure		
Gene symbol	P-Value	Fold change (PB vs Veh)
Hfe	1.81E-04	−8.98
Tnnt3	1.34E-03	−3.00
Opalin	1.87E-04	−2.69
Ccrl2	1.32E-03	−2.00
Pvalb	6.56E-05	−1.79
Plek	1.91E-07	−1.69
Kcng4	1.91E-04	−1.59
Paqr6	3.34E-03	−1.57
Septin1	3.92E-03	−1.54
Nnmt	1.47E-03	−1.49
Top upregulated genes after PB exposure		
Gene symbol	P-Value	Fold change (PB vs Veh)
Impg2	2.74E-03	1.73
Vegfa	3.56E-03	1.77
Cplx3	1.04E-03	1.78
Vegfa	9.33E-04	1.85
Smoc2	7.75E-05	1.91
Cfd	9.90E-04	1.92
Cd68	4.55E-08	1.96
Slc10a1	3.70E-03	2.08
Fmo4	6.97E-04	4.30
Ddx59	3.04E-03	5.15

TABLE 2 Top differentially expressed genes after LEV exposure.

Top downregulated genes after LEV exposure		
Gene symbol	P-Value	Fold change (PB vs Veh)
Hfe	1.42E-04	−9.31
LOC310926	3.38E-05	−1.51
Zbtb20	4.97E-06	−1.42
Rn18s	1.00E-04	−1.42
Pramef8	1.58E-04	−1.40
Slc1a2	2.15E-05	−1.34
Slc4a4	2.96E-09	−1.33
Grin2b	1.13E-06	−1.33
Slc1a2	1.04E-04	−1.26
Top upregulated genes after LEV exposure		
Gene symbol	P-Value	Fold change (PB vs Veh)
Tpcn2	1.58E-06	1.30
Fos	1.73E-04	1.37
Cpne9	2.61E-05	1.49
Npas4	7.50E-06	1.54
Pah	3.75E-06	2.02
Dnmt3a	4.55E-07	2.48
Tpcn2	1.58E-06	1.30

To verify our RNA-seq results we selected general markers of GABAergic cells (*gad1*) and specific markers of parvalbumin expressing GABA cells (*pvalb*) to evaluated by qRT-PCR (Figures 4B, C). *gad1* mRNA levels differed across groups (One Way ANOVA, $F_{2,21} = 18.97$, p-value <0.0001), an effect that was driven by a significant decrease in the PB-treated group (p-value = 0.0007, Holm-Sidak corrected). *gad1* mRNA levels did not differ between LEV and VEH treated animals (p-value = 0.103, Holm-Sidak corrected). We observed a similar pattern with *pvalb* mRNA, with the difference among the groups (One Way ANOVA, $F_{2,21} = 43.34$, p-value <0.0001), driven by a downregulation in the PB treated animals (p-value <0.0001, Holm-Sidak corrected).

To determine if PB causes a reduction in *pvalb* transcripts only, or if this decrease was also associated with changes at the protein level, we performed immunofluorescence of parvalbumin and analyzed the number of expressing cells in the hippocampus (average of CA1, CA3, DG; Figures 4D, E). Similar to our PCR results, we found a significant difference amongst the groups (One Way ANOVA, $F_{2,8} = 11.3$, p-value <0.0047), which was driven by a significant decrease in the number of PV^+ cells compared to the VEH group (p-value = 0.012, Holm-Sidak corrected). LEV treated animals did not differ from VEH treated controls (p-value = 0.736, Holm-Sidak corrected).

3.5 Microglial-enriched genes

Given that CD68, a membrane protein expressed in *activated* microglia, was upregulated in following PB treatment, and PB treatment robustly triggers cell death, which in turn may activate microglia, we further analyzed the effects of ASMs on microglial enriched genes. We examined a curated list of 267 genes enriched in microglia (Supplementary Table S1), and found that five transcripts that were differentially regulated (*Cd68, Cd4, Cd74, C3, and Cd84*). *Cd68* displayed the largest fold change from this list (+1.97, adj. p-value <0.0001) following PB exposure (Figure 5A). No transcripts from the list were differentially expressed in LEV exposed animals.

To confirm RNA-seq results we performed qRT-PCR on general microglial marker *Aif1* (Iba1) (Figure 5B) and activated microglial marker *Cd68* (Figure 5C). We found no difference in *Aif1* transcript levels in either PB or LEV animals as compared to VEH treated animals (One Way ANOVA, $F_{2,21} = 1.287$, p-value = 0.297). However, we found significant differences between groups for *Cd68* transcript levels (One Way ANOVA, $F_{2,21} = 3.53$, p-value = 0.0476). This difference was driven by a significant increase in the PB group when compared to the VEH group (p-value = 0.0296, Holm-Sidak corrected). *cd68* levels in LEV treated animals did not differ from those in VEH treated animals (p-value = 0.153).

We performed immunofluorescence for CD68 and found a significant difference in hippocampal CD68 fluorescence intensity between groups (One Way ANOVA, $F_{2,11} = 12.36$, p-value = 0.0015),

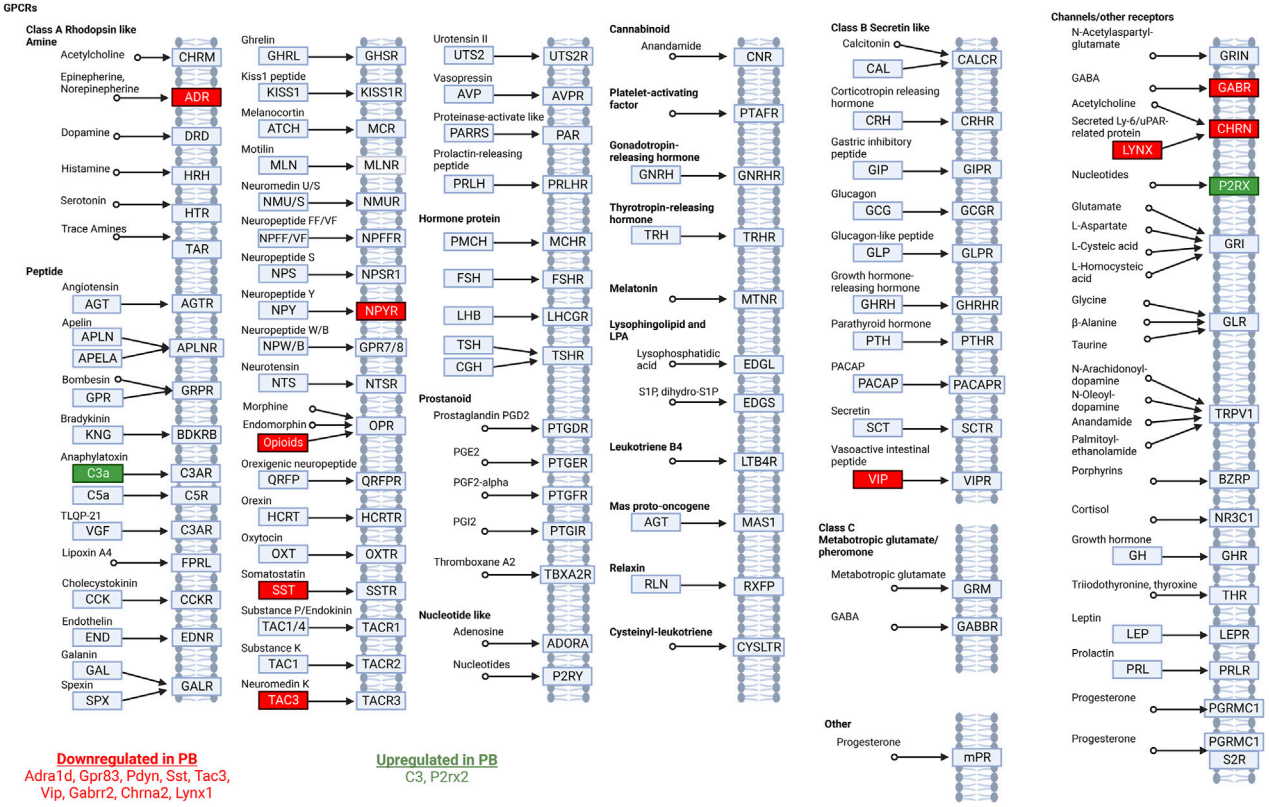

FIGURE 3
Neuroactive ligand-receptor interaction pathway analysis. Modified from the Kyoto Encyclopedia of Genes and Genomes ligand-receptor interaction pathway. Significantly DEGs in this pathway in animals treated with PB are listed at the bottom of the figure. Downregulated transcripts are shown in red and upregulated transcripts are shown in green.

an effect that was driven by a significant increase in the PB exposed group (p-value = 0.016, Holm-Sidak corrected; Figures 5D, E).

3.6 Astrocyte-enriched genes

Astrocytes are a major cell glial type in the CNS; while astrocytes have not been directly linked to developmental toxicity of anti-seizure medications, they play a critical role in regulating synaptic transmission as part of the tripartite synapse, and the developmental trajectory of glutamatergic neurotransmission is altered following even a single exposure to PB. We evaluated a gene list enriched in astrocytes (Supplementary Table S1) and found 13 of 441 were differentially expressed following PB treatment (Figure 6A). Eight transcripts were increased following PB: two *Vegfa* transcripts (variant 7: NM_001287113; variant 9 (non-coding): NR_105011), as well as *Fmo4, Impg2, Pla2g7, Lrrc9, Meis2* and *Col16a1*. Six transcripts were decreased in expression afer PB exposure: *Slc7a10, Slc13a5, Kcne5, Paqr6, and Kcng4*. In the LEV-exposed group, four transcripts (*slc4a4* - NM_053424 and *slc1a2* - NM_001302089 and NM_001035233; and *Zbtb20* - NM_001105880) were downregulated relative to the VEH exposed group, since so few transcripts were differentially regulated with LEV, no volcano plot is shown for that condition.

We assessed *gfap* transcript levels by qPCR (One Way ANOVA, $F_{2,21}$ = 12.15, p-value = 0.0003) and found group differences that were driven by a significant increase in the PB exposed animals (Figure 6B). While in our DESeq analysis, this transcript fell just below the cutoff for fold change (1.24) the p-value was highly significant (p-value = 5×10^{-5}), consistent with our qPCR results (p-value = 0.0011, Holm-Sidak corrected). LEV did not differ from VEH for *gfap* transcript levels (p-value = 0.72).

We found no differences in drug treatments overall on the levels of *vegfa* (One Way ANOVA, $F_{2,21}$ = 1.98, p-value = 0.163; Figure 6C), however this could be due to different transcript variants targeted by PCR amplification (PCR amplicons; NM_001110333, NM_031836, NM_001110334, NM_001110335 and NM_001110336). To identify if altered *Gfap* transcript levels observed in our DESeq analysis resulted in dysregulated GFAP expression in cells, we performed immunofluorescence staining for GFAP in the hippocampus (Figures 6D, E). We used relative fluorescent intensity as a measure of GFAP expression across three regions; the CA1, CA3 and dentate gyrus/hilar regions of the hippocampus, and found an overall effect of drug treatment on GFAP expression by one-way ANOVA ($F_{2,\ 12}$ = 14.19, p-value = 0.0007). Both PB and LEV treated animals had increased fluorescent intensity of GFAP when compared to VEH animals (p-value's = 0.0005 and 0.0019, Holm-Sidak adjusted, respectively).

3.7 Oligodendrocyte-enriched genes

In addition to induction of neuronal apoptosis following PB exposure in neonatal animals (Bittigau et al., 2002), profound

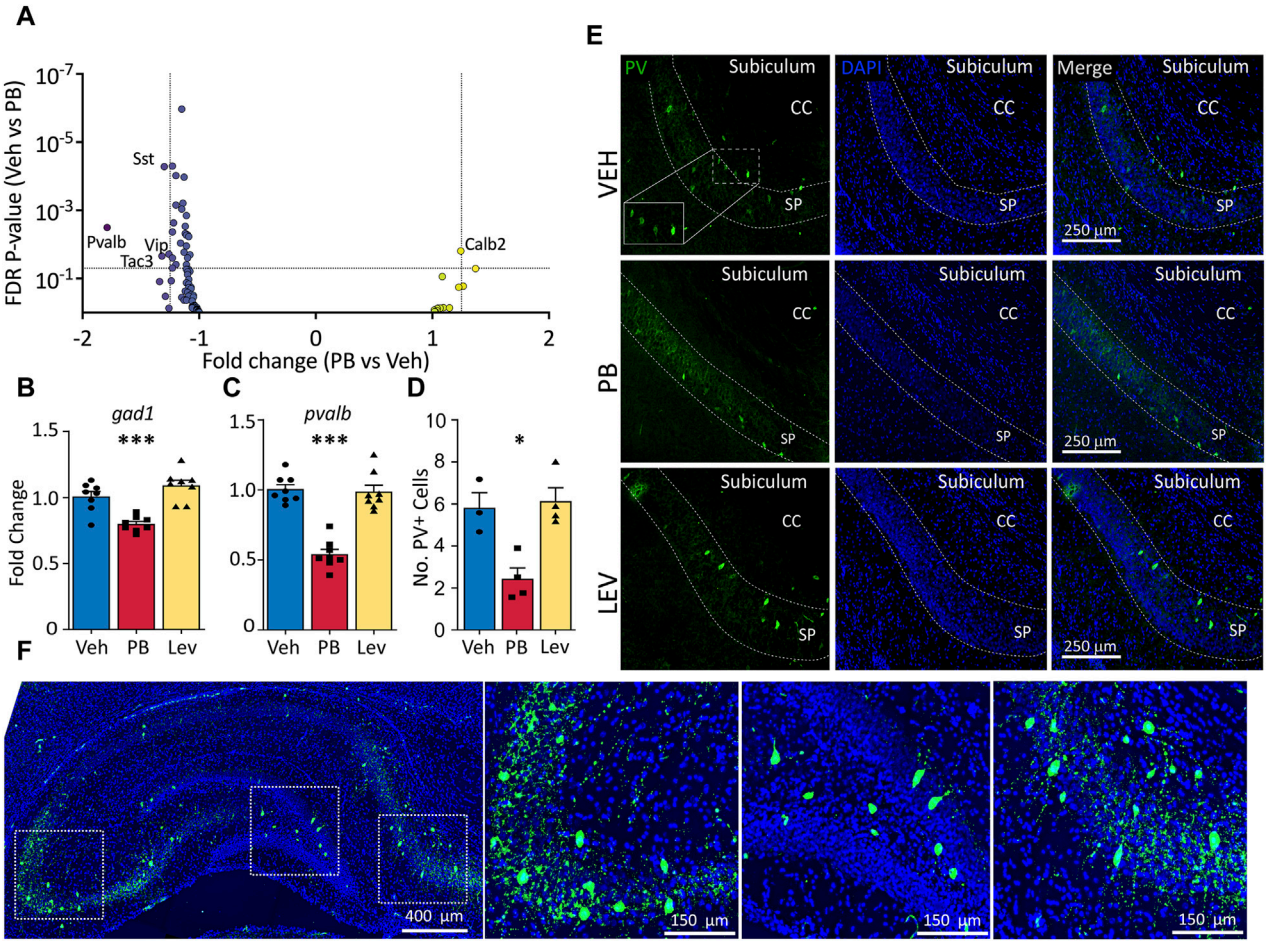

FIGURE 4
Specific decrease in pvalb GABAergic transcripts in PB, but not Lev treated animals. **(A)** Animals treated with PB, but not with LEV showed significant dysregulation of GABAergic neuron related genes. **(B,C)** qPCR analysis confirmed that PB treatment significantly reduced both general GABAergic marker *gad1* transcripts (One Way ANOVA, $F_{2,21}$ = 18.97, *p*-value <0.0001, VEH vs. PB adj. *p*-value = 0.0007 with Holm-Sidak corrected) and reduction of *pvalb* transcripts (One Way ANOVA, $F_{2,21}$ = 43.34, *p*-value <0.0001, VEH vs. PB adj. *p*-value <0.0001, Holm-Sidak corrected). **(D,E)** Representative photomicrographs of parvalbumin (left column) and DAPI (middle column) staining in the hippocampus in animals treated with vehicle (top row), PB (middle row) and LEV (bottom row). Animals treated with PB showed significantly lower levels of immunoreactivity compared to vehicle treated animals (One Way ANOVA, $F_{2,8}$ = 11.3, *p*-value <0.0047, adj. *p*-value = 0.012, Holm-Sidak corrected). CC = corpus callosum, SP = stratum pyramidale of CA1. **(F)** Representative image showing the pattern of PV expression in a whole hippocampus section with enlarged views of subfields.

oligodendrocyte apoptosis has also been observed in developing white matter (Brambrink et al., 2012; Creeley et al., 2013; Creeley et al., 2013; Creeley et al., 2014; Ikonomidou et al., 2019). Interestingly, opalin (also referred to as TMEM10), an oligodendrocyte transmembrane protein, was the transcript with the fifth largest absolute fold change following PB exposure (Fold Change: -2.69; *p*-value <0.001). Opalin is enriched in myelin and its expression is upregulated during oligodendrocyte differentiation. We evaluated, as with neuronal and microglial gene lists, a gene list for oligodendrocytes (Supplementary Table S1) in animals treated with PB as compared to VEH (Figure 7A). Of these transcripts, three were differentially expressed: *Opalin*, *Cdkn1c, and Cndp1*. No transcripts from the list were differentially expressed in LEV exposed animals, so no volcano plot is shown.

We assessed levels of *olig2* by qPCR and found no differences across treatment groups (One Way ANOVA, $F_{2,33}$ = 0.94, *p*-value = 0.40; Figure 7B); by contrast *opalin* differed significantly (One Way ANOVA, $F_{2,21}$ = 12.51, *p*-value = 0.0003; Figure 7C). This effect was driven by a significant decrease in *opalin* transcript levels in the PB exposed group (adj. *p*-value = 0.0146, Holm-Sidak corrected). The LEV group did not differ from the VEH exposed group, although there was a non-significant trend toward increase *opalin* levels in the LEV condition (adj. *p*-value = 0.055). When we assessed Opalin fluorescent intensity, we again found a difference between groups (One Way ANOVA, $F_{2,10}$ = 7.41, *p*-value = 0.0106; Figures 7D, E), which was driven by a decrease in intensity in the PB exposed group (adj-p-value = 0.02, Holm-Sidak corrected) as compared to the VEH group. LEV exposure did not alter opalin immunofluorescence (adj. *p*-value = 0.081).

3.8 Longer-term gene expression profiles

For the transcripts we found to be dysregulated by qPCR in the above experiments, we separately assessed their relative abundance in PB- or LEV-exposed animals 3 months after exposure. *Gfap,*

10.3389/fphar.2024.1340691

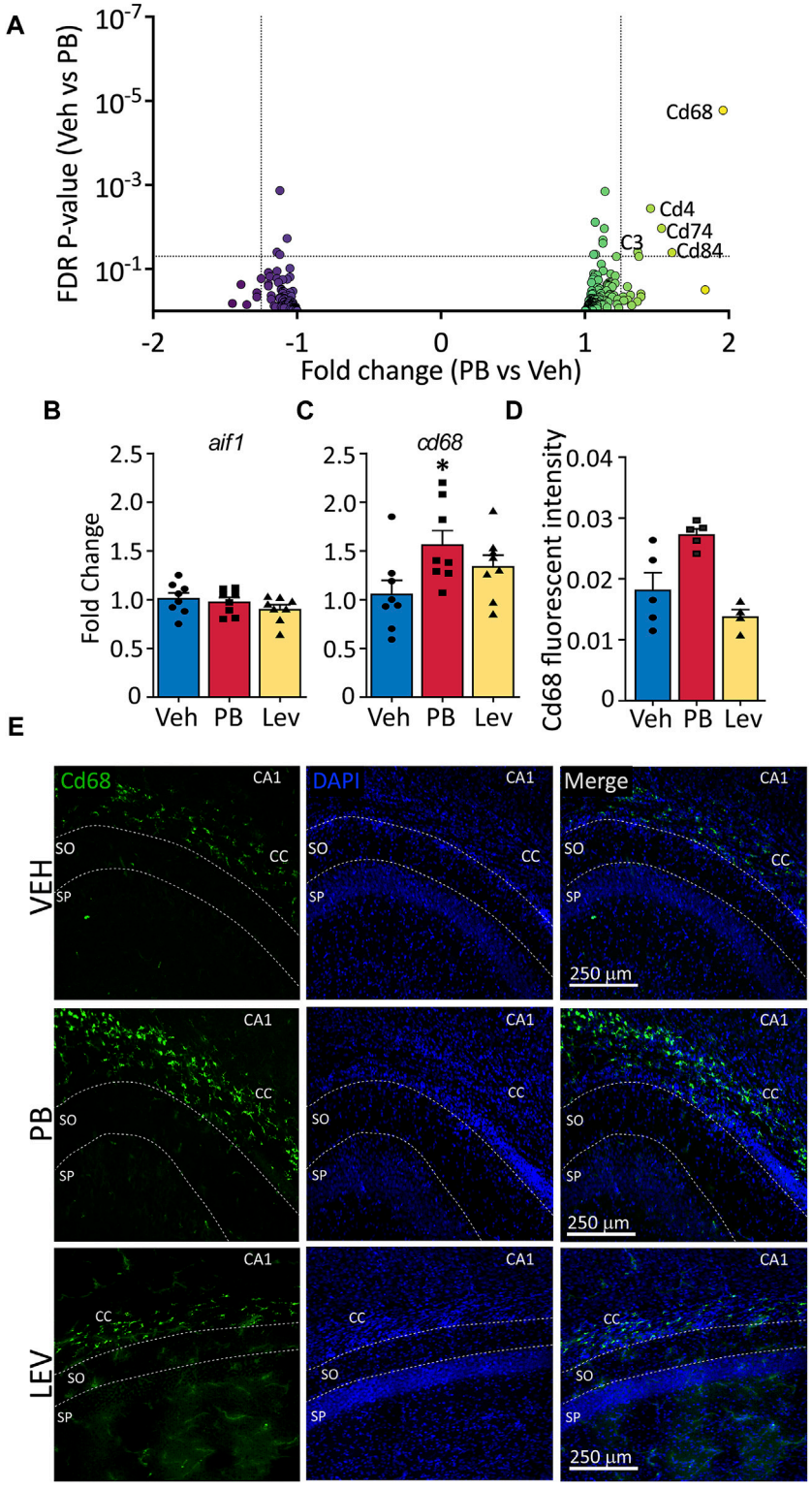

FIGURE 5
The activated microglia marker cd68 is increased following ASM treatment **(A)** Volcano plots of microglial associated genes. PB treated animals showed increased levels of the activated microglial marker, CD68, however no significant changes in any microglial markers were observed in the LEV treated group. **(B)** The general microglial marker *aif1* (iba1) was unchanged in both PB and LEV animals when analysed by qPCR. **(C)** *cd68* transcripts were increased in PB but not LEV treated animals (One Way ANOVA p-value = 0.048, $F_{(2, 21)} = 3.53$. VEH vs. PB adj. p-value = 0.029). **(D,E)** Representative photomicrographs of CD68 (left column) and DAPI (middle column) staining in the corpus collosum in animals treated with vehicle (top row), PB (middle row) and LEV (bottom row). Animals treated with PB showed increased CD68 immunofluorescent intensity in the CC when compared with VEH (One Way ANOVA p-value = 0.0015, $F_{(2, 11)} = 12.36$, VEH vs. PB adj. p-value = 0.016), while there was no difference between LEV and VEH animals. SP = stratum pyramidale of CA1, SO = stratum oriens of CA1. CC = corpus callosum.

10.3389/fphar.2024.1340691

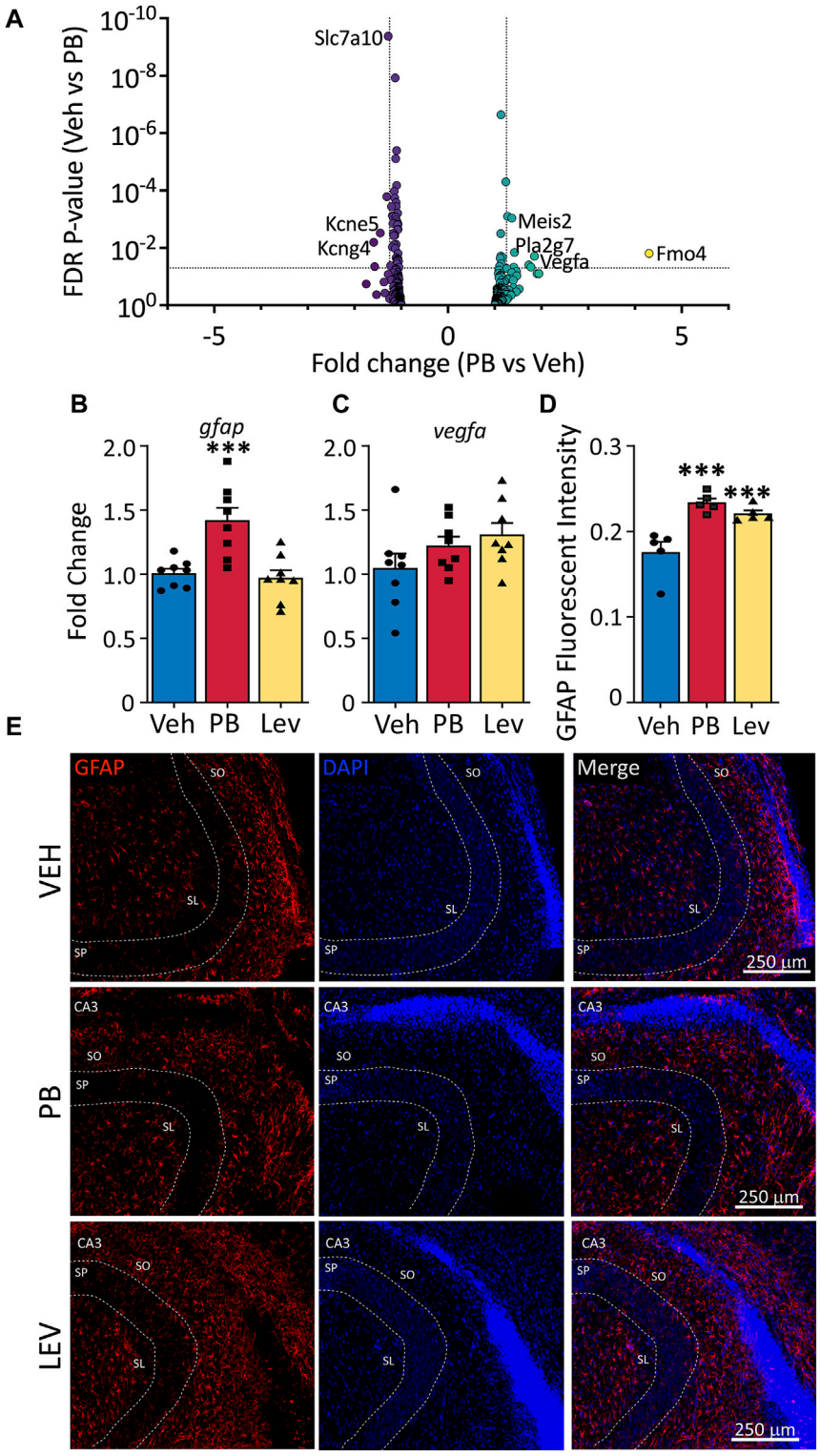

FIGURE 6
Altered astrocytic marker expression following ASM treatment. **(A)** Volcano plots of astrocyte associated genes. Transcripts of *vegfa* were found increased in both PB and LEV treated animals. **(B)** qPCR for *gfap* showed that it was increased in PB treated (One Way ANOVA p-value = 0.0003, $F_{2, 21}$ = 12.15, adj. p-value = 0.001) but not in LEV treated animals. While *vegfa* **(C)** mRNA levels were unchanged in both treatment groups (One Way ANOVA p-value = 0.163, $F_{2, 21}$ = 1.978). **(D,E)** Representative photomicrographs of GFAP (left column) and DAPI (middle column) staining in the CA3 in animals treated with vehicle (top row), PB (middle row) and LEV (bottom row). Fluorescent intensity analysis showed that animals treated with both PB and LEV have increased levels of GFAP$^+$ cells when compared with vehicle treated animals (One Way ANOVA p-value = 0.0007, $F_{2, 12}$ = 14.19, VEH vs. PB adj. p-value<0.001 and VEH vs. LEV adj. p-value<0.005). SP = stratum pyramidale, SO = stratum oriens, SL = stratum lacunosum-moleculare.

10.3389/fphar.2024.1340691

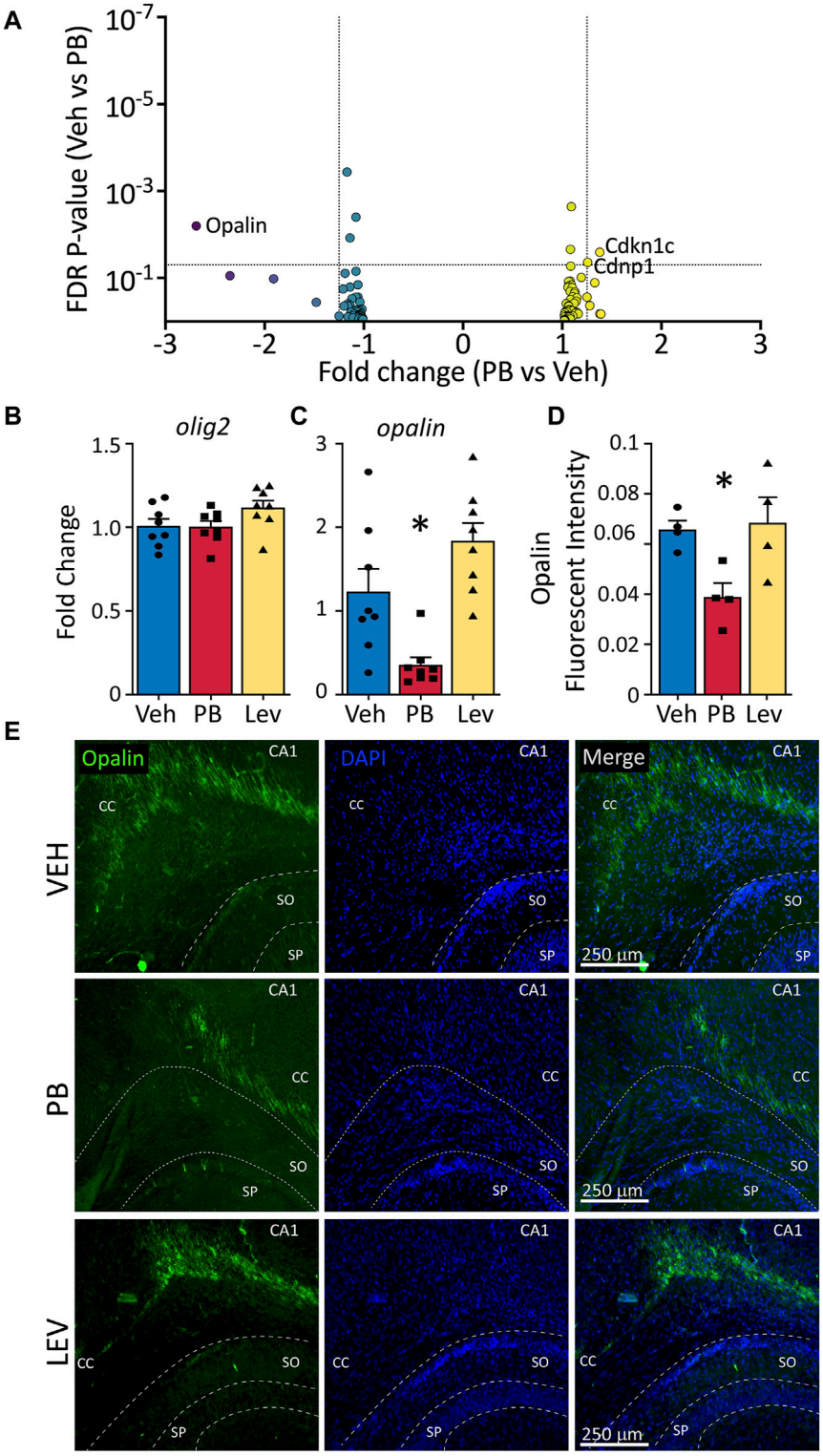

FIGURE 7
Decreased opalin expression in PB treated animals. **(A)** Volcano plots of oligodendrocyte associated genes. **(B)** The mRNA levels of *olig2* were unchanged in both PV and LEV treated animals when analyzed by qPCR (One Way ANOVA p-value = 0.4, $F_{2, 33} = 0.94$), however we observed a significant decrease in the levels of **(C)** *opalin* in PB treated animals when compared to vehicle (One Way ANOVA p-value = 0.0003, $F_{2,21} = 12.51$. adj. p-value = 0.02) **(D,E)** Representative photomicrographs of opalin (left column) and DAPI (middle column) staining in the corpus collosum in animals treated with vehicle (top row), PB (middle row) and LEV (bottom row). Reduced levels of opalin$^+$ fluorescent intensity in the CC of animals treated with PB when compared to vehicle (One Way ANOVA p-value = 0.0106, $F_{2, 10} = 7.416$, VEH vs. PB adj. p-value = 0.02 Holm-Sidak corrected). SP = stratum pyramidale of CA1, SO = stratum oriens of CA1. CC = corpus callosum.

opalin and cd68 did not differ across treatment groups at 3 months post exposure. To our surprise, and differing from what we observed 3 days after exposure, *pvalb* was *increased* in the LEV-treated group compared to vehicle or PB exposure, and the PB-treated group did not differ from controls. *Gad1* transcript levels remained lower in the PB-treated group 3 months after drug exposure, consistent with the pattern observed 3 days after exposure (see Supplementary Figure S1 for results and statistics).

4 Discussion

The choice of anti-seizure medication for use in pregnancy and infancy is complicated by concerns of long-term effects on the developing brain. However, the mechanisms linking acute drug exposure to lasting changes in synaptic function, behavior, and cognitive outcome remain obscure. Here, we examined the two commonly used ASMs for the treatment of neonatal seizures, PB and LEV for effects on the hippocampal transcriptome. PB has well-established neurodevelopmental effects, whereas LEV is commonly thought to be safer. Consistent with this general notion, we found a robust change in the hippocampal transcriptome 72 h after a single exposure to PB: 124 transcripts were differentially expressed in PB-exposed animals compared to vehicle controls. By contrast, only 15 transcripts were differentially expressed in LEV-exposed animals. We followed this analysis with profiling of GABAergic neurons, microglia, astrocytes and oligodendrocytes, and for each cell type found markers that were differentially impacted at the transcript and/or protein level following PB exposure.

The changes we found outlasted the acute drug exposure (P7)—for PB ~6 half-lives passed between treatment and tissue collection (Dingemanse et al., 1989), a point at which only ~1% of the drug is expected to remain. These changes thus may provide a link between acute drug administration and disrupted synaptic development that we have previously reported following PB exposure. For example, P7 exposure to PB disrupts the maturation of inhibitory and excitatory synapses in the striatum and inhibitory synaptic development in hippocampus. In both regions, these effects are evident well after drug is eliminated. In striatum, this effect was manifest by a decrease in inhibitory postsynaptic current (IPSC) frequency (Forcelli et al., 2012a), whereas in the hippocampus we found an initial increase in IPSC frequency, followed by a reduced IPSC frequency at later ages indicating impaired maturation (Al-Muhtasib et al., 2018). In hippocampus, we also observed an increase in tonic GABA currents, and a long-lasting perseverance of giant depolarizing potentials, which are large GABAergic events that are normally absent by the second postnatal week (Al-Muhtasib et al., 2018). Along these lines, it is noteworthy that we identified altered expression of somatostatin, vasoactive intestinal peptide, and parvalbumin transcripts, each of which label populations of GABAergic interneurons in the hippocampus (Pelkey et al., 2017). Moreover, we found that Gpr83, a g-protein coupled receptor that binds the neuropeptide PEN (and may bind neuropeptide Y, as well), which is enriched in parvalbumin interneurons in the amygdala (Lueptow et al., 2018; Fakira et al., 2021). While PEN expression has been reported in the hippocampus, it is unknown what cell types it co-localizes with. Together, these changes suggest that PB impacts inhibitory neurotransmission, and raise the possibility that these changes could in turn, impact PB efficacy–reduced parvalbumin neurons, for example, would be expected to worsen epilepsy outcomes. Suggesting that not only inhibitory transmission may be altered, but also function of excitatory cells, we noted a change in transcript levels for pro-dynorphin, which is enriched in dentate gyrus granule cells in the hippocampus (Chavkin et al., 1985).

Programmed cell death, which is a natural part of postnatal brain development, eliminates neurons that do not establish appropriate synaptic connections. Drugs, such as PB, exacerbate this process, significantly increasing the number of degenerating cells. Microglia play a critical role in the phagocytosis of neurons that undergo programmed cell death (Ferrer et al., 1990; Bessis et al., 2007; Schafer and Stevens, 2015), in fact developmental cell death in the hippocampus requires functional microglial (Wakselman et al., 2008). Neuronal apoptosis drives dynamic changes in microglial states in the retina–and prevention of cell death interestingly *downregulates* cd68 (Anderson et al., 2022). We observed the opposite pattern with PB exposure–CD68 was upregulated at both the transcript and protein level. This effect was not observed in LEV exposed animals, consistent with the induction of cell death by PB, but not by LEV. The impact of prolonged elevation of CD68 beyond the acute injury (the peak detection of degenerating cells after PB exposure is ~24 h), remains unstudied, but given the role for CD68-positive microglia in synaptic pruning (Schafer et al., 2012), raises the possibility that microglial activation may contribute to long-term circuit changes after PB exposure. Assessment of microglial morphology and "activation" state following PB exposure may thus be of future interest.

Interestingly, we observed increased GFAP immunoreactivity–indicative of astrocytosis–in both PB and LEV treated animals, although at the transcript level GFAP was increased only after PB exposure. The functional significance of this increased astrocyte activation is unknown–astrocyte activation is associated with both acute damage responses and repair/plasticity responses to injury (Yang and Wang, 2015). Moreover, why Lev treated animals have increased reactivity to GFAP immunofluorescence, with no detected changes in gfap transcripts remains unclear. We identified an increase in complement C3 after PB exposure (1.37 FC; p-value = 0.04), and astrocytes are a major source of C3 in the brain (Pekna and Pekny, 2021), furthermore C3 may be an important component of astrocyte-microglial cross signaling during states of brain damage. While it is uncertain if the elevated C3 transcript levels we detected is astrocytic in origin, it is worth noting that astrocyte C3 plays an important role in dendritic spine pruning (Lian et al., 2015) and has both putative protective and neurotoxic roles (Pekna and Pekny, 2021). Along these lines, while astrocytes do not appear to undergo programmed cell death, or display increased activation after exposure to isoflurane, an anesthetic agent, this has not been evaluated for anti-seizure medications (Brambrink et al., 2012). However, in astrocyte-neuron co-culture experiments, astrocytes were proposed to play a *critical* role in apoptosis triggered by inhibition of neuronal activity (Shute et al., 2005). In culture, as *in vivo*, ethanol, sodium channel blockers, and NMDA receptor antagonists trigger apoptosis in hippocampal neurons; reducing astrocytes in the cultures protected against this neuronal cell death, and treating cultures with astrocyte conditioned media increased cell death. While the authors of this study determined

that there was a heat-labile component of astrocyte conditioned medium that was responsible for this effect, the identity of this signal remains unknown (Shute et al., 2005). Finally, the increase in Vegf transcripts we detected in our DESeq analysis suggests that blood-brain-barrier and microvascular function merits further investigation after early-life exposure to PB.

In addition to neuronal apoptosis, neonatal drug exposure (including to PB) is associated with increased apoptosis in the developing white matter (Kaushal et al., 2016), predominantly due to apoptosis of immature oligodendrocytes (Brambrink et al., 2012; Ikonomidou et al., 2022). The apoptosis (following anesthesia) preferentially impacts immature oligodendrocytes (O4-positive) (Brambrink et al., 2012); and O4-positive immature oligodendrocytes express opalin at high levels. During periods of brain growth, immature oligodendrocytes require electrical activity of axons to regulate proliferation/oligodendrogenesis (Barres and Raff, 1993), myelination (Gibson et al., 2014), oligodendrocyte precursor survival (Hill et al., 2014), and axon selection (Hines et al., 2015). Similar findings suggest that synaptic vesicle release from neurons is necessary for normal myelination (Mensch et al., 2015). While speculative, it is thus possible that disruptions in the oligodendrocyte linage (consistent with decreased opalin expression), may be a secondary consequence of neuronal inhibition by anti-seizure medications. The degree to which myelination recovers, and the long-term consequences of impaired early myelination after anti-seizure medication exposure remain to be examined.

The only other omics-based study to assess drug toxicity after early-life exposure to PB used a proteomic approach (Kaindl et al., 2008) and identified 45 peptides that were acutely or chronically altered by PB exposure on P6. Of the 45 peptides, two overlap with the transcripts we identified here: parvalbumin, which was identified in our transcriptomic analysis, and GFAP, which was identified in our qPCR/histological analysis. The prior study identified a range of transcripts that were involved in oxidative stress and apoptosis, cell cycle function, and neurite outgrowth. While we did not identify any of the same hits in our transcriptomic analysis, we did note an upregulation of the Foxp2 transcription factor by PB exposure. This transcription factor is strongly associated with speech and language disorders in humans, and it coordinates a gene network that modulates neurite outgrowth (Vernes et al., 2011). Similarly, we found increased transcript levels for Disc1, a gene associated with schizophrenia after PB exposure. Disc1 is critical for neuronal differentiation, migration, and axon/dendrite targeting and growth (Soares et al., 2011). Interestingly, some phenotypes associated with early-life PB exposure are shared with schizophrenia, including impaired sensorimotor gating (Forcelli et al., 2012b; Gutherz et al., 2014), and we have previously reported additive toxicity of PB in the neonatal ventral hippocampal lesion model of schizophrenia (Bhardwaj et al., 2012). Finally, we also noted an increase in Cdkn1a (p21), a cell cycle inhibitor which has been associated with senescence/quiescent cell fates (Jurk et al., 2012; Gillispie et al., 2021), which may impact cell recovery after drug exposure induced injury.

There are several caveats to our present study. First, because our transcriptome-wide assessment was performed 72 h after drug exposure, it remains unclear which, if any of these changes are persistent beyond this period. Of the 5 transcripts we examined 3 months after exposure, *gad1* displayed the same profile as early after exposure (decrease with PB). *Pvalb* was increased in the LEV-treated group at 3 months, but not 3 days, and the decrease observed in the PB treated group at 3 days was absent at 3 months. The other three transcripts (*cd68, opalin, gfap*) each of which were dysregulated by PB at 3 days, did not differ between groups at 3 months. That said, even brief disruptions to developmental processes may set off long-lasting alterations. Moreover, we only evaluated transcript levels at 3 months, not protein expression, and these may be decoupled. Furthermore, we examined only a small set of transcripts at 3 months. Future studies examining later timepoints are therefore warranted. Second, while our focus was on the developing brain, it is unclear which, if any of these transcriptomic changes would also be observed in adult animals treated with AMSs. However, the functional significance of these changes may also differ dramatically between the neonatal and adult brain, as again, brief disruptions to function during development can alter the trajectory of brain development. Third, the present study was conducted in seizure-naïve animals; in a clinical setting these drugs are unlikely to be given to neonates in the absence of seizures or other pathology. However, these findings are also likely relevant to exposure *in utero* as the postnatal day 7 rat models a time range approximately equivalent to the end of the third trimester of pregnancy through early infancy in humans. The degree to which drug exposure interacts with a history of seizures is of clear relevance and is the topic of another ongoing study in our laboratory.

Here we present a transcriptomic profile comparing the effects of early life exposure to the two most common anti-seizure medications used to treat neonatal seizures. PB, is associated with acute neurotoxicity, impaired synaptic development, and long-term behavioral changes, induced changes in gene expression in 124 transcripts; LEV, avoids these toxicities in the developing brain and showed changes in only 15 transcripts. The transcript domains impacted centered around neuroactive receptor-ligand interactions, and transcripts linked to neurons, microglia, oligodendrocytes, and astrocytes. Together these data may provide a link between acute early life toxicity and lasting changes in brain function after exposure to PB.

Data availability statement

The datasets presented in this study can be found in online repositories. The names of the repository/repositories and accession number(s) can be found below: https://www.ncbi.nlm.nih.gov/geo/query/acc.cgi?acc=GSE247577.

Ethics statement

The animal study was approved by the Georgetown University Animal Care and Use Committee. The study was conducted in accordance with the local legislation and institutional requirements.

Author contributions

SQ: Data curation, Writing–review and editing, Writing–original draft, Visualization, Investigation, Formal Analysis, Conceptualization. TK: Writing – review and editing, Investigation. DM: Writing – review and editing, Investigation. CC-R: Writing – review and editing, Investigation. PF: Writing–review and editing, Writing–original draft, Supervision, Project administration, Funding acquisition, Formal Analysis, Data curation, Conceptualization.

Funding

The author(s) declare that financial support was received for the research, authorship, and/or publication of this article. This work was supported by R01HD091994 to PF. TK was supported by F99NS129108. DM was supported by 5T32GM142520. The Genomics and Epigenomics Shared Resource is partially supported by NIH/NCI grant P30-CA051008.

Acknowledgments

We thank the Genomics and Epigenomics Shared Resource at Georgetown for technical assistance.

Conflict of interest

The authors declare that the research was conducted in the absence of any commercial or financial relationships that could be construed as a potential conflict of interest.

The author(s) declared that they were an editorial board member of Frontiers, at the time of submission. This had no impact on the peer review process and the final decision.

Publisher's note

Supplementary material

The Supplementary Material for this article can be found online at: https://www.frontiersin.org/articles/10.3389/fphar.2024.1340691/full#supplementary-material

References

Al-Muhtasib, N., Sepulveda-Rodriguez, A., Vicini, S., and Forcelli, P. A. (2018). Neonatal phenobarbital exposure disrupts GABAergic synaptic maturation in rat CA1 neurons. *Epilepsia* 59, 333–344. doi:10.1111/epi.13990

Anderson, S. R., Roberts, J. M., Ghena, N., Irvin, E. A., Schwakopf, J., Cooperstein, I. B., et al. (2022). Neuronal apoptosis drives remodeling states of microglia and shifts in survival pathway dependence. *Elife* 11, e76564. doi:10.7554/eLife.76564

Barres, B. A., and Raff, M. C. (1993). Proliferation of oligodendrocyte precursor cells depends on electrical activity in axons. *Nature* 361, 258–260. doi:10.1038/361258a0

Bessis, A., Béchade, C., Bernard, D., and Roumier, A. (2007). Microglial control of neuronal death and synaptic properties. *Glia* 55, 233–238. doi:10.1002/glia.20459

Bhardwaj, S. K., Forcelli, P. A., Palchik, G., Gale, K., Srivastava, L. K., and Kondratyev, A. (2012). Neonatal exposure to phenobarbital potentiates schizophrenia-like behavioral outcomes in the rat. *Neuropharmacology* 62, 2337–2345. doi:10.1016/j.neuropharm.2012.02.001

Bittigau, P., Sifringer, M., Genz, K., Reith, E., Pospischil, D., Govindarajalu, S., et al. (2002). Antiepileptic drugs and apoptotic neurodegeneration in the developing brain. *Proc. Natl. Acad. Sci. U. S. A.* 99, 15089–15094. doi:10.1073/pnas.222550499

Bittigau, P., Sifringer, M., and Ikonomidou, C. (2003). Antiepileptic drugs and apoptosis in the developing brain. *Ann. N. Y. Acad. Sci.* 993, 103–114. doi:10.1111/j.1749-6632.2003.tb07517.x

Brambrink, A. M., Back, S. A., Riddle, A., Gong, X., Moravec, M. D., Dissen, G. A., et al. (2012). Isoflurane-induced apoptosis of oligodendrocytes in the neonatal primate brain. *Ann. Neurol.* 72, 525–535. doi:10.1002/ana.23652

Chavkin, C., Shoemaker, W. J., McGinty, J. F., Bayon, A., and Bloom, F. E. (1985). Characterization of the prodynorphin and proenkephalin neuropeptide systems in rat hippocampus. *J. Neurosci.* 5, 808–816. doi:10.1523/JNEUROSCI.05-03-00808.1985

Chen, J., Cai, F., Cao, J., Zhang, X., and Li, S. (2009). Long-term antiepileptic drug administration during early life inhibits hippocampal neurogenesis in the developing brain. *J. Neurosci. Res.* 87, 2898–2907. doi:10.1002/jnr.22125

Coles, L. D., Saletti, P. G., Lisgaras, C. P., Casillas-Espinosa, P. M., Liu, W., Li, Q., et al. (2023). Levetiracetam pharmacokinetics and brain uptake in a lateral fluid percussion injury rat model. *J. Pharmacol. Exp. Ther.* 386, 259–265. doi:10.1124/jpet.122.001377

Creeley, C., Dikranian, K., Dissen, G., Martin, L., Olney, J., and Brambrink, A. (2013a). Propofol-induced apoptosis of neurones and oligodendrocytes in fetal and neonatal rhesus macaque brain. *Br. J. Anaesth.* 110 (1), i29–i38. doi:10.1093/bja/aet173

Creeley, C. E., Dikranian, K. T., Dissen, G. A., Back, S. A., Olney, J. W., and Brambrink, A. M. (2014). Isoflurane-induced apoptosis of neurons and oligodendrocytes in the fetal rhesus macaque brain. *Anesthesiology* 120, 626–638. doi:10.1097/ALN.0000000000000037

Creeley, C. E., Dikranian, K. T., Johnson, S. A., Farber, N. B., and Olney, J. W. (2013b). Alcohol-induced apoptosis of oligodendrocytes in the fetal macaque brain. *Acta Neuropathol. Commun.* 1, 23. doi:10.1186/2051-5960-1-23

Dingemanse, J., van Bree, J. B., and Danhof, M. (1989). Pharmacokinetic modeling of the anticonvulsant action of phenobarbital in rats. *J. Pharmacol. Exp. Ther.* 249, 601–608.

Dobbing, J., and Sands, J. (1979). Comparative aspects of the brain growth spurt. *Early Hum. Dev.* 3, 79–83. doi:10.1016/0378-3782(79)90022-7

Dobin, A., Davis, C. A., Schlesinger, F., Drenkow, J., Zaleski, C., Jha, S., et al. (2013). STAR: ultrafast universal RNA-seq aligner. *Bioinformatics* 29, 15–21. doi:10.1093/bioinformatics/bts635

Edgar, R., Domrachev, M., and Lash, A. E. (2002). Gene Expression Omnibus: NCBI gene expression and hybridization array data repository. *Nucleic Acids Res.* 30, 207–210. doi:10.1093/nar/30.1.207

Fakira, A. K., Lueptow, L. M., Trimbake, N. A., and Devi, L. A. (2021). PEN receptor GPR83 in anxiety-like behaviors: differential regulation in global vs amygdalar knockdown. *Front. Neurosci.* 15, 675769. doi:10.3389/fnins.2021.675769

Farwell, J. R., Lee, Y. J., Hirtz, D. G., Sulzbacher, S. I., Ellenberg, J. H., and Nelson, K. B. (1990). Phenobarbital for febrile seizures--effects on intelligence and on seizure recurrence. *N. Engl. J. Med.* 322, 364–369. doi:10.1056/NEJM199002083220604

Ferrer, I., Bernet, E., Soriano, E., del Rio, T., and Fonseca, M. (1990). Naturally occurring cell death in the cerebral cortex of the rat and removal of dead cells by transitory phagocytes. *Neuroscience* 39, 451–458. doi:10.1016/0306-4522(90)90281-8

Forcelli, P. A., Janssen, M. J., Vicini, S., and Gale, K. (2012a). Neonatal exposure to antiepileptic drugs disrupts striatal synaptic development. *Ann. Neurology* 72, 363–372. doi:10.1002/ana.23600

Forcelli, P. A., Kim, J., Kondratyev, A., and Gale, K. (2011). Pattern of antiepileptic drug-induced cell death in limbic regions of the neonatal rat brain. *Epilepsia* 52, e207–e211. doi:10.1111/j.1528-1167.2011.03297.x

Forcelli, P. A., Kozlowski, R., Snyder, C., Kondratyev, A., and Gale, K. (2012b). Effects of neonatal antiepileptic drug exposure on cognitive, emotional, and motor function in adult rats. *J. Pharmacol. Exp. Ther.* 340, 558–566. doi:10.1124/jpet.111.188862

Frankel, W. N., Valenzuela, A., Lutz, C. M., Johnson, E. W., Dietrich, W. F., and Coffin, J. M. (1995). New seizure frequency QTL and the complex genetics of epilepsy in EL mice. *Mamm. Genome* 6, 830–838. doi:10.1007/BF00292431

Gibson, E. M., Purger, D., Mount, C. W., Goldstein, A. K., Lin, G. L., Wood, L. S., et al. (2014). Neuronal activity promotes oligodendrogenesis and adaptive myelination in the mammalian brain. *Science* 344, 1252304. doi:10.1126/science.1252304

Gillispie, G. J., Sah, E., Krishnamurthy, S., Ahmidouch, M. Y., Zhang, B., and Orr, M. E. (2021). Evidence of the cellular senescence stress response in mitotically active brain cells—implications for cancer and neurodegeneration. *Life* 11, 153. doi:10.3390/life11020153

Gutherz, S. B., Kulick, C. V., Soper, C., Kondratyev, A., Gale, K., and Forcelli, P. A. (2014). Brief postnatal exposure to phenobarbital impairs passive avoidance learning and sensorimotor gating in rats. *Epilepsy Behav.* 37, 265–269. doi:10.1016/j.yebeh.2014.07.010

Hill, R. A., Patel, K. D., Goncalves, C. M., Grutzendler, J., and Nishiyama, A. (2014). Modulation of oligodendrocyte generation during a critical temporal window after NG2 cell division. *Nat. Neurosci.* 17, 1518–1527. doi:10.1038/nn.3815

Hines, J. H., Ravanelli, A. M., Schwindt, R., Scott, E. K., and Appel, B. (2015). Neuronal activity biases axon selection for myelination *in vivo*. *Nat. Neurosci.* 18, 683–689. doi:10.1038/nn.3992

Ikonomidou, C., Kirvassilis, G., Swiney, B. S., Wang, S. H., Huffman, J. N., Williams, S. L., et al. (2019). Mild hypothermia ameliorates anesthesia toxicity in the neonatal macaque brain. *Neurobiol. Dis.* 130, 104489. doi:10.1016/j.nbd.2019.104489

Ikonomidou, C., Scheer, I., Wilhelm, T., Juengling, F. D., Titze, K., Stöver, B., et al. (2007). Brain morphology alterations in the basal ganglia and the hypothalamus following prenatal exposure to antiepileptic drugs. *Eur. J. Paediatr. Neurol.* 11, 297–301. doi:10.1016/j.ejpn.2007.02.006

Ikonomidou, C., Wang, S. H., Fuhler, N. A., Larson, S., Capuano, S., Brunner, K. R., et al. (2022). Mild hypothermia fails to protect infant macaques from brain injury caused by prolonged exposure to Antiseizure drugs. *Neurobiol. Dis.* 171, 105814. doi:10.1016/j.nbd.2022.105814

Johne, M., Römermann, K., Hampel, P., Gailus, B., Theilmann, W., Ala-Kurikka, T., et al. (2021). Phenobarbital and midazolam suppress neonatal seizures in a noninvasive rat model of birth asphyxia, whereas bumetanide is ineffective. *Epilepsia* 62, 920–934. doi:10.1111/epi.16778

Jurk, D., Wang, C., Miwa, S., Maddick, M., Korolchuk, V., Tsolou, A., et al. (2012). Postmitotic neurons develop a p21-dependent senescence-like phenotype driven by a DNA damage response. *Aging Cell* 11, 996–1004. doi:10.1111/j.1474-9726.2012.00870.x

Kaindl, A. M., Koppelstaetter, A., Nebrich, G., Stuwe, J., Sifringer, M., Zabel, C., et al. (2008). Brief alteration of NMDA or GABAA receptor-mediated neurotransmission has long term effects on the developing cerebral cortex. *Mol. Cell Proteomics* 7, 2293–2310. doi:10.1074/mcp.M800030-MCP200

Kanehisa, M., Furumichi, M., Sato, Y., Kawashima, M., and Ishiguro-Watanabe, M. (2023). KEGG for taxonomy-based analysis of pathways and genomes. *Nucleic Acids Res.* 51, D587–D592. doi:10.1093/nar/gkac963

Kanehisa, M., and Goto, S. (2000). KEGG: kyoto encyclopedia of genes and genomes. *Nucleic Acids Res.* 28, 27–30. doi:10.1093/nar/28.1.27

Kaushal, S., Tamer, Z., Opoku, F., and Forcelli, P. A. (2016). Anticonvulsant drug-induced cell death in the developing white matter of the rodent brain. *Epilepsia* 57, 727–734. doi:10.1111/epi.13365

Kim, J., Kondratyev, A., and Gale, K. (2007). Antiepileptic drug-induced neuronal cell death in the immature brain: effects of carbamazepine, topiramate, and levetiracetam as monotherapy versus polytherapy. *J. Pharmacol. Exp. Ther.* 323, 165–173. doi:10.1124/jpet.107.126250

Kubova, H., and Mares, P. (1991). Anticonvulsant effects of phenobarbital and primidone during ontogenesis in rats. *Epilepsy Res.* 10, 148–155. doi:10.1016/0920-1211(91)90007-3

Lian, H., Yang, L., Cole, A., Sun, L., Chiang, A. C.-A., Fowler, S. W., et al. (2015). NFκB-activated astroglial release of complement C3 compromises neuronal morphology and function associated with Alzheimer's disease. *Neuron* 85, 101–115. doi:10.1016/j.neuron.2014.11.018

Love, M. I., Huber, W., and Anders, S. (2014). Moderated estimation of fold change and dispersion for RNA-seq data with DESeq2. *Genome Biol.* 15, 550. doi:10.1186/s13059-014-0550-8

Lueptow, L. M., Devi, L. A., and Fakira, A. K. (2018). Targeting the recently deorphanized receptor GPR83 for the treatment of immunological, neuroendocrine and neuropsychiatric disorders. *Prog. Mol. Biol. Transl. Sci.* 159, 1–25. doi:10.1016/bs.pmbts.2018.07.002

Manent, J.-B., Jorquera, I., Franco, V., Ben-Ari, Y., Perucca, E., and Represa, A. (2008). Antiepileptic drugs and brain maturation: fetal exposure to lamotrigine generates cortical malformations in rats. *Epilepsy Res.* 78, 131–139. doi:10.1016/j.eplepsyres.2007.10.014

Manthey, D., Asimiadou, S., Stefovska, V., Kaindl, A. M., Fassbender, J., Ikonomidou, C., et al. (2005). Sulthiame but not levetiracetam exerts neurotoxic effect in the developing rat brain. *Exp. Neurol.* 193, 497–503. doi:10.1016/j.expneurol.2005.01.006

McKenzie, A. T., Wang, M., Hauberg, M. E., Fullard, J. F., Kozlenkov, A., Keenan, A., et al. (2018). Brain cell type specific gene expression and Co-expression network architectures. *Sci. Rep.* 8, 8868. doi:10.1038/s41598-018-27293-5

Meador, K. J., Baker, G. A., Browning, N., Clayton-Smith, J., Combs-Cantrell, D. T., Cohen, M., et al. (2009). Cognitive function at 3 years of age after fetal exposure to antiepileptic drugs. *N. Engl. J. Med.* 360, 1597–1605. doi:10.1056/NEJMoa0803531

Meador, K. J., Baker, G. A., Browning, N., Cohen, M. J., Bromley, R. L., Clayton-Smith, J., et al. (2012). Effects of fetal antiepileptic drug exposure: outcomes at age 4.5 years. *Neurology* 78, 1207–1214. doi:10.1212/WNL.0b013e318250d824

Meador, K. J., Baker, G. A., Browning, N., Cohen, M. J., Bromley, R. L., Clayton-Smith, J., et al. (2013). Fetal antiepileptic drug exposure and cognitive outcomes at age 6 years (NEAD study): a prospective observational study. *Lancet Neurol.* 12, 244–252. doi:10.1016/S1474-4422(12)70323-X

Mensch, S., Baraban, M., Almeida, R., Czopka, T., Ausborn, J., El Manira, A., et al. (2015). Synaptic vesicle release regulates myelin sheath number of individual oligodendrocytes *in vivo*. *Nat. Neurosci.* 18, 628–630. doi:10.1038/nn.3991

National Research Council (U.S) (2011). *Guide for the care and use of laboratory animals*. 8th ed. Washington, D.C: National Academies Press.

Ozyurek, H., Bozkurt, A., Bilge, S., Ciftcioglu, E., Ilkaya, F., and Bas, D. B. (2010). Effect of prenatal levetiracetam exposure on motor and cognitive functions of rat offspring. *Brain Dev.* 32, 396–403. doi:10.1016/j.braindev.2009.05.003

Pekna, M., and Pekny, M. (2021). The complement system: a powerful modulator and effector of astrocyte function in the healthy and diseased central nervous system. *Cells* 10, 1812. doi:10.3390/cells10071812

Pelkey, K. A., Chittajallu, R., Craig, M. T., Tricoire, L., Wester, J. C., and McBain, C. J. (2017). Hippocampal GABAergic inhibitory interneurons. *Physiol. Rev.* 97, 1619–1747. doi:10.1152/physrev.00007.2017

Pereira de Vasconcelos, A., Colin, C., Desor, D., Divry, M., and Nehlig, A. (1990). Influence of early neonatal phenobarbital exposure on cerebral energy metabolism and behavior. *Exp. Neurol.* 108, 176–187. doi:10.1016/0014-4886(90)90025-n

Pick, C., and Yanai, J. (1984). Long-term reduction in spontaneous alternations after early exposure to phenobarbital. *Int. J. Dev. Neurosci.* 2, 223–228. doi:10.1016/0736-5748(84)90016-9

Polásek, R., Kubová, H., Slamberová, R., Mares, P., and Vorlícek, J. (1996). Suppression of cortical epileptic afterdischarges in developing rats by anticonvulsants increasing GABAergic inhibition. *Epilepsy Res.* 25, 177–184. doi:10.1016/s0920-1211(96)00077-0

Pressler, R. M., Abend, N. S., Auvin, S., Boylan, G., Brigo, F., Cilio, M. R., et al. (2023). Treatment of seizures in the neonate: guidelines and consensus-based recommendations-special report from the ILAE task force on neonatal seizures. *Epilepsia* 64, 2550–2570. doi:10.1111/epi.17745

Qiao, M.-Y., Cui, H.-T., Zhao, L.-Z., Miao, J.-K., and Chen, Q.-X. (2021). Efficacy and safety of levetiracetam vs phenobarbital for neonatal seizures: a systematic review and meta-analysis. *Front. Neurol.* 12, 747745. doi:10.3389/fneur.2021.747745

Reinisch, J. M., Sanders, S. A., Mortensen, E. L., and Rubin, D. B. (1995). *In utero* exposure to phenobarbital and intelligence deficits in adult men. *JAMA* 274, 1518–1525. doi:10.1001/jama.274.19.1518

Rogel-Fuchs, Y., Newman, M. E., Trombka, D., Zahalka, E. A., and Yanai, J. (1992). Hippocampal cholinergic alterations and related behavioral deficits after early exposure to phenobarbital. *Brain Res. Bull.* 29, 1–6. doi:10.1016/0361-9230(92)90002-f

Sanchez Brualla, I., Ghosh, A., Gibatova, V., Quinlan, S., Witherspoon, E., Vicini, S., et al. (2023). Phenobarbital does not worsen outcomes of neonatal hypoxia on hippocampal LTP on rats. *Front. Neurol.* 14, 1295934. doi:10.3389/fneur.2023.1295934

Schafer, D. P., Lehrman, E. K., Kautzman, A. G., Koyama, R., Mardinly, A. R., Yamasaki, R., et al. (2012). Microglia sculpt postnatal neural circuits in an activity and complement-dependent manner. *Neuron* 74, 691–705. doi:10.1016/j.neuron.2012.03.026

Schafer, D. P., and Stevens, B. (2015). Microglia function in central nervous system development and plasticity. *Cold Spring Harb. Perspect. Biol.* 7, a020545. doi:10.1101/cshperspect.a020545

Seol, S., Kwon, J., and Kang, H. J. (2023). Cell type characterization of spatiotemporal gene co-expression modules in Down syndrome brain. *iScience* 26, 105884. doi:10.1016/j.isci.2022.105884

Sharpe, C., Reiner, G. E., Davis, S. L., Nespeca, M., Gold, J. J., Rasmussen, M., et al. (2020). Levetiracetam versus phenobarbital for neonatal seizures: a randomized controlled trial. *Pediatrics* 145, e20193182. doi:10.1542/peds.2019-3182

Shute, A. A., Cormier, R. J., Moulder, K. L., Benz, A., Isenberg, K. E., Zorumski, C. F., et al. (2005). Astrocytes exert a pro-apoptotic effect on neurons in postnatal hippocampal cultures. *Neuroscience* 131, 349–358. doi:10.1016/j.neuroscience.2004.11.025

Soares, D. C., Carlyle, B. C., Bradshaw, N. J., and Porteous, D. J. (2011). DISC1: structure, function, and therapeutic potential for major mental illness. *ACS Chem. Neurosci.* 2, 609–632. doi:10.1021/cn200062k

Stefovska, V. G., Uckermann, O., Czuczwar, M., Smitka, M., Czuczwar, P., Kis, J., et al. (2008). Sedative and anticonvulsant drugs suppress postnatal neurogenesis. *Ann. Neurol.* 64, 434–445. doi:10.1002/ana.21463

Sulzbacher, S., Farwell, J. R., Temkin, N., Lu, A. S., and Hirtz, D. G. (1999). Late cognitive effects of early treatment with phenobarbital. *Clin. Pediatr. (Phila)* 38, 387–394. doi:10.1177/000992289903800702

Tien, Y.-C., Liu, K., Pope, C., Wang, P., Ma, X., and Zhong, X. (2015). Dose of phenobarbital and age of treatment at early life are two key factors for the persistent induction of cytochrome P450 enzymes in adult mouse liver. *Drug Metab. Dispos.* 43, 1938–1945. doi:10.1124/dmd.115.066316

Velísek, L., Kubová, H., Velísková, J., Mares, P., and Ortová, M. (1992). Action of antiepileptic drugs against kainic acid-induced seizures and automatisms during ontogenesis in rats. *Epilepsia* 33, 987–993. doi:10.1111/j.1528-1157.1992.tb01748.x

Vernes, S. C., Oliver, P. L., Spiteri, E., Lockstone, H. E., Puliyadi, R., Taylor, J. M., et al. (2011). Foxp2 regulates gene networks implicated in neurite outgrowth in the developing brain. *PLoS Genet.* 7, e1002145. doi:10.1371/journal.pgen.1002145

Wakselman, S., Béchade, C., Roumier, A., Bernard, D., Triller, A., and Bessis, A. (2008). Developmental neuronal death in hippocampus requires the microglial CD11b integrin and DAP12 immunoreceptor. *J. Neurosci.* 28, 8138–8143. doi:10.1523/JNEUROSCI.1006-08.2008

Yang, Z., and Wang, K. K. W. (2015). Glial fibrillary acidic protein: from intermediate filament assembly and gliosis to neurobiomarker. *Trends Neurosci.* 38, 364–374. doi:10.1016/j.tins.2015.04.003

frontiers | Frontiers in Neurology

TYPE Original Research
PUBLISHED 23 April 2024
DOI 10.3389/fneur.2024.1330102

OPEN ACCESS

EDITED BY
Khojasteh Malekmohammad,
Shiraz University, Iran

REVIEWED BY
Antonio Gambardella,
University of Magna Graecia, Italy
Jerónimo Andrés Auzmendi,
Universidad de Buenos Aires, Argentina

*CORRESPONDENCE
Wen Yujun
1302085222@qq.com
Zhang Rui
zhang.rui@nxmu.edu.cn

†These authors have contributed equally to this work and share first authorship

RECEIVED 30 October 2023
ACCEPTED 26 March 2024
PUBLISHED 23 April 2024

CITATION
Xiaoyu C, Hongzhen Z, Nan P, Tengwei G, Yanan G, Yan G, Haiyan L, Li M, Haiya W, Yujun W and Rui Z (2024) Benzyl isothiocyanate ameliorates cognitive function in mice of chronic temporal lobe epilepsy. *Front. Neurol.* 15:1330102. doi: 10.3389/fneur.2024.1330102

Benzyl isothiocyanate ameliorates cognitive function in mice of chronic temporal lobe epilepsy

Chang Xiaoyu[1,2†], Zhou Hongzhen[3†], Peng Nan[3,4], Gao Tengwei[3,4], Gong Yanan[3], Guo Yan[3], La Haiyan[3], Ma Li[3], Wu Haiya[3,4], Wen Yujun[3*] and Zhang Rui[3,4*]

[1]School of Public Health and Management, Ningxia Medical University, Yinchuan, China, [2]Editorial Board of Journal of Ningxia Medical University, Yinchuan, China, [3]Ningxia Key Laboratory of Cerebrocranial Disease, Incubation Base of National Key Laboratory, Ningxia Medical University, Yinchuan, China, [4]Key Laboratory of Environmental Factors and Chronic Disease Control, Ningxia Medical University, Yinchuan, China

Objective: Temporal lobe epilepsy (TLE) is a prevalent refractory partial epilepsy seen in clinical practice, with most cases originating from the hippocampus and being characterized by impaired learning and memory. Oxidative stress plays a direct role in the development of epilepsy and neurodegeneration while promoting cognitive dysfunction. Previous research indicates that benzyl isothiocyanate (BITC) has antioxidative stress properties and contributes to neuroprotection. In this study, we aimed to investigate the neuroprotective effect of BITC on a lithium-pilocarpine-induced temporal lobe epileptic mice model.

Methods: We conducted Intellicage learning tests, Morris water maze, open field test, and step-down-type passive avoidance tests, respectively. In addition, body weight and brain-to-body ratio were calculated. Nissl staining, real-time quantitative PCR detection of nuclear factor erythroid 2-related factor 2 (Nrf2), heme oxygenase 1 (HO-1) and NAD(P)H dehydrogenase quinone 1(NQO1) were performed. Content of malondialdehyde (MDA) and activities of superoxide dismutase (SOD), glutathione peroxidase (GSH-Px) and total antioxidant capacity (T-AOC) were determined.

Results: Our results demonstrate that BITC enhances cognitive function and motor ability in mice, as determined by Intellicage learning tests, Morris water maze, open field test, and step-down-type passive avoidance tests, respectively. Epilepsy leads to the loss of neurons in the CA3 region, while BITC treatment plays a positive role in neuroprotection, especially in the cortex. In comparison to the control group, the EP group exhibited decreased transcription levels of HO-1 and NQO1, alongside reduced GSH-Px activity, while MDA content was elevated. Conversely, the BITC treatment group, when compared to the EP group, showed enhanced transcription levels of Nrf2, HO-1, and NQO1, along with increased GSH-Px activity, and a decrease in MDA content.

Conclusion: In summary, our study provides evidence that BITC can improve cognitive impairments in pilocarpine-induced epileptic mice, demonstrating significant antioxidant effects and neuroprotective properties. This highlights its potential as a phytochemical for managing the sequelae of epilepsy.

KEYWORDS

temporal lobe epilepsy, benzyl isothiocyanate, neuroprotective effect, cognitive function, Nrf2

1 Introduction

Epilepsy is a clinical syndrome characterized by highly synchronized abnormal neuronal discharges in the brain, resulting from various etiologies (1). It is a common neurological disorder, with approximately 30% of cases being refractory epilepsies (2). Among these, temporal lobe epilepsy is the most prevalent type (3). Patients with temporal lobe epilepsy often exhibit a wide range of cognitive dysfunctions, which significantly impairs their quality of life (4, 5). Good cognitive function is essential for daily activities that require perception, attention, memory, and other cognitive processes (6). However, temporal lobe epilepsy can cause structural abnormalities in multiple cognitive brain areas, slow down cognition, diffuse functional connections, and severely impair patients' cognitive function (7). Additionally, the increase in oxidative stress persists throughout the development of epilepsy, leading to neuronal damage and cognitive impairment (8). Intellicage learning tests, Morris water maze tests, open field tests, and step-down type passive avoidance tests are widely used to evaluate rodents' learning and memory abilities (9). Nerve cells are the most fundamental structural and functional units of the nervous system (10), and the number of nerve cells closely relates to cognitive function and memory ability. The hippocampal region is a vital component of the limbic system, which regulates learning, memory, and behavior (11). Therefore, the number of nerve cells and the results of neurobehavioral tests can reflect the neurodegenerative changes in animals to some extent. While surgery is the preferred method for the treatment of refractory temporal lobe epilepsy, it carries an elevated risk, a high cost, and many factors that affect the outcome (3). Therefore, there is an ongoing need for research and application of economic, safe, and effective antiepileptic drugs in temporal lobe epilepsy.

In recent years, the bioactive substances in cruciferous vegetables have attracted great attention in the field of health and wellness. Phenolic compounds, organic sulfides, carotenoids, and vitamins collectively contribute to the health-promoting attributes of cruciferous vegetables (12). Among these, benzyl isothiocyanate (BITC) is a natural component with remarkable properties. Numerous studies have demonstrated that BITC has a variety of beneficial effects, including anti-inflammatory, antioxidant, anti-cancer, and cytoprotective properties (13–15). BITC has been the subject of several studies due to its potential in modulating the levels of malondialdehyde (MDA), catalase (CAT), superoxide dismutase (SOD), and glutathione peroxidase (GSH-Px), and enhancing the cellular antioxidant defense mechanism (16). The nuclear factor erythroid 2-related factor 2 (Nrf2) pathway plays a vital role in the regulation of antioxidant enzymes (17). Moreover, the ability of BITC to modulate inflammation, oxidative stress, and apoptosis through Nrf2/ heme oxygenase 1 (HO-1) and nuclear factor kappa-B (NF-κB) signaling pathways has been highlighted (13). It has been suggested that some plant-derived phytochemicals, including BITC, could be effective in the prevention and/or management of diseases associated with oxidative stress and inflammation (18). Despite the insights provided by previous studies regarding the molecular role of BITC, there are still significant gaps, particularly in understanding its potential impact on neurological function, especially in pilocarpine-induced epileptic mice. The complex interaction between bioactive compounds and neurological function remains a compelling area of inquiry. Consequently, this study aims to bridge this knowledge gap by investigating whether BITC can indeed improve the cognitive impairment in epileptic mice and play a neuroprotective role. By exploring this unknown aspect, our objective is to contribute valuable insights to the ongoing discussions on the multifaceted benefits of cruciferous vegetables and their potential applications in promoting neurohealth. This investigation is anticipated not only to enhance our comprehension of the impact of BITC, but also to pave the way for new therapeutic interventions in the field of cognitive health.

2 Materials and methods

2.1 Reagent

BITC (purity: ≥ 98.0%), pilocarpine (purity: ≥ 98%), and atropine (purity: ≥ 98.0%) were obtained from Sigma-Aldrich Corporation (St Louis, Missouri); lithium chloride was purchased from Tianjin Haijing Chemical Co. LTD (Tianjin, China); Nissl staining solution was obtained from Beyotime Corporation (Shanghai, China); total RNA extraction kit (Omega), reverse transcription kit, RT-PCR SYBR kit (Dalian Takara); GSH-Px, T-SOD, T-AOC, and MDA assay kits (Nanjing Jiancheng Bioengineering Institute). All other reagents were obtained from commercial sources with the highest purity available.

2.2 Animals and treatment

Healthy 20-week-old C57BL/6J mice were provided by Ningxia Medical University Experimental Animal Center (IACUC Animal code: SCXK (Ning) 2017-0001). Mice were kept in a 12-h cycle of light and dark, with temperatures controlled at 22°C ± 2°C, the humidity of 55% ± 15%, and food and water *ad libitum*. The Animal Care and Use Committee of Ningxia Medical University approved the experiment (no. NXMU2020-021), which complied with the National Institute of Health's Guide for the Care and Use of Laboratory Animals. All efforts were made to minimize suffering and the number of animals.

An acute epilepsy model in mice was established by randomly dividing male mice into three groups (11 per group): a control group, an epilepsy (EP) group, and an EP group treated with BITC (EP + BITC). Mice in the EP + BITC group were administered 10 mg/kg BITC dissolved in corn oil via gavage once daily; mice in the EP and control groups were injected with an equivalent volume of corn oil as a placebo, with the treatment lasting for 7 days. The temporal lobe epilepsy model in mice was induced as follows: first, lithium chloride (130 mg/kg body weight) was injected 18 h before the administration of pilocarpine (290 mg/kg body weight). Then, 2 h later, anesthesia was performed using isoflurane, and the brain was extracted. In each group, 3 mice were selected for perfusion to collect brain tissue, and the remaining 8 were used to obtain fresh brain tissue samples.

Status epileptic mouse model: Male mice were randomly divided into 3 groups ($n = 10$) by weight: a control group and epilepsy (EP) group with or without BITC treatment. Animal treatments are shown in timeline (Figure 1). Temporal lobe epilepsy was induced in epilepsy group and BITC intervention group (EP + BITC) at the beginning of the experiment whereas the mice in control group were treated with saline. The lithium-pilocarpine-induced temporal lobe epileptic mice was carried out as follows: Mice were injected with lithium chloride

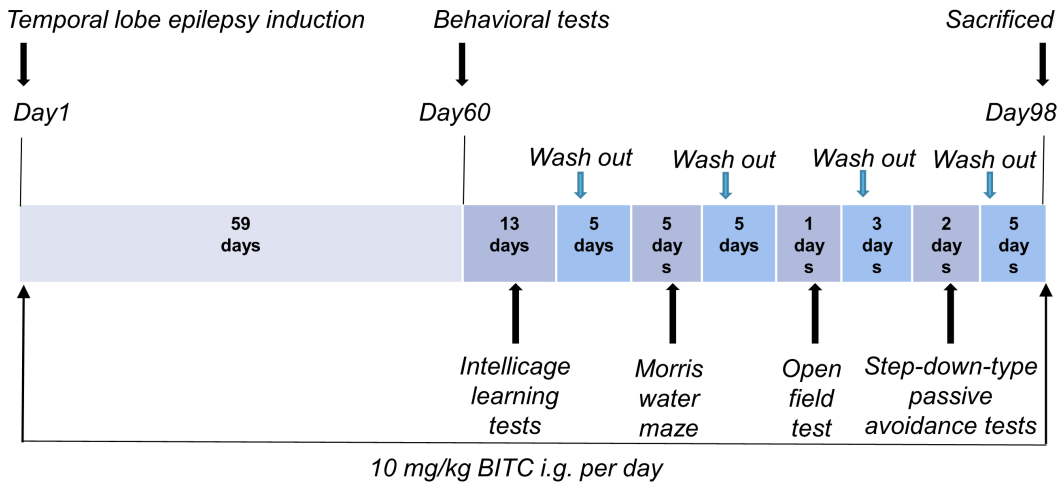

FIGURE 1
Scheme of animal treatments.

(130 mg/kg bodyweight, i.p.) 18 h before pilocarpine (290 mg/kg bodyweight, i.p.) injection. Mice in the EP + BITC group were treatment by gavage with 10 mg/kg BITC (dissolved in corn oil) once a day during the whole experiment, and mice in the EP group and control group were injected with gastric equivalent vehicle. All mice were weighed weekly.

Behavioral tests for mice were performed on the 60th days after treatment, and then animals were sacrificed 5 days after the last behavioral test to calculate brain-to-body weight ratio and to conduct Nissl's Staining.

2.3 Behavioral tests

The behavioral test for mice was performed in a quiet enclosed room at a temperature of 22 ± 2°C. There is a video camera connected to a computer directly above the center of the experimental area during Morris water maze, open field test, step-down-type passive avoidance tests.

2.3.1 Intellicage learning tests

Intellicage (TSE Systems GmbH, Germany) is equipped with four chambers located in four corners. Each chamber contains two water bottles and a transponder reader antenna that registers the microchip of the entering mice. Infrared beam-break sensors were programmed to keep open or closed upon nose-poke response. Microchips were implanted into subcutaneous part of nuchal region of each mouse to ensure data to be separated by each individual mouse. The experimental procedure was as follows [refer to previously described with major modification (19)]:

Divided into 5 parts:

Free exploration: The mice were allowed to explore freely and familiarize themselves with the environment for 3 days. All doors were opened, and all water bottles were available. The number of corner visits and numbers of drinks of each mouse were recorded.

Nose-poke learning: During these 3 days, all doors were closed initially, and mice need to nose-poke to open the door to drink water. The number of corner visits were recorded to calculate corner preference of each mouse.

Behavioral extinguishment: Mice were allowed to do free exploration for 1 day to extinguish the previous learning behavior.

Positive position learning: During 3 days of test, each mouse's least preferred corner was defined as "right" corner, while the remaining corners would be defined as "wrong" corners. The doors would be opened and the mice were allowed to drink after they nose-poked the "right" corner. The number of right visits and number of drinking were recorded to evaluate the positive position learning abilities of the mice.

Reversed position learning: During these 3 days, the opposite corner of the previous "right" corner would be defined as the new "right" corner, while the remaining corner would be defined as new "wrong" corners. The doors would be opened and the mice were allowed to drink after they nose-poked the "right" corner. The number of right visits and number of drinking were recorded to evaluate the reversed position learning abilities of the mice.

All mice were washed out for 5 days at the end of Intellicage learning tests.

2.3.2 Morris water maze

A five-day Morris water maze procedure was carried out as described previously (20) after Intellicage learning tests, and the escape latency in escape trials and the passing times in the probe trials were recorded. And the mice were washed out for 5 days at the end of Morris water maze.

2.3.3 Open field test

The test was executed as described previously (20) after Morris water maze, and immobility time in the central area (latency), times of cross grids, and times of uprights were recorded. A three-day wash-out period would be conducted after the open field test.

2.3.4 Step-down-type passive avoidance tests

YLS-3TB platform recorder (Yiyan Technology, Jinan, China) was used to conduct Step-Down-Type passive avoidance tests follow the

methods we described before (21). Escape latency and numbers of errors in training session and Step-down latency and numbers of errors in retention test were recorded.

The mice would be sacrificed after a five-day wash-out.

2.4 Brain-to-body weight ratio

After anesthetized with isoflurane, the mice were weighed, and brains were quickly isolated and washed with ice-cold saline. The brain-to-body weight ratio were calculated according to the following formula:

$$\text{Brain} - \text{to} - \text{body weight ratio} = \text{Brain mass}\left(\text{mg}\right) / \text{Weight}\left(\text{g}\right)$$

2.5 Nissl's staining

The brains from Bregma −2.5 mm to −3.5 mm were removed, post-fixed with 4% paraformaldehyde (pH 7.4), and dehydrated with 30% sucrose solution. Coronal sections (40 μm) were obtained with a cryostat and washed with phosphate buffer. After stained with crystal violet solution at 56°C for 30 min, followed by washing with distilled water. Sections were differentiated with 1% hydrochloric acid ethanol solution until the backgrounds were nearly colorless. Dehydration was carried out by 70% alcohol, 80% alcohol, and 95% alcohol, respectively, for 2 min, and then by anhydrous alcohol twice for 5 min. Then sections were transparentized with xylene, and sealed. The changes in the morphology and number of nerve cells in hippocampal CA1, CA3, and CORTEX areas were observed with an optical microscope.

2.6 Real-time quantitative PCR

Real-time quantitative PCR was employed to assess the mRNA levels of HO-1, NAD(P)H dehydrogenase quinone 1 (NQO1), and Nrf2 in the hippocampal tissues of diverse mouse groups. Initially, total RNA was extracted from each sample, and the total mRNA concentration was standardized to 500 ng/μL. Subsequently, mRNA underwent reverse transcription to form cDNA. The reverse transcription reaction system comprised: 5X PrimeScript RT Master Mix (Perfect Real Time) 2 μL, total mRNA 1 μL, and sterile water 7 μL.

GAPDH served as the internal reference, followed by PCR amplification. The specific primers were as follows:

HO-1 primers:

Forward: 5'-CAAGCCGAGAATGCTGAGTTCATG-3'

Reverse: 5'-GCAAGGGATGATTTCCTGCCAG-3'

NQO1 primers:

Forward: 5'-AGGATGGGAGGTACTCGAATC-3'

Reverse: 5'-AGGCGTCCTTCCTTATATGCTA-3'

Nrf2 primers:

Forward: 5'-AAAATCATTAACCTCCCTGTTGAT-3'

Reverse: 5'-CGGCGACTTTATTCTTACCTCTC-3'

The PCR amplification system comprised: TB Green Premix Ex Tap II 12.5 μL, forward primer 1 μL, reverse primer 1 μL, Sterile water 8.5 μL and cDNA 2 μL. Reaction conditions were as follows: pre-denaturation at 95°C for 30 s, followed by 40 cycles, each cycle involving denaturation at 95°C for 15 s, annealing at 58°C for 30 s, and extension at 72°C for 30 s.

2.7 Enzymatic assay measurements

Isolate the mouse cortex and use an ultrasonic tissue disruptor to prepare a 10% tissue homogenate, centrifuge at 2000 rpm for 15 min at 4°C, and carefully aspirate the supernatant. The activity of tissue T-SOD, MDA, GSH-Px, and total antioxidant capacity (T-AOC) were determined and calculated as follows. Protein concentration: Take the sample to be tested, add Coomassie Brilliant Blue G-250 solution for color development, mix thoroughly, then use an enzyme-linked immunosorbent assay reader at 595 nm wavelength for colorimetry, record the absorbance value and calculate the protein concentration in the solution based on the standard curve. T-SOD: Dilute the above tissue homogenate to 2.5%, add substrate and incubate at 37°C for 20 min, read with an ELISA reader at 450 nm, and calculate. SOD activity = (OD value after enzyme tube zeroing - OD value after non-enzyme tube zeroing) × 1,000 / (OD value after enzyme tube zeroing × 134 × 2.5% tissue homogenate protein concentration). MDA: Use a 10% tissue homogenate to prepare the reaction system, water bath at 95°C for 40 min, centrifuge at 3800 rpm for 10 min, read with an ELISA reader at 532 nm, and calculate. MDA content = [(OD value after zeroing – OD value after blank zeroing) × 10 / (OD value after standard zeroing – OD value after blank zeroing) × 10% tissue homogenate protein concentration × 10]. GSH-Px: Prepare a 2.5% tissue homogenate, color development after enzymatic reaction for 15 min, read with an ELISA reader at 412 nm, and calculate. GSH-Px activity = (OD value after non-enzyme tube zeroing – OD value after enzyme tube zeroing) × 5 / ((standard zeroing – blank zeroing) × 5 × 0.2 × 0.25% tissue homogenate protein concentration). T-AOC: Use a 10% tissue homogenate to prepare the reaction system, react at room temperature for 10 min, read with an ELISA reader at 520 nm, and calculate. T-AOC = (OD value – concentration after blank zeroing) × 10 / ((concentration after standard zeroing – concentration after blank zeroing) × 10% tissue homogenate protein concentration).

2.8 Statistical analyses

Parametric data were presented as means ± standard error of the means (Mean ± SEM). Data were plotted using GraphPad 9.0 software. If the data were normally distributed and had equal variance, one-way ANOVA was used for analysis, and LSD-t test was used for multiple comparisons between groups. Data that were not normally distributed were analyzed using the Kruskal-Wallis H test. $\alpha = 0.05$, $p < 0.05$ was considered statistically significant.

3 Results

3.1 Effect of BITC on epileptic mouse model and body weights

During the acute phase of epilepsy, there was no significant difference in the latency of seizure onset between the groups of mice ($p > 0.05$) (Supplementary Figure S1D). Compared to the control group, the average power of δ waves increased in the EP group and EP + BITC group ($p < 0.05$); there was no significant difference in the average power of δ waves between the EP group and EP + BITC group ($p > 0.05$) (Supplementary Figure S1E). During the treatment period,

no sign of significant toxicity was observed in all mice, and there were no significant differences ($p > 0.05$) in body weight of mice between groups for each week (Figure 2). The results indicate that the BITC treatment did not impact the latency of seizure onset or the average power of δ waves in mice. Additionally, the BITC treatment did not cause significant physiological alterations or modifications to the growth pattern of mice.

3.2 Intellicage learning tests

As shown in Figure 3, at free exploration part, there was no difference in terms of the number of visits and number of drinks between groups ($p > 0.05$). During positive position learning, mice in EP group with or without BITC treatment exhibited a smaller number of visits and drinks compared with mice in the control group ($p < 0.05$), while mice in EP + BITC group showed increased time of visits and drinks compared with the EP group ($p < 0.05$). During reversed position learning, the number of visits and drinks decreased in EP group compared with the control group ($p < 0.05$), while the number of visits increased in EP + BITC group compared with the EP group ($p < 0.05$). In summary, the Intellicage learning tests indicate that the EP group experienced cognitive deficits, particularly in spatial learning and memory tasks. However, BITC treatment appears to mitigate these deficits, showing a potential cognitive-enhancing effect. These results provide valuable information for understanding the impact of the experimental conditions on cognitive function in the mice.

3.3 Morris water maze

In terms of latency in escape trials of Morris water maze (Figure 4), there was no difference in the escape latency between groups in the first 2 days ($p > 0.05$), form day 3 to day 4, mice in the EP group showed prolonged escape latency compared with mice in the control group ($p < 0.05$), while EP + BITC mice had shorter escape latency compared with the EP mice ($p < 0.05$). In probe trial, the passing time significantly reduced in the EP mice compared with the control mice ($p < 0.05$), while a remarkable increase of passing time was found in the EP + BITC mice compared with the EP mice without BITC ($p < 0.05$). In conclusion, the Morris water maze results indicate that the EP group experienced deficits in spatial learning and memory, particularly during later phases of training and in the probe trial. However, BITC treatment appears to ameliorate these deficits, suggesting a potential therapeutic effect on cognitive function in the context of spatial memory tasks.

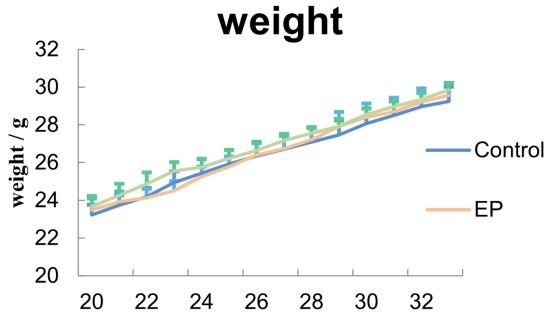

FIGURE 2
Measurement of mice body weight. During the treatment, no significant difference in body wights was observed between control, EP and EP + BITC mice ($n = 10$; mean ± S.E.M.; One-way ANOVA followed by *post hoc* least significant difference [LSD] multiple comparison tests).

3.4 Open field test

The results from open field test were shown in Figure 5. Compared with control, there was an obvious decrease in times of cross grids ($p < 0.05$), a longer latency in the central grid ($p < 0.05$), and a reduced times of upright ($p < 0.05$) in EP group. Meanwhile, a remarkable shorter latency in the central grid ($p < 0.05$) and an increased times of upright ($p < 0.05$) were observed in EP + BITC mice compared with EP mice. However, there is no difference in times of cross grids between EP with or without BITC ($p > 0.05$). To sum up, the open field test results suggest that the EP group exhibited altered exploratory and anxiety-like behaviors, while BITC treatment showed potential ameliorative effects. The anxiolytic-like effects of BITC are indicated by the improved performance in central grid latency and increased times of upright.

3.5 Step-down-type passive avoidance tests

As shown in Figure 6, in training session, EP mice showed longer escape latency ($p < 0.05$), while the mice in EP + BITC group exhibited no difference compared with the controls ($p > 0.05$). However, there was no significant difference in the number of errors between these three groups ($p > 0.05$). In addition, in retention test, there is no remarkable difference between groups ($p > 0.05$). Considering the above, the Step-Down-Type Passive Avoidance Tests indicate that the EP mice initially struggled with learning, as indicated by longer escape latency, but this impairment was mitigated by BITC treatment. The comparable number of errors and performance in the retention test suggest that the quality of learning and memory retention was not significantly affected by the experimental conditions.

3.6 Brain–body ratio

During the treatment, no significant difference in body weights was observed between control, EP and EP + BITC mice ($p > 0.05$) (Figure 7). The brain-to-body ratio results showed the overall health stability of mice throughout the treatment, which was the basis for an accurate explanation of other experimental results and emphasized the safety of the interventions applied.

3.7 Morphological staining

As shown in Immunofluorescence staining of NeuN (Supplementary Figures S2–S4), the mean fluorescence intensities of

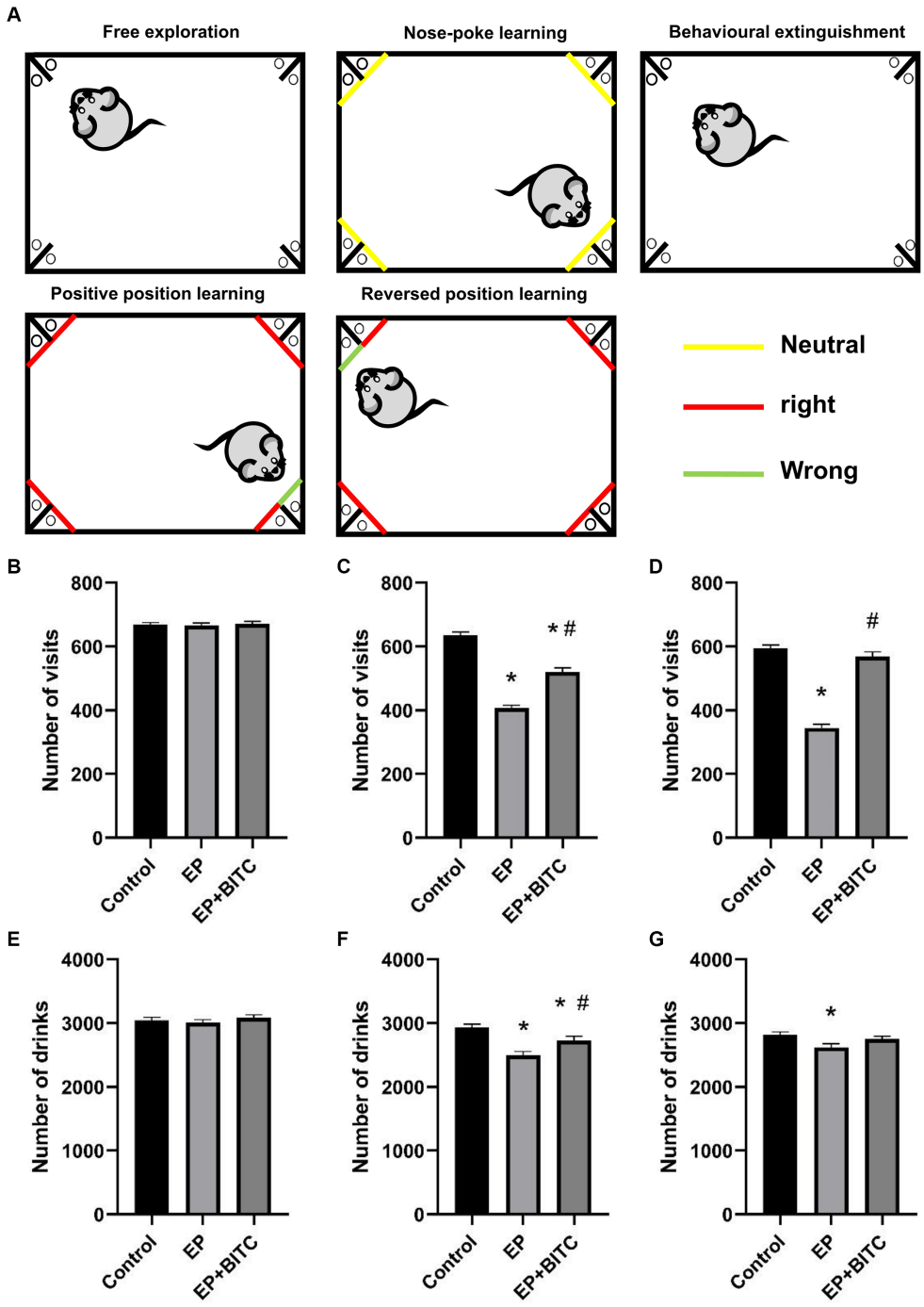

FIGURE 3
Intellicage. Analysis of Intellicage test in mice of control, EP, and EP + BITC ($n = 10$ per group; mean ± S.E.M.). **(A)** Intellicage learning module design. **(B)** The number of visits of three groups of mice in free exploration. No difference between the control, EP, and EP + BITC groups, $p > 0.05$. **(C)** The number of drinks of three groups of mice in free exploration. No difference in weight gain between the control, EP, and EP + BITC groups, $p > 0.05$. **(D)** The number of visits of three groups of mice in position learning. **(E)** The number of drinks of three groups of mice in position learning. **(F)** The number of visits of three groups of mice in reversal position learning. **(G)** The number of drinks of three groups of mice in reversal position learning. * Compared with control group: $p < 0.05$, # compared with EP group: $p < 0.05$. One-way ANOVA followed by *post hoc* least significant difference [LSD] multiple comparison tests.

the hippocampal CA1 and CA3 regions in acute seizure model mice showed no significant difference ($p > 0.05$); compared with the control group and EP group, the mean fluorescence intensity of the cortex in the EP + BITC group decreased slightly ($p < 0.05$). As shown in Nissl's staining of the chronic epilepsy state model (Figure 8), in terms of the number of cells in CA1 region of hippocampus, there was no difference between groups ($p > 0.05$). The EP mice showed decreased cells in CA3 compared with the control mice ($p < 0.05$). In addition,

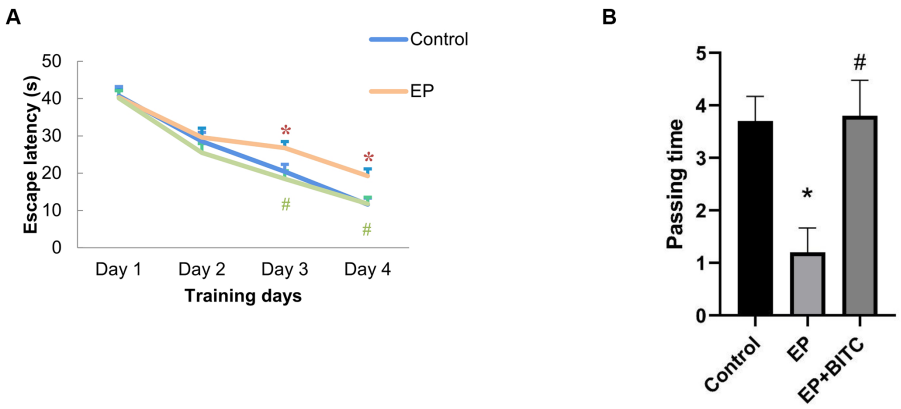

FIGURE 4
Morris water maze. Analysis of Morris water maze test in mice of control, EP, and EP + BITC ($n = 10$ per group; mean ± S.E.M.). **(A)** The escape latency of the three groups of mice during the 4 days of training. **(B)** The number of times the three groups of mice crossed the platform in the explore test. * Compared with control group: $p < 0.05$, # compared with EP group: $p < 0.05$. One-way ANOVA followed by *post hoc* least significant difference [LSD] multiple comparison tests.

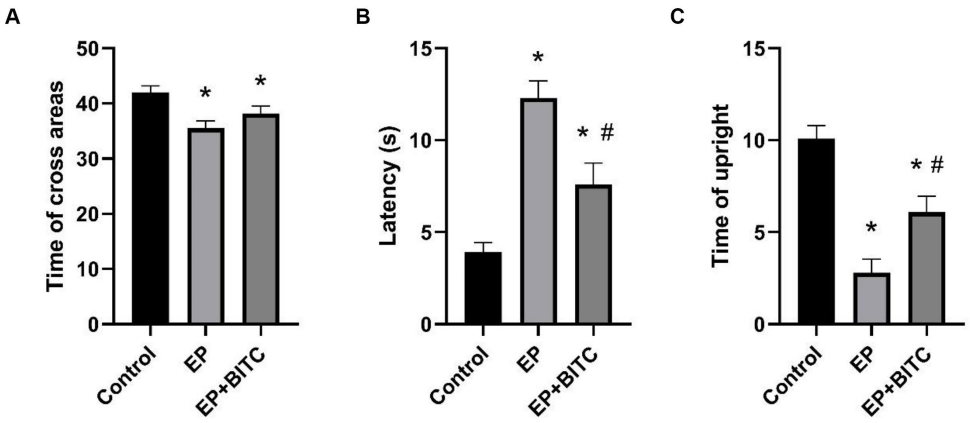

FIGURE 5
Open field test. Analysis of open field test in mice of control, EP, and EP + BITC ($n = 10$ per group; mean ± S.E.M.). **(A)** The three groups of mice crossed the areas times within 3 min. **(B)** The three groups of mice stayed in the central area within 3 min. **(C)** The upright times of three groups of mice within 3 min. * Compared with control group: $p < 0.05$, # compared with EP group: $p < 0.05$. One-way ANOVA followed by *post hoc* least significant difference [LSD] multiple comparison tests.

the number of cells in cortex was increased in EP + BITC group compared with the EP group ($p < 0.05$). These findings highlight the differential effects of epilepsy and BITC treatment on neuronal density in distinct brain regions. While epilepsy appears to induce neuronal loss in the CA3 region of the hippocampus, BITC treatment may exert neuroprotective effects, particularly evident in the cortex.

3.8 Real-time quantitative PCR

We investigated the transcription factor Nrf2, as well as two Nrf2-regulated enzymes, HO-1 and NQO1, in the transcriptional levels within the hippocampus. As shown in Figure 9, compared to the control group, the transcription levels of HO-1 and NQO1 in the EP group were significantly decreased ($p < 0.05$). Additionally, the treatment with BITC markedly increased the transcription levels of Nrf2, HO-1, and NQO1 in epileptic mice ($p < 0.05$). These results suggest that the antioxidant defense mechanism mediated by Nrf2 and its downstream targets may be damaged under epileptic conditions. The treatment of BITC enhanced the expression of Nrf2 and its downstream antioxidant enzymes, which potentially reduced oxidative stress and its harmful effects on hippocampal function in epileptic mice.

3.9 Determination of oxidative stress index in cerebral cortex of mice

In our study, we assessed the MDA levels and the activity of antioxidant enzymes in the cerebral cortex across various mouse groups. Figure 10 illustrates that, relative to the control group, the MDA levels in the EP group were elevated, while GSH-Px activity

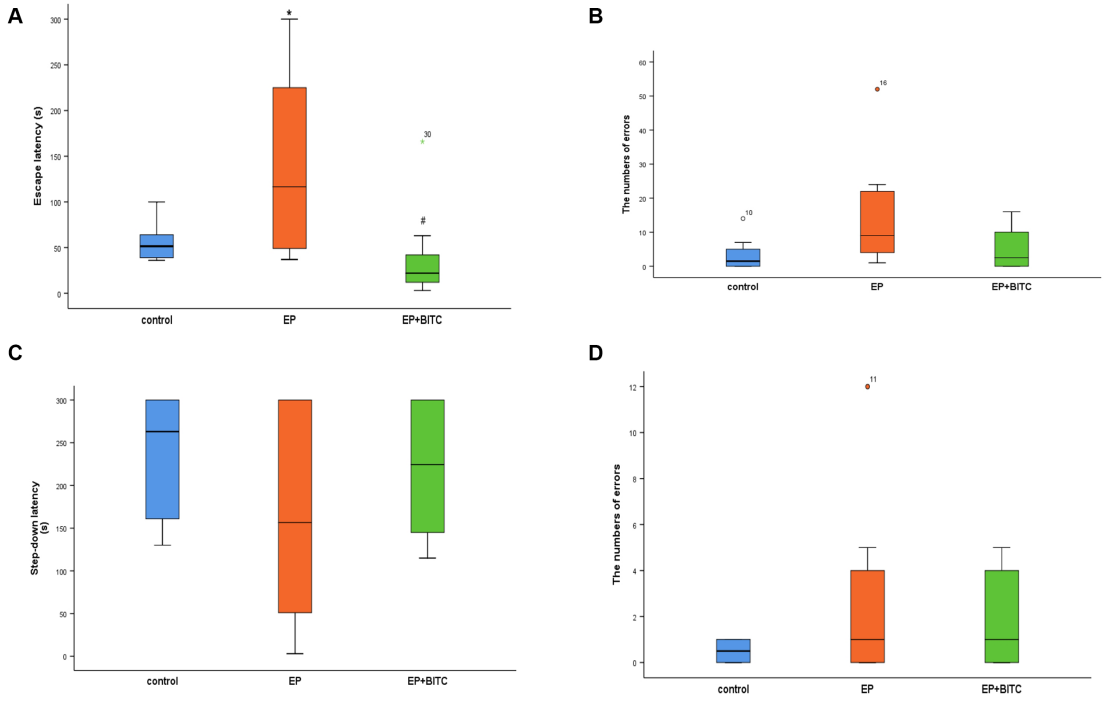

FIGURE 6
Step-down-type passive avoidance tests. Analysis of step-down-type passive avoidance tests in mice of control, EP, and EP + BITC ($n = 10$ per group; mean ± S.E.M.). **(A)** The escape latency of the three groups of mice during the training session. **(B)** The number of errors the three groups of mice jumped off the platform during the training session. **(C)** The Step-down latency of the three groups of mice during the retention session. **(D)** The number of errors the three groups of mice jumped off the platform during the retention session. * Compared with control group: $p < 0.05$, # compared with EP group: $p < 0.05$.; Analysis of significant differences using the Kruskar-Wallis test.

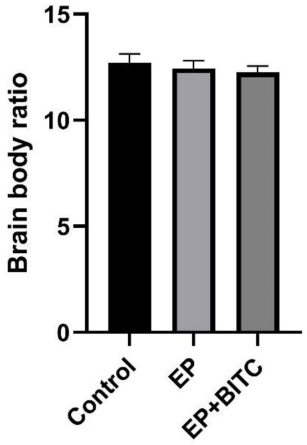

FIGURE 7
Brain-to-body weight ratio. Analysis of brain-to-body weight ratio in mice of control, EP, and EP + BITC. No difference between the control, EP, and EP + BITC groups ($n = 10$ per group; mean ± S.E.M.; $p > 0.05$. One-way ANOVA followed by *post hoc* least significant difference [LSD] multiple comparison tests).

diminished ($p < 0.05$). Conversely, in the BITC intervention group, MDA levels decreased, and GSH-Px activity increased when compared with the EP group ($p < 0.05$). Furthermore, the activities of T-AOC and SOD did not show significant differences across the groups. BITC might enhance the antioxidant defense mechanism, potentially by upregulating GSH-Px activity, thereby reducing lipid peroxidation as indicated by lower MDA levels. This implies that BITC could have therapeutic potential in mitigating oxidative stress-related neuronal damage in epilepsy.

4 Discussion

TLE is the most common form of intractable epilepsy (22). In clinical studies, TLE patients have been shown to have cognitive impairments (23). Chronic central nervous system dysfunction is usually accompanied with persistent and recurrent seizures (24). Reactive oxygen species (ROS) formation and consequent oxidative stress (OS) are reported to show a potential role in seizures and closely linked to neuroinflammation (25, 26). BITC, an extract of cruciferous vegetables, has been shown to have anti-inflammatory and antioxidative stress effects, as well as cytoprotective effects (16, 27). In the present study, we demonstrate that BITC exhibits improvements in cognitive dysfunction and neuroprotective effects in lithium pilocarpine-induced epileptic mice.

The lithium-pilocarpine-induced epilepsy model represents a durable, reliable, and cost-effective method with a short timeframe. Pilocarpine activates the M1 receptor, elevates glutamate levels, triggers NMDA receptor activation in the hippocampus, and induces hippocampal neuronal damage (28, 29). This model reproduces the majority of the clinical neuropathological features of TLE and closely resembles persistent epilepsy in humans (30). Sandro et al. found that long-term memory impairment in rats having early

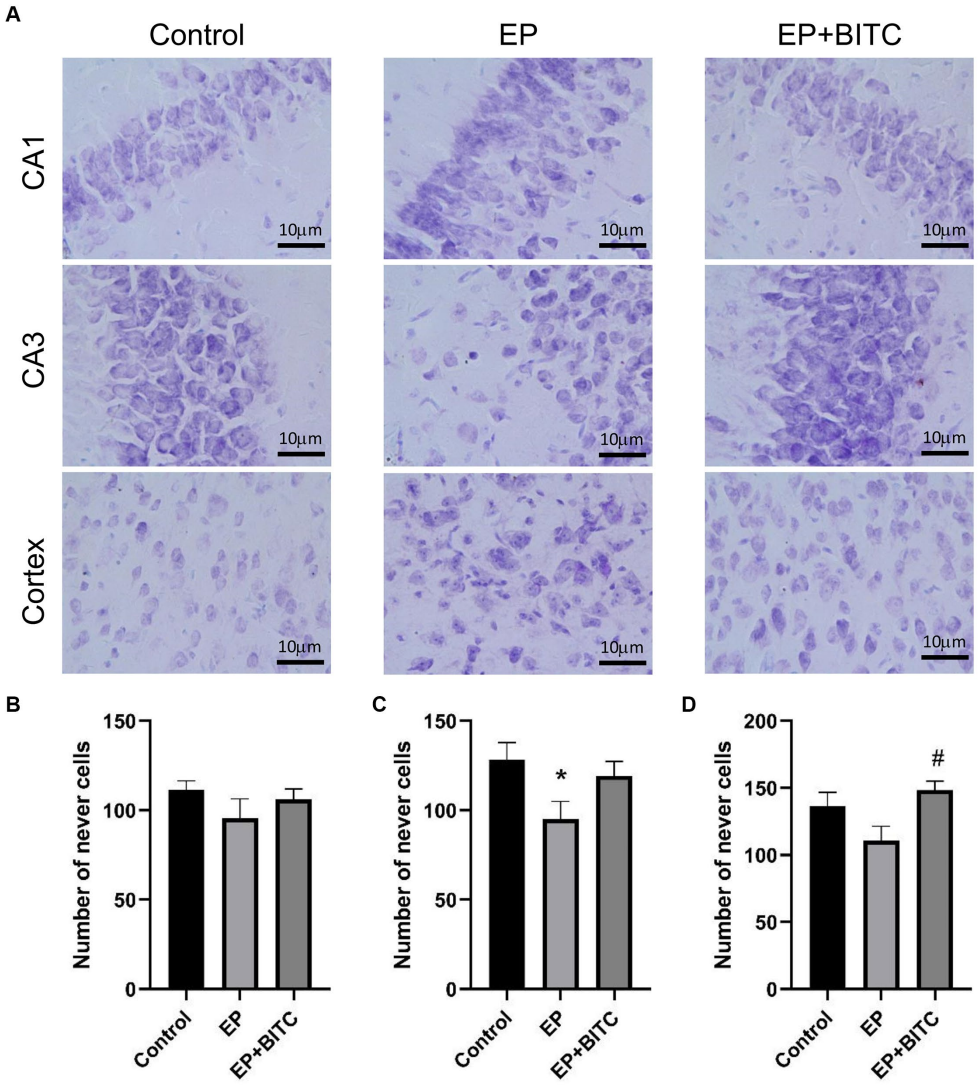

FIGURE 8
Nissl's staining. Analysis of Nissl's staining in mice of control, EP, and EP + BITC ($n = 10$ per group; mean ± S.E.M.). **(B)** The number of nerve cells in the CA1 region in the three groups of mice. No difference between the control, EP, and EP + BITC groups, $p > 0.05$. **(C)** The number of nerve cells in the CA3 region in the three groups of mice. **(D)** The number of nerve cells in the cortex region in the three groups of mice. * Compared with control group: $p < 0.05$, # compared with EP group: $p < 0.05$. One-way ANOVA followed by *post hoc* least significant difference [LSD] multiple comparison tests.

lithium-pilocarpine-induced epilepsy during object recognition tasks (31). Jia et al. used male C57BL/6J mice induced status epilepticus (SE) through pilocarpine hydrochloride injection (320 mg/kg) and conducted behavioral testing within 7–10 days post-surgery. SE reduced the recognition index of new and old objects in mice, leading to increased time spent in the central area during open field tests (32). Wu et al. performed the Morris water maze test on a lithium-pilocarpine-induced epileptic rat model, revealing a significant impairment in spatial memory function (33). The modeling method used in our experiment is similar to that of other experiments, and the results of the behavioral tests are consistent. Four different behavioral detection methods were used in this study. Intellicage learning tests can protect experimental animals from human interference, truly reflect the learning and memory abilities of experimental animals in their natural state and monitor the behavior of multiple experimental animals at the same time, unaffected by time series and other factors (34). Morris water maze is a classical behavioral experiment to study and evaluate the spatial learning and memory abilities of animals (9). Open field test can measure the anxiety, spontaneous activity, and exploratory behavior of experimental animals; Step-down-type passive avoidance tests are based on the fact that mice tend to jump on small platforms that are uncomfortable, and animals inhibit their behavior to avoid electric shocks, which is measured by longer delays or refusing to step down. Delay is used to evaluate memory. In our investigation, compared with the control group, epileptic mice exhibited a reduction in corner visits and drinking episodes, an extended escape latency, diminished occurrences of crossing the original platform, grid crossing, and standing frequency. Meanwhile, treatment with BITC had a positive effect on spatial cognition, exploratory behavior, and learning and memory abilities in epileptic

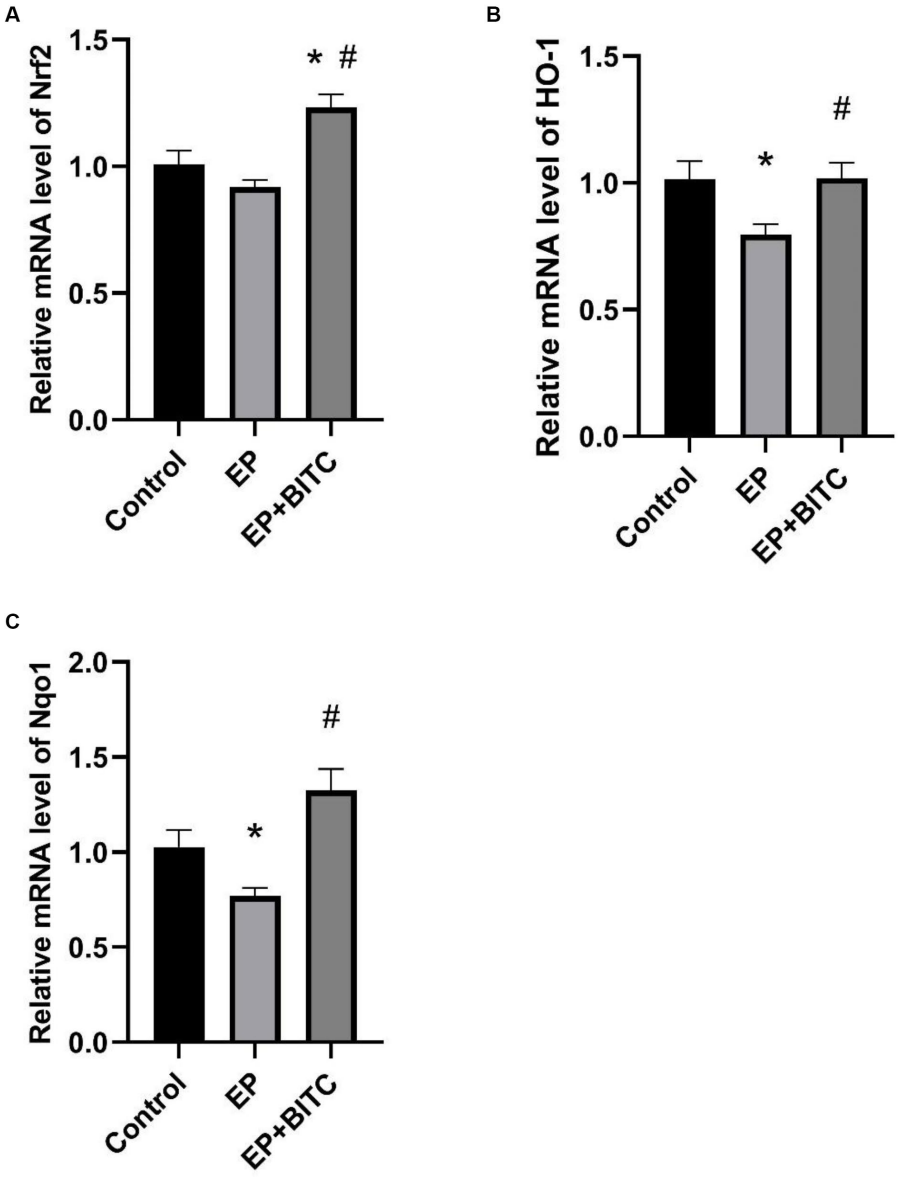

FIGURE 9
Analysis of mRNA levels of Nrf2, HO-1 and NQO1 from hippocampus between groups ($n = 8$ per group; mean ± S.E.M.). **(A)** Nrf2 transcription levels in hippocampus of three groups of mice. **(B)** HO-1 transcription levels in hippocampus of three groups of mice. **(C)** Nqo1 transcription levels in hippocampus of three groups of mice. * Compared with control group: $p < 0.05$, # compared with EP group: $p < 0.05$. One-way ANOVA followed by *post hoc* least significant difference [LSD] multiple comparison tests.

mice, with a significant enhancement in spatial cognition and learning and memory abilities.

The hippocampus plays an important role in spatial working memory (35). Chen et al. used Timm staining and transmission electron microscopy to observe the effect of pilocarpine-induced epilepsy on the CA3 region of the hippocampus in rats, and they observed abnormal mossy fiber sprouting (MFS) and vacuolar degeneration in the CA3 region of the model group (36). Alberto et al. used N-acetylcysteine and sulforaphane (SFN) as a temporary treatment for the epileptic rats and the results showed that it reduced the loss of hippocampal neurons and ameliorated cognitive impairments (37). Nissl staining can indicate the Nissl body of pyramidal cells in purple, and by observing the number of Nissl bodies, we can judge the damage in brain nerve cells and then the cognitive function of the brain. In our study, consistent with previous research, BITC treatment improved the number of neurons in the cortex and CA3 region of the hippocampus in epileptic mice and prevented the loss of neurons.

Cruciferous vegetables are recognized as abundant sources of isothiocyanates (ITCs), including sulforaphane (SFN) and BITC (38). These compounds demonstrate the capability to activate the Nrf2 pathway, associated with antioxidant and anti-inflammatory effects (39). The Nrf2 pathway plays a key role in up-regulating gene expression driven by antioxidant response elements (ARE), thereby reducing inflammation and providing cellular protection against oxidative stress (40, 41). Furthermore, the protective effects of Nrf2

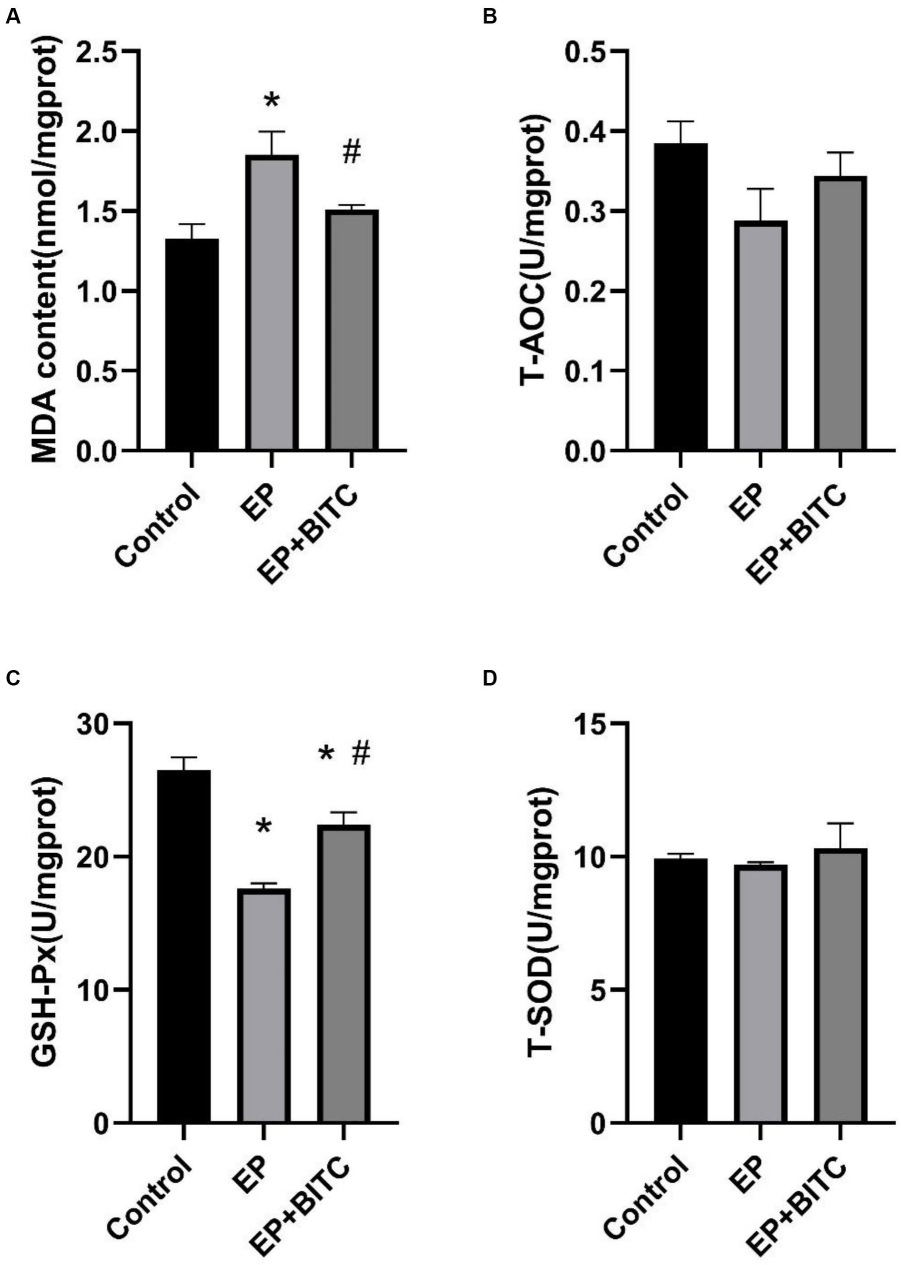

FIGURE 10
Analysis of MDA and anti-oxidative enzymes levels in cortex of mice between groups ($n = 8$ per group; mean ± S.E.M.). **(A)** The content of MDA in three groups of mice. **(B)** T-AOC activity of three groups of mice. No difference between the control, EP, and EP + BITC groups, $p > 0.05$. **(C)** GSH-Px activity of three groups of mice. **(D)** T-SOD activity of three groups of mice. No difference between the control, EP, and EP + BITC groups, $p > 0.05$. * Compared with control group: $p < 0.05$, # compared with EP group: $p < 0.05$. One-way ANOVA followed by *post hoc* least significant difference [LSD] multiple comparison tests.

and its signaling pathway have been confirmed in many disease models, such as vinblastine improving methotrexate-induced nephrotoxicity through Nrf2/HO-1 antioxidant pathway (42). These findings suggest that a targeted approach to Nrf2 holds therapeutic promise in conditions linked to oxidative stress and inflammation. In our experiment, BITC treatment increased the mRNA transcription levels of HO-1, NQO1, and Nrf2 in epileptic mice. This suggests that BITC may target the activation of Nrf2/HO-1 signal pathway in epileptic mice, play antioxidant and anti-inflammatory effects, and then protect hippocampal neurons from lithium pilocarpine-induced damage and improve cognitive impairment.

In summary, BITC exhibits neuroprotective effects on pilocarpine-induced epileptic mice. Treatment with BITC enhances the antioxidant capacity of the brain tissue in epileptic mice, improving cognitive impairments and neuronal damage caused by seizures. Our research provides scientific evidence that BITC is a candidate drug for the prevention and treatment of epilepsy and has great potential and value.

5 Limitations of our study

Due to limitations in funding and data recording, our research showed that BITC had no significant impact during the acute phase of epileptic seizures. However, we believe that BITC's potential in alleviating oxidative stress may provide neuroprotective effects in the chronic stages of epilepsy, emphasizing the need for further research to explore its full therapeutic potential. We highlight the critical role of oxidative stress in neurological diseases, including epilepsy, and the promising antioxidant capabilities of BITC. Although cognitive impairment often co-occurs with epilepsy, the complex interplay between oxidative stress, cognitive dysfunction, and epilepsy indicates potential therapeutic strategies worthy of in-depth investigation. Our goal is to extend our research through comparative analysis of BITC's effects in different epilepsy models, such as the PTZ model, to comprehensively understand its neuroprotective efficacy. Additionally, we plan to conduct seizure threshold tests in both pilocarpine and PTZ models to quantitatively assess BITC's neuroprotective abilities and investigate its mechanism of action, with a focus on its modulation of oxidative stress.

Data availability statement

The raw data supporting the conclusions of this article will be made available by the authors, without undue reservation.

Ethics statement

The animal study was approved by Ningxia Medical University Experimental Animal Center (IACUC Animal code: SCXK (Ning) 2017-0001) The Animal Care and Use Committee of Ningxia Medical University approved the experiment (No. NXMU2020-021). The study was conducted in accordance with the local legislation and institutional requirements.

Author contributions

CX: Writing – review & editing. ZH: Writing – original draft. PN: Writing – original draft. GT: Writing – original draft. GoY: Writing – original draft. GuY: Methodology, Writing – original draft. LH: Methodology, Writing – original draft. ML: Methodology, Writing – original draft. WH: Methodology, Writing – original draft. WY: Supervision, Writing – review & editing. ZR: Writing – review & editing.

Funding

The author(s) declare that financial support was received for the research, authorship, and/or publication of this article. This work was supported by Natural Science Foundation of Ningxia (Nos. 2022AAC05024, 2022AAC03175, and 2023AAC02032), National Natural Science Foundation of China (Nos. 82160617 and 82202431), Natural Science Research Project of Ningxia Medical University (No. XZ2019003), and Innovation and Entrepreneurship Projects for Returnees from Studying Abroad.

Acknowledgments

The authors wish to thank other members of the research group and the Ningxia Key Laboratory of Cerebrocranial Disease for their contributions to the project.

Conflict of interest

The authors declare that the research was conducted in the absence of any commercial or financial relationships that could be construed as a potential conflict of interest.

Publisher's note

Supplementary material

The Supplementary material for this article can be found online at: https://www.frontiersin.org/articles/10.3389/fneur.2024.1330102/full#supplementary-material

References

1. Fisher RS, Bonner AM. The revised definition and classification of epilepsy for neurodiagnostic technologists. *Neurodiagnostic J.* (2018) 58:1–10. doi: 10.1080/21646821.2018.1428455

2. Janmohamed M, Brodie MJ, Kwan P. Pharmacoresistance – epidemiology, mechanisms, and impact on epilepsy treatment. *Neuropharmacology*. (2020) 168:107790. doi: 10.1016/j.neuropharm.2019.107790

3. Milovanovic JR, Jankovic SM, Milovanovic D, Ruzic ZD, Folic M, Kostic M, et al. Contemporary surgical management of drug-resistant focal epilepsy. *Expert Rev Neurother*. (2020) 20:23–40. doi: 10.1080/14737175.2020.1676733

4. Carron S, Dezsi G, Ozturk E, Nithianantharajah J, Jones NC. Cognitive deficits in a rat model of temporal lobe epilepsy using touchscreen-based translational tools. *Epilepsia*. (2019) 60:1650–60. doi: 10.1111/epi.16291

5. Dey S, Dubey V, Dixit AB, Tripathi M, Chandra PS, Banerjee J. Differential levels of tryptophan–kynurenine pathway metabolites in the hippocampus, anterior temporal lobe, and neocortex in an animal model of temporal lobe epilepsy. *Cells*. (2022) 11:3560. doi: 10.3390/cells11223560

6. Johnson EL, Adams JN, Solbakk AK, Endestad T, Larsson PG, Ivanovic J, et al. Dynamic frontotemporal systems process space and time in working memory. *PLoS Biol*. (2018) 16:e2004274. doi: 10.1371/journal.pbio.2004274

7. Chang YA, Marshall A, Bahrami N, Mathur K, Javadi SS, Reyes A, et al. Differential sensitivity of structural, diffusion, and resting-state functional mri for detecting brain alterations and verbal memory impairment in temporal lobe epilepsy. *Epilepsia*. (2019) 60:935–47. doi: 10.1111/epi.14736

8. Wang M, Zhang X, Jia W, Zhang C, Boczek T, Harding M, et al. Circulating glutathione peroxidase and superoxide dismutase levels in patients with epilepsy: a

meta-analysis. *Seizure*. (2021) 91:278–86. doi: 10.1016/j.seizure.2021.07.001

9. Higaki A, Mogi M, Iwanami J, Min LJ, Bai HY, Shan BS, et al. Predicting outcome of Morris water maze test in vascular dementia mouse model with deep learning. *PLoS One*. (2018) 13:e191708. doi: 10.1371/journal.pone.0191708

10. Tsybina Y, Kastalskiy I, Krivonosov M, Zaikin A, Kazantsev V, Gorban AN, et al. Astrocytes mediate analogous memory in a multi-layer neuron–astrocyte network. *Neural Comput & Applic*. (2022) 34:9147–60. doi: 10.1007/s00521-022-06936-9

11. Kessels R, Bergmann HC. What does the hippocampus do during working-memory tasks? A cognitive-neuropsychological perspective. *Cogn Neurosci*. (2022) 13:210–1. doi: 10.1080/17588928.2022.2131745

12. Esteve M. Mechanisms underlying biological effects of cruciferous Glucosinolate-derived isothiocyanates/indoles: a focus on metabolic syndrome. *Front Nutr*. (2020) 7:111–1. doi: 10.3389/fnut.2020.00111

13. El BS, Ogaly HA, Abd-Elsalam RM, Azouz AA. Benzyl isothiocyanates modulate inflammation, oxidative stress, and apoptosis via nrf2/ho-1 and nf-kappab signaling pathways on indomethacin-induced gastric injury in rats. *Food Funct*. (2021) 12:6001–13. doi: 10.1039/d1fo00645b

14. Li Z, Wu H, Liu J, Hao H, Bi J, Hou H, et al. Synergistic effects of benzyl isothiocyanate and resveratrol against listeria monocytogenes and their application in chicken meat preservation. *Food Chem*. (2023) 419:135984. doi: 10.1016/j.foodchem.2023.135984

15. Mitra S, Emran TB, Chandran D, Zidan BMRM, Das R, Mamada SS, et al. Cruciferous vegetables as a treasure of functional foods bioactive compounds: targeting p53 family in gastrointestinal tract and associated cancers. *Front Nutr*. (2022) 9:951935. doi: 10.3389/fnut.2022.951935

16. Chuang WT, Yen CC, Huang CS, Chen HW, Lii CK. Benzyl isothiocyanate ameliorates high-fat diet-induced hyperglycemia by enhancing nrf2-dependent antioxidant defense-mediated irs-1/akt/tbc1d1 signaling and glut4 expression in skeletal muscle. *J Agric Food Chem*. (2020) 68:15228–38. doi: 10.1021/acs.jafc.0c06269

17. Ibrahim A, Al-Hizab FA, Abushouk AI, Abdel-Daim MM. Nephroprotective effects of benzyl isothiocyanate and resveratrol against cisplatin-induced oxidative stress and inflammation. *Front Pharmacol*. (2018) 9:1268. doi: 10.3389/fphar.2018.01268

18. Peluso I, Palmery M. Editorial: therapeutic index for nutraceuticals in inflammation-related diseases: efficacy, bioavailability, metabolism and interactions with drugs. *Front Pharmacol*. (2020) 11:61. doi: 10.3389/fphar.2020.00061

19. Wu N, Wang F, Jin Z, Zhang Z, Wang LK, Zhang C, et al. Effects of gaba(b) receptors in the insula on recognition memory observed with intellicage. *Behav Brain Funct*. (2017) 13:7. doi: 10.1186/s12993-017-0125-4

20. Zhang R, Miao QW, Zhu CX, Zhao Y, Liu L, Yang J, et al. Sulforaphane ameliorates neurobehavioral deficits and protects the brain from amyloid beta deposits and peroxidation in mice with Alzheimer-like lesions. *Am J Alzheimers Dis Other Dement*. (2015) 30:183–91. doi: 10.1177/1533317514542645

21. Zhang R, Zhang J, Fang L, Li X, Zhao Y, Shi W, et al. Neuroprotective effects of sulforaphane on cholinergic neurons in mice with Alzheimer's disease-like lesions. *Int J Mol Sci*. (2014) 15:14396–410. doi: 10.3390/ijms150814396

22. Yakimov AM, Timechko EE, Areshkina IG, Usoltseva AA, Yakovleva KD, Kantimirova EA, et al. MicroRNAs as biomarkers of surgical outcome in mesial temporal lobe epilepsy: a systematic review. *Int J Mol Sci*. (2023) 24:5694. doi: 10.3390/ijms24065694

23. Giovagnoli AR, Franceschetti S, Reati F, Parente A, Maccagnano C, Villani F, et al. Theory of mind in frontal and temporal lobe epilepsy: cognitive and neural aspects. *Epilepsia*. (2011) 52:1995–2002. doi: 10.1111/j.1528-1167.2011.03215.x

24. Lopez-Rivera JA, Smuk V, Leu C, Nasr G, Vegh D, Stefanski A, et al. Incidence and prevalence of major epilepsy-associated brain lesions. *Epilepsy Behav Rep*. (2022) 18:100527. doi: 10.1016/j.ebr.2022.100527

25. Geronzi U, Lotti F, Grosso S. Oxidative stress in epilepsy. *Expert Rev Neurother*. (2018) 18:427–34. doi: 10.1080/14737175.2018.1465410

26. Paudel YN, Shaikh MF, Shah S, Kumari Y, Othman I. Role of inflammation in epilepsy and neurobehavioral comorbidities: implication for therapy. *Eur J Pharmacol*. (2018) 837:145–55. doi: 10.1016/j.ejphar.2018.08.020

27. Park WS, Lee J, Na G, Park S, Seo S, Choi JS, et al. Benzyl isothiocyanate attenuates inflammasome activation in *Pseudomonas aeruginosa* LPS-stimulated THP-1 cells and exerts regulation through the MAPKs/NF-κB pathway. *Int J Mol Sci*. (2022) 23:1228. doi: 10.3390/ijms23031228

28. Kraus KL, Nawreen N, Godale CM, Chordia AP, Packard B, LaSarge CL, et al. Hippocampal glucocorticoid receptors modulate status epilepticus severity. *Neurobiol Dis*. (2023) 178:106014. doi: 10.1016/j.nbd.2023.106014

29. Meller S, Brandt C, Theilmann W, Klein J, Loscher W. Commonalities and differences in extracellular levels of hippocampal acetylcholine and amino acid neurotransmitters during status epilepticus and subsequent epileptogenesis in two rat models of temporal lobe epilepsy. *Brain Res*. (2019) 1712:109–23. doi: 10.1016/j.brainres.2019.01.034

30. André V, Dubé C, François J, Leroy C, Rigoulot MA, Roch C, et al. Pathogenesis and pharmacology of epilepsy in the lithium-pilocarpine model. *Epilepsia*. (2007) 48:41–7. doi: 10.1111/j.1528-1167.2007.01288.x

31. Cordova SD, Loss CM, de Oliveira DL. Low-intensity physical training recovers object recognition memory impairment in rats after early-life induced status epilepticus. *Int J Dev Neurosci*. (2013) 31:196–201. doi: 10.1016/j.ijdevneu.2013.01.002

32. Jia X, Wang Q, Ji J, Lu W, Liu Z, Tian H, et al. Mitochondrial transplantation ameliorates hippocampal damage following status epilepticus. *Anim Model Exp Med*. (2023) 6:41–50. doi: 10.1002/ame2.12310

33. Wu J, Wang L, Huang Y, Wu Q, Luo X, Li Y, et al. Cognitive impairment and mossy fiber sprouting in a rat model of drug-resistant epilepsy induced by lithium-pilocarpine. *Curr Neurovasc Res*. (2021) 18:374–80. doi: 10.2174/1567202618666210917155408

34. Kiryk A, Janusz A, Zglinicki B, Turkes E, Knapska E, Konopka W, et al. Intellicage as a tool for measuring mouse behavior - 20 years perspective. *Behav Brain Res*. (2020) 388:112620. doi: 10.1016/j.bbr.2020.112620

35. Song D, Wang D, Yang Q, Yan T, Wang Z, Yan Y, et al. The lateralization of left hippocampal ca3 during the retrieval of spatial working memory. *Nat Commun*. (2020) 11:2901. doi: 10.1038/s41467-020-16698-4

36. Jia C, Zhang R, Wei L, Xie J, Zhou S, Yin W, et al. Investigation of the mechanism of tanshinone iia to improve cognitive function via synaptic plasticity in epileptic rats. *Pharm Biol*. (2023) 61:100–10. doi: 10.1080/13880209.2022.2157843

37. Pauletti A, Terrone G, Shekh-Ahmad T, Salamone A, Ravizza T, Rizzi M, et al. Targeting oxidative stress improves disease outcomes in a rat model of acquired epilepsy. *Brain*. (2019) 142:e39. doi: 10.1093/brain/awz130

38. Kim SY, Park JE, Kim EO, Lim SJ, Nam EJ, Yun JH, et al. Exposure of kale root to nacl and na(2) seo(3) increases isothiocyanate levels and nrf2 signalling without reducing plant root growth. *Sci Rep*. (2018) 8:3999. doi: 10.1038/s41598-018-22411-9

39. Kubo E, Chhunchha B, Singh P, Sasaki H, Singh DP. Sulforaphane reactivates cellular antioxidant defense by inducing nrf2/are/prdx6 activity during aging and oxidative stress. *Sci Rep*. (2017) 7:14130. doi: 10.1038/s41598-017-14520-8

40. Albarakati A, Baty RS, Aljoudi AM, Habotta OA, Elmahallawy EK, Kassab RB, et al. Luteolin protects against lead acetate-induced nephrotoxicity through antioxidant, anti-inflammatory, anti-apoptotic, and nrf2/ho-1 signaling pathways. *Mol Biol Rep*. (2020) 47:2591–603. doi: 10.1007/s11033-020-05346-1

41. McMahon M, Itoh K, Yamamoto M, Hayes JD. Keap1-dependent proteasomal degradation of transcription factor nrf2 contributes to the negative regulation of antioxidant response element-driven gene expression. *J Biol Chem*. (2003) 278:21592–600. doi: 10.1074/jbc.M300931200

42. Shalaby YM, Menze ET, Azab SS, Awad AS. Involvement of nrf2/ho-1 antioxidant signaling and nf-κb inflammatory response in the potential protective effects of vincamine against methotrexate-induced nephrotoxicity in rats: cross talk between nephrotoxicity and neurotoxicity. *Arch Toxicol*. (2019) 93:1417–31. doi: 10.1007/s00204-019-02429-2

frontiers | Frontiers in Cellular Neuroscience

TYPE Original Research
PUBLISHED 22 May 2024
DOI 10.3389/fncel.2024.1305867

OPEN ACCESS

EDITED BY
Antonio Gambardella,
University of Magna Graecia, Italy

REVIEWED BY
Mattia Bonzanni,
Tufts Medical Center, United States
Khojasteh Malekmohammad,
Shiraz University, Iran

*CORRESPONDENCE
Chaofeng Zhu
✉ zhuchaofeng@fjmu.edu.cn
Huapin Huang
✉ Huang@fjmu.edu.cn

†These authors share first authorship

RECEIVED 02 October 2023
ACCEPTED 15 April 2024
PUBLISHED 22 May 2024

CITATION
Lin M, Gong J, Wu L, Lin X, Zhang Y, Lin W, Huang H and Zhu C (2024) ADCY3: the pivotal gene in classical ketogenic diet for the treatment of epilepsy.
Front. Cell. Neurosci. 18:1305867.
doi: 10.3389/fncel.2024.1305867

ADCY3: the pivotal gene in classical ketogenic diet for the treatment of epilepsy

Mingxing Lin[1†], Jiayin Gong[2†], Luyan Wu[2†], Xin Lin[2], Yuying Zhang[2], Wanhui Lin[2], Huapin Huang[2,3,4*] and Chaofeng Zhu[2*]

[1]Department of Pediatrics, Fujian Medical University Union Hospital, Fuzhou, China, [2]Department of Neurology, Fujian Medical University Union Hospital, Fuzhou, China, [3]Fujian Key Laboratory of Molecular Neurology, Fuzhou, China, [4]Department of Geriatrics, Fujian Medical University Union Hospital, Fuzhou, China

Objective: Epilepsy is a common neurological disorder characterized by recurrent epilepsy episodes. As a non-pharmacological treatment, the ketogenic diet has been widely applied in treating epilepsy. However, the exact therapeutic mechanism of the ketogenic diet for epilepsy remains unclear. This study investigates the molecular mechanisms of the ketogenic diet in regulating fatty acid metabolism and activating the ADCY3-initiated cAMP signaling pathway to enhance neuronal inhibition and thereby treat epilepsy.

Methods and results: Meta-analysis reveals that the ketogenic diet is superior to the conventional diet in treating epilepsy. Animal experiments demonstrate that the ketogenic diet is more effective than the conventional diet in treating epilepsy, with the best results achieved using the classic ketogenic diet. Transcriptome sequencing analysis identifies six essential genes, among which ADCY3 shows increased expression in the ketogenic diet. In vivo experiments confirm that the activation of the cAMP-PKA signaling pathway by ADCY3 enhances neuronal inhibition and improves epilepsy control.

Conclusion: Clinical observations indicate that the ketogenic diet improves patient epilepsy episodes by regulating the ADCY3-initiated cAMP signaling pathway.

KEYWORDS

ketogenic diet, fatty acid metabolism, ADCY3, CAMP signaling pathway, epileptic epilepsy, neuronal inhibition

1 Introduction

Epilepsy remains a prevalent neurological disorder, manifesting in recurrent seizures that significantly impact the quality of life for many individuals (Beghi et al., 2015; Manford, 2017; Thijs et al., 2019; Levin et al., 2021). Although an array of anticonvulsants drugs are available, they fail to provide substantial relief for a significant subset of patients, either due to drug resistance or intolerable adverse effects (Klein et al., 2021). This prevailing issue underlines the pressing need for innovative and effective alternative treatments (Sorkpor and Ahn, 2021). One such promising non-pharmacological approach is the ketogenic diet, which has garnered empirical support for its potential therapeutic benefits in managing epilepsy (Sampaio, 2016; Paoli et al., 2020; Sourbron et al., 2020; Wells et al., 2020). Nonetheless, the intricate mechanisms underpinning its anticonvulsants effects remain partially obscured, necessitating further comprehensive exploration (Zhang et al., 2021a).

The ketogenic diet is fundamentally high in fats, moderate in proteins, and low in carbohydrates. It uniquely simulates a fasting state by inducing the production of β-hydroxybutyrate, a key metabolic product (Youm et al., 2015; Beam et al., 2021; Khoziainova et al., 2022). While the exact mechanisms of the anticonvulsants effects of the ketogenic diet are not fully understood, studies have shown that the diet can influence various metabolic pathways and signaling pathways in the brain, thereby reducing the frequency and severity of seizures (Zarnowska, 2020). Literature reports indicate that the ketogenic diet offers an effective alternative for children and adults with drug-resistant epilepsy, showing particular efficacy in certain epilepsy syndromes such as West syndrome, severe infantile spasms, myoclonic-astatic epilepsy, fever-related epilepsy syndromes, and drug-resistant idiopathic generalized or refractory epilepsy (Elia et al., 2017). Furthermore, in drug-resistant epilepsy, the ketogenic diet has demonstrated utility (Ułamek-Kozioł et al., 2019). Ketogenic diet-induced increase in circulating ketones may assist in the treatment of drug-resistant epileptic episodes (Rogawski et al., 2016). The production of ketone bodies in the liver as a result of the ketogenic diet helps control seizures through its anticonvulsant action (Cicek and Sanlier, 2023). When conventional anticonvulsants medications and anesthetics fail, the ketogenic diet presents a promising new adjunctive strategy for managing acute status epilepticus in the intensive care setting (McDonald and Cervenka, 2020). Research suggests that the ketogenic diet is high in fat and protein content but low in carbohydrates, with β-hydroxybutyrate being the primary ketone body produced during carbohydrate deficiency in the diet, believed to have neuroprotective effects (Polito et al., 2023). Additionally, studies on the ketogenic diet often consider β-hydroxybutyrate as a crucial marker (Lin et al., 2023; Martins et al., 2023; Poorshiri et al., 2023). Moreover, literature indicates that β-hydroxybutyrate is a byproduct of normal fatty acid oxidation metabolism. In animals, β-hydroxybutyrate serves not only as an intermediary metabolite but also as a significant regulatory molecule that can influence gene expression, lipid metabolism, neuronal function, and overall metabolic rate (Mierziak et al., 2021).

Fatty acid metabolism is a central feature of the ketogenic diet (Nagpal et al., 2019; Kraeuter et al., 2020). By enhancing fatty acid metabolism, the ketogenic diet can lead to the production of abundant β-hydroxybutyrate in the body (Koronowski et al., 2021; Basolo et al., 2022; Karagiannis et al., 2022). Recent studies have revealed a close relationship between fatty acid metabolism and epileptic seizures (Samanta, 2021). ADCY3 (Adenylate Cyclase 3), a crucial signaling molecule, is involved in regulating intracellular levels of cyclic adenosine monophosphate (cAMP) (Wu et al., 2016; Son et al., 2022; Gárriz et al., 2023). Research has detected miRNA in the cerebrospinal fluid of subjects, identifying potential target cells of ADCY3 including the choroid plexus, neurons, and microglial cells (Narayan et al., 2020). ADCY3 plays a significant role in neuronal excitability and is associated with severe depression (Yang et al., 2021). Furthermore, a study comparing two weight-loss diets has demonstrated that the ADCY3 gene is involved in regulating various metabolic processes, such as the development and function of adipose tissue, with specific regulatory effects depending on the nutrient intake levels (Goni et al., 2018). Therefore, we hypothesize that the ketogenic diet may regulate ADCY3 by promoting fatty acid metabolism, further activating the cAMP signaling pathway, influencing neuronal inhibition, and improving epileptic seizures.

To test this hypothesis, a comprehensive experimental design was implemented. Initially, a meta-analysis was conducted to evaluate the efficacy of ketogenic diet on epileptic seizures. Subsequently, animal experiments were carried out using an epilepsy mouse model to observe the effects of different types of ketogenic diets on seizure activity, assessing their anticonvulsants effects through indicators such as electroencephalograms. Furthermore, key genes and signaling pathways related to the ketogenic diet were identified through transcriptome sequencing and protein interaction analysis. Lastly, a mouse model overexpressing ADCY3 was constructed, followed by *in vivo* validation using a cAMP inhibitor, to elucidate the role of the ADCY3/cAMP signaling pathway in the ketogenic diet.

Our study results are expected to further elucidate the mechanistic role of ketogenic diet in treating epilepsy, providing a theoretical basis and new therapeutic strategies for its clinical application. Understanding the effects of ketogenic diet on fatty acid metabolism, ADCY3 activation of the cAMP signaling pathway, and regulatory mechanisms of neuronal inhibition holds significant importance for investigating the pathogenesis of epileptic seizures and treating related disorders.

2 Materials and methods

2.1 Meta-analysis

Searching computer databases such as PubMed, Cochrane Library, Embase, and Web of Science. The retrieval is set from the establishment of the database until April 2023. Search is performed using a combination of controlled vocabulary and free words. The retrieval terms primarily include: "Epilepsy" OR"Epilepsies," "Seizure Disorder," "Seizure Disorders," "Awakening Epilepsy," "Epilepsy, Awakening, "Epilepsy, Cryptogenic" OR"Cryptogenic Epilepsies" OR"Cryptogenic Epilepsy" OR"Epilepsies, Cryptogenic" OR"Aura" OR"Auras."

The inclusion criteria for the literature meets the principles of evidence-based medicine PICOS (P-patient, I-intervention, C-comparison intervention, O-outcomes): (1) Patient population: patients diagnosed with epilepsy; (2) Intervention: ketogenic diet (KD); Comparison group: comparison with regular diet or different KDs; (3) Study design: clinical randomized controlled trials; (4) Outcome measures: frequency of epileptic epilepsy, including epilepsy reduction ≥50% or epilepsy reduction ≥90% or no epilepsy; (5) Included literature should include general information about the patients, adverse reactions, follow-up, and number of dropouts.

Exclusion criteria include (1) non-randomized controlled trials (RCTs); (2) studies that do not include relevant outcome measures and treatment methods; (3) incomplete literature data integrity; (4) non-case–control experiments; (5) duplicate publications; (6) guidelines, conference reports, systematic reviews or abstract articles; (7) animal experiments; (8) non-English literature.

The literature included in the study was independently analyzed by two researchers. Use Endnote software to identify relevant literature by reading the titles, abstracts, and full texts to determine if they meet the inclusion criteria. Disagreements are resolved through consensus to ensure the objectivity and integrity of the data.

According to the Jadad scale, the methodological quality of incorporating data is evaluated based on four aspects: random

allocation method (appropriate, unclear, inappropriate), concealment of allocation scheme (appropriate, unclear, inappropriate), blinding method (appropriate, unclear, inappropriate), and follow-up records (present, absent). Scores 1 to 3 indicate low-quality research, while scores 4 to 7 represent high-quality research (Wells et al., 2020).

2.2 Generation of epileptic mouse model and sample acquisition

This experiment used healthy C57BL/6 male mice (weighing 20–30 g, 8–10 weeks old). All mice were purchased from the Experimental Animal Center of Guangdong Province and were housed in SPF-grade laboratories. The housing conditions met the standard requirements, including humidity (44–78%), temperature (17–20°C), lighting (12-h light–dark cycle), and access to food and water. The mice were acclimated to the experimental environment for 1 week. All mice were handled strictly with the ethical requirements for experimental animals and obtained approval from the Animal Ethics Committee for Experimentation.

The mice were randomly divided into six groups: a regular group of 10 mice (Control), a model group of 10 mice with epilepsy (Model), a group of 10 mice on a classical ketogenic diet (Model+KD), a group of mice on a medium-chain triglyceride ketogenic diet (Model+MCT), a group of mice on a modified Atkins diet (Model+MAD), and a group of mice on a low glycemic index ketogenic diet (Model+LGIT).

Proportions of nutrients in different types of ketogenic diets: Classic KD: fat content (80%); low carbohydrate content (5%); protein content (15%) (Neal et al., 2009). MCT: MCT composition contains two fatty acids, caprylic acid (C: 8.60%) and capric acid (C: 10.40%) (Hollis et al., 2018; Guimarães et al., 2019). MAD: carbohydrate content (7.6%), fat content (54.5%), protein (21.2%) (Gupta et al., 2021). LGIT: fat content (65%); low carbohydrate content (25%); protein content (10%) (Karimzadeh et al., 2014).

The KA (kainic acid) model is a classical model that simulates human temporal lobe epilepsy and is widely used in the study of refractory epilepsy drugs. Rodents can induce epileptic status after intraperitoneal injection of KA, which activates the limbic system (Grabenstatter et al., 2005).

Adult mice (20–30 g) were induced with a cell cytotoxic epilepsy model by intraperitoneal injection of KA (kainic acid) (55001ES10, Yeasen). Administer a low dose (5 mg/kg) every hour until mice exhibit a sustained epilepsy lasting longer than 3 h. After inducing epilepsy in each mouse, a subcutaneous injection of approximately 2.5 milliliters of lactated Ringer's solution (approval number: National Medical Products Administration H20059425, Jiseng) was administered (Grabenstatter et al., 2005; Modebadze et al., 2016; Ramazi et al., 2022). Record each mouse's epilepsy severity and convulsion duration according to the Racine Scale. In surviving mice, select mice that exhibit spontaneous and recurrent epilepsy within a few days and continue with subsequent experiments for several weeks. Inject an equivalent dose of normal saline into the control group. The standard experimental group and the epileptic mouse model group were fed a conventional diet, while the mice in different types of ketogenic diet groups were fed with different types of ketogenic feed (Wang et al., 2021) and purchased from the high-tech platform for experimental animal feed. We used a video monitoring method to continuously observe mice for 3 months and recorded information, including the frequency and duration of epileptic epilepsy (Modebadze et al., 2016; Wang et al., 2021).

To collect samples, excessive intraperitoneal injection of 0.5% pentobarbital sodium (controlled substance, contact customer service for purchase) or (P3761, Sigma) was used to euthanize the mice. Harvest the mouse brain hippocampal tissue and quickly wash the surface stains with physiological saline. Remove excess liquid and cut the tissue into specified sizes, collecting them in pre-chilled enzyme-free tubes. Place the tubes in liquid nitrogen and quickly freeze them at −80°C for storage after collecting all the samples (López-Rivera et al., 2023).

2.3 Generation of an animal model of overexpression of ADCY3 in epileptic mice

Divide the mice into four groups: oe-NC (overexpressing lentivirus negative control group), oe-ADCY3 (overexpressing lentivirus ADCY3 group), oe-ADCY3 + DMSO, and oe-ADCY3 + RMI12330A (cAMP inhibitor RMI 12330A) (Guellaen et al., 1977; Grupp et al., 1980; Griebel et al., 1991; Kim et al., 2019). Each group has 10 mice. The design customization service of RMI12330A is provided by Shanghai Yiji Bio-Technology Co., Ltd. Inducing epilepsy in mice using pilocarpine has been described earlier. After confirming the successful establishment of an epileptic mouse model, the ADCY3 overexpression was carried out using the lentiviral transduction method for 4 weeks. Subsequently, OE-ADCY3 + RMI12330A group mice were intraperitoneally injected with RMI 12330A (dissolved in DMSO at 15 mg/kg). The mice in the oe-ADCY3 + DMSO group were also injected with an equivalent dose of DMSO solution (Hong et al., 2013).

2.4 Lentivirus transfection

Epileptic mice overexpressing ADCY3 were constructed using a lentiviral transfection method. Initially, the pAcGFP plasmid vector was appropriately reconstructed by replacing the original CMV promoter with the SYN1 gene promoter. This promoter drives the expression of the SYN1 gene, producing Synapsin I protein, which exhibits specific expression within neurons, enabling the specific expression of ADCY3 in neuronal cells (Wang et al., 2018). Plasmid design, construction, and lentiviral packaging services were provided by Shanghai's Biotech Engineering Company. Four hundred nanogram of pAcGFP-ADCY3 was transfected into HEK293 cells (CL-0005) using Lipofectamine 2000, followed by validation, amplification, and purification to obtain the packaged lentivirus. Mice were secured in appropriate restraint devices, with the injection needle positioned at the base of the tail to ensure entry into the tail vein. Subsequently, the prepared lentivirus was slowly injected into the tail vein of the mice (titer: 5×10^6 TU/mL) once a week for a total of 4 weeks (Hong et al., 2013).

2.5 Ketogenic diet treatment for preparation of mouse models of epilepsy and injection of cAMP inhibitors

The methods for purchasing mice and establishing the epilepsy model were performed as described previously. Mice were randomly

assigned into two groups, with 10 mice in each group: KD group and KD + RMI 12330A group. Following the successful establishment of the epilepsy model, the mice were fed a ketogenic diet for 3 months. On the 90th day, mice in the KD + RMI 12330A group received an intraperitoneal injection of RMI 12330A (a cAMP inhibitor, 15 mg/kg), after which relevant parameters were measured and observed (Guellaen et al., 1977; Grupp et al., 1980; Biondi et al., 1990; Griebel et al., 1991; Hong et al., 2013; Kim et al., 2019).

2.6 Behavioral observation of mice (Racine scoring)

Evaluation criteria: R1: The mildest epileptic epilepsy is manifested as bright, flashing, or unusual sensations in the field of vision, referred to as photosensitivity or visual abnormalities, or localized muscle spasms, also known as focal epilepsy. R2: Mild epileptic epilepsy, characterized by local muscle twitching or jerking, which can spread to adjacent muscles, are called clonic epilepsy. R3: Moderate seizure, manifested as a grand mal seizure, where the patient suddenly loses consciousness, experiences muscle convulsions or stiffness, and may have symptoms such as foaming at the mouth and urinary incontinence. R4: Severe epileptic epilepsy, manifested as grand mal epilepsy, sudden intense emotional reactions such as fear or anger, possibly accompanied by loss of consciousness, muscle convulsions or stiffness, foaming at the mouth, incontinence, rapid breathing, etc. R5: The most severe epileptic epilepsy is characterized by a status epilepticus, which involves a prolonged period of unconsciousness until the epilepsy episode ends and may result in severe brain damage (Van Erum et al., 2019).

2.7 EEG measurements in epileptic mice

Anesthesia was induced in mice by intraperitoneal injection of 0.5% sodium pentobarbital at 50 mg/kg. Bipolar, coated stainless steel electrodes were implanted in the right CA3 region, with a single reference electrode and ground electrode fixed above the mouse brain cortex and cerebellum. Twenty-four hours after the implantation surgery, we used Pinnacle's Nervus EEG recording system to record a 12-h electroencephalogram (EEG). We define an epileptic epilepsy as a sustained high-amplitude rhythmic discharge (such as repeated spike waves, spike-and-wave complexes, and slow waves) lasting at least 5 s, with a frequency greater than 5 Hz and an amplitude greater than twice the baseline (Masino et al., 2011). Later, after 3 months of ketogenic treatment, the brainwave of the mice was recorded.

2.8 High-throughput transcriptome sequencing

Three hippocampal tissue samples were selected from the standard group, the epilepsy model group, and the classic ketogenic diet group, respectively. Each sample was extracted for at least 1 μg total RNA (AM1931, Thermo Fisher Scientific, Netherlands), followed by treatment with DNAse I and silica-membrane purification (74,134, Qiagen, Germany). RNA was quantified using the Qubit RNA HS Assay Kit (Q32852, Thermo Fisher Scientific) and diluted to a concentration of 100 ng/μl. Confirm the quality of total RNA using the Fragment Analyzer (Advanced Analytical Technologies, Germany). For samples with an RNA Quality Number (RQN) greater than or equal to 6, RNA library preparation will be conducted using protocols certified under ISO/IEC 17025 (TruSeq RNA Library Preparation Kit v2, Illumina, United States). After cDNA synthesis of enriched oligo (dT) beads and fragmented mRNA, adapter ligation and PCR amplification are performed. Sequencing with Illumina HiSeq 2500v4 sequencer using a 126 bp paired-end sequencing strategy. According to the manufacturer's protocol, each sample should be sequenced to a minimum depth of 12.5 Gbp, resulting in approximately 50 million read pairs. Perform image analysis, base calling, and quality control using Illumina data analysis pipeline RTA v1.18.64 and Bcl2fastq v1.8.4. RNAseq reads are provided in compressed Sanger FASTQ format.

Each input sample file is analyzed by FastQC (version 0.10.1). Known overexpressed sequences detected by FastQC were subjected to adapter trimming using cutadapt (version 1.2), with a minimum accepted read length set at 20 bp. Next, use a sickle (version 1.33) to trim low-quality bases. Each read is synchronized through a custom Python script to maintain correspondence and merged into a single file. Use the GSNAP alignment tool (version 2014–12–23) to align reads against the human reference genome GRCh38, with the options set for novel splicing discovery (−-novel splicing 1) and unique alignment (−-paths 1 and --quiet-if-excessive). The output SAM file is compressed, position sorted, and indexed using the Picard suite (version 1.141). Differentially expressed genes between the control group, model group, and classical ketogenic diet group samples were filtered using "Limma" in Python script (with thresholds of $|\log FC| > 1$ and p-value <0.05). Use Python script to draw the heatmap of differentially expressed genes, and also draw the volcano plot of differentially expressed genes and perform GO and KEGG enrichment analysis (Saeidian et al., 2020; Arindrarto et al., 2021; Wang et al., 2021).

2.9 RT-qPCR

Extract hippocampal tissues from the control, Model, and classic ketogenic diet group mice. Extract total RNA from hippocampal tissue using TRIzol reagent (15,596,026, ThermoFisher, United States). Reverse transcribe 1 μg of RNA into cDNA using oligo (dT) primer. The primer sequence can be found in Supplementary Table S1, and Shanghai Biochemical Co., Ltd. synthesized it Synthesize cDNA using Maxima Reverse Transcriptase (EP0751, Thermo Scientific). Using SYBR Green (K0222, Thermo Scientific) for RT-qPCR detection, three replicates were set for each sample. GAPDH serves as an internal reference. Calculate relative expression using the $2^{-\Delta\Delta Ct}$ method (Liang et al., 2017; Mazdeh et al., 2018; Wang et al., 2021).

2.10 Western blot

The hippocampus tissue was digested in RIPA buffer (Thermo Scientific, United States). Protein concentration was determined using the BCA (Bicinchoninic Acid) method, and quantification was performed with the BCA1 assay kit (Sigma-Aldrich, United States). The samples are separated on SDS/PAGE and transferred to a PVDF

membrane. Incubate the membrane in TBS buffer containing Tween-20 and 5% skim milk for 1 h. Incubation with the following antibodies was performed overnight at 4°C: MA5-32245 (VAV2, dilution 1:1000), PA5-35382 (ADCY3, dilution 1:2000), MA3-920 (CACNA1S, dilution 1:500), PA5-104261 (CALLM3, dilution 1:1000), MA1-157 (PRKACA, dilution 1:1000), PA5-104261 (GRIN2B, dilution 1:1000), MA1-083 (CREB), and BFNE84953 (pCREB). Incubate the membrane after washing, and then incubate with the HRP-conjugated secondary antibody (ab6721, Abcam, United Kingdom) in the same TBS buffer for 1 h. Wash the membrane with TBST for 5 min; repeat 3 times. For development, protein quantification analysis was performed using the Genesys imaging system (Gene Company Limited, UK) and ImageJ 1.80u software. Protein quantification analysis is performed by calculating the ratio of each protein's grayscale value to the internal reference's grayscale value, GAPDH (Zou et al., 2016; Wang et al., 2021). Repeat the experiment three times each time.

2.11 ELISA

Homogenized samples of mouse hippocampal tissue were collected, and the expression levels of cAMP (ab290713, from the United Kingdom) and PKA (JK-E3114, from Crysto Biotech in China) were detected using an enzyme-linked immunosorbent assay (ELISA) kit following the manufacturer's instructions (Ding et al., 2014; Ma et al., 2014).

2.12 Electrophysiological analysis

Mice were anesthetized with 0.5% pentobarbital sodium for brain extraction. The brain was quickly removed and placed in artificial cerebrospinal fluid (ACSF) for cooling. The ACSF composition consisted of: choline chloride 110 mM, $NaHCO_3$ 26 mM, d-glucose 10 mM, Na-ascorbate 11.6 mM, $MgCl_2$ 7 mM, Na-pyruvate 3.1 mM, KCl 2.5 mM, NaH_2PO_4 1.25 mM, and $CaCl_2$ 0.5 mM (Wickham et al., 2020). The VT-1000S vibrating microtome (Leica, Germany) cut longitudinal hippocampal slices (300 μm) in ACSF and transferred them to a regular ACSF storage chamber. The slices were maintained at a constant temperature of 32°C for 30 min before recording, followed by an additional hour at room temperature. All solutions are saturated with 95% O_2/5% CO_2 (vol/vol). Place the brain slices in the recording chamber and perfuse with ACSF at a 2 mL/min flow rate. Perform whole-cell patch clamp recordings on CA1 pyramidal neurons using an upright microscope with an infrared-sensitive CCD camera (DAGE-MTI, IR-1000E). The resistance value of the pipette is 3–5 MΩ, and the micropipette puller (P-97, Sutter instrument) is used for pulling. The recording was performed using the MultiClamp 700B amplifier and the 1440A digitizer (Molecular Devices). Recorded spontaneous inhibitory postsynaptic currents (sIPSCs) were maintained at −70 mV in the presence of 20 μM CNQX and 100 μM AP-5, and the pipette solution contained (in millimolar): 140 mM CsCl, 10 mM Hepes, 0.2 mM EGTA, 1 mM MgCl2, 4 mM Mg-ATP, 0.3 mM Na-GTP, 10 mM phosphocreatine, and 5 mM QX314 (pH 7.40, 285 mm). Measurements of evoked inhibitory postsynaptic currents (PSCs) were conducted with the stimulating electrode placed on the Schaffer Collaterals (SC)-CA1 pathway, approximately 100 micrometers away from the recording pipette (Wang et al., 2021).

2.13 Calcium imaging technology

Separate and culture neurons from the mouse brain in suspension in a culture medium. Then, add 1 microliter of Fluo4-AM (Beyotime. S1060) to 1 milliliter of DMEM solution and incubate the neurons for 30 min. Remove the Fluo4-AM solution, wash three times with HBSS solution (14170112), excite with fluorescence dye at 480 ± 15 nanometers, and measure fluorescence emission at 535 ± 25 nanometers. Capture images every 2 s using a digital camera (Nikon Corporation, Japan) and analyze them using ImageJ software (Ait Ouares et al., 2020; Yang et al., 2020). The fluorescence intensity of Fluo-4 was quantified in a minimum of 5 fields, each containing at least 100 cells. The average fluorescence intensity was computed for each field. Following this, the average fluorescence intensity of the control group (oe-NC or KD group) in every experiment was normalized to 100%. Subsequently, the relative fluorescence intensity of calcium ions in each experimental group was determined by calculating the ratio of its average fluorescence intensity to that of its respective control group (Wang et al., 2013).

2.14 Blood glucose and blood ketone monitoring

Measure the concentrations of blood ketones (β-hydroxybutyrate) and glucose using Abbott's blood glucose and ketone monitoring system (FreeStyle Optium Neo124434). According to the manufacturer's instructions, disinfect the mouse tail with 70% ethanol, then use clean scissors to cut off the tip and collect a drop of blood. Use Abbott test strips to measure levels of β-hydroxybutyrate or glucose (Wang et al., 2021).

2.15 Recruitment and other processing of clinical samples

This study involved a 6-month clinical observation of 60 epilepsy patients admitted to our hospital between January and June 2023. This study has been approved by the Clinical Ethics Committee of our hospital, and written informed consent has been obtained from the patients and their families, strictly adhering to the Helsinki Declaration. Inclusion criteria include: (1) Meeting the diagnostic criteria for epilepsy, including primary epilepsy, secondary epilepsy, focal epilepsy, and generalized epilepsy; (2) No improvement after treatment with two or more anticonvulsants drugs; (3) Age older than 3 years; (4) The study has obtained approval from the medical ethics committee. Exclusion criteria include: (1) individuals with disorders of lipid metabolism; (2) individuals with severe cardiovascular, pulmonary, renal, and hematologic diseases; (3) individuals with severe hepatic and renal impairment; (4) individuals with mental disorders, behavioral disorders, and language disorders; (5) pregnant women; (6) individuals who have used a ketogenic diet or had changes in anticonvulsants treatment in the past 12 months; (7) individuals who have experienced status epilepticus in the previous 6 months or have undergone surgical resection or vagus nerve stimulator implantation in the previous 12 months; (8) individuals with other conditions prohibiting the use of a ketogenic diet.

Eligible patients were randomly assigned into two groups using a computer-generated random number list: the Conventional Diet

Group (CAU) and the Classic Ketogenic Diet Group (KD), each consisting of 30 individuals. The KD group comprised 12 males and 18 females with a mean age of 14.53 years, while the CAU group included 10 males and 20 females with a mean age of 13.73 years (Neal et al., 2009; Sondhi et al., 2020).

Both groups underwent a one-week baseline observation period, during which each patient recorded detailed medical history and underwent examinations, including measurement of β-hydroxybutyrate, cholesterol, triglycerides, high-density lipoprotein, and low-density lipoprotein levels. The type, frequency, age of onset, family history, developmental status, and treatment history of epilepsy were also recorded. During hospitalization, participants in the diet group received dietary guidance, and family members collected data after patients were discharged. The CAU group received conventional anticonvulsants treatment and standard diet, while the KD group received adjunctive ketogenic diet treatment based on the CAU group's treatment. During the ketogenic diet therapy, daily meals should be prepared according to the principles of the KD diet. The recommended ratio of fats to proteins and carbohydrates is 4:1, with protein intake meeting the minimum requirement suggested by the World Health Organization (WHO). Adequate supplementation of sugar, calcium, and vitamins is also essential. For patients during the ketogenic diet therapy, assess the contraindications and adverse reactions of the ketogenic diet therapy, and evaluate the effectiveness of epilepsy treatment based on the grading criteria of the International League Against Epilepsy (ILAE). The standard is divided into the following four levels: (1) Complete epilepsy control: patients have not experienced any epilepsy for two consecutive years and are not using any anticonvulsants drugs; (2) improvement: patients have a reduction in epilepsy frequency of 75% or more; (3) Some improvement: patients have a reduction in epilepsy frequency of 50 to 74%; (4) Ineffective: patients have a reduction in epilepsy frequency of less than 50%, or there is no improvement in symptoms (Neal et al., 2009; Lambrechts et al., 2017; Kverneland et al., 2018).

During the 6 months of the study, the epilepsy frequency and duration of epileptic patients in the CAU and KD groups were assessed through observation and recording by family members or caregivers. Additionally, regular examinations, such as electroencephalograms, were conducted.

Before and after treatment, we collected peripheral venous blood samples (3 mL) from the patients and measured the levels of β-hydroxybutyrate, triglycerides (TG), cholesterol (HyperChol), high-density lipoprotein (HDL), and low-density lipoprotein (LDL).

Obtain 3 mL of a peripheral venous blood sample using venipuncture into an EDTA preparation tube, and detect the expression levels of ADCY3 (ADCY3, RENJIE), cAMP (ab290713, United Kingdom), and PKA (CB10491-Hu, SCI-BIO) in the sample using enzyme-linked immunosorbent assay (ELISA) kits.

2.16 Statistical analysis

Using the fixed effects model, a Meta-analysis was conducted on direct evidence using R 4.3.0 software and the Meta package. The treatment efficacy of the ketogenic diet in patients with epilepsy was directly compared, and the respective odds ratios (OR) and 95% confidence intervals (CI) for each study were combined to obtain the overall effect size. In addition, Bayesian statistical methods are used for network meta-analysis, comparing the treatment effects through indirect evidence with corresponding risk ratios (RR) and 95% confidence intervals. Create a probability graph of the levels to rank these intervention measures and compare them to choose the best therapeutic effect. The I2 test is used to analyze heterogeneity among different studies. A fixed-effect model is adopted when $p \geq 0.05$ and $I2 < 50\%$. A random-effect model is adopted when $p < 0.05$ and $I2 > 50\%$.

The data was statistically processed using SPSS 26.0 software. The continuous variable is expressed as $\chi \pm s$. The comparison between two groups was conducted using a t-test, while the comparison among multiple groups was performed using a one-way analysis of variance. The categorical variable was analyzed using the chi-square test. Count data is presented as rates or percentages. A significance level of $p < 0.05$ indicates a statistical difference.

3 Results

3.1 The classical ketogenic diet has therapeutic effects in treating epilepsy

The ketogenic diet is a high-fat, low-carbohydrate diet widely used in treating patients with epilepsy. There are several types of ketogenic diets, including the classic ketogenic diet (KD), medium-chain triglyceride ketogenic diet (MCT), modified ketogenic diet, and a low-calorie ketogenic diet (MAD) (Sampaio, 2016; Martin-McGill et al., 2020; Sondhi et al., 2020). The individual variances in patients with epilepsy suggest that their responses to different treatments may vary. A detailed comparison of various ketogenic diets can offer clinicians more specific guidance to assist them in selecting the most suitable dietary treatment plan for each patient based on their specific circumstances (van der Louw et al., 2016).

First, we searched English databases such as PubMed, Cochrane Library, Embase, and Web of Science (Sourbron et al., 2020; Yang et al., 2022). We obtained a total of 1,211 articles, excluding 251 duplicated articles. We then screened out 411 articles, including animal experiment articles, review articles, cohort study articles, and irrelevant articles, by reading the titles and abstracts. Next, we read the full texts of the remaining 122 articles and eventually included eight randomized controlled trial articles (Supplementary Figure S1), totaling 692 patients. Among them, 4 studies compared the ketogenic diet with the conventional diet (CAU), with 111 patients in the ketogenic diet group and 114 patients in the conventional diet group. The detailed characteristics are shown in Supplementary Table S2. Additionally, four studies compared different types of ketogenic diets, including 467 patients. Detailed characteristics are also shown in Supplementary Table S2. Quality assessment for the included 8 literature was conducted (risk bias), and the Jadad score ranged from 4 to 7, indicating all studies were of high quality (Supplementary Table S3). The Cochrane risk of bias assessment results are shown in Supplementary Figure S2.

To verify the efficacy of the ketogenic diet in treating epileptic epilepsy, we analyzed four clinical studies comparing the conventional diet (CAU) with different types of ketogenic diets (KD, MCT, MAD, LGIT), evaluating a total of 225 patients. In these four studies, the ketogenic diet was used as an adjunctive therapy for epileptic epilepsy. In these four studies, the efficacy rate of a 3-month ketogenic diet

treatment was 36.0% (40/111). The I2 test showed no heterogeneity between the groups (I2 = 38%, $p = 0.19$), and the funnel plot showed no obvious publication bias (Figure 1A). When conducting sensitivity analysis, a fixed effects model was used. The results showed that Magnhild Kverneland had an I2 of 54%, indicating slight heterogeneity. The overall pooled risk ratio (RR) was 4.17, with a 95% confidence interval (CI) of [2.16, 8.04]. The p-value was less than 0.05, indicating a statistical difference (Figure 1B). It suggests that the ketogenic diet is superior to the conventional diet in treating epilepsy. Because the ketogenic diet has 4 different types, we conducted subgroup analysis on different types of ketogenic diet subgroups to assess the effectiveness of the ketogenic diet and the heterogeneity of the studies. The results show that when comparing different ketogenic diets with a conventional diet group, the I2 value is less than 50%, indicating acceptable heterogeneity. The relative risk ratio between the KD and CAU groups was 1.69, 95% CI = 1.69[0.59, 4.87], with no statistical difference. The merged relative risk ratio between the MAD group and the CAU group was 5.50, 95% CI = [2.20, 13.74], I2 = 37%, $p = 0.21$, indicating an improvement in treatment effect in the MAD group compared to CAU, but with no statistical difference. The relative risk ratio between the LGIT and CAU groups was 13, 95% CI = [0.78, 216.05], with no statistical difference (Figure 1C).

To compare the differences in the therapeutic effects of different types of ketogenic diets on epilepsy, a network meta-analysis was conducted on the included 8 studies. The therapeutic effects of different ketogenic diets are represented as relationships between nodes in the network graph (Supplementary Figure S3). The greater the number of nodes, the higher the degree of association. The study, analyzing the reduction of epilepsy by 50% in 3 months (including ①②④⑤⑦⑧), found that the ketogenic diet (KD) and modified Atkins diet (MAD) were superior to conventional anticonvulsants drugs (CAU) (Supplementary Table S4; Supplementary Figure S4A). The probability graph suggests that LGIT is better than KD, MCT, and MAD, and KD is better than MAD (Figure 2A). The study analyzing three months of reduced epilepsy by 90% (including ①④⑤⑦⑧) found that KD was superior to CAU (Supplementary Table S5; Supplementary Figure S4B). The level probability graph indicates that KD is superior to CAU (Figure 2B). The study analyzing a 50% decrease in epilepsy over 6 months (including ⑤⑥⑦) found that the KD was superior to CAU (Supplementary Table S4;

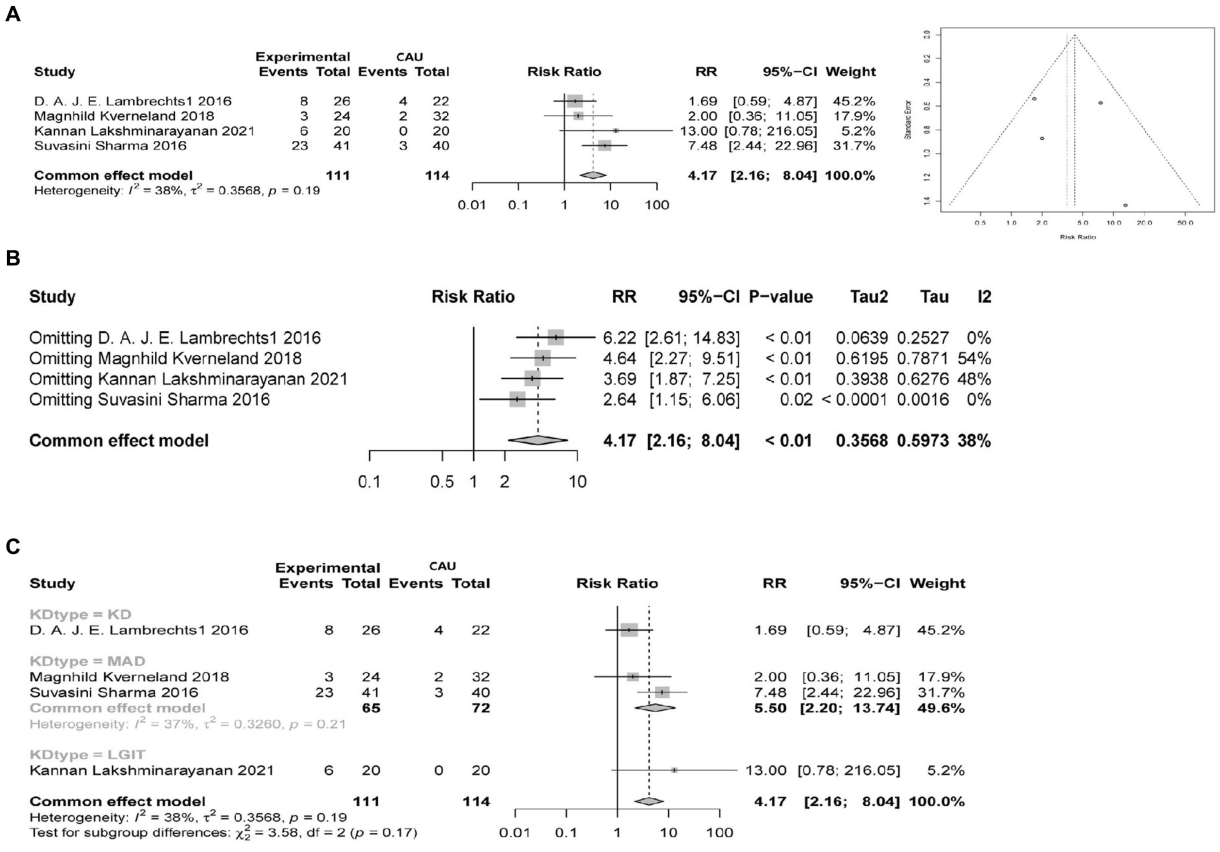

FIGURE 1
Comparison of the therapeutic efficacy between the ketogenic diet and conventional diet control in reducing epilepsy (≥50% reduction in epilepsy). Experimental group refers to the group on a ketogenic diet, with a total sample size of 111 cases, while CAU represents the control group on a conventional diet, with a total sample size of 114 cases. Events indicate the number of cases with a ≥ 50% reduction in epilepsy. RR indicates the relative risk ratio, where RR > 1 indicates that the number of cases with a ≥ 50% reduction in epilepsy in the ketogenic diet group is multiplied by the ratio compared to the control group on a conventional diet. The 95% confidence interval (95%-CI) reflects the possible range of effect sizes to support the results. I2 is used to evaluate the magnitude of heterogeneity between studies, with I2 < 50% indicating an acceptable level of heterogeneity.
(A) Comparison of the therapeutic efficacy of ketogenic and conventional diets in reducing epilepsy by at least 50% at 3 months, with a funnel plot to assess publication bias. **(B)** Sensitivity analysis of the therapeutic efficacy of ketogenic and conventional diets in controlling epilepsy at 3 months, evaluating the source of heterogeneity. **(C)** Subgroup analysis of different types of ketogenic diets to evaluate the heterogeneity of the studies.

Supplementary Figure S4C). MCT, MAD, and LGIT were superior to the CAU group, but the differences were insignificant. The probability graph indicates that the KD group has the best effect (Figure 2C; Supplementary Figure S4B). The study, which analyzed a 90% reduction in epilepsy over 6 months (including ⑤⑥⑦), found that KD, MAD, and LGIT were superior to MCT, while KD and LGIT were superior to MAD (Supplementary Table S5; Supplementary Figure S4D). The difference is not statistically significant, and the rank probability plot indicates that the KD group is superior to the MCT, MAD, and LGIT groups (Figure 2D). The meta-analysis results indicate more robust support for using the conventional ketogenic diet in treating epileptic epilepsy.

3.2 Transcriptome sequencing indicates that the ketogenic diet exerts its therapeutic effect on epilepsy by activating the cAMP signaling pathway

To further validate the results of the aforementioned meta-analysis, this study constructed a chronic epilepsy mouse model and utilized video monitoring to observe spontaneous recurrent seizures in the mice. The results showed that the Racine scoring system was used to assess motor epilepsy activity in epileptic patients. Compared with the Control group, the Model group showed increased epilepsy scores. Compared with the Model group, the group using KD, MCT, MAD, and LGIT, four types of ketogenic diets, showed reduced epilepsy scores (Figure 3A). The EEG results indicated that the amplitude of epilepsy activity in the Model group was increased compared to the Control group. Compared with the Model group, mice using KD, MCT, MAD, and LGIT ketogenic diets reduced the amplitude of epileptic epilepsy activity (Figure 3B). Compared to the Control group, the epilepsy frequency in the Model group increased. Compared with the Model group, the groups using KD, MCT, MAD, and LGIT ketogenic diets demonstrated a decrease in the frequency of epileptic epilepsy. Comparing the frequency of epileptic epilepsy among different types of ketogenic diets, it can be observed that the ketogenic diet (KD) is superior to the medium-chain triglyceride diet (MCT), the modified Atkins diet (MAD), and the low glycemic index treatment (LGIT) (Figure 3C), which is consistent with the results of the meta-analysis.

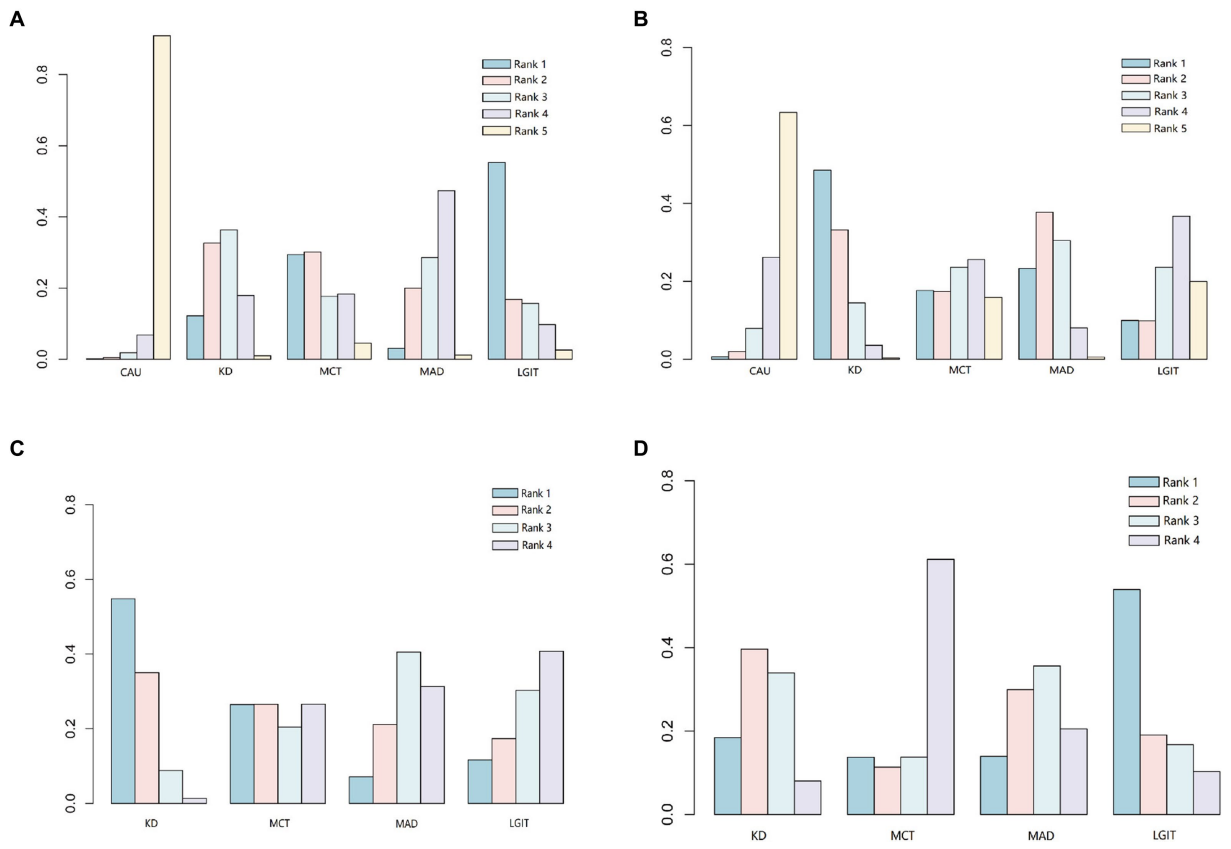

FIGURE 2
Comparison of the probabilities of different types of ketogenic diets at various levels. CAU refers to the control group on a conventional diet, KD represents the group on a classic ketogenic diet, MCT refers to the group on a medium-chain triglyceride ketogenic diet, MAD stands for the group on a modified Atkins diet, and LGIT describes the group on a low glycemic index ketogenic diet. Rank indicates the ranking probability of different types of ketogenic diets at specific levels (1–5). The levels indicate the likelihood of being the best treatment, second-best treatment, and so on, with Level 1 being the best and Level 5 being the worst. **(A)** Comparison of the therapeutic efficacy of different ketogenic diets in reducing epilepsy by at least 50% at 3 months. **(B)** Comparison of the therapeutic efficacy of different ketogenic diets in reducing epilepsy by at least 90% at 3 months. **(C)** Comparison of the therapeutic efficacy of different ketogenic diets in reducing epilepsy by at least 50% at 6 months. **(D)** Comparison of the therapeutic efficacy of different ketogenic diets in reducing epilepsy by at least 90% at 6 months.

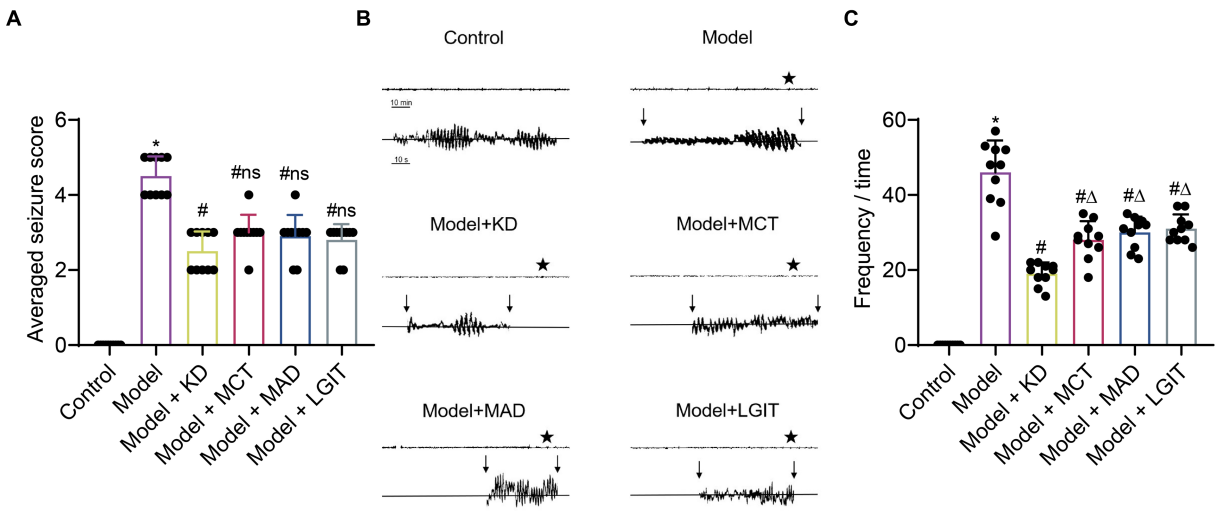

FIGURE 3
Analysis of the therapeutic efficacy of a classic ketogenic diet in controlling epilepsy. Control refers to the standard group, Model represents the epilepsy model group, KD stands for the group on a classic ketogenic diet, MCT refers to the group on a medium-chain triglyceride ketogenic diet, MAD stands for the group on a modified Atkins diet, and LGIT describes the group on a low glycemic index ketogenic diet. Each group had a sample size of n = 10. **(A)** Racine scoring, *denotes a difference compared to the Control group, # denotes a difference compared to the Model group, $p < 0.05$, ns denotes no difference compared to the KD group, $p > 0.05$. **(B)** In EEG analysis of epilepsy controlled by the ketogenic diet, vertical arrows indicate the start and end of epilepsy in mice, the Control group had no epilepsy activity, the Model group represents the baseline epilepsy activity in mice, KD, MCT, MAD, and LGIT groups showed a decrease in epilepsy activity wave amplitude compared to the Model group. **(C)** Comparison of epilepsy frequency in mice with epilepsy, *denotes a difference compared to the Control group, # denotes a difference compared to the Model group, $p < 0.05$, Δ denotes a difference compared to the KD group, $p < 0.05$.

To investigate the potential mechanisms of ketogenic diet therapy in treating epileptic epilepsy, we performed transcriptome sequencing on the Control group, Model group, and KD group. The results indicate that volcano plots can provide an overall view of the distribution of differential genes (Figures 4A,B). The Model group obtained 5,054 upregulated differentially expressed genes and 5,497 down-regulated differentially expressed genes compared with the Control group (Figure 4A). Compared to the Model group, the KD group had 4,693 upregulated differentially expressed genes and 5,038 downregulated differentially expressed genes (Figure 4B). Differential gene expression analysis was conducted using the criteria $|\text{LogFC}| > 1$ and $p < 0.05$ as selection standards (Figures 4C,D). Genes with similar or identical expression patterns were grouped for analysis, where high gene expression levels are represented in red and low levels in blue. By intersecting the differentially expressed genes between the Control and Model groups with those between the Model and KD groups but in opposite trends, a total of 157 intersecting genes were identified (Figure 4E). Protein–protein interaction analysis was conducted on the 157 intersecting genes encoded by these proteins. The top 15 genes, sorted by degree value, are GRIN2B, CALM3, PRKACA, ITPR1, COG1, MYO5A, SPTAN1, ADCY3, ANK1, APOE, CACNA1S, ZW10, CPT1c, GABARAP12, XPO5 (Figure 4F).

The results of GO and KEGG enrichment analysis showed that there were enrichments in biological processes such as response to hypoxia, response to decreased oxygen levels, cellular response to hypoxia, and phospholipid efflux (Figure 4G), as well as in signaling pathways, including Proteoglycans in cancer, cAMP signaling pathway, Calcium signaling pathway, Glucagon signaling pathway, Glutamatergic synapse, GABAergic synapse, and Fatty acid elongation (Figure 4H). After consulting, it was found that the genes enriched in the cAMP signaling pathway were mainly VAV2, CALM3, ADCY3, CACNA1S, PRKACA, and GRIN2B. Among them, 5 genes overlapped with the sorted degree values, suggesting that KD may regulate the cAMP signaling pathway in treating epilepsy by modulating the above genes.

Transcriptome sequencing results indicate that, compared with the Control group, the expression levels of VAV2, CALM3, ADCY3, PRKACA, and GRIN2B are down-regulated, while the expression level of CACNA1S is upregulated. Compared with the Model group, the expression levels of VAV2, CALM3, ADCY3, PRKACA, and GRIN2B were upregulated, while the expression level of CACNA1S was downregulated. To further validate the transcriptome data, we performed RT-qPCR and Western blot experiments to detect the mRNA and protein expression levels of VAV2, CALM3, ADCY3, CACNA1S, PRKACA, and GRIN2B. As shown in Figures 5A–C, the results showed that compared to the Control group, the mRNA and protein levels of VAV2, CALM3, ADCY3, PRKACA, and GRIN2B were downregulated, while the mRNA and protein levels of CACNA1S were upregulated. Compared with the Model group, the mRNA and protein levels of VAV2, CALM3, ADCY3, CACNA1S, PRKACA, and GRIN2B were upregulated, while the mRNA and protein levels of CACNA1S were downregulated, which is consistent with the expression trend observed in the transcriptome sequencing results.

The above results suggest that these six genes, VAV2, CALM3, ADCY3, CACNA1S, PRKACA, and GRIN2B, may be critical genes influencing epileptic epilepsy. KD may improve epileptic epilepsy by regulating the expression of VAV2, CALM3, ADCY3, CACNA1S, PRKACA, and GRIN2B, thereby modulating the cAMP signaling pathway and inhibiting neuronal activity.

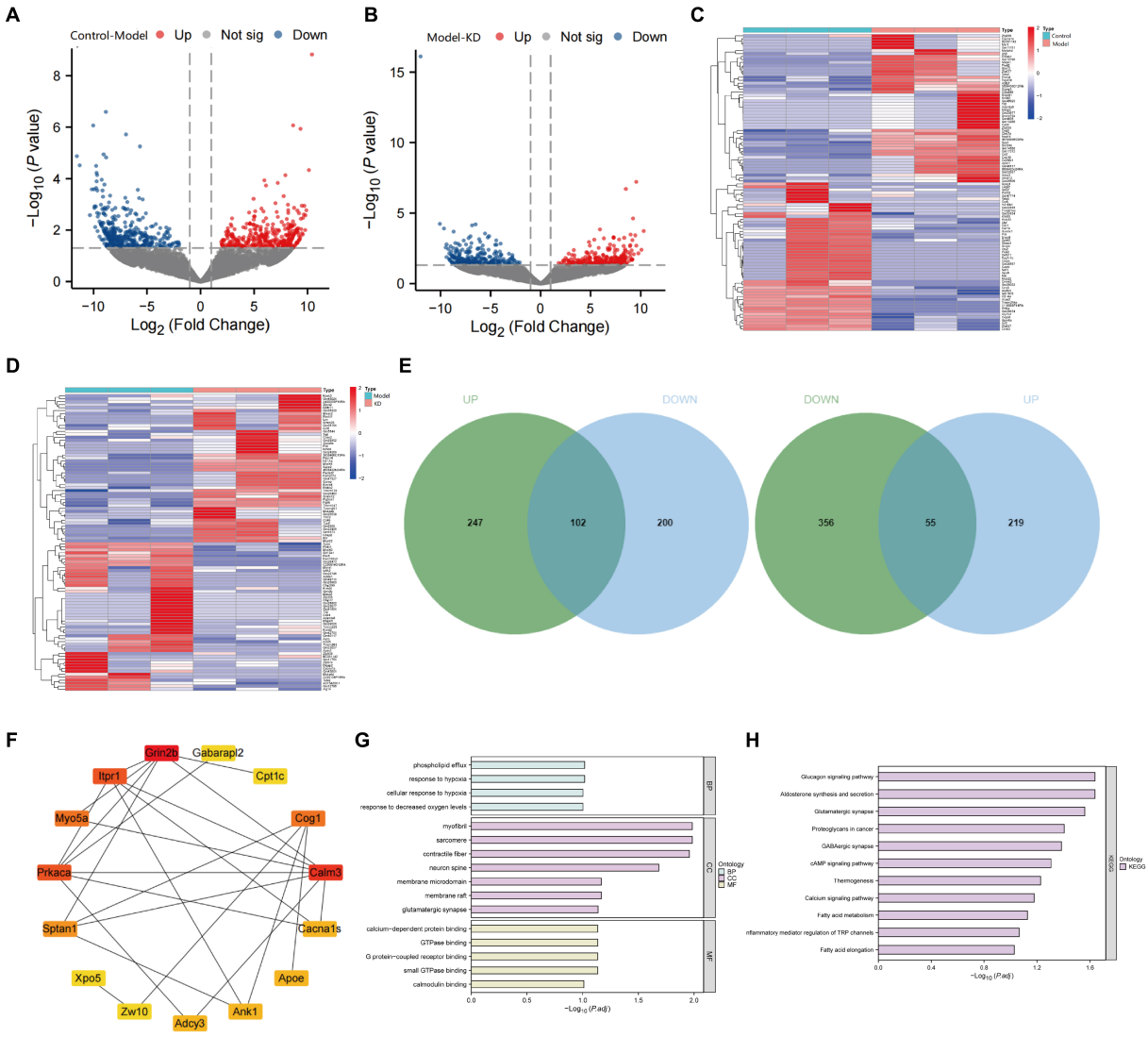

FIGURE 4
Transcriptome sequencing analysis results. Control refers to the standard group, the Model represents the epilepsy model group, and KD stands for the group on a classic ketogenic diet. Each group had a sample size of $n = 3$. **(A)** Comparison of the Model group with the Control group, red dots indicate upregulated gene expression, green dots indicate downregulated gene expression, the p-value represents the significance of differential gene expression, and a higher Log2FC (log2 fold change) indicates a more difference in expression. **(B)** Comparison of the epilepsy model group with the classic KD group, $p < 0.05$, indicating a difference. Red dots indicate upregulated gene expression, green dots indicate downregulated gene expression, the p-value represents the significance of differential gene expression, and a higher Log2FC (log2 fold change) indicates more expression differences. **(C)** Hierarchical clustering analysis of differentially expressed genes between the Control and Model groups. **(D)** Hierarchical clustering analysis of differentially expressed genes between the Model and KD groups. **(E)** Venn diagrams depicting the intersection of upregulated genes in the Model group (compared to the Control group) with downregulated genes in the KD group (upper diagram), and the intersection of downregulated genes in the Model group (compared to the Control group) with upregulated genes in the KD group (lower diagram). Green represents genes differentially expressed between the Control and Model groups, blue represents genes differentially expressed between the Model and KD groups, and the overlapping area indicates intersecting genes. **(F)** Protein interaction analysis among the Control, Model, and KD groups. **(G)** GO enrichment analysis. **(H)** KEGG pathway enrichment analysis.

3.3 ADCY3 activation improves epilepsy onset in epilepsy through the cAMP signaling pathway

To explore the possible mechanisms of the involvement of critical genes such as VAV2, CALM3, ADCY3, and CACNA1S in epileptic epilepsy, we have consulted relevant literature. We found that ADCY3 (adenylate cyclase 3) is an activator of cAMP. Increased expression of ADCY3 can catalyze ATP to generate cAMP, which then binds to the regulatory subunits of PKA, activating the catalytic subunits of PKA and subsequently activating PKA (Hong et al., 2013; Zheng et al., 2023). Therefore, regulating the activity of cAMP plays a crucial role in controlling the excitability of neurons and networks (Zhang et al., 2021b). Based on this, we found that the remaining four genes are downstream in the cAMP signaling pathway, and their expression may be closely associated with cAMP activation.

Research has found that activation of the cAMP signaling pathway in the hippocampal neurons of brain tissue has a neuroprotective

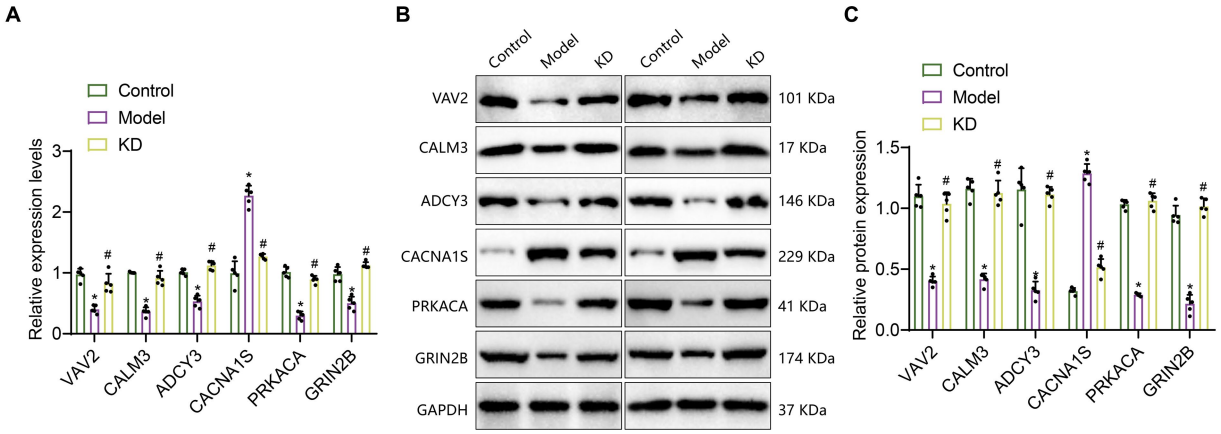

FIGURE 5
The expression of 6 critical genes in the hippocampal tissue of epileptic mice. Control refers to the standard group; Model refers to the epileptic model group; KD refers to the classic ketogenic diet group. The sample size in each group was $n = 5$. **(A)** RT-qPCR analysis, * indicates the difference between the Model group and the Control group ($p < 0.05$); # indicates the difference between the KD group and the Model group ($p < 0.05$); **(B,C)** Western Blot analysis, * indicates the difference between the Model group and the Control group ($p < 0.05$); # indicates the difference between the KD group and the Model group ($p < 0.05$).

effect (Chen et al., 2021; Essam and Kandil, 2023). The expression levels of the ADCY3 gene increase during dietary restriction and ketone body intake (Zhang et al., 2017; Goni et al., 2018). Therefore, ADCY3 may be a potential target for the treatment of epilepsy.

Several studies have indicated that cAMP exhibits dual regulatory effects. It enhances the strength of excitatory neural circuits and, simultaneously, acts locally on postsynaptic GABA receptors to reduce inhibitory synaptic plasticity (Lee, 2015). In the context of epilepsy research, activation of the cAMP-PKA pathway has been shown to have inhibitory effects during seizures (Qi et al., 2019). Furthermore, Forskolin, a adenylyl cyclase activator, has been demonstrated to increase cAMP levels when administered subcutaneously in mice, thereby preventing epileptic seizures (Sano et al., 1984). The findings of these studies align with those of the present study, suggesting that increasing cAMP has antiepileptic effects in the regulation of epilepsy.

To investigate the activation of the ADCY3 in the cAMP signaling pathway and its impact on epileptic seizures (Hosseini-Zare et al., 2011), we established an epileptic mouse model and conducted experimental validation. The experiments were divided into four groups: oe-NC (overexpression lentivirus control group), oe-ADCY3 (overexpression lentivirus ADCY3 group), oe-ADCY3 + DMSO (overexpression lentivirus ADCY3 group with intraperitoneal injection of varying doses of DMSO), and oe-ADCY3 + RMI 12330A (overexpression lentivirus ADCY3 group with intraperitoneal injection of varying doses of cAMP inhibitor, RMI 12330A).

Behavioral observations were conducted on mice, including evaluation of mouse performance using the Racine scoring system, electroencephalogram (EEG) detection, and recording of epilepsy frequencies. Racine scoring results showed that compared to the oe-NC group, the epilepsy score decreased in the oe-ADCY3 group; compared to the oe-ADCY3 + DMSO group, the epilepsy score increased in the oe-ADCY3 + RMI 12330A group (Figure 6A). EEG results showed that compared with the oe-NC group, the amplitude of epileptic EEG activity was reduced in the oe-ADCY3 group; compared with the oe-ADCY3 + DMSO group, the amplitude of epileptic EEG activity was increased in the oe-ADCY3 + RMI 12330A group (Figure 6B). Statistical analysis of the frequency of epileptic seizures revealed a significant reduction in seizure frequency in the oe-ADCY3 group compared to the oe-NC group. Conversely, when comparing mice in the oe-ADCY3 + DMSO group (overexpression lentivirus ADCY3 group with intraperitoneal injection of varying doses of DMSO) to those in the oe-ADCY3 + RMI 12330A group (overexpression lentivirus ADCY3 group with intraperitoneal injection of varying doses of cAMP inhibitor, RMI 12330A), there was an increase in seizure frequency in the oe-ADCY3 + RMI 12330A group (Figure 6C).

To explore the molecular mechanism of treating epileptic epilepsy by activating the cAMP signaling pathway through ADCY3, we utilized the Western blot analysis method to examine the protein expression levels of ADCY3, cAMP-responsive element binding protein (CREB), and phosphorylated CREB (pCREB). Additionally, we employed the ELISA analysis method to measure the expression levels of cAMP and protein kinase A (PKA). The results showed that compared with the oe-NC group, the expression levels of cAMP, PKA, ADCY3, CREB, and pCREB were upregulated in the oe-ADCY3 group. Compared with the oe-ADCY3 + DMSO group, the expression levels of cAMP, PKA, CREB, and pCREB were downregulated in the oe-ADCY3 + RMI 12330A group, while the expression level of ADCY3 showed no difference (Figures 6D,E). These results indicate that overexpression of ADCY3 affects the production of cAMP.

Furthermore, we investigated whether activating the ADCY3/cAMP signaling pathway can enhance neuronal inhibition and improve epilepsy onset in epilepsy. We analyzed the inhibitory properties of neurons using electrophysiological techniques, as described in the methods section. Electrophysiological techniques recorded spontaneous inhibitory postsynaptic currents (sIPSCs) and evoked inhibitory postsynaptic currents (PSCs). UPSC results showed that compared with the oe-NC group, the frequency and amplitude increased in the oe-ADCY3 group, and the inhibitory effect of neurons was enhanced. Compared with the oe-ADCY3 + DMSO group, the amplitude decreased, and the inhibitory effect of neurons was weakened in the oe-ADCY3 + RMI 12330A group (Figure 6F).

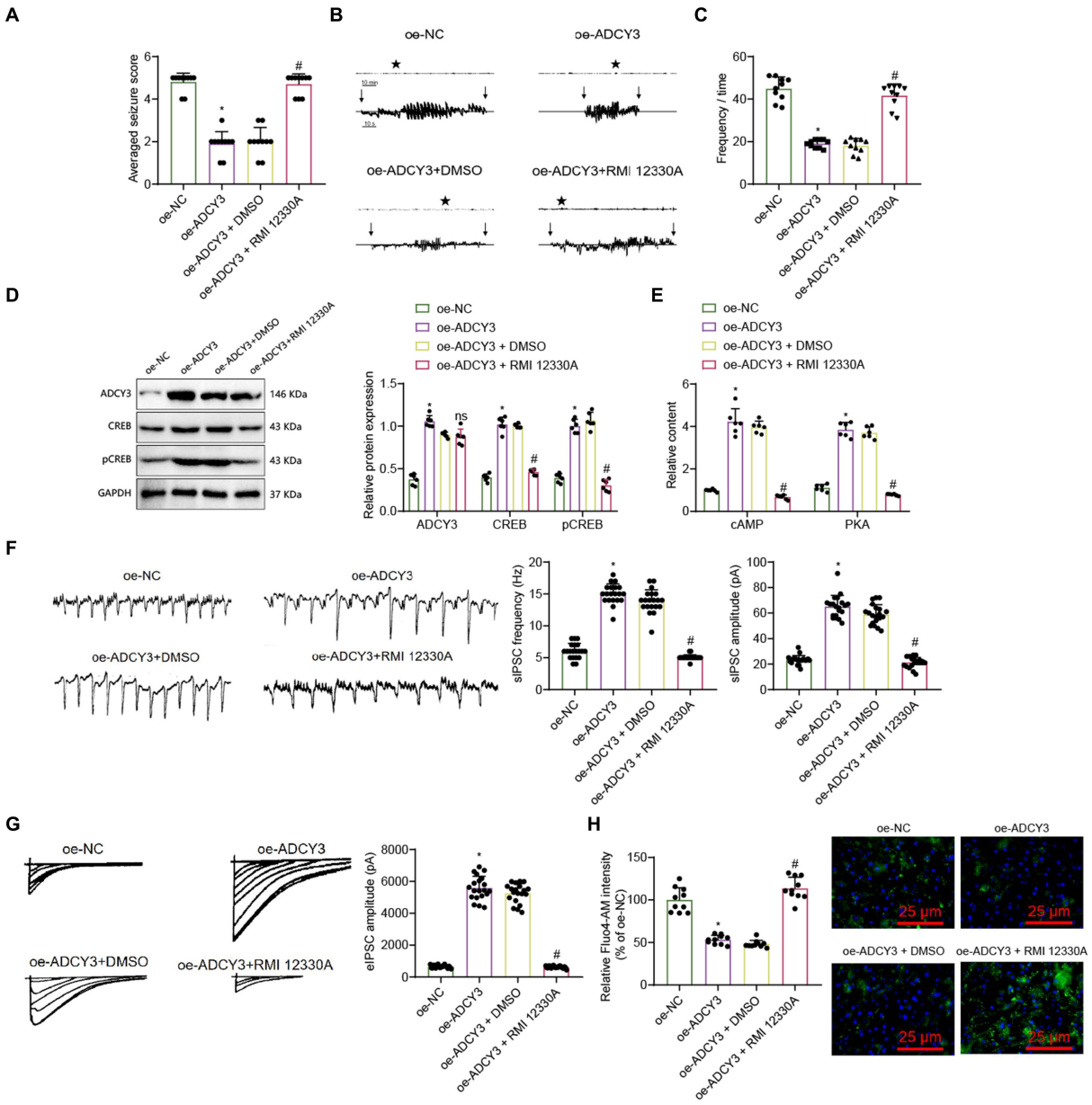

FIGURE 6
Activation of the cAMP signaling pathway by ADCY3 improves epileptic epilepsy. **(A)** Behavioral observation in mice (Racine score), $n = 10$, *indicates difference between the oe-ADCY3 group and the oe-NC group ($p < 0.05$), # indicates difference between the oe-ADCY3 + RMI 12330A group and the oe-ADCY3 + DMSO group ($p < 0.05$). **(B)** Analysis of mouse EEG, Vertical arrows indicate the beginning and end of seizures in mice. **(C)** Frequency of epileptic epilepsy, $n = 10$, *indicates difference between the oe-ADCY3 group and the oe-NC group ($p < 0.05$), # indicates difference between the oe-ADCY3 + RMI 12330A group and the oe-ADCY3 + DMSO group ($p < 0.05$). **(D,E)** Expression levels of ADCY3, CREB, pCREB, cAMP, and PKA in mice as detected by Western Blot and ELISA, $n = 6$, *indicates difference between the oe-ADCY3 group and the oe-NC group ($p < 0.05$), ns indicates no difference between the oe-ADCY3 + RMI 12330A group and the oe-ADCY3 + DMSO group ($p > 0.05$). **(F)** Detection of sIPSC using electrophysiological techniques, scale bar, 100 ms and 1,000 pA, $n = 20$ neurons, bar graph (right) represents frequency and amplitude. **(G)** Detection of eIPSC using electrophysiological techniques, scale bar, 2 s and 20 pA, $n = 20$ neurons, bar graph (right) represents amplitude. **(H)** Measurement of the relative intensity changes of calcium ions in different groups of mice neurons using calcium imaging techniques (scale bar = 25 μm), $n = 10$ cells, *indicates difference between the oe-ADCY3 group and the oe-NC group ($p < 0.05$), # indicates difference between the oe-ADCY3 + RMI 12330A group and the oe-ADCY3 + DMSO group ($p < 0.05$).

The UPSC results showed that compared to the oe-NC group, the frequency and amplitude increased in the oe-ADCY3 group, and the inhibitory effect of the neurons was enhanced. Compared to the oe-ADCY3 + DMSO group, the amplitude decreased, and the inhibitory effect of the neurons was weakened in the oe-ADCY3 + RMI 12330A group (Figure 6G).

Calcium ions are one of the critical mediators for signal transmission in neurons. After the cell membrane is stimulated, calcium ion channels on the membrane can either open or close, resulting in the influx of calcium ions and an increase in calcium ion concentration, which has a particular impact on the excitability of neurons (Ross, 1989). Hence, we utilized calcium imaging analysis to

examine the trends in calcium ion concentration changes in neurons, thereby investigating the impact of ADCY3 activation on neuronal excitability via the cAMP signaling pathway. The results indicate that compared to the oe-NC group, the oe-ADCY3 group exhibited a decreasing trend in calcium ion concentration. Additionally, when comparing the oe-ADCY3 + DMSO group with the oe-ADCY3 + RMI 12330A group, there was an increasing trend in the relative intensity of calcium fluorescence signals in the latter (Figure 6H).

In conclusion, modulating the activation of ADCY3 can enhance inhibitory synaptic transmission, increase neuronal inhibition, and thereby improve epilepsy onset in epilepsy.

3.4 A ketogenic diet regulates ADCY3 to activate the cAMP signaling pathway and improve epileptic epilepsy

To investigate the regulatory effects of the ketogenic diet on ADCY3-mediated activation of the cAMP signaling pathway and its impact on epileptic epilepsy, we further validated the influence of the ketogenic diet on the cAMP signaling pathway and epilepsy occurrence. We established a mouse model of epilepsy and performed experimental verification using a cAMP inhibitor. The experiment is divided into the KD group and the KD + RMI 12330A group.

We conducted behavioral observations on mice, and according to the Racine scoring results, the epilepsy score of the KD + RMI 12330A group was higher compared to the KD group (Figure 7A). The electroencephalogram results showed that compared with the KD group, the amplitude of epileptic brain electrical activity in the KD + RMI 12330A group increased (Figure 7B). Analysis of epilepsy frequency statistics showed that compared to the KD group, the KD + RMI 12330A group had increased epilepsy frequency (Figure 7C).

β-hydroxybutyrate and glucose levels reflect the body's fat metabolism status. Compared to the KD group, the KD + RMI 12330A group showed a decrease in β-hydroxybutyrate concentration and an increase in blood glucose levels (Figures 7D,E), indicating that the ketogenic diet can promote fatty acid metabolism and improve epilepsy disorders.

We used the Western blot analysis to detect cAMP, PKA, ADCY3, CREB, and pCREB protein expression levels. The results showed that compared to the KD group, the expression levels of cAMP, PKA, CREB, and pCREB in the KD + RMI 12330A group were down-regulated, while the expression level of ADCY3 showed no difference (Figure 7F).

We used electrophysiological techniques to analyze spontaneous inhibitory postsynaptic currents (sIPSCs) and evoked inhibitory postsynaptic currents (PSCs). The sIPSC results revealed that, compared to the KD group, the KD + RMI 12330A group exhibited a decreased frequency and significantly reduced amplitude, indicating a marked decrease in neuronal inhibitory function (Figure 7G). The UPSC results showed that compared to the KD group, the amplitude of the KD + RMI 12330A group decreased, and the inhibitory nature of the neurons was weakened (Figure 7H).

We employed calcium imaging analysis to detect the trends in the relative intensity changes of calcium fluorescence signals in neurons. The results revealed that compared to the KD group, the KD + RMI 12330A group exhibited an increasing trend in the relative intensity of calcium fluorescence signals, indicating a decrease in neuronal excitability (Figure 7I).

In summary, by regulating ADCY3 to activate the cAMP signaling pathway and increasing inhibitory synaptic transmission, the ketogenic diet improves epilepsy activity in epilepsy.

3.5 The impact of a classical ketogenic diet on patients with epileptic epilepsy

In order to evaluate the efficacy of the ketogenic diet in patients with epilepsy, we conducted a study involving 60 individuals diagnosed with epilepsy. These participants were randomly assigned to either a control group or an observation group, with each group consisting of 30 individuals. Comparison of the general characteristics between the two groups revealed no significant differences ($p > 0.05$), indicating their comparability (Supplementary Table S6). The Hospital's Medical Ethics Committee has approved this study.

The electroencephalogram (EEG) results of patients with epilepsy showed that compared to the control group, the ketogenic diet group had a decreased amplitude of EEG activity (Figure 8A). Compared with the control group, the ketogenic diet group showed a reduction in the frequency and duration of epileptic epilepsy (Figures 8B,C), indicating that the ketogenic diet can decrease the frequency and duration of epilepsy in epileptic patients, thereby improving their epilepsy condition. Compared with the control group, the ketogenic diet group showed a decrease in glucose levels and an increase in β-hydroxybutyrate levels, indicating that the ketogenic diet can elevate ketone body levels in patients and promote fatty acid metabolism, thereby improving epilepsy in epilepsy (Figures 8D,E). Blood lipid analysis results showed no differences in cholesterol, triglycerides, high-density lipoprotein, and low-density lipoprotein between the ketogenic diet group and the control group (Figure 8F), indicating that the ketogenic diet does not cause harm to patients. In addition, we also assessed the expression levels of ADCY3, cAMP, and PKA in the blood of patients with epilepsy using ELISA. The results showed that in the classical ketogenic diet group, ADCY3, cAMP, and PKA expression levels were upregulated compared to the control group (Figure 8G). It indicates that the classical ketogenic diet regulates the ADCY3-initiated cAMP signaling pathway by promoting fatty acid metabolism, inhibiting neuronal activity and further alleviating patients' epileptic epilepsy.

4 Discussion

In this study, we delved into the molecular mechanisms by which the ketogenic diet regulates fatty acid metabolism, activates ADCY3 to initiate the cAMP signaling pathway, enhances neuronal inhibition, and treats epileptic seizures. Through high-throughput transcriptome sequencing and *in vivo* experiments in mice, we systematically elucidated how the ketogenic diet increases neuronal inhibition and improves seizure control by promoting fatty acid metabolism to regulate ADCY3 activation of the cAMP signaling pathway. The findings of this study align with previous clinical and experimental research, confirming the effectiveness of the ketogenic diet in epilepsy treatment (Wells et al., 2020; Kong et al., 2021).

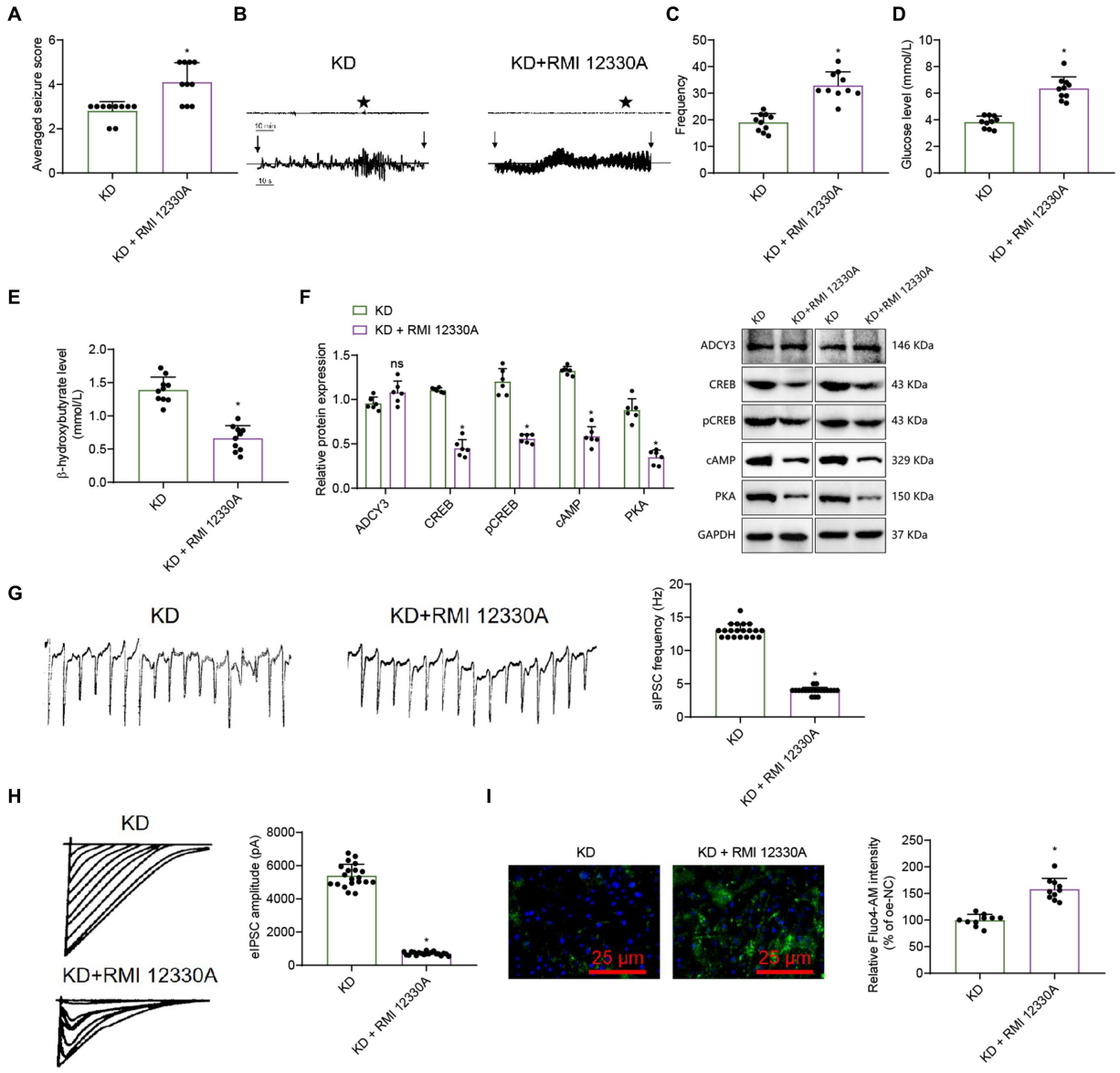

FIGURE 7
The ketogenic diet regulates the cAMP signaling pathway and influences epileptic seizure. **(A)** Behavioral observation in mice (Racine score), $n = 10$, * indicates difference between the KD + RMI 12330A group and the KD group ($p < 0.05$). **(B)** Analysis of mouse EEG, and vertical arrows indicate the beginning and end of seizures in mice. **(C)** Frequency of epileptic epilepsy, $n = 10$, * indicates difference between the KD + RMI 12330A group and the KD group ($p < 0.05$). **(D,E)** Levels of β-hydroxybutyrate and Glucose, $n = 10$, * indicates difference between the KD + RMI 12330A group and the KD group ($p < 0.05$). **(F)** Western Blot analysis of ADCY3, CREB, pCREB, cAMP, and PKA expression levels in mice, $n = 6$, * indicates difference between the KD + RMI 12330A group and the KD group ($p < 0.05$), ns indicates no difference between the KD + RMI 12330A group and the KD group ($p > 0.05$). **(G)** Detection of sIPSC using electrophysiological techniques, bar graph (right) represents frequency and amplitude, scale bar, 100 ms and 1,000 pA, $n = 20$ neurons. **(H)** Detection of eIPSC using electrophysiological techniques, bar graph (right) represents amplitude, scale bar, 2 s and 20 pA, $n = 20$ neurons. **(I)** Measurement of the relative intensity in calcium ion concentrations among the different groups of mice's neurons using calcium imaging techniques (scale bar = 25 μm), $n = 10$ cells, * indicates difference between the KD + RMI 12330A group and the KD group ($p < 0.05$).

Our meta-analysis revealed that the efficacy of the ketogenic diet in treating epilepsy surpasses that of conventional diets, with the classical ketogenic diet demonstrating superior improvement in seizure activity compared to other variants. These results provide robust evidence for clinicians to consider the ketogenic diet as a non-pharmacological treatment option for epilepsy patients, guiding clinical practices coherently with previous research. Both traditional and network meta-analyses support the superior efficacy of the classical ketogenic diet in ameliorating seizure activity compared to other variants (Wang et al., 2022), endorsing the ketogenic diet as a viable non-pharmacological therapeutic approach (Yuan et al., 2020; Sun et al., 2021; Ruan et al., 2022).

The meta-analysis revealed that the classical ketogenic diet may improve epileptic seizures by modulating the expression of VAV2, CALM3, ADCY3, CACNA1S, PRKACA, and GRIN2B, thereby regulating the cAMP signaling pathway to inhibit neuronal activity

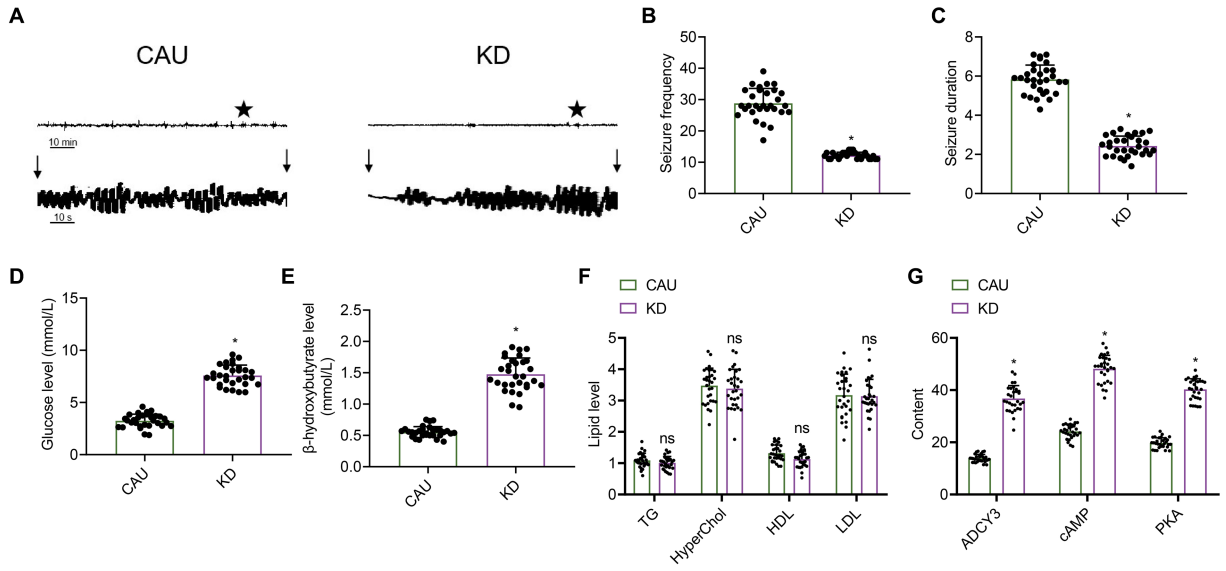

FIGURE 8
Effect of the classical ketogenic diet on epilepsy onset in patients with epilepsy. CAU, conventional epilepsy diet group; KD, classical ketogenic diet group. **(A)** EEG of patients with epilepsy, $n = 30$, and the vertical arrow indicates the beginning and end of epileptic seizures in mice. **(B)** Frequency of epilepsy in patients with epilepsy, $n = 30$, * indicates the comparison between the two groups, $p < 0.05$. **(C)** Duration of epilepsy in patients with epilepsy, $n = 50$, * indicates the comparison between the two groups, $p < 0.05$. **(D)** Glucose concentration levels, $n = 50$, * indicates the comparison between the two groups, $p < 0.05$. **(E)** β-hydroxybutyrate levels, $n = 50$, * indicates the comparison between the two groups, $p < 0.05$. **(F)** Influence of KD on blood lipid levels in patients with epilepsy, $n = 30$, TG (triglycerides), HyperChol (cholesterol), HDL (high-density lipoprotein), LDL (low-density lipoprotein), ns indicates the comparison between the two groups, $p > 0.05$. **(G)** Expression of ADCY3, cAMP, and PKA in the blood of patients with epilepsy detected by ELISA, $n = 30$, * indicates the comparison between the two groups, $p < 0.05$.

(Figures 1–4). Subsequently, the expression of six key genes was examined in the hippocampal tissue of epileptic mice (Figure 5). Based on the literature, ADCY3, identified as a significant adenylyl cyclase, when activated, elevates intracellular cAMP levels and modulates various cellular functions (Son et al., 2022; Gárriz et al., 2023). Consequently, ADCY3 is viewed as a potential therapeutic target for epilepsy treatment. Furthermore, a mouse model was successfully established to validate the findings. It was discovered that modulating ADCY3 to initiate the cAMP signaling pathway could enhance inhibitory synaptic transmission, increasing neuronal inhibition and ameliorating epileptic seizures (Figure 6). This research highlights the critical role of ADCY3 in the ketogenic diet and lays the groundwork for further investigations into its mechanism of action. This finding aligns with existing literature, emphasizing the vital regulatory role of the cAMP signaling pathway in treating epileptic seizures with a ketogenic diet. cAMP influences neuronal function by activating protein kinase A (PKA) and regulating the phosphorylation of the transcription factor CREB (Grigsby et al., 2020). Additionally, delving deeper into the specific regulatory mechanisms of ADCY3 within the cAMP signaling pathway and exploring other potential molecular mechanisms warrants further investigation (Ding et al., 2021).

Subsequently, we validated that the ketogenic diet can improve epileptic seizures by modulating ADCY3 to activate the cAMP signaling pathway (Figure 7). This discovery holds significant importance for gaining a deeper understanding of the molecular mechanisms underlying epileptic seizures and exploring novel therapeutic approaches. This conclusion is consistent with research findings from relevant literature, indicating that through cAMP pathway activation, the ketogenic diet can enhance neuronal inhibition, reducing the likelihood of epileptic seizures (Luo et al., 2022).

Lastly, to ascertain the efficacy of the ketogenic diet in human epilepsy patients, we collected data from 60 epilepsy patients. The results demonstrated that the classical ketogenic diet regulates ADCY3 to initiate the cAMP signaling pathway by promoting fatty acid metabolism, thereby inhibiting neuronal activity and further alleviating the occurrence of seizures in patients (Figure 8). As a non-pharmacological treatment approach, the ketogenic diet exhibits fewer side effects and dependencies, making it a promising option for certain refractory epilepsy patients (Paoli et al., 2020). Future clinical studies could further evaluate the application effectiveness of the ketogenic diet in various types of epilepsy patients and explore its combined use with medication or other treatment modalities (Norwitz et al., 2020). Additionally, long-term follow-up observations can assess the impact of the ketogenic diet on the recurrence rate of epileptic seizures and long-term prognosis, providing stronger evidence for clinical practice (Desli et al., 2022).

In conclusion, we can preliminarily deduce the following outcomes: the classical ketogenic diet enhances neuronal inhibition by promoting fatty acid release, thereby regulating ADCY3 to activate the cAMP signaling pathway, leading to the amelioration of epileptic seizures (Figure 9). This study provides significant scientific and clinical value by delving into the mechanisms of the ketogenic diet in treating epileptic seizures.

However, this study has certain limitations. Although we employed mouse models and transcriptome sequencing for validation, there are inherent methodological constraints. Future research could utilize alternative models such as large animal models or *in vitro* cell models to better mimic the pathological processes of

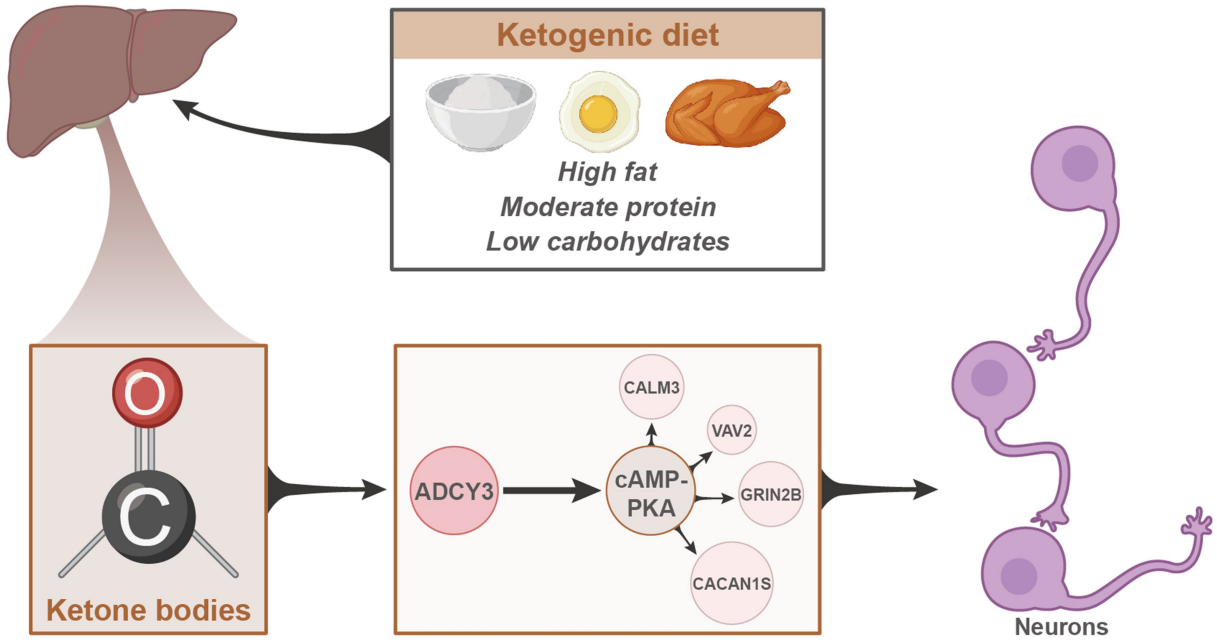

FIGURE 9
Schematic representation of the molecular mechanisms underlying the therapeutic effects of the classical ketogenic diet in epilepsy.

human epilepsy. Moreover, integrating other technologies like single-cell transcriptome sequencing and proteomics analysis could further elucidate the regulatory mechanisms of the ketogenic diet on neuronal inhibition. While this study offers initial insights into the molecular mechanisms of the ketogenic diet in epilepsy treatment, there are numerous aspects that require further exploration, such as investigating the diet's regulatory effects on other epilepsy-related genes and elucidating the specific functions of these genes during seizure onset (Sourbron et al., 2020; Wells et al., 2020; Dashti et al., 2021).

The systemic effects of intraperitoneal administration on *in vivo* validation were not extensively investigated in this study, introducing certain limitations that need exploration in future research. Predominantly based on animal experiments and transcriptome sequencing analyses, large-scale clinical trials have not yet been conducted for verification. Therefore, it is imperative to proceed with further human clinical studies to validate the efficacy and safety of the ketogenic diet in epilepsy patients. Additionally, the limited selection of ketogenic diet types in this study, including the classical ketogenic diet, MAD, LGIT, and MCT, leaves other variants unexplored. Hence, further research is essential to investigate the mechanisms of action of other types of ketogenic diets in epilepsy treatment. Furthermore, Fluo-4 AM is not the optimal dye for measuring the ratio metric of absolute calcium concentrations between independent samples. In future studies, we will consider using calcium indicators like Fura Red AM for ratio metric calcium measurement to enhance the accuracy of our calcium measurements.

Despite its limitations, the results of this study offer promising prospects. Firstly, further research could broaden the spectrum of ketogenic diet types, comparing the efficacy of different types in epilepsy treatment to identify more personalized dietary strategies. Secondly, exploring the therapeutic effects of the ketogenic diet on other neurological disorders such as Parkinson's and Alzheimer's diseases is warranted. Investigating the common mechanisms of action of the ketogenic diet on neurological diseases could extend its applications across various disease domains. Additionally, combining the ketogenic diet with other therapies like drug treatments and neuroregulation techniques could enhance the effectiveness of epilepsy treatment.

In essence, our study provides a profound understanding of the application of the ketogenic diet in epilepsy treatment, offering a non-pharmacological treatment option for epilepsy patients. Future research will refine the application strategies of the ketogenic diet, exploring its potential value in other neurological disorders, fostering new breakthroughs in both neuroscience research and clinical practice.

Data availability statement

The original contributions presented in the study are included in the article/Supplementary material, further inquiries can be directed to the corresponding authors.

Ethics statement

All mice were handled strictly with the ethical requirements for experimental animals and obtained approval from the Animal Ethics Committee for Experimentation (IACUC FJMU 2023-0100). The studies were conducted in accordance with the local legislation and institutional requirements. The participants provided their written informed consent to participate in this study. This study has

been approved by the Clinical Ethics Committee of Fujian Medical University Union Hospital, and written informed consent has been obtained from the patients and their families, strictly adhering to the Helsinki Declaration (2022YF018-01). The study was conducted in accordance with the local legislation and institutional requirements.

Author contributions

ML: Conceptualization, Formal analysis, Methodology, Writing – original draft, Writing – review & editing. JG: Conceptualization, Methodology, Supervision, Validation, Writing – original draft, Writing – review & editing. LW: Conceptualization, Methodology, Supervision, Validation, Writing – review & editing. XL: Data curation, Resources, Validation, Writing – review & editing. YZ: Data curation, Resources, Validation, Writing – review & editing. WL: Formal analysis, Investigation, Supervision, Writing – review & editing. HH: Formal analysis, Investigation, Project administration, Writing – original draft, Writing – review & editing. CZ: Formal analysis, Investigation, Project administration, Writing – original draft, Writing – review & editing.

Funding

The author(s) declare that financial support was received for the research, authorship, and/or publication of this article. This study was supported by the Excellent Young Scholars Cultivation Project of Fujian Medical University Union Hospital (2022XH037), National Natural Science Foundation of China Youth Grant Program 82201604, 81901311), National Natural Science Foundation of China Comprehensive Program (82171445), and Fujian Provincial Natural Science Foundation of China Youth Innovation Program (2023J05148).

Conflict of interest

The authors declare that the research was conducted in the absence of any commercial or financial relationships that could be construed as a potential conflict of interest.

Publisher's note

Supplementary material

The Supplementary material for this article can be found online at: https://www.frontiersin.org/articles/10.3389/fncel.2024.1305867/full#supplementary-material

SUPPLEMENTARY FIGURE S1
Literature screening process.

SUPPLEMENTARY FIGURE S2
Cochrane bias risk assessment. Green represents low risk, red represents high risk, and yellow represents potential high bias risk.

SUPPLEMENTARY FIGURE S3
Network diagram comparing the efficacy of different types of ketogenic diets. **(A)** ≥50% reduction in epilepsy at 3 months; **(B)** ≥90% reduction in epilepsy at 3 months; **(C)** ≥50% reduction in epilepsy at 6 months; **(D)** ≥90% reduction in epilepsy at 6 months. The lines connecting the nodes indicate their correlations, with more lines indicating higher correlations.

SUPPLEMENTARY FIGURE S4
Forest plot of meta-analysis comparing the efficacy of different types of ketogenic diets. **(A)** ≥50% reduction in epilepsy at 3 months; **(B)** ≥90% reduction in epilepsy at 3 months; **(C)** ≥50% reduction in epilepsy at 6 months; **(D)** ≥90% reduction in epilepsy at 6 months.

References

Ait Ouares, K., Jaafari, N., Kuczewski, N., and Canepari, M. (2020). Imaging native calcium currents in brain slices. *Adv. Exp. Med. Biol.* 1131, 73–91. doi: 10.1007/978-3-030-12457-1_4

Arindrarto, W., Borràs, D. M., de Groen, R. A. L., van den Berg, R. R., Locher, I. J., van Diessen, S. A. M. E., et al. (2021). Comprehensive diagnostics of acute myeloid leukemia by whole transcriptome RNA sequencing. *Leukemia* 35, 47–61. doi: 10.1038/s41375-020-0762-8

Basolo, A., Magno, S., Santini, F., and Ceccarini, G. (2022). Ketogenic diet and weight loss: is there an effect on energy expenditure? *Nutrients* 14:1814. doi: 10.3390/nu14091814

Beam, A., Clinger, E., and Hao, L. (2021). Effect of diet and dietary components on the composition of the gut microbiota. *Nutrients* 13:2795. doi: 10.3390/nu13082795

Beghi, E., Giussani, G., and Sander, J. W. (2015). The natural history and prognosis of epilepsy. *Epilept. Disord.* 17, 243–253. doi: 10.1684/epd.2015.0751

Biondi, C., Campi, A. L., Pareschi, M. C., Portolan, A., and Ferretti, M. E. (1990). RMI 12330A, an inhibitor of adenylate cyclase and cyclic AMP-phosphodiesterase activities in the segmental ganglia of the leech *Hirudo medicinalis*. *Neurosci. Lett.* 113, 322–327. doi: 10.1016/0304-3940(90)90605-9

Chen, Y., Wang, H., Wang, W. Z., Wang, D., Skaggs, K., and Zhang, H. T. (2021). Phosphodiesterase 7(PDE7): a unique drug target for central nervous system diseases. *Neuropharmacology* 196:108694. doi: 10.1016/j.neuropharm.2021.108694

Cicek, E., and Sanlier, N. (2023). The place of a ketogenic diet in the treatment of resistant epilepsy: a comprehensive review. *Nutr. Neurosci.* 26, 828–841. doi: 10.1080/1028415X.2022.2095819

Dashti, H. M., Mathew, T. C., and Al-Zaid, N. S. (2021). Efficacy of low-carbohydrate ketogenic diet in the treatment of type 2 diabetes. *Med. Princ. Pract.* 30, 223–235. doi: 10.1159/000512142

Desli, E., Spilioti, M., Evangeliou, A., Styllas, F., Magkos, F., and Dalamaga, M. (2022). The efficacy and safety of ketogenic diets in drug-resistant epilepsy in children and adolescents: a systematic review of randomized controlled trials. *Curr. Nutr. Rep.* 11, 102–116. doi: 10.1007/s13668-022-00405-4

Ding, S., Hua, Y., Wu, J., Xie, A., and Zhu, X. (2014). Family-based analysis of the adiponectin gene polymorphisms and polycystic ovary syndrome. *Zhonghua Fu Chan Ke Za Zhi* 49, 36–41. doi: 10.3760/cma.J.issn.0529-567x.2014.10.009

Ding, Q., Wu, Y., and Liu, W. (2021). Molecular mechanism of reproductive toxicity induced by Tripterygium Wilfordii based on network pharmacology. *Medicine* 100:e26197. doi: 10.1097/MD.0000000000026197

Elia, M., Klepper, J., Leiendecker, B., and Hartmann, H. (2017). Ketogenic diets in the treatment of epilepsy. *Curr. Pharm. Des.* 23, 5691–5701. doi: 10.2174/1381612823666170809101517

Essam, R. M., and Kandil, E. A. (2023). P-CREB and p-DARPP-32 orchestrating the modulatory role of cAMP/PKA signaling pathway enhanced by Roflumilast in rotenone-induced Parkinson's disease in rats. *Chem. Biol. Interact.* 372:110366. doi: 10.1016/j.cbi.2023.110366

Gárriz, A., Morokuma, J., Toribio, D., and Zoukhri, D. (2023). Role of the adenylate cyclase/cyclic AMP pathway in oxytocin-induced lacrimal gland myoepithelial cells contraction. *Exp. Eye Res.* 233:109526. doi: 10.1016/j.exer.2023.109526

Goni, L., Riezu-Boj, J. I., Milagro, F. I., Corrales, F. J., Ortiz, L., Cuervo, M., et al. (2018). Interaction between an ADCY3 genetic variant and two weight-lowering diets

affecting body fatness and body composition outcomes depending on macronutrient distribution: a randomized trial. *Nutrients* 10:789. doi: 10.3390/nu10060789

Grabenstatter, H. L., Ferraro, D. J., Williams, P. A., Chapman, P. L., and Dudek, F. E. (2005). Use of chronic epilepsy models in antiepileptic drug discovery: the effect of topiramate on spontaneous motor seizures in rats with kainate-induced epilepsy. *Epilepsia* 46, 8–14. doi: 10.1111/j.0013-9580.2005.13404.x

Griebel, G., Misslin, R., Vogel, E., and Bourguignon, J. J. (1991). Behavioral effects of rolipram and structurally related compounds in mice: behavioral sedation of cAMP phosphodiesterase inhibitors. *Pharmacol. Biochem. Behav.* 39, 321–323. doi: 10.1016/0091-3057(91)90186-6

Grigsby, K. B., Childs, T. E., and Booth, F. W. (2020). The role of nucleus accumbens CREB attenuation in rescuing low voluntary running behavior in female rats. *J. Neurosci. Res.* 98, 2302–2316. doi: 10.1002/jnr.24698

Grupp, G., Grupp, I. L., Johnson, C. L., Matlib, M. A., Rouslin, W., Schwartz, A., et al. (1980). Effects of RMI 12330A, a new inhibitor of adenylate cyclase on myocardial function and subcellular activity. *Br. J. Pharmacol.* 70, 429–442. doi: 10.1111/j.1476-5381.1980.tb08721.x

Guellaen, G., Mahu, J. L., Mavier, P., Berthelot, P., and Hanoune, J. (1977). RMI 12330 a, an inhibitor of adenylate cyclase in rat liver. *Biochim. Biophys. Acta* 484, 465–475. doi: 10.1016/0005-2744(77)90102-4

Guimarães, J., Bargut, T. C. L., Mandarim-de-Lacerda, C. A., and Aguila, M. B. (2019). Medium-chain triglyceride reinforce the hepatic damage caused by fructose intake in mice. *Prostaglandins Leukot. Essent. Fatty Acids* 140, 64–71. doi: 10.1016/j.plefa.2018.11.005

Gupta, S., Dabla, S., and Kaushik, J. S. (2021). Modified Atkins diet vs low glycemic index treatment for drug-resistant epilepsy in children: an open label. *Random. Contr. Trial. Indian Pediatr.* 58, 815–819. doi: 10.1007/s13312-021-2299-y

Hollis, F., Mitchell, E. S., Canto, C., Wang, D., and Sandi, C. (2018). Medium chain triglyceride diet reduces anxiety-like behaviors and enhances social competitiveness in rats. *Neuropharmacology* 138, 245–256. doi: 10.1016/j.neuropharm.2018.06.017

Hong, S. H., Goh, S. H., Lee, S. J., Hwang, J. A., Lee, J., Choi, I. J., et al. (2013). Upregulation of adenylate cyclase 3 (ADCY3) increases the tumorigenic potential of cells by activating the CREB pathway. *Oncotarget* 4, 1791–1803. doi: 10.18632/oncotarget.1324

Hosseini-Zare, M. S., Salehi, F., Seyedi, S. Y., Azami, K., Ghadiri, T., Mobasseri, M., et al. (2011). Effects of pentoxifylline and H-89 on epileptogenic activity of bucladesine in pentylenetetrazol-treated mice. *Eur. J. Pharmacol.* 670, 464–470. doi: 10.1016/j.ejphar.2011.09.026

Karagiannis, F., Peukert, K., Surace, L., Michla, M., Nikolka, F., Fox, M., et al. (2022). Impaired ketogenesis ties metabolism to T cell dysfunction in COVID-19. *Nature* 609, 801–807. doi: 10.1038/s41586-022-05128-8

Karimzadeh, P., Sedighi, M., Beheshti, M., Azargashb, E., Ghofrani, M., and Abdollahe-Gorgi, F. (2014). Low glycemic index treatment in pediatric refractory epilepsy: the first Middle East report. *Seizure* 23, 570–572. doi: 10.1016/j.seizure.2014.03.012

Khoziainova, S., Rozenberg, G., and Levy, M. (2022). Ketogenic diet and beta-hydroxybutyrate in colorectal cancer. *DNA Cell Biol.* 41, 1007–1011. doi: 10.1089/dna.2022.0486

Kim, N. J., Baek, J. H., Lee, J., Kim, H., Song, J. K., and Chun, K. H. (2019). A PDE1 inhibitor reduces adipogenesis in mice via regulation of lipolysis and adipogenic cell signaling. *Exp. Mol. Med.* 51, 1–15. doi: 10.1038/s12276-018-0198-7

Klein, P., Devinsky, O., French, J., Harden, C., Krauss, G. L., McCarter, R., et al. (2021). Suicidality risk of newer antiseizure medications: a meta-analysis. *JAMA Neurol.* 78, 1118–1127. doi: 10.1001/jamaneurol.2021.2480

Kong, C., Yan, X., Liu, Y., Huang, L., Zhu, Y., He, J., et al. (2021). Ketogenic diet alleviates colitis by reduction of colonic group 3 innate lymphoid cells through altering gut microbiome. *Signal Transduct. Target. Ther.* 6:154. doi: 10.1038/s41392-021-00549-9

Koronowski, K. B., Greco, C. M., Huang, H., Kim, J. K., Fribourgh, J. L., Crosby, P., et al. (2021). Ketogenesis impact on liver metabolism revealed by proteomics of lysine β-hydroxybutyrylation. *Cell Rep.* 36:109487. doi: 10.1016/j.celrep.2021.109487

Kraeuter, A. K., Mashavave, T., Suvarna, A., van den Buuse, M., and Sarnyai, Z. (2020). Effects of beta-hydroxybutyrate administration on MK-801-induced schizophrenia-like behaviour in mice. *Psychopharmacology* 237, 1397–1405. doi: 10.1007/s00213-020-05467-2

Kverneland, M., Molteberg, E., Iversen, P. O., Veierød, M. B., Taubøll, E., Selmer, K. K., et al. (2018). Effect of modified Atkins diet in adults with drug-resistant focal epilepsy: a randomized clinical trial. *Epilepsia* 59, 1567–1576. doi: 10.1111/epi.14457

Lambrechts, D. A., de Kinderen, R. J., Vles, J. S., de Louw, A. J., Aldenkamp, A. P., and Majoie, H. J. (2017). A randomized controlled trial of the ketogenic diet in refractory childhood epilepsy. *Acta Neurol. Scand.* 135, 231–239. doi: 10.1111/ane.12592

Lee, D. (2015). Global and local missions of cAMP signaling in neural plasticity, learning, and memory. *Front. Pharmacol.* 6:161. doi: 10.3389/fphar.2015.00161

Levin, D. N., McClain, C. D., Stone, S. S. D., Madsen, J. R., and Soriano, S. (2021). Anesthetic management and outcomes for MRI-guided laser interstitial thermal therapy (LITT) for seizure focus in pediatrics: a single-Centre experience with 10 consecutive patients. *Paediatr. Anaesth.* 31, 234–236. doi: 10.1111/pan.13929

Liang, N., Li, Y., and Chung, H. Y. (2017). Two natural eudesmane-type sesquiterpenes from Laggera alata inhibit angiogenesis and suppress breast cancer cell migration through VEGF- and angiopoietin 2-mediated signaling pathways. *Int. J. Oncol.* 51, 213–222. doi: 10.3892/ijo.2017.4004

Lin, C., Wang, S., Xie, J., Zhu, J., Xu, J., Liu, K., et al. (2023). Ketogenic diet and β-Hydroxybutyrate alleviate ischemic brain injury in mice via an IRAKM-dependent pathway. *Eur. J. Pharmacol.* 955:175933. doi: 10.1016/j.ejphar.2023.175933

López-Rivera, J. A., Leu, C., Macnee, M., Khoury, J., Hoffmann, L., Coras, R., et al. (2023). The genomic landscape across 474 surgically accessible epileptogenic human brain lesions. *Brain J. Neurol.* 146, 1342–1356. doi: 10.1093/brain/awac376

Luo, Z., Liao, X., Luo, L., Fan, Q., Zhang, X., Guo, Y., et al. (2022). Extracellular ATP and cAMP signaling promote piezo 2-dependent mechanical allodynia after trigeminal nerve compression injury. *J. Neurochem.* 160, 376–391. doi: 10.1111/jnc.15537

Ma, T. C., Barco, A., Ratan, R. R., and Willis, D. E. (2014). cAMP-responsive element-binding protein (CREB) and cAMP co-regulate activator protein 1 (AP1)-dependent regeneration-associated gene expression and neurite growth. *J. Biol. Chem.* 289, 32914–32925. doi: 10.1074/jbc.M114.582460

Manford, M. (2017). Recent advances in epilepsy. *J. Neurol.* 264, 1811–1824. doi: 10.1007/s00415-017-8394-2

Martin-McGill, K. J., Bresnahan, R., Levy, R. G., and Cooper, P. N. (2020). Ketogenic diets for drug-resistant epilepsy. *Cochrane Database Syst. Rev.* 2020:CD001903. doi: 10.1002/14651858.CD001903.pub5

Martins, C., Nymo, S., Aukan, M. I., Roekenes, J. A., Coutinho, S. R., Hunter, G. R., et al. (2023). Association between ß-Hydroxybutyrate plasma concentrations after hypocaloric ketogenic diets and changes in body composition. *J. Nutr.* 153, 1944–1949. doi: 10.1016/j.tjnut.2023.05.010

Masino, S. A., Li, T., Theofilas, P., Sandau, U. S., Ruskin, D. N., Fredholm, B. B., et al. (2011). A ketogenic diet suppresses seizures in mice through adenosine a_1 receptors. *J. Clin. Invest.* 121, 2679–2683. doi: 10.1172/JCI57813

Mazdeh, M., Omrani, M. D., Sayad, A., Komaki, A., Arsang-Jang, S., Taheri, M., et al. (2018). Expression analysis of cytokine coding genes in epileptic patients. *Cytokine* 110, 284–287. doi: 10.1016/j.cyto.2018.01.017

McDonald, T. J. W., and Cervenka, M. C. (2020). Ketogenic diet therapies for seizures and status epilepticus. *Semin. Neurol.* 40, 719–729. doi: 10.1055/s-0040-1719077

Mierziak, J., Burgberger, M., and Wojtasik, W. (2021). 3-Hydroxybutyrate as a metabolite and a signal molecule regulating processes of living organisms. *Biomol. Ther.* 11:402. doi: 10.3390/biom11030402

Modebadze, T., Morgan, N. H., Pérès, I. A., Hadid, R. D., Amada, N., Hill, C., et al. (2016). A low mortality, high morbidity reduced intensity status epilepticus (RISE) model of epilepsy and Epileptogenesis in the rat. *PLoS One* 11:e0147265. doi: 10.1371/journal.pone.0147265

Nagpal, R., Neth, B. J., Wang, S., Craft, S., and Yadav, H. (2019). Modified Mediterranean-ketogenic diet modulates gut microbiome and short-chain fatty acids in association with Alzheimer's disease markers in subjects with mild cognitive impairment. *EBioMedicine* 47, 529–542. doi: 10.1016/j.ebiom.2019.08.032

Narayan, V., Shivapurkar, N., and Baraniuk, J. N. (2020). Informatics inference of exercise-induced modulation of brain pathways based on cerebrospinal fluid MicroRNAs in Myalgic encephalomyelitis/chronic fatigue syndrome. *Netw. Syst. Med.* 3, 142–158. doi: 10.1089/nsm.2019.0009

Neal, E. G., Chaffe, H., Schwartz, R. H., Lawson, M. S., Edwards, N., Fitzsimmons, G., et al. (2009). A randomized trial of classical and medium-chain triglyceride ketogenic diets in the treatment of childhood epilepsy. *Epilepsia* 50, 1109–1117. doi: 10.1111/j.1528-1167.2008.01870.x

Norwitz, N. G., Sethi, S., and Palmer, C. M. (2020). Ketogenic diet as a metabolic treatment for mental illness. *Curr. Opin. Endocrinol. Diabetes Obes.* 27, 269–274. doi: 10.1097/MED.0000000000000564

Paoli, A., Mancin, L., Giacona, M. C., Bianco, A., and Caprio, M. (2020). Effects of a ketogenic diet in overweight women with polycystic ovary syndrome. *J. Transl. Med.* 18:104. doi: 10.1186/s12967-020-02277-0

Polito, R., La Torre, M. E., Moscatelli, F., Cibelli, G., Valenzano, A., Panaro, M. A., et al. (2023). The ketogenic diet and neuroinflammation: the action of beta-hydroxybutyrate in a microglial cell line. *Int. J. Mol. Sci.* 24:3102. doi: 10.3390/ijms24043102

Poorshiri, B., Barzegar, M., Afghan, M., Shiva, S., Shahabi, P., Golchinfar, Z., et al. (2023). The effects of ketogenic diet on beta-hydroxybutyrate, arachidonic acid, and oxidative stress in pediatric epilepsy. *Epilepsy Behav.* 140:109106. doi: 10.1016/j.yebeh.2023.109106

Qi, A. Q., Zhang, Y. H., Qi, Q. D., Liu, Y. H., and Zhu, J. L. (2019). Overexpressed HspB6 underlines a novel inhibitory role in Kainic acid-induced epileptic seizure in rats by activating the cAMP-PKA pathway. *Cell. Mol. Neurobiol.* 39, 111–122. doi: 10.1007/s10571-018-0637-y

Ramazi, S., Fahanik-Babaei, J., Mohamadi-Zarch, S. M., Baluchnejadmojarad, T., and Roghani, M. (2022). Paeonol exerts neuroprotective and anticonvulsant effects in intrahippocampal kainate model of temporal lobe epilepsy. *J. Chem. Neuroanat.* 124:102121. doi: 10.1016/j.jchemneu.2022.102121

Rogawski, M. A., Löscher, W., and Rho, J. M. (2016). Mechanisms of action of Antiseizure drugs and the ketogenic diet. *Cold Spring Harb. Perspect. Med.* 6:a022780. doi: 10.1101/cshperspect.a022780

Ross, W. N. (1989). Changes in intracellular calcium during neuron activity. *Annu. Rev. Physiol.* 51, 491–506. doi: 10.1146/annurev.ph.51.030189.002423

Ruan, Y., Chen, L., She, D., Chung, Y., Ge, L., and Han, L. (2022). Ketogenic diet for epilepsy: an overview of systematic review and meta-analysis. *Eur. J. Clin. Nutr.* 76, 1234–1244. doi: 10.1038/s41430-021-01060-8

Saeidian, A. H., Youssefian, L., Vahidnezhad, H., and Uitto, J. (2020). Research techniques made simple: whole-transcriptome sequencing by RNA-Seq for diagnosis of monogenic disorders. *J. Invest. Dermatol.* 140, 1117–1126.e1. doi: 10.1016/j.jid.2020.02.032

Samanta, D. (2021). Epilepsy in Angelman syndrome: a scoping review. *Brain Dev.* 43, 32–44. doi: 10.1016/j.braindev.2020.08.014

Sampaio, L. P. (2016). Ketogenic diet for epilepsy treatment. *Arq. Neuropsiquiatr.* 74, 842–848. doi: 10.1590/0004-282X20160116

Sano, M., Seto-Ohshima, A., and Mizutani, A. (1984). Forskolin suppresses seizures induced by pentylenetetrazol in mice. *Experientia* 40, 1270–1271. doi: 10.1007/BF01946669

Son, Y., Choi, C., Saha, A., Park, J. H., Im, H., Cho, Y. K., et al. (2022). REEP6 knockout leads to defective β-adrenergic signaling in adipocytes and promotes obesity-related metabolic dysfunction. *Metab. Clin. Exp.* 130:155159. doi: 10.1016/j.metabol.2022.155159

Sondhi, V., Agarwala, A., Pandey, R. M., Chakrabarty, B., Jauhari, P., Lodha, R., et al. (2020). Efficacy of ketogenic diet, modified Atkins diet, and low glycemic index therapy diet among children with drug-resistant epilepsy: a randomized clinical trial. *JAMA Pediatr.* 174, 944–951. doi: 10.1001/jamapediatrics.2020.2282

Sorkpor, S. K., and Ahn, H. (2021). Transcranial direct current and transcranial magnetic stimulations for chronic pain. *Curr. Opin. Anaesthesiol.* 34, 781–785. doi: 10.1097/ACO.0000000000001056

Sourbron, J., Klinkenberg, S., van Kuijk, S. M. J., Lagae, L., Lambrechts, D., Braakman, H. M. H., et al. (2020). Ketogenic diet for the treatment of pediatric epilepsy: review and meta-analysis. *Child Nerv. Syst.* 36, 1099–1109. doi: 10.1007/s00381-020-04578-7

Sun, H. L., Wu, Y. W., Bian, H. G., Yang, H., Wang, H., Meng, X. M., et al. (2021). Function of uric acid transporters and their inhibitors in Hyperuricaemia. *Front. Pharmacol.* 12:667753. doi: 10.3389/fphar.2021.667753

Thijs, R. D., Surges, R., O'Brien, T. J., and Sander, J. W. (2019). Epilepsy in adults. *Lancet* 393, 689–701. doi: 10.1016/S0140-6736(18)32596-0

Ułamek-Kozioł, M., Czuczwar, S. J., Januszewski, S., and Pluta, R. (2019). Ketogenic Diet and Epilepsy. *Nutrients* 11:2510. doi: 10.3390/nu11102510

van der Louw, E., van den Hurk, D., Neal, E., Leiendecker, B., Fitzsimmon, G., Dority, L., et al. (2016). Ketogenic diet guidelines for infants with refractory epilepsy. *Eur. J. Paediatr. Neurol.* 20, 798–809. doi: 10.1016/j.ejpn.2016.07.009

Van Erum, J., Van Dam, D., and De Deyn, P. P. (2019). PTZ-induced seizures in mice require a revised Racine scale. *Epilepsy Behav.* 95, 51–55. doi: 10.1016/j.yebeh.2019.02.029

Wang, Y., Gao, Y., Tian, Q., Deng, Q., Wang, Y., Zhou, T., et al. (2018). TRPV1 SUMOylation regulates nociceptive signaling in models of inflammatory pain. *Nat. Commun.* 9:1529. doi: 10.1038/s41467-018-03974-7

Wang, J., Huang, J., Li, Y. Q., Yao, S., Wu, C. H., Wang, Y., et al. (2021). Neuregulin 1/ErbB4 signaling contributes to the anti-epileptic effects of the ketogenic diet. *Cell Biosci.* 11:29. doi: 10.1186/s13578-021-00536-1

Wang, Z. Y., Li, X. Y., Gou, X. J., Chen, C. L., Li, Z. Y., Zhao, C., et al. (2022). Network Meta-analysis of Acupoint catgut embedding in treatment of simple obesity. *Evid. Based Complement. Alternat. Med.* 2022, 6408073–6408016. doi: 10.1155/2022/6408073

Wang, D., Wong, H. K., Feng, Y. B., and Zhang, Z. J. (2013). Paeoniflorin, a natural neuroprotective agent, modulates multiple anti-apoptotic and pro-apoptotic pathways in differentiated PC12 cells. *Cell. Mol. Neurobiol.* 33, 521–529. doi: 10.1007/s10571-013-9914-y

Wells, J., Swaminathan, A., Paseka, J., and Hanson, C. (2020). Efficacy and safety of a ketogenic diet in children and adolescents with refractory epilepsy-a review. *Nutrients* 12:1809. doi: 10.3390/nu12061809

Wickham, J., Corna, A., Schwarz, N., Uysal, B., Layer, N., Honegger, J. B., et al. (2020). Human cerebrospinal fluid induces neuronal excitability changes in resected human neocortical and hippocampal brain slices. *Front. Neurosci.* 14:283. doi: 10.3389/fnins.2020.00283

Wu, L., Shen, C., Seed Ahmed, M., Östenson, C. G., and Gu, H. F. (2016). Adenylate cyclase 3: a new target for anti-obesity drug development. *Obesity Rev.* 17, 907–914. doi: 10.1111/obr.12430

Yang, X. Y., Ma, Z. L., Storm, D. R., Cao, H., and Zhang, Y. Q. (2021). Selective ablation of type 3 adenylyl cyclase in somatostatin-positive interneurons produces anxiety- and depression-like behaviors in mice. *World J. Psychiatry* 11, 35–49. doi: 10.5498/wjp.v11.i2.35

Yang, L., Ton, H., Zhao, R., Geron, E., Li, M., Dong, Y., et al. (2020). Sevoflurane induces neuronal activation and behavioral hyperactivity in young mice. *Sci. Rep.* 10:11226. doi: 10.1038/s41598-020-66959-x

Yang, C., Yang, Y., Peng, Y., Zhang, L., and Yu, D. (2022). Efficacy and safety of lacosamide in pediatric patients with epilepsy: a systematic review and meta-analysis. *Epilepsy Behav.* 134:108781. doi: 10.1016/j.yebeh.2022.108781

Youm, Y. H., Nguyen, K. Y., Grant, R. W., Goldberg, E. L., Bodogai, M., Kim, D., et al. (2015). The ketone metabolite β-hydroxybutyrate blocks NLRP3 inflammasome-mediated inflammatory disease. *Nat. Med.* 21, 263–269. doi: 10.1038/nm.3804

Yuan, X., Wang, J., Yang, S., Gao, M., Cao, L., Li, X., et al. (2020). Effect of the ketogenic diet on glycemic control, insulin resistance, and lipid metabolism in patients with T2DM: a systematic review and meta-analysis. *Nutr. Diabetes* 10:38. doi: 10.1038/s41387-020-00142-z

Zarnowska, I. M. (2020). Therapeutic use of the ketogenic diet in refractory epilepsy: what we know and what still needs to be learned. *Nutrients* 12:2616. doi: 10.3390/nu12092616

Zhang, J., Lu, C., Wu, X., Nie, D., and Yu, H. (2021a). Neuroplasticity of acupuncture for stroke: an evidence-based review of MRI. *Neural Plast.* 2021, 2662585–2662514. doi: 10.1155/2021/2662585

Zhang, Z., Yang, D., Zhang, M., Zhu, N., Zhou, Y., Storm, D. R., et al. (2017). Deletion of type 3 adenylyl cyclase perturbs the postnatal maturation of olfactory sensory neurons and olfactory cilium ultrastructure in mice. *Front. Cell. Neurosci.* 11:1. doi: 10.3389/fncel.2017.00001

Zhang, J., Zhang, C., Chen, X., Wang, B., Ma, W., Yang, Y., et al. (2021b). PKA-RIIβ autophosphorylation modulates PKA activity and seizure phenotypes in mice. *Commun. Biol.* 4:263. doi: 10.1038/s42003-021-01748-4

Zheng, W., Zhang, T., Zhao, T., Zhu, Z., Qin, S., Yan, H., et al. (2023). cAMP controls the balance between dormancy and activation of primordial follicles in mouse ovaries. *PNAS Nexus* 2:pgad 055. doi: 10.1093/pnasnexus/pgad055

Zou, S., Wang, C., Cui, Z., Guo, P., Meng, Q., Shi, X., et al. (2016). β-Elemene induces apoptosis of human rheumatoid arthritis fibroblast-like synoviocytes via reactive oxygen species-dependent activation of p38 mitogen-activated protein kinase. *Pharmacol. Rep.* 68, 7–11. doi: 10.1016/j.pharep.2015.06.004

frontiers | Frontiers in Pharmacology

TYPE Original Research
PUBLISHED 05 June 2024
DOI 10.3389/fphar.2024.1364353

OPEN ACCESS

EDITED BY
Antonella Riva,
University of Genoa, Italy

REVIEWED BY
Nicola Forte,
National Research Council (CNR), Italy
Wieslawa Agnieszka Fogel,
Polish Academy of Sciences, Poland

*CORRESPONDENCE
Bassem Sadek,
bassem.sadek@uaeu.ac.ae
Salim M. Bastaki,
sbastaki@uaeu.ac.ae

RECEIVED 02 January 2024
ACCEPTED 06 May 2024
PUBLISHED 05 June 2024

CITATION
Bastaki SM, Abdulrazzaq YM, Zidan MA, Shafiullah M, Alaryani SG, Alnuaimi FA, Adeghate E, Mohsin S, Akour A, Siwek A, Łażewska D, Kieć-Kononowicz K and Sadek B (2024), Reproductive and fetal toxicity studies of histamine H3 receptor antagonist DL76 used in mice to prevent maximal electroshock-induced seizure.
Front. Pharmacol. 15:1364353.
doi: 10.3389/fphar.2024.1364353

Reproductive and fetal toxicity studies of histamine H3 receptor antagonist DL76 used in mice to prevent maximal electroshock-induced seizure

Salim M. Bastaki[1,2]*, Yousef M. Abdulrazzaq[3], Marwan Abdelrahim Zidan[4], Mohamed Shafiullah[1,2], Saif Ghdayer Alaryani[5], Fatima Awad Alnuaimi[5], Ernest Adeghate[5], Sahar Mohsin[5], Amal Akour[1], Agata Siwek[6], Dorota Łażewska[7], Katarzyna Kieć-Kononowicz[7] and Bassem Sadek[1,2]*

[1]Department of Pharmacology and Therapeutics, College of Medicine and Health Science, United Arab Emirates University, Al Ain, United Arab Emirates, [2]Zayed Center for Health Sciences, United Arab Emirates University, Al Ain, United Arab Emirates, [3]Department of Paediatrics and Neonatology, College of Medicine and Health Science, United Arab Emirates University, Al Ain, United Arab Emirates, [4]Department of Education, Dubai Health Authority, Dubai, United Arab Emirates, [5]Department of Anatomy, College of Medicine and Health Sciences, United Arab Emirates University, Al Ain, United Arab Emirates, [6]Department of Pharmacobiology, Faculty of Pharmacy, Jagiellonian University Medical College in Kraków, Kraków, Poland, [7]Department of Technology and Biotechnology of Drugs, Faculty of Pharmacy, Jagiellonian University Medical College in Kraków, Kraków, Poland

Introduction: Brain histamine is considered an endogenous anticonvulsant and histamine H1 receptor. H1R antagonists have, in earlier studies, been found to induce convulsions. Moreover, research during the last two decades has provided more information concerning the anticonvulsant activities of histamine H3R (H3R) antagonists investigated in a variety of animal epilepsy models.

Methods: Therefore, the *in vivo* anticonvulsant effect of the H3R antagonist DL76, with proven high *in vitro* affinity, *in vitro* selectivity profile, and high *in vivo* antagonist potency in mice against maximal electroshock (MES)-induced seizures in mice, was assessed. Valproic acid (VPA) was used as a reference antiepileptic drug (AED). In addition, DL76 was tested for its reproductive and fetal toxicity in the same animal species.

Results and discussion: Our observations showed that acute systemic administration (intraperitoneal; i.p.) of DL76 (7.5 mg/kg, 15 mg/kg, 30 mg/kg, and 60 mg/kg, i.p.) provided significant and dose-dependent protection against MES-induced seizures in female and male mice. Moreover, the DL76-provided protective effects were comparable to those offered by the VPA and were reversed when animals were co-administered the CNS-penetrant selective H3R agonist *R*-(α)-methylhistamine (RAM, 10 mg/kg, i.p.). Furthermore, the administration of single (7.5 mg/kg, 15 mg/kg, 30 mg/kg, or 60 mg/kg, i.p.) or multiple doses (3 × 15 mg/kg, i.p.) of H3R antagonist DL76 on gestation days (GD) 8 or 13 failed to affect the maternal body weight of mice when compared with the control mice group. No significant alterations were detected in the average number of implantations and resorptions between the control and DL76-treated groups at the early stages of gestation and the organogenesis period. In addition,

no significant differences in the occurrence of skeletal abnormalities, urogenital abnormalities, exencephaly, exomphalos, facial clefts, and caudal malformations were observed. The only significant abnormalities witnessed in the treated groups of mice were in the length of long bones and body length. In conclusion, the novel H3R antagonist DL76 protected test animals against MES-induced seizures and had a low incidence of reproductive and fetal malformation with decreased long bone lengths *in vivo*, signifying the potential therapeutic value of H3R antagonist DL76 for future preclinical as well as clinical development for use in the management of epilepsy.

KEYWORDS

histamine H3 receptors, antagonist DL76, maximal electroshock, seizures, anticonvulsant, malformation, gestation, mice

1 Introduction

Epilepsy is characterized by seizures that are unpredictable in frequency and is the second most common neurological disorder that affects people of all ages, with onset most often occurring in childhood and older adulthood (Mauritz et al., 2022; Yang et al., 2022; Asadi-Pooya et al., 2023). Epilepsy leads to abnormal behavioral paradigms, necessitating a lifelong treatment with effective antiepileptic drugs (AEDs) (Brigo et al., 2013; Mauritz et al., 2022). The anticipated prevalence rate of epilepsy in the United States and other regions is high. Approximately 1.5 million women with epilepsy give birth to 27,000 infants yearly, with an estimated prevalence of epilepsy in pregnant women of approximately 0.5% (Tomson and Battino, 2007; Thomas et al., 2012; Sadek et al., 2014a; Sadek et al., 2015; Bastaki et al., 2018; Tomson et al., 2018). Clinical observations revealed that approximately 60%–70% of patients diagnosed with epilepsy respond to available treatments with AEDs. However, resistance to monotherapy is not uncommon, and a combination of several AEDs is often inevitable with the possibility of drug–drug interactions (Brigo et al., 2013; Sadek et al., 2014a). Following chronic clinical use of several AEDs, the incidence of major malformations in infants of epileptic parents was found to be twice that of non-epileptic parents (Sadek et al., 2015; Bastaki et al., 2018). In addition, gestational epilepsy is a concern for women with a pre-existing seizure and can lead to a 17% rise in seizure episodes (Tomson et al., 2018). Accordingly, hormonal fluctuations and changes in the pharmacokinetics of AEDs play a crucial role (Thomas et al., 2012). Therapeutic drug monitoring and maintaining strict adherence to AEDs have improved therapeutic management (Pennell et al., 2020), yet the threat of complications for both mother and child persists. Epilepsy can increase maternal mortality fivefold, and *in utero* exposure to AEDs, notably valproic acid (VPA), increases the risk of congenital defects, which is also related to drug type and dosage and is worsened by specific drug combinations (Viale et al., 2015).

The involvement of the brain histaminergic neurotransmitter system in seizure control is well-established, as several previous observations in preclinical experiments demonstrated that brain histamine is capable of modulating seizure trends in both electrically and chemically induced seizure models in animals (Kamei et al., 1993a; Kamei et al., 1993b; Chen et al., 2002; Zhang et al., 2003; Sadek et al., 2014b). Accordingly, the precursor of brain histamine, namely, the amino acid L-histidine, was reported to decrease chemically induced seizure in experimental animals by stimulating the brain histaminergic neurotransmission and increasing the seizure threshold by interactions of brain histamine with postsynaptically located histamine H1 receptors (H1Rs) in the brain (Chen et al., 2002). Moreover, the involvement of central H1Rs in the development of seizures was confirmed by preclinical studies that showed an increased tendency of seizures in mice lacking H1Rs or histidine decarboxylase enzyme responsible for the biosynthesis of histamine in the brain (Jang et al., 2010; Miyata et al., 2011). Clinically, it has been found that the use of high doses of various centrally acting H1R antagonists belonging to old-generation antihistamines, such as diphenhydramine, as antiallergic drugs occasionally increased the risk of convulsions in healthy young children, and this risk was especially observed among long-term users (Ago et al., 2006; Jang et al., 2010; Miyata et al., 2011). Histamine interacts with four G-protein-coupled H1-4R subtypes. H3R, first described in 1983, was found to regulate histamine biosynthesis and release, acting as presynaptic auto-receptors (Arrang et al., 1983; 1987; Brown et al., 2001). Accordingly, H3R antagonists or histamine *N*-methyl transferase (HNMT) inhibitors (e.g., methoprene) were found to increase brain histamine levels and decrease seizures in epileptic patients through interactions with H1Rs (Witkin and Nelson, 2004; Vohora et al., 2010). Hence, the potential of H3R antagonists as future AEDs has begun to be increasingly considered, as mounting evidence from both acute and chronic experimental seizure models demonstrated the anticonvulsant efficacy of numerous imidazole- and non-imidazole-based H3R antagonists, such as thioperamide, 2–18, DL77, E159, and E169 (Brown et al., 2001; Vohora et al., 2010; Witkin and Nelson, 2004; Sadek et al., 2015; Bastaki et al., 2018).

Based on the afore-mentioned preclinical and clinical findings, and in search of potent and selective histamine H3R antagonists with anticonvulsant properties, our research group succeeded in developing the histamine H3R antagonist DL76 [1-(3-(4-tert-butyl-phenoxy) propyl) piperidine] (Figure 1), a non-imidazole-based H3R ligand, which proved to be a highly potent H3R antagonist (human H3R K_i = 22 nM) with good selectivity profile vs. other histamine receptors and high oral potency in mice with an ED_{50} value of 2.8 ± 0.4 mg/kg (Lazewska et al., 2006; Lazewska et al., 2017; Lazewska et al., 2020; Canale et al., 2021) (Figure 1). Moreover, previous research works clearly showed antiparkinsonian effects of H3R antagonist DL76 without inducing *in vitro* toxicity when tested

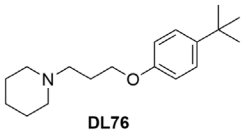

DL76

ED_{50} = 2.8 ± 0.4 mg/kg after p.o. administration to mice[a]
hH_3R K_i = 22 ± 3 nM (in CHO K1 cells; [^{125}I]Iodoproxyfan binding assay)[a]
hH_1R K_i = 849 ± 67 nM (in CHO K1 cells; [^{3}H]pyrilamine)[b]
hH_2R: 2.8 % of inhibition at 1 μM (in CHO cells; [^{125}I]APT)[c]
hH_4R K_i = 65,955 ± 35,702 nM (in Sf9 cells; [^{3}H]histamine)[d]
adrenergic α2 receptor: K_i > 5000 nM[e] (in rat cerebral cortex; [^{3}H]clonidine)[e]
Na^+ channel (site 2): 32% inhibition at 1 μM (in rat cerebral cortex; [^{3}H]batrachotoxin)[c]
hN neuronal α4β2: 3% inhibition at 1 μM (in SH-SY5Y cells; [^{3}H]cystine)[c]

FIGURE 1
Chemical structure, *in vitro* affinities, and *in vivo* H3R antagonist potency of DL76. [a]Data from Lazewska et al. (2006). [b]Measured according to a previous protocol (Lazewska et al., 2017). [c]Radioligand binding studies were performed commercially in Eurofins Cerep Laboratories (Celle-Lévescault, France). [D]Data from Lazewska et al. (2020) and Canale et al. (2021). [e]Measured according to a previous protocol (Canale et al., 2021).

in several cell lines (Canale et al., 2021). In a previous preclinical pharmacokinetic evaluation study in experimental animals, concentrations of DL76 in the cortex, hippocampus, and striatum were found to be significantly higher (44%) than in the whole brain tissues. Following administration of the doses, C_0 values increased from 564 ng/mL (3 mg/kg) to 653 ng/mL (6 mg/kg), while AUC0→∞ was found to be doubled when the tested dose increased from 3 mg/kg to 6 mg/kg (298 ng∘h/mL vs. 685 ng∘h/mL) (Szafarz et al., 2015). Therefore, the H3R antagonist DL76, which has a high *in vitro* H3R antagonist affinity, an excellent *in vitro* selectivity profile, a high *in vivo* H3R antagonist potency, and pharmacokinetics and tissue distribution profiles, was selected for further investigations of its anticonvulsant efficacy in MES-induced seizure models in male and female adult mice. Possible reproductive toxicities in the same animal species were assessed following systemic administration of H3R antagonist DL76 in a wide range of doses.

2 Materials and methods

2.1 Animals

Experiments utilized 8–10-week-old C57BL/6J mice (30–35 g) from The Jackson Laboratory, referred to as C57 mice, of both sexes. Mice were group-housed in standard Plexiglas cages with *ad libitum* access to food and water in a 12-h light/dark cycle (lights on at 6:00 a.m.). Procedures were conducted between 9:00 a.m. and 12:00 p.m., following guidelines of the European Communities Council Directive (86/609/EEC) and approved by the Institutional Animal Ethics Committee for epilepsy (ERA-2017-5535) and teratogenic studies (A14-14) at the College of Medicine and Health Sciences/United Arab Emirates University.

2.2 Drugs

The reference AED VPA and the CNS-penetrant H3R agonist (*R*)-α-methylhistamine (RAM, 10 mg/kg, i.p.) were obtained from Sigma-Aldrich (St Louis, Missouri, USA). The test compound DL76 was synthesized by the Department of Technology and Biotechnology of Drugs (Kraków, Poland) according to previously described synthetic protocols (Lazewska et al., 2006). The test compound DL76, the reference drug VPA (300 mg/kg), and the CNS-penetrant H3R agonist RAM (10 mg/kg) were dissolved in isotonic saline and administered intraperitoneally (i.p.) at a volume of 1 mL/kg for all *in vivo* studies. DL76 was used in a dose range of 7.5 mg/kg, 15 mg/kg, 30 mg/kg, and 60 mg/kg. All doses of used drugs were expressed in terms of the free bases. Eight mice were used to assess the anticonvulsant activity of each compound.

2.3 Maximal electroshock (MES)-induced seizure

As previously described and with a slight modification in the intensity applied, seizures were elicited in mice with a 50-Hz alternating current of 120 mA intensity (Kaminski et al., 2015; Song et al., 2020; Xiao et al., 2021; Hua et al., 2023). The current was applied through ear electrodes for 0.2 s. Protection against the spread of MES-induced convulsion was defined as the abolition of the tonic hind limb extension (THLE) component of the seizure (Kaminski et al., 2015; Song et al., 2020; Xiao et al., 2021; Hua et al., 2023). The animals were divided into the following experimental groups, with eight mice in each: the control group injected with saline, the positive control group injected with 300 mg/kg of VPA (the minimal dose of VPA that protected animals against the spread of MES-induced convulsions without mortality in mice) (Sadek et al., 2015; Bastaki et al., 2018), and four groups that were administered the test compound DL76 at doses of 7.5 mg/kg, 15 mg/kg, 30 mg/kg, or 60 mg/kg. All drugs were administered 30–45 min before the MES challenge. In a further group of eight mice, the most promising and protective dose of DL76 (60 mg/kg, i.p.) was co-injected with RAM (10 mg/kg, i.p.), 30 min apart and 15 min prior to the MES test. Protection against the spread of MES-induced convulsion was defined as the abolition of the THLE component of the convulsion (Sadek et al., 2015; Alachkar et al., 2018; Bastaki et al., 2018).

2.4 Reproductive studies

Reproductive studies were conducted in adult female mice, averaging 30 gm in weight and 6 weeks in age (Padmanabhan et al., 2006; Bastaki et al., 2018). Following successful mating, indicated by vaginal plug observation, the plug-positive day was

10.3389/fphar.2024.1364353

TABLE 1 Morphological effect of systemic treatment of H3R antagonist DL-76 on gestation day (GD-8) in C57/B6 mouse embryos.

		DL76 (mg/kg) on GD-8				
	Control	7.5	15	30	60	3 × 15-dose
Total no. of embryos	38	44	38	51	46	47
Mandible hypoplasia	2 (5.3)	3 (6.8)	3 (7.9)	3 (5.9)	4 (8.7)	3 (6.4)
Maxilla hypoplasia	1 (2.6)	3 (6.8)	1 (2.6)	2 (3.9)*	2 (4.3)	2 (4.3)
Eye open	1 (2.6)	2 (4.5)	3 (7.9)	2 (3.9)	1 (2.2)	4 (8.5)
Microtia/low set microtia	1 (2.6)	2 (4.5)	1 (2.6)	2 (3.9)	2 (4.3)	2 (4.3)
Exomphalos	1 (2.6)	0	1 (2.6)	1 (2.0)	0	0
Left/right kidney hypo/descended	1 (2.6)	1 (2.3)	2 (5.3)	2 ((3.9)	2 (4.3)	2 (4.3)
Undescended testis	0	2 (4.5)	0	0	0	1 (2.1)
Number of male embryos	21 (55.3)	25 (56.8)	18 (47.4)	24 (47.1)	25 (54.3)	23 (48.9)
Number of female embryos	17 (44.7)	19 (43.2)	20 (52.6)	27 (52.9)	21 (45.7)	24 (51.1)
Kinky tail	0	0	0	1 (2.0)	0	0

*$p < 0.05$ compared to the values of the corresponding controls; Parentheses contain percentages. Control mice were administered with saline.

TABLE 2 Morphological effect of systemic treatment of drug DL-76 on gestation day (GD-13) in C57/B6 mouse embryos.

		DL76 (mg/kg) on GD-13				
	Control	7.5	15	30	60	3 × 15-dose
Total no. of embryos	47	50	40	43	32	48
Mandible hypoplasia	3 (6.4)	4 (8.0)	4 (10.0)	3 (7.0)	2 (6.3)	3 (6.3)
Maxilla hypoplasia	2 (4.3)	4 (8.0)*	3 (7.5)	2 (4.7)	2 (6.3)	3 (6.3)
Eye open	0	3 (6.0)	2 (5.0)	0	2 (6.3)	6 (12.5)
Microtia/low set microtia	2 (4.3)	2 (4.0)	2 (5.0)	1 (2.3)	2 (6.3)	3 (6.3)
Exomphalos	0	0	0	1 (2.3)	0	1 (2.1)
Left/right kidney hypo/descended	1 (2.1)	2 (4.0)	1 (2.5)	1 (2.3)	2 (6.3)	2 (4.2)
Undescended testis	0	1 (2.0)	1 (2.5)	0	2 (6.3)	0
Number of male embryos	22 (46.8)	23 (46.0)	22 (55.0)	19 (44.2)	15 (46.9)	24 (50.0)
Number of female embryos	25 (53.2)	27 (54.0)	18 (45.0)	24 (55.8)	17 (53.1)	24 (50.0)
Kinky tail	0	0	0	0	0	1 (2.1)

*$p < 0.05$ compared to the values of the corresponding controls; Parentheses contain percentages. Control mice were administered with saline.

considered gestation day 0 (GD-0). DL76 was administered at various doses (7.5 mg/kg, 15 mg/kg, 30 mg/kg, and 60 mg/kg) through single i.p. injections and three 15 mg/kg injections in 1 day to mouse groups on GD-8 and GD-13 (Tables 1, 2). The control group was injected with normal saline. Appropriate formation of different organs occurs in specific periods of the development of the mouse. These two periods were selected because GD-8 is known to be a critical period for the induction of neural tube defects, craniofacial malformations, and the development of other organs, whereas on GD-13, the retina and other parts are being formed, and most other organs have been formed. The number of implantations, fetal deaths, and resorptions was recorded. Fetal and placental weights were documented separately. After blotting dry, the fetuses were weighed and fixed in 95% ethanol. The reproductive toxicological effects of DL76 were assessed by observing gross and visceral malformations, following Sterz and Lehmann (1985), Abdulrazzaq et al. (1997), Padmanabhan et al. (2003), and Padmanabhan et al. (2006).

2.4.1 Method of whole embryo observation

Deformities of the embryos were identified according to a modified method of Sterz and Lehmann (1985), Abdulrazzaq et al. (1997), and Bass et al. (2020). Accordingly, the embryos were removed from the 95% ethanol, and the lower part of the

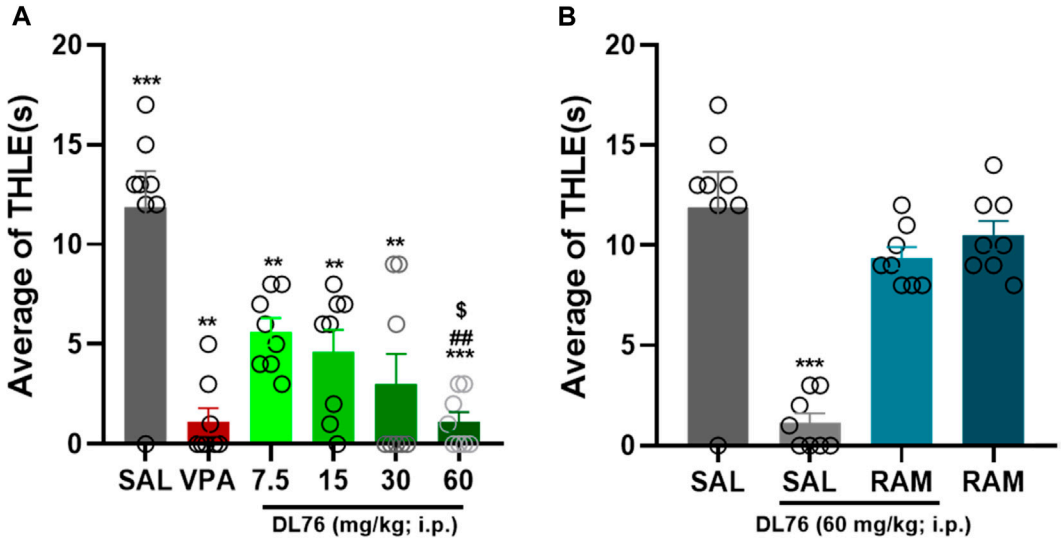

FIGURE 2
Anticonvulsant effect of acute systemic administration of H3R antagonist DL76 on MES-induced seizure in male adult mice. **(A)** Anticonvulsant effects of valproic acid (VPA, 300 mg/kg, i.p.) and test compound DL76 (7.5 mg/kg, 15 mg/kg, 30 mg/kg, and 60 mg/kg, i.p.) on the duration of tonic hind limb extension (THLE) induced in an MES model in male adult mice. **(B)** Effect of CNS-penetrant H3R agonist RAM (10 mg/kg, i.p.) pretreatment on the protection by H3R antagonist DL76 (60 mg/kg, i.p.) on MES-induced convulsions in male adult mice. Each value represents mean ± SEM (n = 8). ***$p < 0.001$ *versus* saline- and DL76 (7.5 mg/kg)-treated groups. $^{\#\#}p < 0.001$ *versus* DL76 (7.5 mg/kg)- and DL76 (15 mg/kg)-treated groups. $^{\$}p < 0.05$ *versus* DL76 (30 mg/kg)-treated group.

abdomen was cut using a razor blade. All organs were checked for abnormalities with a stereo dissecting microscope, and finally, the organs were removed by using forceps.

2.4.2 Double staining methods

After isolating fetuses from viscera and skin, they underwent a fat-removal process by immersion in acetone for 1–3 days. The resulting transparent specimens underwent a sequence of glycerin solutions (50% and 80%) before being finally stored in 100% glycerin for observation of malformations using a stereo dissecting microscope (McLeod, 1980; Sterz and Lehmann, 1985; Abdulrazzaq et al., 1997; Bass et al., 2020). Following this, specimens were processed and stained with Alizarin Red-S and Alcian blue (McLeod, 1980; Sterz and Lehmann, 1985; Abdulrazzaq et al., 1997; Bass et al., 2020) to identify bone and cartilage deformities.

2.5 Statistics

Statistical analyses employed SPSS 26.0 (IBM Middle East, Dubai, UAE). Data were presented as means ± SEM. Convulsion effects, measured by THLE in seconds, and reproductive toxicities were assessed using one-way ANOVA with treatment (vehicle or test compound) and dose (test compound) as between-subjects factors, followed by least significant difference (LSD) *post hoc* analysis. Fetal abnormality data were presented as counts and percentages. Fisher's exact test compared the percentages of abnormalities between the control group (saline) and the different dose groups. All tests were two-tailed, and significance was set at $p < 0.05$.

3 Results

3.1 Protective effects of H3R antagonist DL76 against MES-induced convulsions in male adult mice

The acute systemic administration of a dose range of DL76 (7.5 mg/kg, 15 mg/kg, 30 mg/kg, and 60 mg/kg, i.p.) exhibited a protective effect on MES-induced convulsions [$F(7,56) = 16.54$; $p < 0.0001$] (Figure 2). The results show that there are substantial protective effects of all doses of DL76 (i.e., 7.5 mg/kg, 15 mg/kg, 30 mg/kg, and 60 mg/kg when compared with saline (all p values <0.0001) (Figure 2). Among the doses tested, the 60 mg/kg dose of DL76 showed the most promising protection in an MES model in adult male mice when compared with the saline-, DL76 (7.5 mg/kg)-, DL76 (15 mg/kg)-, and DL76 (30 mg/kg)-treated groups [mean difference of THLE 6.25 s, 7.25 s, 8.88 s, and 10.75 s; respectively, all $p < 0.0001$] (Figure 2). Notably, the protection provided by H3R antagonist DL76 at the higher dose (60 mg/kg, i.p.) was comparable to that provided by the reference drug VPA ($p = 1.000$) (Figure 2) and was reversed following co-injection with the CNS-penetrant histamine H3R agonist RAM (10 mg/kg, i.p.) 15 min before the MES challenge, with a mean difference of 2.5 s (p-value = 0.094), for the comparison of saline vs. DL76+RAM (Figure 2). Interestingly, RAM (10 mg/kg, i.p.), when injected alone, did not affect MES-induced convulsions ($p = 0.602$ saline + saline vs. DL76 (60 mg/kg) + RAM) (Figure 2). Figure 2 represents the significant differences between all doses of DL76 and compared to VPA (300 mg/kg), RAM, and DL76 60 mg/kg + RAM observed in adult male mice.

10.3389/fphar.2024.1364353

TABLE 3 Effect of systemic treatment of H3R antagonist DL-76 on gestation day (GD-8) in C57/B6 mouse embryos.

			DL76 (mg/kg)				
	Non-Treat. Con	Control	7.5	15	30	60	3 × 15-dose
Number of litters	7	6	7	6	7	7	7
Fetuses/litter	9.143 ± 1.574	7.333 ± 2.066	7.714 ± 1.890	7.167 ± 2.317	8.429 ± 0.787	7.286 ± 1.380	8.143 ± 0.690
Live fetus/litter	8.143 (89.06)	6.333 (86.36)	6.289 (81.48)	6.338 (88.37)	7.286 (86.44)	6.571 (90.20)	6.714 (82.46)
Resorption/litter	1.000 (10.94)	1.000 (13.64)	1.429 (18.51)	0.833 (11.62)	1.143 (13.56)	0.714 (9.80)	1.429 (17.54)
Fetal weight/							
Litter (g) (Mean ± SD)	1.009 ± 0.012	1.050 ± .0.071	1.143 ± 0.107	0.993 ± 0.106	1.004 ± 0.047	1.048 ± .0156	1.037 ± 0.101
IUGR −1SD	1/57 (1.75)	1/38 (2.63)	0	0	1/51 (1.96)	0	3/47 (6.38)
IUGR −2SD	0	1/38 (2.63)	0	2/38 (5.26)	0	2/51 (4.35)	0
Placental weight/							
Litter (g) (mean ± SD)	0.104 ± .011	0.104 ± 0.014	0.109 ± 0.11	0.105 ± 0.009	0.097 ± 0.019	0.101 ± 0.010	0.092 ± 0.007
IUGR −1SD	1/57 (1.75)	1/38 (2.63)	0	0	2/51 (3.92)	1/51 (2.17)	3/47 (4.26)
IUGR −2SD	0	0	0	0	1/51 (1.96)	0	0

Note: Non-Treat. Con = Non-treated control; Parentheses contain percentages. Control mice were administered with saline.

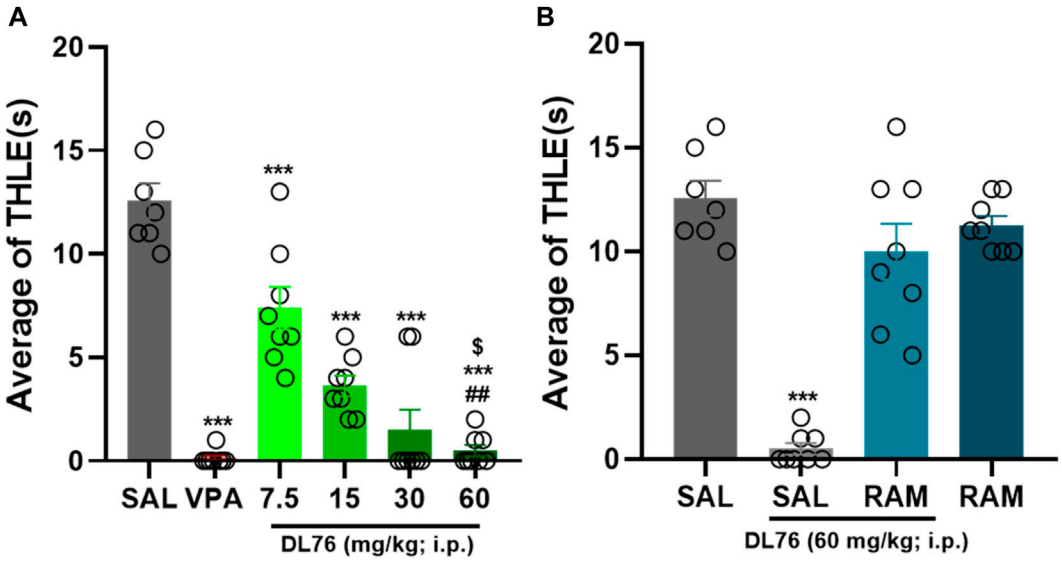

FIGURE 3
Anticonvulsant effect of acute systemic administration of H3R antagonist DL76 on MES-induced seizure in female adult mice. **(A)** Anticonvulsant effects of valproic acid (VPA, 300 mg/kg, i.p.) and test compound DL76 (7.5 mg/kg, 15 mg/kg, 30 mg/kg, and 60 mg/kg, i.p.) on the duration of tonic hind limb extension (THLE) induced in an MES model in female adult mice. **(B)** Effect of CNS-penetrant H3R agonist RAM (10 mg/kg, i.p.) pretreatment on the protection by H3R antagonist DL76 (60 mg/kg, i.p.) on MES-induced convulsions in female adult mice. Each value represents mean ± SEM (n = 8). ***$p < 0.001$ *versus* saline- and DL76 (7.5 mg/kg)-treated groups. $^{\#\#}p < 0.001$ *versus* DL76 (7.5 mg/kg)- and DL76 (15 mg/kg)-treated groups. $^{\$}p < 0.05$ *versus* DL76 (30 mg/kg)-treated group.

3.2 Protective effects of H3R antagonist DL76 against the MES-induced convulsion model in female adult mice

The results showed that VPA (300 mg/kg) and DL76 (7.5–60 mg/kg, i.p.) significantly protected animals against MES-induced convulsions [F (7,56) = 51.78; $p < 0.0001$] (Figure 3). In addition, the results showed that DL76 at a dose of 60 mg/kg significantly provided the highest protection in an MES model in female adult mice when compared with the saline-, DL76 (7.5 mg/kg)-, DL76 (15 mg/kg)-, and DL76 (30 mg/kg)-treated groups [mean difference in THLE of 12.13 s, 10.63 s, and 3.13 s; respectively ($p < 0.05$)] (Figure 3). Similarly, the protection provided by DL76 at the highest dose used in the current study (60 mg/kg, i.p.)

was comparable to that provided by the reference drug VPA (300 mg/kg) (p = 0.72) and was abrogated following acute systemic co-administration of RAM (10 mg/kg, i.p.) 15 min before the MES challenge [mean difference = 1.33; p = 0.17, for the comparison of saline + saline vs. DL76 + RAM] (Figure 3). Data showed that RAM alone in female adult mice generated results similar to those witnessed in male adult mice (10 mg/kg, i.p.; p = 0.91 saline-saline vs. saline-RAM) (Figure 3). Interestingly, no significant differences were observed for the protective effects provided in male and female mice after acute systemic administration of VPA (300 mg/kg, i. p.) or H3R antagonist DL76 at doses of 7.5 mg/kg, 15 mg/kg, 30 mg/kg, and 60 mg/kg, i.p. [F (1,14) = 2.15; p = 0.164, for the comparison of saline + VPA in male mice vs. saline + VPA in female mice], [F (1,14) = 0.156; p = 0.70, for the comparison of saline + DL76 (7.5 mg/kg) in male mice vs. saline + DL76 (7.5 mg/kg) in female mice], [F (1,14) = 0.17; p = 0.685, for the comparison of saline + DL76 (15 mg/kg) in male mice vs. saline + DL76 (15 mg/kg) in female mice], [F (1,14) = 2.31; p = 0.151, for the of comparison saline + DL76 (30 mg/kg) in male mice vs. saline + DL76 (30 mg/kg) in female mice], and [F (1,14) = 0.76; p = 0.398, for the comparison of saline + DL76 (60 mg/kg) in male mice vs. saline + DL76 (60 mg/kg) in female mice], respectively.

3.3 Results of reproductive studies

There was no sign of maternal toxicity in any of the mice from all groups in both the GD-8 and GD-13 treated animals. The number of fetuses in each litter was not significantly different between all study groups, nor was the number of live fetuses. The resorption rate was not significantly different between all the groups. The mean fetal weight in each litter was not significantly different between all treatment groups and the controls. The mean placental weights were also not significantly different between the treated groups and the controls. The incidence of gross morphological anomalies in the treated fetuses of the single- and multiple-dose groups given i.p. was not significantly different from that in the control group. There was no significant difference in the incidence of exencephaly and craniofacial malformations, such as mandibular and maxillary hypoplasia, exomphalos, low set microtia, exophthalmia, eye remaining open, posterior bilateral palate, posterior unilateral palate, hydronephrosis, descended kidney, undescended testis, or kinky tail, between any of the groups studied (Tables 1, 3).

3.4 Results of skeletal malformations

Observations of skeletal defects showed that mean crown-to-rump length decreased significantly in the 7.5 mg/kg-, 30 mg/kg-, and 60 mg/kg-treated groups when compared to control groups. Humerus and ulna lengths were reduced in the 30 mg/kg and 60 mg/kg groups, with only the 30 mg/kg group showing a significant decrease in radius length. Femur length significantly decreased in the 7.5 mg/kg and 60 mg/kg groups; a non-significant decrease (p = 0.06) occurred in the 30 mg/kg group. Tibia and fibula lengths significantly decreased in the 7.5 mg/kg, 30 mg/kg, and 60 mg/kg groups when compared to the controls (Tables 1, 2). No significant differences were observed in skull or facial bones (Tables 1, 2). In addition, in the vertebrae, our observed results showed that there were no differences in the number of centra or the number of unossified/hypoplastic bodies in all the DL-76-treated groups. There was no hypoplasia or poor ossification of the caudal vertebrae in any of the groups. The number of coccygeal vertebral bodies was the same in all tested mice groups (Tables 1, 2). The cervical ribs were attached to the seventh cervical vertebra and ended free anteriorly, becoming the first thoracic ribs. The lumbar ribs attached to the first lumbar vertebra were shorter than the last pair of thoracic ribs. The incidence of lumbar ribs in the DL76-treated group was not significantly different when compared to the saline-treated control mice groups. In addition, there was no fusion of ribs, reduction in number and size, or splitting and forking of ribs in either the control or the DL76-treated mice groups. Notably, 13 pairs of thoracic ribs were observed in both control and experimental embryos (Tables 1, 2). Furthermore, the sternum of the control fetuses consisted of seven sternebrae. There was no significant difference in the fifth sternebrium between the DL76-treated and control mice groups with regards to the absence or the occurrence of hypoplasia. We did not observe any malalignment, hemilateral or unilateral agenesis, scrambling, or fusion, or any cases of bifid sternebrae in any of the groups (Tables 1, 2). Figure 4 shows some of the malformations seen in the embryos.

4 Discussion

H3R antagonist DL76 showed very promising results in terms of its ability to exert protective effects against MES-induced convulsions in male and female adult mice, especially when mice were pretreated with 60 mg/kg i.p., as compared with the saline-treated groups or other mice groups that received lower doses (Figures 2–4). Therefore, the results demonstrated a dose–response relationship of the protective effects provided by H3R antagonist DL76 against convulsions in adult mice of both sexes (Figure 2, 3). Notably, the DL76 (60 mg/kg)-provided protective effect was similar to that observed for the reference drug VPA (300 mg/kg, i.p.) (Figure 2, 3). The latter observations are in harmony with previous preclinical studies that showed dose-dependent protective effects of a couple of H3R antagonists against MES convulsions induced in several animal models (Sadek et al., 2013; Sadek et al., 2014a; Sadek et al., 2014b; Sadek et al., 2015; Sadek et al., 2016a; Sadek et al., 2016b).

In a very recent study, a group of compounds known as 6-aminoalkoxy-3,4-dihydroquinolin-2(1H)-ones were synthesized to evaluate their potential as H3R antagonists and their ability to prevent seizures (Hua et al., 2023). The synthesized compounds exhibited strong H3R antagonism. Specifically, compounds labeled 2a, 2c, 2h, and 4a demonstrated exceptionally potent H3R antagonistic activities, with half-maximal inhibitory concentrations (IC_{50}) of 0.52 μM, 0.47 μM, 0.12 μM, and 0.37 μM, respectively. When tested in the MES model, three compounds—2h, 4a, and 4b—were identified as having antiseizure properties. Molecular docking studies involving compounds 2h, 4a, and a reference compound PIT with the H3R protein were conducted to predict how these molecules might interact with the H3R binding site. The docking results indicated

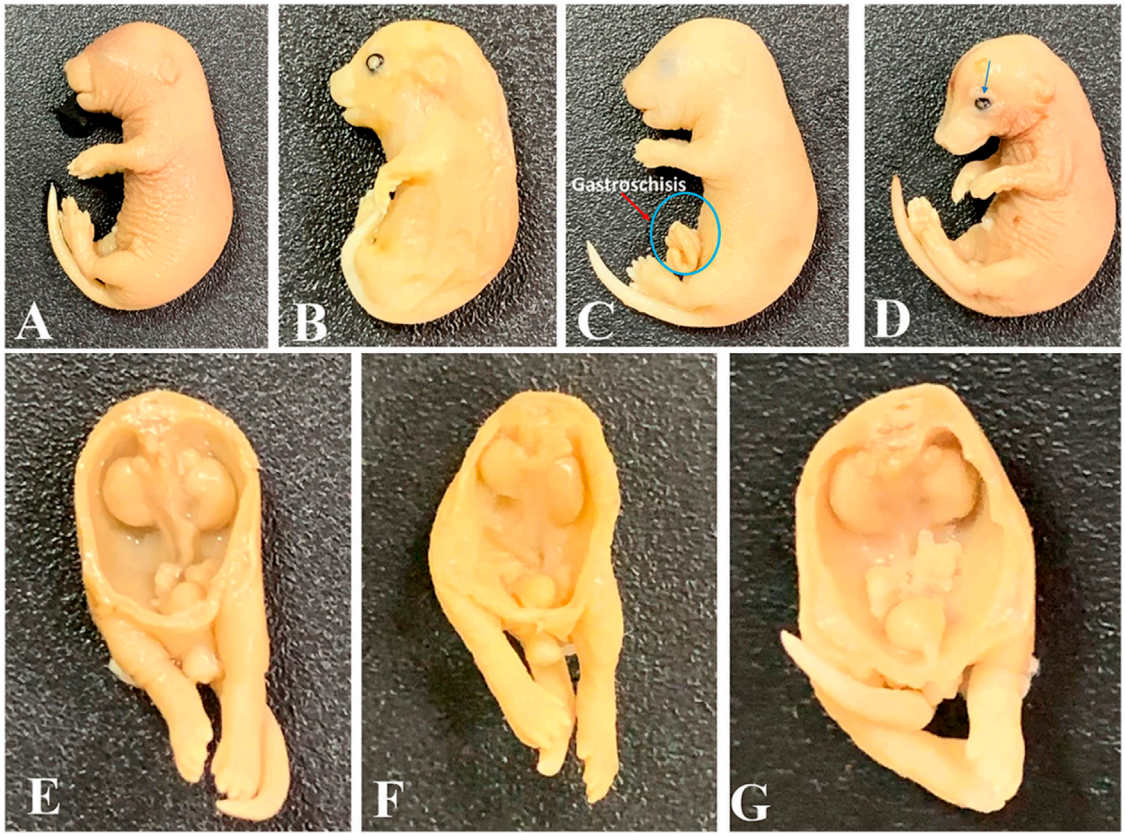

FIGURE 4
Some abnormalities detected in tested mice embryos at gestational day 18. **(A)** Normal embryo; **(B)** mandibular and maxillary hypoplasia with an open eye; **(C)** embryo with gastroschisis; **(D)** intrauterine growth restriction (IUGR) and open eye; **(E)** normal urogenital system; **(F)** embryo with a hypoplastic right kidney and a descended left kidney; **(G)** embryo with undescended testes. Magnification: ×1.25.

that 2h, 4a, and PIT likely share a similar binding mode to the H3R, providing insights into the molecular basis for their antagonistic effects (Hua et al., 2023).

In addition, several non-imidazole H3R antagonists have been tested and, of these, some, such as E159 and E177, emerged as particularly effective, reducing the duration of THLE in a dose-dependent manner in MES-induced seizures in rats (Sadek et al., 2014b; Alachkar et al., 2018). Previous clinical studies showed that the H3R antagonist PIT exhibited protective effects against the photosensitivity seizure model in adult patients (Lamb, 2020).

The current study showed that the protection observed for H3R antagonist DL76 was almost nullified when animals were co-injected with the CNS-penetrant histamine H3R agonist RAM (10 mg/kg i.p.) (Figure 2B, 3B). However, when injected alone, RAM (10 mg/kg) showed neither a protective nor an epileptogenic activity in mice challenged by the MES-induced convulsion (Figure 2B, 3B). These results suggest that the protective effects of H3R antagonist DL76 in the MES-induced convulsions are mediated, at least in part, through an H3R blockade, which is consistent with the formerly observed protective activities of various H3R antagonists (Brigo et al., 2013; Sadek et al., 2014b; Mauritz et al., 2022). These later effects can be devised from the inhibitory effect of H3Rs on the biosynthesis and release of histamine in the presynaptic histaminergic terminals (Sadek et al., 2014b). Subsequently, blockage of these H3 auto-receptors by selective antagonists, such as our compound H3R antagonist DL76, would result in an enhanced neuronal release of brain histamine, providing the proposed protective effect in the MES-induced convulsion status in mice. Notably, the abrogation effect on numerous previously assessed H3R antagonists brought about either by H3R agonists or by CNS-penetrant H1- or H2R antagonists was described, providing further evidence about the role of the H3R antagonism-released brain histamine (Sadek et al., 2013; Sadek et al., 2014a; Sadek et al., 2014b; Sadek et al., 2015; Sadek et al., 2016a; Sadek et al., 2016b). Interestingly, no significant differences were observed for the reference drug VPA (300 mg/kg, i.p.) and the 30 mg/kg and 60 mg/kg doses of the H3R antagonist DL76 in both sexes of adult mice, but there was a significant difference between the THLE values of VPA and the lower doses of DL76 (i.e., the 7.5 mg/kg, and 15 mg/kg, i.p.). The latter results are discrepant with previous studies in which there was a variation in seizure threshold between both sexes due to differences in levels of steroids and steroidal derivatives, such as 3α-hydroxylated pregnane steroids, which can interact with GABA receptor complex, and therefore, decrease seizure susceptibility in female adult mice (Belelli et al., 1990a; Belelli et al., 1990b; Lan et al., 1990; Maguire et al., 2005). In a further series of experiments, H3R antagonist DL76 was administered at various doses to groups of mice on gestational days 8 and 13 (Tables 1–4). The observed results showed that there was no difference in the abnormalities that

TABLE 4 Effect of systemic treatment of H3R antagonist DL-76 on gestation day (GD-13) in C57/B6 mouse embryos.

	Non-Treat. Con	Saline control	DL76 (mg/kg)				
			7.5	15	30	60	3 × 15-dose
Number of litters	7	7	7	7	7	6	7
Fetuses/litter	9.143 ± 1.574	7.571 ± 0.900	8.000 ± 1.291	7.571 ± 1.272	7.000 ± 1.155	7.000 ± 1.414	8.286 ± 1.704
Live fetus/litter	8.143 (89.06)	6.714 (88.68)	7.143 (76.19)	5.714 (75.47)	6.143 (87.76)	5.333 (76.19)	6.857 (82.76)
Resorption/litter	1.000 (10.94)	0.857 (11.32)	0.857 (10.71)	1.857 (24.53)	.857 (12.24)	1.667 (23.81)	1.429 (17.24)
Fetal weight							
Litter (g) (Mean ± SD)	1.006 ± 0.012	1.040 ± 0.090	1.018 ± 0.103	0.998 ± 0.063	1.069 ± 0.082	1.051 ± 0.122	1.051 ± 0.031
IUGR −1SD	1/57 (1.75)	1/47 (2.13)	1/50 (2.00)	1/40 (2.50)	1/43 (2.33)	0	0
IUGR −2SD	0	1/47 (4.26)	0	0	0	0	0
Placental weight/							
Litter (g) (mean ± SD)	0.104 ± .011	0.101 ± 0.007	0.105 ± 0.011	0.113 ± 0.015	0.103 ± 0.006	0.097 ± 0.010	0.110 ± 0.012
IUGR −1SD	1/57 (1.75)	1/47 (2.13)	1/50 (2.00)	1/40 (2.50)	1/43 (2.33)	1/32 (3.13)	1/48 (2.08)
IUGR −2SD	0	0	0	0	0	1/32 (3.13)	0

Note: Non-treat. Con = Non-treated control; Parentheses contain percentages.

occurred in the fetuses. The latter observation is crucial, as all AEDs, including the third-generation agents given to pregnant women, have been shown to have deleterious effects on fetuses in numerous worldwide studies (Abdulrazzaq et al., 1997; Holmes et al., 2001; Padmanabhan et al., 2003; Kaplan, 2004; Padmanabhan et al., 2006).

Although some abnormalities were detected in some of the embryos, their numbers were not different than those in the control groups, except for the crown–rump length and lengths of the long bones of the extremities, which seemed to be affected at the higher doses of 30 mg/kg, 60 mg/kg, and 15 mg/kg × 3. No significant signs of maternal toxicity or fetal resorption were seen in the treated groups (Figure 4). The absence of significant abnormalities in the embryos of mice treated with H3R antagonist DL76 in this study is similar to the lack of teratogenic effects of H3R antagonist 2–18 on mice; the only difference is the adverse effects on the bones of the extremities, which seemed to be shorter in the higher dose groups than the controls (Bastaki et al., 2018). Many women abandon AEDs during pregnancy for fear of their effects on the fetus and are, therefore, at great risk of seizure occurrence and morbidity in both the mother and fetus. The H3R antagonist DL76 appears to be relatively safe except for its effects on the length of the long bones of the extremities at high doses. One of the limitations of this study was that it should have compared the antiseizure and anti-toxicity activities of DL76 to a reference H3R antagonist drug. This will be considered in future experiments.

Unfortunately, it is difficult to extrapolate these findings to humans, and therefore, it is difficult to select a dose that would be safe in humans. Considering these findings, it is reasonable to conclude that the safety profile of H3R antagonist DL76 is obviously higher than that of the other AEDs and comes close to the safety profile of other H3R antagonists like 2–18 (Bastaki et al., 2018).

In conclusion, the H3R antagonist DL76 shows the prospect of being a useful protective anticonvulsant drug with potential use during pregnancy, given the fact that AED VPA was described to induce malformations in C57BL/6 mice (Chateauvieux et al., 2010). Nevertheless, further preclinical studies are necessary to determine if these findings can be replicated when administering the H3R antagonist DL76 throughout the entire gestation period, both in the same species and in other animal models.

Data availability statement

The original contributions presented in the study are included in the article/Supplementary Material; further inquiries can be directed to the corresponding authors.

Ethics statement

The animal study procedures were conducted following guidelines of the European Communities Council Directive (86/609/EEC) and approved by the Institutional Animal Ethics Committee for epilepsy (ERA-2017-5535) and teratogenic studies (A14-14) at the College of Medicine and Health Sciences/United Arab Emirates University. The study was conducted in accordance with the local legislation and institutional requirements.

Author contributions

SB: conceptualization, investigation, supervision, writing–original draft, writing–review and editing, data curation, formal analysis, methodology, software, and validation. YA: investigation, writing–original draft, and writing–review and editing. MZ: formal analysis, investigation, validation, writing–original draft, and writing–review and editing. MS: investigation, writing–original draft, and writing–review and

editing. SA: investigation, writing–original draft, and writing–review and editing. FA: investigation, writing–original draft, and writing–review and editing. EA: investigation, writing–original draft, and writing–review and editing. SM: investigation, writing–original draft, and writing–review and editing. AA: writing–original draft and writing–review and editing. AS: investigation, writing–original draft, and writing–review and editing. DL: investigation, writing–original draft, and writing–review and editing. KK-K: investigation, writing–original draft, and writing–review and editing. BS: conceptualization, data curation, formal analysis, funding acquisition, investigation, methodology, project administration, resources, software, supervision, validation, visualization, writing–original draft, and writing–review and editing.

Funding

The author(s) declare that financial support was received for the research, authorship, and/or publication of this article. The Office of Graduate Studies and Research of UAE University is thanked for the support provided to BS with funds (12M099, 12R207). This study was also supported by statutory funds from the Faculty of Pharmacy Jagiellonian University Medical College, Kraków, Poland [N42/DBS/000300 (DL)].

Conflict of interest

The authors declare that the research was conducted in the absence of any commercial or financial relationships that could be construed as a potential conflict of interest.

Publisher's note

References

Abdulrazzaq, Y. M., Bastaki, S. M., and Padmanabhan, R. (1997). Teratogenic effects of vigabatrin in TO mouse fetuses. *Teratology* 55, 165–176. doi:10.1002/(SICI)1096-9926(199703)55:3<165::AID-TERA1>3.0.CO;2-1

Ago, J., Ishikawa, T., Matsumoto, N., Ashequr Rahman, M., and Kamei, C. (2006). Mechanism of imipramine-induced seizures in amygdala-kindled rats. *Epilepsy Res.* 72, 1–9. doi:10.1016/j.eplepsyres.2006.06.022

Alachkar, A., Lazewska, D., Latacz, G., Frank, A., Siwek, A., Lubelska, A., et al. (2018). Studies on anticonvulsant effects of novel histamine H3R antagonists in electrically and chemically induced seizures in rats. *Int. J. Mol. Sci.* 19, 3386. doi:10.3390/ijms19113386

Arrang, J. M., Garbarg, M., and Schwartz, J. C. (1983). Auto-inhibition of brain histamine release mediated by a novel class (H3) of histamine receptor. *Nature* 302, 832–837. doi:10.1038/302832a0

Arrang, J. M., Garbarg, M., and Schwartz, J. C. (1987). Autoinhibition of histamine synthesis mediated by presynaptic H3-receptors. *Neuroscience* 23, 149–157. doi:10.1016/0306-4522(87)90279-x

Asadi-Pooya, A. A., Brigo, F., Lattanzi, S., and Blumcke, I. (2023). Adult epilepsy. *Lancet* 402, 412–424. doi:10.1016/S0140-6736(23)01048-6

Bass, J. S., Tuo, A. H., Ton, L. T., Jankovic, M. J., Kapadia, P. K., Schirmer, C., et al. (2020). On the digital psychopharmacology of valproic acid in mice. *Front. Neurosci.* 14, 594612. doi:10.3389/fnins.2020.594612

Bastaki, S. M., Abdulrazzaq, Y. M., Shafiullah, M., Wiecek, M., Kiec-Kononowicz, K., and Sadek, B. (2018). Anticonvulsant and reproductive toxicological studies of the imidazole-based histamine H3R antagonist 2-18 in mice. *Drug Des. Devel Ther.* 12, 179–194. doi:10.2147/DDDT.S144730

Belelli, D., Lan, N. C., and Gee, K. W. (1990a). Anticonvulsant steroids and the GABA/benzodiazepine receptor-chloride ionophore complex. *Neurosci. Biobehav Rev.* 14, 315–322. doi:10.1016/s0149-7634(05)80041-7

Belelli, D., Mccauley, L., and Gee, K. W. (1990b). Heterotropic cooperativity between putative recognition sites for progesterone metabolites and the atypical benzodiazepine Ro 5-4864. *J. Neurochem.* 55, 83–87. doi:10.1111/j.1471-4159.1990.tb08824.x

Brigo, F., Ausserer, H., Tezzon, F., and Nardone, R. (2013). When one plus one makes three: the quest for rational antiepileptic polytherapy with supraadditive anticonvulsant efficacy. *Epilepsy Behav.* 27, 439–442. doi:10.1016/j.yebeh.2013.03.010

Brown, R. E., Stevens, D. R., and Haas, H. L. (2001). The physiology of brain histamine. *Prog. Neurobiol.* 63, 637–672. doi:10.1016/s0301-0082(00)00039-3

Canale, V., Kotanska, M., Dziubina, A., Stefaniak, M., Siwek, A., Starowicz, G., et al. (2021). Design, sustainable synthesis and biological evaluation of a novel dual α2a/5-HT7 receptor antagonist with antidepressant-like properties. *Molecules* 26, 3828. doi:10.3390/molecules26133828

Chateauvieux, S., Morceau, F., Dicato, M., and Diederich, M. (2010). Molecular and therapeutic potential and toxicity of valproic acid. *J. Biomed. Biotechnol.* 2010, 479364. doi:10.1155/2010/479364

Chen, Z., Li, W. D., Zhu, L. J., Shen, Y. J., and Wei, E. Q. (2002). Effects of histidine, a precursor of histamine, on pentylenetetrazole-induced seizures in rats. *Acta Pharmacol. Sin.* 23, 361–366.

Holmes, L. B., Harvey, E. A., Coull, B. A., Huntington, K. B., Khoshbin, S., Hayes, A. M., et al. (2001). The teratogenicity of anticonvulsant drugs. *N. Engl. J. Med.* 344, 1132–1138. doi:10.1056/NEJM200104123441504

Holmes, L. B., and Hernandez-Diaz, S. (2012). Newer anticonvulsants: lamotrigine, topiramate and gabapentin. *Birth Defects Res. A Clin. Mol. Teratol.* 94, 599–606. doi:10.1002/bdra.23028

Hua, Y., Song, M., Guo, Q., Luo, Y., Deng, X., and Huang, Y. (2023). Antiseizure properties of histamine H(3) receptor antagonists belonging 3,4-dihydroquinolin-2(1H)-Ones. *Molecules* 28, 3408. doi:10.3390/molecules28083408

Jang, D. H., Manini, A. F., Trueger, N. S., Duque, D., Nestor, N. B., Nelson, L. S., et al. (2010). Status epilepticus and wide-complex tachycardia secondary to diphenhydramine overdose. *Clin. Toxicol. (Phila)* 48, 945–948. doi:10.3109/15563650.2010.527850

Kamei, C., Okumura, Y., and Tasaka, K. (1993a). Influence of histamine depletion on learning and memory recollection in rats. *Psychopharmacol. Berl.* 111, 376–382. doi:10.1007/BF02244955

Kamei, C., Okumura, Y., Tsujimoto, S., and Tasaka, K. (1993b). Role of hypothalamic histamine in stimulating the corticosterone release in rats. *Arch. Int. Pharmacodyn. Ther.* 325, 35–50.

Kaminski, K., Rapacz, A., Luszczki, J. J., Latacz, G., Obniska, J., Kiec-Kononowicz, K., et al. (2015). Design, synthesis and biological evaluation of new hybrid anticonvulsants derived from N-benzyl-2-(2,5-dioxopyrrolidin-1-yl)propanamide and 2-(2,5-dioxopyrrolidin-1-yl)butanamide derivatives. *Bioorg Med. Chem.* 23, 2548–2561. doi:10.1016/j.bmc.2015.03.038

Kaplan, P. W. (2004). Reproductive health effects and teratogenicity of antiepileptic drugs. *Neurology* 63, S13–S23. doi:10.1212/wnl.63.10_suppl_4.s13

Kasteleijn-Nolst Trenite, D., Parain, D., Genton, P., Masnou, P., Schwartz, J. C., and Hirsch, E. (2013). Efficacy of the histamine 3 receptor (H3R) antagonist pitolisant (formerly known as tiprolisant; BF2.649) in epilepsy: dose-dependent effects in the human photosensitivity model. *Epilepsy Behav.* 28, 66–70. doi:10.1016/j.yebeh.2013.03.018

Lamb, Y. N. (2020). Pitolisant: a review in narcolepsy with or without cataplexy. *CNS Drugs* 34, 207–218. doi:10.1007/s40263-020-00703-x

Lan, N. C., Chen, J. S., Belelli, D., Pritchett, D. B., Seeburg, P. H., and Gee, K. W. (1990). A steroid recognition site is functionally coupled to an expressed GABA(A)-benzodiazepine receptor. *Eur. J. Pharmacol.* 188, 403–406. doi:10.1016/0922-4106(90)90201-8

Lazewska, D., Kaleta, M., Schwed, J. S., Karcz, T., Mogilski, S., Latacz, G., et al. (2017). Biphenyloxy-alkyl-piperidine and azepane derivatives as histamine H(3) receptor ligands. *Bioorg Med. Chem.* 25, 5341–5354. doi:10.1016/j.bmc.2017.07.058

Lazewska, D., Ligneau, X., Schwartz, J. C., Schunack, W., Stark, H., and Kiec-Kononowicz, K. (2006). Ether derivatives of 3-piperidinopropan-1-ol as non-imidazole histamine H3 receptor antagonists. *Bioorg Med. Chem.* 14, 3522–3529. doi:10.1016/j.bmc.2006.01.013

Lazewska, D., Olejarz-Maciej, A., Reiner, D., Kaleta, M., Latacz, G., Zygmunt, M., et al. (2020). Dual target ligands with 4-tert-Butylphenoxy scaffold as histamine H(3) receptor antagonists and monoamine oxidase B inhibitors. *Int. J. Mol. Sci.* 21, 3411. doi:10.3390/ijms21103411

Maguire, J. L., Stell, B. M., Rafizadeh, M., and Mody, I. (2005). Ovarian cycle-linked changes in GABA(A) receptors mediating tonic inhibition alter seizure susceptibility and anxiety. *Nat. Neurosci.* 8, 797–804. doi:10.1038/nn1469

Mauritz, M., Hirsch, L. J., Camfield, P., Chin, R., Nardone, R., Lattanzi, S., et al. (2022). Acute symptomatic seizures: an educational, evidence-based review. *Epileptic Disord.* 24, 26–49. doi:10.1684/epd.2021.1376

Mcleod, M. J. (1980). Differential staining of cartilage and bone in whole mouse fetuses by alcian blue and alizarin red S. *Teratology* 22, 299–301. doi:10.1002/tera.1420220306

Miyata, I., Saegusa, H., and Sakurai, M. (2011). Seizure-modifying potential of histamine H1 antagonists: a clinical observation. *Pediatr. Int.* 53, 706–708. doi:10.1111/j.1442-200X.2011.03328.x

Padmanabhan, R., Abdulrazzaq, Y. M., Bastaki, S. M., Shafiullah, M., and Chandranath, S. I. (2003). Experimental studies on reproductive toxicologic effects of lamotrigine in mice. *Birth Defects Res. B Dev. Reprod. Toxicol.* 68, 428–438. doi:10.1002/bdrb.10042

Padmanabhan, R., Shafiullah, M., Benedict, S., and Nagelkerke, N. (2006). Effect of maternal exposure to homocystine on sodium valproate-induced neural tube defects in the mouse embryos. *Eur. J. Nutr.* 45, 311–319. doi:10.1007/s00394-006-0600-4

Pennell, P. B., French, J. A., May, R. C., Gerard, E., Kalayjian, L., Penovich, P., et al. (2020). Changes in seizure frequency and antiepileptic therapy during pregnancy. *N. Engl. J. Med.* 383, 2547–2556. doi:10.1056/NEJMoa2008663

Sadek, B., Kuder, K., Subramanian, D., Shafiullah, M., Stark, H., Lazewska, D., et al. (2014a). Anticonvulsive effect of nonimidazole histamine H3 receptor antagonists. *Behav. Pharmacol.* 25, 245–252. doi:10.1097/FBP.0000000000000042

Sadek, B., Saad, A., Latacz, G., Kuder, K., Olejarz, A., Karcz, T., et al. (2016a). Non-imidazole-based histamine H3 receptor antagonists with anticonvulsant activity in different seizure models in male adult rats. *Drug Des. Devel Ther.* 10, 3879–3898. doi:10.2147/DDDT.S116192

Sadek, B., Saad, A., Schwed, J. S., Weizel, L., Walter, M., and Stark, H. (2016b). Anticonvulsant effects of isomeric nonimidazole histamine H3 receptor antagonists. *Drug Des. Devel Ther.* 10, 3633–3651. doi:10.2147/DDDT.S114147

Sadek, B., Saad, A., Subramanian, D., Shafiullah, M., Lazewska, D., and Kiec-Kononowiczc, K. (2015). Anticonvulsant and procognitive properties of the non-imidazole histamine H3 receptor antagonist DL77 in male adult rats. *Neuropharmacology* 106, 46–55. doi:10.1016/j.neuropharm.2015.10.023

Sadek, B., Schwed, J. S., Subramanian, D., Weizel, L., Walter, M., Adem, A., et al. (2014b). Non-imidazole histamine H3 receptor ligands incorporating antiepileptic moieties. *Eur. J. Med. Chem.* 77, 269–279. doi:10.1016/j.ejmech.2014.03.014

Sadek, B., Shehab, S., Wiecek, M., Subramanian, D., Shafiullah, M., Kiec-Kononowicz, K., et al. (2013). Anticonvulsant properties of histamine H3 receptor ligands belonging to N-substituted carbamates of imidazopropanol. *Bioorg Med. Chem. Lett.* 23, 4886–4891. doi:10.1016/j.bmcl.2013.06.075

Schwartz, J. C. (2011). The histamine H3 receptor: from discovery to clinical trials with pitolisant. *Br. J. Pharmacol.* 163, 713–721. doi:10.1111/j.1476-5381.2011.01286.x

Song, M., Yan, R., Zhang, Y., Guo, D., Zhou, N., and Deng, X. (2020). Design, synthesis, and anticonvulsant effects evaluation of nonimidazole histamine H(3) receptor antagonists/inverse agonists containing triazole moiety. *J. Enzyme Inhib. Med. Chem.* 35, 1310–1321. doi:10.1080/14756366.2020.1774573

Sterz, H., and Lehmann, H. (1985). A critical comparison of the freehand razor-blade dissection method according to Wilson with an *in situ* sectioning method for rat fetuses. *Teratog. Carcinog. Mutagen* 5, 347–354. doi:10.1002/tcm.1770050505

Szafarz, M., Kryczyk, A., Lazewska, D., Kiec-Kononowicz, K., and Wyska, E. (2015). Pharmacokinetics and tissue distribution of the new non-imidazole histamine H3 receptor antagonist 1-[3-(4-tert-butylphenoxy) propyl]piperidine in rats. *Xenobiotica* 45, 912–920. doi:10.3109/00498254.2015.1025117

Thomas, S. V., Syam, U., and Devi, J. S. (2012). Predictors of seizures during pregnancy in women with epilepsy. *Epilepsia* 53, e85–e88. doi:10.1111/j.1528-1167.2012.03439.x

Tomson, T., and Battino, D. (2007). Pharmacokinetics and therapeutic drug monitoring of newer antiepileptic drugs during pregnancy and the puerperium. *Clin. Pharmacokinet.* 46, 209–219. doi:10.2165/00003088-200746030-00002

Tomson, T., Battino, D., Bonizzoni, E., Craig, J., Lindhout, D., Perucca, E., et al. (2018). Comparative risk of major congenital malformations with eight different antiepileptic drugs: a prospective cohort study of the EURAP registry. *Lancet Neurol.* 17, 530–538. doi:10.1016/S1474-4422(18)30107-8

Veroniki, A. A., Rios, P., Cogo, E., Straus, S. E., Finkelstein, Y., Kealey, R., et al. (2017). Comparative safety of antiepileptic drugs for neurological development in children exposed during pregnancy and breast feeding: a systematic review and network meta-analysis. *BMJ Open* 7, e017248. doi:10.1136/bmjopen-2017-017248

Viale, L., Allotey, J., Cheong-See, F., Arroyo-Manzano, D., Mccorry, D., Bagary, M., et al. (2015). Epilepsy in pregnancy and reproductive outcomes: a systematic review and meta-analysis. *Lancet* 386, 1845–1852. doi:10.1016/S0140-6736(15)00045-8

Vohora, D., Saraogi, P., Yazdani, M. A., Bhowmik, M., Khanam, R., and Pillai, K. K. (2010). Recent advances in adjunctive therapy for epilepsy: focus on sodium channel blockers as third-generation antiepileptic drugs. *Drugs Today (Barc)* 46, 265–277. doi:10.1358/dot.2010.46.4.1445795

Witkin, J. M., and Nelson, D. L. (2004). Selective histamine H3 receptor antagonists for treatment of cognitive deficiencies and other disorders of the central nervous system. *Pharmacol. Ther.* 103, 1–20. doi:10.1016/j.pharmthera.2004.05.001

Xiao, F., Yan, R., Zhang, Y., Wang, S., Chen, S., Zhou, N., et al. (2021). Synthesis and antiseizure effect evaluation of nonimidazole histamine H(3) receptor antagonists containing the oxazole moiety. *Arch. Pharm. Weinh.* 354, e2000298. doi:10.1002/ardp.202000298

Yang, L., Wang, Y., and Chen, Z. (2022). Central histaminergic signalling, neural excitability and epilepsy. *Br. J. Pharmacol.* 179, 3–22. doi:10.1111/bph.15692

Zhang, L. S., Chen, Z., Huang, Y. W., Hu, W. W., Wei, E. Q., and Yanai, K. (2003). Effects of endogenous histamine on seizure development of pentylenetetrazole-induced kindling in rats. *Pharmacology* 69, 27–32. doi:10.1159/000071263

Frontiers in Pharmacology

Explores the interactions between chemicals and living beings

The most cited journal in its field, which advances access to pharmacological discoveries to prevent and treat human disease.

Discover the latest Research Topics

See more →

Frontiers

Avenue du Tribunal-Fédéral 34
1005 Lausanne, Switzerland
frontiersin.org

Contact us

+41 (0)21 510 17 00
frontiersin.org/about/contact